Investigating the Immunomodulatory Effect of Novel Fermentates for the Development of a Functional Food Ingredient for the Management of Inflammatory Bowel Disorders and Support against Viral Infection

A thesis submitted by

Dearbhla Finnegan, BSc.

For the degree of Doctor of Philosophy (Ph.D.)

July 2024

Based on research carried out at Dublin City University

School of Biotechnology

Under the supervision of Professor Christine Loscher

and Associate Professor Michael Freeley

I hereby certify that this material, which I now submit for assessment on the programme of study leading to the award of Doctor of Philosophy is entirely my own work, and that I have exercised reasonable care to ensure that the work is original, and does not to the best of my knowledge breach any law of copyright, and has not been taken from the work of others save and to the extent that such work has been cited and acknowledged within the text of my work.

Signed: Candidate I.D: 16780929 Date: 5th July 2024

“Today is your day!

Your mountain is waiting.

So…*get on your way*!”

-Dr.Seuss

For you Nanny, and Grandad.

Acknowledgements:

A lot of time and effort has gone into creating this thesis and for those of you who helped me along the way I appreciate every bit of energy you have given me in order to get me this far.

I would like to thank my supervisor Professor Christine Loscher for all her support throughout the years, encouraging me throughout my journey, and never failing to pick me up me up or spur me on especially when things were not going as planned/hoped. You allowed me to really make this project my own, and your willingness to listen and hear me out made this not only one of the most important experiences in my life but also such an enjoyable one.

I would also like to thank Professor Michael Freeley, my co-supervisor, for his guidance and support in completing the final stages of my Ph.D., always being available to answer my frenzied questions no matter how big or small. Thank you both for your time, patience and expertise that has enabled me to get to this far.

I would like to thank my colleagues in Food for Health Ireland (FHI), in particular Nessa Noronha, for providing me with the funding and opportunity to contribute to science and health in such a meaningful way. I would like to thank the DCU support team for the School of Biotechnology, especially Mary Rafter, Graham Dodrill, Deirdre Curtain, and Allison Tipping. I would like to extend my greatest gratitude to postdoctoral researchers Dr. Restituto Tocmo, and Dr. Roya Hakimjavadi for supporting me throughout my Ph.D..

I would like to thank my friends in work, who have kept me sane throughout these last few years. Doing a Ph.D. more so than anything is a mental challenge, a test of your ability to persevere, and to continue showing up even when things have been failing for weeks, if not months at a time. The only reason I have been able to do this is because of my colleagues Helena, Sarah, and Conor, so thanks for being there for me when I needed it most.

Finally, I want to thank those outside of work who listened to me vent about things I'm sure they couldn't have been less interested in, so a special thanks to my parents Lucia and Aidan who have provided unconditional support always and forever, my brothers Conor and Kevin, as well as Dara, as without all of your love and support I wouldn't have been able to get to this point today. A special thank you to Teddy, and Polly who provided some much needed distraction throughout the last few years. I would like to thank my partner Juan who was always there to listen to me and reassure me of my progress through the many highs and lows, while always being the first to celebrate any achievement no matter how big or small. Lastly I would like to thank my friends outside of college that were there to help me tune out of all things immunology, with a special shoutout to Amy, and Sophie, I'd have been lost without you.

I am forever grateful for all of your support.

Research Dissemination:

1) Research Day, Biological Research Society, Dublin City University, May 2022: Poster Presentation
2) Discovery Day, Food For Health Ireland, May 2022: Poster Presentation
3) Research Day, Biological Research Society, Dublin City University, April 2023: Poster Presentation
4) Research on Walls, Dublin City University, September 2023: Image Presentation
5) British Society for Immunology Congress, Belfast, December 2023: Poster Presentation
6) Food Science and Technology Conference, Dublin, December 2023: Poster Presentation
7) Research Day, Biological Research Society, Dublin City University, April 2024: Poster Presentation

Outreach Initiatives:

1) Dublin City University, Youth outreach with local primary school, March 2022
2) Dublin City University, Youth outreach with local primary school, March 2023

Publications:

1) Akintola, Conor P., Dearbhla Finnegan, Niamh Hunt, Richard Lalor, Sandra O'Neill, and Christine Loscher. "Nutrition Nutraceuticals: A Proactive Approach for Healthcare." In *Advances in Nutraceuticals and Functional Foods*, pp. 123-172. Apple Academic Press, 2022.
2) Finnegan, Dearbhla, Restituto Tocmo, and Christine Loscher. 2023. "Targeted Application of Functional Foods as Immune Fitness Boosters in the Defense against Viral Infection" *Nutrients* 15, no. 15: 3371. https://doi.org/10.3390/nu15153371
3) Sørensen, Helena Mylise, Dearbhla Finnegan, Susan Maye, George MacLeod, Dermot Brabazon, Christine Loscher, and Brian Freeland. 2024. "Optimisation of Dairy-Based Media Using Response Surface Modelling to Increase Yields of Probiotic L. Rhamnosus Promoting an Enhanced Immune Response". In *SSRN*. http://dx.doi.org/10.2139/ssrn.4744874
4) Finnegan, Dearbhla, Monica A. Mechoud, Jamie A. FitzGerald, Tom Beresford, Harsh Mathur, Paul D. Cotter, and Christine Loscher. 2024. "Novel Fermentates Can Enhance Key Immune Responses Associated with Viral Immunity" *Nutrients* 16, no. 8: 1212. https://doi.org/10.3390/nu16081212
5) Under review*:* Finnegan, Dearbhla.; Monica A. Mechoud, Claire Connolly, Jamie A FitzGerald, Tom Beresford, Harsh Mathur, Lorraine Brennan, Paul D. Cotter, Christine Loscher. 2024. "Novel Dairy Fermentates Have Differential Effects on Key Immune Responses Associated with Viral Immunity and Inflammation." *Nutrients*. https://doi.org/10.20944/preprints202404.0455.v1
6) Pending Submission: Finnegan, Dearbhla.; Monica A. Mechoud, Michael Freeley, Tom Beresford, Harsh Mathur, Lorraine Brennan, Paul D. Cotter, Christine Loscher. "Novel dairy fermentates enhance key T cell immune responses with a role in enhanced viral immunity and anti-inflammatory responses for the control of chronic inflammation".

Table of Contents

ACKNOWLEDGEMENTS: ..... **III**

RESEARCH DISSEMINATION: ..... **IV**

OUTREACH INITIATIVES: ..... **IV**

PUBLICATIONS: ..... **V**

ABBREVIATIONS: ..... **X**

LIST OF FIGURES: ..... **XIII**

LIST OF TABLES: ..... **XXII**

ABSTRACT: ..... **XXIV**

1 CHAPTER 1 ..... **1**

GENERAL INTRODUCTION **1**

1.1 INTRODUCTION: 2

1.1.1 Viral infection: *6*

1.1.2 Inflammatory Bowel Disorders: *7*

1.1.3 Overview of the Immune System: *8*

1.1.4 How the immune system reacts to viral invasion: *11*

1.1.5 What is IBD and how it affects the immune system: *19*

1.1.6 What are fermentates: *22*

1.1.7 Immune receptors: *25*

1.1.8 Key Cytokines being examined: *31*

1.2 AIMS AND OBJECTIVES 48

2 CHAPTER 2 ..... **49**

MATERIALS AND METHODS **49**

2.1 MATERIALS 50

2.1.1 Cell Culture: *50*

2.1.2 Sample Preparation and Supernatant generation: *52*

2.1.3 MTS: *53*

2.1.4 ELISA: *53*

2.1.5 M1/M2 Polarisation: *55*

2.1.6 Flow Cytometry and Cell Staining: *56*

2.1.7 Phagocytosis Assay: *58*

2.1.8 Migration assay: *59*

2.1.9 Immune synapse assay: *59*

2.1.10 Lysate Preparation: *59*
2.1.11 BCA protein Quantification: *60*
2.1.12 SDS-PAGE: *60*
2.1.13 Western Blot: *61*
2.1.14 Cells Used: *61*
2.1.15 Buffers/Gels Used: *62*
2.2 METHODS 64
2.2.1 Cell Culture: *64*
2.2.2 Preparation of Cell Stocks: *64*
2.2.3 Revival from Frozen Stocks: *64*
2.2.4 JAWSII Murine Dendritic Cell: *65*
2.2.5 J774.A.1 Murine Macrophage: *65*
2.2.6 Primary-Derived Bone Marrow Dendritic Cells (BMDCs): *66*
2.2.7 Primary-Derived Bone Marrow Macrophages (BMDMs): *67*
2.2.8 Isolation of Primary-Derived T Cells: *68*
2.2.9 T cell polarisation: *70*
2.2.10 JURKAT Human T cell line: *71*
2.2.11 Cell Numeration: *71*
2.2.12 Sample Preparation: *72*
2.2.13 MTS Cell Viability Assay: *73*
2.2.14 Enzyme Linked Immunosorbent Assay (ELISA): *74*
2.2.15 Macrophage M1/M2 polarisation assay: *76*
2.2.16 Flow Cytometry *78*
2.2.17 Migration assay: *82*
2.2.18 Immune synapse assay: *82*
2.2.19 Cell Lysate Preparation: *83*
2.2.20 BCA Protein Quantification Assay: *84*
2.2.21 Western Blot Sample Lysate Preparation: *84*
2.2.22 SDS-PAGE Procedure: *85*
2.2.23 Western Blot: *85*
2.2.24 Statistical analysis: *87*
2.2.25 Ethical Statement: *87*
3 CHAPTER 3 88
PHASE 1 FERMENTATE SCREENING 88
3.1 INTRODUCTION 89
3.2 CHAPTER AIMS 91
3.3 RESULTS: 93

3.3.1 Establishing a dendritic cell model for assessment of fermentate effect on dendritic cell function *93*
3.3.2 Round 1 screening of the bank of fermentate samples in viral immune activated LOX dendritic cells *100*
3.4 DISCUSSION: 144
4 CHAPTER 4 152
PHASE 2 FERMENTATE SCREENING 152
4.1 INTRODUCTION 153
4.2 CHAPTER AIMS: 154
4.3 RESULTS 156
Round 2 screening of top 4 candidate immune boosting fermentates *156*
4.3.1 ..... *156*
4.3.2 Establishing a macrophage model for examination of immune profile of candidate immune boosting fermentates *171*
4.4 DISCUSSION 212
5 CHAPTER 5 224
PHASE 3 FERMENTATE SCREENING 224
5.1 INTRODUCTION 225
5.2 CHAPTER AIMS: 228
5.3 RESULTS 230
5.3.1 Screening of Overall Top 19 bioactive Fermentates from all bioassay groups for anti-inflammatory candidate fermentates *230*
5.3.2 Screening of Top 5 bioactive fermentate candidates *239*
5.3.3 Extended Screening of Top 4 Immunomodulatory candidate fermentates *245*
5.3.4 Regeneration of fermentates has little effect on fermentate bioactivity *252*
5.4 DISCUSSION 268
6 CHAPTER 6 274
PHASE 3 FERMENTATE EXAMINATION 274
6.1 INTRODUCTION 275
6.2 CHAPTER AIMS: 277
6.3 RESULTS 279
6.3.1 CD4+ T cells can be isolated from the spleen of Balb/C mice via magnetic separation, and express CD4, CD3 and, CD25 ..... *279*
6.3.2 CD4+ T cells can be polarised to Th1, Th2, Th17, and Treg cells expressing signature cytokine profiles and transcription factor expression *284*

6.3.3 Stimulation of differentiated T cells with raw fermentates doesn't affect cell viability 291

6.3.4 Stimulation of differentiated T cells with Aerobic R0033, and SC40 affects secretion of cytokines 292

6.3.5 T Cell Functionality 297

6.4 DISCUSSION 324

7 CHAPTER 7 337

FINAL DISCUSSION 337

7.1 PROJECT OVERVIEW 338

7.2 DIET, GLOBAL THREATS, AND IMMUNE FITNESS: 339

7.3 TRADITIONAL FERMENTED FOODS AND OUR NOVEL FERMENTATES: 342

7.4 THE FUTURE OF FUNCTIONAL FOOD INGREDIENTS: 345

REFERENCES 351

APPENDIX 416

Abbreviations:

Full name	Abbreviation
Inflammatory Bowel Disorder	IBD
Human Immunodeficiency Virus 1	HIV-1
Hepatitis C Virus	HCV
Hepatitis B Virus	HBV
Type I IFN	IFN-I
Crohn's Disease	CD
Ulcerative Colitis	UC
Lactic Acid Bacteria	LAB
Generally Regarded As Safe	GRAS
Angiotensin-Converting Enzyme	ACE
Interleukin	IL
Interferon-gamma	IFN-γ
Immunoglobin	Ig
Natural Killer	NK
Toll-Like Receptor	TLR
Tumor Necrosis Factor-alpha	TNF-α
Macrophage inflammatory protein	MIP
Polymorphonuclear Leukocyte	PMN
Major Histocompatibility Complex	MHC
Antigen Presenting Cells	APC
T Cell Receptor	TCR
T helper cell	Th
Retinoic Acid Receptor-Related Orphan Receptor	ROR
Signal Transducer and Activator of Transcription	STAT
Transforming Growth Factor-beta	TGF-β
Antibody Dependant Cellular Cytotoxicity	ADCC
Intestinal Epithelial Cells	IECs
Nucleotide-binding Oligomerisation Domain	NOD

Caspase Recruitment Domain-Containing protein	CARD
Cluster differentiated	CD
Pathogen-Associated Molecular Pattern	PAMP
Lipopolysaccharide	LPS
Plasmacytoid Dendritic Cells	pDCs
IFN Producing Cells	IPCs
Natural IFN-Producing Cells	NIPCs
IFN Regulatory Factor	IRF
PolyI:polyC	PIC
Loxoribine	LOX
Cytosine-Guanine Dinucleotide	CpG
Epstein-Barr virus induced gene 3	EBI3
IL-1β receptor 1	IL-1R1
Nuclear Factor-Kappa B	NF-κB
Toll-IL-1 receptor	TIR
Herpes Simplex Virus	HSV
Granulocyte Macrophage Colony Stimulating Factor	GM-CSF
TNF Receptors	TNFR
Cytokine Synthesis Inhibitory Factor	CSIF
Ethylenediaminetetraacetic acid	EDTA
Stromal cell-derived factor-1 chemokine	SDF-1
Bovine Serum Albumin	BSA
European Collection of Authenticated Cell Cultures	ECACC
Bone Marrow Derived Dendritic Cells	BMDCs
Bone marrow Derived Macrophage Cells	BMDMs
Enzyme Linked Immunosorbent Assay	ELISA
Reagent Diluent	RD
N-(1-Naphthyl) ethylenediamine dihydrochloride	NED
Fixable Viability Dye	FVD
Mean Phagocytosis Index	MPI
Mean Fluorescence Index	MFI

Food for Health Ireland	FHI
Dublin City University	DCU
Reconstituted Skim Milk	RSM
University City Dublin	UCD
Peripheral Blood Mononuclear Cells	PBMC
Mitogen-Activated Protein Kinase	MAPK
Poly Unsaturated Fatty Acids	PUFA
Specialized Pro-resolving lipid Mediator	SPM
Eicosapentaenoic Acid	EPA
Docosahexaenoic Acid	DHA
Arachidonic Acid	AA
Protectin D1 isomer	PDX
Acute Respiratory Distress Syndrome	ARDS
Vitamin D Receptor	VDR
Virgin Coconut Oil	VCO
Extra Virgin Olive Oil	EVOO
Short-Chain Fatty Acid	SCFA

List of Figures:

Figure 1: Retail sales value of functional foods in Europe in 2021. 4

Figure 2: Percentage hold of various regions of the worldwide functional food market size for 2021. 5

Figure 3: Overview of innate and adaptive immunity. 10

Figure 4: How the immune system responds to viral infection. 18

Figure 5: How the immune system responses to IBD. 21

Figure 6: Health Benefits of functional foods. 23

*Figure 7: **TLRs, their associated Ligands and agonists.*** 30

*Figure 8: **Structural units of the IL-12 family of cytokines, respective signalling transducers and signalling pathways, showing main functional immune response.*** 33

*Figure 9: **BMDM and BMDC Schematic.*** 68

*Figure 10: **ELISA Schematic.*** 75

Figure 11: Summary of Chapter 3 Aims. 92

Figure 12: Exposure of JAWS to different concentrations of TLR ligands affects cell viability. 95

*Figure 13: **Exposure of JAWS to different concentrations of TLR ligands results in the secretion of cytokines.*** 96

*Figure 14: **Exposure of BMDC to different TLR ligands doesn't affect cell viability.*** 98

Figure 15: Exposure of BMDC to different TLR ligands results in the secretion of cytokines. 99

*Figure 16: **Exposure of JAWS to pre-treated fermentates SC6, SC15, SC17 and SC40 doesn't affect cell viability.*** 102

*Figure 17: **Exposure of JAWS to pre-treated fermentates SC6, and SC16 affects cytokine secretion.*** 104

*Figure 18: **Exposure of JAWS to pre-treated fermentates SC17, and SC40 affects cytokine secretion.*** 105

Figure 19: Exposure of JAWS to dose response of raw sample fermentates SC6, SC15, SC17 and SC40 doesn't affect cell viability. 107

*Figure 20: **Exposure of JAWS to dose response of filtered sample fermentates SC6, SC15, SC17 and SC40 doesn't affect cell viability.*** 108

*Figure 21: **Exposure of JAWS to dose response of raw sample fermentate SC6 and SC15 affects cytokine secretion.*** 110

*Figure 22: **Exposure of JAWS to dose response of raw sample fermentate SC17 and SC40 affects cytokine secretion.*** 111

*Figure 23: **Exposure of JAWS to dose response of filtered sample fermentate SC6 and SC15 affects cytokine secretion.*** 112

Figure 24: Exposure of JAWS to dose response of filtered sample fermentate SC17 and SC40 affects cytokine secretion. 113

Figure 25: ***Exposure of JAWS to raw sample fermentates SC6, SC15, SC17 and SC40 and TLRs LPS, CpG and PIC affects cell viability.*** 115
Figure 26: ***Exposure of JAWS to panel of TLRs and raw fermentate SC6 and SC15 affects cytokine secretion.*** 117
Figure 27: ***Exposure of JAWS to panel of TLRs and raw fermentate SC17 and SC40 affects cytokine secretion.*** 117
Figure 28: ***Exposure of BMDC to dose range of filtered fermentates SC6, SC15, SC17 and SC40 doesn't affect cell viability.*** 120
Figure 29: ***Exposure of LOX activated BMDC to filtered sample SC6 results in the secretion of cytokines.*** 122
Figure 30: ***Exposure of LOX activated BMDC to filtered sample SC15 results in the secretion of cytokines.*** 123
Figure 31: ***Exposure of LOX activated BMDC to filtered sample SC17 results in the secretion of cytokines.*** 123
Figure 32: ***Exposure of LOX activated BMDC to filtered sample SC40 results in the secretion of cytokines.*** 124
Figure 33: ***Exposure of BMDC to dose response of raw or filtered SC16, SC18, SC63, SC72, SC51, SC52, DPC1178, and DPC1817 sample fermentates doesn't affect cell viability.*** .. 125
Figure 34:**Exposure of LOX activated BMDC to raw or filtered sample SC16 results in the secretion of cytokines.** 128
Figure 35:**Exposure of LOX activated BMDC to raw or filtered sample SC18 results in the secretion of cytokines.** 129
Figure 36:**Exposure of LOX activated BMDC to raw or filtered sample SC51 results in the secretion of cytokines.** 130
Figure 37:**Exposure of LOX activated BMDC to raw or filtered sample SC52 results in the secretion of cytokines.** 131
Figure 38:**Exposure of LOX activated BMDC to raw or filtered sample SC63 results in the secretion of cytokines.** 132
Figure 39:**Exposure of LOX activated BMDC to raw or filtered sample SC72 results in the secretion of cytokines.** 133
Figure 40: ***Exposure of LOX activated BMDC to raw or filtered sample DPC1178 results in the secretion of cytokines.*** 134
Figure 41: ***Exposure of LOX activated BMDC to raw or filtered sample DPC1817 results in the secretion of cytokines.*** 135
Figure 42: ***Exposure of BMDC to 25mg/ mL raw and filtered LC10, Aerobic R0033, Anaerobic R0033, Aerobic R0070, HA136, HA119, HA108, SC71, LH88, P200209, R0389, HA196, R0419 and HA179 fermentates doesn't affect cell viability.*** 138

Figure 43: ***Exposure of LOX activated BMDC to sample LC10, Aerobic R0033, Anaerobic R0033, Aerobic R0070 and Anaerobic R0070 results in the secretion of cytokines.*** 140
Figure 44: ***Exposure of LOX activated BMDC to sample HA136, HA119, HA108, SC71 and LH88 results in the secretion of cytokines.*** 141
Figure 45: ***Exposure of LOX activated BMDC to sample P200209, R0389, HA196, R0419 and HA179 results in the secretion of cytokines.*** 142
Figure 46:**Schematic representation of Chapter 3 workflow.** 144
Figure 47:**Summary of Chapter 4 Aims for objective 1.** 155
Figure 48**: Summary of Chapter 4 Aims for objective 2.** 155
Figure 49: ***Exposure of BMDC to LPS, CpG, and PIC TLRs and 25mg/mL raw immune boosting fermentates doesn't affect cell viability.*** 157
Figure 50:**Exposure of LOX and LPS activated BMDC to 25mg/mL raw samples doesn't affect cell viability.** 158
Figure 51: ***Exposure of LPS, CpG and Pic activated BMDC to 25mg/mL raw sample Aerobic R0033 results in the secretion of cytokines IL-1b, IL-6, IL-10, TNF-a, IL-12p40, IL-12p70, IL-23 and IL-27.*** 160
Figure 52: ***Exposure of LPS, CpG and Pic activated BMDC to 25mg/mL raw sample Anaerobic R0033 results in the secretion of cytokines IL-1b, IL-6, IL-10, TNF-a, IL-12p40, IL-12p70, IL-23 and IL-27.*** 161
Figure 53:**Exposure of LPS, CpG and Pic activated BMDC to 25mg/mL raw sample SC40 results in the secretion of cytokines IL-1b, IL-6, IL-10, TNF-a, IL-12p40, IL-12p70, IL-23 and IL-27.** .. 162
Figure 54: ***Exposure of LPS, CpG and Pic activated BMDC to 25mg/mL raw sample R0419 results in the secretion of cytokines IL-1b, IL-6, IL-10, TNF-a, IL-12p40, IL-12p70, IL-23 and IL-27.*** 163
Figure 55: ***Exposure of LOX activated BMDC to 25mg/mL raw Aerobic R0033, Anaerobic R0033, SC40 and R0419 results in the secretion of cytokines IL-1b, IL-6, IL-10 , TNF-a, IL-12p40, IL-12p70, IL-23 and IL-27.*** 166
Figure 56: ***Exposure of LPS activated BMDC to 25mg/mL raw Aerobic R0033, Anaerobic R0033, SC40 and R0419 results in the secretion of cytokines IL-1b, IL-6, IL-10, TNF-a, IL-12p40, IL-12p70, IL-23 and IL-27.*** 167
Figure 57: ***Exposure of LOX activated BMDC to 25mg/mL LC10, R0215, HA118 and P200622 results in the secretion of cytokines IL-1b, IL-6, IL-10, TNF-a, IL-12p40, IL-12p70, IL-23 and IL-27.*** 169
Figure 58: ***Exposure of LPS activated BMDC to 25mg/mL LC10, R0215, HA118 and P200622 results in the secretion of cytokines IL-1b, IL-6, IL-10, TNF-a, IL-12p40, IL-12p70, IL-23 and IL-27.*** 170
Figure 59:**Exposure of LOX, LPS, CpG, and PIC activated J774.A.1 cells to 25mg/mL raw sample Aerobic R0033, Anaerobic R0033, SC40 and R0419 doesn't affect cell viability.** 173

Figure 60: ***Exposure of LOX and PIC activated J774.A.1 cells to TLRs and 25mg/mL raw sample results in the secretion of for IL-1B, IL-6, IL-10, and TNF-A.*** 175

Figure 61: ***Exposure of LPS and CpG activated J774.A.1 cells to 25mg/mL raw sample results in the secretion of IL-1B, IL-6, IL-10, and TNF-A.*** 175

Figure 62: ***Exposure of J774.A.1 to TLR and incubation at 37°C and 4°C affects MFI.*** 179

Figure 63: ***Exposure of J774.A.1 to TLR and incubation at 37°C and 4°C affects percentage phagocytosing cells.*** 180

Figure 64: ***Exposure of J774.A.1 cells to TLR and incubation at 37°C and 4°C affects phagocytosis.*** 181

Figure 65: ***Exposure of J774.A.1 cells to LOX and LPS results in phagocytosis.*** 184

Figure 66:**Exposure of J774.A.1 cells to LOX and LPS results in phagocytosis.** 187

Figure 67: ***Exposure of LOX and LPS activated J774.A.1 cells to 25mg/mL sample affects MFI.*** . 190

Figure 68: ***Exposure of LOX and LPS activated J774.A.1 cells to 25mg/mL sample affects percentage of phagocytosing cells.*** 193

Figure 69: ***Exposure of LOX and LPS activated J774.A.1 cells to 25mg/mL sample affects MPI.*** . 196

Figure 70: ***Exposure of LOX activated J774.A.1 cells to 25mg/mL sample affects Cell Surface Marker Expression.*** 199

Figure 71: ***Exposure of LPS activated J774.A.1 cells to 25mg/mL sample affects Cell Surface Marker Expression.*** 200

Figure 72: ***Isolated BMDM Express Key Surface Markers of the Macrophage Lineage F4/80.*** ... 202

Figure 73: ***Exposure of BMDM to panel of TLRs and 25mg/mL raw sample Aerobic R0033, Anaerobic R0033, SC40 and R0419 doesn't affect cell viability.*** 204

Figure 74: ***Exposure of LOX activated BMDM to 25mg/mL raw sample results in the secretion of cytokines.*** 206

Figure 75: ***Exposure of PIC activated BMDM to 25mg/mL raw sample results in the secretion of cytokines.*** 207

Figure 76: ***Exposure of LPS activated BMDM to 25mg/mL raw sample results in the secretion of cytokines.*** 207

Figure 77: ***Exposure of CpG activated BMDM to 25mg/mL raw sample results in the secretion of cytokines.*** 208

Figure 78: ***Exposure of LOX and PIC activated BMDM to 25mg/mL raw sample results in the secretion of chemokines.*** 210

Figure 79: ***Exposure of LPS and CpG activated BMDM to 25mg/mL raw sample results in the secretion of chemokines.*** 211

Figure 80: **Polarisation of M0 macrophage to M1, and M2 macrophage and their subsequent phenotypes .** 227

Figure 81: ***Summary of Chapter 5 Aims.*** 229

Figure 82: ***Exposure of LPS activated BMDC to 25mg/mL of top 19 Regenerated raw samples doesn't affect cell viability.*** 232
Figure 83: ***Exposure of LPS activated BMDC to 25mg/mL to top 19 raw sample fermentates results in the secretion of cytokines IL-1β, IL-6, IL-10 and TNF-α.*** 235
Figure 84: ***Exposure of LPS activated BMDC to 25mg/mL to top 19 raw sample fermentates results in the secretion of cytokines IL-1β, IL-6, IL-10 and TNF-α.*** 236
Figure 85: ***Exposure of LPS activated BMDC to 25mg/mL to top 19 raw sample fermentates results in the secretion of cytokines IL-12p40, IL-12p70, IL-23 and IL-27.*** 237
Figure 86: ***Exposure of LPS activated BMDC to 25mg/mL to top 19 raw sample fermentates results in the secretion of cytokines IL-12p40, IL-12p70, IL-23 and IL-27.*** 238
Figure 87: ***Exposure of LOX and LPS activated BMDC to 25mg/mL top 5 bioactive fermentates doesn't affect cell viability.*** 240
Figure 88: ***Exposure of LOX activated BMDC to 25mg/mL top 5 fermentate candidates results in the secretion of cytokines IL-1β, IL-6, IL-10, TNF-α, IL-12p40, IL-12p70, IL-23, and IL-27*** .. 242
Figure 89: ***Exposure of LPS activated BMDC to 25mg/mL top 5 fermentate candidates results in the secretion of cytokines IL-1β, IL-6, IL-10, TNF-α, IL-12p40, IL-12p70, IL-23, and IL-27.*** 243
Figure 90: ***Exposure of M0, M1, and M2 BMDM to 25mg/mL top 4 raw samples affects production of NO.*** 246
Figure 91: ***Exposure of M0, M1, and M2 BMDM to 25mg/mL top 4 raw samples affects arginase activity.*** 248
Figure 92: ***Exposure of M1/M2 polarised BMDMs to 25mg/mL top 4 Fermentate samples results in the secretion of cytokines IL-6, TNF-α, and IL-10.*** 250
Figure 93: **Exposure of BMDM and BMDC to panel of TLRs and 25mg/mL differentially generated raw SC40 doesn't affect cell viability.** 253
Figure 94: **Exposure of LOX activated BMDC to 25mg/mL differentially generated SC40 raw sample results in the secretion of cytokines IL-1β, IL-6, IL-10, TNF-α, IL-12p40, IL-12p70, IL-23, and IL-27** 256
Figure 95: **Exposure of PIC activated BMDC to 25mg/mL differentially generated SC40 raw sample results in the secretion of cytokines IL-1β, IL-6, IL-10, TNF-α, IL-12p40, IL-12p70, IL-23, and IL-27** 257
Figure 96: **Exposure of LPS activated BMDC to 25mg/mL differentially generated SC40 raw sample results in the secretion of cytokines IL-1β, IL-6, IL-10, TNF-α, IL-12p40, IL-12p70, IL-23, and IL-27** 258
Figure 97: **Exposure of CpG activated BMDC to 25mg/mL differentially generated SC40 raw sample results in the secretion of cytokines IL-1β, IL-6, IL-10, TNF-α, IL-12p40, IL-12p70, IL-23, and IL-27** 259

FIGURE 98: EXPOSURE OF LOX ACTIVATED BMDM TO 25MG/ML DIFFERENTIALLY GENERATED SC40 RAW SAMPLE RESULTS IN THE SECRETION OF CYTOKINES IL-1β, IL-6, IL-10, TNF-α, IL-12P40, IL-12P70, IL-23, AND IL-27 262
FIGURE 99: EXPOSURE OF PIC ACTIVATED BMDM TO 25MG/ML DIFFERENTIALLY GENERATED SC40 RAW SAMPLE RESULTS IN THE SECRETION OF CYTOKINES IL-1β, IL-6, IL-10, TNF-α, IL-12P40, IL-12P70, IL-23, AND IL-27 263
FIGURE 100: EXPOSURE OF LPS ACTIVATED BMDM TO 25MG/ML DIFFERENTIALLY GENERATED SC40 RAW SAMPLE RESULTS IN THE SECRETION OF CYTOKINES IL-1β, IL-6, IL-10, TNF-α, IL-12P40, IL-12P70, IL-23, AND IL-27 264
FIGURE 101: EXPOSURE OF CPG ACTIVATED BMDM TO 25MG/ML DIFFERENTIALLY GENERATED SC40 RAW SAMPLE RESULTS IN THE SECRETION OF CYTOKINES IL-1β, IL-6, IL-10, TNF-α, IL-12P40, IL-12P70, IL-23, AND IL-27 265
FIGURE 102: SCHEMATIC REPRESENTATION OF T CELL DIFFERENTIATION. 276
FIGURE 103:SUMMARY OF CHAPTER 6 AIMS. 278
FIGURE 104: SPLEENOCYTES DO NOT EXPRESS CD4, WHILE ISOLATED T CELLS EXPRESS CD4. 281
FIGURE 105: ISOLATED UNDIFFERENTIATED T CELLS EXPRESS CD4 AND CD3. 282
FIGURE 106: ACTIVATED CD4+ T CELLS EXPRESS CD25. 283
FIGURE 107: EXPOSURE OF UNDIFFERENTIATED CD4+ T CELLS TO POLARISATION FACTORS RESULTS IN THE SECRETION OF CYTOKINES IFN-Γ, IL-2, IL-4, IL-6, IL-10, IL-13, IL-17, AND TGF-β. 286
FIGURE 108: TH1 CELLS EXPRESS HIGH LEVELS OF TBET. 287
FIGURE 109: TH2 CELLS EXPRESS HIGH LEVELS OF GATA. 288
FIGURE 110: TH17 CELLS EXPRESS HIGH LEVELS OF RORYT. 289
FIGURE 111: TREG CELLS EXPRESS HIGH LEVELS OF FOXP3. 290
FIGURE 112:EXPOSURE OF POLARISED T CELLS TO AEROBIC R0033, AND SC40 DOESN'T AFFECT CELL VIABILITY. 292
FIGURE 113:EXPOSURE OF TH1, TH2, AND TH 17 CELLS TO 25MG/ML AEROBIC R0033, AND SC40 RESULTS IN THE SECRETION OF CYTOKINES IL-2, IL-4, IL-6, IL-10, IL-13, IL-17, TGF-β, AND IFN-Γ. 294
FIGURE 114:EXPOSURE OF TH1, TH2, AND TREG CELLS TO 25MG/ML AEROBIC R0033, AND SC40 RESULTS IN THE SECRETION OF CYTOKINES IL-2, IL-4, IL-6, IL-10, IL-13, IL-17, TGF-β, AND IFN-Γ. 295
FIGURE 115: EXPOSURE OF JURKAT CELLS TO DOSE RANGE OF RSM, SC40, AND AEROBIC R0033 INFLUENCES CELL PROLIFERATION. 298
FIGURE 116: EXPOSURE OF JURKAT CELLS TO PLATE BOUND T CELL ACTIVATION AFFECTS CELL PROLIFERATION. 299
FIGURE 117: EXPOSURE OF ACTIVATED JURKAT CELLS TO FERMENTATES AFFECTS CELL PROLIFERATION. 301
FIGURE 118: EXPOSURE OF JURKAT CELLS TO PLATE BOUND T CELL ACTIVATION AFFECTS SECRETION OF CYTOKINES.. 302
FIGURE 119: EXPOSURE OF ACTIVATED JURKAT CELLS TO FERMENTATES AFFECTS SECRETION OF CYTOKINES 304

FIGURE 120: **EXPOSURE OF JURKAT CELLS TO DOSE RANGE OF SDF-1 CHEMOATTRACTANT RESULTS IN THE MIGRATION OF CELLS.** 305
FIGURE 121: **EXPOSURE OF JURKAT CELLS TO DOSE RANGE OF SRSM, SC40, AND AEROBIC R0033 RESULTS IN THE MIGRATION OF CELLS.** 307
FIGURE 122: **JURKAT CELLS CAN BE STAINED BY FLUORESCENT MICROSCOPY TO IMAGE THE T CELL, THE NUCLEUS, AND THE ACTIVATED F-ACTIN OF THE IMMUNE SYNAPSE.** 311
FIGURE 123: **EXPOSURE OF JURKAT CELLS TO T CELL ACTIVATION BEADS RESULTS IN IMMUNE SYNAPSE INTERACTION.** 311
FIGURE 124: **EXPOSURE OF JURKAT CELLS TO T CELL ACTIVATION BEADS RESULTS IN IMMUNE SYNAPSE INTERACTION.** 313
FIGURE 125: **PROTEIN QUANTIFICATION OF JURKAT CELLS ACTIVATED WITH PLATE BOUND ANTIBODIES.** 315
FIGURE 126: **TOTAL ERK 1/2 ARE EXPRESSED IN JURKAT CELLS ACTIVATED WITH PLATE BOUND ANTIBODIES.** 316
FIGURE 127: **PHOSPHO ERK 1/2 ARE EXPRESSED IN JURKAT CELLS ACTIVATED WITH PLATE BOUND ANTIBODIES.** 317
FIGURE 128:**TOTAL AND PHOSPHO ERK 1/2 ARE EXPRESSED IN JURKAT CELLS ACTIVATED WITH PLATE BOUND ANTIBODIES.** 318
FIGURE 129: **PROTEIN QUANTIFICATION OF JURKAT CELLS ACTIVATED WITH PLATE BOUND ANTIBODIES AND FERMENTATES.** 319
FIGURE 130: **TOTAL ERK 1/2 ARE EXPRESSED IN ACTIVATED JURKAT CELLS STIMULATED WITH FERMENTATES RSM, SC40, AND AEROBIC R0033.** 321
FIGURE 131: **PHOSPHO ERK 1/2 ARE EXPRESSED IN ACTIVATED JURKAT CELLS STIMULATED WITH FERMENTATES RSM, SC40, AND AEROBIC R0033.** 322
FIGURE 132: **TOTAL AND PHOSPHO ERK 1/2 ARE EXPRESSED IN ACTIVATED JURKAT CELLS STIMULATED WITH FERMENTATES RSM, SC40, AND AEROBIC R0033.** 323
*FIGURE 133: **DIAGRAMMATIC REPRESENTATION OF PROJECT.*** 338
*FIGURE 134: **EXPOSURE OF JAWS TO DOSE RESPONSE OF RAW OR FILTERED FERMENTATES DOESN'T AFFECT CELL VIABILITY.*** 417
*FIGURE 135: **EXPOSURE OF LOX ACTIVATED JAWS TO SAMPLE SC16, SC18, SC51, AND SC52 RESULTS IN THE SECRETION OF CYTOKINES.*** 418
*FIGURE 136: **EXPOSURE OF LOX ACTIVATED JAWS TO SAMPLE SC63, SC72, DPC1178, AND DPC1817 RESULTS IN THE SECRETION OF CYTOKINES.*** 419
*FIGURE 137: **EXPOSURE OF BMDC TO 25MG/ML RAW AND FILTERED SAMPLES DOESN'T AFFECT CELL VIABILITY.*** 420
*FIGURE 138: **EXPOSURE OF LOX ACTIVATED BMDC TO SAMPLE LPC58, SC76, ST115, ST906 AND LN34 RESULTS IN THE SECRETION OF CYTOKINES.*** 421
*FIGURE 139: **EXPOSURE OF LOX ACTIVATED BMDC TO SAMPLE R1039, R0215, R0052, HA110 AND HA118 RESULTS IN THE SECRETION OF CYTOKINES.*** 422

Figure 140: ***Exposure of LOX activated BMDC to sample R0422, P200622, P200524, P2006175 and P200427 results in the secretion of cytokines.*** 423
Figure 141: ***Exposure of LOX activated BMDC to sample ST765, R1058, HA114 and HA274 results in the secretion of cytokines.*** 424
Figure 142: ***Exposure of J774.A.1 to time course of LOX and LPS activated TLRs results in phagocytosis.*** 425
Figure 143: ***Activation of J774.A.1 Macrophage time course of LOX and inflammatory LPS TLRs affects phagocytic activity.*** 426
Figure 144: ***Exposure of J774.A.1 to 25mg/mL RSM sample and LOX or LPS activated TLRs results in phagocytosis.*** 427
Figure 145: ***Activation of J774.A.1 Macrophage with sample and viral TLR LOX affects phagocytic activity.*** 428
Figure 146: ***Activation of J774.A.1 Macrophage with sample and inflammatory TLR LPS affects phagocytic activity.*** 429
Figure 147: ***Exposure of J774.A.1 to LOX and LPS TLRs and 25mg/mL sample affects phagocytosis.*** 430
Figure 148: ***Stimulation of LOX and LPS activated J774.A.1 Macrophage with RSM, Aerobic R0033 and Anaerobic R0033 affects phagocytic activity.*** 431
Figure 149: ***Stimulation of LOX and LPS activated J774.A.1 Macrophage with RSM, R0419 and SC40 affects phagocytic activity.*** 432
Figure 150: ***Cell Surface Marker Expression Profile is affected by Specific TLR Activation and RSM presence.*** 433
Figure 151: ***Cell Surface Marker Expression Profile is affected by Specific TLR Activation and RSM presence.*** 434
Figure 152: ***Cell Surface Marker Expression Profile is affected by Specific TLR Activation and Aerobic R0033 presence.*** 435
Figure 153: ***Cell Surface Marker Expression Profile is affected by Specific TLR Activation and Aerobic R0033 presence.*** 436
Figure 154: ***Cell Surface Marker Expression Profile is affected by Specific TLR Activation and Anaerobic R0033 presence.*** 437
Figure 155: ***Cell Surface Marker Expression Profile is affected by Specific TLR Activation and Anaerobic R0033 presence.*** 438
Figure 156: ***Cell Surface Marker Expression Profile is affected by Specific TLR Activation and SC40 presence.*** 439
Figure 157: ***Cell Surface Marker Expression Profile is affected by Specific TLR Activation and SC40 presence.*** 440
Figure 158: ***Cell Surface Marker Expression Profile is affected by Specific TLR Activation and R0419 presence.*** 441

Figure 159: ***Cell Surface Marker Expression Profile is affected by Specific TLR Activation and R04190 presence.*** 442

Figure 160: ***Exposure of LPS activated BMDC to 25mg/mL Original or Regenerated raw samples doesn't affect cell viability.*** 443

Figure 161: ***Exposure of LPS activated BMDC to 25mg/mL Original or Regenerated raw Aerobic R0033 results in the secretion of cytokines IL-1β, IL-6, IL-10, TNF-α, IL-12p40, IL-12p70, IL-23, and IL-27.*** 443

Figure 162: ***Exposure of LPS activated BMDC to 25mg/mL Original or Regenerated raw Anaerobic R0033 results in the secretion of cytokines IL-1β, IL-6, IL-10, TNF-α, IL-12p40, IL-12p70, IL-23, and IL-27.*** 444

Figure 163: ***Exposure of LPS activated BMDC to 25mg/mL Original or Regenerated R0419 results in the secretion of cytokines IL-1β, IL-6, IL-10, TNF-α, IL-12p40, IL-12p70, IL-23, and IL-27.*** 444

Figure 164: **Exposure of JURKAT cells to T cell activation beads results F-ACTIN.** 445

Figure 165: **Exposure of JURKAT cells to T cell activation beads results in immune synapse interaction.** 447

List of Tables:

Table 1: ***Functional Food Market Size in Ireland, Eastern Europe, Western Europe and the World.*** 4

Table 2: ***Summary of Cytokine Functions.*** 42

Table 3: ***All Tissue and Cell culture materials and reagents, corresponding sources and product codes.*** 50

Table 4: ***All Sample and Supernatant generation materials and reagents, corresponding sources and product codes.*** 52

*Table 5 :****All Cell Viability materials and reagents, corresponding sources and product codes.*** . 53

Table 6: ***All ELISA materials and reagents, corresponding sources and product codes.*** 53

Table 7: ***All M1/M2 polarisation, Griess Assay and Arginase Assay materials and reagents corresponding sources and product codes.*** 55

*Table 8****: All Flow Cytometry materials and reagents, corresponding sources and product codes.*** 56

Table 9: ***All Phagocytosis materials and reagents, corresponding sources and product codes.*** 58

*Table 10****: All migration assay materials and reagents, corresponding sources and product codes.*** 59

*Table 11****: All immune synapse assay materials and reagents, corresponding sources and product codes.*** 59

Table 12**: All lysate preparation materials and reagents, corresponding sources and product codes.** 59

Table 13**: All Protein Purification materials and reagents, corresponding sources and product codes.** 60

Table 14**: All SDS-PAGE materials and reagents, corresponding sources and product codes.** ...60

Table 15**: All western blot materials and reagents, corresponding sources and product codes.** 61

*Table 16****: All Cell Names, Cell Types used and corresponding sources.*** 61

Table 17: ***Composition of most commonly used buffers and gels.*** 62

Table 18: ***Polarisation factors for differentiation towards Th1, Th2, Th17, and Treg cells.*** 70

Table 19**:FHI list of fermentate sample strains and sample names.** 90

Table 20: **Summary of the cytokines secreted in the presence of SC6, SC15, SC17, and SC40 in the presence of PIC, LPS, and CpG activated JAWS cells.** 118

Table 21: **Summary of the cytokines secreted in the presence of SC16, SC18, SC51, SC52, SC63, SC72, DPC1178, and DPC1817 at 10mg/mL or 25mg/mL raw and filtered doses.** 136

Table 22: **Summary of the cytokines secreted in the presence of LC10, Aerobic R0033, Anaerobic R0033, Aerobic R0070, Anaeerobic R0070, HA136, HA119, HA108, SC71, LH88, P200622, R0389, HA196, R0419, and HA179 in their raw and filtered 25mg/mL form.** 142

*TABLE 23: **SUMMARY TABLE OF THE CYTOKINES PRODUCED BY BMDC CELLS ACTIVATED WITH LOX, PIC, LPS, AND CPG, IN THE PRESENCE OF SAMPLES AEROBIC R0033, ANAEROBIC R0033, SC40 AND, R0419.*** 163

*TABLE 24: **TOP 19 BIOACTIVE FERMENTATES.*** 226

TABLE 25: **SUMMARY CYTOKINE SECRETION FOR BMDCS IN THE PRESENCE OF TOP 5 BIOACTIVE FERMENTATES.** 244

TABLE 26:**SUMMARY OF THE EFFECTS ON CYTOKINE SECRETION, NO PRODUCTION, AND ARGINASE ACTIVITY IN THE PRESENCE OF FERMENTATES IN M0, M1, AND M2 MACROPHAGE.** 251

TABLE 27: **SUMMARY OF THE CYTOKINES SECRETED IN THE PRESENCE OF SPIN-OFF SC40 FERMENTATES IN LOX, PIC, LPS, AND CPG ACTIVATED BMDC AND BMDMS.** 266

TABLE 28: **SUMMARY OF FERMENTATE EFFECT ON KEY CYTOKINES IN T CELL SUBSETS.** 296

Abstract:

Dearbhla Finnegan

Investigating the Immunomodulatory Effect of Novel Fermentates for the Development of a Functional Food Ingredient for the Management of Inflammatory Bowel Disorders and Support against Viral Infection

The aim of this project was to assess the immunomodulatory capabilities of a bank of 46 dairy fermentates derived from lactic acid bacteria. Initially screening the 46 fermentates in the context of viral immunity assessing their viability, and cytokine secretion profiles in JAWS and bone marrow derived dendritic cells (BMDC), highlighted 4 immune boosting candidates Aerobic R0033, R0419, SC40, and Anaerobic R0033. A more in depth screening was carried out on these fermentates to assess their effect in additional immune cells key to innate immunity, macrophage cell line J774.A.1 and primary bone marrow derived macrophage (BMDM). A range of cell functions were assessed including cell viability, cytokine and chemokine secretion, phagocytosis, and cell surface marker expression. A multidisciplinary review from Food for health Ireland (FHI), and its collaborators collated the top 19 fermentates in the context of candidate anti-inflammatory samples to support gut health. An initial screening assessed these 19 fermentates in the context of anti-inflammatories assessing cell viability and cytokine secretion in both BMDM, and BMDCs, to highlight 4 candidate anti-inflammatory fermentates. The top 5 immune boosting and anti-inflammatory fermentates were deduced and a comparative screening in BMDC, highlighted the top 4 candidates, two immune boosting (Aerobic R0033, R0419) and two anti-inflammatory fermentates (SC40, LH88). Theses fermentates were assessed for nitric oxide production, arginase activity, and cytokine secretion in unpolarised and M1, M2 polarised macrophage, to highlight the two most promising immune boosting and anti-inflammatory fermentate, Aerobic R0033, and SC40 respectively. These two samples underwent extensive analysis in murine derived naïve, Th1, Th2, Th17, and Treg cells for viability, and cytokine secretion to establish sample effect on adaptive immunity. From there these two samples were assessed for their effect on cell functionality in the human T cell line JURKAT cells, assessing their effect on cytokine secretion, cell proliferation, cell migration, immune synapse interactions, and downstream signalling. This project highlighted sample Aerobic R0033, and SC40 as the most promising fermentates for their immune boosting, and anti-inflammatory capabilities respectively.

1 Chapter 1

General Introduction

1.1 Introduction:

In recent years there has been a clear shift in the interest of consumers in food for health, with people more than ever before being aware of the ancient old saying, thought to be stated by Hippocrates in 400BC “Let food be thy medicine and medicine be thy food”. Food is a critical factor in a healthy, disease free, quality of life. Food is fundamental for longevity, with global dietary risk factors estimated to cause 11 million deaths and 255 million disability-adjusted life years annually (Fadnes et al., 2022). Thus, only serving to prove the importance of a healthy well-balanced diet for sustained quality of life. It is a long known fact that what we eat influences our body, and vital nutrients are essential for growth, cellular function, tissue development, energy and immune defence (Koithan & Devika, 2010). There is growing evidence and increased research in the science of food as immunomodulators, the study of nutritional immunology, whereby increased intake of certain nutrients above the recommended daily dose has been highlighted to optimize immune function to improve immune defence function and increase resistance to infection, while maintaining tolerance (Wu et al., 2018). Furthermore, deficiency in nutrients leads to malnutrition and results in the development of disease. Often this disease results from the nutritional inadequacies which impair immune function and put the individual at greater risk of disease development or increased susceptibility to infection.

The increased popularity and global explosion within the Health and Wellbeing industry can be seen through the booming economic figures based on data from 2015-2017 showing a growth rate of 6.4% (Wellness Creative Co, 2019). This growth was expected to continue at this pace with the UK Health and Wellbeing industries net worth of €24.1 billion as of 2019, only expected to grow more in the following years, within the global wellness market with its estimated $4.75 trillion net worth in 2019. Of this network it is the Healthy Eating, Nutrition and Weight Loss sector that comes to an estimated $702 billion, making it the second largest sector of the

industry, only to be ruled by the Personal Care, Beauty, and Anti-aging sector, with an estimated worth of $1,083 billion based on data form 2015-2017.

These trends in the health and wellbeing industry reflect trends seen in the food industry, with an increasing demand for healthy foods, in turn impacting and sparking the revolution that is the development of food products that can impart health benefits to their consumers, *i.e.*, the functional food industry. The functional food industry is growing at a phenomenal rate with a worldwide growth rate of 10.34% from 2016-2021 based on data gathered from Euromonitor (Euromonitor International, a market research provider, 2022). Furthermore, this growth rate is expected to increase further, nearly doubling that of 2016-2021, with an expected worldwide growth rate of 19.17% from 2021-2026 (Euromonitor International, a market research provider, 2022). Figure 1 represents the retail sales value of the functional food industry in Europe in 2021, with the UK holding the largest value followed by France and Germany (Sørensen et al., 2022). The popularity of functional foods worldwide is on the increase, with the USA, Europe and Japan being the regions holding the greatest retail sales values (Sørensen et al., 2022).

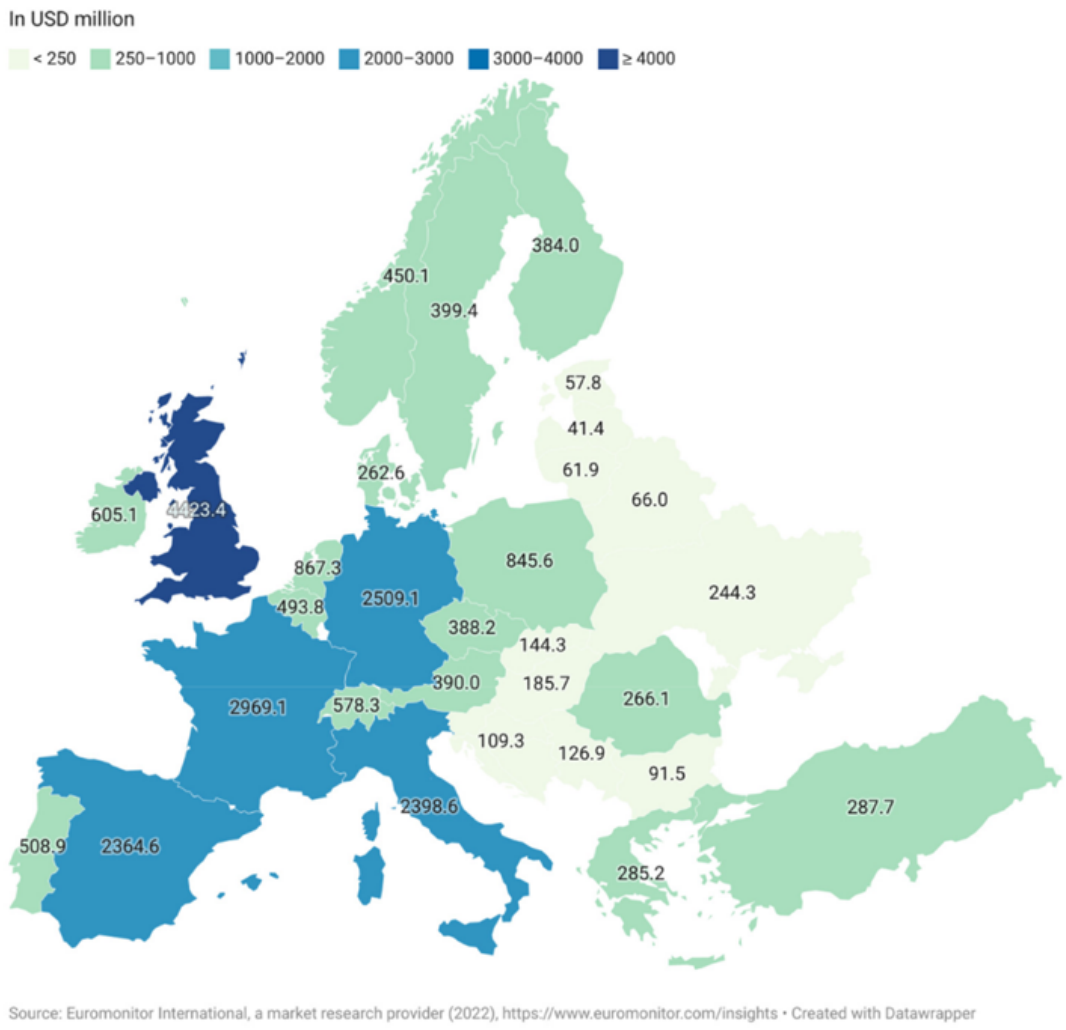

*Figure 1**: Retail sales value of functional foods in Europe in 2021.** (Sørensen et al., 2022).*

Table 1 presents the annual increase in market size for Ireland, Eastern and Western Europe, USA, and Worldwide, in million USD from 2016-2021, with future predictions in market size for 2022-2026.

*Table 1: **Functional Food Market Size in Ireland, Eastern Europe, Western Europe and the World.** Market values from 2016-2021 in million USD. Predicted market values for 2022-2026 in million USD.*

Year	2016	2017	2018	2019	2020	2021	2022	2023	2024	2025	2026
Ireland	495	511	520	532	554	585	586	592	618	647	679
Eastern Europe	4,142	4,727	4,968	4,999	4,921	5,212	5,531	5,746	5,977	6,234	6,498
Western Europe	20,690	20,696	21,569	20,662	21,537	23,032	23,527	23,907	24,444	25,131	25,804
USA	31,903	31,709	31,008	30,957	32,054	31,512	32,941	34,148	35,240	36,211	37,164
World	159,040	164,365	168,157	168,478	168,919	177,395	184,465	192,846	201,417	210,356	219,468

Figure 2 represents the percentage hold Ireland, Eastern and Western Europe and USA have in the worldwide functional food market, with Europe and the USA making up over a third of the worldwide functional food market at a combined 33.67% of the total market size.

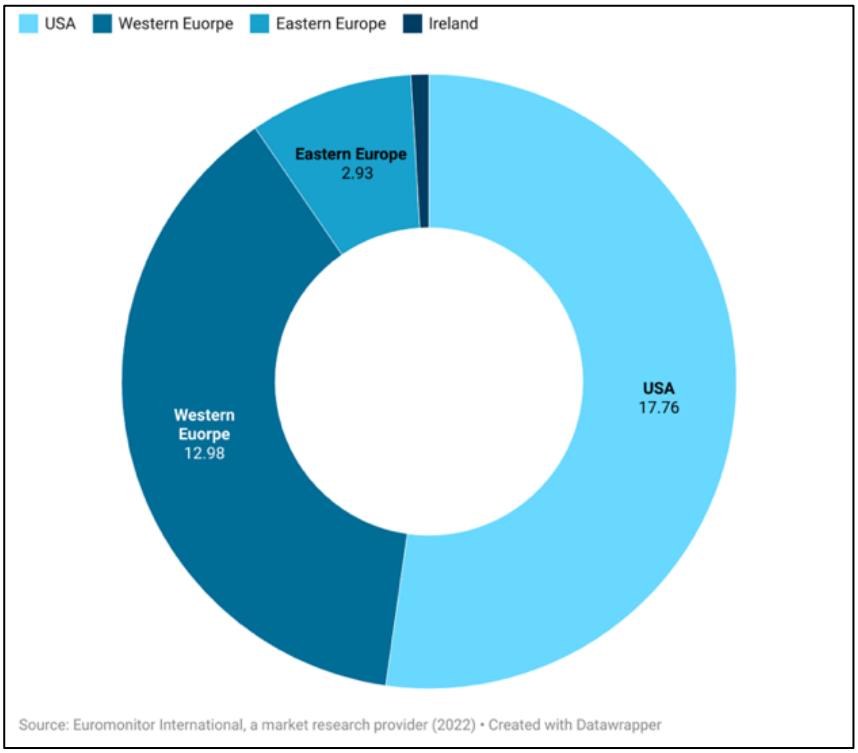

*Figure 2**: Percentage hold of various regions of the worldwide functional food market size for 2021.** Data obtained from Euromonitor International, a market research provider (2022). Figure created with Datawrapper.*

This annual growth rate was expected to continue for the foreseeable future, however, in late 2019 and early 2020 the catastrophic news of a global COVID-19 pandemic further ignited the global interest in the Health and Wellness industry. This rapid growth and boom within the functional food industry is clear evidence that global civilisation is now looking to food to support immune function. Seeking functional foods sources with immunomodulatory capabilities could potentially be a game changer to aid in a natural way of tackling viral infection and chronic illness. Due to the current economic climate, the immune support and health supplements market is expected to grow even further, at a compound annual growth rate of over 9% from 2019-2025 (Research and Markets, 2021). This is due to the impact of COVID-19, sparking and rejuvenating interest in food components to be used as major sources of immune boosting ingredients.

1.1.1 Viral infection:

In late 2019 and early 2020 the catastrophic news of a global pandemic further ignited the global interest in the Health and Wellness industry and the Functional Food industry. With an estimated six month immunity provided by the vaccines as antiviral therapy for the prevention of COVID-19 infection, alternative methods to augment protection against viral invasion are highly desirable (Health Service Executive, 2021; Thomas et al., 2021). Immune boosting health foods have been of utmost interest in protecting global civilisation against the devasting effects of such a dangerous and fatal viral attack.

As a result of such devastating damage and loss caused by the Coronavirus, humanity more than ever, is looking for every way possible to keep themselves as healthy and protected against viral attack. Novel ways of using food ingredients has recently become an intriguing area of research to achieve such a goal due to the lengthy process that is implemented for the development of safe and efficacious anti-viral vaccines and the rapid mutation rate of the virus. Therefore, there is a keen interest in the maintenance and protection from viral infection in the form of naturally sourced food ingredients.

Nowadays trends on the market clearly indicate that people are looking for ways to boost the immune system and fortify it against potentially deadly viral invasion. The uncertainty within the public surrounding new vaccines like that of the Sars-CoV-2 virus and the subsequent COVID-19 vaccine, and the rate of mutations means that finding a way to boost the immune system in a natural way is highly sought after. Likewise, chronic viral infections such chronic viral infections include human immunodeficiency virus 1 (HIV-1), hepatitis C virus (HCV) and hepatitis B virus (HBV) together affect more than 500 million individuals worldwide (Wilson & Brooks, 2011) and occur in the form of persistently replicating viruses that cause lifelong health challenges (Harker et al., 2018). Similarly seasonal flu viruses pose significant threat to human life with 26-50million flu illness from October 2022 through April 2023, 12-24 million medical visits, 290,00-670,000 flu hospitalisations, and 17,000-98,000 flu deaths (CDC, 2023). Current viral treatments often result in highly regulated immune responses aiming to keep the

virus as suppressed as possible without causing the human host any fatal immunopathological effects. However such responses include hypofucntionality of CD4+ and CD8+T cells, delayed antibody production and attenuated type I IFN (IFN-I) responses (Harker et al., 2018), thus leaving the patient in a state of highly weakened immunity. Therefore, immune boosting health foods have been of utmost interest in protecting global civilisation against the potentially devasting effects of dangerous and fatal viral invasion.

1.1.2 Inflammatory Bowel Disorders:

With the modern diet consisting of greater meat and animal product consumption, observational studies have linked such dietary patterns to the risk and development of IBDs like that of Crohn's Disease (CD) and Ulcerative Colitis (UC) (Lewis, 2016). IBDs are issues within the body associated with gut discomfort as a result of immunological imbalances within the intestinal mucosa associated with cells of the adaptive immune system (de Mattos et al., 2015). IBDs arise as a result of the immune system responding to self-antigens and triggering chronic inflammation in patients with diseases like UC and CD. These chronic digestive diseases affect over 10 million people worldwide and have no known cause or cure (EFCCA, 2022). IBDs result in common symptoms including severe abdominal pain, diarrhoea, gas, fatigue, weight loss as well as mucus or bloody stool (CDC, 2022b; Cleveland Clinic, 2022).

Dietary treatments for IBDs include enteral nutrition in the form of hydrolysed or intact protein formulas, however there is much interest in identifying more palatable and easier to use diets for the long term treatment of IBDs (Lewis, 2016). Other nonsurgical IBD treatments involve medications to control symptoms. They include Aminosalicylates, antibiotics, biologics and corticosteroids (Cleveland Clinic, 2022). Significant side effects are often associated with such medications and therefore a need for a more natural intervention is highly sought after (Head & Jurenka, 2004). Otherwise surgical treatments for IBDs involve removal of diseased bowel segment in CD patients or a colectomy in UC patients whereby the colon is

removed and an ileal pouch is attached externally (Cleveland Clinic, 2022). The prevalence of IBDs is on the increase (Alatab et al., 2020; CDC, 2022a) and thus finding a functional food, that could aid in the control and management of such a prevalent and debilitating disease, in a natural way, would be of huge medical significance.

1.1.3 Overview of the Immune System:

A well-functioning immune system is critical for survival, in the protection against invading pathogens, in the ability to distinguish self from non-self, and furthermore decipher non- self-molecules which could potentially be harmful to the body to those innocuous molecules which present no danger. The immune system is comprised of the innate and adaptive immune response.

The innate immune system is the first line of defence in protecting the body against invading pathogens. It is non-specific, meaning it attacks pathogens without knowing their specific species/strain. The innate immune system is therefore less efficient but quick acting, recognising pathogens through common features conserved only to specific pathogen species, via pathogen recognition receptors. The innate immune system provides fast acting immune responses acting within 0-4 hours to remove pathogens via the first line of cellular innate immunity, or with early induced response calling on innate immune cells at 4-96 hours. The innate immune system consists of physical barriers such as the skin, sweat and mucus's, such as those found at the epithelial barrier, and consists of cells such as phagocytic cells like macrophages, NK cells and neutrophils which are the first cells on site in the attack of a pathogen, as well as other cells such as dendritic and mast cells. The innate immune response also plays a key role in the activation of the adaptive immune response, with dendritic cells being the key link between the innate and adaptive immune systems.

The adaptive immune response is called into action when the innate response cannot overcome the initial attack on the immune system, and is generally initiated after 96 hours. The adaptive immune system is specific and

recognises pathogen species in order to destroy them. It is much more efficient in its protection against invading pathogens as cells of the adaptive immune response have the ability to “remember” previous pathogens that have invaded the body and prevent them eliciting an immune response second time round. The cells of the adaptive immune response consist of lymphocytes such as B and T cells, which hold this memory capacity and are antigen specific. T cells include cytotoxic T cells with the CD8 receptor, important in direct cell killing, T helper cells with the CD4 receptor, which are important for coordinating responses of other immune cells and T regulatory cells (Treg), which also contain CD4 receptors and modulate immune tolerance. Th1 and Th2 are subsets of Th cells defined by the cytokines they produce, with Th1 profiles being immune boosting and promoting secretion of an M1 pro-inflammatory phenotype for anti-viral effect, while Th2 promote an M2 phenotype whereby cytokine secretion is anti-inflammatory and aids in disease resolution, similarly Treg cells suppress inflammatory cytokines and exert an anti-inflammatory immune response. B cells are required for antibody production in order to attack, bind and kill pathogens via the production of immunoglobulin (Ig) classes IgM, IgD, IgA, IgG and IgE.

It is these responses of both the innate and adaptive immune systems that lead to inflammation, noted by redness, swelling, heat, and discomfort which are caused by pressure being exerted on nerves resulting in pain, that signal the immune system is at work on healing affected tissue. Figure 3 shows an overview of the innate and adaptive immune mechanisms, detailing the cells involved in each.

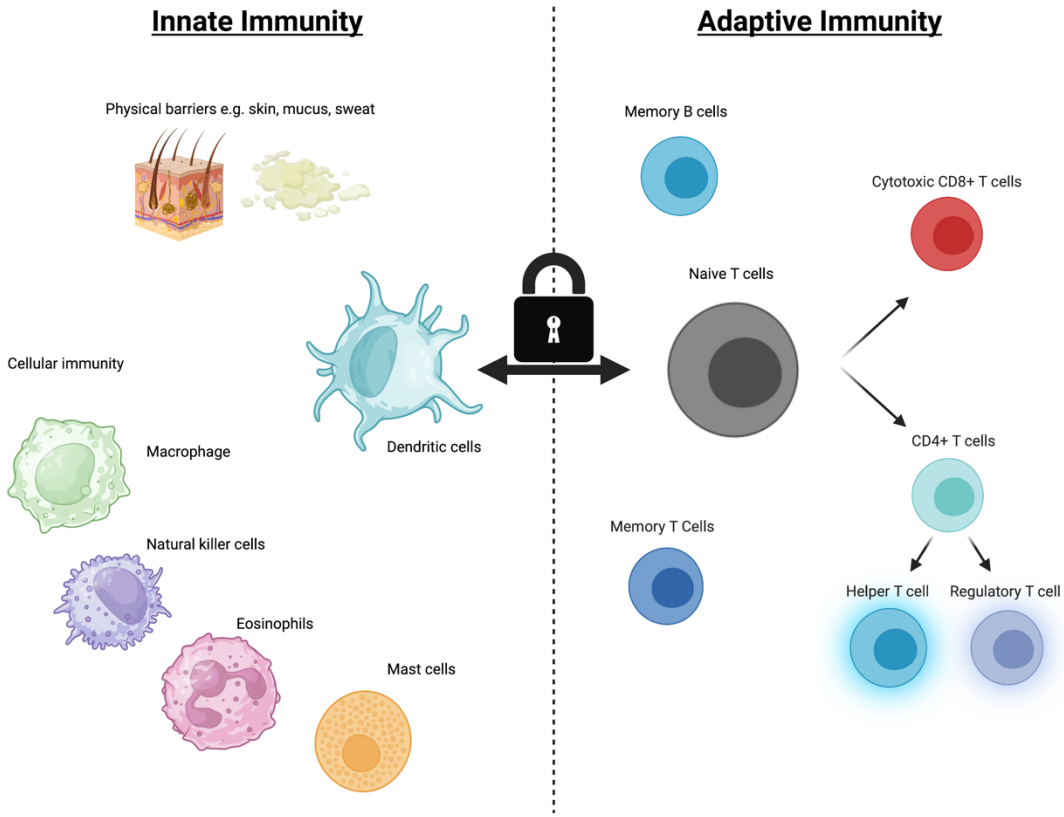

*Figure 3:**Overview of innate and adaptive immunity.** Overview of the physical and cellular immunity involved in the innate and adaptive immune systems, specifying the cells involved in each. Dendritic cell and naïve T cell shown as the key link between the innate and adaptive immune responses. Created using BioRender.com.*

1.1.4 How the immune system reacts to viral invasion:

A typical viral immune response is mounted in a host when a viral pathogen manages to invade the cells of the host, where it remains in order to survive and replicate (Laing & Fred Hutchinson Cancer Research Centre, 2020). Viruses are therefore considered obligate intracellular parasites hijacking their host cells in order to replicate and aid in their spread of infection. Almost all viral infections cause the induction of the immune response in the form of recruitment and activation of inflammatory cells including macrophage and neutrophils, which in turn cause the generation of a range of molecules such as cytotoxic cytokines, cationic proteins, lipid mediators, metalloproteinases and components of the oxygen burst (Rouse & Sehrawat, 2010).

During a viral infection the immune system is triggered to produce

1) the early, nonspecific immune response in the form of nonspecific inhibition, Natural Killer (NK) cell activity and interferon activity to limit viral multiplication following acute phase of the viral attack, with subsequent

2) initiation of the specific adaptive immune response in the form of the humoral and cell-mediated immune responses that function to aid in the elimination of the virus and in maintenance of specific resistance to reinfection (Klimpel, 1996).

More than 95% of living organisms use the innate immune mechanisms for survival compared to less than 5% which depend on T and B cell functions of the adaptive immune response (Dinarello, 2018).

1.1.4.1 Innate immune mechanisms:

Virus transmission occurs in the host, having been confronted with many physical and chemical barriers upon entry. Mechanical barriers like that of the skin and mucosal surfaces are most effective as well as the chemical hostility provided by the gut (Mueller & Rouse, 2008). Other routes of entry include genitourinary tract, respiratory tract, gastrointestinal and ocular

routes of entry. Once in the body the virus then attaches to cellular receptors and fuses with the cell membrane, the cell becomes endocytosed thus gains entry to the cell cytoplasm or nucleus by fusing with the vesicular membrane of enveloped viruses, or can translocate across the cell membrane or induce cell lysis of the endocytic vesicle once in the cytoplasm for nonenveloped viruses (Marsh & Helenius, 2006). Once they've gained entry into the cell they then hijack the cells machinery combined with their own unique specialised viral encoded proteins to replicate rapidly within the cell. From here the infection transmits if not tackled already and spreads inconspicuously through various mechanisms of virus release strategies such as budding or secretion into extracellular space via cytolysis (Marsh & Helenius, 2006). This process of attachment to host cell, assembly of viral particles within the cell, release to extracellular space and entry into new cell is the basis of the spread of viral infection within the host body.

Innate cellular immune responses come into play in the case of failure of physical and chemical barriers within the first 24 hours of viral invasion (Mueller & Rouse, 2008). This involves initiation via the pathogen recognition receptors of the Toll-like receptor (TLR) family or DExD/H box RNA helicases (Kawai & Akira, 2006) to promote expression of type I IFN and a multitude of IFN-stimulated genes and inflammatory cytokines (Garcia-Sastre & Biron, 2006). IFN-I receptor binding to create antiviral proteins like that of α/β IFNs results in the transcription of more than 100 IFN-stimulated genes, leading to an antiviral state for the inhibition of cell protein synthesis and prevention of viral replication as well as the activation of NK cells and various other cytokines to produce a proinflammatory response to kill infected cells and interact with dendritic cells (Mueller & Rouse, 2008). Many other leukocytes aid in the innate immune defence system like that of macrophage, dendritic cells and neutrophils, while similarly, many other host proteins function in antiviral defence, including natural antibodies and complement proteins as well as other cytokines like Tumour necrosis factor (TNF)-α, IFN-γ and IL-6 and chemokines such as Macrophage inflammatory protein (MIP)-1α (Mueller & Rouse, 2008).

Thus overall the innate immune system protects against viral invasion through a series of physical and chemical barriers as well as a nonspecific cellular immune defence mechanism to protect against viral infection by blocking, protecting and destroying the invading virus.

1.1.4.2Adaptive immune mechanisms:

In the case that a virus cannot be cleared the adaptive immune system kicks into action, in the form of a more targeted and specific attack on the invading virus, providing recognition of self from non self and furthermore provides a memory to prevent repeated viral attack. Adaptive immunity relies on antigen-specific receptors expressed on clonally expanded T and B lymphocytes, cell mediated response and a humoral response respectively (Kawai & Akira, 2006).

1.1.4.2.1 Cell mediated

1.1.4.2.1.1 T cells:

T cells or T lymphocytes, are a type of leukocyte or white blood cell that are essential for the effective functioning of the immune system (The Editors of Encyclopaedia, 2020). T cells are one of the two key lymphocytes involved in the initiation and specificity of the immune response to antigens invading a host, B cells being the other. T cells get their name as they originate in the bone marrow however mature in the thymus, where they are then able to multiply and differentiate into a range of subsets of T cells depending on the required immune response needed to clear, control and prevent pathogen invasion and infection. These subsets are the helper T cells, cytotoxic T cells, regulatory T cells and memory T cells.

1.1.4.2.1.1.1 Th cells:

Helper T cells or Th cells are needed to coordinate effector functions to lead to the destructive responses of the immune system for pathogen clearance, however likewise can also be the source of autoimmunity when overexpressed (Bacchetta, 2016). Th cells are vital for activation of CD8+ cytotoxic T cells and macrophage,

maturation of B cells into plasma and memory B cells, antibody production, recruitment of polymorphonuclear leukocyte

(PMN) such as neutrophils, eosinophils and basophils at the source of infection or inflammation, amplification of microbiocidal activity of macrophage, and likewise involved in the detrimental effects of the immune system in the form of tolerance development and suppression of inflammatory responses (Pahl & Vaziri, 2015).

Th cells become activated by recognising a peptide of antigen, via the major histocompatibility complex (MHC) II, presented on antigen presenting cells (APC) through the interaction with the T cell receptor (TCR) (Kaiko et al., 2008) and via co-stimulation caused by the binding of B7 proteins on the dendritic cell to the CD28 on the T cells (*How The Body Reacts To Viruses*, 2021). This is carried out when these cells travel through the circulation to reach the lymph nodes where activation can then occur (*How The Body Reacts To Viruses*, 2021). Following activation naïve Th cells can then begin to divide and further differentiate into effector cells specific to the MHCII complex (Goldsby et al., 2003). These effector cells are CD4+ and can be classed under three main subdivisions, each with their own unique cytokine secretion phenotypes, that ultimately each elicit a distinct immune function (Kaiko et al., 2008). These subdivisions are; Th type-1 (Th1), Th type-2 (Th2) and Th type-17 (Th17) cells. These effector cells then leave the lymph nodes and travel through the circulation to carry out immune functions (*How The Body Reacts To Viruses*, 2021).

1.1.4.2.1.2 Th1, Th2, Th17, and Treg immune responses and differences:

Th1:

Such cells are involved in cellular immunity (Saito et al., 2010). Cellular immunity is a slow acting adaptive immune response that destroys infected cells from working inside the cell, thus destroying intracellular pathogens by cell lysis, phagocytosis or pinocytosis (Rachna, 2019). Th1 cells produce cytokines including **IFN-γ**, IL-2, **IL-12** and **TNF-α**, thus a cell mediated pro-inflammatory response (Xu et al., 2016). Th1 cells mainly produce IFN-γ and IL-2 and are the key regulators of the type 1 immune response against intracellular pathogens like that of viral infections, as

well as tumours (Xu et al., 2013). They are characterised by the transcriptional factor T-bet (Peck & Mellins, 2010).

Th2:

Th2 cells produce cytokines including IL-4, IL-5, **IL-6**, **IL-10** and IL-13, thus elicit an anti-inflammatory response and immune suppression by inhibition of Th1 cytokine production (Wei et al., 2004; Xu et al., 2016). Furthermore they are associated with allergic response (Dong, 2006) and are involved in humoral immunity or antibody development (Saito et al., 2010). These cells are characterised by the transcription factor GATA-3 (Peck & Mellins, 2010).

Th17:

Such cells are critical elements for the induction of inflammation (Saito et al., 2010). Th17 cells produce the pro-inflammatory cytokines IL-17 as well as other cytokines including IL-21, IL-22, IL-26 (Dong, 2006), **IL-6**, **IL-1**, **IL-23** (Peck & Mellins, 2010) and **TNF-α** (Korn et al., 2009). Th17 cells have been linked to the development of autoimmune diseases, acute transplant rejections (Saito et al., 2010) and allergic reaction (Maruyama et al., 2010). The Th17 cell lineage is associated with the retinoic acid receptor-related orphan receptor (ROR) and signal transducer and activator of transcription 3 (STAT3) transcriptional factors (Peck & Mellins, 2010).

Treg:

Such cells inhibit other Th cells like that of Th1, Th2 and Th17 cells by virtue of their direct contact with cells and release of cytokines such as IL-10 and Transforming Growth Factor (TGF)-β to maintain immune tolerances (Y. Huang & Chen, 2016). They are specialised subpopulations of T cells that act mainly to supress the immune response to maintain homeostasis and self-tolerance via their ability to remain unresponsive to self-antigens, inhibit T cell proliferation and cytokine production, playing a critical role in preventing autoimmunity, allergy or IBDs (Kondělková et al., 2010; Rocamora-Reverte et al., 2021; Yamada et al., 2016). The Treg cell lineage is associated with the Foxp3 intracellular marker (Kondělková et al., 2010).

1.1.4.2.2 Humoral

The humoral or anti-body mediated adaptive immune response is much quicker upon reinfection, acting against invading pathogens by producing antibodies against antigens present on the outside of infected cells or free circulating in the bloodstream, thus attacking extracellular pathogens (Rachna, 2019). They provide a memory for subsequent reinfection by the same invading pathogen through the generation of memory B cells, while the circulating antibodies produced provide protection. B cells are derived in the bone marrow, where each naïve B cell expresses its own unique membrane bound B cell receptor with unique specificity to recognise different antigens. B cells lead to antibodies that can also respond to infected cells by binding and activating the complement system and causing an inflammatory response (Rouse & Sehrawat, 2010). The main function of B cells is to produce antibodies which are specialised proteins that can bind to many different kinds of antigens, however consist of the same basic structural component with variable antigen recognition sites from one B cell clone to another (*How The Body Reacts To Viruses*, 2021). Processed peptides displayed on the MHC of the B cell allow for interaction with activated helper T cells to signal the B cell to become activated and allow for secretion of cytokines. Assisted by the follicular Th cell the activated B cell undergoes clonal expansion to create many B cells with B cell receptors specific to the displayed protein, to then differentiate into plasma cells, producing antibodies with the same antigen binding site of the original B cell receptor (*How The Body Reacts To Viruses*, 2021). B cells undergo affinity maturation and isotype switching (Mueller & Rouse, 2008) to become any of five main antibody isotype groups, IgM, IgA, IgD, IgG and IgE each producing an array of different functions. Some of these functions include (*How The Body Reacts To Viruses*, 2021):

i) IgM, IgG and IgA have the ability to neutralise a virus by binding to the antigen and preventing it from interacting with other cells, preventing a virus entering and invading its host. IgA being predominantly secreted and protective in humans, especially at mucosal surfaces (Mueller & Rouse, 2008).

ii) IgG and IgM can carry out complement fixation whereby these antibodies activate a series of proteins known as the complement system, aiding in opsonization for easy target recognition and ingestion, as well as the formation of the membrane attack complex and eventual cell lysis.

iii) IgG carries out antibody dependant cellular cytotoxicity (ADCC) to target NK cells to initiate cell death

iv) IgG provides neonatal immunity from mother to baby through the placenta to the foetus protecting the baby from infections for approximately 6 months after birth

Thus it is through the use of the innate and adaptive immune systems, and the cell-mediated and humoral components of such, allow for the identification, attack, destruction and removal of invading viral pathogens from the body. Through the mechanisms outlined above the body finds ways of overcoming foreign attack. By identifying such mechanisms one has the possibility to further enhance such mechanisms to potentially further aid in protection against viruses. It is important however to consider the balance between the pro-inflammatory and anti-inflammatory mechanisms as too much pro-inflammatory status with little anti-inflammatory influence leads to tissue damage while viral persistence is a result of the opposite (Rouse & Sehrawat, 2010).

Figure 4 highlights how the immune system responds to viral infection.

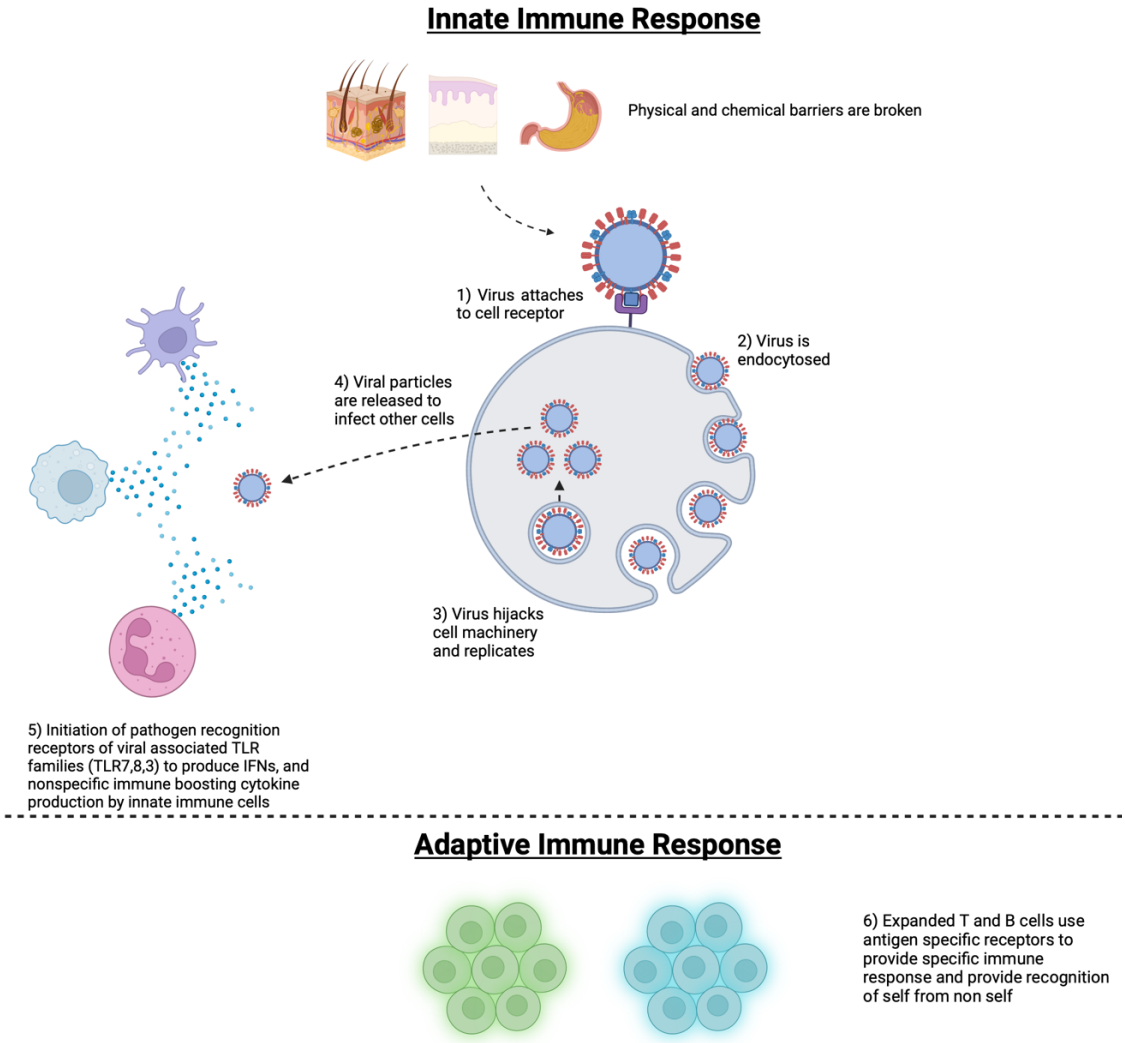

Figure 4: ***How the immune system responds to viral infection.*** *Diagrammatic representation of the process by which the virus gains entry to the cell and viral replication occurs when physical and chemical barriers are broken, and the subsequent release of viral associated cytokines for infection resolution.*

1.1.5 What is IBD and how it affects the immune system:

In order for the immune system to function correctly there needs to be a homeostatic balance between the innate and adaptive immune systems. Dysregulation of this intestinal mucosa, along with cellular, environmental and genetic factors are what is associated with the aetiology of IBD (de Mattos et al., 2015). When the gut microbiome becomes dysregulated this results in the development of IBDs.

1.1.5.1 Innate immune mechanisms:

The intestinal mucosa provides innate immunity by virtue of the gut associated lymphoid tissue, constituted by Peyer's patches, lymphoid follicles and mesenteric lymph nodes (Faria et al., 2012). IBD is associated with the disruption of the integrity of the epithelial cells of the intestinal lumen bacteria which are necessary to communicate with the immune system (Hisamatsu et al., 2013). Intestinal epithelial cells (IECs) are key players within the mucosal barrier, preventing the influx of antigens, the invasion of pathogens and commensal microorganisms, maintaining tolerance to alimentary antigens and commensal microbiota while also playing a crucial role in the activation of cellular innate and adaptive immune responses producing cytokines and chemokines, along with keeping the epithelial barrier in tact (Hisamatsu et al., 2013; Silva et al., 2016).

Macrophage play a crucial role in the regulation of gut homeostasis within the intestinal mucosa, and when this macrophage function becomes disrupted this leads to chronic intestinal inflammation (Hisamatsu et al., 2013). Regulation of intestinal gut inflammation is largely down to the M2 macrophage producing IL-10 cytokine (Hisamatsu et al., 2013). Dysregulation in IL-10 function leads to decrease in secretion of this anti-inflammatory cytokine and is therefore linked to the pathogenesis of IBDs particularly for UC (Franke et al., 2008).

Nucleotide-binding oligomerisation domain (NOD) 2 is a protein encoded by the caspase recruitment domain-containing protein (CARD) 15, that is an intracellular microbial sensor that acts as a potent activator and regulator of inflammation (de Mattos et al., 2015). NOD2 mutation or deficient expression is often associated with IBDs including CD through increased expression of inflammatory factors (Negroni et al., 2018).

TLR signalling helps protect the epithelial barrier and aid in tolerance to commensal bacteria, however malfunction in the TLR signalling associated with IBDs induces an intestinal inflammatory response through the activation of the NF-kB transcription factor that regulates the expression of key inflammatory cytokines IL-1, IL-2, IL-6, IL-12, and TNF-α (Silva et al., 2016).

1.1.5.2Adaptive immune mechanisms:

1.1.5.2.1 Cell mediated

Inflammatory disorders like that of IBDs largely associated with issues with the adaptive immune system and consist of alterations in the autophagy of cells, antigen processing, regulation of cell signalling and T cell homeostasis (de Mattos et al., 2015). The imbalance of Th1 and Th2 cytokine release by the intestinal mucosa determines the development and persistence of inflammatory responses leading to chronic inflammatory disease (Neurath et al., 1996). Key Th1 cytokines linked to the development of IDBs are TNF-α (Kam & Targan, 2000), TGF-β (G. Monteleone et al., 2008), IFN-γ (Ghosh et al., 2006), IL-6 (Hisamatsu et al., 2013), IL-12 and IL-18 (Y. Huang & Chen, 2016) as well as the response to self-antigens (de Mattos et al., 2015).

Similarly Th17 related cytokines such as IL-17 and IL-22 play a role in the development and establishment of IBDs (Y. Huang & Chen, 2016; I. Monteleone et al., 2012). Thus T cell and their subsets may have excessive increases in the chemokines and cytokines that lead to the worsening or maintenance of mucosal inflammation (Y. Huang & Chen, 2016).

Treg cells are associated with the pathogenesis of IBD (Yamada et al., 2016). Cluster differentiated (CD)4+ and CD25+ Treg cells play a role in immune regulation

and IBD treatment in mice models, whereby these cells are recruited to the intestinal lymphatic tissues and lamina propria playing a key role in maintaining intestinal homeostasis (Y. Huang & Chen, 2016; Izcue et al., 2006). Reduction of Treg cells can result in the development of IBD (Boden & Snapper, 2008).

1.1.5.2.2 Humoral

In patients with IBDs there is a dysregulation in the amount of antibodies produced and secreted from B cells (MacDermott et al., 1981). UC is characterised by the infiltration of IgG-producing plasma cells via the CD184 receptor of inflamed mucosa, further exacerbating inflammation through the activation of intestinal CD14+ macrophages (Hisamatsu et al., 2013) (Uo et al., 2013). CD is characterised by high levels of IgG1, IgG2 and IgG3 in both serum and intestinal mucosa (Tsianos & Katsanos, 2009). Similarly higher levels of IgM are associated with IBD pathogenesis (Hodgson & Jewell, 1978).

Figure 5 highlights how the immune system responds in IBD pathogenesis.

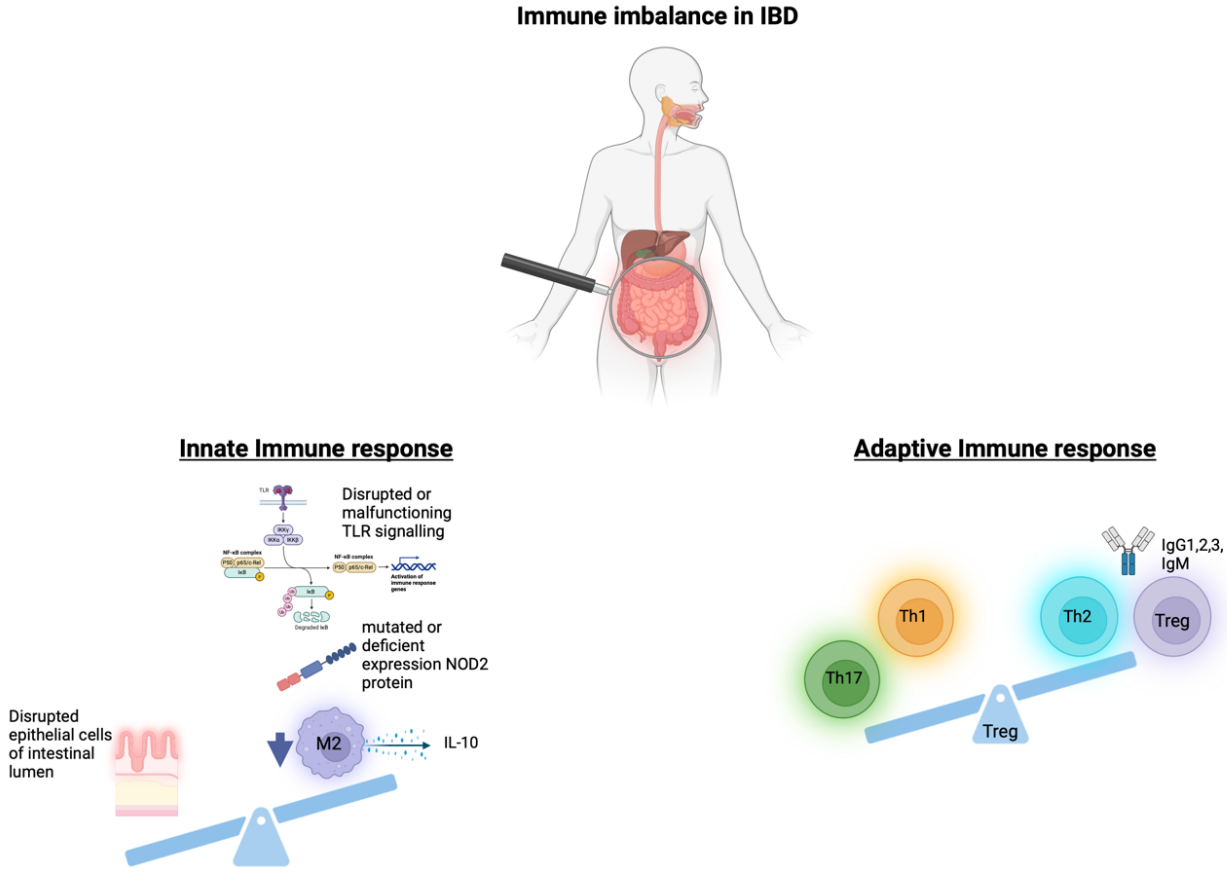

Figure 5: ***How the immune system responses to IBD.*** *Diagrammatic representation of how the innate and adaptive immune responses are affected in IBD.*

1.1.6 What are fermentates:

Fermentates generally refers to a preparation "derived from a fermented [food] product and which can contain the fermenting microorganisms, components of these microorganisms, culture supernatants, fermented substrates, and a range of metabolites and bioactive components" (Mathur et al., 2020). In recent years the consumption of such fermented food products produced as a by-product of the fermentation process, have been of huge interest. This increased curiosity has sparked the revolution of research into their potential health benefits for the human body, in maintaining and controlling human disease, as an alternative approach to conventional modern medicine. Such research is in its early stages, however, already fermentates have been found to be associated with a range of potential health benefits (Mathur et al., 2020).

Lactic acid bacteria (LAB) are a common group of bacteria found in fermented food products including; dairy such as milk, yoghurt and cheese (Pessione, 2012), fermented vegetable with products such as kimchi (H.-Y. Kim et al., 2016) in fermented meat when used as starter cultures for dry sausage products (Papamanoli et al., 2003) and fermented cereals for the generation of products such as bakery goods including sourdough bread (Zhao et al., 2015). Common LAB genera include most commonly *Lactobacilli, Lactococci*, *Enterococci*, *Streptococci*, *Leuconostoc*, and *Pediococci*, of which *Lactobacilli* and *Lactococci* are considered GRAS (generally regarded as safe) (Pessione, 2012), thus are considered to have the most potential as functional food and health boosting components. Each different strain of LAB can produce different fermentation products, with the common feature that is they are alive in the product, thus can interact with microorganisms during intestinal transit and have the ability to therefore interact with the cells of the intestinal wall (Granier et al., 2013). We however have generated novel fermentates whereby the LAB underwent a heat killing phase, creating a fermentate or postbiotic ingredient that has bioactivity associated with the secondary metabolites present, opposed to a viable LAB strain. This quality makes them ideal components for the development of a large range of novel health-promoting consumable products, as functional foods and potential

nutraceuticals (García-Burgos et al., 2020), with particular interest for viral immunity and management of IBDs.

Such LAB fermentations yield by-products with a broad range of bioactivity of which can result in health-promoting effects as outlined in Figure 6, "including protection against infectious agents, immunomodulatory effects, anti-allergenic effects, anti-obesity effects, anti-oxidant effects, enhancing the bioavailability of vitamins/minerals, anti-anxiety effects, among others" (Mathur et al., 2020).

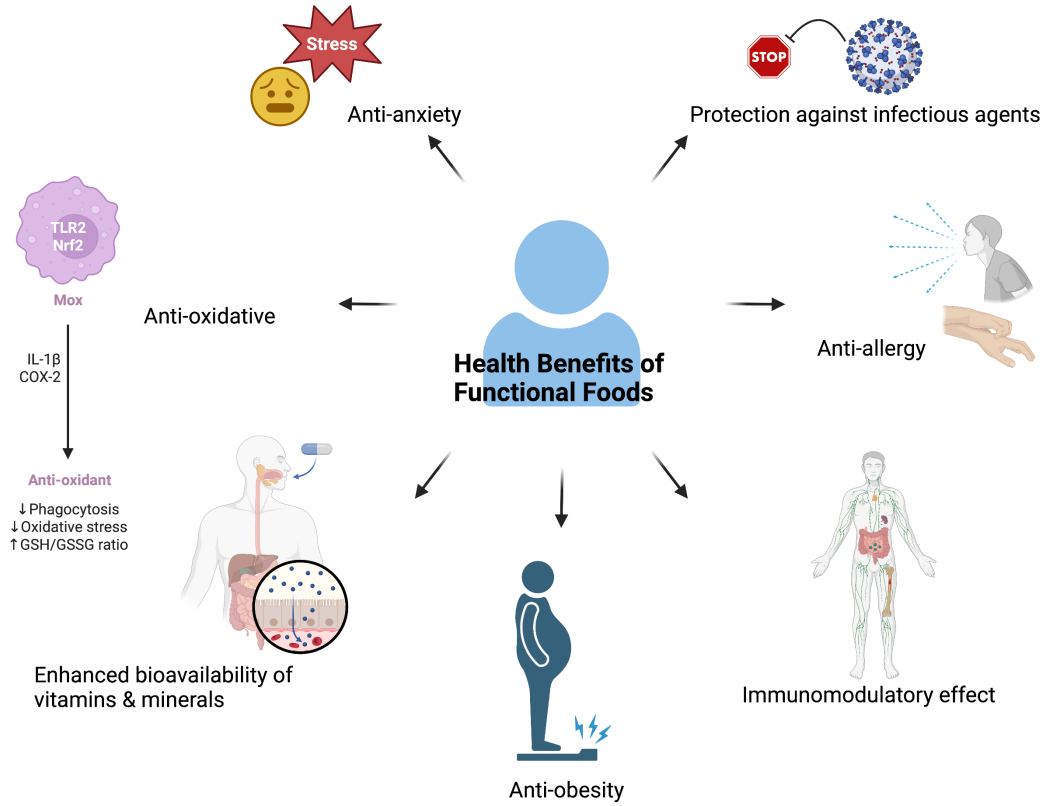

*Figure 6:**Health Benefits of functional foods**. Created using BioRender.com.*

Several studies have proven that LAB fermentation bi-products can modulate intestinal microbiota, often seen through increase in *Bifidobacterium*, ergo improving barrier function and immune priming as well as for the proper maturation of the immune system (García-Burgos et al., 2020). These studies include examination of faeces of children fed with fermented milk formulas opposed to standard formulas (Mullié et al., 2004), as well as examining increased colonization of Bifidobacterium in breastfed children opposed to formula fed children (Granier et al., 2013). Furthermore, fermented dairy products like kefir produced through

fermentation of milk by LAB and yeasts have been shown to exhibit a range of health benefits such as cholesterol metabolism, angiotensin-converting enzyme (ACE) inhibition, antimicrobial activity, tumour suppression, increased wound healing capabilities, and modulation of the immune system including allergy and asthma alleviation (Bourrie et al., 2016). Yogurts and LAB have shown to have anti-carcinogenic effects including the reduction of the inflammatory response through increased interleukin (IL)-10 secreting cells, apoptosis and decline on procarcinogenicas enzymes seen upon consumption of yogurt in colon cancer cell models (De Moreno de LeBlanc & Perdigón, 2010). The immunomodulatory effects of novel fermentates is a relatively new area of research. However, already fermentation products, such as fermented infant milk, have been shown to modify immune responses with particular emphasis on the Th1 response or Treg induction and IL-10 secretion, with significantly higher levels of Interferon (IFN)-γ, IL-12p40 and IL-10 being found in mice fed with fermented infant milk (Granier et al., 2013). IL-10 being a key cytokine for anti-inflammatory regulation in the control of IBDs, while IFN-γ and IL-12p40 are key pro-inflammatory cytokines associated with viral immunity. In the same study it was shown that probiotic cultured milk enhanced bifidobacterial in the intestinal microbiota, number of macrophage, dendritic and immunoglobin (Ig)A cells. Interestingly, the *Saccharomyces cerevisiae* fermentate, EpiCor®, has already been investigated and shown to have anti-inflammatory qualities which significantly reduced microvascular inflammatory responses to histamine-induced skin inflammation (Jensen et al., 2015) thus further suggesting the potential for fermentates as potent anti-inflammatory immunomodulators.
This suggests that such fermentates likely have potential as immunomodulatory functional food components, which could enhance viral immunity as well as aid in the regulation and control of inflammatory diseases like that of CD or UC.

Thus regardless of the only new found interest, fermentates are quickly proving to be of huge benefit already, ergo, warranting further investigation into their immunomodulatory capabilities, as anti-inflammatories for IBDs like CD and UC, as well as for viral immunity to provide protection against invading viruses, both providing possible health enhancing qualities to its consumers.

1.1.7 Immune receptors:

TLRs are cell surface or endosomal membrane-bound proteins that are expressed by a variety of cells including macrophage, dendritic cells, lymphocytes and parenchymal cells (Kopp & Medzhitov, 2003). TLRs play a vital role in induction of both the innate and adaptive immune responses by virtue of their ability to recognise specific molecular patterns found in pathogens including bacteria and viruses, allowing for the initiation of an inflammatory and antiviral responses, dendritic cell maturation to ultimately target and destroy the invading pathogen (Kawai & Akira, 2006). To date there have been ten TLRs identified in humans that enable the detection of a broad range of pathogens (Christmas, 2010). TLRs are composed of a transmembrane protein which acts as a receptor that recognises conserved microbial structures known as pathogen-associated molecular patterns (PAMPs) unique to specific classes of microorganisms (Kopp & Medzhitov, 2003). Thus, different TLRs recognise specific viral components such as single-stranded or double-stranded RNA by TLR7/8 and TLR3 respectively (Mueller & Rouse, 2008), through the recognition of CpG DNA motifs of microbial DNA (Carty & Bowie, 2010) and through recognition of bacterial structural components such as lipopolysaccharide (LPS) via TLR4 recognition (Park & Lee, 2013). These are therefore antigen-independent innate immune responses that act within hours and provide a frontline attack against invading pathogens (Lester & Li, 2014). Once the pathogen is recognised by the TLR this triggers an intracellular signalling pathway that results in the activation of the immune response to induce inflammatory cytokine production, a type I IFN and chemokine response, as well as signalling to induce upregulation of costimulatory molecules on dendritic cells in the process of DC maturation, in order to incite the pathogen-specific adaptive immune response (Kawai & Akira, 2006). It is in this way that TLRs and dendritic cells are key players in linking both the innate and adaptive immune system, essential for host protection against invading viral agents.

DCs act as the link between innate and adaptive immunity. Plasmacytoid dendritic cells (pDCs) play a crucial role in the antiviral immunity described via proficient type I IFN producing cells (IPCs) to induce the cellular antiviral responses in order to

restrict viral replication and viral spread and eventual infection (Sugimura et al., 2013). pDCs are considered the natural IFN-producing cells (NIPCs) as they are the most potent producers of IFN-α/β, which upon stimulation of endosomal TLRs are prompted to further enhance this production (Theofilopoulos et al., 2005). Furthermore pDCs serve to function in differentiation and maturation of DCs to induce Th1 responses and cross-presentation of antigens to $CD8^+$ T cells, promote $CD8^+$ T cell function and polarization of $CD4^+$ T cells into Th1 cells, play roles in mucosal T cell independent IgA production, while in non-IPCs they produce chemokines and recruit $CD4^+$ and $CD8^+$ cells to sites of infection (Sugimura et al., 2013). pDCs express the two distinct TLR types TLR7 and TLR9 (Gilliet et al., 2008).

Of the TLRs identified to date there are several that are key to antiviral immunity, these are: **TLR3**, **TLR7**, **TLR8** and **TLR9** which detect distinct forms of viral nucleic acids and thus are crucial to recognising viral genetic materials in endolysosomal compartments and initiate antiviral responses (Lester & Li, 2014), as well as TLR2 and TLR4 that recognise viral structural and non-structural proteins leading to inflammatory cytokine production (Mogensen & Paludan, 2005). Similarly, eliciting an immune response via a TLR can deduce the anti-inflammatory capabilities a sample may have on the immune system and thus give insight into the potential for a sample to act as an anti-inflammatory for use in gut comfort and IBD models.
Figure 7 below illustrates the distinct signalling cascades induced by each respective TLR in response to viral and bacterial invasion, showing the overlapping regulatory mechanisms, dependant on coordinated activation of cytosolic transcriptional factors, largely IFN regulatory factors (IRFs), IRF3 and IRF7 and nuclear factor-kappa B (NF-κB) (Lester & Li, 2014).

1.1.7.1TLR3:

TLR3 is a receptor for double-stranded RNA and some DNA viruses that generate dsRNA during their lifecycle (Yoneyama & Fujita, 2010). Expressed in endosomes of myeloid dendritic cells or on cell surfaces of fibroblasts and epithelial cells (Matsumoto & Seya, 2008). Through the TRIF-dependent pathway induces proinflammatory cytokines, chemokines and type I or type III IFNs via NF-κB and

IRF3 activation (Alexopoulou et al., 2001). polyI:polyC (PIC) is a large dsRNA-like synthetic polymer used to induce TLR3 for activation of the immune response through mimicking of viral invasion (Jelinek et al., 2011).

1.1.7.2TLR7/8:

TLR7 and TLR8 are highly homologous, related phylogenetically and functionally that detect single-stranded RNA (Carty & Bowie, 2010). This receptor immunity is derived from TLR-7 expressing pDCs and TLR8 expressing myeloid DCs (Diebold, 2008). Anti-viral sensors initiate MyD88-dependant pathway for production of type I and type III IFNs and proinflammatory mediators via activation of IFN7 and NF-κB depending on cell type (Kawai et al., 2004). TLR7 can be induced by the TLR agonist Loxoribine (LOX), a guanine nucleoside analog (Z. Zhang et al., 2017). TLR7/8 recognize guanosine or uridine nucleosides and oligoribonucleotides which are considered RNA degradation products (Z. Zhang et al., 2016). Processes like that of endocytosis, phagocytosis and autophagy, of viruses, bacteria, immune complexes, cell debris, and artificial nucleic acids, from extracellular space and the cytosol are important ligand sources for viral genetic material, nucleic acids, and thus prompt the immune response through recognition via these nucleic acid sensing TLRs (Z. Zhang et al., 2017).

Thus, due to the antiviral immune responses that the presence of TLRs outlined above induce, one can deduce that by increasing and driving the presence of these TLRs in the body one could potentially help in the protection of a host from viral invasion by virtue of their pro-inflammatory inducing status or vice versa for their anti-inflammatory status.

Similarly antibacterial immunity may be driven through the promotion of the presence of bacterial related TLRs such as **TLR4**, again inducing a pro-inflammatory immune response to prompt the body into defence to highlight, target and destroy invading bacteria. TLR4 is also a key TLR for the development and persistence of

IBDs via LPS inducible intestinal inflammation and thus a crucial TLR for the examination of anti-inflammatory potentials of fermentates

1.1.7.3TLR4:

TLR4 signal transduction is produced in response to recognition of the hexaacyl lipid A moiety, from the key structural component of most gram-negative bacteria of the outer membrane, the LPS, to induce the innate immune signalling pathway via NF-κB activation to ultimately trigger the release of proinflammatory cytokine and other inducible inflammatory factors (Vargas-Caraveo et al., 2017, 2020). The LPS signalling pathway triggers changes in immune responses, largely consisting in the increase in intestinal inflammation (Head & Jurenka, 2004). Similarly CD14 is crucial for LPS recognition along with TLR4 which are present in most cells (Vargas-Caraveo et al., 2020).

Some TLRs can recognise components of both viruses and bacteria and therefore are of use in promoting an immune response to either a viral or bacterial attack. Thus through driving expression of such TLRs one can recognise pathogens and induce an immune response in a timely manner in order to help clear microbial or viral pathogens from the body and prevent infection of either nature. Similarly driving of TLR4 via the LPS signalling pathway one can induce a model for intestinal inflammation and therefore test for anti-inflammatory capabilities of a functional food.

1.1.7.4TLR9:

TLR9 can sense hypomethylated cytosine-guanine dinucleotide (CpG) motifs of microbial DNA or viral DNA and thus can activate the immune response to either bacterial or viral invasion (Carty & Bowie, 2010; Latz et al., 2004). TLR9 recognises such unmethylated CpG motifs expressed in intracellular vesicles of prokaryotic cells, including the endoplasmic reticulum, endosomes and lysosomes (Nigar & Shimosato, 2019). Immune activated expression of TLR9 occurs in many cells including neutrophils, monocytes and $CD4^+$ T cells, as well as non-immune cells like epithelial cells expressing TLR9 (Carty & Bowie, 2010). It is also constitutively expressed on B cells and plasmacytoid DCs (Vollmer & Krieg, 2009). Anti-viral

responses produce large amounts of type I IFNs (Carty & Bowie, 2010) via TLR9-MyD88 signalling pathway (Lester & Li, 2014). Non-methylated CpG-dinucleotides are more abundant in microbial DNA however and therefore more often associated with evoking a bacterial immune response (Latz et al., 2004).

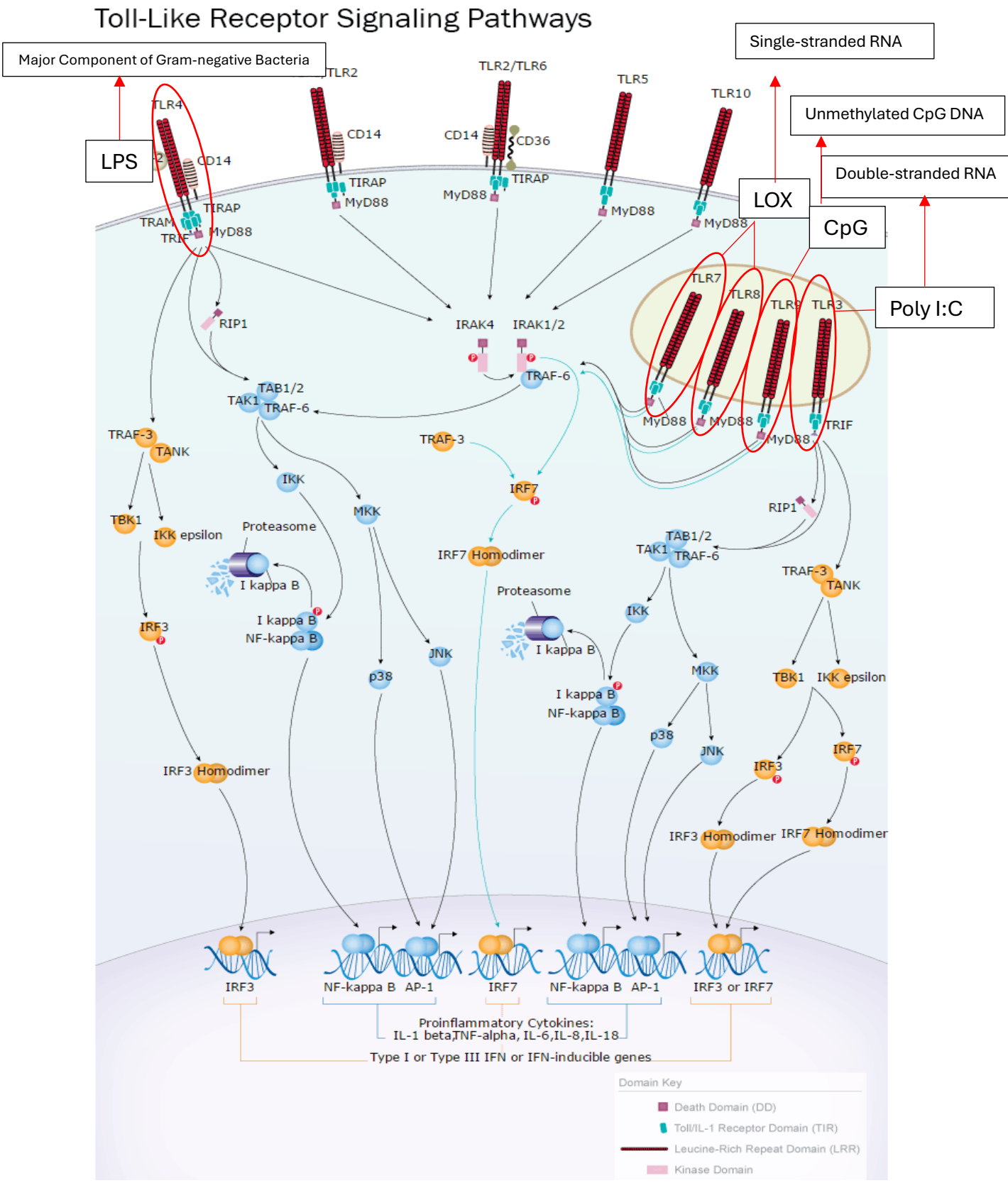

Figure 7: ***TLRs, their associated Ligands and agonists.*** *TLRs expressed due to immune activation response by TLR ligand stimulation derived from their associated viral agonist, or inflammatory agonist showing resulting signalling cascade, transcription factors and secretion of a range of pro-inflammatory and anti-inflammatory cytokines and immune responses. Adapted from (R&D Systems Inc., 2012).*

1.1.8 Key Cytokines being examined:

1.1.8.1 IL-12:

The bioactive IL-12p70 from the IL-12 family consists of a 70kD heterodimer composed of 35 and 40kD peptides (Wolf et al., 1994), while the IL-12p40 form can work in the absence of the 35kD subunit (Akdis et al., 2016).

IL-12 is a potent regulator of cell mediated immune responses, providing a crucial link between innate resistance and adaptive immunity, preventing/reducing severity of infection and control/cure of infection, respectively (Trinchieri, 2003).

Secreted by activated inflammatory cells including monocytes, macrophage and dendritic cells, it induces a pro-inflammatory cytokine response to pathogen invasion (Trinchieri, 2003).

IL-12 is a critical cytokine for the proliferation of Th1 cells and for the continuous production of IFN-γ (Bae et al., 2016). Induces IFN-γ production by NK and T cells when naïve T cells differentiate into Th1 cells, while also upregulating a variety of cell surface molecules on NK cells (Thomson, 1996). IL-12 works to induce IFN-γ at a high efficiency at low concentrations, while working in synergy with many other activating stimuli, like that of IL-2 and IL-12 working together for T cells, for rapid, efficient production of IFN-γ through stimulation of TCR-CD3 complex and CD28 receptor (Chan et al., 1992). Furthermore, IL-12 has been noted to amplify CD8 responders, enhance production of neutralizing IgG2a antibodies and ultimately, halting viral replication and providing clearance of the viral pathogen from the host cells (Komastu et al., 1998).

1.1.8.2 IL-23:

This pro-inflammatory cytokine is part of the IL-12 family of cytokines, composed of two subunits, IL-23p19 and IL-12p40, it therefore resembles IL-12 in structure due to the presence of IL-12p40 and thus likewise takes after IL-12 in function also (Guo et al., 2019). This cytokine is different from IL-12 due to their unique p35 and p19 subunits present in IL-12 and IL-23, respectively (Oppmann et al., 2000). This means that not only does IL-23 share similar function to IL-12 in its Th1-mediated

immune response but also, shows its own unique regulation of T cell mediated immunity (Kohyama et al., 2007).

IL-23 is essential for Th17 cell expansion and function (Bettelli et al., 2006). Such Th17 cells produce a range of cytokines including IL-17, IL-6 and TNF-α, however they do not produce cytokines like that of IFN-γ or IL-4, thus making them a different subset from that of the Th1 or Th2 classical responses (Harrington et al., 2005).The IL-23/Th17/IL-17 axis is often associated with inflammatory autoimmune diseases such as rheumatoid arthritis, multiple sclerosis, asthma and psoriasis (Schön & Erpenbeck, 2018) due to IL-17's proinflammatory cytokine and chemokine induction properties (Kohyama et al., 2007). While IL-23 drives and maintains differentiation of Th17 lymphocytes, it is only recently unveiled that regulation of IL-23 and subsequently IL-17, is not only from Th17 cell differentiation but also from IL-23 independent production of IL-17, as well as from the innate immune system (Schön & Erpenbeck, 2018).

1.1.8.3IL-27:

This is a heterodimeric cytokine that is structurally similar to the IL-12 family, composed of the IL-27p28 and Epstein-Barr virus induced gene 3 (EBI3) subunits (Harker et al., 2018). It is produced by macrophage, dendritic cells and epithelial cells in response to inflammatory activation (Villarino & Hunter, 2004) with APCs as the main source of IL-27 to target and abolish viral infections (Guo et al., 2019).

Initially noted for being a pro-inflammatory cytokine due to its shared IL-12 role in the promotion of Th1 differentiation, IL-27 functions through the induction of T-bet expression and downstream targeting of IL-12Rβ2 to enhance responsiveness to IL-12 and subsequent IFN-γ production, while unable to drive IFN-γ production on its own (Lucas et al., 2003).

IL-27 differs from IL-12 and IL-23 in that it has both pro and anti-inflammatory effect (Guo et al., 2019). IL-27 induces production of IL-1β, TNF- α, IL-18 (Villarino & Hunter, 2004) and IL-21 in helper T cells (Harker et al., 2018). On the other hand IL-27 has recently been associated with suppressive effects on the inflammatory response through the ability to inhibit some key inflammatory processes (Villarino & Hunter, 2004). Such abilities include the inhibition of Th17 differentiation,

restriction of IL-2 production, but moreover IL-27's ability to promote the inhibitory cytokine IL-10 (Wehrens et al., 2018).Furthermore, IL-27 appears to have direct inhibitory effects on Th2 mucosal responses independent of its ability to enhance IFN-γ production (Villarino & Hunter, 2004). However, due to its proinflammatory cytokine production and early role in IFN-γ induction it is important not to over stimulate this cytokines as in doing so could lead to autoimmune inflammatory diseases.

Thus IL-12, IL-23 and IL-27 can be useful in the protection against viral invasion and subsequent infection through their abilities to enhance cytokine, chemokine and antibody production, to limit and control viral replication, to ultimately clear viral pathogens from the body. On the contrary though it is important to ensure that their production is not over heightened as this in itself can lead to the development of inflammatory autoimmune diseases. Autoimmune diseases are for the most part caused by a dysregulation of the adaptive immune response and because of pathologic antibodies or autoreactive T cells , while in contrast autoinflammatory diseases can be caused by genetic defect in the innate immune systems and inflammatory pathways (Dinarello, 2011).

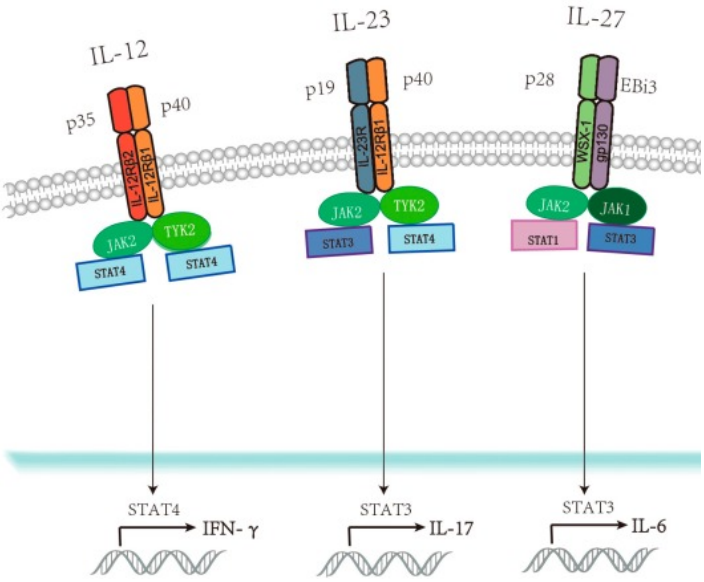

Figure 8: ***Structural units of the IL-12 family of cytokines, respective signalling transducers and signalling pathways, showing main functional immune response.*** *Adapted from (Guo et al., 2019).*

1.1.8.4IFN-γ:

This is a homodimeric glycoprotein with pleiotropic immunological functions (Tau & Rothman, 1999). It too is a pro-inflammatory cytokine that's overproduction can be associated with many chronic inflammatory and autoimmune diseases such as insulin-dependent diabetes mellitus (Mühl & Pfeilschifter, 2003). IFN-γ is largely secreted by activated T cells and NK cells to promote macrophage activation, mediate both antiviral and antibacterial immunity, activate the innate immune system, enhance antigen presentation by increasing expression of MHC antigens by immune cells to T cells (Griffin, 2008), upregulating expression of both class I and class II MHC molecules (Xu et al., 2013), regulate Th1 and Th2 balance and regulate cellular proliferation and apoptosis (Boehm et al., 1997). It is the only type II IFN and signals through the IFN-γ receptor, to produce IFN-γ by specialised immune cells, to elicit a response by binding nearly all cell types (Payne, 2017). IFN-γ inhibits the proliferation of Th2 cells such as IL-4 and IL-10, which themselves otherwise would block the proliferation and cytokine release of Th1 cells (Bae et al., 2016).

IFN-γ has been noted for its dual role by presenting with anti-inflammatory properties that include its ability to reduce IL-1 and IL-8 production, induce IL-1Ra and IL-18BP release which is critical to the etiology of inflammatory diseases (Mühl & Pfeilschifter, 2003) as well as being known for their antiproliferative, pro-apoptotic, antitumour mechanisms and antiviral properties (Castro et al., 2018). IFN-γ was reported as far back as 1965 to have been noted for its ability to inhibit viral replication and thus a key cytokine in the study of viral infections and viral immunity (Wheelock, 1965). IFN-γ has been shown to be crucial in the host defence against viral infections such as vaccinia virus (Kohyama et al., 2007).

1.1.8.5IL-1β:

This is a proinflammatory cytokine belonging to the large IL-1 family of cytokines, consisting of 11 members with both pro and anti-inflammatory properties (Dinarello, 2018). IL-1β has been proposed to promote retroviral replication, immune activation and pathogenesis in the form of a positive feedback loop in response to infection (Browne, 2015). It is a pleiotropic cytokine with its main

effects on inflammation, immunity and hemopoiesis (Apte et al., 2006). IL-1β is produced by a range of hematopoietic cells such as monocytes, macrophage, dendritic cells and microglia in response to TLR ligands, activated complement molecule and other cytokines like that of TNF α and other IL-1 members itself (Dinarello, 2011) and can affect many different immune lineages (Garlanda et al., 2013).

IL-1β binds to and activates the IL-1β receptor 1 (IL-1R1) and results in the potent stimulation of transcription factor Nuclear Factor-Kappa B (NF-κB) (Browne, 2015). This is carried out through the recruitment of MyD88 to the Toll-IL-1 receptor (TIR) domain to ultimately result in a large inflammatory response profile (Dinarello, 2011) required for immune-mediated inflammation, effective adaptive immunity and anti-viral control (Aarreberg et al., 2018). IL-1 is largely linked to the innate immune response due to the cytoplasmic domain of the IL-1R1 being highly homologous to the cytoplasmic domains of all TLRs, resulting in indistinguishable inflammatory responses from both IL-1 and TLR ligands (Dinarello, 2009). Elevated levels of IL-1β have been associated with autoimmune and autoinflammatory diseases (Garlanda et al., 2013) as well as in the promotion of tumorigenesis (Apte et al., 2006).

1.1.8.6IL-6:

IL-6 is again a pleotropic cytokine that is produced in response to tissue damage and infections, that aids in host defence through activation of acute phase responses, haematopoiesis and immune response actions (Tanaka et al., 2014). Produced by a range of cell types including macrophage, dendritic cells, T cells and B cells, ergo making it a crucial cytokine in the activation and regulation of the immune response (Velazquez-Salinas et al., 2019).

IL-6 is largely considered a pro-inflammatory cytokine promoting neutrophilia, while blocking regulatory Treg differentiation (Covarrubias & Horng, 2014). IL-6 supports differentiation of naïve CD4 T cells, making it a critical link between the innate and adaptive immune system, in combination with TGF-β is needed for Th17 differentiation from naïve CD4 T cells, promotes T-follicular helper-cell differentiation and IL-21 production which is needed for regulation of

immunoglobulin synthesis particularly IgG4 production, induces differentiation of CD8 T cells to cytotoxic T cells, as well as being able to induce differentiation of activated B cells into Ab-producing plasma cells (Tanaka et al., 2014). IL-6 is largely associated with induction of the Th17 pathogenic immune response (Hou et al., 2009) and thus with IL-6, is associated with the development of autoimmune disorders and cancer progression, as well as being linked to chronic viral infection (Hou et al., 2014). It does so due to IL-6 directly playing an important role in the inhibition of cellular apoptosis, as well as being able to promote the growth and survival of various cells like that of cancer cells (Hideshima et al., 2001). Excessive levels of IL-6 lead to autoimmune disorders like that of diabetes, rheumatoid arthritis and psoriasis (Ishihara & Hirano, 2002). Furthermore IL-6 and IL-17 together support the upregulated expression of prosurvival molecules, thus inhibiting target cell destruction by virus-specific CD8 T cells, preventing cellular apoptosis through both STAT3 and NF-κB activation via distinct cytokine-dependant pathways (Hou et al., 2014). Therefore, IL-6 when overexpressed, generates Th17 cells which results in the upregulation of IL-6 and IL-17 cytokines, in turn leading to viral persistence by virtue of their synergistic abilities to protect virus infected cells from apoptosis and CD8 T cell-mediated target destruction(Hou et al., 2014).

1.1.8.7TNF-α:

TNF-α is a homotrimer proinflammatory cytokine (Atzeni & Sarzi-Puttini, 2013).
This cytokine again has pleiotropic functions of which its main function includes the modulation of the inflammatory response, host resistance to pathogens and the pathogenesis of many chronic inflammatory diseases like that of rheumatoid arthritis (Atzeni & Sarzi-Puttini, 2013; Horiuchi et al., 2010). TNF-α is produced by many cells including, activated macrophage, T and B lymphocytes, NK cells, endothelial cells, epithelial and some tumour cells to name a few, with CD4 and CD8 T cells being a critical source of TNF-α (Seo & Webster, 2002a). TNF-α expression has been linked to the ability to inhibit replication of viruses including vesicular stomatitis, encephalomyocarditis, herpes simplex virus (HSV) and influenza virus (Seo & Webster, 2002a).

The antiviral protective roles of TNF-α are long known. TNF-α has an anti-viral effect which is a result of their ability to be produced by such a wide range of immune cells to protect against both RNA and DNA viruses, while working in synergy with IFN-γ to promote its antiviral activities (Rook et al., 1991; Ruby et al., 1997). Similarly TNF-α has been noted for its ability to kill virally infected cells, which in itself can prove both beneficial and detrimental depending on how many cells of the body become infected with a virus, resulting in its ultimate destruction by TNF-α via its cytotoxic activity (Rook et al., 1991). TNF-α is a critical cytokine in controlling infection with it being needed for leukocyte trafficking, immune complex clearance, as well as playing a major role in the defence of intracellular organisms against invading viruses and pathogens (Atzeni & Sarzi-Puttini, 2013). Furthermore TNF-α has been noted for its ability to activate endothelial cells, cause B cell proliferation and immunoglobulin production, activate T cells to express HLA-DR and produce granulocyte macrophage colony stimulating factor (GM-CSF) in addition with CD25 cell surface marker expression, as well as adipocyte differentiation, NK cell stimulation and cytokine production, like that of IL-10, from monocytes (Horiuchi et al., 2010), all of which is mediated through both the p55 and p75 TNF receptors (TNFR) (Ruby et al., 1997). However, as with the aforementioned cytokines, TNF-α likewise, when dysregulated can lead to autoimmune disorders like that of rheumatoid arthritis or inflammatory bowel disorders, whereby there is an overexpression of TNF-α causing a hyperactive immune responses and thus a chronic inflammatory response (Kollias & Kontoyiannis, 2002).

1.1.8.8IL-10:

This cytokine was originally known as cytokine synthesis inhibitory factor (CSIF) due to its opposing immunoregulatory effects than the other cytokines examined, being identified as a CD4 produced Th2 cytokine with the ability to indirectly suppress Th1 responses (Wilson & Brooks, 2011). It does so by downregulating antigen presenting capacities of APC (Rojas et al., 2017). IL-10 is produced by a multitude of cell types including dendritic cells, B cells, macrophage, CD4 T cells, CD8 T cells, NK cells as well as Treg cells (Moore et al., 2001). IL-10 can inhibit activation and effector function of T cells, monocytes, and macrophage, with a range of effects on

most hemopoietic cell types (Moore et al., 2001). IL-10 is largely considered an immunosuppressive cytokine with potent anti-inflammatory function (Wilson & Brooks, 2011). IL-10 plays a critical role in limiting host immune response to invading pathogens, ultimately preventing damage to the host from over activation of the pro-inflammatory molecules thus preventing inflammatory and autoimmune pathologies such as IBDs, rheumatoid arthritis and psoriasis (Iyer & Cheng, 2012). On the other hand, viruses can exploit this IL-10 pathway to evade immunity which can result in a persistent or latent infection (Rojas et al., 2017). IL-10 is considered the master negative regulator of inflammation, however also plays a supportive role in effective virus clearance, which is seen particularly in influenza and CNS infection clearance, by supporting the adaptive immune response and controlling IL-10 producing T cells to improve virus control via both direct and indirect effects of the cytokine (Rojas et al., 2017).

1.1.8.9IL-2:

This cytokine is a proinflammatory cytokines involved in the survival and differentiation of CD4+ T helper subsets and CD4+ T regulatory cells (T. Wang et al., 2018). It is also responsible for activation of effector lymphocytes, boosting cytolytic activity of NK cells, T cells, augmenting production of activated B cells and influencing memory T cells and effector T cells and monocytes (Arenas-Ramirez et al., 2015; T. Wang et al., 2018). IL-2 is also responsible for mediation of activation-induced cell death (Liao et al., 2011). IL-2 modulates Th cell differentiation through the expression of receptors and/or inhibition of cytokine cascades correlating to each Th cell subsets developmental state (T. Wang et al., 2018). IL-2 promotes naïve T cell differentiation into Th1 and Th2 cells while inhibiting Th17 cell development (Liao et al., 2011; T. Wang et al., 2018). Regardless of its proinflammatory qualities, IL-2 due to its T cell growth and expansion has been linked to treatment of moderate to severe UC at low doses and therefore of key interest in the treatment of IBDs including UC and CD (Allegretti et al., 2021).

1.1.8.10 IL-4 and IL-13:

These are key anti-inflammatory cytokines and signature cytokines of the type II inflammatory response, triggered by invading parasites or allergens (Chatterjee et al., 2014; de Vries, 1998; Junttila, 2018). IL-4 and IL-13 share many biological activities due to the fact that IL-13 and IL-4 receptor complexes share the IL-4 receptor α-chain, important for signal transduction (de Vries, 1998). These cytokines are secreted by a range of cell types including CD4 + T cells, basophils, eosinophils, mast cells and NK cells (Junttila, 2018). IL-4 is important for regulation of antibody production, haematopoiesis, inflammation and development of effector T cell responses (Brown & Hural, 1997). IL-4 induces Th2 cell differentiation unlike IL-13, while IL-13 is required for optimal IgE synthesis, indirectly affects Th1 differentiation through inhibition of proinflammatory cytokine and chemokine production, particularly IL-12, and is responsible for IgE mediated allergic responses (de Vries, 1998). Decreased production of IL-4 and IL-13 is linked to defective immunosuppression and anti-inflammatory mechanisms and can contribute to IBD disease pathogenesis (Hoving, 2018; West et al., 1996).

1.1.8.11 TGF-β:

TGF-β is considered both a pro-inflammatory and an anti-inflammatory cytokine, depending on the amount of TGF-β presented to cells, as well as intracellular or local extracellular factors (Travis & Sheppard, 2014). TGF-β is a ubiquitous cytokine playing a crucial role in numerous pathways regulating cellular and tissue homeostasis, of which nearly all cells secrete latent TGF-β and express the TGF-β receptors (Fleisch et al., 2006). TGF-β allows for distinct context dependant roles in T cell development, homeostasis, tolerance and differentiation (Oh & Li, 2013). TGF-β regulates several biological processes including inflammation, tissue repair, tumorigenesis, developmental processes, immunity, carcinogenesis, and fibrosis (Wahl, 1994; Yun et al., 2019). TGF-β is critical for the differentiation of Th17 cells and the subsequent production of inflammatory cytokine IL-17, a key cytokine associated with autoimmunity, while simultaneously inhibiting differentiation of Th1 and Th2 cells (Veldhoen & Stockinger, 2006). TGF-β is the master regulator in

the driving of fibrosis in all organs including the intestine and is therefore linked to the development of fibrosis occurring in IBDs (Speca et al., 2012; Yun et al., 2019). TGF-β levels are increased in patients with IBDs, in particular CD patients (Babyatsky et al., 1996). Thus IDB pathogenesis can be linked to this cytokine and thus controlling the expression of TGF-β in IBD patients may aid in the management and treatment of diseases like UC and CD.

1.1.8.12 IL-17:

IL-17 is a potent pro-inflammatory cytokine with key functions in maintain homeostatic conditions through the stimulation of neutrophils, potent chemotactic effects on neutrophils, production of mucous and antimicrobial peptides, bridging the innate and adaptive immune responses through interactions with epithelial integrity via secretions of claudins and the production and interaction with other inflammatory cytokines and chemokines (Ruiz de Morales et al., 2020). IL-17 is characteristic of the Th17 subset of CD4 lymphocytes which is dependent on the presence of IL-6, IL-1β and TGF-β cytokines (Ruiz de Morales et al., 2020). IL-17 can also be induced by other cells including γδT cells, NK T cells, group 3 innate lymphoid cells (ILC3s), CD8+ cells, neutrophils, microglia, mast cells, myeloid cells in the lung and kidneys, and Paneth cells in the intestine (Ge et al., 2020). IL-17 leads to the pathogenesis's of many inflammatory conditions including IBDs, psoriasis, psoriatic arthritis, rheumatoid arthritis, ankylosing spondylitis, cardiovascular disorders, non-alcoholic fatty liver disease, multiple sclerosis, uveitis, haematological and solid cancer (Ruiz de Morales et al., 2020). In patients with UC and CD there are increased levels of IL-17 expression in the inflamed mucosa and sera of patients with active disease, and is likely associated with altered immune and inflammatory responses of the intestinal mucosa (Fujino et al., 2003). Thus controlling expression of IL-17 may aid in the management and treatment of diseases like UC and CD.

Therefore, overall one would aim to enhance and boost IL-12, IL-23, IL-27, IFN-γ, IL-1β, IL-6 and TNF-α production as all are linked with beneficial antiviral properties

which aid in the protection, destruction and removal of viral pathogens from the body in their own unique ways as outlined above. It is crucial however that these levels of cytokine production are not overexpressed or driven too much as this in itself would lead to detrimental effects in the form of autoimmune disorders, tumorigenesis or even viral persistence as already discussed.

Aiming to maintain IL-10 cytokine secretion levels would ensure that the host has sufficient capabilities to protect the host from chronic inflammation by virtue of the increased proinflammatory molecules, thus ensuring to prevent against chronic inflammation or autoimmune disorders by limiting pro-inflammatory immune status.

On the other hand, limiting the production of pro-inflammatory cytokines like that of IL-12, IL-7, IL-23, IL-27, IFN-γ, IL-1β, IL-6 , TNF-α and TGF-β in patients with IBDs, while simultaneously increasing the IL-4, IL-10, IL-13, and maintaining low doses of IL-2 cytokine concentrations, may aid in the management of chronic inflammation and IBDs. This is by virtue of the dampening of the already heightened proinflammatory profile seen with IBDs, while simultaneously increasing concentrations of anti-inflammatory cytokines to overall bring homeostatic balance to the body.

Table 2: ***Summary of Cytokine Functions.*** *This table summarises the key functions of each of the core cytokines examined, detailing their immune phenotype, be it immune boosting and/or anti-inflammatory, as well as summarising their key effect on immune function.*

Cytokine Name	Phenotype	Immune Function	References
IL-12 (IL-12p40/ IL-12p70)	Immune Boosting	- Regulator of cell mediated immune responses - Provides crucial link between innate resistance and adaptive immunity - Prevents/reduces severity of infection control/cure of infection - Aids in proliferation of Th1 cells and continuous production of IFN-γ - Upregulates cell surface molecules on NK cells - Amplifies CD8 responders - Enhances production of neutralizing IgG2a antibodies - Aids in halting viral replication and providing clearance of the viral pathogen	(Bae et al., 2016; Komastu et al., 1998; Thomson, 1996; Trinchieri, 2003)
IL-23	Immune Boosting	- Similar function to IL-12 in particular to Th1 mediation - Promotes Th17 cell expansion and function producing cytokines IL-17, IL-6 and TNF-α, but not IFN-γ or IL-4 - Independent IL-23 production of cytokine IL-17	(Bettelli et al., 2006; Guo et al., 2019; Harrington et al., 2005; Schön & Erpenbeck, 2018)
IL-27	Immune Boosting/ Anti-inflammatory	- Similar function to IL-12 in particular to Th1 mediation, induced via T-bet expression to enhance responsiveness of IL-12 and IFN-γ production - Induces production of IL-1β, TNF- α, IL-18, and IL-21 - Inhibits Th17 differentiation	(Guo et al., 2019; Harker et al., 2018; Lucas et al., 2003; Villarino & Hunter,

		- Restricts IL-2 production - Promotes the inhibitory cytokine IL-10 - Inhibitory effects on Th2 mucosal responses	2004; Wehrens et al., 2018)
IFN-γ	Immune Boosting/ Anti-inflammatory	- Promotes macrophage activation - Mediates both antiviral and antibacterial immunity - Activates the innate immune system - Enhances antigen presentation by increasing expression of MHC I and II molecules - Regulates Th1 and Th2 balance - Regulates cellular proliferation and apoptosis - Inhibits the proliferation of Th2 cells such as IL-4 and IL-10 - Reduces IL-1 and IL-8 production - Induces IL-1Ra and IL-18BP release - Antiproliferative - Pro-apoptotic - Antitumour mechanisms - Antiviral properties - Inhibits viral replication	(Bae et al., 2016; Boehm et al., 1997; Castro et al., 2018; Griffin, 2008; Mühl & Pfeilschifter, 2003; Wheelock, 1965; Xu et al., 2013)

IL-1β	Immune Boosting/ Anti-inflammatory	- Promotes retroviral replication - Immune activation and pathogenesis main effects on inflammation, immunity and hemopoiesis - Required for immune-mediated inflammation, effective adaptive immunity and anti-viral control	(Aarreberg et al., 2018; Apte et al., 2006; Browne, 2015; Dinarello, 2011, 2018)
IL-6	Immune Boosting	- Promotes neutrophilia - Blocks Treg differentiation - Activates acute phase responses, haematopoiesis and immune response actions - Supports differentiation of naïve CD4 T cells, making it a critical link between the innate and adaptive immune system - In combination with TGF-β is needed for Th17 differentiation from naïve CD4 T cells - Promotes T-follicular helper-cell differentiation and IL-21 production needed for regulation of immunoglobulin synthesis - Induces differentiation of CD8 T cells to cytotoxic T cells - Induces differentiation of activated B cells into Ab-producing plasma cells - Th17 pathogenic immune response - Role in the inhibition of cellular apoptosis	(Covarrubias & Horng, 2014; Hideshima et al., 2001; Hou et al., 2009, 2014)05/07/2024 09:50:00

		- Promotes the growth and survival - Supports the upregulated expression of prosurvival molecules - Inhibits CD8 T cell-mediated target destruction	
TNF-α	Immune Boosting	- Modulates inflammatory response, host resistance to pathogens - Inhibits replication of viruses - Antiviral protective roles to protect against both RNA and DNA viruses, working in synergy with IFN-γ to promote its antiviral activities, via cytotoxic activity - Leukocyte trafficking - Immune complex clearance - Activates endothelial cells, cause B cell proliferation and immunoglobulin production - Activates T cells to express HLA-DR and produce GM-CSF in addition with CD25 cell surface marker expression, adipocyte differentiation, NK cell stimulation and cytokine production	(Atzeni & Sarzi-Puttini, 2013; Horiuchi et al., 2010; Rook et al., 1991; Ruby et al., 1997; Seo & Webster, 2002a)
IL-10	Anti-inflammatory	- CD4 produced Th2 cytokine with the ability to indirectly suppress Th1 responses - Downregulates antigen presenting capacities of APC	(Iyer & Cheng, 2012; Moore et al., 2001; Rojas et al., 2017; Wilson & Brooks, 2011)

		- Inhibits activation and effector function of T cells, monocytes, and macrophage - Limiting host immune response to invading pathogens, ultimately preventing damage to the host from over activation of the pro-inflammatory molecules - Supportive role in effective virus clearance	
IL-2	Immune Boosting	- Survival and differentiation of CD4+ T helper subsets and CD4+ T regulatory cells - Activates effector lymphocytes - Boosts cytolytic activity of NK cells, T cells - Augments production of activated B cells - Influences memory T cells and effector T cells and monocytes - Mediates activation-induced cell death - Modulates Th cell differentiation through the expression of receptors and/or inhibition of cytokine cascades - Promotes naïve T cell differentiation into Th1 and Th2 cells while inhibiting Th17 cell development	(Arenas-Ramirez et al., 2015; Liao et al., 2011; T. Wang et al., 2018, 2018)
IL-4	Anti-inflammatory	- Regulates antibody production, haematopoiesis, inflammation and development of effector T cell responses - Induces Th2 cell differentiation	(Brown & Hural, 1997; de Vries, 1998)

IL-13	Anti-inflammatory	- Similar function to that of IL-4 - Indirectly affects Th1 differentiation through inhibition of proinflammatory cytokine and chemokine production, particularly IL-12, and is responsible for IgE mediated allergic responses	(Brown & Hural, 1997; de Vries, 1998)
TGF-β	Immune Boosting/ Anti-inflammatory	- Regulates cellular and tissue homeostasis - Distinct context dependant roles in T cell development, homeostasis, tolerance, and differentiation - Regulates inflammation, tissue repair, tumorigenesis, developmental processes, immunity, carcinogenesis, and fibrosis - Induces differentiation of Th17 cells and the subsequent production of inflammatory cytokine IL-17 - Inhibits differentiation of Th1 and Th2 cells	(Oh & Li, 2013; Travis & Sheppard, 2014; Veldhoen & Stockinger, 2006; Wahl, 1994; Yun et al., 2019)
IL-17	Immune Boosting	- Maintains homeostatic conditions through the stimulation of neutrophils - Potent chemotactic effects on neutrophils - Influences production of mucous and antimicrobial peptides - Bridges the innate and adaptive immune responses through interactions with epithelial integrity via secretions of claudins and the production and interaction with other inflammatory cytokines and chemokines	(Ruiz de Morales et al., 2020).

1.2 Aims and Objectives

While the area of fermentates is only of emerging interest, novel LAB fermentation products have already been highlighted for their potential as immunomodulatory functional foods. Therefore, we concluded that further research into their capabilities could provide information about their potential use in viral immunity and for anti-inflammatories in IBD management. Food for Health Ireland (FHI) is a national full service scientific organisation that aims to give companies a competitive edge in the global food and ingredients market, This project was funded by FHI and Enterprise Ireland (Grant #: TC20180025), in conjunction with industry partners in Teagasc, to generate a bank of 46 novel fermentates for assessment of their bioactivity, for commercial development by commercial industry partners Kerry, Carberry, and Tirlán. Such fermentates were generated using skim milk powder, reconstituted in distilled water to generate the reconstituted skim milk (RSM) starting material, which then was inoculated with individual strains of LAB to generate unique fermentates.

We hypothesised that novel fermentates can be used for the modulation of the immune system, to:

1) Boost the immune system to provide protection against viral infection,

and

2) Act as an anti-inflammatory for the control, management and prevention of chronic IBDs including UC and CD

Our aims were:

1) Screen bank of FHI fermentate samples *in vitro*
2) Discover novel proinflammatory immune boosting samples *in vitro*
3) Discover novel anti-inflammatory immune suppressive samples *in vitro*
4) Investigate candidate proinflammatory/anti-inflammatory samples immunomodulatory profiles *in vitro* in a range of immune cell types

2 Chapter 2

Materials and Methods

2.1 Materials

2.1.1 Cell Culture:

Table 3: ***All Tissue and Cell culture materials and reagents, corresponding sources and product codes.***

Materials and Reagents	Supplier	Catalogue number
25 Litre IMS Industrial Methylated Spirits (IMS) 25 L	Lennox	CRTSI0330716
T75 Cell Culture Flasks	Thermo Fisher Scientific	156499
T25 Cell Culture Flasks	Fisher	TKT-130-170F
Petri Dishes	Fisher	TKT-310-020W
MEM alpha, nucleosides Cell Culture Media	Bio-sciences	22571020
DMEM cell culture medium	Biosciences	41965039
FBS	Biosciences	10270106
Pen/Strep	Biosciences	10378016
rGMCSF from mouse	Sigma Aldrich	G0282-50UG
Mouse M-CSF Recombinant Protein	Biosciences	PMC2044
1X DPBS	Biosciences	14190094
Trypsin-EDTA Solution 0.25%	Sigma-Aldrich	T4049-500 ML
Cell Scrapper	Sarstedt	83.1831
50 mL Conical centrifuge tube conical centrifuge tube	Sarstedt	62.559.001
15 mL Conical centrifuge tube conical centrifuge tube	Sarstedt	62.554.502
5 mL Pipette	Merck Life Sciences	CLS4051-200EA
10 mL Pipette	Merck Life Sciences	CLS4101-200EA
25 mL Pipette	Merck Life Sciences	CLS4251-200EA

1.5 mL sterile screw-cap microcentrifuge tubes.	Sarstedt	72.692.005
1.5 mL microcentrifuge tubes.	Sarstedt	72.690.001
Trypan Blue 100 mL	Sigma-Aldrich	T8154
Long cover slips (1000pc)	VWR	631-0664
Bright-Line haemocytometer	Sigma-Aldrich	Z359629-IEA
Pipette tip, 10 µl	Sarstedt	70.3010.200
Pipette tip, 200 µl	Sarstedt	70.3030.200
Pipette tip, 300 µl	Sarstedt	70.3040.305
Pipette tip, 1000 µl	Cruinn	S1112-1020
Nunc 6 Well Plate	Fischer Scientific	10119831
Nunc 24 Well Plate	Fischer Scientific	10604903
Nunc 96 Well Plate	Fischer Scientific	10212811
Automated Cell counter	Lennox	EZ1
Acella 100, Cell Counter Slides, PK25	Lennox	A-10085
RPMI 1640 Medium, no glutamine	Biosciences	31870-074
10 mL Syringe	Lennox	ASY225.40BX
Sterile Transfer Pipettes	Sarstedt	86.1171.001
19G Needles	VWR	613-3939
27G Needles	VWR	613-3832
Tissue Roll	Lennox	ACL730.15CT24
Cryogenic vials	Lennox	ATP456.13
Ultra-LEAF™ Purified anti-mouse IL-4 Antibody	MSC	504121
Recombinant Mouse IL-4 (carrier-free)	MSC	574302
Ionomycin	Stemcell	73722
Lympholyte®-M Cell Separation Media	Tebu Bio	CL5031

Mouse CD4+ T Cell Enrichment Column, Small, Pack of 4	Biotechne (R&D Systems)	MCD4C-1000
Anti-mouse IFN-γ, clone XMG1.2	Biolegend	505834
eBioscience™ Permeabilization Buffer (10X)	Thermo Fischer Scientific	00-8333-56
Ultra-LEAF™ Purified anti-mouse CD3ε Antibod	Biolegend	100340
Ultra-LEAF™ Purified anti-mouse CD28 Antibody	Biolegend	102116
Recombinant Mouse IL-23 (carrier-free)	Biolegend	589002
Recombinant Mouse IL-2 (carrier-free)	Biolegend	575402
Recombinant Human TGF-β1 (carrier-free)	Biolegend	781802
Phorbol 12-myristate 13-acetate	Stemcell	74042
EasySep™ Mouse Naïve CD4+ T Cell Isolation Kit	Cruinn	19765
Dynabeads™ Human T-Activator CD3/CD28 for T Cell Expansion and Activation	Thermo Fisher Scientific	11161D

2.1.2 Sample Preparation and Supernatant generation:

Table 4: ***All Sample and Supernatant generation materials and reagents, corresponding sources and product codes.***

Materials and Reagents	Supplier	Catalogue number
Weigh Boats	Lennox	AWB100SQ/AS
15 mL Conical centrifuge tubes	Sarstedt	62.554.502
1.5 mL microcentrifuge tubes	Sarstedt	72.690.001

Sterile Transfer Pipettes	Sarstedt	86.1171.001
Water: Nuclease-Free Water, for Molecular Biology	Sigma-Aldrich	W4502-1L
MSC-Advantage Class II BSC, 1.2 m	Thermo Scientific	51025411
ODN 1826 (10mg)	Invivogen	tlrl-1826-1
Poly(I:C) (HMW) (10 mg)	Invivogen	tlrl-pic
Loxoribin	Invivogen	tlrl-lox
LPS E.coli serotype R515	Enzo life science	ALX-581-007-L002
p10 tips	Sarstedt	70.113
p200 tips	Sarstedt	70.760.002

2.1.3 MTS:

*Table 5 :**All Cell Viability materials and reagents, corresponding sources and product codes.***

Materials and Reagents	Supplier	Catalogue number
MTS CellTiter 96 AQueous One Solution Cell Proliferation Assay 1000 assays	My Bio (Promega)	G3580
Dimethyl Sulphoxide (DMSO)	Sigma-Aldrich	D8418-250 ML
DMSO Filters	Sigma-Aldrich	WHA67861302
Versamax™ 96-well plate reader	VWR	735-0348

2.1.4 ELISA:

*Table 6: **All ELISA materials and reagents, corresponding sources and product codes.***

Materials and Reagents	Supplier	Catalogue number
ELISA plates - Clear Flat-Bottom Immuno Nonsterile 96-Well Plates	Biosciences	442404
IL-6 Duoset ELISA kit	Biotechne (R&D Systems)	DY406
IL-1B Duoset ELISA kit	Biotechne (R&D Systems)	DY401

IL-10 Duoset ELISA kit	Biotechne (R&D Systems)	DY417
TNF-alpha Duoset ELISA kit	Biotechne (R&D Systems)	DY410
IFN-γ Duoset ELISA kit	Biotechne (R&D Systems)	DY485
IL-27p28 Duoset ELISA kit	Biotechne (R&D Systems)	DY1834
IL-12p70 Duoset ELISA kit	Biotechne (R&D Systems)	DY419
IL-23 Duoset ELISA kit	Biotechne (R&D Systems)	DY1887
IL-12p40 Duoset ELISA kit	Biotechne (R&D Systems)	DY499
IL-2 Duoset ELISA kit	Biotechne (R&D Systems)	DY402
IL-4 Duoset ELISA kit	Biotechne (R&D Systems)	DY404
IL-13 Duoset ELISA kit	Biotechne (R&D Systems)	DY413
TGF-β Duoset ELISA kit	Biotechne (R&D Systems)	DY1679
Bovine Serum Albumin (BSA)	Sigma-Aldrich	A7906-100G
Tween20	Sigma-Aldrich	P2287-500 ML
10XPBS reagents	Merck	11666789001
TMB 600 mL	BD Biosciences	555214
Sulfuric acid	Merck	258105
Weigh Boats	Lennox	AWB100SQ/AS
50 mL Conical centrifuge tubes	Sarstedt	62.559.001
5 mL Pipette	Merck	CLS4051-200EA
10 mL Pipette	Merck	CLS4101-200EA

25 mL Pipette	Merck	CLS4251-200EA
1.5 mL microcentrifuge tubes	Sarstedt	72.690.001
96 well Round Bottom Tissue Culture Non-Sterile	Sarstedt	1852.5
MCP ELISA Duokit	R&D Systems	DY479
MIP-1 ELISA Duokit	R&D Systems	DY450
MIP-2 ELISA Duokit	R&D Systems	DY452
ELISA Flex Human IL-2	2Bscientific	3445-1A-20

2.1.5 M1/M2 Polarisation:

Table 7: ***All M1/M2 polarisation, Griess Assay and Arginase Assay materials and reagents corresponding sources and product codes.***

Materials and Reagents	Supplier	Catalogue number
6 well plates	Biosciences	10119831
96 well plates	Biosciences	10212811
1.5 mL microcentrifuge tubes	Sarstedt	72.690.001
Cell Scrapper	Sarstedt	83.1831
1X DPBS	Biosciences	14190094
LPS	Enzo life sciences	ALX-581-007-L002
rIFN-γ	Peprotech	315-05
rIL-4	Peprotech	214-14
rIL-13	Peprotech	210-13
rTGF-β	BD Biosciences	240-B-002/CF
Greiss Reagent System	Promega (MyBio)	G2930
Arginase 1 Assay	Merck	MAK112-1KT
Pepstatin A	Merck	P5318-50mg
Leupeptin	Merck	L9783-50mg
Triton X-100	Merck	T8787

2.1.6 Flow Cytometry and Cell Staining:

*Table 8**: All Flow Cytometry materials and reagents, corresponding sources and product codes.***

Materials and Reagents	**Supplier**	**Catalogue number**
Cell Scrapper	Sarstedt	83.1831
15 mL Conical centrifuge tubes	Sarstedt	62.554.502
FBS	Biosciences	10270106
Whatman Filters Cellulose Acetate	Sigma-Aldrich	WHA69012502
10 mL Syringe	Lennox	ASY225.40BX
Sodium azide (NaN_3)	Sigma-Aldrich	S2002-500G
1X DPBS	Biosciences	14190094
Ethylenediaminetetraacetic acid (EDTA)	Sigma-Aldrich	200-449-4
96 Well Round Bottom Tissue Culture Non-Sterile	Sarstedt	1852.5
Anti-Mouse TLR4/MD-2 Complex PE	Biosciences	12-9924-82
MHC Class I (H-2Kd/H-2Dd) Monoclonal Antibody (34-1-2S), PE	Thermo Fisher scientific	12-5998-82
CD14-FITC antibody	eBioscience	11-0141-82
Mouse CD40/ TNFRSF5 affinity purified polyclonal Ab 100ug	R&D Systems	AF440
CD11c Monoclonal Antibody (N418), FITC	Thermo Fisher scientific	11-0114-85
APC hamster anti-mouse CD11c	*BD Biosciences*	550261
BD Pharmingen FITC anti-mouse CD86	*BD Biosciences*	553691
BD Pharmingen PE hamster anti-mouse CD80	*BD Biosciences*	553769
I-A/I-E FITC (MHC II)	BD Biosciences	553623
Mouse TLR2 FITC	eBiosciences	11-9021-82

CD11b Monoclonal Antibody (M1/70), PE	Thermo Fisher scientific	12-0112-82
F4/80 APC	MSC	123116
Formalin	Sigma-Aldrich	HT501128-4L
FACS tubes	VWR	734-0443
Mouse CD4+ T Cell Enrichment Column, Small, Pack of 4	R&D Systems	MCD4C-1000
TLR7 Polyclonal Antibody, FITC	Biosciences	PA5-23127
CD283 (TLR3) Monoclonal Antibody (TLR3.7), PE, eBioscience™	Biosciences	12-9039-82
Mouse Erythrocyte Lysing Kit	R&D Systems	WL2000
Mouse CD4 APC-conjugated Antibody	R&D Systems	FAB554A-100
Human/Mouse ROR gamma t/RORC2/NR1F3 PE-conjugated Antibody	R&D Systems	IC6006P-100
T-bet Monoclonal Antibody (eBio4B10 (4B10)), PE, eBioscience™	Thermo Fisher scientific	12-5825-82
Gata-3 Monoclonal Antibody (TWAJ), Alexa Fluor™ 488, eBioscience™	Thermo Fisher scientific	53-9966-42
FOXP3 Monoclonal Antibody (FJK-16s), PE, eBioscience™	Thermo Fisher scientific	12-5773-82
Hanks' Balanced Salt solution	Sigma-Aldrich	H9394
APC/Cyanine7 anti-mouse CD4 Antibody	Biolegend	100413
Propidium Iodide Solution	Biolegend	421301
eBioscience™ Fixable Viability Dye eFluor™ 455UV	Thermo Fischer Scientific	65-0868-14
TruStain FcX™ PLUS	Biolegend	156603
CFSE Cell Division Tracker Kit	Biolegend	423801
FITC anti-mouse IFN-γ Antibody	Biolegend	505805
APC anti-mouse IL-4 Antibody	Biolegend	504105

PE anti-mouse IL-17A Antibody	Biolegend	506903
FITC anti-mouse CD3 Antibody	Biolegend	100204
APC/Cyanine7 anti-mouse CD4 Antibody	Biolegend	100414
PerCP/Cy5.5 anti-mouse IL-10 25 µg	Biolegend	505027
Pacific BlueTM anti-mouse F4/80 25 µg	Biolegend	123123
7-AAD Viability Staining Solution	eBioscience	00-6993-50
Zombie Violet™ Fixable Viability Kit	Biolegend	423113
Monensin Solution (1,000X)	Biolegend	420701
eBioscience™ Foxp3 / Transcription Factor Fixation/Permeabilization Concentrate and Diluent	Thermo Fischer Scientific	00-5521-00

2.1.7 Phagocytosis Assay:

Table 9: ***All Phagocytosis materials and reagents, corresponding sources and product codes.***

Materials and Reagents	**Supplier**	**Catalogue number**
LPS E.coli serotype R515	Enzo life science	ALX-581-007-L002
Loxoribin	Invivogen	tlrl-lox
Phagocytosis Beads, Latex beads, carboxylate-modified polystyrene, fluorescent yellow-green	Sigma-Aldrich	L4655-1 mL
Cell Scrapper	Sarstedt	83.1831
Sodium azide (NaN_3)	Sigma-Aldrich	S2002-500G
1X DPBS	Biosciences	14190094
Ethylenediaminetetraacetic acid (EDTA)	Sigma-Aldrich	03620-50G

96 well round bottom tissue culture non-sterile	Sarstedt	1852.5
FBS	Biosciences	10270106
Round-bottom polystyrene tubes, disposable, Falcon	VWR	734-0443

2.1.8 Migration assay:

Table 10: ***All migration assay materials and reagents, corresponding sources and product codes.***

Materials and Reagents	Supplier	Catalogue Number
5uM pore transwell plate	Neuroprobe	106-5
stromal cell-derived factor-1 chemokine (SDF-1)	Biotechne (R&D systems)	6448-SD-025
Hoechst 33258 solution	Merck	94403-1 mL
Paraformaldehyde 8%	VWR	MFCD00133991

2.1.9 Immune synapse assay:

Table 11: ***All immune synapse assay materials and reagents, corresponding sources and product codes.***

Materials and Reagents	Supplier	Catalogue number
8 well chamber slide	Thermo scientific	16250681
Poly-lysine	Merck	P4707
Dynabeads	Thermo Fischer Scientific	11131D
phalloidin-TRITC	Merck	P1951-.1MG

2.1.10 Lysate Preparation:

Table 12: ***All lysate preparation materials and reagents, corresponding sources and product codes.***

Material and Reagents	Supplier	Catalogue number
NP40	Sigma-Aldrich	56741

500 mM Tris-HCl (pH 7.4)	Sigma-Aldrich	T-1503
1 M NaCl	Sigma-Aldrich	S-7653
100 mM NaF	Sigma-Aldrich	S-7920
100 mM Sodium Pyrophosphate decahydrate	Sigma-Aldrich	223168
100 mM EDTA	Sigma-Aldrich	100933T
100 mM EGTA	Sigma-Aldrich	E0396
100 mM PMSF	Sigma-Aldrich	P7626
1 mg/ mL leupeptin	Sigma-Aldrich	L8511
100 mM Na_3VO_4 (sodium orthovanadate)	Sigma-Aldrich	S-6508

2.1.11 BCA protein Quantification:

Table 13: ***All Protein Purification materials and reagents, corresponding sources and product codes.***

Material and Reagents	Supplier	Catalogue number
Bovine Serum Albumin	Sigma-Aldrich	A7906-100G
1 SET BCA PROTEIN ASSAY KIT, 1L KIT	Fisher	10741395
96 Well Round Bottom Tissue Culture Non-Sterile	Sarstedt	1852.5
1.5 mL microcentrifuge tubes	Sarstedt	72.690.001

2.1.12 SDS-PAGE:

Table 14: ***All SDS-PAGE materials and reagents, corresponding sources and product codes.***

Material and Reagents	Supplier	Catalogue number
30 % acrylamide	Sigma-Aldrich	A3699
10 % w/v ammonium persulphate (10 % APS)	Sigma-Aldrich	A3678
1.5 M Tris-HCl (pH 8.8)	Sigma-Aldrich	T-1503
1.0 M Tris-HCl (pH 6.8)	Sigma-Aldrich	T-1503

10 % w/v SDS	Sigma-Aldrich	L-5750
TEMED	Sigma-Aldrich	T-9281
Isobutanol	Sigma-Aldrich	58448
15.1 g TRIZMA	Sigma-Aldrich	T-1503
Glycine	Sigma-Aldrich	G-8898
PageRuler™ Plus Prestained Protein Ladder, 10 to 250 kDa	Thermo Fisher Scientific	26619
4X Bolt™ LDS *Sample Buffer*	Invitrogen	B0007
10X Bolt™ *Sample Reducing Agent*	Invitrogen	B0009

2.1.13 Western Blot:

Table 15: ***All western blot materials and reagents, corresponding sources and product codes.***

Material and Reagents	Supplier	Catalogue number
5% w/v milk powder	Tesco	N/A
30% H_2O_2	BDH labs	285194F
250 mM luminol	Sigma	09253
90 mM 4-Iodophenylboronic acid	Sigma-Aldrich	471933-5G

2.1.14 Cells Used:

*Table 16****: All Cell Names, Cell Types used and corresponding sources.***

Cell Name	Cell Type	Purchased
J774A.1	Macrophage cell line	ECACC
JAWSII	Dendritic cell line	ECACC
BMDM (Balb/C)	Primary Macrophage	Charles River
BMDC (Balb/C)	Primary Dendritic cells	Charles River
T cells (Balb/C)	Primary T cells	Charles River
JURKAT	Human T cell line	Queens University Belfast

2.1.15 Buffers/Gels Used:

Table 17: ***Composition of most commonly used buffers and gels.***

Buffer	Composition
10 X PBS	8 mM Na2HPO4, 1.5 M KH2PO4, 137 Mm NaCl, 2.7 mM KCL, pH 7.4
ELISA Wash Buffer	500 mL 10XPBS, 4500 mL Deionised Water, 2-3 mL Tween 20
FACS Buffer	10 mL FCS, 0.25g NaN_3, 500 mL PBS, 1000µl EDTA 0.5M
1X column wash buffer T cell isolation	7.5 mL 10X column wash buffer, 67.5 mL Sterile distilled water
Lysis wash Buffer T cell isolation	5 mL 10X wash, 45 mL Sterile distilled water
Lyse Buffer T cell isolation	1 mL 10X lyse, 9 mL Sterile distilled water
Cell lysis buffer for western blot	1 mL of NP40 solution, 15 mL of 1M NaCl, 4 mL of 500 mM Tris-HCl (pH 7.4), 10 mL glycerol, 5 mL of 100 mM NaF, 5 mL of 100 mM NaPP, 5 mL of 100 mM EDTA, 5 mL of 100 mM EGTA
10% acrylamide gel	dH_20 7.9 mL, 30 % Acrylamide 6.7 mL, 1.5 M Tris-HCl (pH 8.8), 5.0 mL, 10 % w/v sodium dodecyl sulfate (SDS), 200ul, 10 % w/v Ammonium Persulfate (APS), tetramethylethylenediamine (TEMED) 8 µL
Stacking gel	dH_20 3.4 mL, 30 % Acrylamide 0.83 mL, 1.0 M Tris-HCl (pH 6.8) 0.63 mL, 10 % w/v SDS 50 µL, 10 % w/v APS 50 µL, TEMED 5 µL
5X SDS-PAGE running buffer	15.1 g Trizma, 94 g Glycine, 50 mL of 10 % w/v SDS, dH_20 to 1 litre
Western blot transfer buffer	5.8 g Trizma base, 2.9 g Glycine, 0.37 g of SDS or 8 mL 10 % w/v SDS, 200 mL, Methanol, dH_20 to 1

	L
10X TBS for western blot	24.2g Trizma base, 80g NaCl, 900 mL dH_20 pH solution to 7.6 with HCl, Add dH_20 to 1L.
Western blot wash buffer	1X TBS with 0.1% v/v Tween-20 (TBS-T)
Western blot blocking buffer	5 % w/v milk powder (Marvel) in Western blot wash buffer (TBS-T)
HRP development solution for western blot	24 mL of 100 mM Tris-HCl (pH 8.5), 14.4 µL of 30 % H_2O_2, 120 µL of 250 mM luminol, 532 µL of 90 mM 4-Iodophenylboronic acid

2.2 Methods

2.2.1 Cell Culture:

Cell culturing was carried out in a Holton Air Laminar Flow Class II Biosafety cabinet. Sterile, aseptic conditions were maintained throughout all cell culturing activities using aseptic techniques. Cleaning of the biosafety cabinet was conducted with 70% IMS before use and similarly, all materials entering the biosafety cabinet were sterilised with 70% IMS. Cells were maintained in cell culture flasks within incubator at 37°C, with 5% CO_2 and 95% humidified air.

2.2.2 Preparation of Cell Stocks:

Cells were grown to a state of sub-confluency and harvested and counted as outlined in section on cell numeration (Section 2.2.11 Cell numeration). Cells were resuspended in 1 mL cryoprotectant (10% v/v DMSO and 90% cell suspension) at a concentration of $1x10^7$ cells/ mL and were transferred to dated and labelled cryovials. Cryovials were placed in freeze wheel containing Isopropyl alcohol and were placed at -80°C overnight before transferring to storing long term in a liquid nitrogen vessel.

2.2.3 Revival from Frozen Stocks:

Cryovials were carefully removed from liquid nitrogen vessel and quickly thawed in 37°C water bath with agitation. Thawed cells were transferred to 10 mL cell culture media and carefully resuspended. Cells were spun at 1200RPM for 5 minutes, removing excess DMSO. Supernatant was discarded and cells were resuspended in 1 mL prewarmed cell culture media and transferred to T75 flask with appropriate supplemented media for optimal cell growth.

2.2.4 JAWSII Murine Dendritic Cell:

Jaws II Dendritic cell line, now referred to as JAWS, purchased from European Collection of Authenticated Cell Cultures (ECACC) were maintained in αMEM with 10% non-heat inactivated FBS, 1% Pen-Strep Antibiotic, 50ng/ mL GM-CSF, cultured in T25 and sub-cultured in T75 culture vessel. Cells were passaged every three to four days at a confluency of 70%-80%. Suspending cells were transferred to 50 mL conical centrifuge tube. Adherent cells were washed twice with sterile PBS. Trypsin was added to flask and incubated for five minutes at 37°C. αMEM was added and suspension containing floating cells was added to 50 mL conical centrifuge tube. Cell suspension was centrifuged at 1,000rpm for ten minutes at 4°C. Supernatant was discarded and pellet was resuspended in 3 mL αMEM containing GM-CSF. Sub-culturing of cells at ratio 1:3 was carried out. Cells were counted as outlined (Section 2.2.11 Cell numeration). Cell seeding for experimentation was carried out at concentration of $1x10^6$cells/ mL. Cells were left overnight to settle before proceeding with experimentation.

2.2.5 J774.A.1 Murine Macrophage:

J774.A.1 Murine Macrophage, now referred to as J774, purchased from ECACC were maintained in DMEM with 10% heat inactivated FBS, 1% Pen-Strep Antibiotic. Cells were cultured in a T75 culture vessel. Cells were passaged every three to four days at a confluency of 80-90%. Adherent cells were scrapped from bottom of T75 using sterile cell scrapper into the culture media. Cell suspension was collected in 50 mL conical centrifuge tube and centrifuged at 1200 RPM for 5 minutes at room temperature. Supernatant was discarded and pellet was resuspended in 10 mL DMEM. Cells were Sub-cultured at 1:10 ratio. Cells were counted as outlined (Section 2.2.11 Cell numeration). Cell seeding for experimentation was carried out at concentration of $1x10^6$ cells/ mL. Cells were left overnight to settle before proceeding with experimentation.

2.2.6 Primary-Derived Bone Marrow Dendritic Cells (BMDCs):

This procedure was carried out to isolate primary-derived dendritic cells from the bone marrow of Balb/C mice. On Day 1 cells were harvested by carefully removing legs and trimming off the flesh off mice and collected in 50 mL conical centrifuge tube containing 50 mLs RPMI1640, 5% FCS and 2% Pen-Strep, left to soak for 30 minutes. Legs and media were poured into petri dish and remaining flesh and fat precisely removed so ends of bones were visible. Femur and tibia were separated, and each bone flushed using a 10 mL syringe, equipped with a 27G needle, filled with media. Each bone was flushed one at a time, using a tweezers to hold in the middle of the bone, cutting either end of the bone exposing marrow and flushing with media. Flushed media was collected containing bone marrow, into new 50 mL conical centrifuge tube. Sterilising tweezers and scissors were carried out after each bone, filling syringe with media before repeating on next bone. The conical centrifuge tube was then spun at 1200RPM for 5 minutes. Media was prepared for plating with RPMI1640, 10% FCS, 2% Pen-Strep and GMCSF for DC induction. 1 Petri dish per 1 bone with 10 mLs media per plate was prepared. Pellet checked and supernatant removed into waste before resuspending cells in amount of media required for plating. Cells were plated in sterile petri dishes and incubated at 37%, 5% CO_2 until Day 4. On Day 4 media was prepared as described before with GMCSF for 10 mLs media per plate. Excess media was removed in so much as possible without disturbing film of cells and then gently added the new media. Plates were incubated at 37%, 5% CO_2. On Day 7 the cells were carefully scraped with cell scraper and collected using disposable pipette into 50 mL conical centrifuge tube. Spun at 1200RPM for 5 minutes. Emptied media into waste and resuspended cells in 5 mLs RPMI media without GMCSF. Counted cells (Section 2.2.11 Cell numeration). Cell seeding for experimentation was carried out at concentration of $1x10^6$cells/ mL. Cells were left overnight to settle before proceeding with experimentation.

2.2.7 Primary-Derived Bone Marrow Macrophages (BMDMs):

This process was designed to isolate primary derived macrophage cells from the bone marrow of Balb/C mice. On Day 1 cells were harvested by carefully removing legs and trimming off the flesh off mice and collected in 50 mL conical centrifuge tube containing 50 mL RPMI1640, 5% FCS and 2% Pen-Strep, left to soak for 30 minutes. Legs and media were poured into petri dish and remaining flesh and fat precisely removed so ends of bones are visible. Femur and tibia were separated, and using a 10 mL syringe, equipped with a 27G needle, was filled with media each bone was flushed. Each bone was flushed one at a time, using tweezers to hold in the middle, cutting either end of the bone exposing marrow and flushing with media. Collected flushed media and bone marrow into new 50 mL conical centrifuge tube. Sterilised tweezers and scissors after each bone and filled syringe with media before repeating on next bone. The conical centrifuge tube was then centrifuged at 1200RPM for 5 minutes. Prepared media for plating with RPMI1640, 10% FCS, 2% Pen-Strep and 25ng/ mL rM-CSF for macrophage induction. Used 1 Petri dish per 1 bone with 10 mL media per plate. Checked pellet and emptied media into waste before resuspending cells in suitable volume of media required for plating the cells. Plated cells in sterile petri dishes and incubated at 37%, 5% CO_2 until Day 3. On Day 4 made up media as described before with 25ng/ mL rM-CSF for 10 mL media per plate. Gently added 10 mL of the new media without disturbing layer of old cells for a total of 20 mL of media per plate. Incubated at 37%, 5% CO_2. On Day 6 carefully scraped cells with cell scraper and collected using disposable pipette into 50 mL conical centrifuge tube. Spun at 1200 RPM for 5 minutes. The supernatant was discarded into waste and the cell pellet was resuspended in 10 mL RPMI/10% FCS/2% Pen-strep/25 ng/ mL rM-CSF. Cells were counted (Section 2.2.11 Cell numeration). Cell seeding for experimentation was carried out at concentration of $1x10^6$ cells/ mL. Cells were left overnight to settle before proceeding with experimentation.

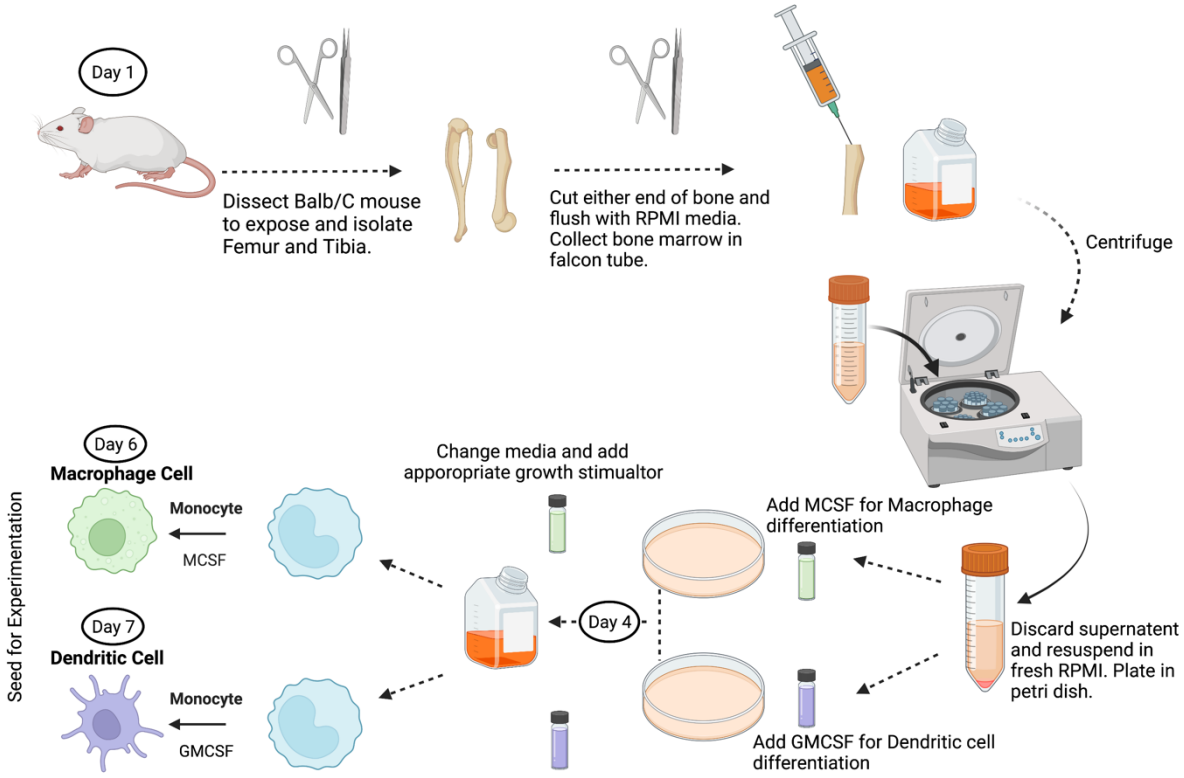

Figure 9: ***BMDM and BMDC Schematic.*** *Protocol for the isolation of bone marrow from a Balb/C mouse and differentiation of bone marrow derived macrophage and bone marrow derived dendritic cells. Created with BioRender.com.*

2.2.8 Isolation of Primary-Derived T Cells:

On the day prior to isolation, 24-well ELISA plates were coated with 1000 µL of sterile PBS and CD3/mix, and 96-well ELISA plates were coated with 200 µL of the mix, then incubated overnight at 4°C. A 6-well plate was similarly coated with 2000 µL of sterile PBS and CD3 mix and left to incubate overnight at 4°C. To isolate the T cells, the spleen was harvested from the mouse, gently disaggregated in PBS using a 40 µm cell strainer and a Petri dish. The suspension was centrifuged for 10 minutes at 300 g (approximately 1500 rpm). The pellet was then resuspended in RoboSep Buffer, counted, and its viability assessed via FACS.

2.2.8.1 EasySep Mouse CD4+ T cell Isolation Method:

Cells were prepared at ratio of 1 mL per spleen in 5 mL FACS tubes. A volume of 10 µL FcR blocker was added to the cells. Subsequently, 50 µL/ mL of isolation cocktail was added to the cell suspension, mixed and incubated at room temperature for 7.5 minutes. A 50 µL depletion cocktail was added to the cells, mixed and incubated at room temperature for 2.5 minutes. The Rapidspheres were vortexed for 30 seconds, and 75 µL per mL of cell suspension was added. The mixture was then incubated at room temperature for 2.5 minutes after thorough mixing. The cell suspension was then brought up to a total volume of 2.5 mL by adding 1.32 mL of the medium recommended by RoboSep. The tube was placed into the magnet and incubated at room temperature for 10 minutes. The enriched cell suspension was then carefully pipetted into a new tube. and 2% penicillin-streptomycin. This was followed by centrifugation for 10 minutes at 300g or 1500rpm. The cells were resuspended cells in complete RPMI, supplemented with 10% heat inactivated FBS and 2% penicillin streptomycin.

2.2.8.2 Mouse CD4+ T Cell Enrichment Column Method:

The supernatant was discarded and the cells were resuspended in lyse buffer at a ratio of 2 mL per spleen and vortexed quickly. Incubated for 10 minutes at room temperature. Filled the tube with 1X wash buffer lysing. Spun cells via centrifugation for 10 minutes at 200g or 1200rpm. Resuspended cells in small volume 1X column wash buffer. Counted cells and adjusted to concentration 1-2x10^8 cell/ mL using 1X column wash buffer. Added antibody cocktail (1 mL) in 15 mL falcon to all 1-2 mL cells and column wash buffer mix. Mixed gently and incubated at RT for 15 minutes. Prepared the column by taking off top cap then bottom cap of column and drain into 15 mL falcon. Washed column with 10 mL of 1X column wash buffer and centrifuged 2000rpm for 10minutes. Resuspended in 2 mL 1X column wash buffer. The antibody-treated cells were introduced into the column, where they were allowed to suspend within the matrix, and incubated for 10 mins at room temperature. Eluted cells from column using total 10 mL of column wash buffer until eluate appeared clear. Centrifuged collected cells at 1750rpm for

5 minutes. Discarded supernatant and resuspended cells in appropriate buffer or cell culture media RPMI containing 5% pen strep, and 10% HIFBS.
Counted cells, polarised for Th1, Th2, Th17, Treg, and seeded for experimentation.

2.2.9 T cell polarisation:

On the day of T cell isolation, the CD3 coated plates were washed three times with PBS. Polarisation components were then added to the media as follows:

Table 18: ***Polarisation factors for differentiation towards Th1, Th2, Th17, and Treg cells.***

Th1	**Th2**	**Th17**	**Treg**
3ug/ mL Anti-mouse CD28	3ug/ mL Anti-mouse CD28	3ug/ mL Anti-mouse CD28	3ug/ mL Anti-mouse CD28
10ug/ mL anti-mouse IL-4	20ng/ mL IL-2	2ng/ mL Human TGFb	20ng/ mL IL-2
20ng/ mL IL-2	10ug/ mL Anti-IFNy	20ng/ mL IL-23	2ng/ mL Human TGFb
20ng/ mL IL-12	50ng/ mL IL-4	10ug/ mL anti-mouse IL-4	10mM all trans retinoic acid (ATRA)
		10ug/ mL Anti-IFNy	
		50ng/ mL IL-6	

After centrifuging, the cells were resuspended in media containing the specified polarization components. The cells were then seeded at a concentration of 1 x 10^6 cells/mL: 500 µL per well in a 24-well plate or 150 µL per well in a 96-well plate. The plates were incubated for 30 minutes at 37°C with 5% CO2. Following this initial incubation, samples were added to each well. The plates were then incubated at 37°C with 5% CO_2 for three days, during which time the cells were exposed to the appropriate polarization components as outlined in Table 18. On Day 2 T cell polarisation, complete RPMI media containing the specified polarization

components was prepared. Cells were restimulated by adding 250 µL of the new media/polarization mix per well in 24 well plates or 75 µL for 96 well plate. Samples were then added for restimulation. The culture continued until Day 4. On Day 4, for intracellular staining, the test cells were stimulated with 25 ng/ mL PMA, 1µg/ mL ionomycin, and 10ug/ mL Brefeldin A. The cells were incubated for 4 hours at 37^{O}C with 5% $CO_{2.}$ Afterwards, the cells were collected and pooled into a 15 mL conical centrifuge tube, then centrifuged and counted . After incubation, the procedure continued with intracellular staining. Alternatively on Day 5, supernatants were collected for ELISA analysis.

2.2.10 JURKAT Human T cell line:

JURKAT Human T cell line, attained from Queens University Belfast, were maintained in RPMI with 10% heat inactivated FBS, 1% Pen-Strep Antibiotic. Cells were cultured in a T25 culture vessel. Cells were passaged every three to four days at a confluency of 80-90%. Suspension cell line thus cells were sub-cultured at a ratio of 1:9 replacing old media with fresh complete RPMI. The cells were counted as outlined (Section 2.2.11 Cell numeration). Cell seeding for experimentation was carried out at concentration of 1x10^{6}cells/ mL. Cells were left overnight to settle before proceeding with experimentation.

2.2.11 Cell Numeration:

This method was used to determine the count of viable cells present in a suspension, facilitating their use across various experimental procedures.

2.2.11.1 Trypan Blue Method:

Cell suspensions were counted on a haemocytometer. 100 µL of cell suspension was added to a 1.5 mL Microcentrifuge tube containing 150 µL sterile 1x PBS and 250 µL of Trypan Blue staining solution. This was mixed and incubated at room temperature for five minutes. Haemocytometer was sterilised with 70% IMS and

glass cover slip placed on top of grid. 10µL of the Trypan Blue mix was carefully placed underneath the coverslip, ensuring no air bubbles form. Counted cells in each of the four gridded sections and determine average value for all (N). The following equation is used to calculate cell concentration where "N" is the average cell count, "5" is the dilution factor and "10^4"corresponds to the surface area of the haemocytometer and remains constant.

$$N \times 5 \times 10^4 = X \text{ cells/ mL}$$

2.2.11.2 Automatic Cell Counter Method:

50 µL of cell suspension was added to a 1.5 mL microcentrifuge tube. 20 µL of cell suspension was added to glass cover slide. Automatic cell counter was turned on, turned slide up-side-down and slide placed in machine. Selected option to read cells/ mL in cell suspension.

Either allows for the calculated cells to then be diluted to the desired concentration in the appropriate cell culture medium.

2.2.12 Sample Preparation:

Fermentate samples received from Teagasc in 50 mL liquid form where skim milk powder was used as a substrate for the generation of the fermentates used in this study. Skim milk powder was reconstituted at 10% w/v in distilled water to generate RSM, autoclaved, cooled and stored at 4°C for a maximum of 7 days. An inoculum of frozen mother culture stocks of the individual strains was added to 10% RSM and incubated for 24hrs at 37°C without agitation, to generate these individual fermentates. From these cultures, a further inoculum was added to 10% w/v RSM and incubated for 24hrs at 37°C again without agitation. These fermentates were subjected to a heat treatment step to generate the fermentates. After cooling to room temperature, the pH of the fermentates was neutralized. These fermentates were aliquoted and immediately frozen at -80°C until further analysis. Non-fermented RSM samples subjected to the same heat-treatment mentioned above were used as negative controls for all experiments described herein.

Upon receipt at DCU samples were left to defrost at 4^{O}C over 48hours. Samples were aliquoted into smaller single use aliquots of 0.5g liquid sample in 1.5 mL microcentrifuge 's or 1g liquid sample in 15 mL conical centrifuge tubes and stock refrozen and stored at -20 ^{O}C for short term storage or -80 ^{O}C for long term storage. Sample was made fresh on the day of use by defrosting single use sample. Based on previous work conducted at Teagasc it was determined that the fermentates contained 10% protein on a weight basis and therefore 1 mL of molecular grade water was added to dilute 0.5 g liquid sample for a stock concentration of 50mg/ mL or similarly 2 mL molecular grade water to 1g liquid sample. Sample mixed by repeat pipetting. Desired working concentration was then calculated for experimentation.

2.2.13 MTS Cell Viability Assay:

The assay system used was the CellTiter 96® AQueous One Solution Cell Proliferation Assay and conducted as per manufacturer's instructions. This assay was used to determine cytotoxicity as well as cell proliferation. Herein the reference to "cell viability" additionally refers to cell proliferation, where anything above 100% cell viability demonstrated enhanced cell proliferation, while anything below 100% cell viability demonstrated a cytotoxic affect. Each assay was performed in triplicate, with a positive and negative control of untreated cells and 10% DMSO respectively. 100µl of appropriate cell line was seeded at a concentration of 1 x 10^6 cells/ mL to a flat bottom 96-well plate, incubated for 24 hours at 37°C in a humidified, 5% CO_2 atmosphere. Specific "treatment" added to the cells and the plate incubated at the specified length of time, under the same conditions. The following day, 20 µl of the thawed CellTiter96® Aqueous One Solution was added to each well of the 96-well plate. The plate was then incubated at 37°C for 1-3 hours in a humidified atmosphere containing 5% CO_2. Absorbance recorded at 490 nm using Versamax™ 96-well plate reader after three hours. Cell viability of each sample calculated by treating the absorbance of the vehicle control

as 100% and comparing the remaining samples to this to then express results as percentage viability.

2.2.14 Enzyme Linked Immunosorbent Assay (ELISA):

2.2.14.1 Murine:

The concentrations of cytokines IL-1β, IL-2, IL-4, IL-6, IL-10, IL-13, TNF-α, IL-12p40, IL-12p70, IL-23, IL-27, IFN-γ, and TGF-β or chemokines MCP-1, MIP-1 and MIP-2 were determined via ELISA kits, provided by R&D Systems and performed according to the manufacturer's instructions. Functioning as a sandwich ELISA, the capture antibody was diluted to appropriate concentration with PBS and 50 µL/well added to each well of a 96 well NuncTM microtitre plate. Plates covered with clingfilm and incubated at room temperature overnight. Plates washed 3 times with wash buffer. 200 µL reagent diluent added to block wells and overcome non-specific binding for minimum 1 hour at room temperature or overnight at 4^{O}C. Plates washed with wash buffer 3 times and 50 µL/well of appropriately diluted standard and sample added to each well: 25 µL of RD each well, 25 µL of serially diluted standard and 25µL appropriately diluted supernatant as per plate plan with each sample and standard carried out in triplicate. Incubated at 4^{o}C overnight. The plates were washed three times with wash buffer. Added 50 µL/well of appropriately diluted biotinylated detection antibody made up with RD. Incubated at room temperature for 2 hours in the dark. Washed plates 3 times with wash buffer. Added 50 µL/well of a 1:40 streptavidin-horse radish peroxidase (HRP) solution for 20 minutes, at room temperature in the dark. Plated washed 3 times with wash buffer. 50 µL/well of fresh TMB substrate added and incubate for 20-25 minutes, at room temperature, protected from light. Blue colour starts to develop and 25 µL/well of 2N sulphuric acid added, to stop the reaction. Optical density was determined using VersamaxTM microplate reader at wavelength of 450 nm.

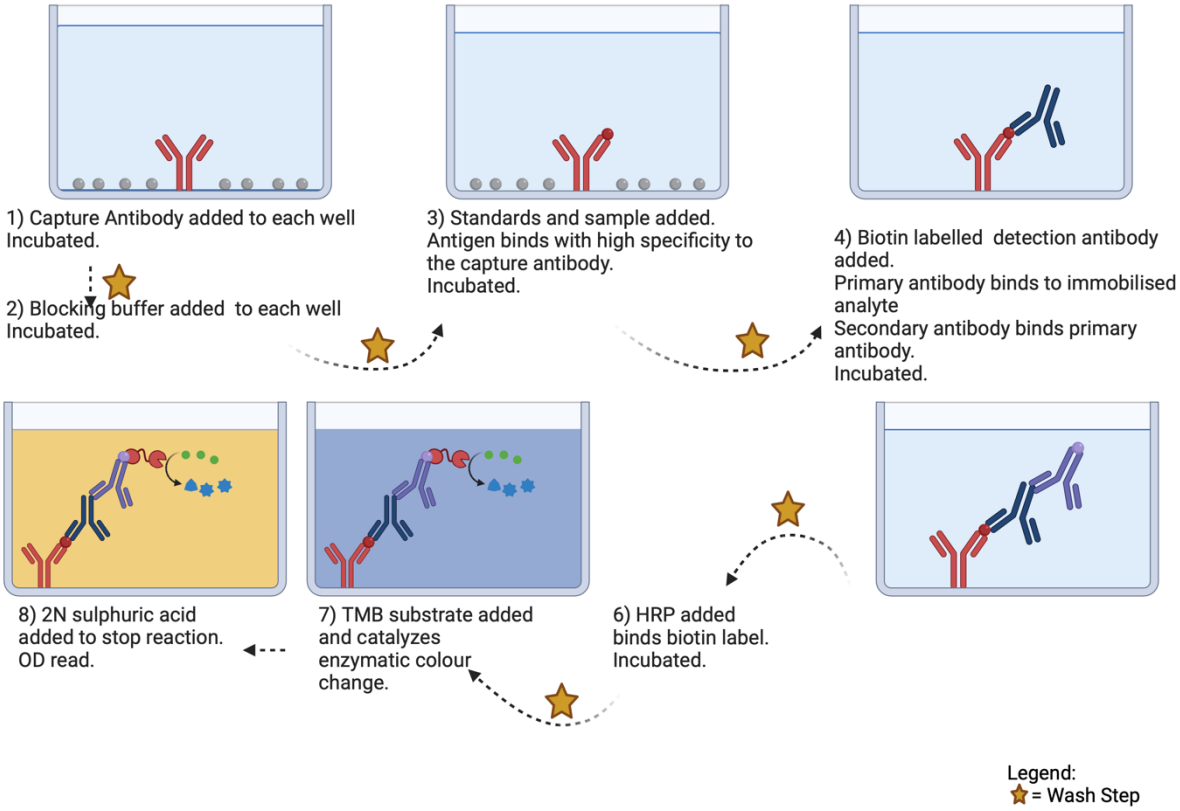

*Figure 10**: ELISA Schematic.** Protocol for ELISA to quantitatively determine cytokine concentrations produced by a range of cells in response to TLRs and samples present. Cytokines examined include IL-1β, IL-2, IL-4, IL-6, IL-10, TNF-α, IL-12p40, IL-12p70, IL-13, IL-23, IL-27, TGFβ and IFN-γ. Created with BioRender.com.*

2.2.14.2 Human:

The concentrations of cytokines IL-2, IL-6, IL-10, and IL-13, were determined via human ELISA kits, provided by 2Bscientific and performed according to the manufacturer's instructions. Functioning as a sandwich ELISA, the capture antibody was diluted to appropriate concentration with PBS and 100 µL/well added to each well of a 96 well NuncTM microtitre plate. Plates covered with clingfilm and incubated at 4-8^{O} C overnight. Plates were washed 2 times with wash buffer. 200 µL reagent diluent (RD) added to block wells and overcome non-specific binding allowing it to sit for minimum 1 hour at room temperature. Plates were washed with wash buffer 5 times and 100 µL/well of appropriately diluted standard and sample added to each well and carried out in triplicate. Plates were incubated at room temperature for 2 hours, then plates were washed 5 times with wash buffer. After washing, 100 µL of appropriately diluted biotinylated detection antibody prepared

with RD was added to each well.. The plates were incubated at room temperature for 1 hours in the dark, then plates were washed 5 times with wash buffer. After washing, 100µL/well of a 1:1000 dilution of streptavidin-HRP solution was added and incubated for 1 hour, at room temperature in the dark. Plates washed 5 times with wash buffer. 100µL/well of fresh TMB substrate added and incubate for 20-25 minutes, at room temperature, protected from light. Blue colour started to develop and 25µL/well of 2N sulphuric acid added, to stop the reaction. Optical density was determined using VersamaxTM microplate reader at wavelength of 450nm.

2.2.15 Macrophage M1/M2 polarisation assay:

Used to determine the effect of sample on the polarisation of macrophage to either an M1 or M2 phenotype. Seeded 1 mL BMDM cells at a concentration of 500,000 cells per well in 24-well plates and incubated for 30 minutes-1 hr at 37 C. Added sample for 3 hours, incubated at 37^{O}C. Polarized cells towards M1 macrophages by adding LPS (100 ng/ mL) in the presence of 20 ng/ mL rIFN-γ or towards M2 cells by adding 20 ng/ mL rIL-4, 20 ng/ mL IL-13, and 20 ng/ mL rTGF-B and incubated for 24 h at 37 C. Harvested media and stored at -20^{o} C for cytokine analysis (ELISA) and for NO2- (nitrite) measurement by Griess Assay, and after collecting the supernatants, immediately prepared and analysed cell lysates for Arginase activity using a commercial kit.

2.2.15.1 Griess Assay: M1 phenotype

This method was used to quantify the production of nitric oxide by inducible nitric oxide synthases in response to fermentate, when cells are activated with LPS in presence of IFN-γ. Supernatant was harvested from M1/M2 polarized plates that had been previously prepared . A nitrite standard curve was established using a serial dilution of Nitrite standard at 1:1000 dilution in media. Then 50 µL of standard solutions and 50 µL of the sample were added to a 96-well plate according to the plate layout. Next, 50 µL of sulfanilamide solution was added to each well, followed by a 10-minute incubation in the dark. Afterwards, 50 µL of N-(1-Naphthyl) ethylenediamine dihydrochloride (NED) solution was added, and the plate was

incubated again for 10 minutes in the dark. Finally, the absorbance was read at 548 nm.

2.2.15.2 Arginase Assay: M2 phenotype

This method was used to quantify the amount of arginase activity in a cell, via the proportional detection of urea, a direct result of arginase catalysing the conversion of arginine to urea and ornithine, when cells are induced with IL-4, TGFβ, and IL-13. Harvested supernatant from already prepared M1/M2 polarised plates. Supernatants were frozen for ELISA and Griess assay. Washed the plate with 1 mL PBS carefully and discarded. Added 0.5 mL PBS to plates and scraped cells. Harvested cells in PBS and transferred to microcentrifuge tubes. Centrifuged cells at 1000g, for 10 minutes at 4^{O}C. Discarded supernatant and retained pellet. Made up lysing buffer: Adding 500 µL of 1M Tris to 49.5 mL of molecular grade water to make a 10mM tris buffer, 1uM Lepeptin and 1uM Pepstatin, and 200 µL for a 0.4% Triton X-100 to make the complete lysing buffer. Added 100 µL of the Lysing buffer to each tube. Vortexed each tube for 30 seconds. Left to stand for 10 minutes at room temperature. Centrifuged at 13000g for 10 minutes at 4 ^{O}C. Harvested supernatant and discarded pellet. Froze lysates in -80 ^{O}C if needed for future use. Prepared blank buffer using 0.4%(w/v) Triton X, 10mM Tris HCl, 1uM leupeptin, and 1uM pepstatin. Prepared Urea standard to a 1mM concentration. Prepared 5X substrate buffer constituting of 8 parts Arginine buffer and 2 parts Mn buffer. Added 20 µL samples in duplicate according to plate plan, included 50 µL Urea standard well, 50 µL deionized water well, and blank buffer well consisting of 20 µL deionised water and 20 µL blank buffer. Added 10 µL of 5X substrate buffer to all wells, excluding blank buffer well. Incubated for 2 hours at 37^{O}C. Prepared Urea Reagent at a 1:1 ratio Reagent A and Reagent B. Added 200 µL Urea reagent to every well. Added 10 µL Substrate buffer to buffer blank. Incubated at room temperature for 1 hour. Measured absorbance at 430nm. Calculated activity based on following equation:

$$Activity\ \left(\frac{units}{L}\right) = \frac{(\ sample_{abs(430)_{\square}} - buffer\ blank\ _{abs(430)_{\square}})}{(Urea\ standard_{abs(430)_{\square}} - deionised\ water\ _{abs(430)_{\square}})} x \frac{1mMx50x10^3}{sample\ vol(uL)\ x\ reaction\ time(mins)}$$

Where: 1mM is the Urea standard concentration, 50 is the 50 µL reaction volume, and 10^3 is the conversion from mM to µM.

2.2.16 Flow Cytometry

2.2.16.1 Cell Surface marker Staining:

This method was used to identify cell surface markers through staining. Cells that were seeded in a 6-well plate and stimulated with appropriate treatments were scraped and transferred to a 15 mL conical centrifuge tube. To block non-specific binding, 2 mL of filtered FCS was added, and the mixture was left at room temperature for 15 minutes. The cells were then centrifuged at 2000 RPM for 5 minutes at 4°C. Cells were resuspended in 1 mL of FACS buffer consisting of 2 mL FCS, 0.05 g NaN_3, 100 mL PBS, and 200 µL of 0.5 M EDTA. 200 µL of this cell suspension was distributed into the appropriate wells of a 96-well round bottom plate according to the treatment plan for each antibody, including compensation steps if required. The plate was centrifuged at 2000 rpm at 4°C for 5 minutes, and the supernatant was aspirated. Cells were then resuspended in 100 µL of a 1:1000 dilution of the respective antibodies and incubated for 30 minutes at 4°C. After another spin at 2000 rpm for 5 minutes, the cells were washed three times with FACS buffer, involving resuspension in 200 µL of FACS buffer and repeated centrifugation. Once washing was complete, cells were fixed in 1% formaldehyde fixing buffer for potential overnight storage. This was achieved by resuspending the cells in 100 µL of fixing buffer (composed of 9 mL FACS buffer and 1 mL 37% formaldehyde), allowing them to sit for 15 minutes at room temperature, followed by a centrifugation at 1200 rpm for 5 minutes with one repeat wash. Finally, cells were resuspended in 100 µL of FACS buffer and stored overnight at 4°C. The next day, cells were transferred to FACS loading tubes containing 400 µL of FACS buffer

to make a total volume of 500 µL. Cells were then analysed using a BD FACSAria I system flow cytometer. The raw fcs files were processed, and the data graphed using FlowJo software, version 10.0.

2.2.16.2 Intracellular transcription factor staining:

A single-cell suspension was prepared, and non-specific Fc-mediated interactions were blocked. For primary cells the cells were pre-incubated with 0.5–1 µg of anti-Mouse CD16/CD32 antibody per 100 µL for 10–20 minutes at 2–25°C before staining. Cells were then resuspended in 50 µL of eBioscience Flow Cytometry Staining Buffer. Additionally, the cells were pre-incubated with 2 µL of 2% rat serum per 100 µL of mouse cells, and incubated for 15 minutes at 2–25°C. The cells were not washed prior to staining cells with antibodies. Cells were stained with a Fixable Viability Dye (FVD) by adding 1µL of FVD per 1 mL of cells and immediately vortexed. Then cells were Incubated for 30 minutes at 2-8°C, protected from light. Cells were washed twice with Flow Cytometry Staining Buffer. Cells were stained for surface markers following the protocol previously described (section 2.2.16.1 Cell Surface Marker Staining). After the final wash, the supernatant was discarded and pulse vortexed the sample. Then to each well 200 µL of Fixation/Permeabilization working solution was added and incubated for 30-60 minutes at 2-8°C or room temperature, protected from light. Samples were centrifuged at 400-600 xg for 5 minutes at room temperature. Then the Supernatant was discarded and 200 µL 1X Permeabilization Buffer was added to each well and centrifuged samples at 400-600 xg for 5 minutes at room temperature. Discarded the supernatant. Centrifuged samples at 400-600 xg for 5 minutes at room temperature. Discarded the supernatant. Resuspended pellet in residual volume and adjust volume to 100 µL with 1X Permeabilization Buffer. Blocked with 2% normal mouse/rat serum by adding 2 µL directly to the cells. Incubated for 15 minutes at room temperature. Without washing, added the recommended amount of directly conjugated antibody for detection of intracellular antigen(s) to cells and incubated for at least 30 minutes at room temperature. Protected from light. Added 200 µL of 1X Permeabilization Buffer to each well and centrifuged samples at 400-600 x g for 5 minutes at room temperature. Discarded

the supernatant. Again, without washing, added the recommended amount of directly conjugated antibody for detection of intracellular antigen(s) to cells and incubated for at least 30 minutes at room temperature. Protected from light. Resuspended stained cells in an appropriate volume of Flow Cytometry Staining Buffer. Analysed by flow cytometer.

2.2.16.3 BMDC and BMDM Purity Assay:

This method was used to determine the differentiation of bone marrow derived cells into dendritic cells (BMDC) or macrophage (BMDM). Cells were seeded onto a 6 well plates were scraped and added to 15 mL conical centrifuge tube. 2 mL of filtered FCS added and left at room temperature for 15 minutes to block non-specific binding. Cells were centrifuged at 2000 rpm for 5 minutes at 4°C. Cells were resuspended in 1 mL of FACS buffer (containing 2 mL FCS, 0.05g NaN_3, 100 mL PBS, 200µL EDTA 0.5M). 200µL of this cell suspension was added to appropriate well of a 96 well round bottom plate, as per plate plan for treatment for each antibody. Plate was centrifuged at 2000rpm at 4°C for 5 minutes. Supernatant was aspirated, and cells resuspended in 100µL of 1:1000 dilutions of respective antibodies and incubated for 30 minutes at 4°C. Spun at 2000rpm at 4°C for 5 minutes. Cells were washed 3 times in FACS buffer by resuspension in 200µL of FACs buffer and repeat centrifugation. Cells were transferred to FACS loading tubes containing 400µL of FACs buffer, for total volume 500µL. Cells were analysed using BD FACSAria 1 system flow cytometer. Raw FCS files were analysed, and data was graphed using V10.0 FlowJo software.

2.2.16.4 Phagocytosis Assay:

This assay was used to determine the amount of phagocytosis carried out by the cells. J774A.1 macrophages were seeded at $1x10^6$ cells/ mL in 6 well plates and incubated overnight at 37°C in a humidified, 5% CO_2 atmosphere. Cells were stimulated with sample for 1 hour with sample and left incubated under the same conditions. Subsequently cells were stimulated with 100ng/ mL LPS and LOX at different exposure times. Cells were subsequently incubated with 1µm fluorescent

latex beads at a concentration of 20 beads per cell, for 1 hour at 37°C in a humidified, 5% CO_2 atmosphere. Cells were then scrapped from the cell culture plate and pelleted via centrifugation at 4°C at 2000RPM for 5minutes. Cells were resuspended and washed twice in 1 mL FACs buffer via centrifugation at 4°C at 2000RPM for 5minutes. Cells were resuspended in 200 µL of FACs buffer and added to FACs tubes. The uptake of beads was measured by flow cytometry on a FACSAria™ flow cytometer. Data was analysed using FlowJo software (Treestar).

Data was represented as the Mean Phagocytosis Index (MPI). This is a representation to encapsulate the mean fluorescence (MFI) from the phagocytosed beads as well as the percentage of phagocytosing cells in the viable population of cells and comparing to the control, which represents baseline phagocytosis. The MPI is calculated as follows:

$$MPI = \frac{\%\ phagocytes\ x\ MFI}{control\ phagocytes\ x\ control\ MFI}$$

2.2.16.5 4°C incubation for halting Phagocytosis:

A 4°C incubation was used to halt phagocytosis following a 55-minute incubation at 37°C with phagocytic beads. J774A.1 macrophages were seeded at $1x10^6$ cells/ mL in 6 well plates and incubated overnight at 37°C in a humidified atmosphere with 5% CO_2. Cells were stimulated with 100 ng/ mL LPS and 0.5mM LOX for 6 hours. Cells were subsequently incubated with 1 µm fluorescent latex beads at a concentration of 20 beads per cell, for 55 minutes at 37°C in a humidified atmosphere with5% CO_2. Cells then were either left to continue incubation at 37°C in incubator or at 4°C for 5 minutes in fridge to stop phagocytosis. Cells were then scrapped from the cell culture plate and pelleted via centrifugation at 4°C at 2000 RPM for 5minutes. Cells were resuspended and washed twice in 1 mL FACS buffer via centrifugation at 4°C at 2000 RPM for 5minutes. Cells were resuspended in 200 µL of FACs buffer and added to FACs tubes. The uptake of beads was measured by flow cytometry on a FACSAria™ flow cytometer. Data were analysed using FlowJo software (Treestar).

2.2.17 Migration assay:

JURKAT cells were centrifuged at 1500 rpm for 5 minutes at room temperature. The cells were then resuspended in RPMI medium alone. After counting, the cells were washed once with RPMI and subsequently resuspended in 0.2 µm filtered 0.5% BSA/RPMI-1640 at the required concentration for the assay, which is 1 x 10^6 cells/mL.. Cells were serum-starved by incubating for 1 hour at 37°C in 0.5% BSA/RPMI-1640 to deplete them of chemokines and cytokines. This was followed by stimulation with fermentate samples for an additional hour at the same temperature. Subsequently, 30 µL of chemotaxis medium containing various concentrations of the chemoattractant SDF-1 was added to the lower wells of a transwell plate, with the chemokine diluted in 0.5% BSA/RPMI-1640. The filter was then placed back on top of the 96-well plate, and 25 µL of cells were added to the top of the filters. The lid was replaced over the 96-well transwell plate, and the assembly was incubated for 2 hours at 37°C.The cells were removed from the top of the filters and discard. The filter was removed, and the migrated cells were recovered from the wells. The migrated cells were added to standard 96-well plates where an additional 70 µL RPMI/0.5% BSA was added. The percentage of migrated cells was determined by placing 25 µL of total cells from the assay directly into the standard 96-well plates and treating as above. 100 µL of 8% paraformaldehyde containing 2 µg/ mL Hoechst 33258 made up in RPMI-1640, was added to each well and the plate was incubated overnight at 4°C. The cells were imaged using a fluorescent-based imager e.g. Images were captured using a Nikon TiE microscope and analysed with Mipar V4.4.00 (1) software. This software facilitated batch processing and counting of fluorescent cells based on DAPI fluorescence.

2.2.18 Immune synapse assay:

8 well chamber slides were coated with poly-lysine and incubated overnight in the at 4°C. JURKAT cells were spun down at 1500 rpm for 5 minutes at room temperature. Cells were resuspended in RPMI only. Cells were counted the cells

and washed once in RPMI to then be resuspended in 0.2um filtered 0.5% BSA/RPMI-1640 at the required concentration for the assay 5 x 10^5 cells/ mL. Cells were serum starved via incubation for 1 hour at 37°C to deplete the cells of chemokines and cytokines in 0.5% BSA/RPMI-1640, before stimulating with fermentate samples and incubated for a further 1 hour at 37°C. The poly-lysine was removed and 200 µL of cells were added to the appropriate wells and incubated for 30 minutes at 37°C. Dynabeads were washed in PBS and negatively selected for using a magnet. The beads were reconstituted for a ratio of 1 bead to every 1 cell. The Dynabeads were added to the cells in the chamber and incubated for either 0, 15, 30 minutes, or 1 hour or 4 hours. Equal volumes of warm 8% PFA solution was added for 15min at 37°C. PFA/media was removed and a 1/500 dilution of phalloidin-TRITC (labels F-actin) and 1/1000 dilution of Hoechst 33258 (labels nucleus) in 3% BSA/PBS for 30 minutes at room temperature was added to the chambers. Chambers were washed twice in PBS and imaged under TRITC microscopy filter. The cells were imaged using a fluorescent-based imager e.g. Nikon TiE microscope. Images captured were analysed using software ImageJ and counted the fluorescent cells based on DAPI, and TRITC fluorescence. Data is represented as percentage immune synapse interaction.

2.2.19 Cell Lysate Preparation:

To prepare the cell lysates, 6-well plates were coated overnight with anti-mouse IgG using 1 mL of IgG solution per well, prepared in PBS. Plates were incubated overnight at 4°C covered with parafilm. IgG was removed and the wells were washed once with sterile PBS before being coated with CD3/CD28 made up in PBS for 1 hour at 37°C. JURKAT cells were centrifuged at 1500rpm for 5minutes at 18 °C and counted for a concentration of 5x10^5 cells/ mL. Plates were washed with PBS once before seeding 5 mLs of cells for 0, 30 minutes, 4 hours. Fermentate sample was added at appropriate time point. Cell supernatant was removed and centrifuged at 1500rpm for 5minutes at 18°C. Plate bound cells had 1 mL of lysis buffer added (with PI cocktail and SoV added fresh on day to the lysis buffer). The

cell pellet was collected and resuspended in the cell lysis buffer and all cells were harvested in microcentrifuge 's. These cell lysates were incubated on ice for 30 minutes, vertexing every 5 minutes. The cell lysates were centrifuged at 10,000 rpm for 5 minutes at 4°C and the supernatants were collected in fresh microcentrifuge tubes. Procedure for quantifying protein was carried out on each sample. Procedure for SDS-PAGE and Western blot was carried out on the cell lysates to analyse samples effect on Total and Phospho ERK1/2 protein.

2.2.20 BCA Protein Quantification Assay:

Used to determine the concentration of protein present in cell lysates. Bovine Serum Albumin (BSA) diluted standards were prepared ranging in concentration from 2000µg/ mL to 0 µg/ mL using appropriate diluent. BCA working reagent prepared at ratio 50 parts Reagent A to 1 part Reagent B. 25 µL of each known standard or unknown sample added to 96 well plate as per plate plan, carried out in duplicate. 200 µL of the prepared working reagent added to each well. The plate was thoroughly mixed on a plate shaker for 30 seconds, then covered and incubated for 30 minutes at 37°C.Plate is cooled for 5 minutes at room temperature and absorbance read at 562 nm on VersamaxTM microplate reader.

2.2.21 Western Blot Sample Lysate Preparation:

Depending on the desired protein concentration for SDS-PAGE, a specific volume of lysates was mixed with 5 µL of a combination of 4x sample buffer and 10x DTT. The samples were then adjusted with distilled water to achieve a final volume of 20 µL for addition to each well. Samples were boiled for 5 mins at 100°C with a pierced hole in top of pipette. Samples were then ready to be added to the wells.

2.2.22 SDS-PAGE Procedure:

The electrophoresis plates were cleaned with ethanol and the rubber gaskets attached to notched plates and fastened with the green clips to each side. Combs were added between the plates and the glass was marked 1 cm down from the bottom of the comb, before removing and preparing 10 % acrylamide resolving gel. The resolving gel solution was mixed and quickly poured between the glass plates up to the 1 cm mark. 1 mL of isobutanol was added to the top of the gel to block out oxygen, to allow the gel to set for approximately 40 minutes at room temperature. After this the isobutanol was removed and the top of the gel wash washed with dH_20, removing any excess water with paper towel. The stacking gel was the prepared, mixed, and quickly added to the top of the resolving gel until the solution reached the top of the plate. The combs were added and stacking gel was left to set for approximately 40 minutes at room temperature. The following day the green clips and rubber gaskets were removed, and the glass plates placed into the electrophoresis rig and fastened with the clear plastic holders. The 1X SDS-PAGE running buffer was prepared and poured into the electrophoresis rig and between the glass plates in the centre of the electrophoresis rig. The combs were removed carefully, and wells were straightened with a gel-loading tip before washing each well by pipetting up and down. The protein samples were loaded (approx 20 µL) and molecular weight markers (approx 5 µL) into the wells. The leads were attached, and the gel was run at 250V and 50 mAmps for approximately 1.5hours.

2.2.23 Western Blot:

Four sets of filter paper were cut (10 sheets in each set) and 2 pieces of PVDF membrane. The PVDF membrane was activated by soaking in methanol for 30 seconds and then placed it in Western blot transfer buffer. When the SDS-PAGE gel completed its run, the plates were prised apart, stacking gel was removed with a scalpel and discarded. On the Atto Western blot transfer system, one set of filter papers were soaked in Western blot transfer buffer and placed on the bottom of the

rig. The activated PVDF membrane was placed on top of the filter papers and more Western blot transfer buffer added on top. The SDS-PAGE gel was immersed it in Western blot transfer buffer briefly and placed on top of the PVDF membrane. The additional 1 set of filter papers was added to the top of this stack, having previously been soaked in Western blot transfer buffer. Excess transfer buffer on the bottom of the rig was removed with paper towel. The top piece of the transfer system was lowered onto the stack, the leads connected and ran at 100 V and 100 mAmp per gel stack for 1 hour. After the hour the filter papers on top of gel stack were removed along with the SDS-PAGE gel and discarded. The molecular weight marker lane was cut off with a scalpel and incubated with Coomassie stain solution overnight, and de-stained with Coomassie de-staining solution the following day to show up the molecular weight ladder. Any relevant lanes on the PVDF membrane were marked with a pencil and incubated with Western blot blocking buffer for 1 hour at room temperature on a shaker. The PVDF membrane was washed three times with Western blot wash buffer (5 minutes washes) at room temperature. The PVDF membrane was incubated with primary antibody (diluted according to manufacturer's instructions in appropriate buffer i.e. 1:1000 in 5% BSA in TBS-T for Phospho-ERK 1/2, and Total Phospho-ERK 1/2) overnight at 4 degrees with gentle agitation. The following day the PVDF membrane was three times with Western blot wash buffer (5 minutes washes) at room temperature. The PVDF membrane was incubated with HRP-labelled secondary antibody (diluted according to manufacturer's instructions i.e. 1:5000 in Western blot blocking buffer) for 1 hour at room temperature with gentle agitation. The PVDF membrane was washed three times with Western blot wash buffer (5 minutes washes) at room temperature. The fresh HRP development solution was prepared. The PVDF membranes were placed on cling film, and the HRP development solution was added and incubated for 60 seconds. The solution was drained off, and the PVDF membranes transferred to fresh cling film, and covered with clingfilm. Using the G-box and Genesys software the blots were placed inside the machine and the image of the blots was captured for 1 minute capture time. ImageJ was used for image analysis to calculate intensity of the ERK1/2 bands.

2.2.24 Statistical analysis:

Statistical analysis was carried out using a one-way ANOVA to compare variance among the means of different sample groups. A Newman-Keuls post-test was used to determine significance among the samples. Newman-Keuls post-test was used due to the increased power useful for the analysis of a large panel of screening samples. The level of statistical significance was indicated by * ($p<0.05$), ** ($p<0.01$) and *** ($p<0.001$).

2.2.25 Ethical Statement:

The care, treatment, and experiments involved in this study were approved by the Research Ethics Committee (REC) of Dublin City University (Approval ID: DCUREC/2011/008, and DCUREC/2023/187).

3 Chapter 3

Phase 1 Fermentate Screening

3.1 Introduction

Within the Food for Health Ireland (FHI) programme, 46 fermentate samples were generated by the Technology Team and then sent to us for assessment of their potential as bioactive candidate samples for future commercial development. A number of different research teams, within FHI analysed a variety of bioactivities of the fermentate samples in this large collaborative multidisciplinary project. These teams included; Dublin City University (DCU) investigating sample potential as immune boosting samples for the enhancement of viral immunity; University College Dublin (UCD), investigating sample potential as anti-inflammatory samples for aiding in management of chronic inflammation, and Teagasc, investigating sample effects on the microbiome and gut barrier integrity for enhanced gut comfort. The samples, generated at Teagasc or outsourced from different companies, were supplied to each of the teams at the same time over the course of a year for assessment of bioactivity. Due to the large screening required for these 46 samples , a literature review was carried out to identify LAB strains which have been documented as immune boosting or anti-inflammatory fermentates to date, for the identification of candidate fermentates to bring forward for initial testing to narrow down the selection process for a more targeted experimental investigation. Priority was given to the samples of interest outlined by the literature review initially as samples were provided in bulk, however as the project continued smaller batches of samples were received and thus were assessed based on production rate.

Table 19 below is a list of fermentate samples made for assessment by the FHI and Teagasc teams for investigation for their potential anti-viral properties and/or anti-inflammatory properties chosen based on an initial literature review of current scientific research into LAB strains and their immunomodulatory properties.

*Table 19:**FHI list of fermentate sample strains and sample names.** List of fermentate samples made and named by FHI and generated/acquired by Teagasc with their corresponding bacterium strain and respective control samples. Green highlight denotes strains of interest observed through initial literature review.*

Strain	Sample Name
L. lactis	SC15
L. lactis	SC17
L. lactis	SC18
Lb. delbrueckii subsp. bulgaricus	SC40
Lb. acidophilus	SC63
Lb. paraplantarum	SC72
Lb. helveticus	SC6
L. lactis	SC16
Lb. helveticus	SC46
L. lactis	SC51
L. lactis	SC52
S. thermophilus	DPC1178
S. thermophilus	DPC1817
Lb. paraplantarum	SC71
S. thermophilus	DPC1168
S. thermophilus	DPC1798
S. thermophilus	DPC1836
S. thermophilus	SC46
L. lactis ssp. cremoris	SL69
L. lactis	SL119
Lb. helveticus	LH13
Lb. helveticus	LH45
S. thermophilus	ST765

Strain	Sample Name
S. thermophilus	ST906
L. lactis	SC15 Dialysed
L. lactis	SC17 Dialysed
Lb. delbrueckii	SC40 Dialysed
Lb. acidophilus	SC63 Dialysed
Lb. delbrueckii	SC40 Infogest
Lb. acidophilus	SC63 Infogest
Lb. paraplantarum	SC72 Infogest
Lb. helveticus	R0389
Lb. rhamnosus	HA114
S. thermophilus	HA110
Lb. paracasei	HA196
Lb. fermentum	HA179
B.breve	R0070 (Aerobic fermentation)
Lb. paracasei	HA274
L. lactis	R1058
Lactobacillus helveticus	R0419
B. infantis	R0033 (Aerobic fermentation)
Lb helveticus	R0033 (Anaerobic fermentation)
Lb helveticus	R0033 (Aerobic fermentation)
B. breve	R0070 (Anaerobic fermentation)
B. breve	R0070 (Aerobic fermentation)

As identified in the literature the following LAB strains were of interest to us in DCU, due to the capabilities of such LAB strains to aid in antiviral and immune boosting properties associated with increased viral immunity, *Lactococcus lactis (L. lactis*), and *Bifidobacterium breve* (*B. breve*). So initially, these strains of LAB used to generate our novel fermentates were targeted, however, as the rate of receiving fermentates slowed down, the screening process was then carried out in order of when samples were received.

3.2 Chapter Aims

The purpose of this chapter was to investigate the panel of 46 fermentates for their potential as viral immune boosting immunomodulators. Samples were assessed in dendritic cells using the cell line JAWS, followed by primary BMDCs, using the TLR agonist LOX to mimic the exposure to a virus. This was to provide insight into the potential of these fermentates to act as functional food ingredients which can boost the immune system in response to viral immune activation, compared to the raw starting material (RSM). The RSM is the starting material from which the fermentates are derived from. Thus, in order to establish bioactivity from the fermentates, analysis was carried out comparing each fermentate to RSM, to establish further beneficial bioactivity over and above that attributed to the RSM. The main goal was to assess the effect of each sample on cytokine secretion from DCs , when challenged with a viral ligand, LOX, mimicking an immune response similar to that elicited during a viral infection (Figure 11).

The specific objectives include:

- Establishment of a model for the assessment of fermentate effects in immune cells.
- Assessment of fermentates in JAWS cells to confirm sample bioactivity.
- Assessment of fermentates in JAWS cells to optimise sample pre-treatment and dose response of fermentates from a range of 5mg/ mL – 50mg/ mL.
- Assessment of cytotoxicity of fermentates in both JAWS and BMDCs to ensure that samples were not negatively impacting on cell viability.
- Assessment of fermentates in LOX activated BMDCs at 2 doses of 10mg/ mL and 25mg/ mL of both raw unprocessed fermentate and filtered fermentate to study the fermentates ability to modulate cytokine secretion, and effect of filtration on this cytokine production.

- Assessment of 1 dose of 25mg/ mL of both raw and filtered fermentate to assess remaining sample cytokine secretion profiles in more high throughput manner.

Data was analysed following exposure of cells to LOX and fermentates, and potential viral immune boosting samples were highlighted for further investigation when compared against the RSM.

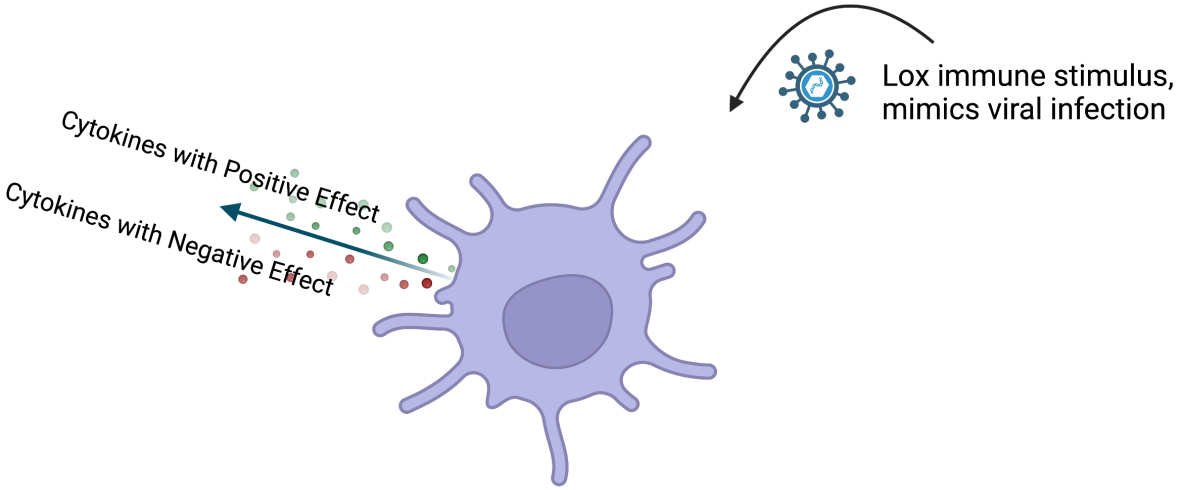

*Figure 11:**Summary of Chapter 3 Aims.** Assessing effect of sample presence on cytokine secretion profiles in dendritic cells activated with viral immune stimulus LOX.*

3.3 Results:

The aim of this screening chapter was to establish a model for the assessment of fermentate effects in immune cells. The establishment of an appropriate model for fermentate assessment was critical at this point to provide a solid basis for all further screening that was carried out in subsequent chapters. Prior to investigation of the fermentate effects on immune cells, it was important to optimise the model to be used for viability, and cytokine assessment in the two dendritic cell models that were used throughout the project. Therefore an initial project optimisation was carried out. Once the concentrations of TLR were confirmed for optimal cell viability and cytokine secretion, the assessment of sample effect on dendritic cells began. An initial pilot study was carried out in JAWS cells, as these cells are easy to use, a good measure of how dendritic cells behave *in vivo*, allow for high throughput analysis, and were cost effective. From there, and based on pilot study findings, assessment was expanded in the high throughput screening phase in the primary cells BMDCs, as these are an even better model of how the fermentates behaved *in vivo*, as well as being easy to use, and highly recognised in the field of immunology.

3.3.1 Establishing a dendritic cell model for assessment of fermentate effect on dendritic cell function

3.3.1.1 Project Optimisation:

Prior to screening of fermentates, it was important to optimise concentrations of TLRs that were used in the assessment of immunological function, in response to cells being challenged with different immune stimuli. This project optimisation allowed us to develop an appropriate model for the use of TLRs in initially JAWS cells, and then BMDCs, to allow for subsequent assessment of fermentate affect. Previous work in our group had already established the optimal dose of various

TLRs required to elicit appropriate immune responses in both JAWS and BMDCs. Therefore we aimed to confirm this concentration for CpG, PIC, and LOX, using a dose range of each TLR, prior to the screening of the fermentates. Based on extensive use of LPS in the laboratory the concentration of LPS used to elicit an immune response was known and didn't require revalidation. Importantly LOX activates TLR7/8, PIC activates TLR3, LPS activates TLR4, and CpG activates TLR9.

3.3.1.1.1 JAWS dendritic cell model

The dendritic cell line JAWS was chosen as a model to represent dendritic cell function as it is a good representative of how such cells behave *in vivo* and are an easy cell line to work with. Optimisation was carried out to identify the optimal concentrations of each of the TLR ligands in the chosen cell line to elicit an optimum immune responses, without affecting the viability of the cells. An MTS assay was used to assess effect on cell viability and an ELISA to assess the effect of TLR ligand activation in JAWS cells on cytokine secretion.

3.3.1.1.1.1 Cell viability is affected by a dose response of TLRs

JAWS cells were seeded at a concentration of $1x10^6$ cells/ mL, incubated for 24 hours before adding respective concentrations of TLR ligands and subsequently incubated under the same conditions at 37^0C in 5% CO_2: CpG 1µM, 2 µM, 5 µM and 10 µM; PIC 500ng/ mL, 1µg/ mL, 10µg/ mL and 15µg/ mL ; and LOX 0.5mM, 1mM, 2mM and 5mM. After 24 hours an MTS assay was performed as previously outlined (section 2.2.13 MTS Cell Viability Assay),

Figure 12 demonstrates that at varying concentrations of each TLR ligand, JAWS cell viability may become negatively affected. The positive control 10% DMSO induced cell death and thus provided a clear distinction of the cytotoxic effects on cell viability compared with the negative control of the untreated control sample. Similarly the graduated DMSO concentrations acted as a vehicle control for the LOX TLR ligand due to its composition in 100% DMSO. Cell viability is largely unaffected by varied concentrations of CpG and PIC. Optimal cell viability was present at higher CpG concentrations of 5 µM and 10µM, while PIC is optimal at lower concentrations of 500ng/ mL and 1µg/ mL. LOX and its vehicle control of DMSO showed that cell

viability was optimal at a lower concentration of 0.5mM, while increasing concentrations negatively affected cell viability.

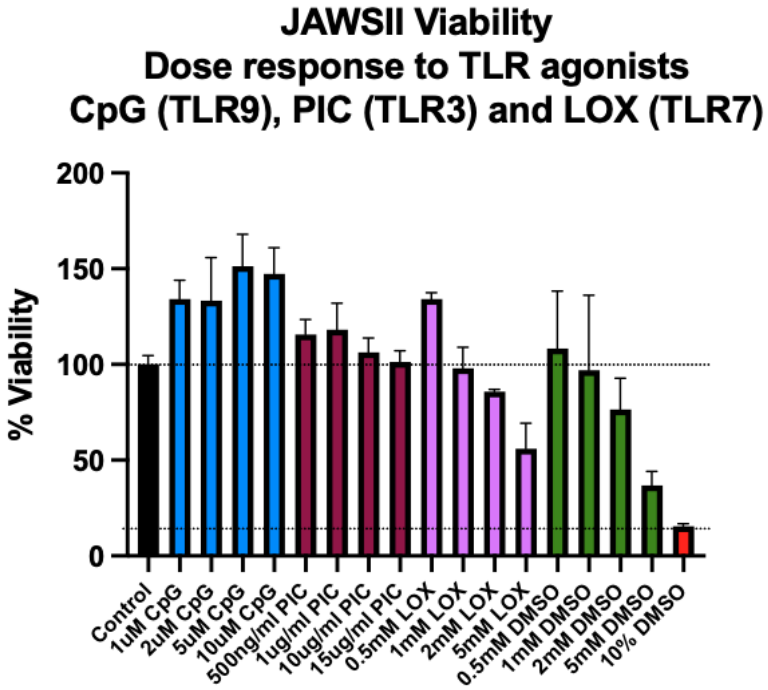

Figure 12: ***Exposure of JAWS to different concentrations of TLR ligands affects cell viability.*** *JAWS cells were seeded at 1x10⁶ cells/ mL and exposed to Toll ligands at the following concentrations: CpG 1µM, 2 µM, 5 µM and 10 µM, PIC 500ng/ mL, 1µg/ mL, 10µg/ mL and 15ng/ mL, LOX 0.5mM, 1mM, 2mM and 5mM. A vehicle control of DMSO was included at 0.5mM, 1mM, 2mM and 5mM in conjunction with LOX, while 10% DMSO was included as a positive control to induce cell death. Cells were incubated with MTS cell titre aqueous one solution for 3 hours at 37⁰C in 5% CO_2. Viability is represented as a percentage compared to viable, untreated cells (Control). Data is presented as mean ± SD of three replicates.*

3.3.1.1.1.2 Cytokine profile is affected by a dose response of TLRs

JAWS cells were seeded at a concentration of $1x10^6$ cells/ mL, incubated for 24 hours before adding respective concentrations of TLR ligands and subsequently incubated under the same conditions at 37⁰C in 5% CO_2: CpG 1µM, 2 µM, 5 µM and 10 µM; PIC 500ng/ mL, 1µg/ mL, 10µg/ mL and 15µg/ mL; and LOX 0.5mM, 1mM, 2mM and 5mM. After 24 hours supernatants removed and ELISA preformed for cytokines IL-1β, IL-6, IL-10 and TNF-α according to the manufacturer's instructions (section 2.2.14 Enzyme Linked Immunosorbent Assay (ELISA)).

Figure 13 demonstrates that JAWS cells secreted varying levels of IL-1β, IL-6, IL-10 and TNF-α compared to untreated control cells when stimulated with the TLR ligands CpG, PIC and LOX. Cells stimulated with LOX 0.5mM, 1mM, 2mM secreted

IL-1β significantly (p<0.001), while CpG and PIC stimulated cells had nonsignificant levels, however higher concentrations of both CpG and PIC resulted in increased IL-1β secretion. This same profile is observed for TNF-α secretion. Cells stimulated with LOX 0.5mM and 1mM secreted IL-6 significantly (p<0.001), while 2mM LOX still promoted IL-6 secretion but to a lesser extent (p<0.002). Higher concentrations of CpG and PIC resulted in secretion of more IL-6, similar to what we observed with IL-1β and TNF-α. Secretion of IL-10 for cells stimulated with CpG, PIC and LOX remained similar to untreated control cells. The vehicle control of DMSO for LOX does not promote cytokine secretion from the cells.

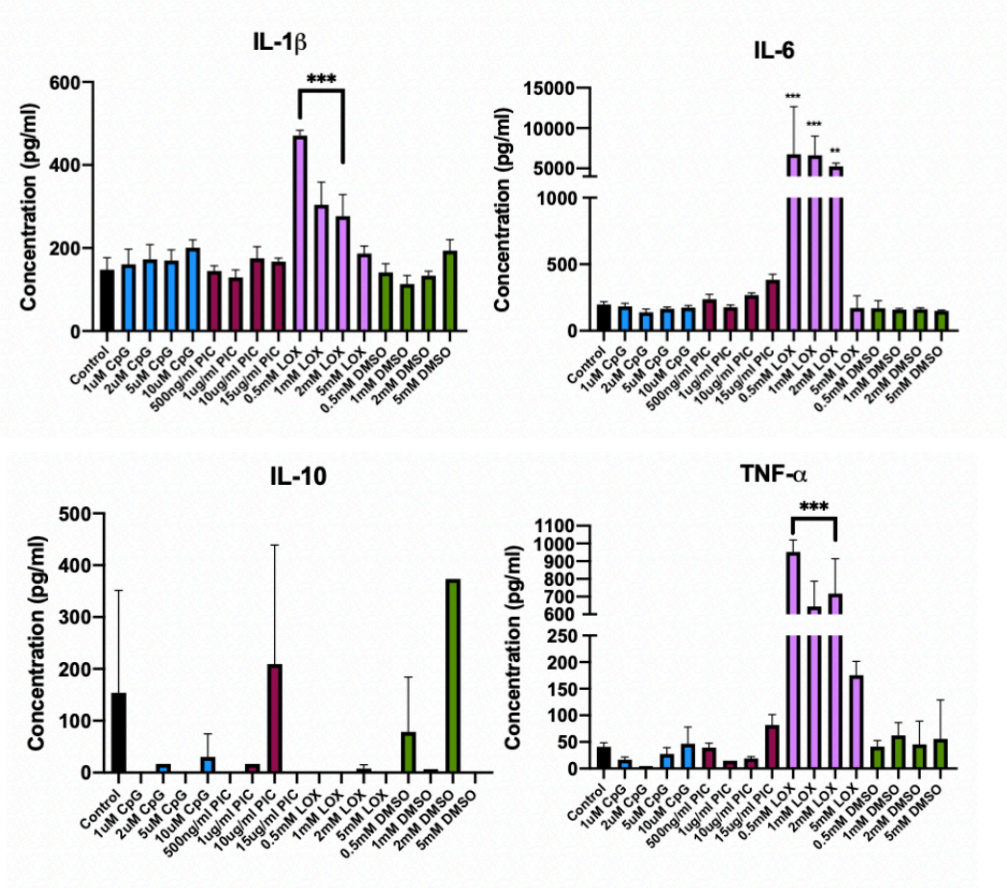

Figure 13: ***Exposure of JAWS to different concentrations of TLR ligands results in the secretion of cytokines****. JAWS cells were seeded at 1x10⁵ cells/ mL and exposed to Toll ligands at the following concentrations: CpG 1μM, 2 μM, 5 μM and 10 μM, PIC 500ng/ mL, 1μg/ mL, 10μg/ mL and 15ng/ mL, LOX 0.5mM, 1mM, 2mM and 5mM. A vehicle control of DMSO was included at 0.5mM, 1mM, 2mM and 5mM in conjunction with LOX. Supernatants were removed after 24 hours and ELISA was performed for cytokines IL-1β, IL-6, IL-10 and TNF-α. Data is presented as mean ± SD of three replicates. Significance determined using one- way ANOVA with a Newman-Keuls post-test. Output P value style APA: .12 (ns), .033 (*), .002(**) and <.001 (***) comparing unstimulated control cells to TLR stimulated cells.*

Thus we were able to establish optimal concentrations for TLRs CpG 5 µM, PIC 10µg/ mL and LOX 0.5mM, were required to elicit an appropriate immune response while not hindering cell viability in the JAWS cell line. From here we then were able to expand our optimisation of TLRs to examine their effects in the BMDC cell.

Here we examined our previously highlighted optimal TLR doses for CpG, PIC, and LOX from our JAWS investigation, as well as including LPS at a known bioactive concentration, of 100ng/ mL, frequently used within the lab, for confirmation of their effects in BMDCs.

3.3.1.1.2 BMDC dendritic cell model

Due to the limitations of the JAWS cell line in its limited ability to secrete certain cytokines, primary dendritic cells, BMDC, were chosen as a model to represent dendritic cell function as it is a better representative of how such cells behave *in vivo*. Prior to the screening of sample fermentates, optimisation was carried out to confirm the optimal concentrations of each of the TLR ligands ensuring viability of the cells is not affected.

The optimal dose highlighted from our JAWS data was used to assess CpG 5 µM, PIC 10µg/ mL and LOX 0.5mM, in addition to a known LPS concentration of 100ng/ mL, to assess effect on cell viability via an MTS assay, and an ELISA to assess the effect of TLR ligand activation on cytokine secretion, in BMDC.

3.3.1.1.2.1 Cell viability is not affected by TLRs

BMDC were seeded at a concentration of $1x10^6$ cells/ mL, incubated for 24 hours before adding respective concentrations of TLR ligands and subsequently incubated under the same conditions at 37^0C in 5% CO_2: CpG 5 µM, PIC 10µg/ mL and LOX 0.5mM. After 24 hours an MTS assay was performed as previously outlined (section 2.2.13 MTS Cell Viability Assay).

Figure 14 demonstrates that there was no significant change in cell viability following exposure of the cells to any of the TLR ligands. The use of the positive control of 10% DMSO provided a clear distinction between the cytotoxic effects on cell viability with the untreated control sample, as DMSO induced cell death.

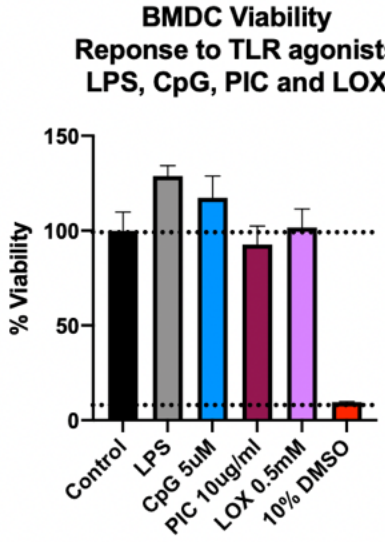

Figure 14: ***Exposure of BMDC to different TLR ligands doesn't affect cell viability.*** *BMDC cells were seeded at 1x10^6 cells/ mL and exposed to Toll ligands at the following concentrations: LPS 100ng/ mL, CpG 5 µM, PIC 10µg/ mL and LOX 0.5mM. 10% DMSO was included as a positive control to induce cell death. Cells were incubated with MTS cell titre aqueous one solution for 3 hours at 37^{0}C in 5% CO_2. Viability is represented as a percentage compared to viable, untreated cells (Control). Data is presented as mean ± SD of six replicates.*

3.3.1.1.2.2 Cytokine profile is affected by stimulation with a range of TLRs

BMDC were seeded at a concentration of 1x10^6 cells/ mL, incubated for 24 hours before adding respective concentrations of TLR ligands and subsequently incubated under the same conditions at 37^{0}C in 5% CO_2: CpG 5 µM, PIC 10µg/ mL and LOX 0.5mM. After 24 hours, supernatants were removed and ELISA performed for cytokines IL-1β, IL-6, IL-10, TNF-α, IL-12p40, IL-12p70, IL-23 and IL-27 according to the manufacturer's instructions (section 2.2.14 Enzyme Linked Immunosorbent Assay (ELISA).Figure 15 demonstrates that LOX was a significant inducer of IL-1β, IL-6, IL-10, TNF-α, IL-27 ($p<0.001$) and IL-12p40 ($p<0.033$), while IL-12p70 and IL-23 were non-significantly increased. CpG induced significant production of IL-6, IL-10, TNF-α, IL-12p70, IL-27 ($p<0.001$), IL-23 ($p<0.002$) and IL-12p40 ($p<0.033$), while only non-significantly increasing IL-1β production. LPS significantly promoted IL-10, TNF-α and IL-27 ($p<0.001$) secretion and IL-6 ($p<0.033$), and non-significantly

promoted the secretion of IL-12p40, IL-12p70 and IL-23. PIC non-significantly increased IL-6, TNF-α and IL-23.

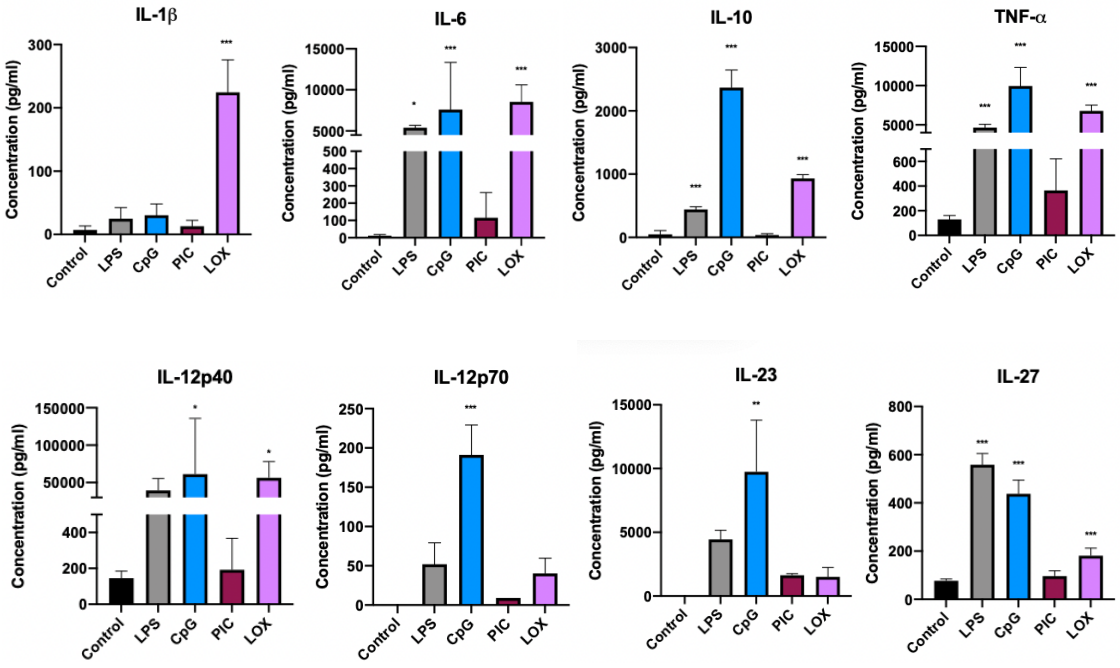

*Figure 15:**Exposure of BMDC to different TLR ligands results in the secretion of cytokines.** BMDC cells were seeded at 1x10^6 cells/ mL and exposed to Toll ligands at the following concentrations: LPS 100ng/ mL, CpG 5 μM, PIC 10μg/ mL and LOX 0.5mM. Supernatants were removed after 24 hours and ELISA was performed for cytokines IL-1β, IL-6, IL-10, TNF-α, IL-12p40, IL-12p70, IL-23, and IL-27. Data is presented as mean ± SD of three replicates. Significance determined using one- way ANOVA with a Newman-Keuls post-test. Output P value style APA: .12 (ns), .033 (*), .002(**) and <.001 (***) comparing unstimulated control cells to TLR stimulated cells.*

Therefore we were able to confirm these concentrations were the optimal concentrations of TLRs needed for maintenance of cell viability, and induction of immunological responses in both JAWS cells, and BMDC, and thus this knowledge formed the basis of all subsequent analysis. We could commence screening of the bank of fermentates based on this knowledge.

Having established a targeted experimental investigation strategy identifying sample strains of most interest, a screening phase for all 46 samples commenced. An appropriate model needed to be established to effectively assess all 46 samples in a timely manner to gather data on fermentates bioactivity as immune boosting samples. Based on our data gathered in our optimisation of TLRs and based on our previous lab knowledge, we used these parameters to assess the requirements for sample preparation needed to maintain optimal bioactivity, and to determine the optimal dose required to observe any effect on the immune response. The sample preparation parameters included assessing samples bioactivity when the sample was pretreated either by centrifugation, filtering, centrifugation and filtering, or be it in its raw unprocessed form. These forms of pretreatment were assessed based on previous lab work with other samples like the milk hydrolysates where filtering this sample was needed form optimal bioactivity. Initially this was carried out in JAWS cells via a pilot study, then expanding to BMDCs for our high throughput screening phase. For this pilot study and screening phase, cells were stimulated with LOX, to mimic the effects of viral infection on a cell as finding fermentates that could boost viral immunity was the main goal of the project at that time.

3.3.2 Round 1 screening of the bank of fermentate samples in viral immune activated LOX dendritic cells

3.3.2.1 Pilot Study:

In setting up a model for the assessment of fermentate effects on immune cells, it was critical to first establish that fermentates do not negatively impact on cell viability, inducing cell death. Once this was established the fermentates effect on bioactivity was examined knowing that the fermentates were not harmful to the immune cells, we were then able to establish whether they had an immunological

benefit to the cell. Thus initial screening always involved assessment of cell viability via MTS, followed by assessment of cytokine secretion via ELISA.

Based on previous research from our laboratory, we know that different forms of biological samples have varying optimal performance based on their form of processing prior to application to living cells. Thus, initially it was important to pre-treat the fermentate samples to establish which form of pre-treatment provided optimal bioactivity within cells of the immune system, primarily the dendritic cell. Fermentates were therefore prepared either as filtered, centrifuged, centrifuged and filtered, or left raw unprocessed, before being tested for their immunological effect in the form of cytokine secretion, on dendritic cells activated with LOX to mimic viral infection.

Initially all screening was carried out in JAWS cells in a pilot study in preparation for screening at a more high throughput rate in BMDCs. Fermentates were initially screened at a 10mg/mL based on previous lab knowledge of other samples having optimal bioactivity at this dose, in addition ensuring that sample stocks were preserved for further analysis.

3.3.2.1.1 JAWS screening

3.3.2.1.1.1 Pre-treatment of fermentates doesn't affect cell viability

JAWS were seeded at a concentration of $1x10^6$ cells/ mL, incubated for 24 hours before pre-treatment with 10mg/ mL either filtered, centrifuged, centrifuged and filtered or raw sample for 1 hour then stimulated with 0.5mM LOX TLR ligand and subsequently incubated at 37^0C in 5% CO_2. After 24 hours an MTS assay was performed as previously outlined (section 2.2.13 MTS Cell Viability Assay). Figure 16 demonstrates that there was no significant change in cell viability following exposure of the cells to LOX or any of the differently processed fermentates. The RSM acted as the whole fermentate control for comparison of effects induced by each independent sample. The use of the positive control of 10% DMSO provided a

clear distinction between the cytotoxic effects on cell viability with the untreated control sample, as DMSO induced cell death.

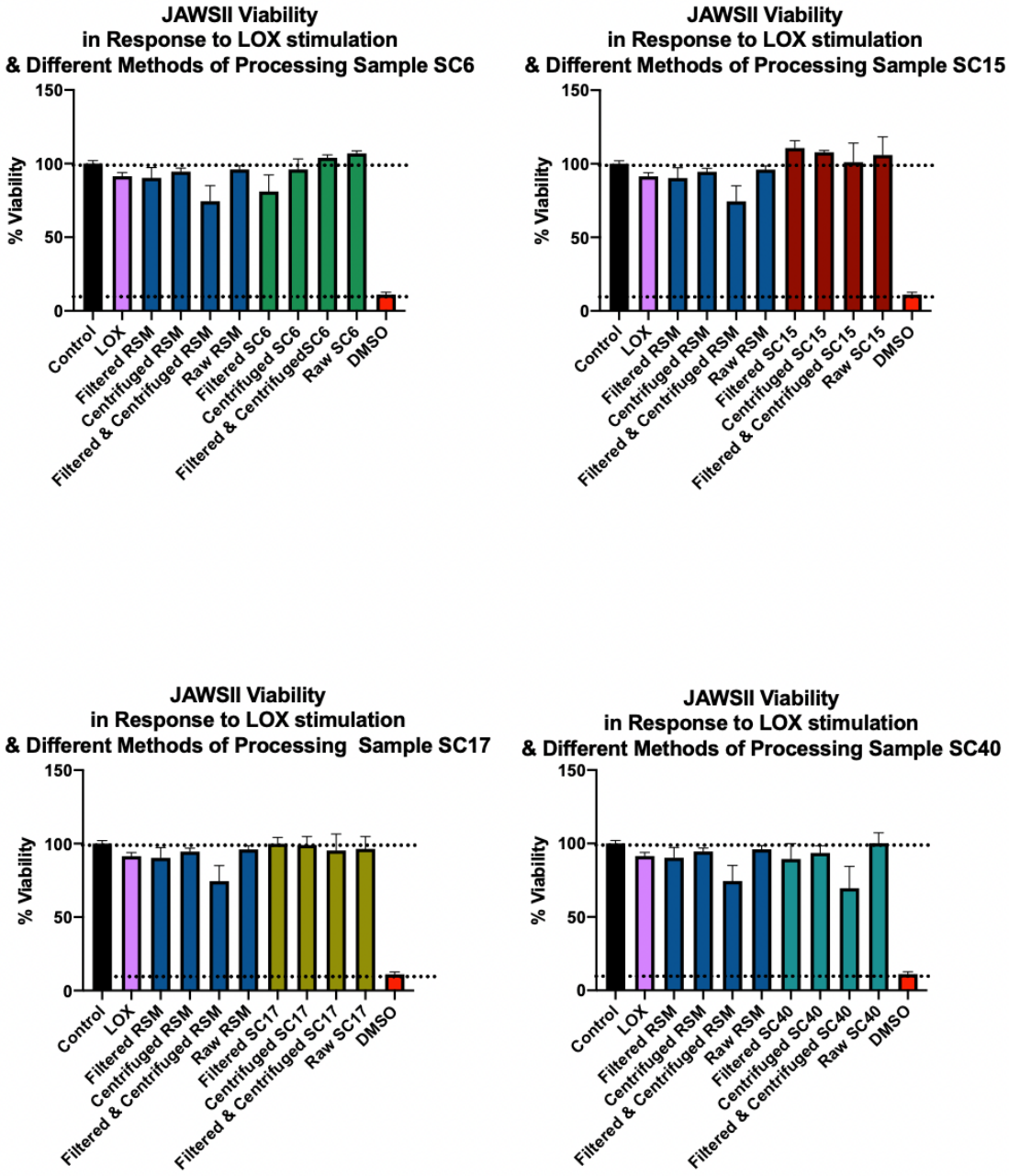

Figure 16: ***Exposure of JAWS to pre-treated fermentates SC6, SC15, SC17 and SC40 doesn't affect cell viability.*** *JAWS cells were seeded at 1x10⁶ cells/ mL and left overnight at 37°C in 5% CO_2. The following day cells were stimulated with 10mg/ mL appropriately processed fermentate, incubated for 1 hour at 37°C in 5% CO_2 and subsequently exposed to LOX 0.5mM for viral TLR activation before incubating overnight under the same conditions. RSM is the fermentate control. 10% DMSO was included as a positive control to induce cell death. Cells were incubated with MTS cell titre aqueous one solution for 3 hours at 37°C in 5% CO_2. Viability is represented as a percentage compared to viable, untreated cells (Control). Data is presented as mean ± SD of three replicates.*

3.3.2.1.1.2 Pre-treatment of fermentates effects cytokine secretion

JAWS cells were seeded at a concentration of $1x10^6$ cells/ mL, incubated for 24 hours before adding 10mg/ mL of differently processed fermentates, incubated for 1 hour at 37^0C in 5% CO_2 before exposure to 0.5mM LOX and subsequently incubated under the same conditions overnight. Sample processing includes sample being either filtered only, centrifuged only, both filtered and centrifuged or left raw unprocessed. After 24 hours supernatants were removed and ELISA procedure for cytokines IL-1β, IL-6, IL-10 and TNF-α were performed according to the manufacturer's instructions (section 2.2.14 Enzyme Linked Immunosorbent Assay (ELISA)).

Figure 17 and Figure 18 demonstrate that processing of samples, affected cytokine secretion in response to LOX, when compared to the RSM. LOX exposure increased the secretion of IL-1β, IL-6 and TNF-α versus unstimulated control cells. Processing of SC6 had little effect on cytokine secretion. Processing of SC15 resulted in the highest cytokine secretion when sample was left raw. SC17 resulted in a significant increase in IL-1β and IL-6 when filtered ($p<0.001$; $p<0.033$) and SC40 resulted in a significant increase in IL-1β when filtered, and when centrifuged ($p<0.033$). Interestingly the RSM secreted the highest concentrations of IL-1β and IL-6 when left raw, while when filtered and centrifuged had increased TNF-α.

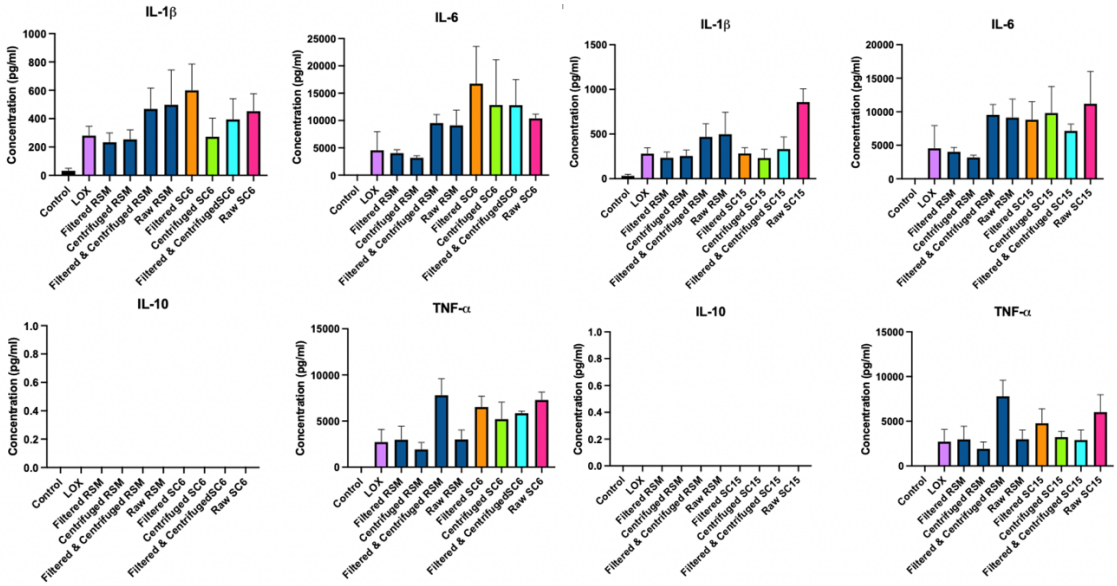

Figure 17: ***Exposure of JAWS to pre-treated fermentates SC6, and SC16 affects cytokine secretion.*** *JAWS cells were seeded at 1x10⁶ cells/ mL and left overnight at 37°C in 5% CO_2. The following day cells were stimulated with 10mg/ mL sample SC6 and SC15, incubated for 1 hour at 37°C in 5% CO_2 and subsequently exposed to LOX 0.5mM for viral TLR activation before incubating overnight under the same conditions. RSM is the fermentate control. Supernatants were removed after 24 hours and ELISA was performed for cytokines IL-1β, IL-6, IL-10 and TNF-α. Data is presented as mean ± SD of three replicates. Significance determined using one- way ANOVA with a Newman-Keuls post-test. Output P value style APA: .12 (ns), .033 (*), .002(**) and <.001 (***) comparing processed sample to processed RSM counterpart.*

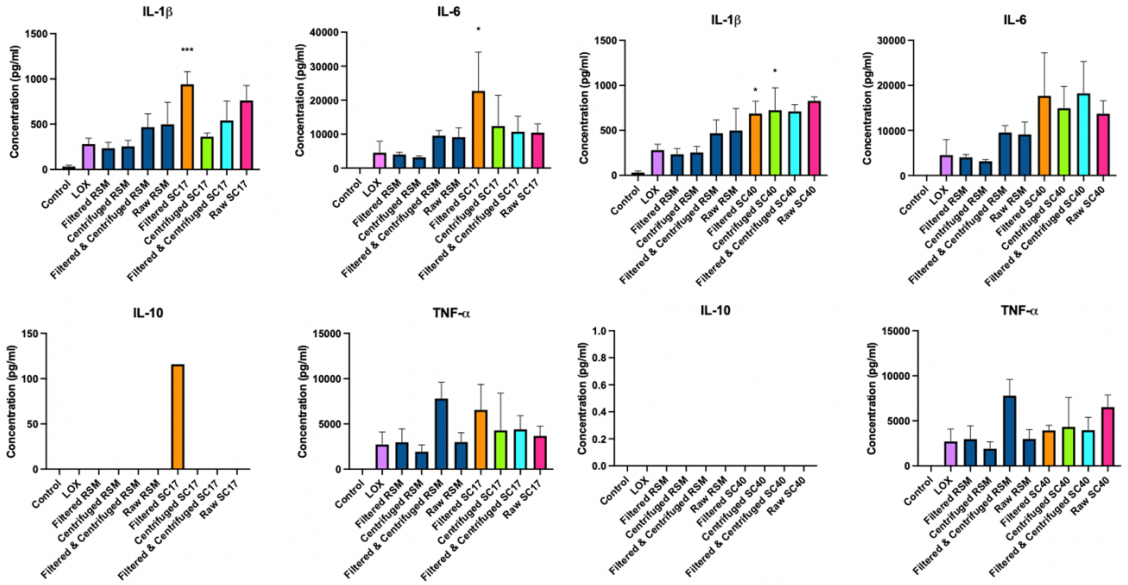

Figure 18: ***Exposure of JAWS to pre-treated fermentates SC17, and SC40 affects cytokine secretion.*** *JAWS cells were seeded at 1x10⁶ cells/ mL and left overnight at 37°C in 5% CO_2. The following day cells were stimulated with 10mg/ mL sample SC17 and SC40, incubated for 1 hour at 37°C in 5% CO_2 and subsequently exposed to LOX 0.5mM for viral TLR activation before incubating overnight under the same conditions. RSM is the fermentate control. Supernatants were removed after 24 hours and ELISA was performed for cytokines IL-1β, IL-6, IL-10 and TNF-α. Data is presented as mean ± SD of three replicates. Significance determined using one-way ANOVA with a Newman-Keuls post-test. Output P value style APA: .12 (ns), .033 (*), .002(**) and <.001 (***) comparing processed sample to processed RSM counterpart.*

We can therefore conclude that based on the RSM, and supported by the fermentate sample results that the raw unprocessed, and potentially the filtered version of the fermentate were optimal for cell viability and induction of sufficient cytokine secretion and subsequent immunological effect.

It was now important to establish the optimal concentration of fermentate sample required to exert the desired immunomodulatory effect in LOX activated dendritic cells. A dose range of 5mg/ mL, 10mg/ mL, 25mg/ mL, and 50mg/ mL was used to assess the effects of fermentate concentrations on JAWS cells. Filtered and raw pre-treatments were examined to provide contrast and confirm bioactivity. Importantly, based on previous research carried out in the lab where milk protein hydrolysates required filtering in order to confer bioactivity we included the filtered version of fermentates in addition to the raw sample to ensure no bioactivity was missed in the screening phase.

3.3.2.1.1.3 Dose range of fermentates does not affect cell viability

JAWS cells were seeded at a concentration of $1x10^6$ cells/ mL, incubated for 24 hours before stimulating with a dose range of 5mg/ mL, 10mg/ mL, 25mg/ mL and 50mg/ mL filtered and raw fermentate sample for 1 hour followed by 0.5mM LOX TLR ligand and subsequently incubated at 37^0C in 5% CO_2. After 24 hours an MTS assay was performed as previously outlined (section 2.2.13 MTS Cell Viability Assay).

Figure 19 and Figure 20 demonstrate that there was no significant change in cell viability following exposure of the cells to LOX or any dose response of raw or filtered fermentate samples SC6, SC15, SC17 and SC40. The RSM acted as the whole fermentate control for comparison of effects induced by each independent sample i.e., SC6, SC15, SC17 and SC40. The use of the positive control of 10% DMSO provided a clear distinction between the cytotoxic effects on cell viability with the untreated control sample, as DMSO induced cell death.

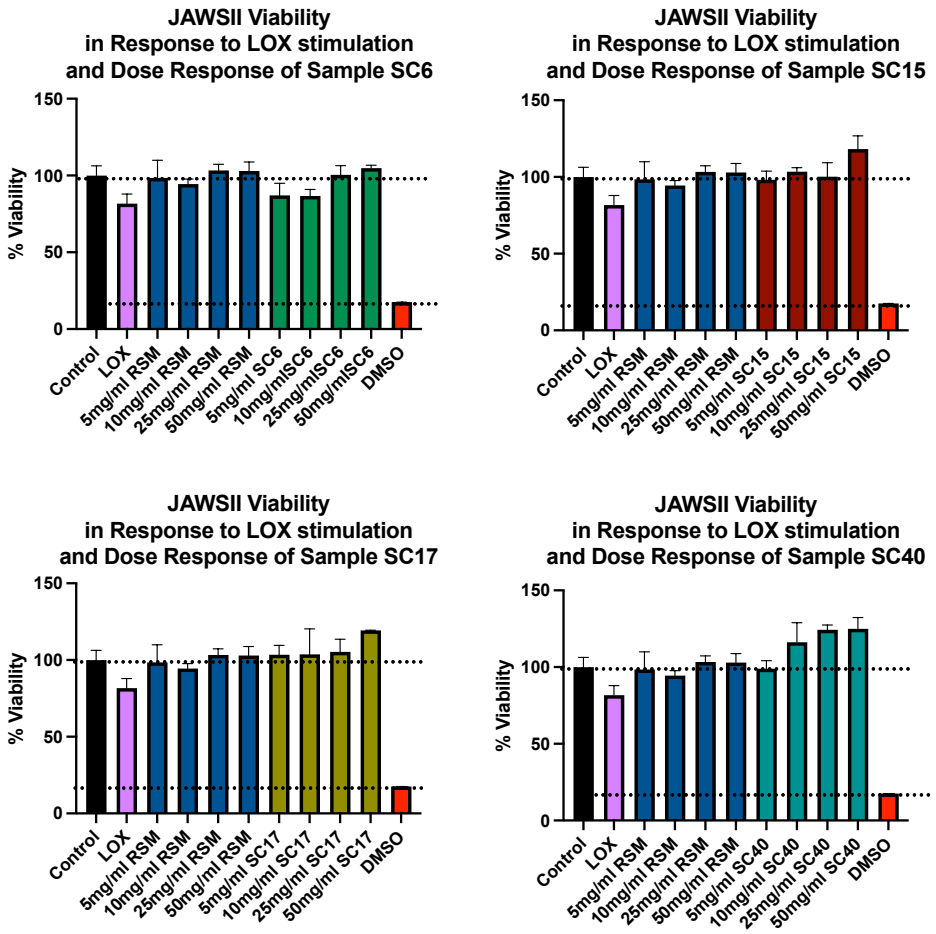

Figure 19: ***Exposure of JAWS to dose response of raw sample fermentates SC6, SC15, SC17 and SC40 doesn't affect cell viability****. JAWS cells were seeded at 1x10⁶ cells/ mL and left overnight at 37°C in 5% CO_2. The following day cells were stimulated with appropriate dose range of raw fermentate, incubated for 1 hour at 37°C in 5% CO_2 and subsequently exposed to LOX 0.5mM for viral TLR activation before incubating overnight under the same conditions. RSM is the fermentate control. 10% DMSO was included as a positive control to induce cell death. Cells were incubated with MTS cell titre aqueous one solution for 3 hours at 37°C in 5% CO_2. Viability is represented as a percentage compared to viable, untreated cells (Control). Data is presented as mean ± SD of three replicates.*

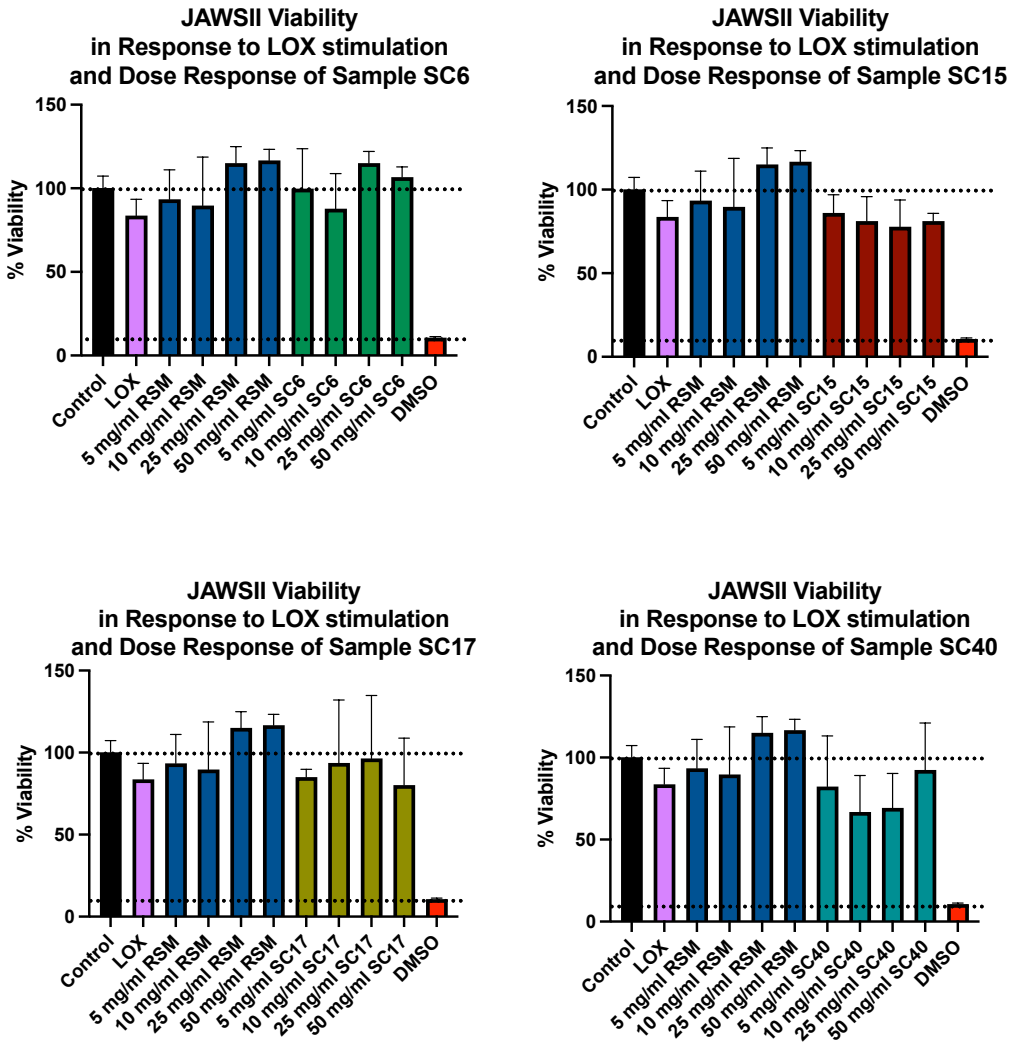

Figure 20: ***Exposure of JAWS to dose response of filtered sample fermentates SC6, SC15, SC17 and SC40 doesn't affect cell viability****. JAWS cells were seeded at 1x10⁵ cells/ mL and left overnight at 37°C in 5% CO_2. The following day cells were stimulated with appropriate dose range of filtered fermentate, incubated for 1 hour at 37°C in 5% CO_2 and subsequently exposed to LOX 0.5mM for viral TLR activation before incubating overnight under the same conditions. RSM is the fermentate control. 10% DMSO was included as a positive control to induce cell death. Cells were incubated with MTS cell titre aqueous one solution for 3 hours at 37°C in 5% CO_2. Viability is represented as a percentage compared to viable, untreated cells (Control). Data is presented as mean ± SD of three replicates.*

3.3.2.1.1.4 Dose range of raw fermentates affects cytokine secretion

JAWS cells were seeded at a concentration of $1x10^6$ cells/ mL, incubated for 24 hours before adding appropriate dose range of raw sample SC6, SC15, SC17, and SC40, incubated for 1 hour at 37^0C in 5% CO_2 before exposure to 0.5mM LOX and subsequently incubated under the same conditions overnight. Sample dose range included 5mg/ mL, 10mg/ mL, 25mg/ mL and 50mg/ mL of raw sample. After 24 hours supernatants were removed and ELISA procedure for cytokines IL-1β, IL-6, IL-10 and TNF-α were performed according to the manufacturer's instructions (section 2.2.14 Enzyme Linked Immunosorbent Assay (ELISA)).

Figure 21 and Figure 22 demonstrate that fermentate samples significantly affected the secretion of cytokines, in response to LOX, when compared to the RSM. LOX significantly increased the secretion of cytokines IL-1β ($p<0.033$) and non-significantly increased IL-6 and TNF-α. SC6 significantly increased IL-1β at concentrations of 5mg/ mL ($p<0.033$), 25mg/ mL and 50mg/ mL ($p<0.002$). SC15 significantly increased IL-1β at concentrations of 10mg/ mL ($p<0.033$), 25mg/ mL ($p<0.002$) and 50mg/ mL ($p<0.001$). SC17 significantly increased IL-1β at concentrations of 5mg/ mL ($p<0.002$), 25mg/ mL and 50mg/ mL ($p<0.001$). SC40 significantly increased IL-1β at concentrations of 10mg/ mL ($p<0.002$), 25mg/ mL and 50mg/ mL ($p<0.001$) and SC40 increased IL-6 at 10mg/ mL ($p<0.033$) and TNF-α at concentrations of 25mg/ mL and 50mg/ mL ($p<0.001$). Otherwise there was little difference between cytokine secretion of samples compared to the RSM.

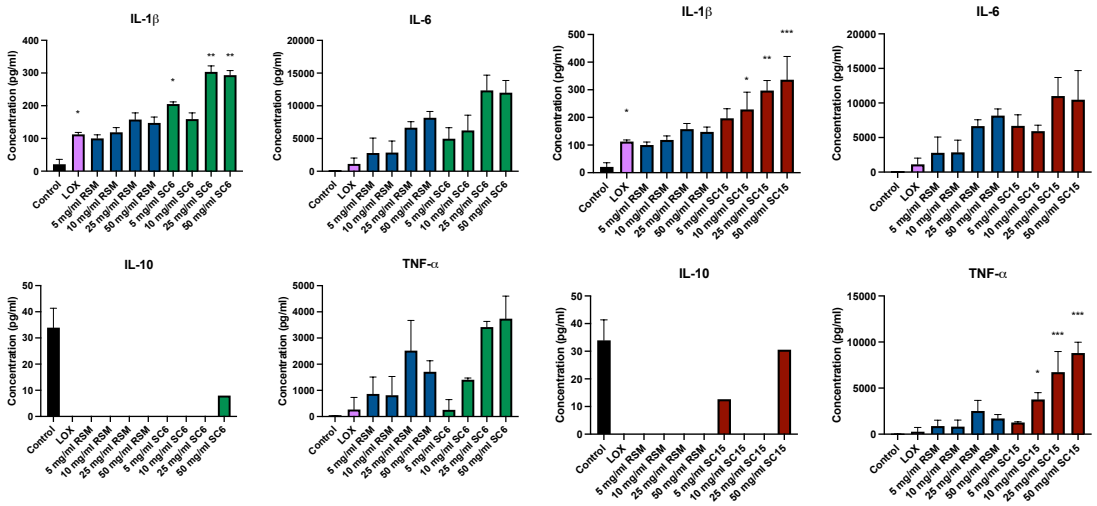

Figure 21: ***Exposure of JAWS to dose response of raw sample fermentate SC6 and SC15 affects cytokine secretion.*** *JAWS cells were seeded at 1x10⁶ cells/ mL and left overnight at 37°C in 5% CO_2. The following day cells were stimulated with dose range of 5mg/ mL, 10mg/ mL, 25mg/ mL and 50mg/ mL sample SC6, incubated for 1 hour at 37°C in 5% CO_2 and subsequently exposed to LOX 0.5mM for viral TLR activation before incubating overnight under the same conditions. RSM is the fermentate control. Supernatants were removed after 24 hours and ELISA was performed for cytokines IL-1β, IL-6, IL-10 and TNF-α. Data is presented as mean ± SD of three replicates. Significance determined using one- way ANOVA with a Newman-Keuls post-test. Output P value style APA: .12 (ns), .033 (*), .002(**) and <.001 (***) comparing unstimulated control cells to TLR stimulated cells and comparing sample to respective RSM counterpart.*

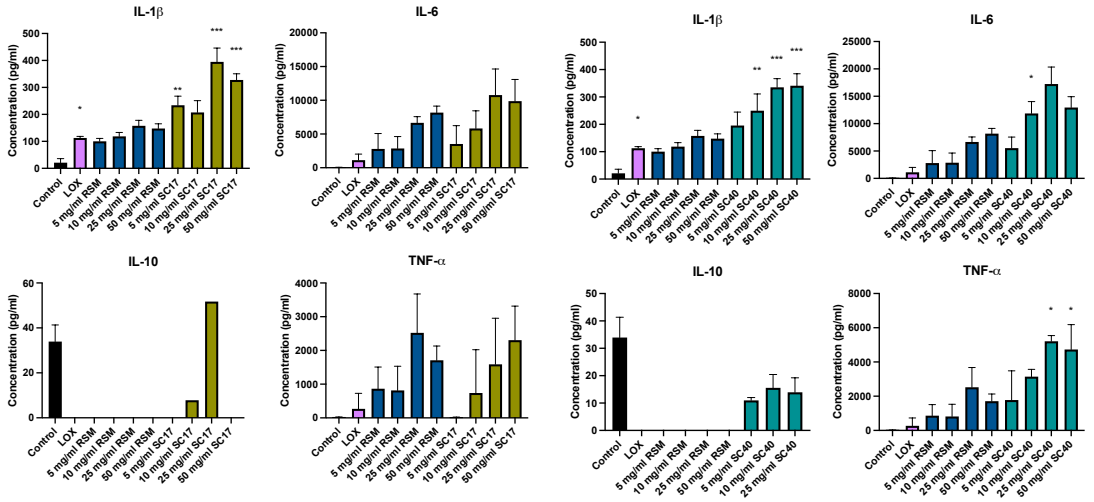

Figure 22: ***Exposure of JAWS to dose response of raw sample fermentate SC17 and SC40 affects cytokine secretion.*** *JAWS cells were seeded at 1x10⁶ cells/ mL and left overnight at 37⁰C in 5% CO_2 The following day cells were stimulated with dose range of 5mg/ mL, 10mg/ mL, 25mg/ mL and 50mg/ mL sample SC40, incubated for 1 hour at 37⁰C in 5% CO_2 and subsequently exposed to LOX 0.5mM for viral TLR activation before incubating overnight under the same conditions. RSM is the fermentate control. Supernatants were removed after 24 hours and ELISA was performed for cytokines IL-1β, IL-6, IL-10 and TNF-α. Data is presented as mean ± SD of three replicates. Significance determined using one- way ANOVA with a Newman-Keuls post-test. Output P value style APA: .12 (ns), .033 (*), .002(**) and <.001 (***) comparing unstimulated control cells to TLR stimulated cells and comparing sample to respective RSM counterpart.*

3.3.2.1.1.5 Dose range of filtered fermentates affects cytokine secretion

JAWS cells were seeded at a concentration of $1x10^6$ cells/ mL, incubated for 24 hours before adding appropriate dose range of samples SC6, SC15, SC17 and SC40, incubated for 1 hour at 37^0C in 5% CO_2 before exposure to 0.5mM LOX and subsequently incubated under the same conditions overnight. Sample dose range included 5mg/ mL, 10mg/ mL, 25mg/ mL and 50mg/ mL of filtered sample. After 24 hours supernatants were removed and ELISA procedure for cytokines IL-1β, IL-6, IL-10 and TNF-α were performed according to the manufacturer's instructions (section 2.2.14 Enzyme Linked Immunosorbent Assay (ELISA)).

Figure 23 and Figure 24 demonstrate that fermentate samples significantly affected the secretion of cytokines, in response to LOX, when compared to the RSM. LOX significantly increased the secretion of cytokines IL-1β, IL-6 and TNF-α ($p<0.001$). SC6 significantly increased IL-6 production at concentrations of 5mg/ mL, 10mg/ mL, 25mg/ mL ($p<0.001$) and 50mg/ mL ($p<0.002$). SC15 significantly increased IL-6 production at concentrations of 10mg/ mL ($p<0.033$), 25mg/ mL and 50mg/ mL

(p<0.002). SC17 significantly increased IL-6 production at concentrations of 10mg/ mL (p<0.001), 25mg/ mL (p<0.002) and 50mg/ mL (p<0.033). SC40 significantly increased IL-6 production at concentrations of 10mg/ mL, 25mg/ mL and 50mg/ mL (p<0.002) and SC6 increased TNF-α at concentrations of 10mg/ mL (p<0.002), 25mg/ mL and 50mg/ mL (p<0.001). Otherwise there was little difference between cytokine secretion of samples compared to the RSM.

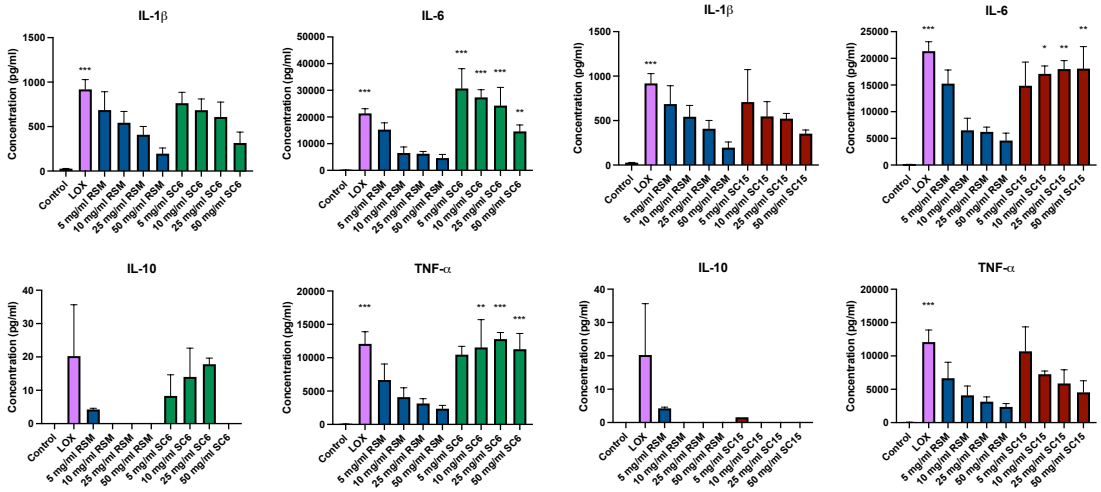

Figure 23: ***Exposure of JAWS to dose response of filtered sample fermentate SC6 and SC15 affects cytokine secretion****. JAWS cells were seeded at 1x10⁶ cells/ mL and left overnight at 37°C in 5% CO_2. The following day cells were stimulated with dose range of 5mg/ mL, 10mg/ mL, 25mg/ mL and 50mg/ mL sample SC6, incubated for 1 hour at 37°C in 5% CO_2 and subsequently exposed to LOX 0.5mM for viral TLR activation before incubating overnight under the same conditions. RSM is the fermentate control. Supernatants were removed after 24 hours and ELISA was performed for cytokines IL-1β, IL-6, IL-10 and TNF-α. Data is presented as mean ± SD of three replicates. Significance determined using one- way ANOVA with a Newman-Keuls post-test. Output P value style APA: .12 (ns), .033 (*), .002(**) and <.001 (***) comparing unstimulated control cells to TLR stimulated cells and comparing sample to respective RSM counterpart.*

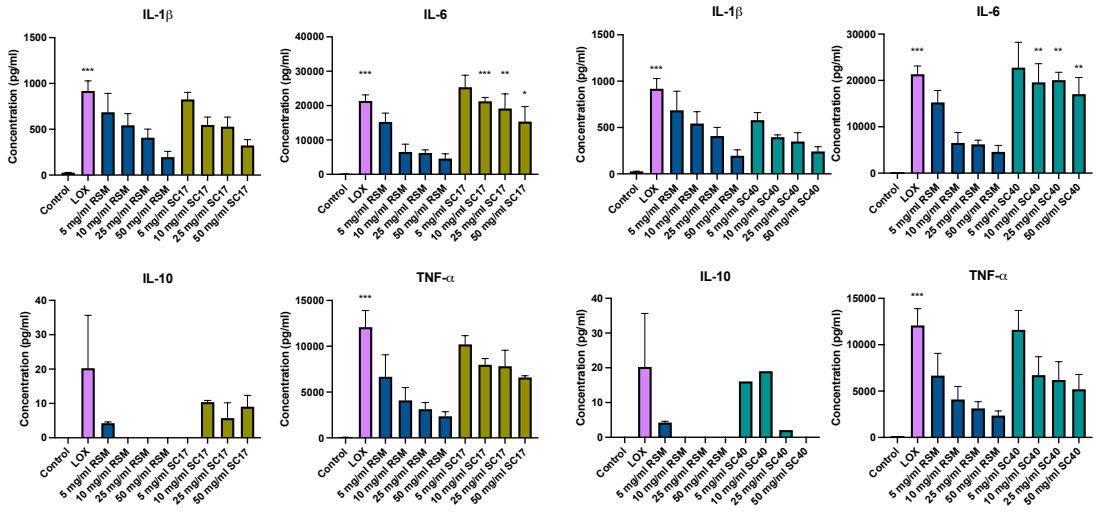

*Figure 24:**Exposure of JAWS to dose response of filtered sample fermentate SC17 and SC40 affects cytokine secretion.** JAWS cells were seeded at 1x10⁶ cells/ mL and left overnight at 37°C in 5% CO_2 The following day cells were stimulated with dose range of 5mg/ mL, 10mg/ mL, 25mg/ mL and 50mg/ mL sample SC40, incubated for 1 hour at 37°C in 5% CO_2 and subsequently exposed to LOX 0.5mM for viral TLR activation before incubating overnight under the same conditions. RSM is the fermentate control. Supernatants were removed after 24 hours and ELISA was performed for cytokines IL-1β, IL-6, IL-10 and TNF-α. Data is presented as mean ± SD of three replicates. Significance determined using one- way ANOVA with a Newman-Keuls post-test. Output P value style APA: .12 (ns), .033 (*), .002(**) and <.001 (***) comparing unstimulated control cells to TLR stimulated cells and comparing sample to respective RSM counterpart.*

We have clearly shown that a dose of either 10mg/ mL, 25mg/ mL, or 50mg/ mL fermentate was sufficient to generate an immune response optimal for viral immunity via the increased secretion of viral associated cytokines including IL-6, and TNF-α. In the interest of commercial production the 50mg/ mL dose was considered to be ruled out due to high cost of production.. Importantly it was the 25mg/ mL that provided the optimal cytokine secretion, however the lower dose of 10mg/ mL was of interest due to ease of production, sufficient cytokine secretion, as well as previous insight into the use of this dose for immunological effect in previous lab work with milk hydrolysates. Therefore the 10mg/ mL, and 25mg/ mL dose were examined further.

Before proceeding with the high throughput screening, we wanted to examine the effect of fermentates when immune cells were activated with different immune stimuli. Examination of fermentates in a range of TLR activated dendritic cells allowed for confirmation of bioactivity and specificity of fermentates, when dendritic cells are challenged with a variety of immune stimuli, mimicking viral infection (PIC, in addition to the already examined LOX),and chronic inflammation (LPS, and CpG). For the purpose of this confirmation of bioactivity, the lower dose of 10mg/ mL fermentate was used in the interest of preserving sample stock, and reagent resources.

3.3.2.1.1.6 Stimulation of JAWS with raw fermentates and activation of with panel of TLRs doesn't affect cell viability

JAWS cells were seeded at a concentration of $1x10^6$ cells/ mL, incubated for 24 hours before stimulating with a dose range of 10mg/ mL raw fermentate samples for 1 hour followed by exposure to 100ng/ mL LPS, 5uM CpG and 10µg/ mL PIC and subsequently incubated at 37^0C in 5% CO_2. After 24 hours an MTS assay was performed as previously outlined (section 2.2.13 MTS Cell Viability Assay).

Figure 25 demonstrates that there was no significant change in cell viability following exposure of the cells to LPS, CpG or PIC for samples SC6, SC15, SC17 and SC40. The RSM acted as the whole fermentate control for comparison of effects induced by each independent sample. The use of the positive control of 10% DMSO provides a clear distinction between the cytotoxic effects on cell viability with the untreated control sample, as DMSO induced cell death.

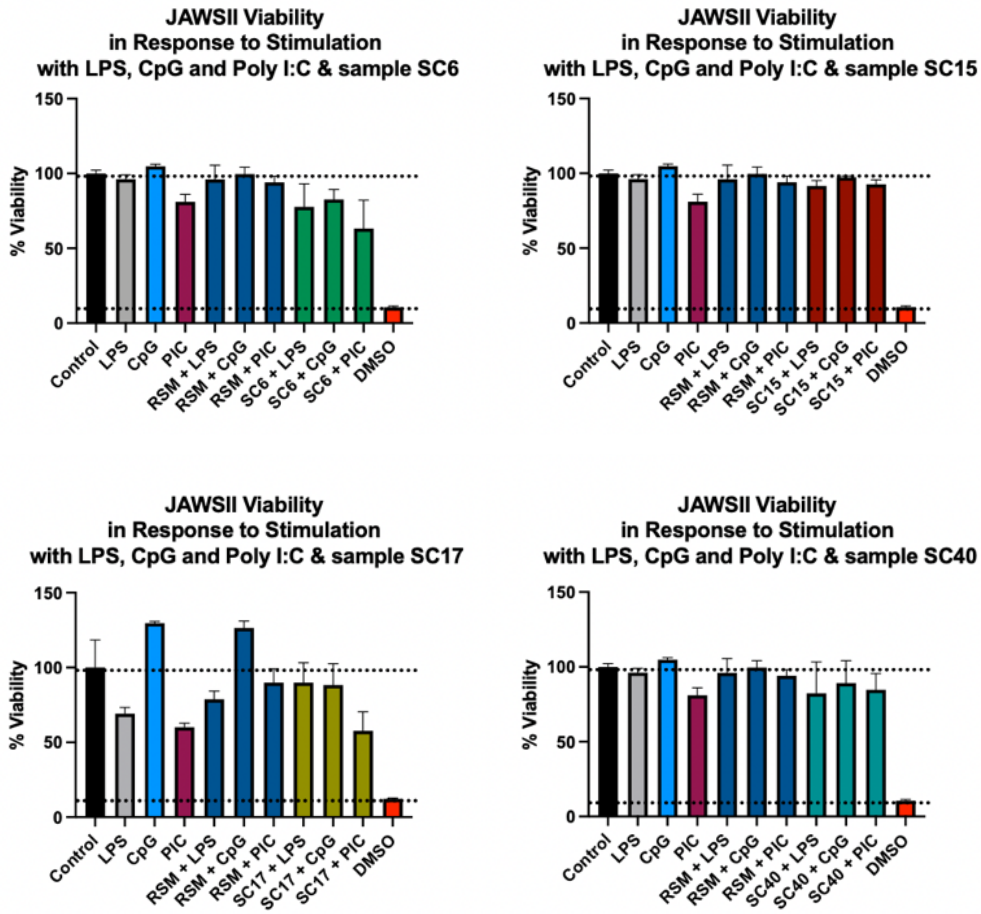

Figure 25: ***Exposure of JAWS to raw sample fermentates SC6, SC15, SC17 and SC40 and TLRs LPS, CpG and PIC affects cell viability.*** *JAWS cells were seeded at 1x10^6 cells/ mL and left overnight at 37^{0}C in 5% CO_2. The following day cells were stimulated with 10mg/ mL raw fermentate, incubated for 1 hour at 37^{0}C in 5% CO_2 and subsequently exposed to 100ng/ mL LPS, 5uM CpG and 10µg/ mL PIC for TLR activation before incubating overnight under the same conditions. RSM is the fermentate control.* 10% *DMSO was included as a positive control to induce cell death. Cells were incubated with MTS cell titre aqueous one solution for 3 hours at 37^{0}C in 5% CO_2. Viability is represented as a percentage compared to viable, untreated cells (Control). Data is presented as mean ± SD of three replicates.*

3.3.2.1.1.7 Stimulation of JAWS with raw fermentates and activation of with panel of TLRs affects cytokine secretion

JAWS cells were seeded at a concentration of $1x10^6$ cells/ mL, incubated for 24 hours before stimulating with a dose range of 10mg/ mL raw fermentate samples SC6, SC15, SC17, and SC40, for 1 hour followed by exposure to 100ng/ mL LPS, 5uM CpG and 10µg/ mL PIC and subsequently incubated at 37^0C in 5% CO_2. After 24 hours supernatants were removed and ELISA was performed for cytokines IL-1β, IL-6, IL-10 and TNF-α according to the manufacturer's instructions (section 2.2.14 Enzyme Linked Immunosorbent Assay (ELISA)). Figure 26 and Figure 27 demonstrate that fermentate samples significantly affected the secretion of cytokines, in response to LPS, CpG and PIC stimulation, when compared to the RSM. LPS significantly increased production of IL-1β, IL-6, and TNF-α ($p<0.001$), while PIC resulted in a small non-significant increase in IL-6 and TNF-α. SC6 significantly increased IL-1β and IL-6 when activated with LPS and PIC ($p<0.001$) and TNF-α when activated with LPS ($p<0.001$) and PIC ($p<0.033$). SC15 significantly increased IL-1β when activated with PIC ($p<0.033$). SC17 significantly increased IL-1β, IL-6, and TNF-α ($p<0.001$) when activated with LPS, and IL-1β ($p<0.002$) and IL-6 ($p<0.033$) when activated with PIC. SC40 significantly increased IL-1β, IL-6, and TNF-α ($p<0.001$) when activated with LPS, IL-1β and IL-6 ($p<0.001$) and TNF-α when activated with PIC, as well as IL-1β ($p<0.033$) when activated with CpG.

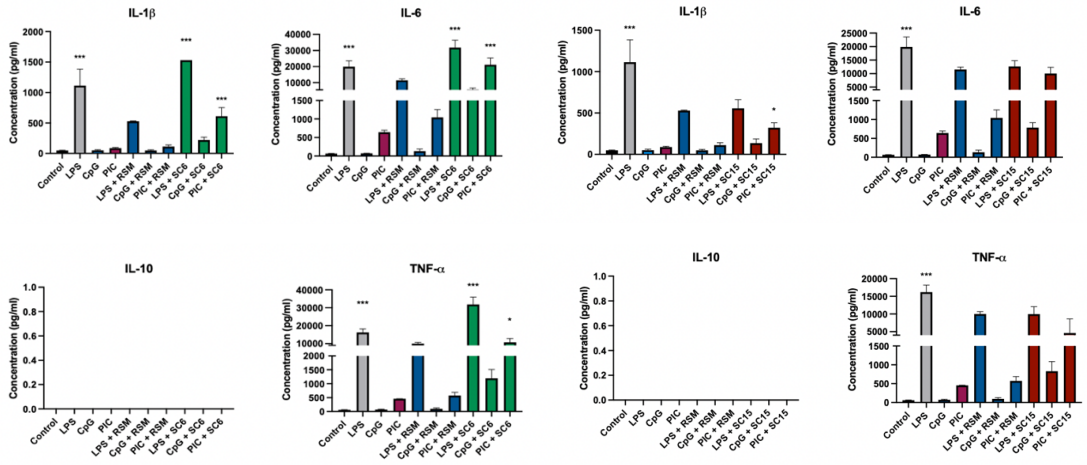

Figure 26: ***Exposure of JAWS to panel of TLRs and raw fermentate SC6 and SC15 affects cytokine secretion.*** *JAWS cells were seeded at 1x10^6 cells/ mL and left overnight at 37^{0}C in 5% CO_2. The following day cells were exposed to 10mg/ mL sample , incubated for 1 hour at 37^{0}C in 5% CO_2 and subsequently exposed to 100ng/ mL LPS, 5uM CpG and 10µg/ mL PIC for TLR activation before incubating overnight under the same conditions. RSM is the fermentate control. Supernatants were removed after 24 hours and ELISA was performed for cytokines IL-1β, IL-6, IL-10 and TNF-α. Data is presented as mean ± SD of three replicates. Significance determined using one- way ANOVA with a Newman-Keuls post-test. Output P value style APA: .12 (ns), .033 (*), .002(**) and <.001 (***) comparing unstimulated control cells to TLR stimulated cells and comparing sample to respective RSM counterpart.*

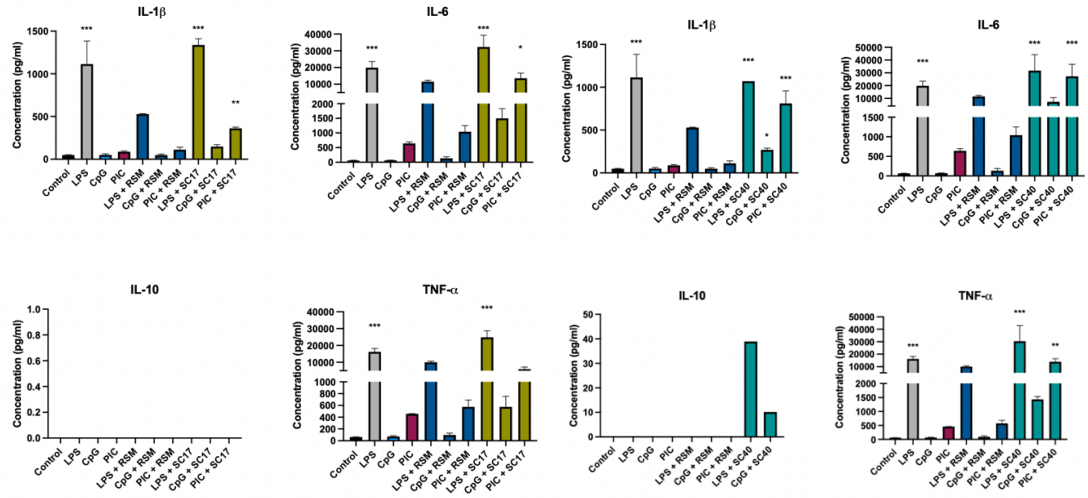

Figure 27: ***Exposure of JAWS to panel of TLRs and raw fermentate SC17 and SC40 affects cytokine secretion.*** *JAWS cells were seeded at 1x10^6 cells/ mL and left overnight at 37^{0}C in 5% CO_2. The following day cells were exposed to 10mg/ mL sample, incubated for 1 hour at 37^{0}C in 5% CO_2 and subsequently exposed to 100ng/ mL LPS, 5uM CpG and 10µg/ mL PIC for TLR activation before incubating overnight under the same conditions. RSM is the fermentate control. Supernatants were removed after 24 hours and ELISA was performed for cytokines IL-1β, IL-6, IL-10 and TNF-α. Data is presented as mean ± SD of three replicates. Significance determined using one- way ANOVA with a Newman-Keuls post-test. Output P value style APA: .12 (ns), .033 (*), .002(**) and <.001 (***) comparing unstimulated control cells to TLR stimulated cells and comparing sample to respective RSM counterpart.*

We clearly demonstrated that fermentate bioactivity was specific to the mode in which the immune cell was activated, be it LOX or PIC induced viral infection, or LPS, or CpG induced chronic inflammation. Thus, fermentate bioactivity was unique and specific to each individual sample, suggesting an individualised role for fermentates not only in viral immunity, but also potentially as anti-inflammatories. As highlighted in Table 20 fermentates are specific. For example, SC40 enhanced IL-1β, IL-6, IL-10 and TNF-α in PIC activated cells but only enhanced IL-1β in CpG activated cells. Therefore, we were now able to expand our screening beyond the pilot study and into examination of fermentate effect in BMDCs.

Table 20: ***Summary of the cytokines secreted in the presence of SC6, SC15, SC17, and SC40 in the presence of PIC, LPS, and CpG activated JAWS cells****. Summary of cytokines secreted in the absence/ presence of fermentates in LOX and LPS activated BMDCs. Significance determined using one- way ANOVA with a Newman-Keuls post-test. Output P value style APA: .12 (ns), .033 (*), .002(**) and <.001 (***); where samples in the presence of TLR were compared to TLR alone. Green indicates increased cytokine production, and red indicates decreased cytokine production.*

Fermentates in BMDCs	SC6	SC15	SC17	SC40	
+PIC	***	*	**	***	IL-1β
	***		*	***	IL-6
					IL-10
	*			***	TNF-α
+LPS	***		***	***	IL-1β
	***		***	***	IL-6
					IL-10
	***			***	TNF-α
+CpG			**	*	IL-1β
					IL-6
					IL-10
					TNF-α

3.3.2.2 High Throughput Screening:

3.3.2.2.1 Confirmation of Pilot Study in BMDC

The pilot study in JAWS cells allowed us to see that the fermentates do have unique bioactivity, which is important to establish prior to examination in primary cells for ethical reasons. Having established the optimal pre-treatments, and doses of fermentates required for optimal bioactivity in the JAWS cells, a similar approach was taken using the raw and filtered fermentates, at a dose of 10mg/ mL, and 25mg/ mL to assess bioactivity in the primary dendritic cells BMDCs. This allowed for the high throughput screening of the bank of fermentates in a primary dendritic cell when challenged with the viral immune stimulus LOX. BMDCs are a better representation of how a dendritic cell behaves *in vivo*. Similar to the pilot study in JAWS cells, we were able to confirm bioactivity and specificity of the fermentates in LOX activated BMDCs.

Initially, based on previous lab research with milk hydrolysates we decided to examine the effects of filtered fermentates on cell viability and cytokine secretion, whereby filtering samples was optimal for cytokine secretion in BMDCs. It was important to first confirm that bioactivity could be seen from fermentates and thus a complete dose range of 5mg/ mL, 10mg/ mL, 25mg/ mL and 50mg/ mL fermentate was used to ensure this. Doing this allowed us to support and validate the findings of the pilot study carried out in JAWS cells.

3.3.2.2.1.1 Dose range of filtered fermentates doesn't affect cell viability

BMDC were seeded at a concentration of $1x10^6$ cells/ mL, incubated for 24 hours before stimulating with a dose range of 5mg/ mL, 10mg/ mL, 25mg/ mL and 50mg/ mL filtered fermentate sample for 1 hour followed by 0.5mM LOX TLR ligand and subsequently incubated at 370C in 5% CO2. After 24 hours an MTS assay was performed as previously outlined (section 2.2.13 MTS Cell Viability Assay).

Figure 28 demonstrates that there was no significant change in cell viability following exposure of the cells to LOX or any dose range of fermentates. The RSM

acted as the whole fermentate control for comparison of effects induced by each independent sample. The use of the positive control of 10% DMSO provided a clear distinction between the cytotoxic effects on cell viability with the untreated control sample, as DMSO induced cell death.

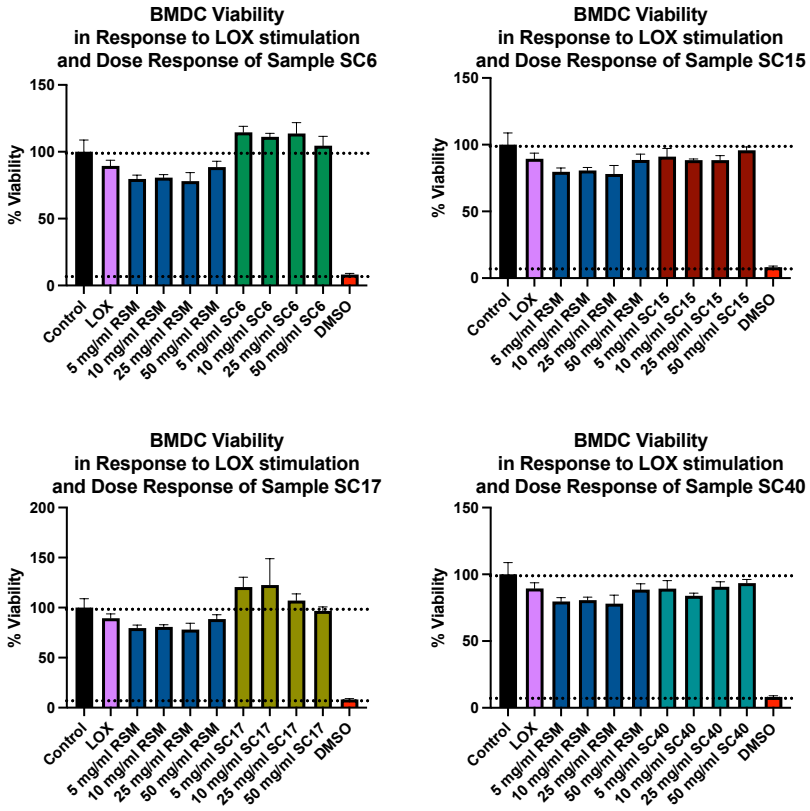

Figure 28: ***Exposure of BMDC to dose range of filtered fermentates SC6, SC15, SC17 and SC40 doesn't affect cell viability.*** *BMDC cells were seeded at 1x10^6 cells/ mL and left overnight at 37^{0}C in 5% CO_2. The following day cells were stimulated with appropriate dose range of fermentate, incubated for 1 hour at 37^{0}C in 5% CO_2 and subsequently exposed to LOX 0.5mM for viral TLR activation before incubating overnight under the same conditions. RSM is the fermentate control.* 10% *DMSO was included as a positive control to induce cell death. Cells were incubated with MTS cell titre aqueous one solution for 3 hours at 37^{0}C in 5% CO_2. Viability is represented as a percentage compared to viable, untreated cells (Control). Data is presented as mean ± SD of three replicates.*

3.3.2.2.1.2 Dose range of filtered fermentates affects cytokine secretion

BMDC were seeded at a concentration of $1x10^6$ cells/ mL, incubated for 24 hours before adding appropriate dose range of filtered sample, incubated for 1 hour at 37^0C in 5% CO_2 before exposing to 0.5mM LOX and subsequently incubated under the same conditions overnight. Sample dose range includes 5mg/ mL, 10mg/ mL, 25mg/ mL and 50mg/ mL of filtered sample. After 24 hours supernatants were removed and ELISA was performed for cytokines IL-1β, IL-6, IL-10 , TNF-α, IL-12p40, IL-12p70, IL-23 and IL-27 according to the manufacturer's instructions (section 2.2.14 Enzyme Linked Immunosorbent Assay (ELISA)).
Figure 29-Figure 32 demonstrate that samples significantly affected the secretion of cytokines, in response to LOX, when compared to the RSM. LOX significantly increased IL-1β and IL-10 ($p<0.001$), IL-6 and TNF-α ($p<0.002$), and IL-27 ($p<0.033$), while non-significantly increasing IL-12-40 and IL-23.
Figure 29 shows SC6 significantly increased IL-1β at concentrations of 5mg/ mL ($p<0.002$), 10mg/ mL ($p<0.001$) and 25mg/ mL ($p<0.002$). SC6 significantly increased IL-10 and IL-27 at concentrations of 25mg/ mL and 50mg/ mL ($p<0.001$). SC6 significantly increased TNF-α and IL-23 at concentrations of 25mg/ mL ($p<0.033$) and SC6 non-significantly increased IL-6 and IL-12p40 for all doses 5mg/ mL-50mg/ mL.
Figure 30 shows SC15 significantly increased IL-1β at concentrations of 5mg/ mL ($p<0.033$). SC15 significantly increased IL-27 at concentrations of 25mg/ mL and 50mg/ mL ($p<0.002$). SC15 non-significantly increased IL-6 and IL-12p40 for all doses 5mg/ mL-50mg/ mL.
Figure 31 shows that SC17 largely had no effect on cytokine secretion with only IL-1β significantly secreted at concentrations of 50mg/ mL ($p<0.033$) and IL-23 at 25mg/ mL ($p<0.033$). SC17 non-significantly increased IL-12p40 for all doses 5mg/ mL-50mg/ mL.
Figure 32 shows SC40 significantly increased IL-1β at concentrations of 5mg/ mL, 10mg/ mL and 25mg/ mL ($p<0.002$). SC40 significantly increased IL-6 for all doses, 5mg/ mL ($p<0.002$), 10mg/ mL and 25mg/ mL ($p<0.001$), and at 50mg/ mL ($p<0.033$). SC40 significantly increased IL-10 at 25mg/ mL ($p<0.002$) and 50mg/ mL ($p<0.033$).

SC40 significantly increased TNF-α at concentrations of 25mg/ mL ($p<0.002$),increased IL-12p40 at 5mg/ mL and 25mg/ mL ($p<0.001$) and increased IL-27 at concentrations of 10mg/ mL ($p<0.033$), 25mg/ mL ($p<0.002$), and 50mg/ mL ($p<0.033$).

For Figure 29 – Figure 32 remaining cytokine profiles varied. Fermentate presence had varying effects which were inconsistent or displayed no affect versus the RSM counterpart.

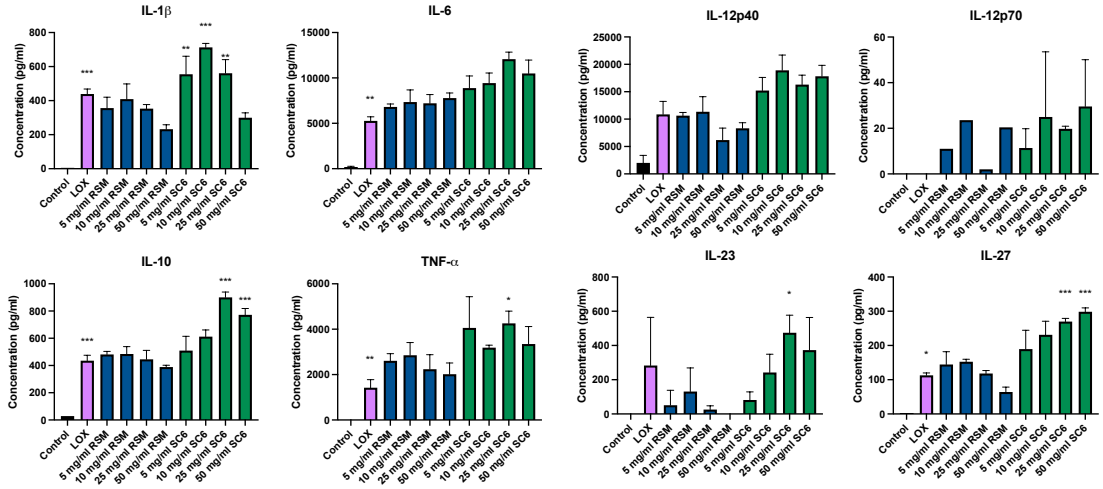

Figure 29: ***Exposure of LOX activated BMDC to filtered sample SC6 results in the secretion of cytokines.*** *BMDC cells were seeded at 1x10^6 cells/ mL and exposed a dose range of SC6 at the following concentrations; 5mg/ mL, 10mg/ mL, 25mg/ mL and 50mg/ mL then activated with 0.5 mM LOX. Supernatants were removed after 24 hours and ELISA was performed for cytokines IL-1β, IL-6, IL-10, TNF-α, IL-12p40, IL-12p70, IL-23, IL-27. Data is presented as mean ± SD of three replicates. Significance determined using one- way ANOVA with a Newman-Keuls post-test. Output P value style APA: .12 (ns), .033 (*), .002(**) and <.001 (***) comparing unstimulated control cells to LOX TLR stimulated cells and comparing respective dose of sample SC6 to its appropriate RSM counterpart.*

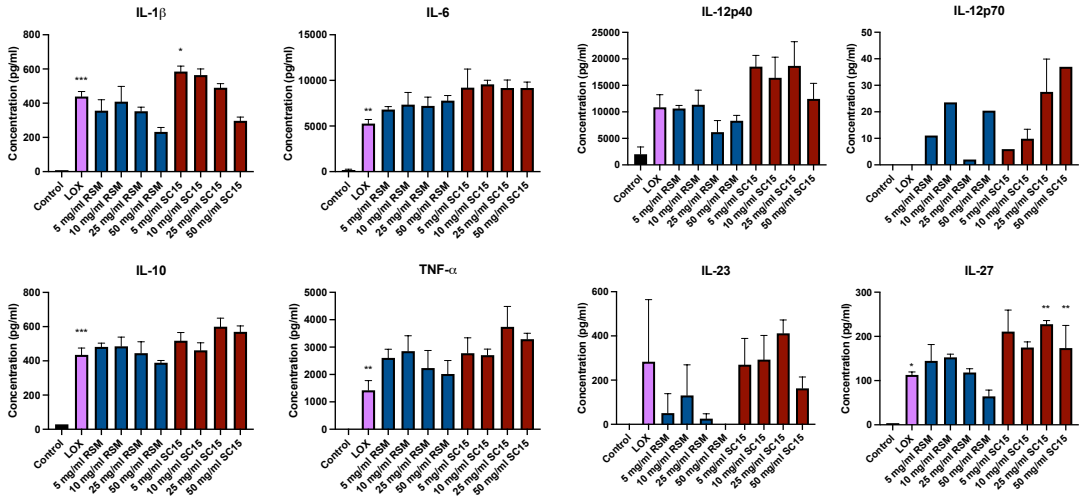

Figure 30: ***Exposure of LOX activated BMDC to filtered sample SC15 results in the secretion of cytokines.*** *BMDC cells were seeded at 1x10^6 cells/ mL and exposed a dose range of SC6 at the following concentrations; 5mg/ mL, 10mg/ mL, 25mg/ mL and 50mg/ mL then activated with 0.5 mM LOX. Supernatants were removed after 24 hours and ELISA was performed for cytokines IL-1β, IL-6, IL-10, TNF-α, IL-12p40, IL-12p70, IL-23, IL-27. Data is presented as mean ± SD of three replicates. Significance determined using one- way ANOVA with a Newman-Keuls post-test. Output P value style APA: .12 (ns), .033 (*), .002(**) and <.001 (***) comparing unstimulated control cells to LOX TLR stimulated cells and comparing respective dose of sample SC6 to its appropriate RSM counterpart.*

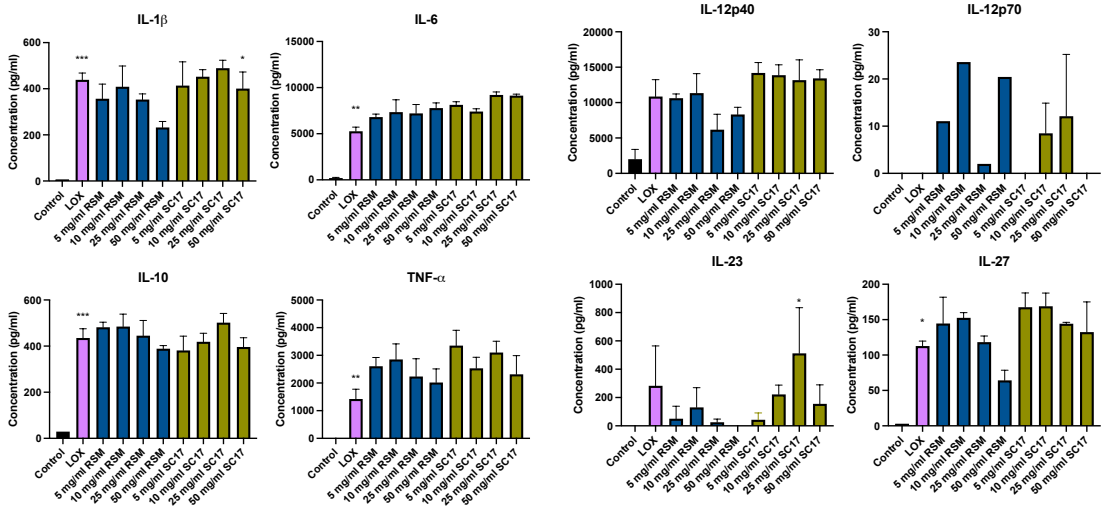

Figure 31: ***Exposure of LOX activated BMDC to filtered sample SC17 results in the secretion of cytokines.*** *BMDC cells were seeded at 1x10^6 cells/ mL and exposed a dose range of SC6 at the following concentrations; 5mg/ mL, 10mg/ mL, 25mg/ mL and 50mg/ mL then activated with 0.5 mM LOX. Supernatants were removed after 24 hours and ELISA was performed for cytokines IL-1β, IL-6, IL-10, TNF-α, IL-12p40, IL-12p70, IL-23, IL-27. Data is presented as mean ± SD of three replicates. Significance determined using one- way ANOVA with a Newman-Keuls post-test. Output P value style APA: .12 (ns), .033 (*), .002(**) and <.001 (***) comparing unstimulated control cells to LOX TLR stimulated cells and comparing respective dose of sample SC17 to its appropriate RSM counterpart.*

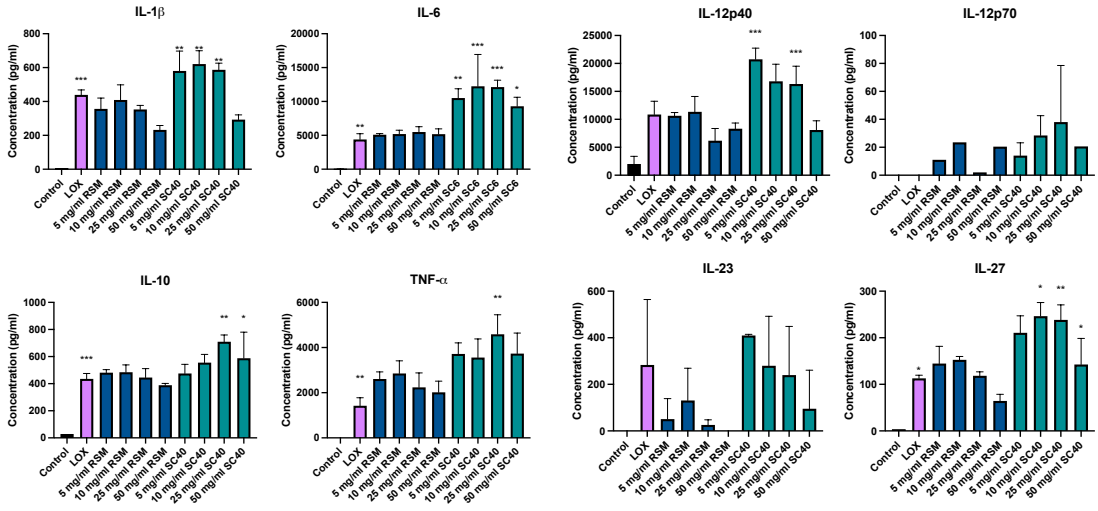

Figure 32: ***Exposure of LOX activated BMDC to filtered sample SC40 results in the secretion of cytokines.*** *BMDC cells were seeded at 1x10^6 cells/ mL and exposed a dose range of SC40 at the following concentrations; 5mg/ mL, 10mg/ mL, 25mg/ mL and 50mg/ mL then activated with 0.5 mM LOX. Supernatants were removed after 24 hours and ELISA was performed for cytokines IL-1β, IL-6, IL-10, TNF-α, IL-12p40, IL-12p70, IL-23, IL-27. Data is presented as mean ± SD of three replicates. Significance determined using one- way ANOVA with a Newman-Keuls post-test. Output P value style APA: .12 (ns), .033 (*), .002(**) and <.001 (***) comparing unstimulated control cells to LOX TLR stimulated cells and comparing respective dose of sample SC40 to its appropriate RSM counterpart.*

Therefore, we proved that the fermentates examined had no negative impact on cell viability, as well as positively effecting the secretion of cytokines in response to viral induced LOX activated BMDCs, corroborating our findings in the pilot study. From here we were then able to commence our screening of fermentates in BMDCs having confirmed 10mg/ mL, and 25mg/ mL as the optimal doses in BMDCs, as expected from our data in JAWS cells.

Having now confirmed our findings of 10mg/ mL and 25mg/ mL as optimal doses we now wanted to confirm the pre-treatment needed for optimal cytokine secretion to bring forward for the establishment of our final fermentate model. Therefore we continued to screen fermentates as raw and filtered at both doses. This formed the basis of the remaining screening in order to ensure nothing was missed in the initial screening to ensure all samples were given enough scope to assess their bioactivity.

3.3.2.2.2 High throughput screening of fermentates in BMDC:

3.3.2.2.2.1 Stimulation of BMDC with raw or filtered dose range of fermentates doesn't affect cell viability

BMDC were seeded at a concentration of $1x10^6$ cells/ mL, incubated for 24 hours before stimulating with a dose range of 10mg/ mL and 25mg/ mL raw or filtered fermentate sample for 1 hour followed by 0.5mM LOX TLR ligand and subsequently incubated at 37^0C in 5% CO_2. After 24 hours an MTS assay was performed as previously outlined (section 2.2.13 MTS Cell Viability Assay).

Figure 33 demonstrates that there was no significant change in cell viability following exposure of the cells to LOX or any dose response or processing of fermentates. The RSM acted as the whole fermentate control for comparison of effects induced by each independent sample. The use of the positive control of 10% DMSO provided a clear distinction between the cytotoxic effects on cell viability with the untreated control sample, as DMSO induces cell death.

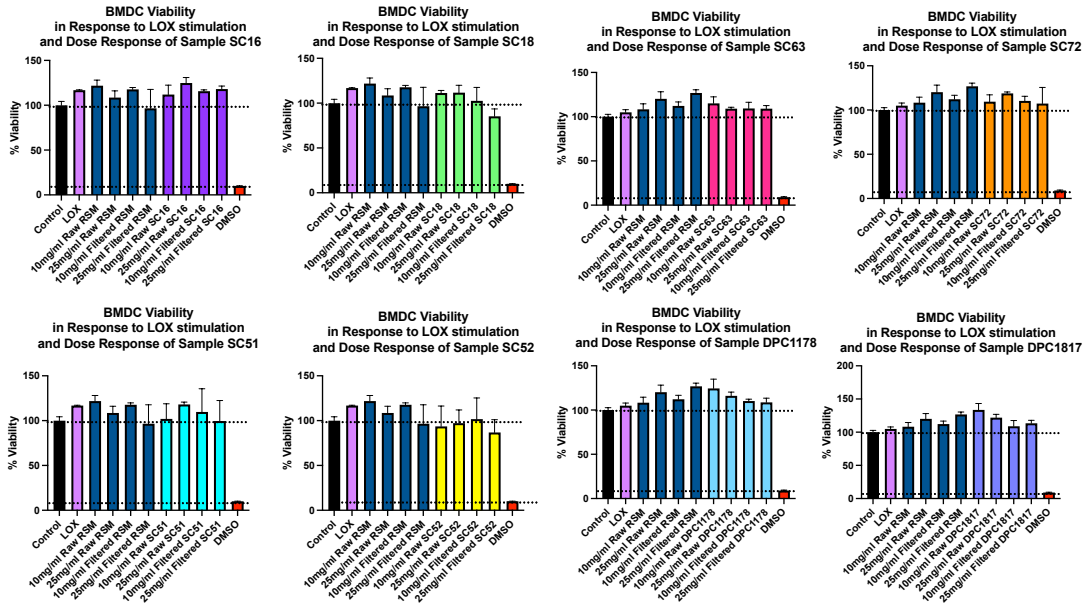

Figure 33: ***Exposure of BMDC to dose response of raw or filtered SC16, SC18, SC63, SC72, SC51, SC52, DPC1178, and DPC1817 sample fermentates doesn't affect cell viability.*** *BMDC cells were seeded at 1x10^6 cells/ mL and left overnight at 37^{0}C in 5% CO_2. The following day cells were stimulated with appropriate dose range of fermentate, incubated for 1 hour at 37^{0}C in 5% CO_2 and subsequently exposed to LOX 0.5mM for viral TLR activation before incubating overnight under the same conditions. RSM is the fermentate control.* 10% *DMSO was included as a positive control to induce cell death. Cells were incubated with MTS cell titre aqueous one solution for 3 hours at 37^{0}C in 5% CO_2. Viability is represented as a percentage compared to viable, untreated cells (Control). Data is presented as mean ± SD of three replicates.*

3.3.2.2.2.2 Stimulation of BMDC with raw or filtered dose range of fermentates affects cytokine secretion

BMDC were seeded at a concentration of $1x10^6$ cells/ mL, incubated for 24 hours at 37^0C in 5% CO_2 before stimulating with 10mg/ mL and 25mg/ mL raw or filtered fermentate sample for 1 hour followed by exposure to 0.5mM LOX TLR ligand and subsequently incubated under the same conditions overnight. After 24 hours supernatants were removed and ELISA was performed for cytokines IL-1β, IL-6, IL-10, TNF-α, IL-12p40, IL-12p70, IL-23, and IL-27 according to the manufacturer's instructions (section 2.2.14 Enzyme Linked Immunosorbent Assay (ELISA)).

Figure 34- Figure 41 demonstrate that samples significantly affect the secretion of cytokines, in response to LOX, when compared to the RSM. Figure 34 - Figure 37 demonstrates that LOX significantly increases IL-1β ($p<0.002$), IL-6, IL-10 and TNF-α ($p<0.001$), and Figure 38 - Figure 41 demonstrates that LOX significantly increased IL-1β and IL-6 ($p<0.001$), and non-significantly increased IL-12-40, IL-23 and IL-27. Figure 34 shows that at 25mg/ mL SC16 significantly increased IL-1β for raw ($p<0.001$), and filtered samples ($p<0.002$), and at concentrations of 10mg/ mL raw sample ($p<0.001$). At 25mg/ mL SC16 significantly increased IL-23 and IL-27 for raw sample ($p<0.002$; $p<0.001$) and at 10mg/ mL significantly increased IL-27 for raw sample ($p<0.033$), and filtered sample ($p<0.001$). Figure 35 shows SC18 significantly increased IL-10, TNF-α, IL-23, and IL-27 for raw fermentate sample at concentrations of 25mg/ mL ($p<0.001$; $p<0.033$; $p<0.002$; $p<0.002$), and increased IL-10 and IL-27 at 10mg/ mL raw sample ($p<0.001$; $p<0.002$). Figure 36 shows SC51 significantly increased TNF-α, IL-12p40 and IL-27 for raw sample at concentrations of 25mg/ mL ($p<0.033$; $p<0.001$; $p<0.001$). and increased IL-27 at concentrations of 10mg/ mL filtered sample ($p<0.002$). Figure 37 shows SC52 significantly increased IL-6, IL-10, TNF-α, IL-23 and IL-27 for raw sample at concentrations of 25mg/ mL ($p<0.002$; $p<0.002$; $p<0.001$; $p<0.033$; $p<0.001$) and significantly increased IL-12p40 for filtered sample at concentrations of 10mg/ mL ($p<0.033$), while 25mg/ mL of filtered SC52 significantly reduced IL-6 concentrations ($p<0.033$).

Figure 38 shows SC63 at 10mg/ mL and 25mg/ mL significantly increased IL-1β for filtered sample ($p<0.033$), and for raw sample increased IL-6 and IL-12p40 ($p<0.001$; $p<0.033$). SC63 significantly increased IL-23 for raw samples at concentrations of 10mg/ mL ($p<0.002$) and 25mg/ mL ($p<0.001$) and non-significantly increased IL-10 for 10mg/ mL and 25mg/ mL doses.

Figure 39 shows SC72 significantly increased IL-6 and IL-23 for raw sample at concentrations of 25mg/ mL ($p<0.001$), and IL-23 at 10mg/ mL ($p<0.033$).

Figure 40 shows DPC1178 significantly increased IL-6, IL-10, and IL-23 for raw sample at concentrations of 10mg/ mL and 25mg/ mL ($p<0.001$), while at 10mg/ mL increased TNF-α and IL-12p40 ($p<0.033$; $p<0.002$) and at 25mg/ mL ($p<0.002$; $p<0.001$). DPC1178 significantly increased IL-12p70 for raw samples at concentrations of 25mg/ mL ($p<0.033$).

Figure 41 shows DPC1817 significantly increased IL-10, and IL-23 for raw sample at concentrations of 10mg/ mL and 25mg/ mL ($p<0.001$), while at 10mg/ mL and 25mg/ mL increased IL-6 ($p<0.001$; $p<0.002$) and TNF-α ($p<0.033$; $p<0.001$). DPC1178 significantly increased IL-12p40 for raw samples at concentrations of 25mg/ mL ($p<0.033$).

Figure 34- Figure 41 demonstrate that filtering of samples had clear significant negative impact on the secretion of cytokines.

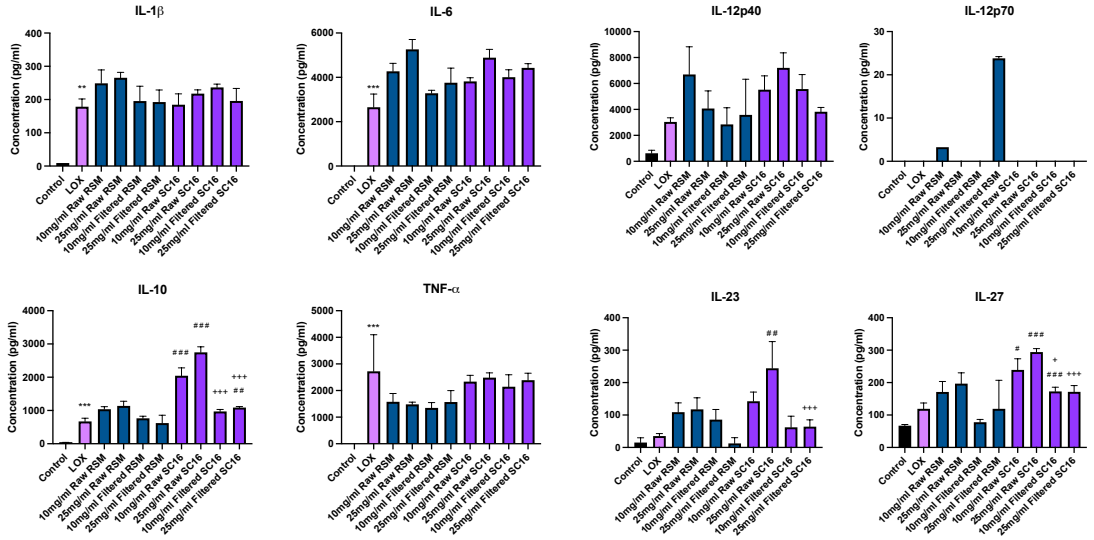

*Figure 34:**Exposure of LOX activated BMDC to raw or filtered sample SC16 results in the secretion of cytokines.** BMDC cells were seeded at 1x10^6 cells/ mL and left overnight at 37^{0}C in 5% CO_2. The following day cells were stimulated with 10mg/ mL and 25mg/ mL raw and filtered sample fermentate, incubated for 1 hour at 37^{0}C in 5% CO_2 and subsequently exposed to LOX 0.5mM for viral TLR activation before incubating overnight under the same conditions. RSM is the fermentate control. Supernatants were removed after 24 hours and ELISA was performed for cytokines IL-1β, IL-6, IL-10, TNF-α, IL-12p40, IL-12p70, IL-23 and IL-27. Data is presented as mean ± SD of three replicates. Significance determined using one- way ANOVA with a Newman-Keuls post-test. Output P value style APA: .12 (ns), .033 (*), .002(**) and <.001 (***) comparing unstimulated control cells to LOX TLR stimulated cells "*", comparing respective dose and processing of sample SC16 to its appropriate RSM counterpart "#" and comparing filtered dose to raw unprocessed sample dose "+".*

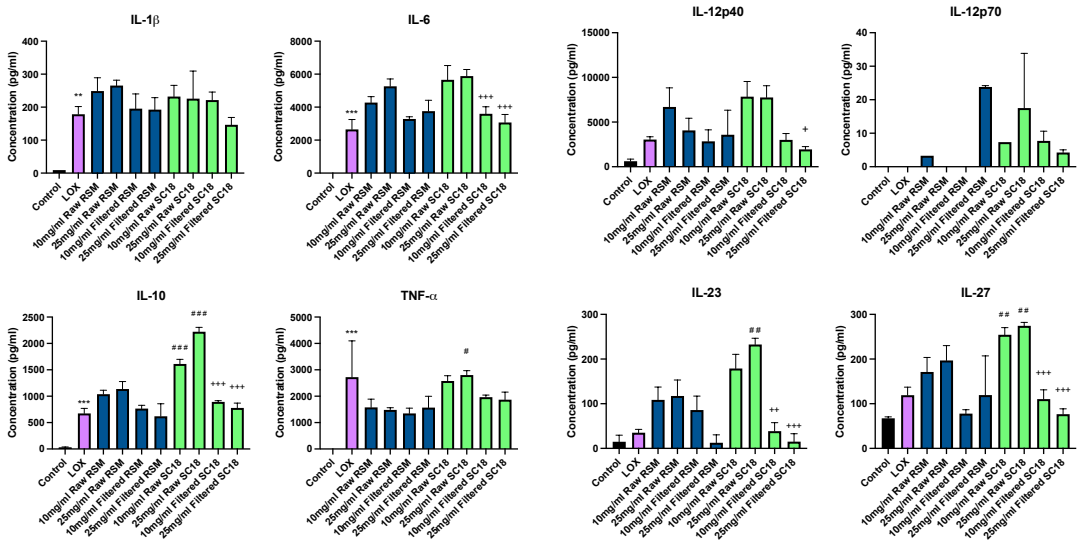

*Figure 35:**Exposure of LOX activated BMDC to raw or filtered sample SC18 results in the secretion of cytokines.** BMDC cells were seeded at 1x10^6 cells/ mL and left overnight at 37^{0}C in 5% CO_2. The following day cells were stimulated with 10mg/ mL and 25mg/ mL raw and filtered sample fermentate, incubated for 1 hour at 37^{0}C in 5% CO_2 and subsequently exposed to LOX 0.5mM for viral TLR activation before incubating overnight under the same conditions. RSM is the fermentate control. Supernatants were removed after 24 hours and ELISA was performed for cytokines IL-1β, IL-6, IL-10, TNF-α, IL-12p40, IL-12p70, IL-23 and IL-27. Data is presented as mean ± SD of three replicates. Significance determined using one- way ANOVA with a Newman-Keuls post-test. Output P value style APA: .12 (ns), .033 (*), .002(**) and <.001 (***) comparing unstimulated control cells to LOX TLR stimulated cells "*", comparing respective dose and processing of sample SC18 to its appropriate RSM counterpart "#" and comparing filtered dose to raw unprocessed sample dose "+".*

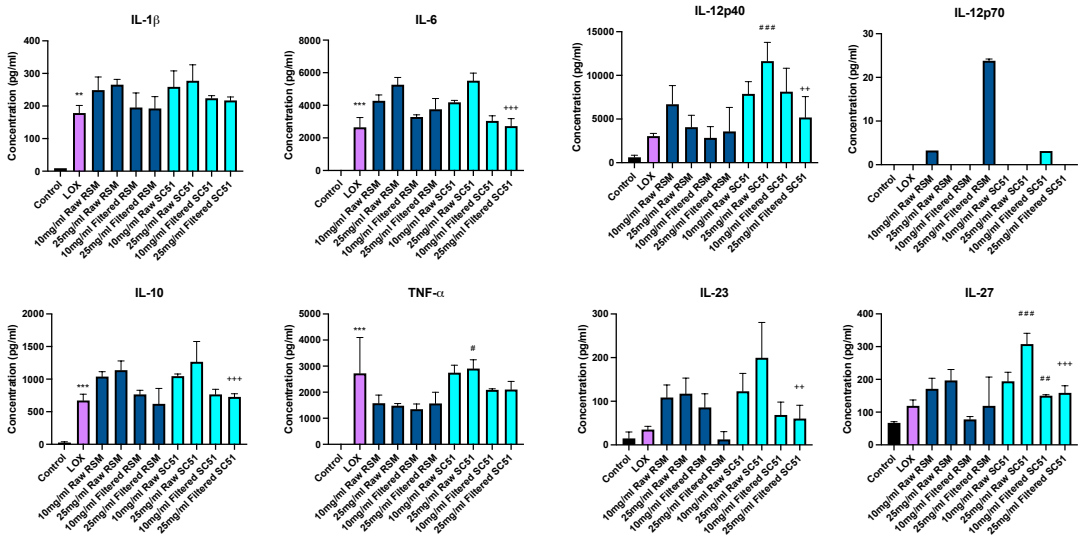

*Figure 36:**Exposure of LOX activated BMDC to raw or filtered sample SC51 results in the secretion of cytokines.** BMDC cells were seeded at 1x10^6 cells/ mL and left overnight at 37^{0}C in 5% CO_2. The following day cells were stimulated with 10mg/ mL and 25mg/ mL raw and filtered sample fermentate, incubated for 1 hour at 37^{0}C in 5% CO_2 and subsequently exposed to LOX 0.5mM for viral TLR activation before incubating overnight under the same conditions. RSM is the fermentate control. Supernatants were removed after 24 hours and ELISA was performed for cytokines IL-1β, IL-6, IL-10, TNF-α, IL-12p40, IL-12p70, IL-23 and IL-27. Data is presented as mean ± SD of three replicates. Significance determined using one- way ANOVA with a Newman-Keuls post-test. Output P value style APA: .12 (ns), .033 (*), .002(**) and <.001 (***) comparing unstimulated control cells to LOX TLR stimulated cells "*", comparing respective dose and processing of sample SC51 to its appropriate RSM counterpart "#" and comparing filtered dose to raw unprocessed sample dose "+".*

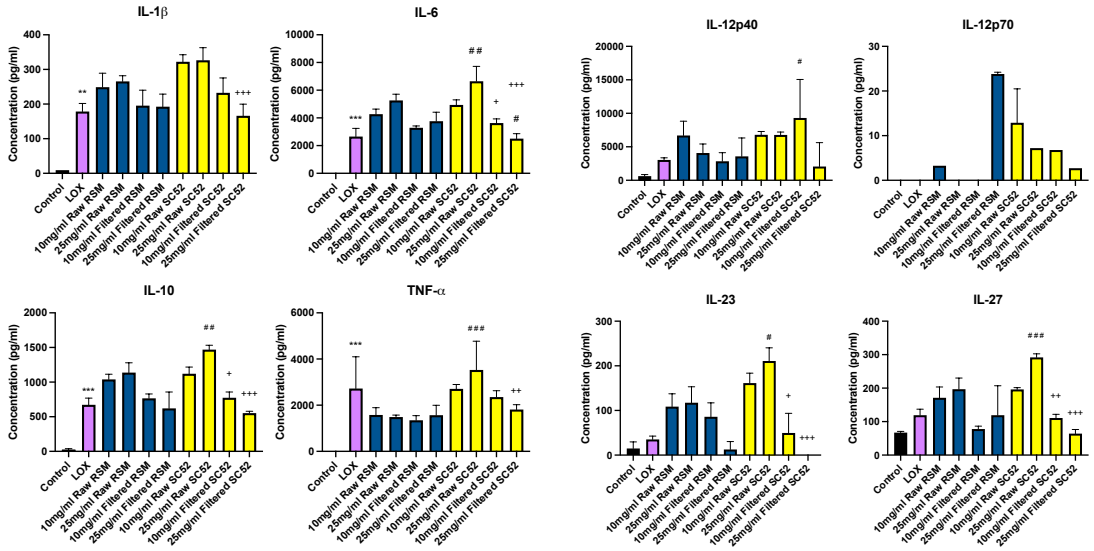

*Figure 37:**Exposure of LOX activated BMDC to raw or filtered sample SC52 results in the secretion of cytokines.** BMDC cells were seeded at 1x10^6 cells/ mL and left overnight at 37^{0}C in 5% CO_2. The following day cells were stimulated with 10mg/ mL and 25mg/ mL raw and filtered sample fermentate, incubated for 1 hour at 37^{0}C in 5% CO_2 and subsequently exposed to LOX 0.5mM for viral TLR activation before incubating overnight under the same conditions. RSM is the fermentate control. Supernatants were removed after 24 hours and ELISA was performed for cytokines IL-1β, IL-6, IL-10, TNF-α, IL-12p40, IL-12p70, IL-23 and IL-27. Data is presented as mean ± SD of three replicates. Significance determined using one- way ANOVA with a Newman-Keuls post-test. Output P value style APA: .12 (ns), .033 (*), .002(**) and <.001 (***) comparing unstimulated control cells to LOX TLR stimulated cells "*", comparing respective dose and processing of sample SC52 to its appropriate RSM counterpart "#" and comparing filtered dose to raw unprocessed sample dose "+".*

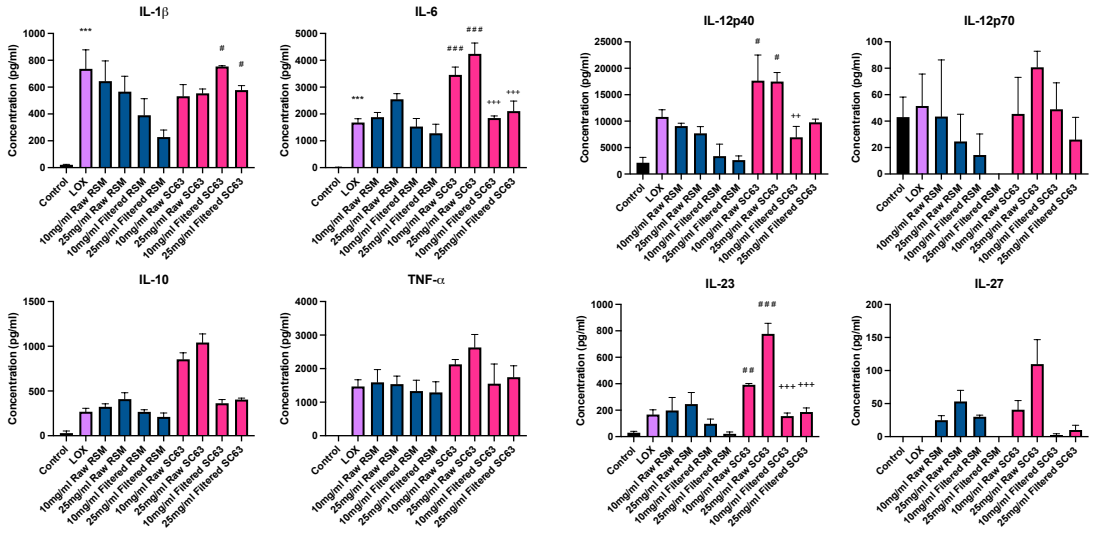

*Figure 38:**Exposure of LOX activated BMDC to raw or filtered sample SC63 results in the secretion of cytokines.** BMDC cells were seeded at 1x10^6 cells/ mL and left overnight at 37^{0}C in 5% CO_2. The following day cells were stimulated with 10mg/ mL and 25mg/ mL raw and filtered sample fermentate, incubated for 1 hour at 37^{0}C in 5% CO_2 and subsequently exposed to LOX 0.5mM for viral TLR activation before incubating overnight under the same conditions. RSM is the fermentate control. Supernatants were removed after 24 hours and ELISA was performed for cytokines IL-1β, IL-6, IL-10, TNF-α, IL-12p40, IL-12p70, IL-23 and IL-27. Data is presented as mean ± SD of three replicates. Significance determined using one- way ANOVA with a Newman-Keuls post-test. Output P value style APA: .12 (ns), .033 (*), .002(**) and <.001 (***) comparing unstimulated control cells to LOX TLR stimulated cells "*", comparing respective dose and processing of sample SC63 to its appropriate RSM counterpart "#" and comparing filtered dose to raw unprocessed sample dose "+".*

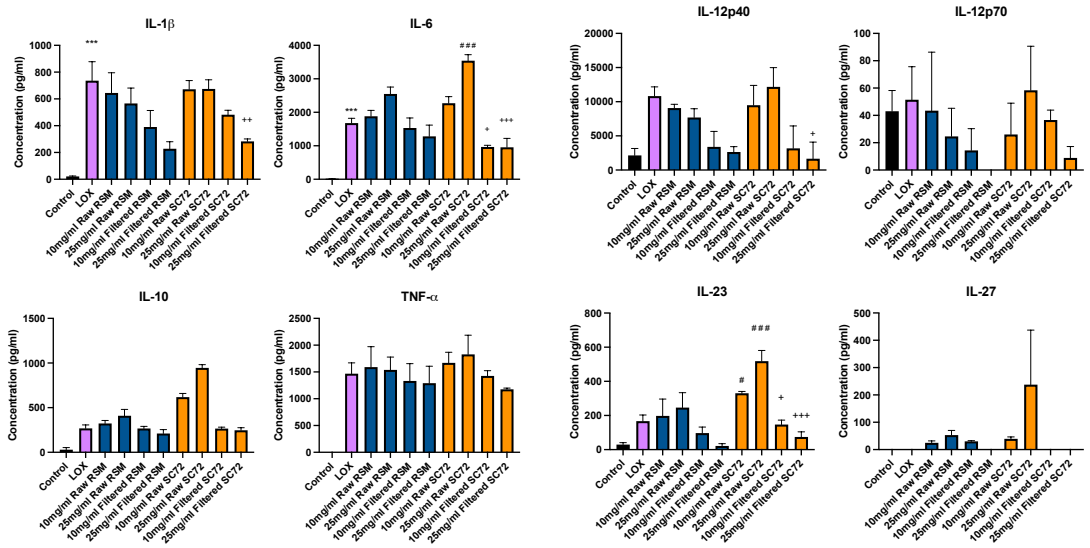

Figure 39: ***Exposure of LOX activated BMDC to raw or filtered sample SC72 results in the secretion of cytokines.*** *BMDC cells were seeded at 1x10^6 cells/ mL and left overnight at 37^{0}C in 5% CO_2. The following day cells were stimulated with 10mg/ mL and 25mg/ mL raw and filtered sample fermentate, incubated for 1 hour at 37^{0}C in 5% CO_2 and subsequently exposed to LOX 0.5mM for viral TLR activation before incubating overnight under the same conditions. RSM is the fermentate control. Supernatants were removed after 24 hours and ELISA was performed for cytokines IL-1β, IL-6, IL-10, TNF-α, IL-12p40, IL-12p70, IL-23 and IL-27. Data is presented as mean ± SD of three replicates. Significance determined using one- way ANOVA with a Newman-Keuls post-test. Output P value style APA: .12 (ns), .033 (*), .002(**) and <.001 (***) comparing unstimulated control cells to LOX TLR stimulated cells "*", comparing respective dose and processing of sample SC72 to its appropriate RSM counterpart "#" and comparing filtered dose to raw unprocessed sample dose "+".*

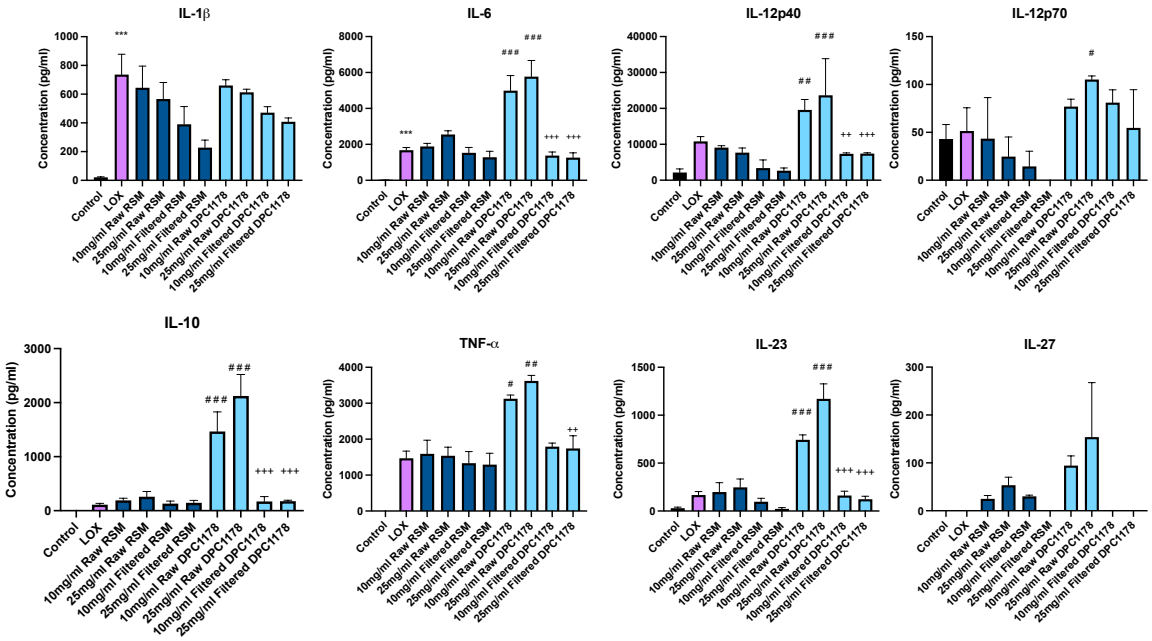

Figure 40: ***Exposure of LOX activated BMDC to raw or filtered sample DPC1178 results in the secretion of cytokines.*** *BMDC cells were seeded at 1x10^6 cells/ mL and left overnight at 37^{0}C in 5% CO_2. The following day cells were stimulated with 10mg/ mL and 25mg/ mL raw and filtered sample fermentate, incubated for 1 hour at 37^{0}C in 5% CO_2 and subsequently exposed to LOX 0.5mM for viral TLR activation before incubating overnight under the same conditions. RSM is the fermentate control. Supernatants were removed after 24 hours and ELISA was performed for cytokines IL-1β, IL-6, IL-10, TNF-α, IL-12p40, IL-12p70, IL-23 and IL-27. Data is presented as mean ± SD of three replicates. Significance determined using one- way ANOVA with a Newman-Keuls post-test. Output P value style APA: .12 (ns), .033 (*), .002(**) and <.001 (***) comparing unstimulated control cells to LOX TLR stimulated cells "*", comparing respective dose and processing of sample DPC1178 to its appropriate RSM counterpart "#" and comparing filtered dose to raw unprocessed sample dose "+".*

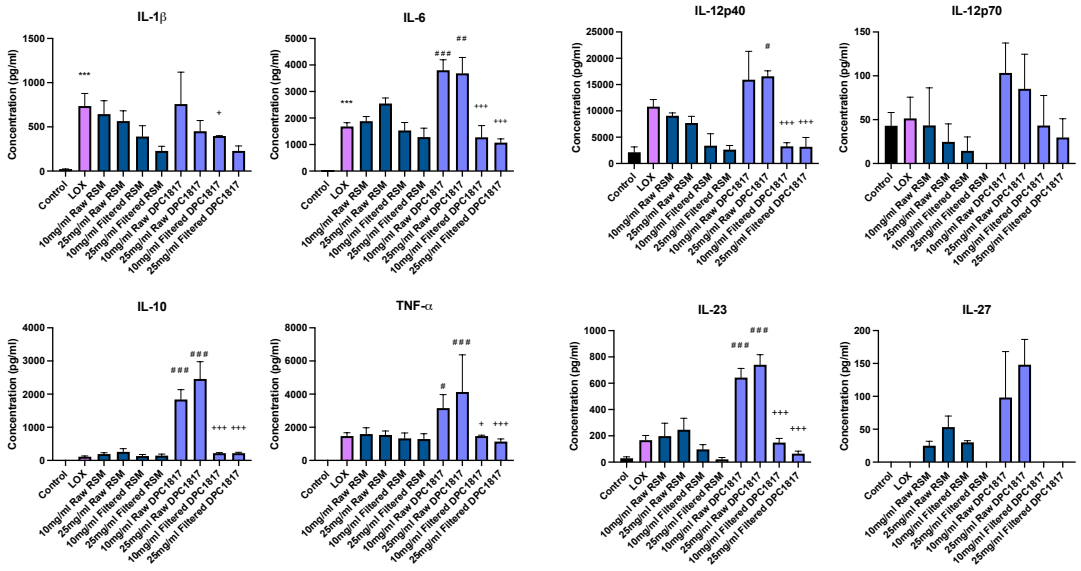

Figure 41: ***Exposure of LOX activated BMDC to raw or filtered sample DPC1817 results in the secretion of cytokines.*** *BMDC cells were seeded at 1x10^6 cells/ mL and left overnight at 37^{0}C in 5% CO_2. The following day cells were stimulated with 10mg/ mL and 25mg/ mL raw and filtered sample fermentate, incubated for 1 hour at 37^{0}C in 5% CO_2 and subsequently exposed to LOX 0.5mM for viral TLR activation before incubating overnight under the same conditions. RSM is the fermentate control. Supernatants were removed after 24 hours and ELISA was performed for cytokines IL-1β, IL-6, IL-10, TNF-α, IL-12p40, IL-12p70, IL-23 and IL-27. Data is presented as mean ± SD of three replicates. Significance determined using one- way ANOVA with a Newman-Keuls post-test. Output P value style APA: .12 (ns), .033 (*), .002(**) and <.001 (***) comparing unstimulated control cells to LOX TLR stimulated cells "*", comparing respective dose and processing of sample DPC1817 to its appropriate RSM counterpart "#" and comparing filtered dose to raw unprocessed sample dose "+".*

As summarised in Table 21 it was clear from assessing this large selection of fermentates that the 25mg/ mL dose was optimal for cytokine secretion. Thus, we decided that in the interest of high-throughput screening, and appropriate use of resources, that screening at the one dose of 25mg/ mL was the most efficient.

Table 21: ***Summary of the cytokines secreted in the presence of SC16, SC18, SC51, SC52, SC63, SC72, DPC1178, and DPC1817 at 10mg/mL or 25mg/mL raw and filtered doses.*** *Summary of cytokines secreted in presence of fermentates in LOX activated BMDCs. Significance determined using one- way ANOVA with a Newman-Keuls post-test. Output P value style APA: .12 (ns), .033 (*), .002(**) and <.001 (***); where each fermentate dose and pretreatment was compared to the respective RSM dose and pretreatment, Green indicates increased cytokine production, and red indicates decreased cytokine production.*

Fermentate	SC16	SC18	SC51	SC52	SC63	SC72	DPC1178	DPC1817	
10mg/mL Raw									IL-1β
					***		***	***	IL-6
	***	***					***	***	IL-10
							*	*	TNF-α
					*		**		IL-12p40
									IL-12p70
					**	*	***	***	IL-23
	*	**							IL-27
25mg/mL Raw									IL-1β
				**	***	***	***	**	IL-6
	***	***		**			***	***	IL-10
		*	*	***			**	***	TNF-α
			***		*		***	*	IL-12p40
							*		IL-12p70
	**	**		*	***	***	***	***	IL-23
	***	**	***	***					IL-27
10mg/mL Filtered					*				IL-1β
									IL-6
				*					IL-10
									TNF-α
									IL-12p40
									IL-12p70
									IL-23
	***		**						IL-27
25mg/mL Filtered					*				IL-1β
				*					IL-6
	**								IL-10
									TNF-α
									IL-12p40
									IL-12p70
									IL-23
									IL-27

In the interest of ensuring no sample bioactivity went unnoticed we decided to continue screening for both raw and filtered fermentates at the one dose. This was important as based on previous lab knowledge we had seen that some samples do preform best when filtered, and thus didn't want to rule out the possibility of some of these fermentates behaving the same. Therefore we processed each fermentate as a novel fermentate with the potential for unique bioactivity in its raw or filtered form.

3.3.2.2.2.3 Stimulation of BMDC with raw or filtered 25mg/ mL fermentates doesn't affect cell viability

BMDC were seeded at a concentration of $1x10^6$ cells/ mL, incubated for 24 hours before stimulating with a dose of 25mg/ mL raw or filtered fermentate sample for 1 hour followed by 0.5mM LOX TLR ligand and subsequently incubated at 37^0C in 5% CO_2. After 24 hours an MTS assay was performed as previously outlined (section 2.2.13 MTS Cell Viability Assay).

Figure 42 demonstrates that there was no significant change in cell viability following exposure of the cells to LOX or 25mg/ mL raw or filtered fermentates. The RSM acted as the whole fermentate control for comparison of effects induced by each independent sample. The use of the positive control of 10% DMSO provided a clear distinction between the cytotoxic effects on cell viability with the untreated control sample, as DMSO induced cell death.

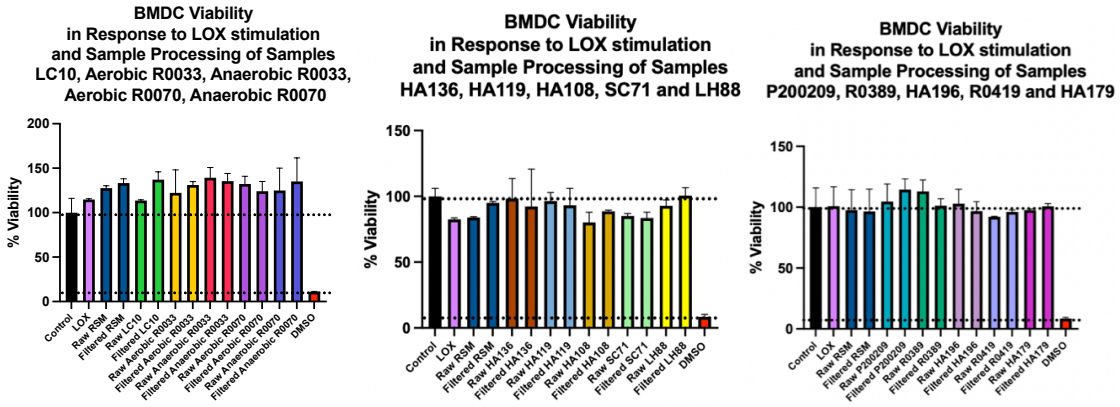

Figure 42: ***Exposure of BMDC to 25mg/ mL raw and filtered LC10, Aerobic R0033, Anaerobic R0033, Aerobic R0070, HA136, HA119, HA108, SC71, LH88, P200209, R0389, HA196, R0419 and HA179 fermentates doesn't affect cell viability.*** *BMDC cells were seeded at 1x10^6 cells/ mL and left overnight at 37^{0}C in 5% CO_2. The following day cells were stimulated with 25mg/ mL sample fermentate, incubated for 1 hour at 37^{0}C in 5% CO_2 and subsequently exposed to LOX 0.5mM for viral TLR activation before incubating overnight under the same conditions. RSM is the fermentate control. 10% DMSO was included as a positive control to induce cell death. Cells were incubated with MTS cell titre aqueous one solution for 3 hours at 37^{0}C in 5% CO_2. Viability is represented as a percentage compared to viable, untreated cells (Control). Data is presented as mean ± SD of three replicates.*

3.3.2.2.2.4 Stimulation of BMDC with raw or filtered 25mg/ mL fermentates affects cytokine secretion

BMDC were seeded at a concentration of 1x10^6 cells/ mL, incubated for 24 hours before stimulating with a dose of 25mg/ mL raw or filtered fermentate sample for 1 hour followed by 0.5mM LOX TLR ligand and subsequently incubated at 37^{0}C in 5% CO_2. After 24 hours supernatants were removed and ELISA was performed for cytokines IL-1β, IL-6, IL-10, TNF-α, IL-12p40, IL-12p70, IL-23, and IL-27 according to the manufacturer's instructions (section 2.2.14 Enzyme Linked Immunosorbent Assay (ELISA)). Due to large numbers of samples, samples of interest have been highlighted below and the data for the remaining samples are included in the appendix.

Figure 43 - Figure 45 demonstrate that fermentate samples significantly affected the secretion of cytokines, in response to LOX, when compared to the RSM. Figure 43 demonstrates that LOX significantly increased IL-1β, IL-10, TNF-α ($p<0.001$), and IL-6 ($p<0.033$). Raw LC10 significantly increased IL-10 ($p<0.001$). Raw Aerobic R0033 significantly increased IL-6, TNF-α, IL-12p40, IL-12p70, IL-23 and IL27 ($p<0.001$), and to a lesser extent increased IL-1β ($p<0.002$), and IL-10

(p<0.033). Raw Aerobic R0070 significantly increased IL-1β (p<0.001),IL-6, IL-10, IL-23 (p<0.001) and TNF-α (p<0.033), while filter Anaerobic R0070 increased TNF-α (p<0.002) and IL-6 (p<0.033).

Figure 44 demonstrates that LOX significantly increased IL-1β (p<0.001), IL-6, IL-10 (p<0.002), and non-significantly increased TNF-α and IL-12p40. Raw HA136 significantly increased IL-6, IL-10, IL-12p40, IL-12p70, IL-23, IL-27 (p<0.001) and TNF-α (p<0.033), while reducing IL-1β (p<0.001). Raw HA108 significantly increased IL-6, IL-10, TNF-α, IL-12p70, IL-27 (p<0.001), and to a lesser extent increased IL-12p40 (p<0.033). Raw LH88 significantly increased IL-10 (p<0.001) and TNF-α (p<0.002), while significantly reducing IL-1β (p<0.033), IL-12p40 (p<0.002), and IL-27 (p<0.001). Filtered LH88 increased IL-6 (p<0.001) and TNF-α (p<0.002).

Figure 45 demonstrates that LOX significantly increased IL-6, IL-10, TNF-α (p<0.001), and non-significantly increased IL-1β, IL-12p40, IL-23 and IL-27. Raw P200209 significantly increased IL-10 (p<0.001). Raw R0389 significantly increased IL-6 and IL-10 (p<0.001). Raw HA136 significantly increased IL-1β, IL-10 and IL-23 (p<0.001). Raw R0419 increased IL-1β, TNF-α, IL-23 (p<0.001) and IL-6 (p<0.002) and Filtered R0419 increased IL-6 (p<0.033).

Figure 43 - Figure 45 demonstrate that filtering of samples had a clear significant negative impact on the secretion of cytokines.

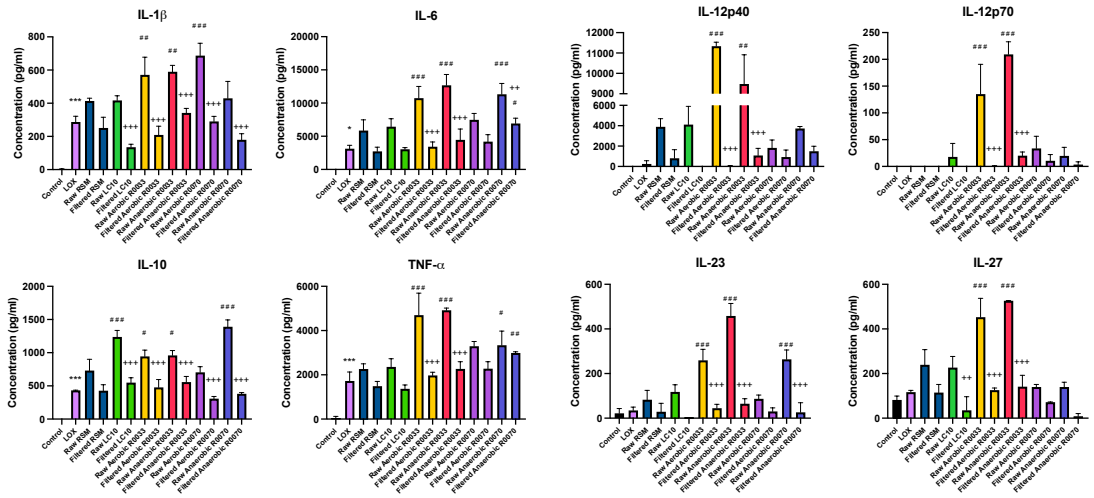

Figure 43: ***Exposure of LOX activated BMDC to sample LC10, Aerobic R0033, Anaerobic R0033, Aerobic R0070 and Anaerobic R0070 results in the secretion of cytokines.*** *BMDC cells were seeded at 1x10^6 cells/ mL and left overnight at 37^{0}C in 5% CO_2. The following day cells were stimulated with 25mg/ mL raw and filtered sample fermentate, incubated for 1 hour at 37^{0}C in 5% CO_2 and subsequently exposed to LOX 0.5mM for viral TLR activation before incubating overnight under the same conditions. RSM is the fermentate control. Supernatants were removed after 24 hours and ELISA was performed for cytokines IL-1β, IL-6, IL-10, TNF-α, IL-12p40, IL-12p70, IL-23 and IL-27. Data is presented as mean ± SD of three replicates. Significance determined using one- way ANOVA with a Newman-Keuls post-test. Output P value style APA: .12 (ns), .033 (*), .002(**) and <.001 (***) comparing unstimulated control cells to LOX TLR stimulated cells "*", comparing processed or unprocessed sample LC10, Aerobic R0033, Anaerobic R0033, Aerobic R0070 and Anaerobic R0070 to its appropriate RSM counterpart "#" and comparing filtered sample to raw unprocessed sample "+".*

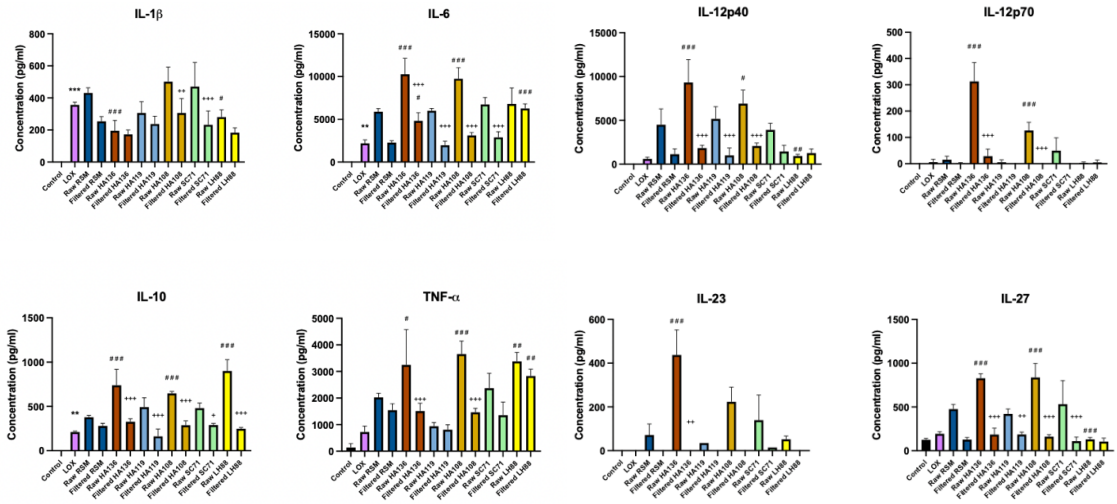

Figure 44: ***Exposure of LOX activated BMDC to sample HA136, HA119, HA108, SC71 and LH88 results in the secretion of cytokines.*** *BMDC cells were seeded at 1x10^6 cells/ mL and left overnight at 37^{0}C in 5% CO_2. The following day cells were stimulated with 25mg/ mL raw and filtered sample fermentate, incubated for 1 hour at 37^{0}C in 5% CO_2 and subsequently exposed to LOX 0.5mM for viral TLR activation before incubating overnight under the same conditions. RSM is the fermentate control. Supernatants were removed after 24 hours and ELISA was performed for IL-1β, IL-6, IL-10, TNF-α, IL-12p40, IL-12p70, IL-23 and IL-27. Data is presented as mean ± SD of three replicates. Significance determined using one- way ANOVA with a Newman-Keuls post-test. Output P value style APA: .12 (ns), .033 (*), .002(**) and <.001 (***) comparing unstimulated control cells to LOX TLR stimulated cells "*", comparing processed or unprocessed sample HA136, HA119, HA108, SC71 and LH88 to its appropriate RSM counterpart "#" and comparing filtered sample to raw unprocessed sample "+".*

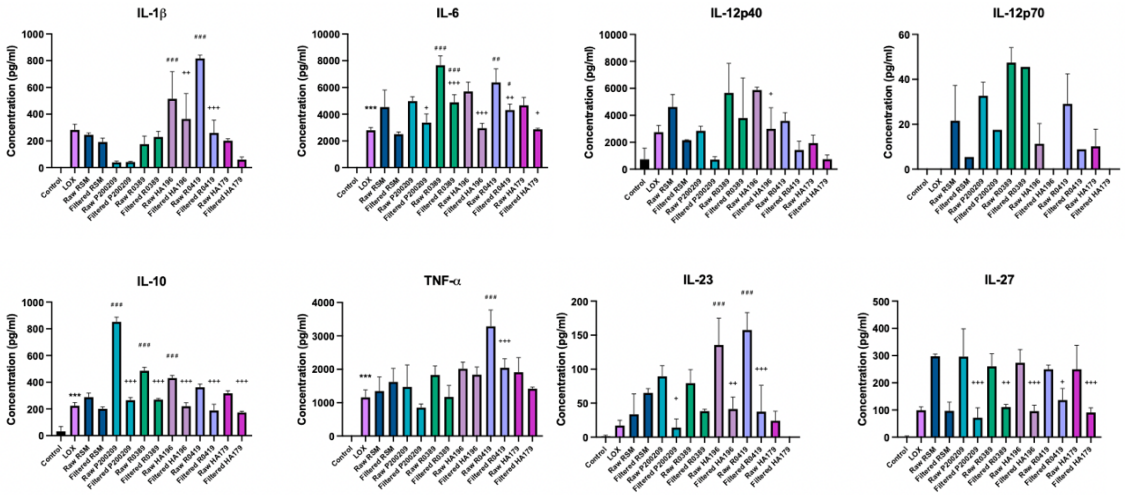

Figure 45: ***Exposure of LOX activated BMDC to sample P200209, R0389, HA196, R0419 and HA179 results in the secretion of cytokines.*** *BMDC cells were seeded at 1x10^6 cells/ mL and left overnight at 37^{0}C in 5% CO_2. The following day cells were stimulated with 25mg/ mL raw and filtered sample fermentate, incubated for 1 hour at 37^{0}C in 5% CO_2 and subsequently exposed to LOX 0.5mM for viral TLR activation before incubating overnight under the same conditions. RSM is the fermentate control. Supernatants were removed after 24 hours and ELISA was performed for IL-1β, IL-6, IL-10 TNF-α, IL-12p40, IL-12p70, IL-23 and IL-27. Data is presented as mean ± SD of three replicates. Significance determined using one- way ANOVA with a Newman-Keuls post-test. Output P value style APA: .12 (ns), .033 (*), .002(**) and <.001 (***) comparing unstimulated control cells to LOX TLR stimulated cells "*", comparing processed or unprocessed sample P200209, R0389, HA196, R0419 and HA179 to its appropriate RSM counterpart "#" and comparing filtered sample to raw unprocessed sample "+".*

As summarised in Table 22 we can clearly see that throughout the screening of the remaining samples at the one dose of 25mg/ mL, that leaving the fermentate raw is the optimal form for increased cytokine secretion in viral immune challenged BMDCs. Having completed the screening process we were now able to confidently establish our fermentate model with an optimal dose of 25mg/ mL, and being left unprocessed in its raw form. This was then able to form the basis of the remaining study, which was able to further delve into fermentate immunomodulatory capabilities.

Table 22: ***Summary of the cytokines secreted in the presence of LC10, Aerobic R0033, Anaerobic R0033, Aerobic R0070, Anaerobic R0070, HA136, HA119, HA108, SC71, LH88, P200622, R0389, HA196, R0419, and HA179 in their raw and filtered 25mg/mL form.*** *Summary of cytokines secreted in presence of fermentates in LOX activated BMDCs. Significance determined using one- way ANOVA with a Newman-Keuls post-test. Output P value style APA: .12 (ns), .033 (*), .002(**) and <.001 (***); where each fermentate dose and pretreatment was compared to the respective RSM dose and pretreatment, Green indicates increased cytokine production, and red indicates decreased cytokine production.*

Fermentate	LC10	Aerobic R0033	Anaerobic R0033	Aerobic R0070	Anaerobic R0070	HA136	HA119	HA108	SC71	LH88	P200622	R0389	HA196	R0419	HA179	
25mg/mL Raw		**	**	***		***				*			***	***		IL-1β
		***	***		***	***	***					***		**		IL-6
	***	*	*		***	***		***		***	***	***	***			IL-10
		***	***		*	*		***		**				***		TNF-α
		***	**			***		*		**						IL-12p40
		***	***			***		***								IL-12p70
		***	***		***	***							***	***		IL-23
		***	***			***		***		***						IL-27
25mg/mL Filtered																IL-1β
					*	*				***		***		*		IL-6
																IL-10
					**					**						TNF-α
																IL-12p40
																IL-12p70
																IL-23
																IL-27

3.4 Discussion:

Figure 46 is a schematic representation of the workflow carried out in this chapter needed for the establishment of an optimal model for assessment of fermentate bioactivity, to form the basis of our subsequent chapters.

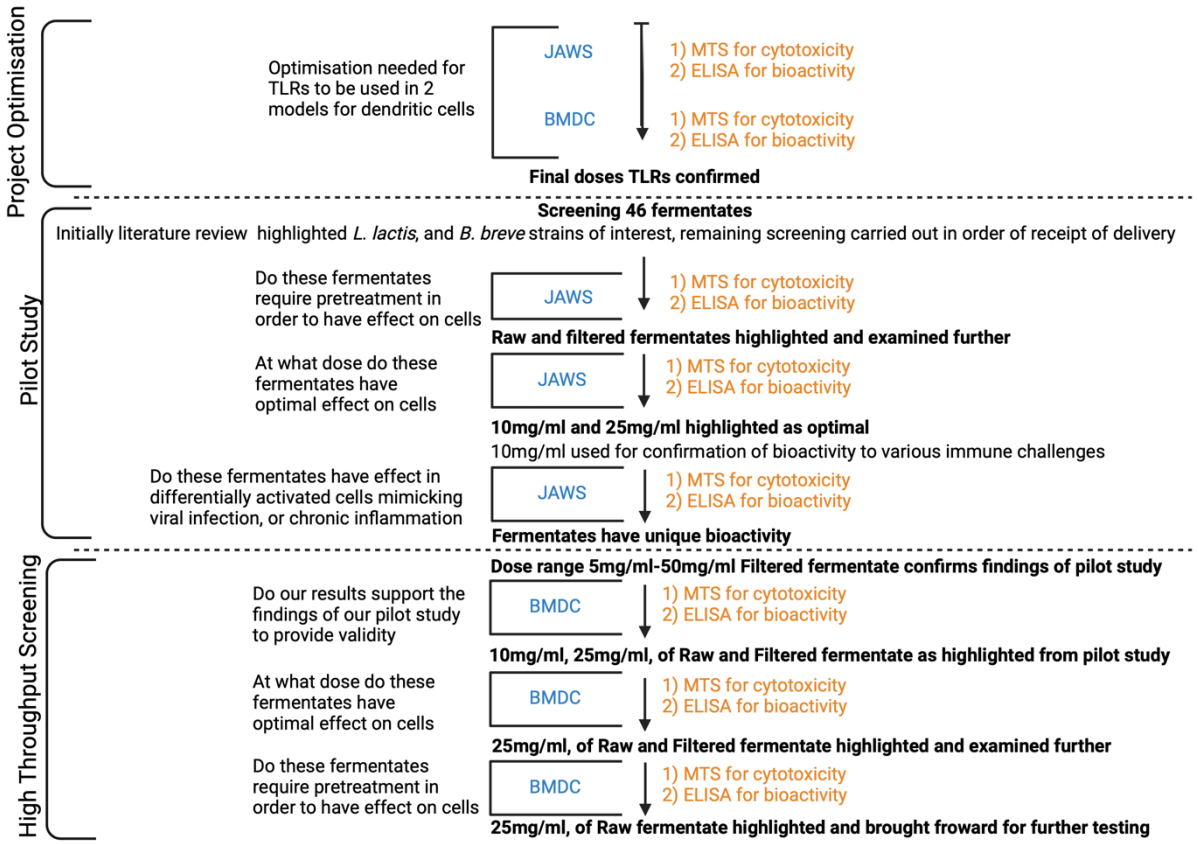

*Figure 46:**Schematic representation of Chapter 3 workflow.** Initially a project optimisation was carried out to confirm concentrations of TLRs needed for cell viability, and cytokine secretion in JAWS cell and BMDCs. Fermentates were then screened via pilot study to determine pre-treatment needed for fermentate bioactivity, as well as dose for optimal cytokine secretion and cell viability. Screening with a panel of TLRs determined unique specificity and bioactivity of fermentates. High throughput screening in BMDCs commenced starting with a confirmation of pilot study results. 10mg/ mL, and 25mg/ mL dose of raw and filtered sample confirmed as optimal for immune boosting bioactivity. Further screening deduced 25mg mL raw or filter sample as optimal for bioactivity. Screening of all fermentates confirms that raw fermentate is best for optimal viral immunological responses. Cells used highlighted in blue, assay highlighted in orange and section outcomes highlighted in **bold**. Created using BioRender.com.*

In order to fully assess the immunomodulatory properties of the bank of fermentates a number of steps had to be followed. The first of these steps was to assess if there was any bioactivity in a cell line that was easy to use i.e. the JAWS cell line, having established optimal TLR concentrations for immune response induction as part of the project optimisation. After the project optimisation, an initial pilot study was carried out in these cells which clearly showed that there was activity in the fermentates. This included a number of steps to optimise a number of different parameters of the fermentates. The first step was based on previous work conducted in the lab whereby the form of preparation that the sample underwent effected the bioactivity of the sample. Previous research in the lab involved sample preparation whereby the sample underwent either centrifugation, filtration, centrifugation combined with filtration, or was left raw unprocessed prior to sample addition to cells. Again due to the exploratory nature we used 10mg/ mL of fermentate in order to assess pre-treatment required for fermentates, as this was the dose previously found to be optimal for milk hydrolysate studies, as well as ensuring stocks were preserved for further downstream assessment. As this was the first time such fermentate samples had been tested on within this laboratory, a similar approach for sample preparation was carried out. Previous work with milk hydrolysates required filtration of sample in order to observe bioactivity, as the filtration of sample is based on size, and only the smaller particles resulted in bioactivity. My findings were also similar to that of the milk hydrolysates in that the centrifugation, and filtered and centrifugation, resulted in decreased bioactivity. In contrast, my findings resulted in decreased bioactivity when the sample was filtered also, with only the raw sample maintaining optimal bioactivity. This is due to the fact that the fermentate sample is much larger in size, and filtering effectively removes the bioactive components present, resulting in altered bioactivity with decreased cytokine output. This means that the resulting bioactivity was as a result of larger particles present in the sample that would've been largely filtered out by the 0.2um filter. However, in order to provide every sample with the best chance of having observed activity, treating them each as unique compounds, the filtered version of the sample continued to be assessed, in order provide contrast, as well as ensuring no bioactivity was lost. DPC1178 and DPC1817 are good examples of

how filtration of fermentates resulted in the decrease of bioactivity at both the 10mg/ mL and 25mg/ mL doses compared to when fermentates are left raw (Figure 40 and Figure 41). Samples LC10, Aerobic R0033, Anaerobic R0033, Aerobic R0070 and Anaerobic R0070 clearly demonstrated that filtering of the sample results in bioactivity similar to, or often less than that of the filtered RSM, and thus filtering samples is of no further interest beyond this screening chapter (Figure 43). Both filtered and raw samples were assessed for bioactivity on all 46 samples to ensure that no sample by either processing stage was overlooked for initial screening as each novel fermentate was treated as a unique compound with bioactive potential in both pretreated forms.

The fact that the sample had enhanced bioactivity when unprocessed impacts the final sample that will be produced at the manufacturing stage. Fermentates that are needed raw are much easier to produce, requiring less manufacturing time and costs, with overall less processing. Raw unprocessed samples are considered the best final ingredient for industry needs, as well as being the most bioactive in the case of such fermentates.

Similarly, having determined that the raw and filtered samples were to be studied beyond the pilot study, the next step was to confirm the optimal dose at which these fermentates had this bioactivity. This involved the assessment of the effect of the dose of the sample whereby previous work in the lab had demonstrated that different bioactive samples required different doses for optimal bioactivity. Original dose range from 5mg/ mL-50mg/ mL was examined to establish a dose at which optimal bioactivity could be obtained. Previous studies in the laboratory established milk hydrolysates with optimal doses of 10mg/ mL. However the fermentates being a new unstudied material in the laboratory showed a range of 10mg/ mL, 25mg/ mL, and 50mg/ mL for optimal bioactivity, with 5mg/ mL and 50mg/ mL resulting in little bioactivity. Therefore, for the high throughput screening phase we narrowed this dose range to include two doses of 10mg/ mL and 25mg/ mL, in the interest of commercial production and based on previous lab research where 10mg/ mL sample had previously resulted in optimal bioactivity.

The final stage of the pilot study involved the assessment of the fermentates when activated by a number of different TLRS. This examination allowed us to confirm that the bioactivity observed from the fermentates was in fact unique, and specific to the novel fermentate depending on the immune scenario they were challenged with.

Having established that the 10mg/ mL, and 25mg/ mL doses of raw and filtered samples were to be brought for the high throughput screening in the primary cells BMDCs, a better representation of how the fermentates behaved *in vivo*, we first needed to confirm their bioactivity in this cell. To do this we examined the total dose range of 5-50mg/ mL filtered fermentate, where we confirmed the findings of the pilot study where the 10mg/ mL and 25mg/ mL fermentate provided optimal bioactivity.

From here we then proceeded with the high throughput screening phases where we examined a large portion of the fermentates at the 10mg/ mL, and 25mg/ mL doses of raw and filtered fermentates. We further established that the 25mg/ mL dose of fermentate was optimal for bioactivity, and thus going forward the 25mg/ mL raw and filtered fermentate was examined for the remaining high through put screening of samples. We continued to include the raw and filtered versions of the fermentate to ensure no bioactivity was being missed, treating each individual fermentate as a unique compound with the potential to impact on bioactivity dependant on pretreatment used.

Our fermentates showed consistent effects on the secretion of cytokines associated with viral immunity as this was the main focus of the project at this time. LOX was used in order to mimic an immune response to a viral particle, in order to determine which samples could enhance the immune response to viral invasion through an increase in viral specific cytokines, which samples would have no effect on cytokines, and which samples would suppress cytokine secretion. Our fermentates had the ability to increase key viral associated cytokines including IL-6, and TNF-α, IL-12p40, and IL-23 while simultaneously supporting small increases In anti-inflammatory IL-10 which is important to provide immune homeostasis.

Viral infections like that of COVID-19 are characterised by increases in pro-inflammatory IL-6, TNF-α, IL-12p40, and IL-23 (Hasanvand, 2022; Montazersaheb et al., 2022), while the flu and HIV-1 are characterised by increased IL-1β, IL-6, and TNF-α (Brydon et al., 2005; Kedzierska & Crowe, 2001). These cytokines are released in an attempt from the immune system to prevent or resolve the infection caused by the invading virus and clear it from the host. As outlined in Chapter 1, IL-6, TNF-α, IL-12p40 and IL-23 are proinflammatory cytokines with key immunomodulatory and anti-viral roles, including supporting CD4+ and CD8+ cell differentiation, B cell activation, promoting additional cytokine secretion, inhibition of viral replication, leukocyte trafficking, immune complex clearance, and defence of intracellular organisms against invading viruses and pathogens (Atzeni & Sarzi-Puttini, 2013; Bae et al., 2016; Harrington et al., 2005; Horiuchi et al., 2010; Rook et al., 1991; Ruby et al., 1997; Seo & Webster, 2002a; Tanaka et al., 2014). When increased to a small degree IL-10 plays a supportive role in viral clearance, through regulation of the adaptive immune response and IL-10 secreting T cells (Kawashima et al., 2018; Rojas et al., 2017). Thus, through increasing the production of such cytokines in the body of an otherwise healthy individual, one can assume that an enhanced immune response will be elicited, and subsequent removal of invading virus particles can occur, with increased overall viral immunity against such pathogens. Other cytokines examined are included for holistic view of fermentates effect on cytokine profile, but are not considered as important for viral immunity (as highlighted in Table 2).

My findings show that in the context of fermentates as immunomodulators, samples SC40, Aerobic R0033, Anaerobic R0033, and R0419, enhance the immune response to viral particles, in a dose specific manner. Increased secretion of key viral associated cytokines IL-6, TNF-α, IL-12p40, IL-23, resulted in the presence of 25mg/ mL Raw Aerobic R0033, and Raw Anaerobic R0033, with additional increases in general immunity associated cytokines IL-1β, IL-10, IL-12p70 and IL-27 (Figure 43). Increased secretion of key cytokines IL-6, TNF-α,and IL-23, results in the presence of 25mg/ mL Raw R0419, with additional increases for IL-1β (Figure 45). Increased secretion of key cytokines IL-6, TNF-α, and IL-12p40, results in the

presence of 25mg/ mL Filtered SC40, with additional increases for IL-1β, IL-10, and IL-27 (Figure 32). Already knowing that filtering reduces bioactivity, one can assume that SC40's antiviral capabilities exceed this of the filtered, and thus are to be investigated further.

The literature clearly documents the viral immune boosting capabilities of other compounds through cytokine modulation similar to that seen in our data. In a randomized, double-blind, placebo-controlled clinical trial by Kawashima et al., five strains of LAB were assessed, with *Pediococcus acidilactici* K15, shown to increase levels of both IL-6 and IL-10, ultimately increasing sIgA concentrations at mucosal sites in humans, aiding in host defence against pathogens and maintaining symbiosis with microorganisms present in the small intestine (Kawashima et al., 2018). In a recent study by Zhu et al., Jasmin, found in the Chinese herbal medicine of Jasmin tea, was found to have antiviral activity *in vitro* (X. Zhu et al., 2022). Increased production of TNF-α from RAW 264.7 cells in the presence of Jasmin resulted at higher concentrations of the compound , ultimately showing antiviral activity against HSV-1 shown via a plaque reduction assay (X. Zhu et al., 2022). Other studies by Takeda et al. showed that LAB, in particular strain *Lactobacillus plantarum* 06CC2, from Cow cheese, increased the production of IL-12, and IL-12p40 *in vitro* and *in vivo* (Takeda et al., 2013). *Lactobacillus plantarum* 06CC2 has been associated with the enhancement of the Th1 response, and resulted in the alleviation of influenza virus infection in mice (Takeda et al., 2011). Panax ginseng Meyer, or white ginseng, has the ability to increase for IL-1β, IL-6, TNF-α, and IL-23, via activation of the MAPK kinase (MKK)4-c-Jun N-terminal kinase (JNK)-c-Jun signalling pathway. (T.-G. Lim et al., 2016; Um et al., 2020). This is important considering viral infections like that of the influenza virus decrease innate IL-23 and IL-12p70 concentrations, to ultimately decrease IL-17 and IFN- γ responses, making the host more susceptible to further infection (Loughran et al., 2018).

Thus as the literature demonstrates, many natural food ingredients have been shown to increase cytokines IL-6, TNF-α, IL-12p40, IL-23 as well as smaller increases in IL-10, supporting viral clearance and protection of host from invading pathogens. Ergo, suggesting that fermentates SC40, Aerobic R0033, Anaerobic

R0033, and R0419 have the potential to act as an antiviral, supporting the hosts defence against viral infection due to their ability to increase these antiviral immune boosting cytokines. Furthermore, this specificity seen, whereby the samples increase some of the cytokines examined but not all, is critical in establishing a sample that is targeted to the clearance of viral pathogens, and not just generally immune boosting for all cytokines.

Thus the overall aim of this study was to screen the fermentate samples for immunomodulatory activity in order to establish whether some of the fermentates could boost the immune response to a virus. The LAB strains used to generate the unique fermentates that enhance key components associated with viral immunity, contrasts the hypothesised strains of LAB expected to boost viral immunity identified in the literature review carried out prior to commencement of the pilot study. As not all 46 samples were received at the same starting point, this literature review allowed for the targeted analysis of hypothesised viral enhancing immunomodulatory fermentates received from the large initial batch, which was then followed by smaller batches of samples analysed at the rate of production. The literature review revealed that *L.lactis* and *B.breve*, which were two of the strains received, were of particular interest due to their already well documented antiviral immunomodulatory properties. These two strains have demonstrated critical antiviral activity for protection against viruses including common colds, seasonal influenza, respiratory viruses, as well as for the coronavirus (Fujii et al., 2017; Jounai et al., 2015; Shibata et al., 2016; Sugimura et al., 2013, 2015). Therefore we proposed that samples SC15, SC16, SC17, SC18, SC51, SC52, SL119, R1058, Aerobic and Anaerobic R0070 were to be brought forward for initial testing based on the literature. Additionally, in collaboration with colleagues working in UCD samples SC6, SC15, SC17 and SC40 were highlighted as anti-inflammatories for the purpose of their research into candidate samples with anti-inflammatory effect. Thus we prioritised these samples also for a holistic view of the fermentates true immunomodulatory capabilities.

However having conducted the total screening of all 46 fermentates we found that in contrast to the hypothesised *L.lactis* and *B.breve* strains, we found that *Lb. delbrueckii* (SC40), and *Lb helveticus* (R0419, Aerobic R0033, and Anaerobic R0033) strains were in fact of most interest due to their viral immune boosting properties. Interestingly, upon further investigation of the literature we found that these strains also had documented antiviral properties. *Lb. delbrueckii* has been found to have antiviral activity against influenza, and other viruses including New Castle disease virus, as well as increasing natural killer cell activity in elderly populations experiencing respiratory tract viruses (Makino et al., 2010; Öztürk & Özel, 2020; Saeed et al., 2007; Serkedjieva et al., 2000). Interestingly, *Lb. helveticus* was found to have only limited documented antiviral properties including the ability to reduce disease severity of rotavirus, and trends in the reduction of influenza like illness in the elderly (Azagra-Boronat et al., 2020; Koesnoe et al., 2021). While in contrast it has been reported to have little to no effect on viral induced acute gastroenteritis (Freedman et al., 2020). *Lb. helveticus* was however well documented as an anti-inflammatory compound to aid in inflammatory conditions including arthritis, and a suggested role in enhancing gut microbiota and treatment of UC through increased anti-inflammatory cytokine secretion (Farahmnandi et al., 2023; C. Huang et al., 2023; Yamashita et al., 2017). Furthermore *Lb. helveticus* is also long documented for its antihypertensive function (Jauhiainen et al., 2005; Maeno et al., 1996).

In this chapter we have now determined that novel fermentates generated from these strains of LAB have immune boosting bioactivity in support of viral immunity. We concluded from this screening that the optimal dose for further analysis at the phase 2 fermentate screening (Chapter4) is a 25mg/ mL dose of raw fermentate. SC40, R0419, Aerobic R0033, and Anaerobic R0033. SC40, R0419, Aerobic R0033, and Anaerobic R0033 were found to enhance bioactivity in support of viral immunity through the enhanced secretion of viral immunity associated cytokine IL-6, TNF-α, IL-12p40, IL-23. This was of critical importance for the establishment of the appropriate fermentate model and for the successful continuation of the in depth study on the now highlighted viral immune boosting fermentates.

4 Chapter 4

Phase 2 Fermentate Screening

4.1 Introduction

As part of the initial screening phase, 4 samples were identified to be of interest as immune boosting fermentates for enhancement of viral immunity. These samples were Aerobic R0033, Anaerobic R0033, SC40, and R0419. Therefore at this point in the project the next step was to carry out a more extensive investigation of these 4 fermentates in order to get a more in depth view of these samples and their bioactivity. The first objective of this chapter was to investigate the sample's activity in a range of immune cells to include both dendritic cells and macrophage. Both of these cell types are critical to immune regulation and protection from viral infection, which was induced via immune cell activation with LOX or PIC. Choosing an additional immune cell allowed us to assess our fermentates in another key innate immune cell the macrophage, which are critical to proper immune function. Thus examining the effect of our fermentates on these cells was important to ensure overall first line immune defences were not hindered in the presence of the fermentates which could otherwise be detrimental to the host. In addition to this, our investigation was expanded to include screening of the samples' effects on cells when challenged with inflammatory stimuli, which mimics an immune response similar to that seen in chronic inflammation, induced via immune cell activation with LPS or CpG. This enabled us to have a more holistic view of the fermentates' potential as both immune boosting and/or anti-inflammatory fermentates. This allowed us to assess the specificity of the samples, assessing the unique context dependant bioactivity in the presence of viral or inflammatory challenges. Narrowing the investigation to 4 samples allowed us also to analyse additional parameters affected by the fermentates. The second objective of our investigation was therefore to include not only the cytokine profiles in dendritic cells as provided in the initial screening, but to also include cytokine profiles in macrophage, chemokine profiles in dendritic cells and macrophage, effects on phagocytosis in macrophage, as well as effects on cell surface marker expression in macrophage, all in response to both viral and inflammatory immune challenges.

4.2 Chapter aims:

The purpose of this chapter was to investigate further the 4 immune boosting fermentates identified during the initial viral challenge screening, at a dose of 25mg/mL raw fermentate highlighted as the optimal fermentate model in the previous chapter. Samples were assessed in primary dendritic cells BMDC, and macrophage in both the cell line J774s and the primary cells BMDM. There were two main objectives:

1) To establish whether our samples Aerobic R0033, Anaerobic R0033, SC40 and R0419 had similar effects in additional innate immune cells when these cells were activated through a variety of different TLRs, mimicking different immune scenarios (Figure 47).
2) To explore further the effects of our samples Aerobic R0033, Anaerobic R0033, SC40 and R0419 on macrophage function by examining their effects on phagocytosis, cell surface marker expression and chemokine secretion (Figure 48).

The specific objectives included:

- Assessment of cytotoxicity of the fermentates in BMDCs, J774.A.1s, and BMDMs to ensure that samples were not negatively impacting on cell viability.
- Assessment of the effects of the fermentates in BMDCs when challenged with a range of TLRs mimicking both viral and inflammatory challenges to the cell.
- Assessment of cytokine secretion in both J774.A.1s and BMDMs with a range of immune challenges.
- Assessment of the effects of fermentates on phagocytosis and cell surface marker expression in J774.A.1 cells.
- Assessment of the effects of fermentates on chemokine secretion in BMDM.

Data gathered from this analysis established the candidate samples that were to be brought forward for investigation as the most promising fermentates with immune boosting capabilities.

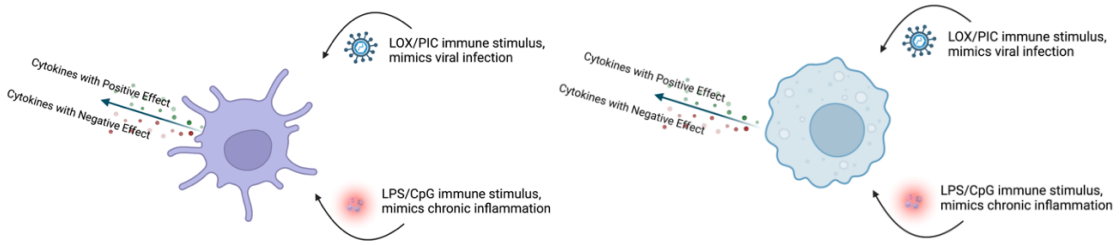

*Figure 47:**Summary of Chapter 4 Aims for objective 1**. Assessing effect of sample presence on cytokine secretion profiles in dendritic cells (purple), and macrophage (blue), when activated with viral immune stimulus LOX/PIC or inflammatory stimulus LPS/CpG.*

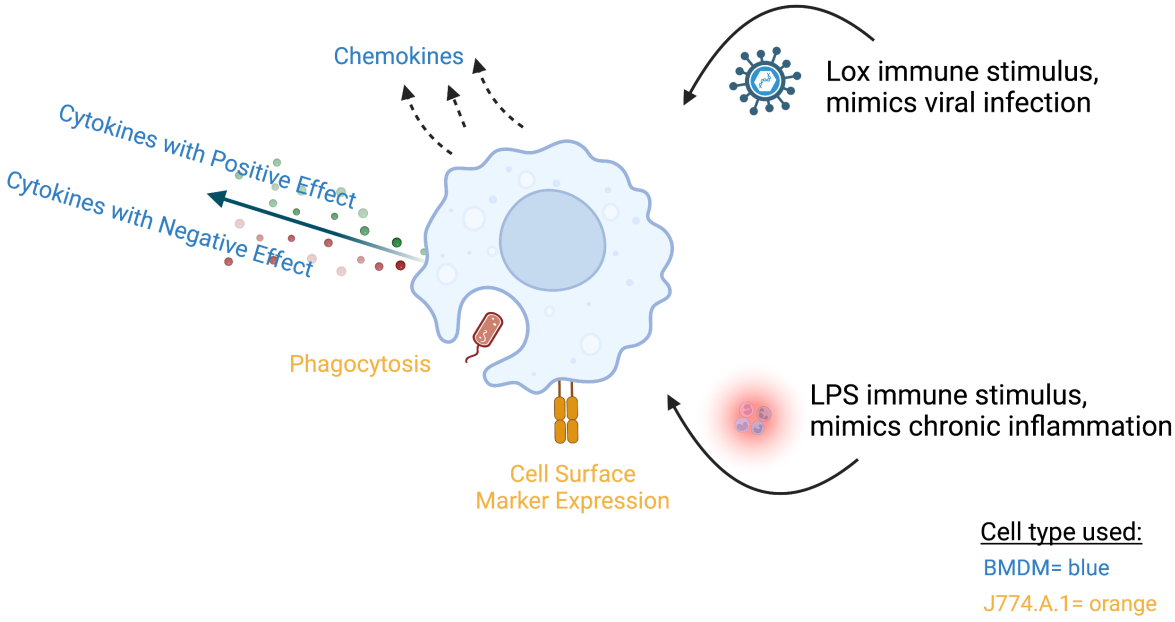

Figure 48**: Summary of Chapter 4 Aims for objective 2**. *Assessing effect of sample presence on cytokine/chemokine secretion profiles, phagocytosis, and cell surface marker expression, in macrophage, when activated with viral immune stimulus LOX or inflammatory stimulus LPS.*

4.3 Results

4.3.1 Round 2 screening of top 4 candidate immune boosting fermentates

4.3.1.1 BMDC screening

Initially we wanted to expand on the immune scenarios which were used to activate the cells mimicking a variety of immune scenarios. Firstly in order to do so and expand the scope of assessment of fermentate function, we examined fermentates in response to an additional viral immune stimulus, PIC, as well as inflammatory immune scenario inducers LPS, and CpG. LPS and CpG mimic inflammation characteristic of that seen in inflammatory disorders like UC, and CD. Due to the availability of resources in the lab PIC, and CpG were also included providing additional information to our analysis of fermentate function, however LOX and LPS were the two key contrasting immune stimuli of interest. Therefore, we next examined a direct contrast between specificity of fermentates and unique bioactivity, in LOX and LPS activated cells. For the purpose of this assessment we included fermentates highlighted in the initial screening to be of little interest for boosting viral immunity, or had little to no bioactivity. This allowed us to confirm the 4 viral immune boosting fermentates unique bioactivity and not general bioactivity induced via the presence of any fermentate following any immune stimulus.

4.3.1.1.1 Stimulation of LOX, LPS, CpG, and PIC activated BMDCs with 25mg/mL raw samples doesn't affect cell viability

BMDC were seeded at a concentration of $1x10^6$ cells/mL, incubated for 24 hours before stimulating with a dose of 25mg/mL raw fermentate sample for 1 hour followed by various TLR ligands as follows: LOX 0.5mM, LPS 100ng/mL, CpG 5 µM, and PIC 10µg/mL, and subsequently incubated at 37^0C in 5% CO_2. After 24 hours an MTS assay was performed as previously outlined (section 2.2.13 MTS Cell Viability Assay).

Figure 49 and Figure 50 demonstrates that there was no significant change in cell viability following exposure of the cells to 25mg/mL raw fermentate when stimulated with LOX, LPS, CpG or PIC. The RSM acted as the whole fermentate control for comparison of effects induced by each independent sample. The use of the positive control of 10% DMSO provided a clear distinction between the cytotoxic effects on cell viability with the untreated control sample, as DMSO induced cell death.

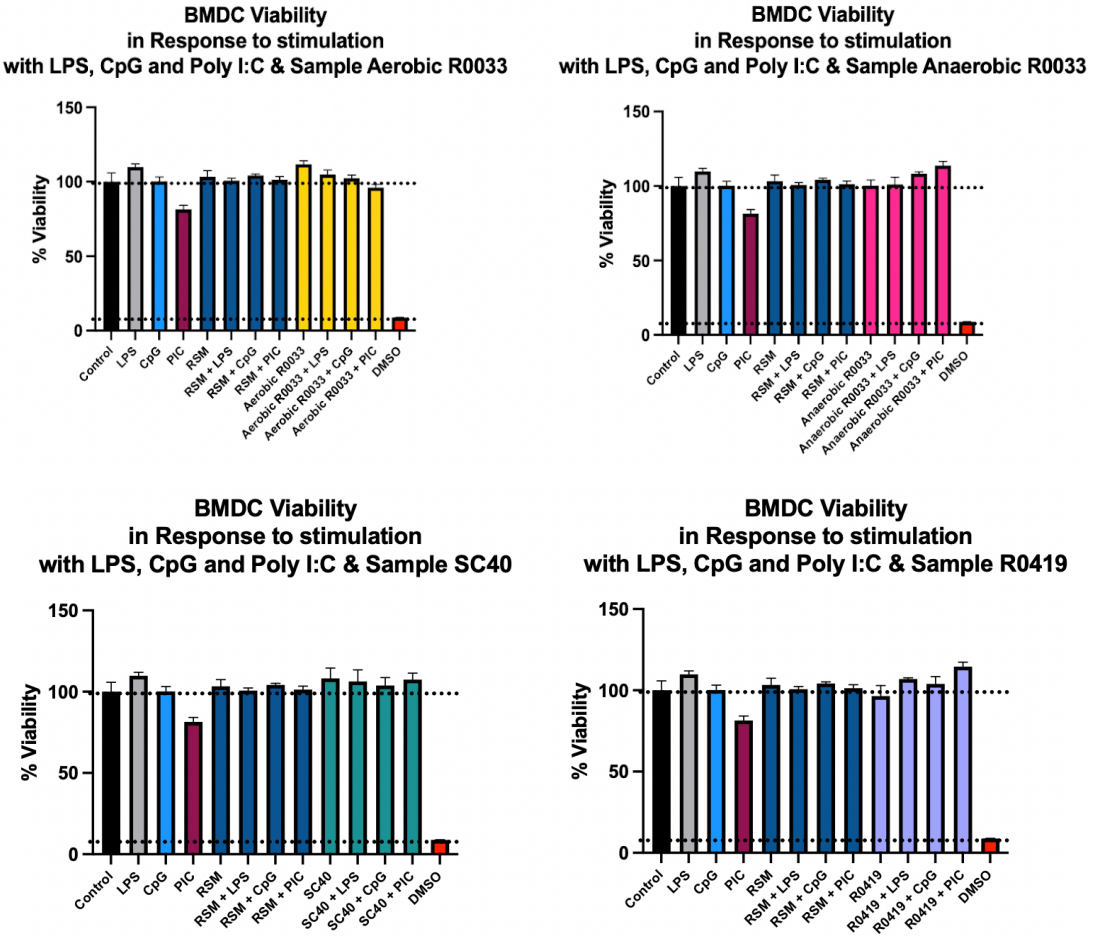

Figure 49: ***Exposure of BMDC to LPS, CpG, and PIC TLRs and 25mg/mL raw immune boosting fermentates doesn't affect cell viability****. BMDC cells were seeded at 1x10⁶ cells/mL and left overnight at 37°C in 5% CO_2. The following day cells were stimulated with 25mg/mL Aerobic R0033, Anaerobic R0033, SC40 and R0419, incubated for 1 hour at 37°C in 5% CO_2 and subsequently exposed to the following concentrations of TLRs: LPS 100ng/mL, CpG 5 µM, PIC 10µg/mL for TLR activation before incubating overnight under the same conditions. RSM is the fermentate control. 10% DMSO was included as a positive control to induce cell death. Cells were incubated with MTS cell titre aqueous one solution for 3 hours at 37°C in 5% CO_2. Viability is represented as a percentage compared to viable, untreated cells (Control). Data is presented as mean ± SD of three replicates.*

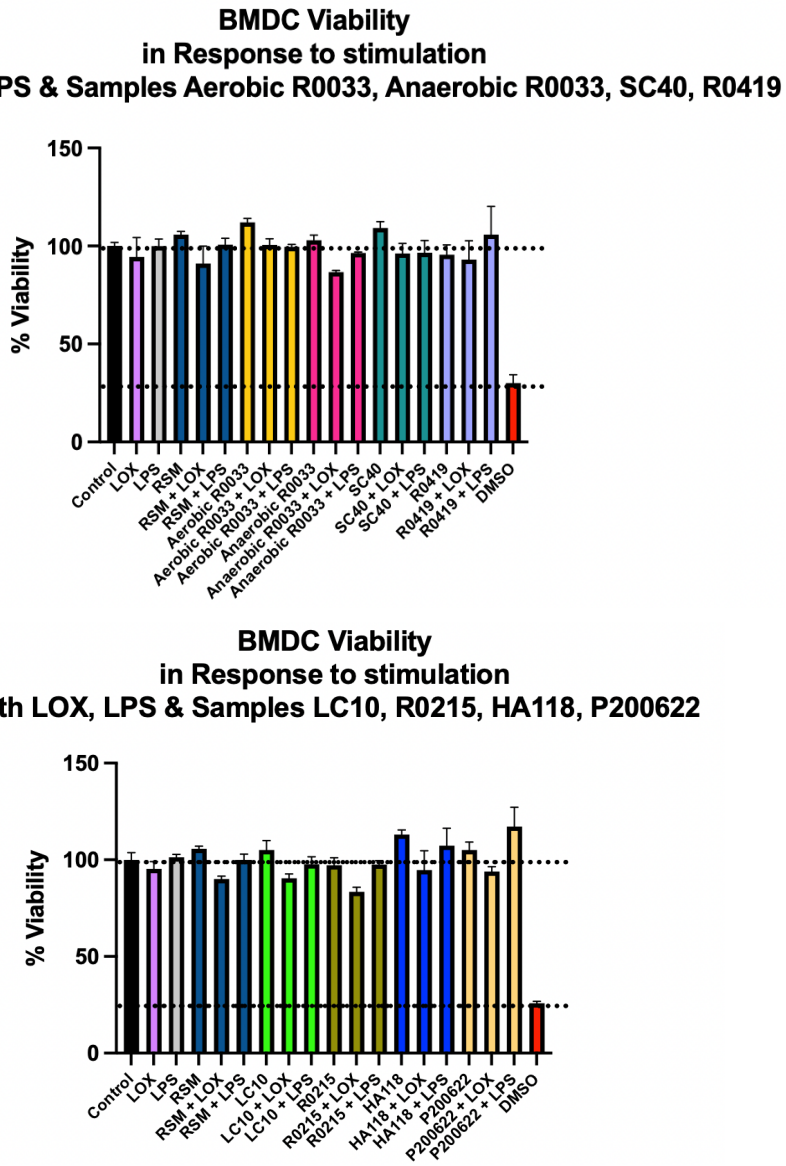

*Figure 50:**Exposure of LOX and LPS activated BMDC to 25mg/mL raw samples doesn't affect cell viability.** BMDC cells were seeded at 1x10⁶ cells/mL and left overnight at 37°C in 5% CO_2 The following day cells were stimulated with 25mg/mL sample fermentate, incubated for 1 hour at 37°C in 5% CO_2 and subsequently exposed to the following concentrations of TLRs: LOX 0.5mM, LPS 100ng/mL for TLR activation before incubating overnight under the same conditions. RSM is the fermentate control. 10% DMSO was included as a positive control to induce cell death. Cells were incubated with MTS cell titre aqueous one solution for 3 hours at 37°C in 5% CO_2. Viability is represented as a percentage compared to viable, untreated cells (Control). Data is presented as mean ± SD of three replicates.*

4.3.1.1.2 Stimulation of LPS, CpG and PIC activated BMDCs with 25mg/mL raw samples Aerobic R0033, Anaerobic R0033, SC40 and R0419 effects cytokine secretion

BMDC were seeded at a concentration of $1x10^6$ cells/mL, incubated for 24 hours before stimulating with a dose of 25mg/mL raw fermentate sample for 1 hour followed by various TLR ligands as follows: LPS 100ng/mL, CpG 5 µM, PIC 10µg/mL and subsequently incubated at 37^0C in 5% CO_2. After 24 hours supernatants were removed and ELISA procedure for cytokines IL-1β, IL-6, IL-10 , TNF-α, IL-12p40, IL-12p70, IL-23 and IL-27 was performed according to the manufacturer's instructions (section 2.2.14 Enzyme Linked Immunosorbent Assay (ELISA)).

Figure 51 - Figure 54 demonstrates that samples significantly affected the secretion of cytokines in response to immune challenges LPS, CpG, and PIC, when compared to the RSM. IL-1β, IL-6 , TNF-α and IL-27 were significantly increased in the presence of LPS ($p<0.002$; $p<0.001$; $p<0.033$; $p<0.001$), IL-6, IL-10, TNF-α, IL-12p40, IL-23 and IL-27 were increased in the presence of CpG ($p<0.001$) and, IL-27 is increased in the presence of PIC ($p<0.001$).

In the presence of Aerobic R0033, LPS activated cells had significantly increased IL-1β ($p<0.001$). CpG activated cells had significantly increased IL-1β, TNF-α ($p<0.001$), IL-6 and IL-12p70 ($p<0.002$). PIC activated cells had significantly increased IL-1β, IL-6, TNF-α and IL-27 ($p<0.001$). Aerobic R0033 alone significantly increased IL-1β, TNF-α ($p<0.001$) and IL-6 ($p<0.002$).

In the presence of Anaerobic R0033, LPS activated cells had significantly increased IL-1β, IL-6, TNF-α ($p<0.001$), and IL-23 ($p<0.002$). CpG activated cells had significantly increased IL-6 ($p<0.002$) and TNF-α ($p<0.033$), while having decreased IL-12p40 ($p<0.001$). PIC activated cells had significantly increased IL-6, IL-10 , TNF-α, IL-27 ($p<0.001$), and IL-1β ($p<0.033$). Anaerobic R0033 alone significantly increased TNF-α, IL-23 ($p<0.001$), IL-6 ($p<0.002$), IL-1β and IL-27 ($p<0.033$).

In the presence of SC40, LPS activated cells had significantly increased IL-1β, IL-10, TNF-α ($p<0.001$), IL-6 ($p<0.033$) and IL-27 ($p<0.002$). CpG activated cells had significantly increased IL-1β, IL-10 ($p<0.001$), with decreased IL-12p40, IL-12p70, IL-27 ($p<0.001$) and IL-23 ($p<0.033$). PIC activated cells had significantly

increased IL-1β, IL-6, IL-10, TNF-α ($p<0.001$), IL-23 and IL-27 ($p<0.002$). SC40 alone significantly increased IL-1β, IL-6, IL-10, TNF-α and IL-27 ($p<0.001$).

In the presence of R0419, LPS activated cells had significantly increased IL-10 ($p<0.001$), TNF-α and IL-27 ($p<0.033$). CpG activated cells had significantly increased IL-23 ($p<0.002$), with decreased IL-12p40, IL-12p70 ($p<0.001$), and IL-27 ($p<0.002$). PIC activated cells had significantly increased IL-6, IL-10, TNF-α and IL-27 ($p<0.001$). R0419 alone significantly increased IL-6, TNF-α, IL-27 ($p<0.001$), IL-1β and IL-10 ($p<0.002$).

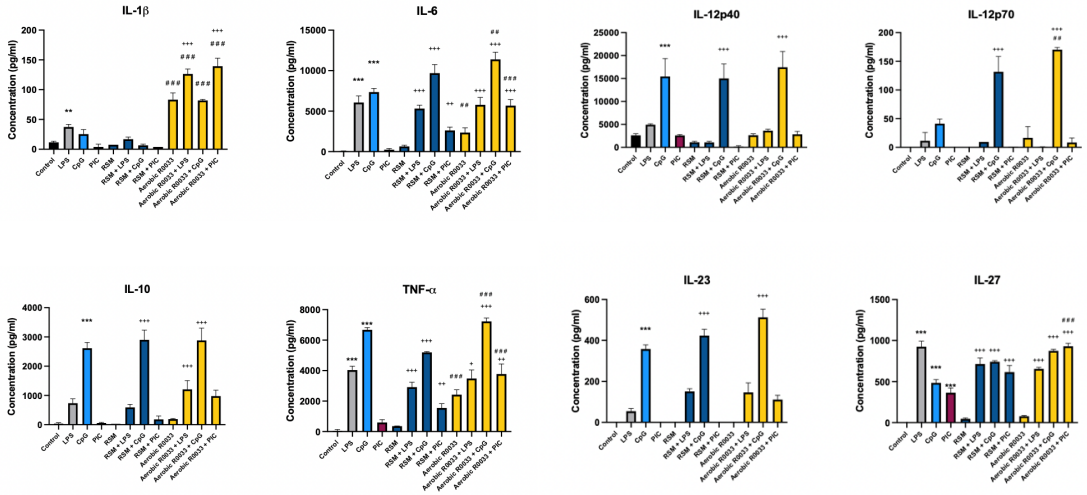

Figure 51: ***Exposure of LPS, CpG and Pic activated BMDC to 25mg/mL raw sample Aerobic R0033 results in the secretion of cytokines IL-1β, IL-6, IL-10, TNF-α, IL-12p40, IL-12p70, IL-23 and IL-27.*** *BMDC cells were seeded at 1x10⁶ cells/mL and left overnight at 37°C in 5% CO_2. The following day cells were stimulated with 25mg/mL raw sample fermentate, incubated for 1 hour at 37°C in 5% CO_2 and 5% CO_2 and subsequently exposed to the following concentrations of TLRs: LPS 100ng/mL, CpG 5 µM, PIC 10µg/mL for TLR activation before incubating overnight under the same conditions. RSM is the fermentate control. Supernatants were removed after 24 hours and ELISA was performed for cytokines IL-1β, IL-6, IL-10, TNF-α, IL-12p40, IL-12p70, IL-23 and IL-27. Data is presented as mean ± SD of three replicates. Significance determined using one- way ANOVA with a Newman-Keuls post-test. Output P value style APA: .12 (ns), .033 (*), .002(**) and <.001 (***); 1) comparing unstimulated control cells to each TLR stimulated cell "*", 2) comparing sample + TLR to unstimulated sample cells "+" and 3) comparing TLR + sample to the each respective TLR + RSM counterpart "#".*

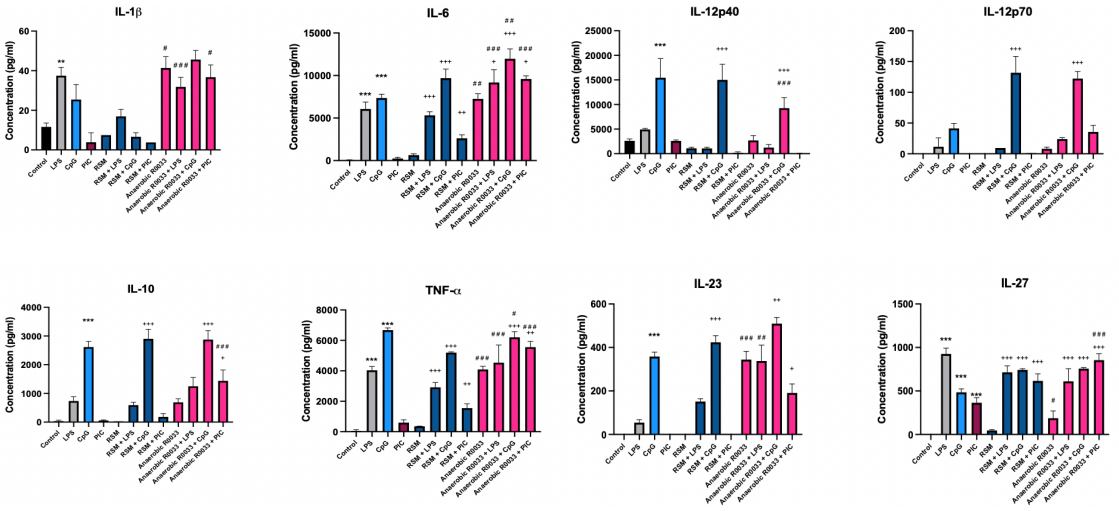

Figure 52: ***Exposure of LPS, CpG and Pic activated BMDC to 25mg/mL raw sample Anaerobic R0033 results in the secretion of cytokines IL-1β, IL-6, IL-10, TNF-α, IL-12p40, IL-12p70, IL-23 and IL-27.*** *BMDC cells were seeded at 1x10⁶ cells/mL and left overnight at 37°C in 5% CO_2. The following day cells were stimulated with 25mg/mL raw sample fermentate, incubated for 1 hour at 37°C in 5% CO_2 and % CO_2 and subsequently exposed to the following concentrations of TLRs: LPS 100ng/mL, CpG 5 µM, PIC 10µg/mL for TLR activation before incubating overnight under the same conditions. RSM is the fermentate control. Supernatants were removed after 24 hours and ELISA was performed for cytokines IL-1β, IL-6, IL-10, TNF-α, IL-12p40, IL-12p70, IL-23 and IL-27. Data is presented as mean ± SD of three replicates. Significance determined using one- way ANOVA with a Newman-Keuls post-test. Output P value style APA: .12 (ns), .033 (*), .002(**) and <.001 (***); 1) comparing unstimulated control cells to each TLR stimulated cell "*", 2) comparing sample + TLR to unstimulated sample cells "+" and 3) comparing TLR + sample to the each respective TLR + RSM counterpart "#".*

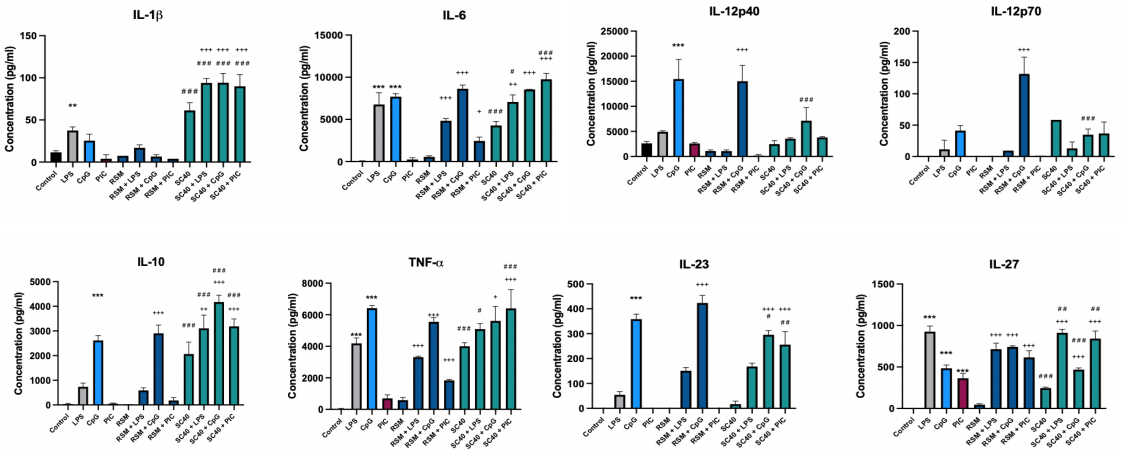

*Figure 53:**Exposure of LPS, CpG and Pic activated BMDC to 25mg/mL raw sample SC40 results in the secretion of cytokines IL-1β, IL-6, IL-10, TNF-α, IL-12p40, IL-12p70, IL-23 and IL-27.** BMDC cells were seeded at 1x10^6 cells/mL and left overnight at 37°C in 5% CO_2 The following day cells were stimulated with 25mg/mL raw sample fermentate, incubated for 1 hour at 37°C in 5% CO_2 and % CO_2 and subsequently exposed to the following concentrations of TLRs: LPS 100ng/mL, CpG 5 µM, PIC 10µg/mL for TLR activation before incubating overnight under the same conditions. RSM is the fermentate control. Supernatants were removed after 24 hours and ELISA was performed for cytokines IL-1β, IL-6, IL-10, TNF-α, IL-12p40, IL-12p70, IL-23 and IL-27. Data is presented as mean ± SD of three replicates. Significance determined using one- way ANOVA with a Newman-Keuls post-test. Output P value style APA: .12 (ns), .033 (*), .002(**) and <.001 (***); 1) comparing unstimulated control cells to each TLR stimulated cell "*", 2) comparing sample + TLR to unstimulated sample cells "+" and 3) comparing TLR + sample to the each respective TLR + RSM counterpart "#".*

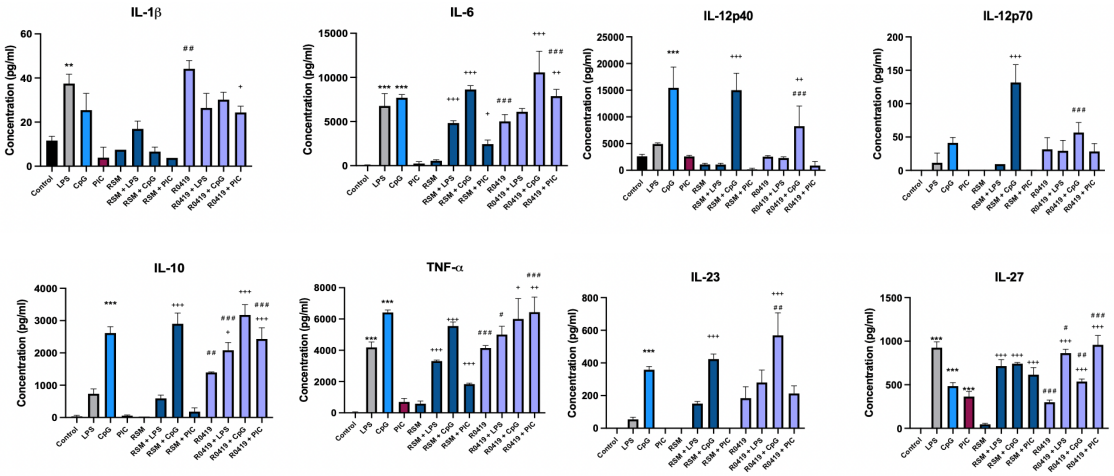

Figure 54: ***Exposure of LPS, CpG and Pic activated BMDC to 25mg/mL raw sample R0419 results in the secretion of cytokines IL-1β, IL-6, IL-10, TNF-α, IL-12p40, IL-12p70, IL-23 and IL-27.*** *BMDC cells were seeded at 1x10^6 cells/mL and left overnight at 37°C in 5% CO_2. The following day cells were stimulated with 25mg/mL raw sample fermentate, incubated for 1 hour at 37°C in 5% CO_2 and % CO_2 and subsequently exposed to the following concentrations of TLRs: LPS 100ng/mL, CpG 5 µM, PIC 10µg/mL for TLR activation before incubating overnight under the same conditions. RSM is the fermentate control. Supernatants were removed after 24 hours and ELISA was performed for cytokines IL-1β, IL-6, IL-10, TNF-α, IL-12p40, IL-12p70, IL-23 and IL-27.. Data is presented as mean ± SD of three replicates. Significance determined using one- way ANOVA with a Newman-Keuls post-test. Output P value style APA: .12 (ns), .033 (*), .002(**) and <.001 (***); 1) comparing unstimulated control cells to each TLR stimulated cell "*", 2) comparing sample + TLR to unstimulated sample cells "+" and 3) comparing TLR + sample to the each respective TLR + RSM counterpart "#".*

Table 23 summarises these effects of Aerobic R0033, Anaerobic R0033, SC40, and R0419 on BMDCs challenged with each different immune stimulus.

Table 23: ***Summary table of the cytokines produced by BMDC cells activated with LOX, PIC, LPS, and CpG, in the presence of samples Aerobic R0033, Anaerobic R0033, SC40 and, R0419.*** *↓ indicates decrease in cytokine secreted from the cell, ↑ indicates increase in cytokine secreted from cell, when comparing sample stimulated with TLR to RSM stimulated with TLR. RSM is used as the fermentate control to highlight additional benefits from unique fermentate samples. LOX results gathered in Ch3 and collated with results from Ch4 PIC, LPS, and CpG BMDC data for samples Aerobic R0033, Anaerobic R0033, SC40 and, R0419.*

TLR Present	Aerobic R0033	Anaerobic R0033	SC40	R0419	Cytokine
+LOX	↑	↑	↑	↑	IL-1β
	↑	↑	↑	↑	IL-6
	↑	↑	↑	-	IL-10
	↑	↑	↑	↑	TNF-α
	↑	↑	↑	-	IL-12p40
	↑	↑	-	-	IL-12p70
	↑	↑	-	↑	IL-23
	↑	↑	↑	-	IL-27
+PIC	↑	↑	↑	-	IL-1β
	↑	↑	↑	↑	IL-6
	-	↑	↑	↑	IL-10
	↑	↑	↑	↑	TNF-α
	-	-	-	-	IL-12p40
	-	-	-	-	IL-12p70
	-	-	↑	-	IL-23
	↑	↑	↑	↑	IL-27
+LPS	↑	↑	↑	-	IL-1β
	-	↑	↑	-	IL-6
	-	-	↑	↑	IL-10
	-	↑	↑	↑	TNF-α
	-	-	-	-	IL-12p40
	-	-	-	-	IL-12p70
	-	-	-	-	IL-23
	-	-	↑	↑	IL-27
+CpG	↑	-	↑	-	IL-1β
	↑	↑	-	-	IL-6
	-	-	↑	-	IL-10
	↑	↑	-	-	TNF-α
	-	↑	↓	↓	IL-12p40
	↑	-	↓	↓	IL-12p70
	-	-	↓	↑	IL-23
	-	-	↓	↓	IL-27

Therefore we established that when challenged with different immune stimuli (LOX, PIC, LPS, and CpG) these fermentates behave differently with differential bioactivity depending on the immune scenario they're challenged with mimicking either viral infection or inflammation. This confirmed that our fermentates were unique to one another and specific depending on the immune scenario they're challenged with.

Next a direct comparison of the differing profiles was used to assess the samples role as immune boosting and/or anti-inflammatory samples in BMDCs activated with LOX (viral immune challenge), or LPS (inflammatory challenge). This enabled the assessment and direct comparison of sample specificity, dependant on the two key immune scenarios we were investigating.

4.3.1.1.3 Stimulation of LOX and LPS activated BMDCs with 25mg/mL raw samples Aerobic R0033, Anaerobic R0033, SC40 and R0419 effects cytokine secretion

BMDC were seeded at a concentration of $1x10^6$ cells/mL, incubated for 24 hours before stimulating with a dose of 25mg/mL raw fermentate sample for 1 hour followed by various TLR ligands as follows: LOX 0.5mM or LPS 100ng/mL, and subsequently incubated at 37^0C in 5% CO_2. After 24 hours supernatants were removed and ELISA procedure for cytokines IL-1β, IL-6, IL-10 , TNF-α, IL-12p40, IL-12p70, IL-23 and IL-27 was performed according to the manufacturer's instructions (section 2.2.14 Enzyme Linked Immunosorbent Assay (ELISA)).

Figure 55 and Figure 56 show that samples significantly affected the secretion of cytokines in response to immune challenges LOX and LPS, when compared to the RSM. Figure 55 demonstrates IL-1β, IL-6, and IL-12p40 were significantly increased in the presence of LOX ($p<0.001$), and IL-10, TNF-α, IL-23 and IL-27 were non-significantly increased. Figure 56 demonstrates IL-6, IL-12p40, IL-27 ($p<0.001$) and TNF-α ($p<0.033$) were significantly increased in the presence of LPS, and IL-1β, IL-10 and IL-23 were non-significantly increased.

In the presence of LOX, Aerobic R0033 increased IL-1β and IL-12p40 ($p<0.001$), Anaerobic R0033 increased IL-6 ($p<0.001$), TNF-α ($p<0.002$), and IL-12p40 ($p<0.033$), SC40 increased IL-10 ($p<0.001$), but SC40 and R0419 decreased IL-6, IL-12p40 and IL-27 ($p<0.001$). Unstimulated SC40 increased IL-6, IL-10, TNF-α and IL-27 ($p<0.001$), and unstimulated Anaerobic R0033 increased IL-6 ($p<0.001$) and IL-27 ($p<0.033$).

In the presence of LPS, Aerobic R0033 and Anaerobic R0033 increased TNF-α ($p<0.033$; $p<0.001$), SC40 increased IL-10, TNF-α ($p<0.001$), IL-1β ($p<0.002$) and IL-27 ($p<0.033$), and R0419 increased IL-10 and TNF-α ($p<0.001$). Unstimulated SC40 increased IL-10, TNF-α ($p<0.001$), IL-6 ($p<0.002$) and IL-27 ($p<0.033$), and unstimulated Anaerobic R0033 increased IL-6 ($p<0.002$).

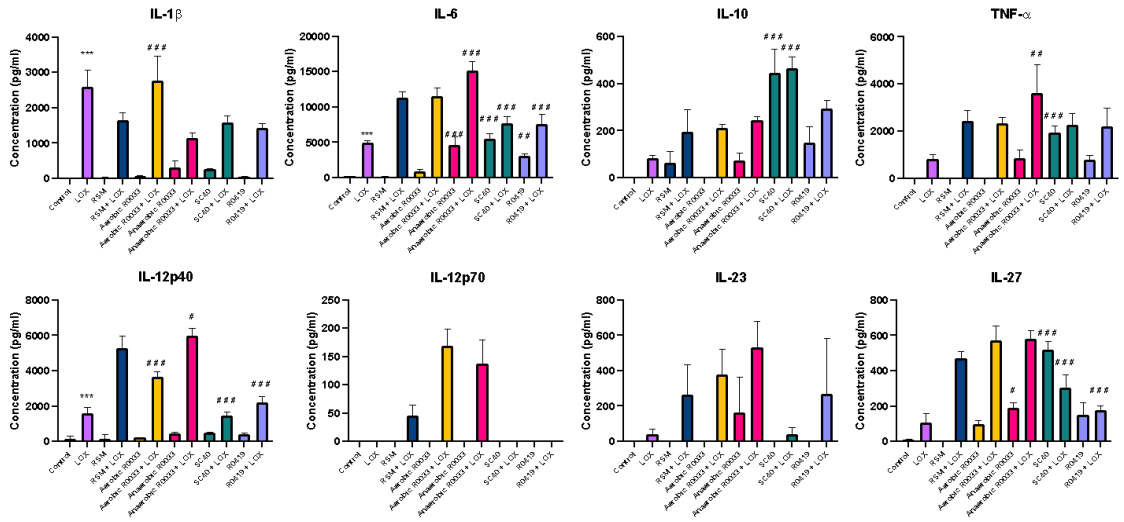

Figure 55: ***Exposure of LOX activated BMDC to 25mg/mL raw Aerobic R0033, Anaerobic R0033, SC40 and R0419 results in the secretion of cytokines IL-1β, IL-6, IL-10 , TNF-α, IL-12p40, IL-12p70, IL-23 and IL-27.*** *BMDC cells were seeded at 1x10⁶ cells/mL and left overnight at 37°C in 5% CO_2. The following day cells were stimulated with 25mg/mL raw sample fermentate, incubated for 1 hour at 37°C in 5% CO_2 and % CO_2 and subsequently exposed to the following concentrations of TLR: LOX 0.5mM for TLR activation before incubating overnight under the same conditions. RSM is the fermentate control. Supernatants were removed after 24 hours and ELISA was performed for IL-1β, IL-6, IL-10, TNF-α, IL-12p40, IL-12p70, IL-23 and IL-27. Data is presented as mean ± SD of three replicates. Significance determined using one- way ANOVA with a Newman-Keuls post-test. Output P value style APA: .12 (ns), .033 (*), .002(**) and <.001 (***); 1) comparing unstimulated control to TLRs "*",and 2) comparing RSM to sample equivalent "#"*

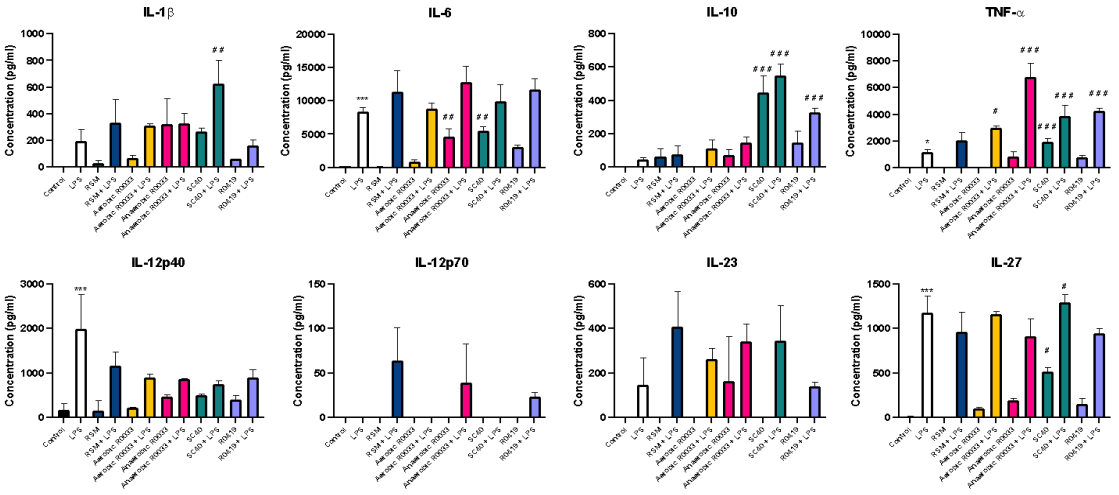

Figure 56: ***Exposure of LPS activated BMDC to 25mg/mL raw Aerobic R0033, Anaerobic R0033, SC40 and R0419 results in the secretion of cytokines IL-1β, IL-6, IL-10, TNF-α, IL-12p40, IL-12p70, IL-23 and IL-27.*** *BMDC cells were seeded at 1x10⁶ cells/mL and left overnight at 37°C in 5% CO_2 The following day cells were stimulated with 25mg/mL raw sample fermentate, incubated for 1 hour at 37°C in 5% CO_2 and % CO_2 and subsequently exposed to the following concentrations of TLR: LPS 100ng/mL for TLR activation before incubating overnight under the same conditions. RSM is the fermentate control. Supernatants were removed after 24 hours and ELISA was performed for IL-1β, IL-6, IL-10, TNF-α, IL-12p40, IL-12p70, IL-23 and IL-27. Data is presented as mean ± SD of three replicates. Significance determined using one- way ANOVA with a Newman-Keuls post-test. Output P value style APA: .12 (ns), .033 (*), .002(**) and <.001 (***); 1) comparing unstimulated control to TLRs "*",and 2) comparing RSM to sample equivalent "#"*

In order to determine whether the candidate immune boosting samples (Aerobic R0033, Anaerobic R0033, SC40 and R04019) had specific bioactivity we next compared them to samples LC10, R0215, HA118, and P200622 which we previously established in Chapter 3 had no specific anti-viral activity.

4.3.1.1.4 Stimulation of LOX and LPS activated BMDCs with 25mg/mL raw samples LC10, R0215, HA118 and P200622 effects cytokine secretion

BMDC were seeded at a concentration of $1x10^6$ cells/mL, incubated for 24 hours before stimulating with a dose of 25mg/mL raw fermentate sample for 1 hour followed by various TLR ligands as follows: LOX 0.5mM or LPS 100ng/mL, and subsequently incubated at 37^0C in 5% CO_2. After 24 hours supernatants were removed and ELISA procedure for cytokines IL-1β, IL-6, IL-10 , TNF-α, IL-12p40, IL-12p70, IL-23 and IL-27 was performed according to the manufacturer's instructions (section 2.2.14 Enzyme Linked Immunosorbent Assay (ELISA)).

Figure 57 and Figure 58 show that samples significantly affected the secretion of cytokines in response to immune challenges LOX and LPS, when compared to the RSM. Contrasting samples below confirmed bioactivity in identified candidate immune boosting samples. Figure 57 demonstrates IL-1β, IL-6, TNF-α and IL-12p40 were significantly increased in the presence of LOX ($p<0.001$), and non-significantly increased for IL-10, IL-12p70, IL-23 and IL-27. Figure 58 demonstrates IL-6, TNF-α, IL-12p40, and IL-27 ($p<0.001$) were significantly increased in the presence of LPS, and were non-significantly increased for IL-1β, IL-12p70 and IL-23.

In the presence of LOX, R0215 increased IL-10, IL-12p70 and IL-23 ($p<0.033$) while decreasing IL-1β ($p<0.002$), HA118 decreased IL-12p40 ($p<0.001$), IL-6 and IL-23 ($p<0.002$), and P200622 decreased IL-1β, IL-6, IL-23 ($p<0.001$) and IL-27 ($p<0.002$) while increasing IL-10 ($p<0.001$). Unstimulated HA118 and P200622 increased IL-6, and TNF-α ($p<0.001$), and P200622 increased IL-10 ($p<0.001$).

In the presence of LPS, LC10 increased IL-1β and IL-23 ($p<0.033$), R0215 increased IL-12p40 and IL-12p70 ($p<0.001$), HA118 decreased IL-1β and IL-23

(p<0.002), and P200622 increased IL-10 and TNF-α (p<0.001) while decreasing IL-23 (p<0.002). Unstimulated HA118 increased IL-6, and TNF-α (p<0.033; p<0.001), and P200622 increased IL-10, TNF-α (p<0.001) and IL-6 (p<0.033).

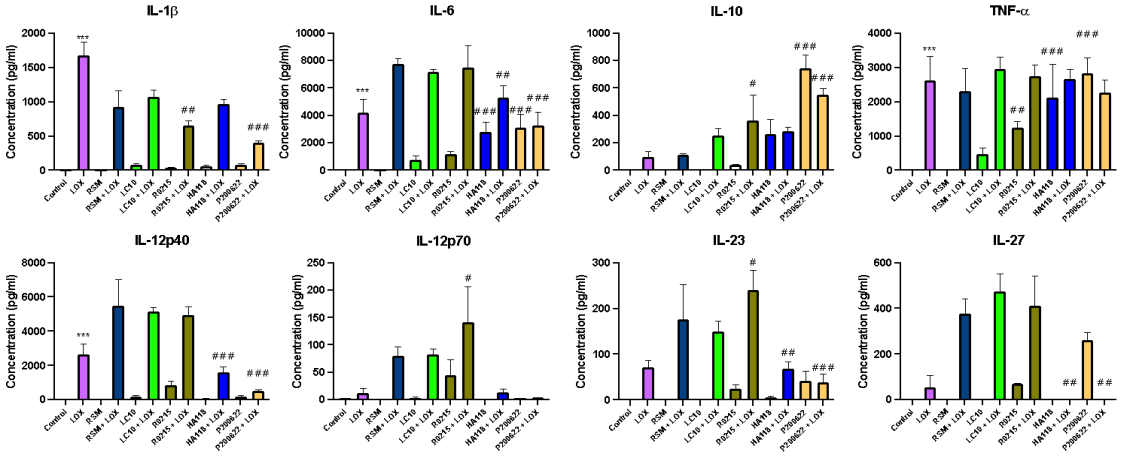

Figure 57: ***Exposure of LOX activated BMDC to 25mg/mL LC10, R0215, HA118 and P200622 results in the secretion of cytokines IL-1β, IL-6, IL-10, TNF-α, IL-12p40, IL-12p70, IL-23 and IL-27.*** *BMDC cells were seeded at 1x10⁶ cells/mL and left overnight at 37°C in 5% CO_2. The following day cells were stimulated with 25mg/mL raw sample fermentate, incubated for 1 hour at 37°C in 5% CO_2 and % CO_2 and subsequently exposed to the following concentrations of TLR: LOX 0.5mM for TLR activation before incubating overnight under the same conditions. RSM is the fermentate control. Supernatants were removed after 24 hours and ELISA was performed for IL-1β, IL-6, IL-10, TNF-α, IL-12p40, IL-12p70, IL-23 and IL-27. Data is presented as mean ± SD of three replicates. Significance determined using one- way ANOVA with a Newman-Keuls post-test. Output P value style APA: .12 (ns), .033 (*), .002(**) and <.001 (***); 1) comparing unstimulated control to TLRs "*",and 2) comparing RSM to sample equivalent "#"*

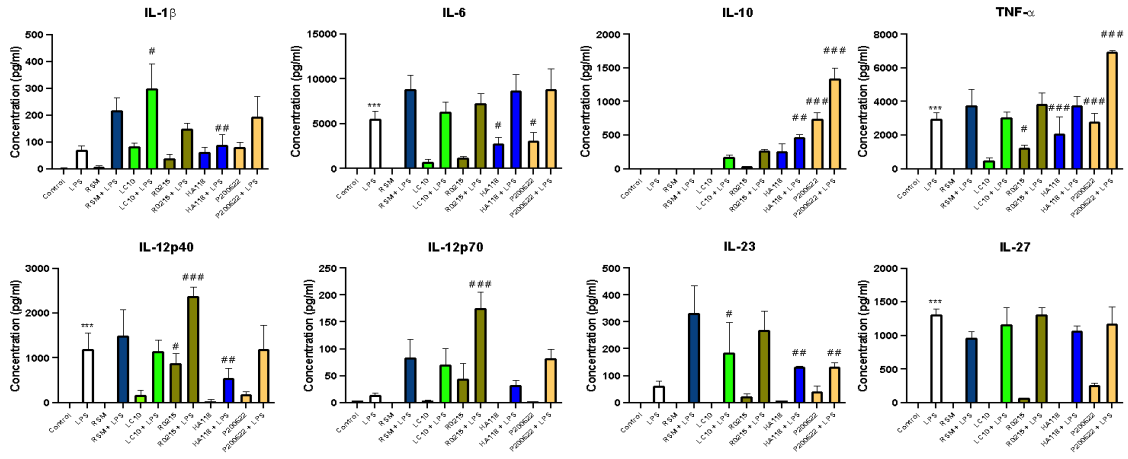

Figure 58: ***Exposure of LPS activated BMDC to 25mg/mL LC10, R0215, HA118 and P200622 results in the secretion of cytokines IL-1β, IL-6, IL-10, TNF-α, IL-12p40, IL-12p70, IL-23 and IL-27.*** *BMDC cells were seeded at 1x10⁶ cells/mL and left overnight at 37°C in 5% CO_2. The following day cells were stimulated with 25mg/mL raw sample fermentate, incubated for 1 hour at 37°C in 5% CO_2 and % CO_2 and subsequently exposed to the following concentrations of TLR: LPS 100ng/mL for TLR activation before incubating overnight under the same conditions. RSM is the fermentate control. Supernatants were removed after 24 hours and ELISA was performed for IL-1β, IL-6, IL-10, TNF-α, IL-12p40, IL-12p70, IL-23 and IL-27. Data is presented as mean ± SD of three replicates. Significance determined using one- way ANOVA with a Newman-Keuls post-test. Output P value style APA: .12 (ns), .033 (*), .002(**) and <.001 (***); 1) comparing unstimulated control to TLRs "*",and 2) comparing RSM to sample equivalent "#"*

Therefore we can clearly see that fermentates Aerobic R0033, Anaerobic R0033, SC40, and R0419 had unique bioactivity in BMDCs activated with not only LOX, but also LPS, PIC, and CpG. These contrasting fermentates had little to no effect on key viral associated cytokines IL-6, and TNF-α, but also decreased secretion of other key viral immune supportive cytokines IL-12p40, IL-23, and IL-27. From here we were then able to expand our research on these 4 immune boosting fermentates in another core immune cell, the macrophage.

The next step involved the establishment of a macrophage model for the assessment of fermentate effect on a variety of different functions within these core immune cells.

4.3.2 Establishing a macrophage model for examination of immune profile of candidate immune boosting fermentates

Having highlighted the top 4 candidate immune boosting samples in BMDCs in response to a variety of immune challenges both viral and inflammatory it was necessary to examine each of these samples in response to a variety of immune challenges in macrophage. Macrophage are key innate immune cells. They are huge players in the secretion of cytokines in response to initial immune activation, with these cytokines triggering the recruitment of chemokines to aid in mounting an appropriate immune response. They are responsible for the direct killing of invading pathogens, through the process of phagocytosis. This is the process whereby the macrophage targets the invading pathogen, engulfs it and destroys it. J774.A.1 cells and BMDMs were stimulated with both viral and inflammatory immune challenges, mimicking viral immune infection and an inflammatory state in the cell respectively, to assess the fermentates capabilities in response to various immune scenarios. This allowed us to establish the fermentate effects on not only cytokine profiles in macrophage cells, but also chemokine profiles, phagocytosis, and cell surface marker expression in macrophage.

4.3.2.1 J774.A.1. cell screening

Initially assessment was carried out in J774.A.1 cells as they are easy to use, and allowed for the confirmation of sample effect in a macrophage cell type. In addition to this, due to the high volume of cells required for analysis of parameters including phagocytosis, and cell surface marker expression, it would otherwise not be feasible to carry out in a primary cell such as BMDMs where only limited cell concentrations were harvested.

4.3.2.1.1 LOX and LPS TLR activated macrophage stimulated with 25mg/mL raw fermentate doesn't affect cell viability

J774.A.1 macrophage were seeded at a concentration of $1x10^6$ cells/mL, incubated for 24 hours before stimulating with a dose of 25mg/mL raw fermentate sample for 1 hour followed by viral TLR ligand: LOX 0.5mM, PIC 10µg/mL or inflammatory TLR: LPS 100ng/mL or CpG 5 µM respectively and subsequently incubated at 37^0C in 5% CO_2. After 24 hours an MTS assay was performed as previously outlined (section 2.2.13 MTS Cell Viability Assay).

Figure 59 demonstrates that there was no significant change in cell viability following exposure of the cells to 25mg/mL raw fermentate samples Aerobic R0033, Anaerobic R0033, SC40 and R0419 to either LOX or LPS, or PIC or CpG TLR ligand activation. The RSM acted as the whole fermentate control for comparison of effects induced by each independent sample i.e., Aerobic R0033, Anaerobic R0033, SC40 and R0419. The use of the positive control of 10% DMSO provided a clear distinction between the cytotoxic effects on cell viability with the untreated control sample, as DMSO induced cell death.

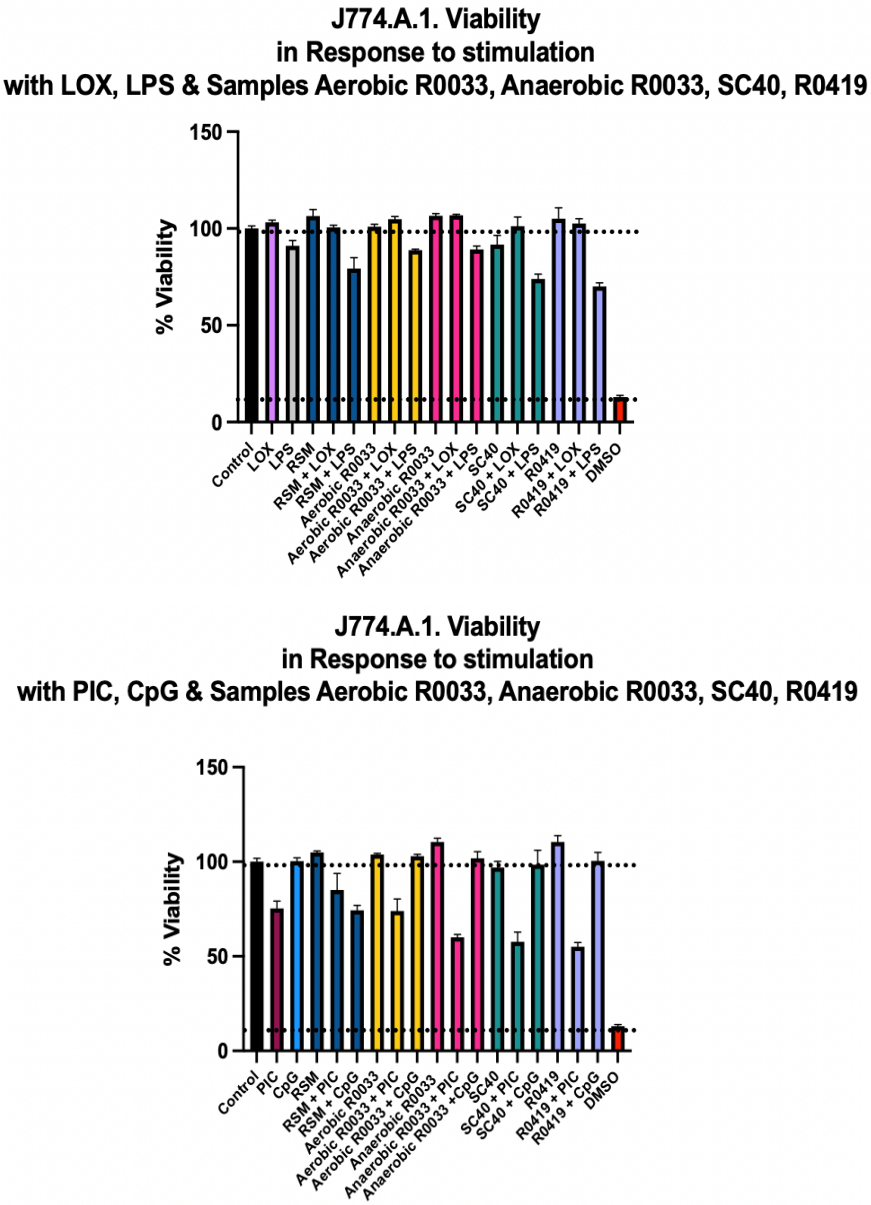

*Figure 59:**Exposure of LOX, LPS, CpG, and PIC activated J774.A.1 cells to 25mg/mL raw sample Aerobic R0033, Anaerobic R0033, SC40 and R0419 doesn't affect cell viability**. J774.A.1. cells were seeded at 1x10^6 cells/mL and left overnight at 37^{0}C in 5% CO_2. The following day cells were stimulated with 25mg/mL sample fermentate, incubated for 1 hour at 37^{0}C in 5% CO_2 and subsequently exposed to the following concentrations of TLRs: LOX 0.5mM, LPS 100ng/mL, CpG 5 µM, PIC 10µg/mL for TLR activation before incubating overnight under the same conditions. RSM is the fermentate control. 10% DMSO was included as a positive control to induce cell death. Cells were incubated with MTS cell titre aqueous one solution for 3 hours at 37^{0}C in 5% CO_2. Viability is represented as a percentage compared to viable, untreated cells (Control). Data is presented as mean ± SD of three replicates.*

4.3.2.1.2 LOX and LPS TLR activated macrophage stimulated with 25mg/mL raw fermentate effects cytokine secretion

J774.A.1 macrophage were seeded at a concentration of $1x10^6$ cells/mL, incubated for 24 hours before stimulating with a dose of 25mg/mL raw fermentate sample for 1 hour followed by viral TLR challenge: LOX 0.5mM, PIC 10µg/mL or inflammatory TLR challenge: LPS 100ng/mL or CpG 5 µM respectively and subsequently incubated at 37^0C in 5% CO_2. After 24 hours supernatants were removed and ELISA procedure for cytokines IL-1β, IL-6, IL-10 , and TNF-α was performed according to the manufacturer's instructions (section 2.2.14 Enzyme Linked Immunosorbent Assay (ELISA)).

Figure 60 and Figure 61 demonstrate that samples significantly affected the secretion of cytokines in response to immune challenges LOX, PIC, LPS and, CpG when compared to the RSM. IL-10, and TNF-α were significantly increased in the presence of LOX ($p<0.002$; $p<0.001$) and PIC ($p<0.002$; $p<0.033$). and LPS ($p<0.001$; $p<0.001$), and CpG ($p<0.001$; $p<0.002$).

In the presence of LOX, SC40 increased IL-6 ($p<0.033$)and R0419 increased IL-10 ($p<0.001$). SC40 alone increased IL-6 ($p<0.02$), IL-10 ($p<.001$) and TNF-α ($p<0.001$), and R0419 increased IL-10 ($p<0.001$) and TNF-α ($p<0.002$).

In the presence of PIC, Aerobic R0033 increased TNF-α, and IL-10 ($p<0.001$; $p<0.033$), Anaerobic R0033 increased TNF-α, and IL-10 ($p<0.001$; $p<0.002$), SC40 and R0419 increased IL-1β, IL-6, IL-10 and TNF-α ($p<0.001$). Unstimulated Anaerobic R0033, SC40 and R0419 samples alone increased IL-10 ($p<0.001$).

In the presence of LPS, Aerobic R0033 increased IL-1β ($p<0.001$), SC40 increased IL-6 and IL-10 ($p<0.002$; $p<0.001$), and R0419 increased IL-10 ($p<0.001$). SC40, R0419 and Anaerobic R0033 alone increased IL-10 ($p<0.001$; $p<0.001$; $p<0.002$), and SC40 increased TNF-α ($p<0.033$).

In the presence of CpG, Aerobic R0033 increased TNF-α and IL-10 ($p<0.001$; $p<0.033$), SC40, R0419 and Anaerobic R0033 increased IL-10 ($p<0.002$; $p<0.002$; $p<0.033$). SC40, R0419 and Anaerobic R0033 alone increased IL-10 ($p<0.001$; $p<0.001$; $p<0.002$), and SC40 increased IL-6 ($p<0.001$).

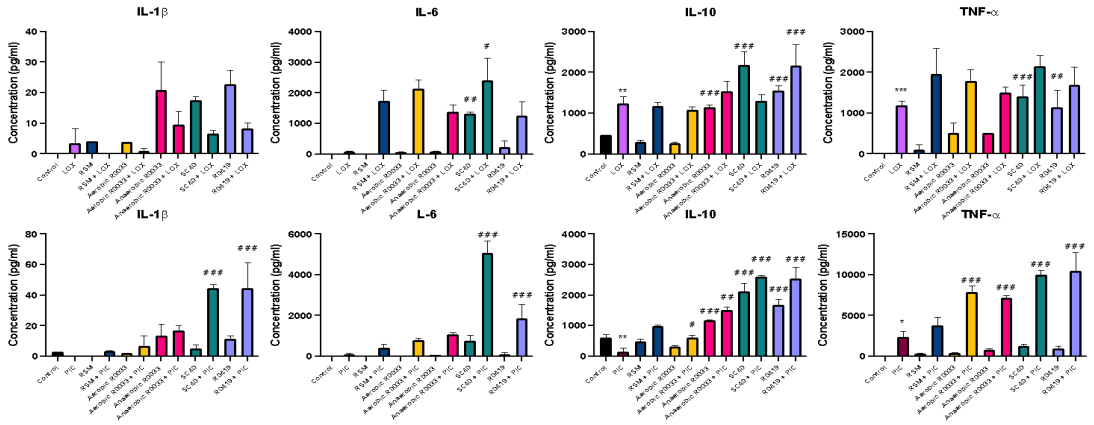

Figure 60: ***Exposure of LOX and PIC activated J774.A.1 cells to TLRs and 25mg/mL raw sample results in the secretion of for IL-1β, IL-6, IL-10, and TNF-α.*** *J774.A.1. cells were seeded at 1x10⁶ cells/mL and left overnight at 37°C in 5% CO_2. The following day cells were stimulated with 25mg/mL raw sample fermentate, incubated for 1 hour at 37°C in 5% CO_2 and % CO_2 and subsequently exposed to the following concentrations of TLRs: LOX 0.5mM, PIC 10µg/mL for TLR activation before incubating overnight under the same conditions. RSM is the fermentate control. Supernatants were removed after 24 hours and ELISA was performed for IL-1β, IL-6, IL-10, and TNF-α. Data is presented as mean ± SD of three replicates. Significance determined using one- way ANOVA with a Newman-Keuls post-test. Output P value style APA: .12 (ns), .033 (*), .002(**) and <.001 (***); 1) comparing unstimulated control cells to each TLR stimulated cell "*", 2) comparing sample + TLR to unstimulated sample cells "+" and 3) comparing TLR + sample to the each respective TLR + RSM counterpart "#".*

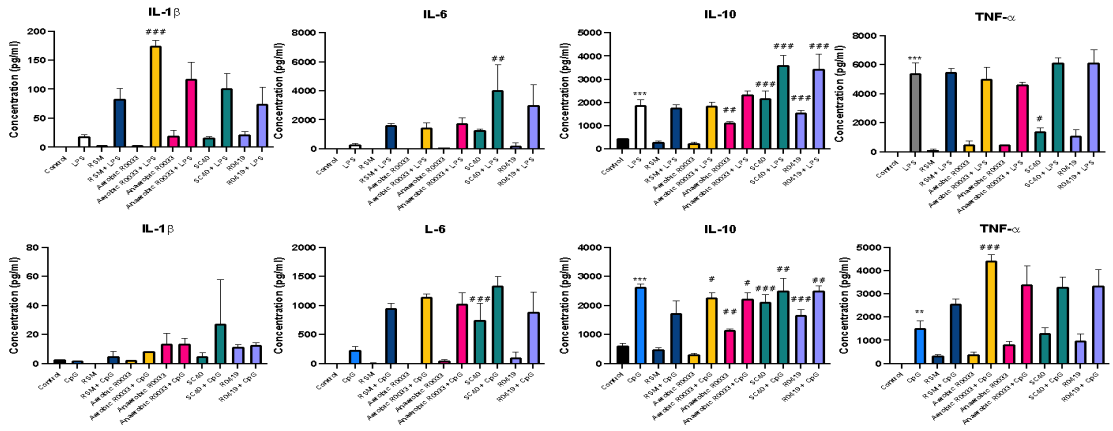

Figure 61: ***Exposure of LPS and CpG activated J774.A.1 cells to 25mg/mL raw sample results in the secretion of IL-1β, IL-6, IL-10, and TNF-α.*** *J774.A.1. cells were seeded at 1x10⁶ cells/mL and left overnight at 37°C in 5% CO_2. The following day cells were stimulated with 25mg/mL raw sample fermentate, incubated for 1 hour at 37°C in 5% CO_2 and subsequently exposed to the following concentrations of TLRs: LPS 100ng/mL, CpG 5 µM, for TLR activation before incubating overnight under the same conditions. RSM is the fermentate control. Supernatants were removed after 24 hours and ELISA was performed for IL-1β, IL-6, IL-10, and TNF-α. Data is presented as mean ± SD of three replicates. Significance determined using one- way ANOVA with a Newman-Keuls post-test. Output P value style APA: .12 (ns), .033 (*), .002(**) and <.001 (***); 1) comparing unstimulated control cells to each TLR stimulated cell "*", 2) comparing sample + TLR to unstimulated sample cells "+" and 3) comparing TLR + sample to the each respective TLR + RSM counterpart "#".*

Therefore, we clearly saw that the bioactive effects seen in dendritic cells were relatively conserved and translated to the effects seen in macrophage at a dose of 25mg/ml raw fermentate. With this knowledge we were able to further examine the fermentates effects on other key macrophage functions including phagocytosis, chemokine secretion and cell surface marker expression.

Having established the cytokine secretion profiles of the samples in macrophage in response to viral and immune challenges, the next step was to investigate the effect of candidate immune boosting samples, on phagocytosis, in LOX and LPS activated J774.A1 macrophage. Phagocytosis is the process whereby the macrophage targets, engulfs and destroys the invading pathogens. In order investigate phagocytosis, two parameters were measured:

1) The mean fluorescence index (MFI). This is a measure of the mean fluorescence within the macrophage cell, as a direct result of the cell, engulfing the fluorescent latex bead.
2) The percentage of phagocytosing cells. This is a measure of the percentage of actively phagocytosing cells versus non-phagocytosing cells within the population of macrophage being assessed.

In order to get a more comprehensive result the mean phagocytosing index (MPI) was created. This combined the two measurable outputs of the MFI and the percentage phagocytosing index, to create the MPI as a more representative model for phagocytosis of a macrophage cell.

Initially it was important to confirm that an appropriate model for the measurement of phagocytosis was in place. Therefore the initial optimisation of the phagocytosis model began with establishing that phagocytosis could be halted via incubation at $4^{O}C$. This allowed for confirmation of MPI activity as a direct result of sample/activation effect and not latent phagocytotic activity. It was then necessary to establish the optimal LOX and LPS stimulation time to promote phagocytosis before stimulating the macrophage with fermentate sample, to assess fermentate

effect on phagocytosis. This was carried out by using a variety of exposure times of TLRs to confirm which exposure time of TLR promoted optimal phagocytic activity, and therefore was carried through for assessment of fermentate effect. This again allowed for confirmation of fermentate effect on phagocytosis rather than TLR effect on phagocytosis. Once the optimal exposure time was confirmed for both LOX and LPS, we now wanted to assess the impact of addition of fermentate at each of the TLR agonist exposure times. In the interest of time efficiency, and sample and resource preservation, RSM as the starting material for all fermentates was used in order to confirm the exposure time needed for phagocytosis assessment. RSM was added 1 hour prior to incubation with TLR agonists at various exposure times. This was done in order to follow a similar approach to the models used for the assessment of cytokine secretion, where sample was added 1 hour prior to activation with immune stimuli. Altogether this then established the appropriate phagocytosis model where the addition of sample could now be assessed for determination of fermentate effect on phagocytosis.

4.3.2.1.3 Exposure of J774.A.1 to incubation at 37^{O}C and 4^{O}C affects phagocytosis of cells

J774.A.1 cells were seeded 1x10^{6} cells/mL and incubated overnight at 37^{0}C in 5% $CO_{2.}$ After 24 hours cells were stimulated for 1 hour to the following concentrations of TLR ligands: LPS 100ng/mL and LOX 0.5mM. The procedure for phenotypic analysis of cell phagocytosis when stimulated with TLR ligands was carried out as previously described (section 2.2.16.4 Phagocytosis Assay) using 1µm fluorescent FITC latex beads Figure 62 -Figure 64 demonstrates that incubation for 5 minutes on ice halted phagocytosis. Figure 62 and Figure 63 are representative figures for the generation of the MFI and percentage phagocytosing cell data used for the remainder of section 4.3.2.1. See appendix for remaining raw MFI and percentage of phagocytosis cells for section 4.3.2.1.

Figure 62 demonstrates the generation of the MFI from the raw flow cytometry data where the mean of the FITC+ cells was gathered from the count of the viable cell population.

Figure 63 demonstrates the gating strategy used for the measurement of percentage phagocytosing cells, where cells to the right expressed FITC and were therefore cells that had phagocytosed the fluorescently labelled FITC latex bead. Cells to the left were FITC negative cells that had not engulfed the labelled bead. We clearly saw that incubation at $4^{O}C$ halts phagocytosis while incubation at $37^{O}C$ did not halt this process.

Figure 64A shows the MFI was significantly reduced for control cells when exposed to $4^{O}C$ incubation compared to $37^{O}C$ control ($p<0.033$). When LOX and LPS were present MFI was reduced when exposed to $4^{O}C$ incubation compared to $37^{O}C$ TLR controls ($p<0.001$). There was a significant increase in MFI observed when comparing control cells to both the LOX and LPS activated cells only when exposed to $37^{O}C$ incubation ($p<0.002$), while there was no difference in control, LOX or LPS MFI at $4^{O}C$.

Figure 64B shows the percentage of phagocytosing cells were significantly reduced for control cells, as well as for LOX and LPS activated cells when exposed to $4^{O}C$ incubation compared to $37^{O}C$ controls ($p<0.001$). There was a significant increase in % phagocytes observed when comparing control cells to both the LOX and LPS activated cells only when exposed to $37^{O}C$ incubation ($p<0.001$), while there was no difference in control, LOX or LPS MFI at $4^{O}C$.

Figure 64C shows the MPI which was a product of the MFI and percentage phagocytosis cells combined. The MPI was significantly reduced for LOX and LPS activated cells when exposed to $4^{O}C$ incubation ($p<0.001$; $p<0.002$), while control cells were reduced but to no significant degree. There was a significant increase MPI observed when comparing control cells to both the LOX and LPS activated cells only when exposed to $37^{O}C$ incubation ($p<0.002$), while there was no difference in control, LOX or LPS MFI at $4^{O}C$. Both the LOX and LPS at $37^{O}C$ had an MPI over three times that of the control cells, while the $4^{O}C$ control, LOX and LPS cells which had an MPI less than 0.07 of the $37^{O}C$ control.

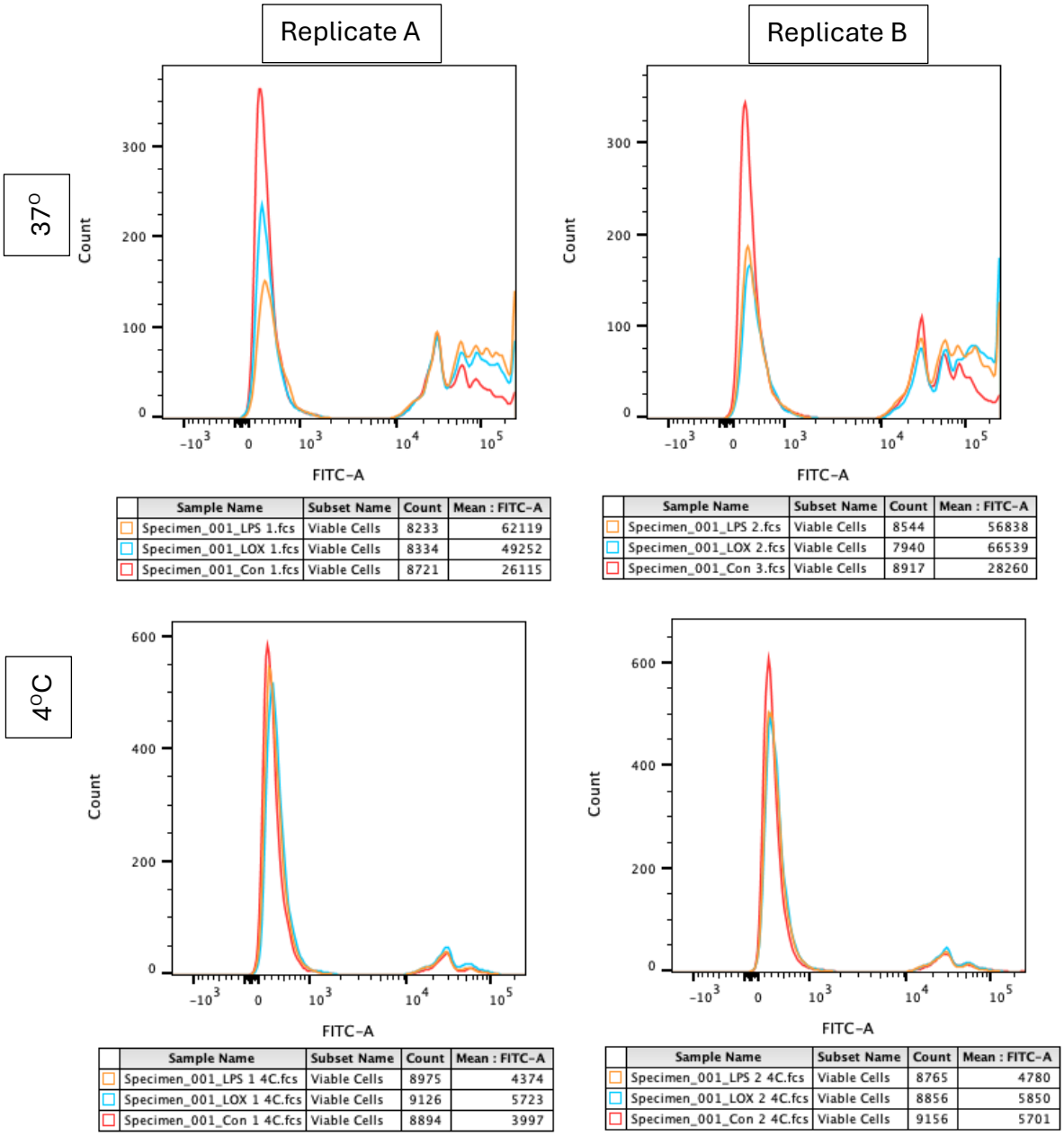

Sample Name	Subset Name	Count	Mean : FITC-A
Specimen_001_LPS 1.fcs	Viable Cells	8233	62119
Specimen_001_LOX 1.fcs	Viable Cells	8334	49252
Specimen_001_Con 1.fcs	Viable Cells	8721	26115

Sample Name	Subset Name	Count	Mean : FITC-A
Specimen_001_LPS 2.fcs	Viable Cells	8544	56838
Specimen_001_LOX 2.fcs	Viable Cells	7940	66539
Specimen_001_Con 3.fcs	Viable Cells	8917	28260

Sample Name	Subset Name	Count	Mean : FITC-A
Specimen_001_LPS 1 4C.fcs	Viable Cells	8975	4374
Specimen_001_LOX 1 4C.fcs	Viable Cells	9126	5723
Specimen_001_Con 1 4C.fcs	Viable Cells	8894	3997

Sample Name	Subset Name	Count	Mean : FITC-A
Specimen_001_LPS 2 4C.fcs	Viable Cells	8765	4780
Specimen_001_LOX 2 4C.fcs	Viable Cells	8856	5850
Specimen_001_Con 2 4C.fcs	Viable Cells	9156	5701

Figure 62: ***Exposure of J774.A.1 to TLR and incubation at 37°C and 4°C affects MFI.*** *J774.A.1. cells were seeded at 1x10^6 cells/mL and left overnight at 37°C in 5% CO_2. The following day cells were stimulated with the following concentrations of TLRs: LPS 100ng/ml, LOX 0.5mM, incubated for 6 hours at 37°C in 5% CO_2. Cell suspensions were retained, and cells were stimulated with 1µm fluorescent latex beads at a concentration of 20 beads per cell, for 55 minutes at 37°C in 5% CO_2, cells were then incubated for a further 5 minutes at either 37°C or 4°C. Cells were analysed using BD FACSAria 1 system flow cytometer, raw FCS files analysed, data graphed using V10.0 FlowJo software.*

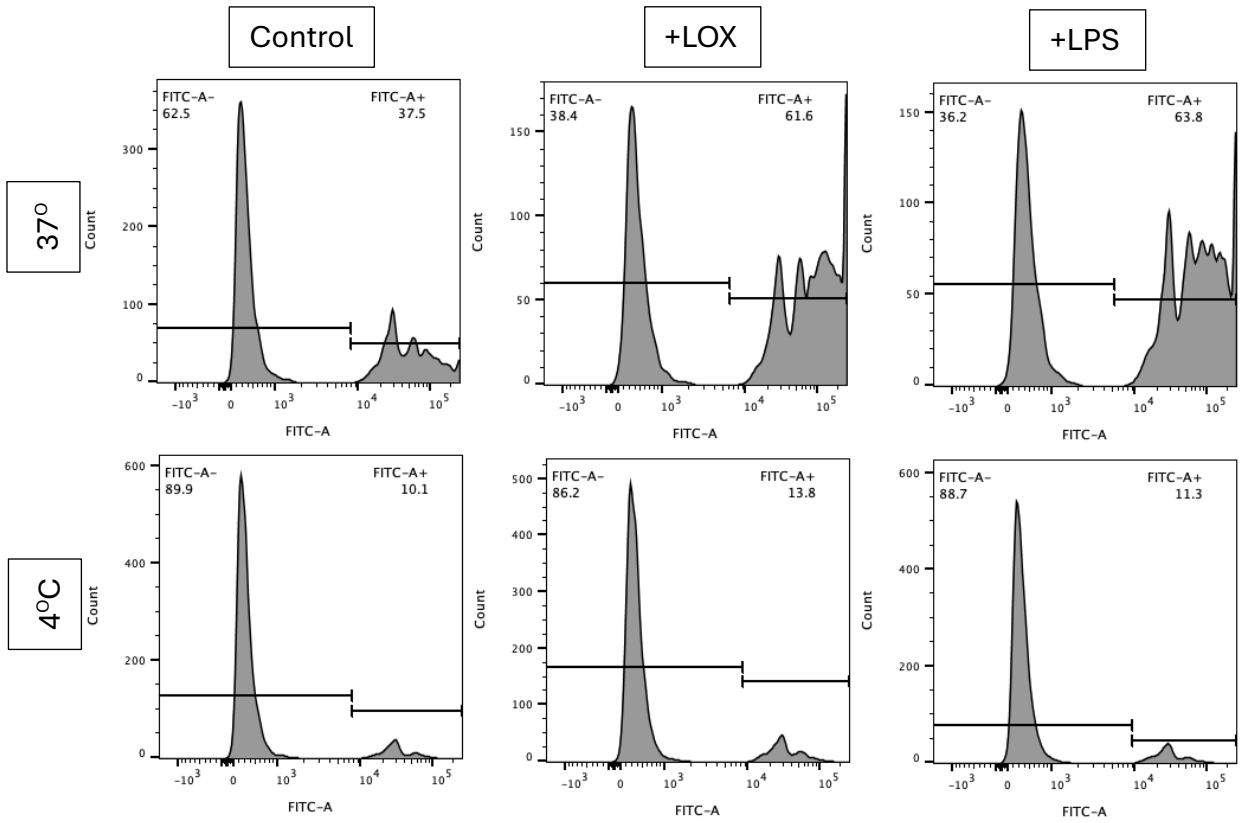

Figure 63: ***Exposure of J774.A.1 to TLR and incubation at 37°C and 4°C affects percentage phagocytosing cells.*** *J774.A.1. cells were seeded at 1x10^6 cells/mL and left overnight at 37°C in 5% CO_2. The following day cells were stimulated with the following concentrations of TLRs: LPS 100ng/ml, LOX 0.5mM, incubated for 6 hours at 37°C in 5% CO_2. Cell suspensions were retained, and cells were stimulated with 1µm fluorescent latex beads at a concentration of 20 beads per cell, for 55 minutes at 37°C in 5% CO_2, cells were then incubated for a further 5 minutes at either 37°C or 4°C. Cells were analysed using BD FACSAria 1 system flow cytometer, raw FCS files analysed, data graphed using V10.0 FlowJo software. Data is presented as mean ± SD of two replicates. Histograms represent FITC-A- the % cells that do not contain beads (non-phagocytes) vs. FITC-A+ representing the % of cells containing beads (phagocytes) within the viable cell population.*

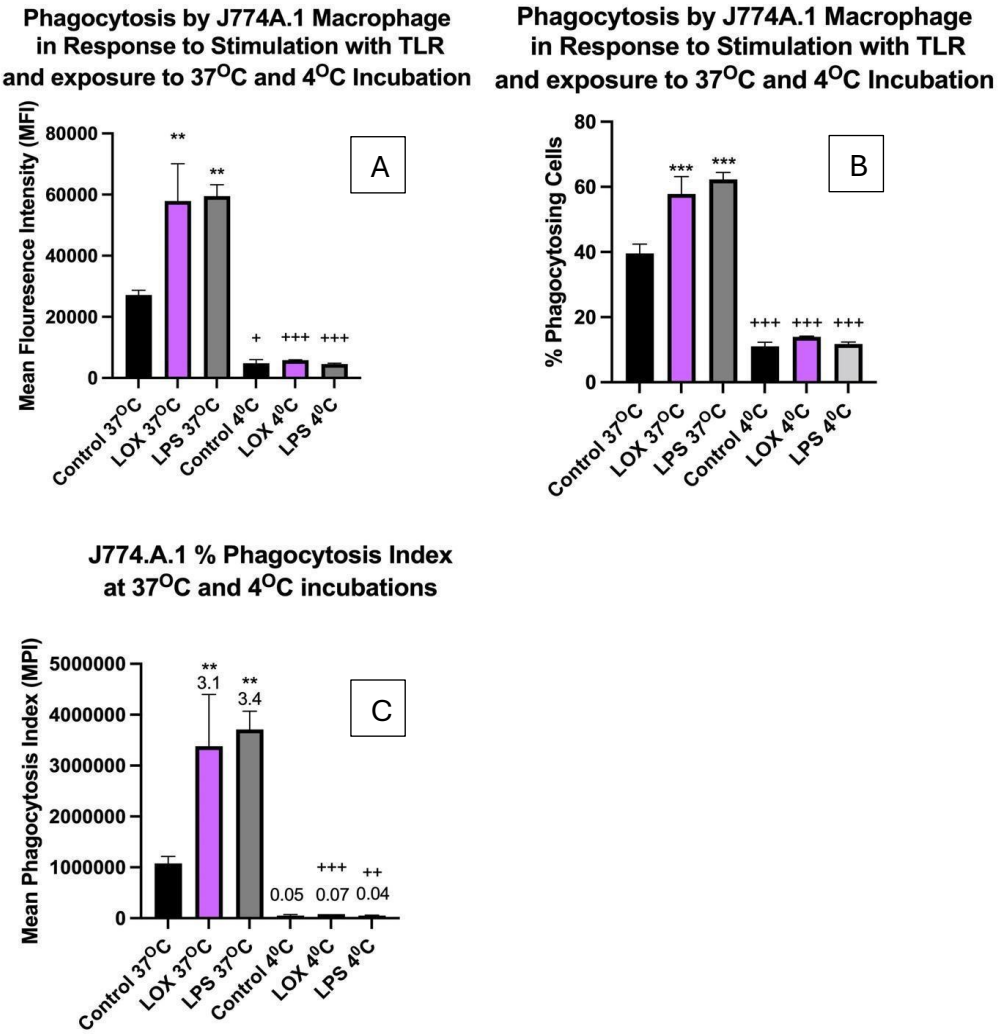

Figure 64: ***Exposure of J774.A.1 cells to TLR and incubation at 37°C and 4°C affects phagocytosis.*** *J774.A.1. cells were seeded at 1x10⁶ cells/mL and left overnight at 37°C in 5% CO_2. The following day cells were stimulated with the following concentrations of TLRs: LPS 100ng/ml, LOX 0.5mM, incubated for 6 hours at 37°C in 5% CO_2. Cell suspensions were retained, and cells were stimulated with 1µm fluorescent latex beads at a concentration of 20 beads per cell, for 55 minutes at 37°C in 5% CO_2, cells were then incubated for a further 5 minutes at either 37°C or 4°C. Cells were analysed using BD FACSAria 1 system flow cytometer, raw FCS files analysed, data graphed using V10.0 FlowJo software. Data is presented as mean ± SD of two replicates. A-B) Significance determined using one- way ANOVA with a Newman-Keuls post-test. Output P value style APA: .12 (ns), .033 (*), .002(**) and <.001 (***); 1) comparing unstimulated control cells to each TLR stimulated cell for respective temperatures" *" and 2) comparing each corresponding control/TLR at 37°C and 4°C "+". C) Data analysed to examine MPI as outlined in section 2.2.16.4 Phagocytosis Assay to include percentage phagocytosing cells and MFI. Number indicated above bar is the MPI compared to the 37°C control cells represented as 1.*

Having established that at 4°C phagocytosis was halted, we now assessed the exposure times needed to promote optimal phagocytic activity in the presence of LOX and LPS.

As there were two different modes of activation of phagocytosis, it was important to assess the TLR incubation times needed to promote phagocytic activity, in LOX and LPS activated cells. LPS activation of phagocytosis was less documented in the literature and thus a confirmation of this in conjunction to the LOX activation was carried out in the interest of continuity of the comparative effects of fermentates under differing immune stimuli.

4.3.2.1.4 Activation of J774.A.1 with LPS and LOX for 1, 3, 4 and 6 hours affects phagocytosis of cells

J774.A.1 cells were seeded $1x10^6$ cells/mL and incubated overnight at 37^0C in 5% CO_2. After 24 hours cells were stimulated for 1, 3, 4 or 6 hours exposure to the following concentrations of TLR ligands: LPS 100ng/mL and LOX 0.5mM. Procedure for phenotypic analysis of cell phagocytosis when stimulated with TLR ligands was carried out as previously described (section 2.2.16.4 Phagocytosis Assay) using 1µm fluorescent FITC latex beads. Figure 65A-C demonstrates that activation with time course of TLR ligands affected phagocytosis. See appendix for raw MFI and percentage of phagocytosis cells.

LOX activated cells had a significant increase in MFI from 3hours to 4hours ($p<0.001$) and from 4 hours to 6 hours ($p<0.001$). LPS activation of the cells led to a stepwise significant increase in MFI for each time point i.e. from 1hour to 3hours, 3hours to 4hours, 4 hours to 6 hours ($p<0.002$; $p<0.001$; $p<0.001$). At the 1hour and 3hour interval MFI was significantly reduced for both LOX and LPS activated cells compared to the control ($p<0.001$), versus the significant increase at the 4 and 6 hour time points ($p<0.001$) (Figure 65A).

LOX activated cells observed a significant increase in % phagocytes from 3hours to 4hours ($p<0.001$) and from 4 hours to 6 hours ($p<0.002$). LPS activation of the cells led to a stepwise significant increase in % phagocytes for each time point i.e. from 1hour to 3hours ($p<0.002$), 3hours to 4hours ($p<0.001$), 4 hours to 6 hours ($p<0.001$). At the 1hour and 3hour interval % phagocytes was significantly less than the unstimulated control for LPS ($p<0.001$; $p<0.033$) and LOX ($p<0.001$), while at the

4 and 6 hour time points % phagocytes was significantly increased for both LOX and LPS activated cells versus the control ($p<0.001$). (Figure 65B).

LOX activation of the cells observed a significant increase in MPI from 3hours to 4hours ($p<0.001$) and from 4 hours to 6 hours ($p<0.001$), while at the lower intervals from 1 to 3 hours there was no significant effect on MPI. LPS activation of the cells led to a stepwise significant increase in MPI for each time point i.e. from 1hour to 3hours ($p<0.033$), 3hours to 4hours ($p<0.001$), 4 hours to 6 hours ($p<0.001$). At the 1hour and 3hour interval MPI was significantly reduced comparing to the control, for LOX ($p<0.001$), and LPS ($p<0.001$; $p<0.002$ respectively), while at the 4 and 6 hour time points MFI was significantly increased ($p<0.001$).

For both LOX and LPS it is only at the 4 and 6 hour time points that the MPI exceeded that of the control, with LOX and LPS 4hour having an index of 1.4, while LOX 6 hour was 1.8 and LPS 6hour was 2.5. Both the 1 and 3 hour LOX had an index of 0.5, half of that of the control cells, while LPS had a 0.4 and 0.7 index for 1 and 3 hour stimulations (Figure 65C).

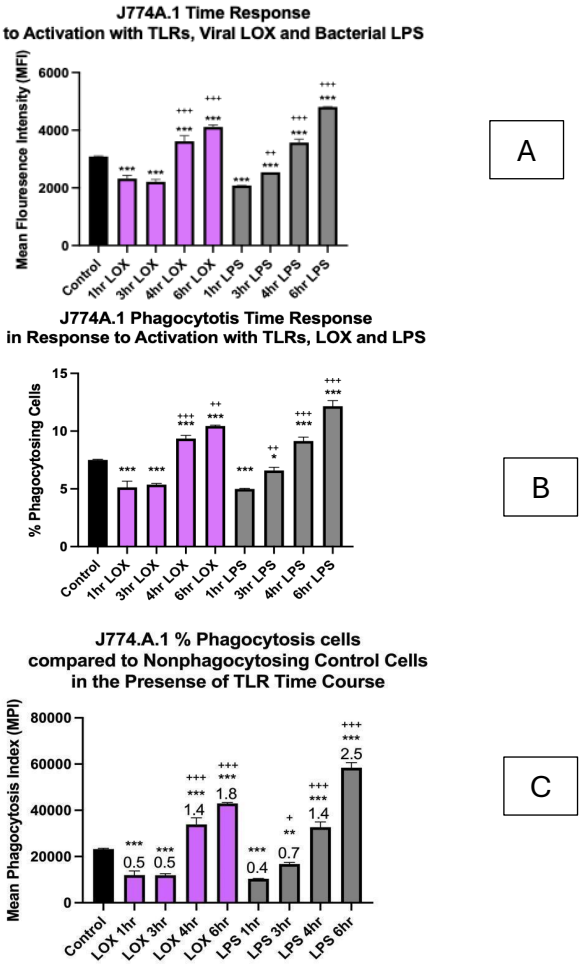

Figure 65: ***Exposure of J774.A.1 cells to LOX and LPS results in phagocytosis.*** *J774.A.1. cells were seeded at 1x10⁶ cells/mL and left overnight at 37°C in 5% CO_2. The following day cells were stimulated with the following concentrations of TLRs: LPS 100ng/ml, LOX 0.5mM, incubated for 1, 3, 4 and 6 hours at 37°C in 5% CO_2. Cell suspensions were retained, and cells were stimulated with 1µm fluorescent latex beads at a concentration of 20 beads per cell, for 1 hour at 37°C in 5% CO_2. Cells were analysed using BD FACSAria 1 system flow cytometer, raw FCS files analysed, data graphed using V10.0 FlowJo software. Data is presented as mean ± SD of two replicates. A-B) Significance determined using one- way ANOVA with a Newman-Keuls post-test. Output P value style APA: .12 (ns), .033 (*), .002(**) and <.001 (***); 1) comparing unstimulated control cells to each TLR stimulated cell "*" and 2) comparing each time point to the previous time point"+". , C) Data analysed to examine MPI as outlined in section 2.2.16.4 Phagocytosis Assay, to include percentage phagocytosing cells and MFI. Number indicated above bar is the MPI compared to the control cells represented as 1.*

We clearly saw that the 4 and 6 hour incubations were sufficient in promoting an appropriate phagocytic response in the J774.A.1 macrophage, and thus we moved forward with assessing the effect of the addition of fermentates in conjunction with the various TLR ligand exposure times on the macrophage. This allowed us to determine the one optimal exposure time to be used in the assessment of each candidate fermentate to be examined.

Prior to assessment of fermentates effect on phagocytosis, the RSM was used in order to establish optimal exposure time for phagocytosis in the presence of both immune challenges, LOX and LPS. This then allowed us to examine the effect of fermentate presence in immune challenged cells at each TLR ligand exposure time, analysing their impact on MFI, percentage phagocytosing cells, and MPI, for determination of optimal fermentate/TLR exposure time. RSM was added 1 hour prior to the incubation with TLRs at various exposure times, to provide continuity in assessment models used for cytokine secretion.

4.3.2.1.5 Activation of J774.A.1with RSM and LOX or LPS TLR for 1, 3, 4 and 6 hours affects phagocytosis of cells

J774.A.1 cells were seeded $1x10^6$ cells/mL and incubated overnight at 37^0C in 5% CO_2. After 24 hours cells were stimulated for 1 hour with 25mg/mL raw sample before being exposed to the following concentrations of TLR ligands for 1, 3, 4 and 6 hours: LPS 100ng/mL and LOX 0.5mM. The Procedure for phenotypic analysis of cell phagocytosis when stimulated with TLR ligands was carried out as previously described (section 2.2.16.4 Phagocytosis Assay) using 1µm fluorescent FITC latex beads. See appendix for raw MFI and percentage of phagocytosis cells. Figure 66A-C demonstrates that at 1, 3, and 4 hours, LOX significantly increased MFI, MPI ($p<0.001$), and % phagocytes ($p<0.002$; $p<0.001$; $p<0.001$).

Figure 66C-F demonstrates at 1, 3, and 4 hours, LPS significantly increased MFI, % phagocytes and MPI ($p<0.001$; $p<0.001$; $p<0.002$).

Figure 66A-C demonstrates that RSM in the presence of LOX significantly decreased MFI and MPI for 1, 3, and 4 hours ($p<0.001$), while % phagocytes was decreased at 1, 3, and 4 hours ($p<0.002$; $p<0.001$; $p<0.002$) versus the LOX 1, 3, and 4 hour time points. Unstimulated RSM at 6 hours significantly decreased % phagocytes versus the control cells ($p<0.002$).

Figure 66C-D demonstrates that RSM in the presence of LPS significantly decreased MFI and MPI for 1, 3, and 4 hours ($p<0.001$; $p<0.001$; $p<0.033$), while % phagocytes was decreased at 1, and 3 hours ($p<0.002$; $p<0.033$) versus the LPS 1,

and 3 hour time points. Unstimulated RSM at 6 hours significantly decreases % phagocytes versus the control cells ($p<0.002$).

There was a trending increase in MPI from 1-4 hours observed for RSM in the presence of LPS (1.3; 2.1; 2.3), followed by a drop at 6 hours (0.8), while with LOX there was little or no difference at the 1 and 3 hour time points (0.9; 0.7) followed by an increase at 4 hours (1.4) and similarly a drop at the 6 hour time point (0.6). For RSM alone there was a stepwise decrease observed in MPI for each time interval for 1, 3, 4 and 6 hour activations in the absence of TLR (1.1; 0.9; 0.7; 0.3).

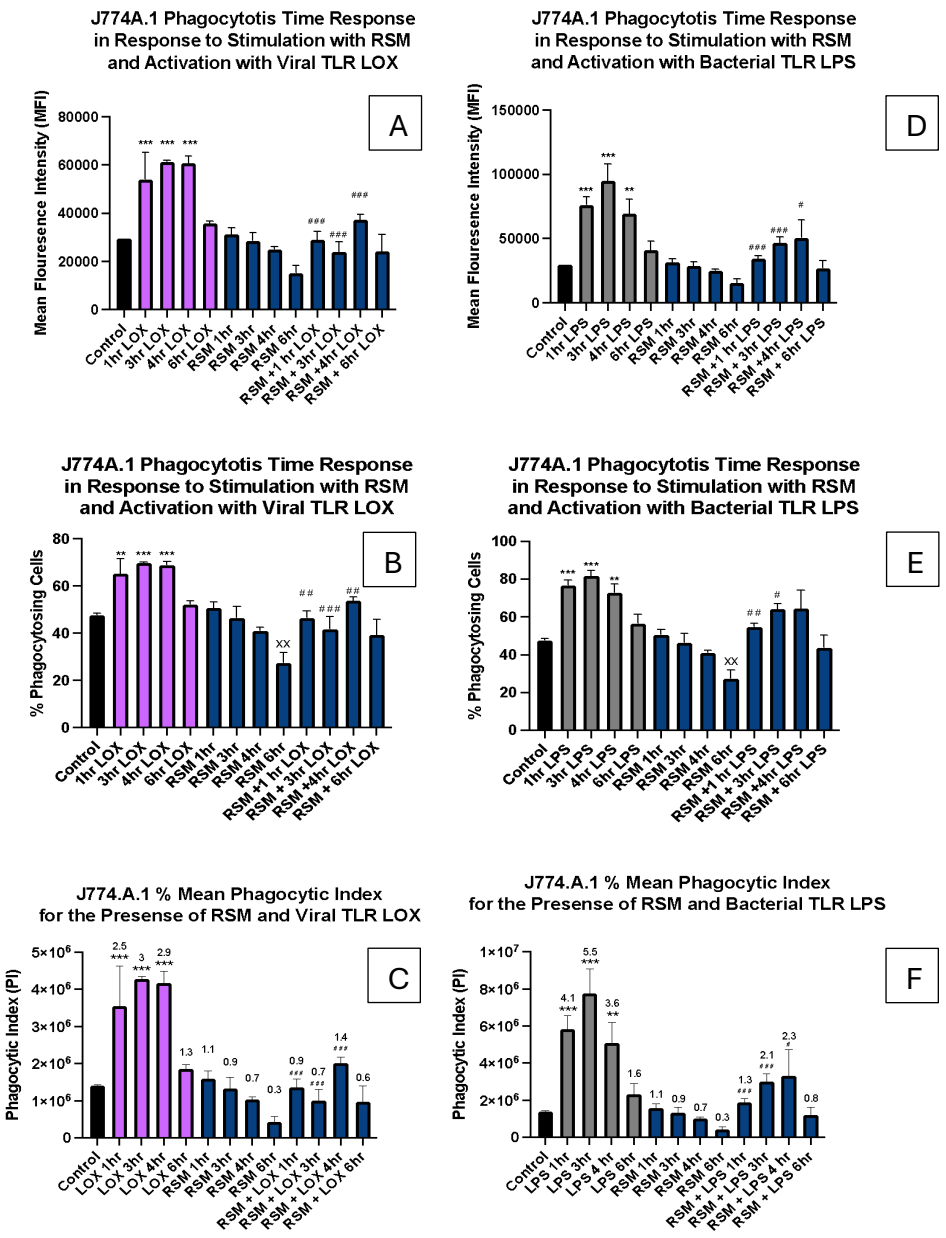

Figure 66: ***Exposure of J774.A.1 cells to LOX and LPS results in phagocytosis.*** *J774.A.1. cells were seeded at 1x10⁶ cells/mL and left overnight at 37°C in 5% CO_2. The following day cells were stimulated for 1 hour with 25mg/mL raw RSM fermentate prior to stimulation with the following concentrations of TLRs: LPS 100ng/ml, LOX 0.5mM, incubated for 1, 3, 4 and 6 hours at 37°C in 5% CO_2. Cell suspensions were retained, and cells were stimulated with 1µm fluorescent latex beads at a concentration of 20 beads per cell, for 1 hour at 37°C in 5% CO_2. Cells were analysed using BD FACSAria 1 system flow cytometer, raw FCS files analysed, data graphed using V10.0 FlowJo software. Data is presented as mean ± SD of two replicates. Significance determined using one- way ANOVA with a Newman-Keuls post-test. A-F) Output P value style APA: .12 (ns), .033 (*), .002(**) and <.001 (***); 1) comparing to TLRs to control cells "*", 2) comparing control TLR time point to corresponding RSM time point "#" and 3) comparing unstimulated RSM time points to control "x". E-F) Data analysed to examine MPI as outlined section 2.2.16.4 Phagocytosis Assay, to include percentage phagocytosing cells and MFI. Number indicated above bar is the MPI compared to the control cells represented as 1.*

We demonstrated that the addition of RSM 1 hour prior to the 4-hour TLR ligand incubation was optimal for phagocytosis in J774.A.1 macrophage. We therefore established the phagocytosis model to be used for candidate fermentate assessment.

In carrying out the assessment of the fermentates on phagocytosis we continued to examine fermentate effect in LOX, and LPS activated cells where fermentate was added 1 hour prior to a 4 hour incubation with respective TLRs.

4.3.2.1.6 Stimulation of LPS and LOX activated J774.A.1 with 25mg/mL RSM, Aerobic R0033, Anaerobic R0033, SC40 and R0419 affects MFI

J774.A.1 cells were seeded $1x10^6$ cells/mL and incubated overnight at 37^0C in 5% CO_2. After 24 hours cells were stimulated for 1 hour with 25mg/mL raw sample before being exposed to the following concentrations of TLR ligands for 4 hours: LPS 100ng/mL and LOX 0.5mM. The procedure for phenotypic analysis of cell phagocytosis when stimulated with TLR ligands was carried out as previously described (section 2.2.16.4 Phagocytosis Assay) using 1µm fluorescent FITC latex beads. See appendix for raw MFI.

Figure 67A-E demonstrates that LOX significantly increased MFI ($p<0.033$) and LPS does so to a varied extent from boosting effect to significance ($p<0.033$; $p<0.002$).

The presence of RSM had no effect when comparing sample alone, or when activated with LOX or LPS, to unstimulated control cells. RSM in the presence of LOX significantly reduced MFI compared to LOX activated cells ($p<0.033$). RSM in the presence of LPS showed a small non-significant decrease in MFI compared to LPS activated control cells. (Figure 67A).

The presence of Aerobic R0033 had no effect when comparing sample alone to unstimulated control cells, while a small non-significant increase was seen for Aerobic R0033 in the presence of LOX or LPS. Aerobic R0033 in the presence of LOX

non-significantly reduced MFI compared to LOX activated cells. Aerobic R0033 in the presence of LPS remained unchanged compared to LPS activated cells alone. (Figure 67B).

The presence of Anaerobic R0033 alone, as well as LOX and LPS activated Anaerobic R0033 non-significantly increased MFI when to unstimulated control cells. Anaerobic R0033 in the presence of LOX non-significantly reduced MFI compared to LOX activated cells. Anaerobic R0033 in the presence of LPS showed no difference in MFI compared to LPS activated cells. (Figure 67C).

The presence of SC40 significantly increased MFI when comparing sample alone, as well as in the presence of LOX and LPS, to unstimulated control cells ($p<0.002$). SC40 in the presence of LOX and LPS non-significantly increased MFI compared to LOX and LPS activated control cells. (Figure 67D).

The presence of R0419 had a small non-significant increase when comparing sample alone to unstimulated control cells, as well as for R0419 in the presence of LOX or LPS. R0419 in the presence of LOX slightly reduced MFI compared to LOX activated cells. R0419 in the presence of LPS significantly decreased in MFI compared to LPS activated cells alone ($p<0.002$). (Figure 67E).

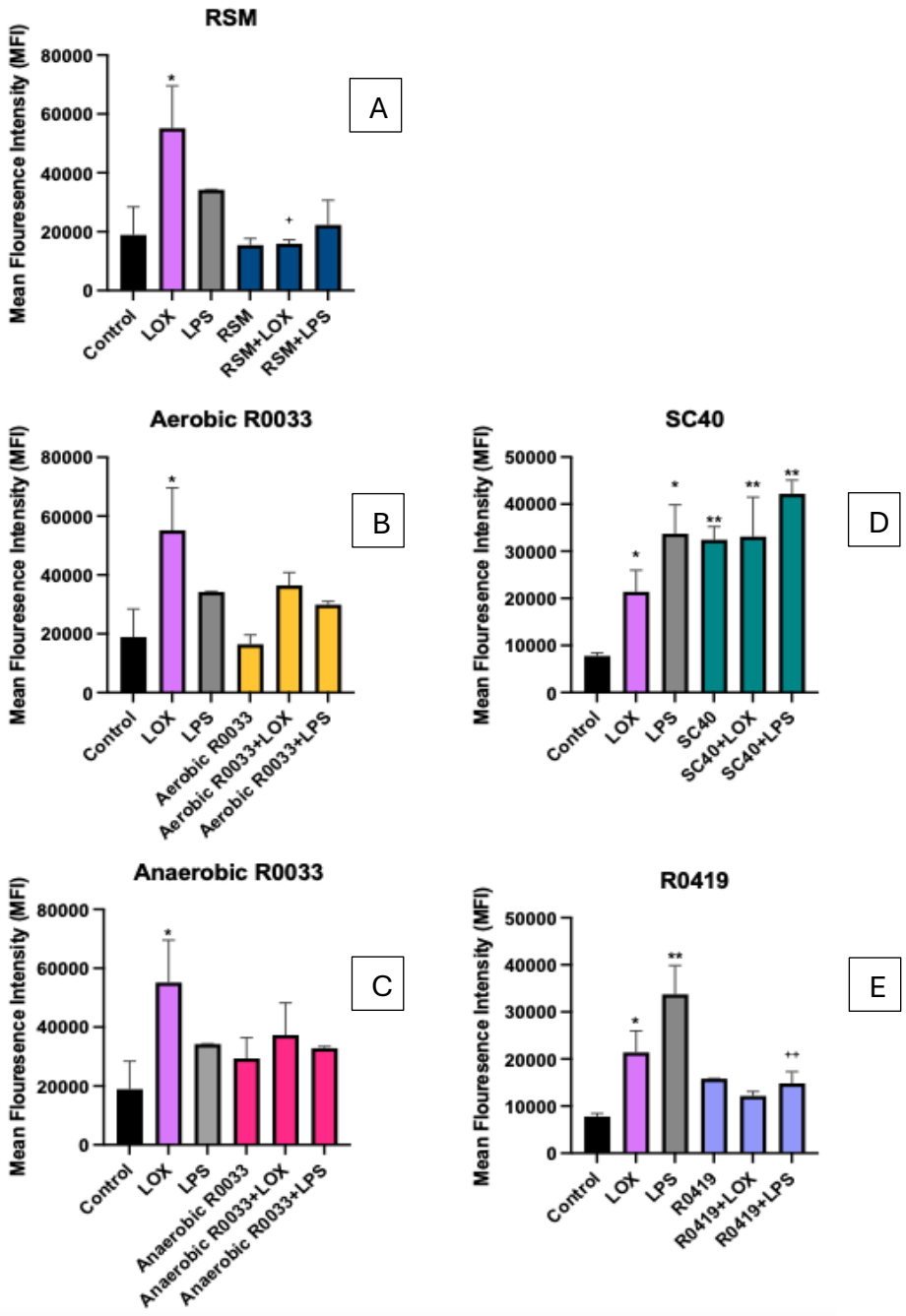

Figure 67: ***Exposure of LOX and LPS activated J774.A.1 cells to 25mg/mL sample affects MFI****. J774.A.1. cells were seeded at 1x10⁶ cells/mL and left overnight at 37°C in 5% CO_2. The following day cells were stimulated with 25mg/mL RSM, Aerobic R0033, Anaerobic R0033, SC40 and R0419 for 1 hour before activating with the following concentrations of TLRs: LPS 100ng/ml, LOX 0.5mM, and incubated for 4 hours at 37°C in 5% CO_2. Cell suspensions were retained, and cells were stimulated with 1µm fluorescent latex beads at a concentration of 20 beads per cell, for 1 hour at 37°C in 5% CO_2. Cells were analysed using BD FACSAria 1 system flow cytometer, raw FCS files analysed, data graphed using V10.0 FlowJo software. Data is presented as mean ± SD of two replicates. Significance determined using one- way ANOVA with a Newman-Keuls post-test. Output P value style APA: .12 (ns), .033 (*), .002(**) and <.001 (***); 1) comparing unstimulated control cells to each test cell "*", 2) comparing each corresponding Sample+TLR to TLR alone "+".*

4.3.2.1.7 Stimulation of J774.A.1with RSM, Aerobic R0033, Anaerobic R0033, SC40 and R0419 and activation with LOX or LPS for 4 hours affects percentage of phagocytosing cells

J774.A.1 cells were seeded $1x10^6$ cells/mL and incubated overnight at 37^0C in 5% CO_2. After 24 hours cells were stimulated for 1 hour with 25mg/mL raw sample before being exposed to the following concentrations of TLR ligands for 4 hours: LPS 100ng/mL and LOX 0.5mM. Procedure for phenotypic analysis of cell phagocytosis when stimulated with TLR ligands was carried out as previously described (section 2.2.16.4 Phagocytosis Assay) using 1µm fluorescent FITC latex beads. See appendix for raw percentage phagocytosing cell data.

Figure 68A-E demonstrates that LOX increased % phagocytosing cells to a varied degree from boosting to increased significance ($p<0.002$), as does LPS ($p<0.001$).

The presence of RSM had no effect on % phagocytes when comparing sample alone, as well as RSM activated with LOX or LPS, to unstimulated control cells. RSM in the presence of LOX non-significantly reduced % phagocytes compared to LOX activated cells. RSM in the presence of LPS had no significant effect on % phagocytes compared to LPS activated cells. (Figure 68A).

The presence of Aerobic R0033 had no effect on % phagocytes when comparing sample alone to unstimulated control cells, while Aerobic R0033 in the presence of LOX and LPS resulted in a non-significant increase in % phagocytes. Aerobic R0033 in the presence of LOX and LPS remained unchanged in % phagocytes compared to LOX and LPS activated cells alone(Figure 68B).

The presence of Anaerobic R0033 non-significantly increased % phagocytes when comparing sample alone to unstimulated control cells, as well as Anaerobic R0033 in the presence of LOX and LPS. Anaerobic R0033 in the presence of LOX non-significantly reduced % phagocytes compared to LOX activated cells, while Anaerobic R0033 in the presence of LPS remained unchanged compared to LPS activated cells. (Figure 68C).

The presence of SC40 had a significant boosting effect when comparing sample alone to unstimulated control cells, as well as SC40 in the presence of LOX or LPS ($p<0.001$). SC40 in the presence of LOX significantly increased % phagocytes

compared to LOX activated cells ($p<0.033$). SC40 in the presence of LPS non-significantly increased % phagocytes compared to LPS activated cells. (Figure 68D).

The presence of R0419 significantly increased % phagocytes when comparing sample alone to unstimulated control cells ($p<0.002$), as well as for R0419 in the presence of LOX and LPS ($p<0.033$; $p<0.002$). R0419 in the presence of LOX non-significantly reduced % phagocytes compared to LOX activated cells, while R0419 in the presence of LPS significantly decreased % phagocytes compared to LPS activated cells ($p<0.002$). (Figure 68E).

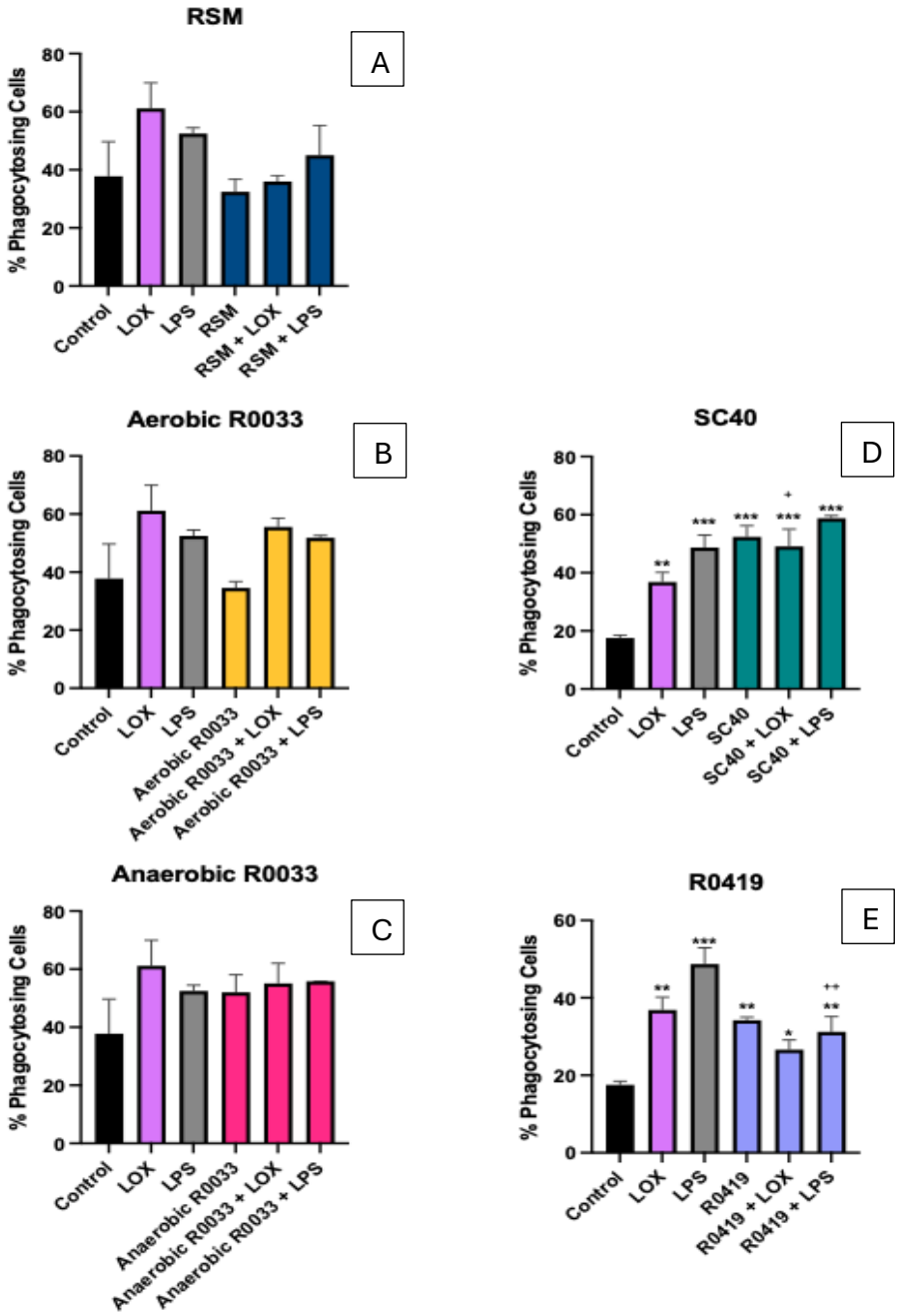

*Figure 68**: Exposure of LOX and LPS activated J774.A.1 cells to 25mg/mL sample affects percentage of phagocytosing cells.** J774.A.1. cells were seeded at 1x10⁶ cells/mL and left overnight at 37°C in 5% CO_2. The following day cells were stimulated for 1 hour with 25mg/mL raw sample fermentate prior to activation with LOX 0.5mM or LPS 100ng/mL and incubated for 4 hours at 37°C in 5% CO_2. Cell suspensions were retained, and cells were stimulated with 1µm fluorescent latex beads at a concentration of 20 beads per cell, for 1 hour at 37°C in 5% CO_2. Cells were analysed using BD FACSAria 1 system flow cytometer, raw FCS files analysed, data graphed using V10.0 FlowJo software. Data is presented as mean ± SD of two replicates. Significance determined using one- way ANOVA with a Newman-Keuls post-test. Output P value style APA: .12 (ns), .033 (*), .002(**) and <.001 (***); 1) comparing unstimulated control cells to each test cell "*", 2) comparing each corresponding Sample+TLR to TLR alone "+".*

4.3.2.1.8 MPI is affected by the presence of samples RSM, Aerobic R0033, Anaerobic R0033, SC40 and R0419 in LOX and LPS activated J744 macrophage

J774.A.1 cells were seeded $1x10^6$ cells/mL and incubated overnight at 37^0C in 5% CO_2. After 24 hours cells were stimulated for 1 hour with 25mg/mL raw sample before being exposed to the following concentrations of TLR ligands for 4 hours: LPS 100ng/mL and LOX 0.5mM. Procedure for phenotypic analysis of cell phagocytosis when stimulated with TLR ligands was carried out as previously described (section 2.2.16.4 Phagocytosis Assay) using 1µm fluorescent FITC latex beads. See appendix for raw MFI and percentage phagocytosing cell data.

Figure 69A-E demonstrates that LOX increased % phagocytosing cells to a varied degree from boosting to increased significance ($p<0.033$), as does LPS ($p<0.033$; $p<0.001$).

The presence of RSM had no significant effect on MPI when comparing sample alone to unstimulated control cells (0.6), or for RSM in the presence of LOX (0.7) or LPS (1.3). RSM in the presence of LOX significantly reduced MPI compared to LOX activated cells (0.7 RSM LOX vs. 4.4 LOX) ($p<0.033$). RSM in the presence of LPS showed a small non-significant decrease in MPI compared to LPS activated cells (1.3 RSM LPS vs. 2.3 LPS). (Figure 69A).

The presence of Aerobic R0033 had no significant effect on MPI when comparing sample alone to unstimulated control cells (0.7), while Aerobic R0033 in the presence of LOX and LPS doubled that of the control (2.6; 2.0). Aerobic R0033 in the presence of LOX reduced MPI compared to LOX activated cells (2.6 Aerobic LOX vs. 4.4 LOX). The MPI of Aerobic R0033 in the presence of LPS remained unchanged compared to LPS activated cells alone (2.0 Aerobic LPS vs. 2.3 LPS). (Figure 69B).

The presence of Anaerobic R0033 non-significantly increased MPI when comparing sample alone to unstimulated control cells (2), while Anaerobic R003 in the presence of LOX and LPS doubled that of the control (2.7; 2.3). Anaerobic R0033 in the presence of LOX reduced MPI compared to LOX activated cells (2.7 Anaerobic LOX vs. 4.4 LOX), while Anaerobic R0033 in the presence of LPS remained unchanged compared to LPS activated cells (2.3 Anaerobic LPS vs. 2.3 LPS). (Figure 69C).

The presence of SC40 significantly increased MPI when comparing sample alone (12.4) to unstimulated control cells ($p<0.033$), as well as for SC40 in the presence of LOX (12.0)and LPS (18.1) ($p<0.033$; $p<0.002$). SC40 in the presence of LOX slightly increased MPI compared to LOX activated cells (12.0 SC40 LOX vs. 5.8 LOX). SC40 in the presence of LPS increased MPI compared to LPS activated cells alone (18.1 SC40 LPS vs. 12.1 LPS). (Figure 69D).

The presence of R0419 non-significantly increased MPI when comparing sample alone (3.9) to unstimulated control cells, as well as for R0419 in the presence of LOX (2.3) and LPS (3.4). R0419 in the presence of LOX reduced MPI compared to LOX activated cells (2.3 R0419 LOX vs. 5.8 LOX). R0419 in the presence of LPS showed a significant decrease in MPI compared to LPS activated cells alone (3.4 R0419 LPS vs. 12.1 LPS) ($p<0.002$). (Figure 69E).

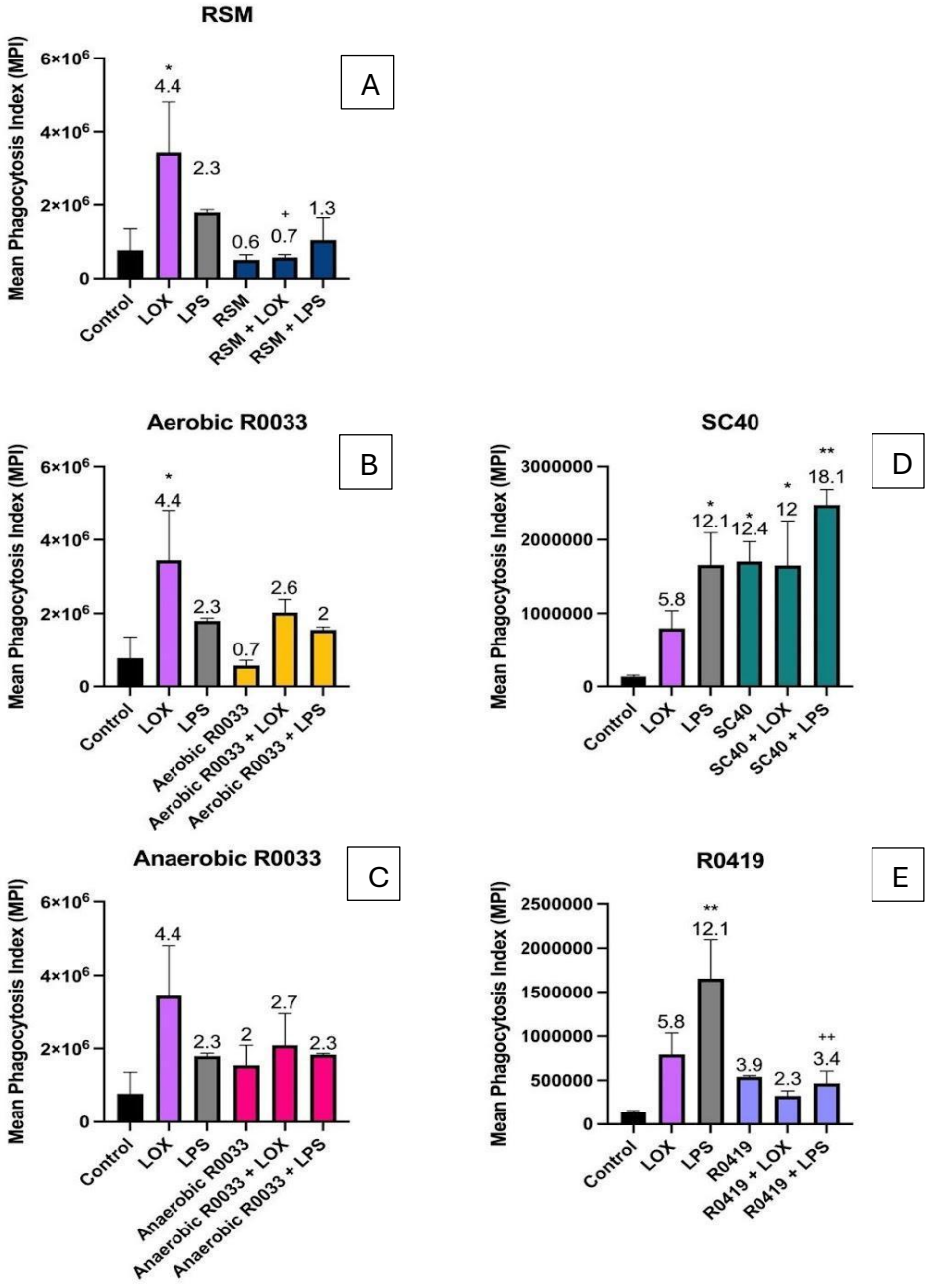

Figure 69: ***Exposure of LOX and LPS activated J774.A.1 cells to 25mg/mL sample affects MPI.*** *J774.A.1. cells were seeded at 1x10⁶ cells/mL and left overnight at 37°C in 5% CO_2. The following day cells were stimulated with 25mg/mL raw sample RSM, Aerobic R0033, Anaerobic R0033, SC40 and R0419 for 1 hour prior to activation with LOX 0.5mM and LPS 100ng/mL and incubated for 4 hours at 37°C in 5% CO_2. Cell suspensions were retained, and cells were stimulated with 1µm fluorescent latex beads at a concentration of 20 beads per cell, for 1 hour at 37°C in 5% CO_2. Cells were analysed using BD FACSAria 1 system flow cytometer, raw FCS files analysed, data graphed using V10.0 FlowJo software, data analysed to examine MPI as outlined in section 2.2.16.4 Phagocytosis Assay, to include percentage phagocytosing cells and MFI. Data is presented as mean ± SD of two replicates. Number indicated above bar is the MPI compared to the control cells represented as 1. Significance determined using one- way ANOVA with a Newman-Keuls post-test. Output P value style APA: .12 (ns), .033 (*), .002(**) and <.001 (***); 1) comparing unstimulated control cells to each test cell "*", 2) comparing each corresponding Sample+TLR to TLR alone "+".*

Thus using the MFI, percentage phagocytosing cells, and combined MPI, we were able to establish that fermentates Aerobic R0033, Anaerobic R0033, SC40, and R0419 affected phagocytic activity. Not only this but the differing effect on phagocytosis was observed in differentially activated cells, activated with viral immune challenge LOX, and inflammatory immune challenge LPS.

Expanding the scope of the study the effect of fermentates on macrophage function on cell surface marker expression was also examined. These cell surface markers are critical for cell to cell interactions and proper immune functioning, and thus are important.

4.3.2.1.9 J774.A.1 cell surface marker expression is affected by the presence of sample RSM, Aerobic R0033, Anaerobic R0033, SC40 and R0419

J774.A.1 cells were seeded $1x10^6$ cells/mL and incubated for 1 hour at 37^0C in 5% CO_2. Then stimulated for 1 hour with 25mg/mL raw sample before being exposed to the following concentrations of TLR ligands for 24 hours: LPS 100ng/mL and LOX 0.5mM. Procedure for phenotypic analysis of cell surface marker expression when stimulated with TLR ligands was carried out as previously described (section 2.2.16.1 Cell Surface marker Staining) using fluorescently labelled antibodies FITC, APC, and PE. See appendix for raw MFI data.

Figure 70 and Figure 71 show that samples significantly affected the expression of cell surface markers in response to immune challenges LOX, and LPS when compared to the RSM. LOX significantly increased the expression of CD86, CD14, CD40, TLR4 ($p<0.001$), CD80 ($p<0.002$), and MHCII ($p<0.033$), and decreased MHCI ($p<0.001$). LPS significantly increased the expression of MHCII, CD86, CD80, CD40, TLR2, MHCI ($p<0.001$), and CD14 ($p<0.002$), while decreasing TLR4 ($p<0.001$).

Figure 70 demonstrates in the presence of LOX, Aerobic R0033, Anaerobic R0033, SC40 and R0419 decreased the expression of MHCII, TLR4, CD86 ($p<0.001$), and TLR2 ($p<0.001$; $p<0.001$; $p<0.002$; $p<0.001$). Aerobic R0033 and Anaerobic

R0033 decreased CD80, CD14, CD40, and MHCI ($p<0.001$). Aerobic R0033, Anaerobic R0033, SC40 and alone decreased MHCII ($p<0.001$), and TLR4 ($p<0.033$; $p<0.001$; $p<0.001$; $p<0.001$). Aerobic R0033 and Anaerobic R0033 alone decreased CD86 and MHCI ($p<0.001$), while R0419 decreased MHCI ($p<0.001$). In contrast SC40 increased CD80, CD14, CD40, and TLR2 ($p<0.001$), and R0419 increased CD14 and CD40 ($p<0.002$).

Figure 71 demonstrates in the presence of LPS, Anaerobic R0033, SC40 and R0419 decreased MHCII, TLR4, CD86 ($p<0.001$), as well as Aerobic R0033 decreasing CD86 ($p<0.001$). Anaerobic R0033 increased CD40 and MHCI ($p<0.002$), SC40 and R0419 increased CD40 ($p<0.001$; $p<0.002$), and Aerobic R0033 increased MCHI ($p<0.033$). Aerobic R0033, Anaerobic R0033, SC40 and R0419 alone decreased MHCII, TLR4 ($p<0.001$). Aerobic R0033 and Anaerobic R0033 alone decreased CD86 ($p<0.002$; $p<0.001$) and MHCI ($p<0.033$; $p<0.002$). SC40 alone increased CD80, CD14, CD40 and TLR2 ($p<0.001$), while R0419 increased CD40 and CD14 ($p<0.002$; $p<0.033$) but decreased MCHI ($p<0.002$).

However when comparing samples activated with LOX and LPS to the respective TLR control, samples significantly affect the expression of cell surface markers.

Figure 70 demonstrates in the presence of LOX, RSM increased the expression of MHCII, TLR4, CD86, CD80, CD14, CD40, TLR2 and MHCI ($p<0.001$). Aerobic R0033 and Anaerobic R0033 decreased CD14 ($p<0.033$; $p<0.001$). SC40 and R0419 increased CD14, CD40, CD86, TLR2, CD80, and MHCI ($p<0.001$). Anaerobic R0033 decreased CD40 and TLR2 ($p<0.001$; $p<0.002$). RSM, Aerobic R0033, Anaerobic R0033, SC40 and R0419 alone increased CD14, CD40, CD86, TLR2, CD80 and MHCI ($p<0.001$), and MHCII ($p<0.001$; $p<.001$; $p<0.001$; $p<0.002$; $p<0.002$).RSM and Aerobic R0033 alone increased TLR4 ($p<0.001$; $p<0.033$).

Figure 71 demonstrates in the presence of LPS, RSM, Aerobic R0033, Anaerobic R0033, SC40 and R0419 increased the expression of MHCII, TLR4, CD86, CD14, TLR2 ($p<0.001$), CD80 ($p<0.002$; $p<0.033$; $p<0.002$; $p<0.001$; $p<0.001$), and CD40 ($p<0.033$; $pp<0.002$; $p<0.001$; $p<0.001$; $p<0.001$). Aerobic R0033 and Anaerobic R0033 increased MHCI ($p<0.033$; $p<0.002$).

RSM, Aerobic R0033, Anaerobic R0033, SC40 and R0419 alone increased MCHII, CD14, CD40, CD86, TLR2, MHCI ($p<0.001$), TLR4 ($p<0.001$; $p<.001$; $p<0.001$; $p<0.002$; $p<0.002$), and CD80 ($p<0.002$; $p<.002$; $p<0.002$; $p<0.001$; $p<0.001$).

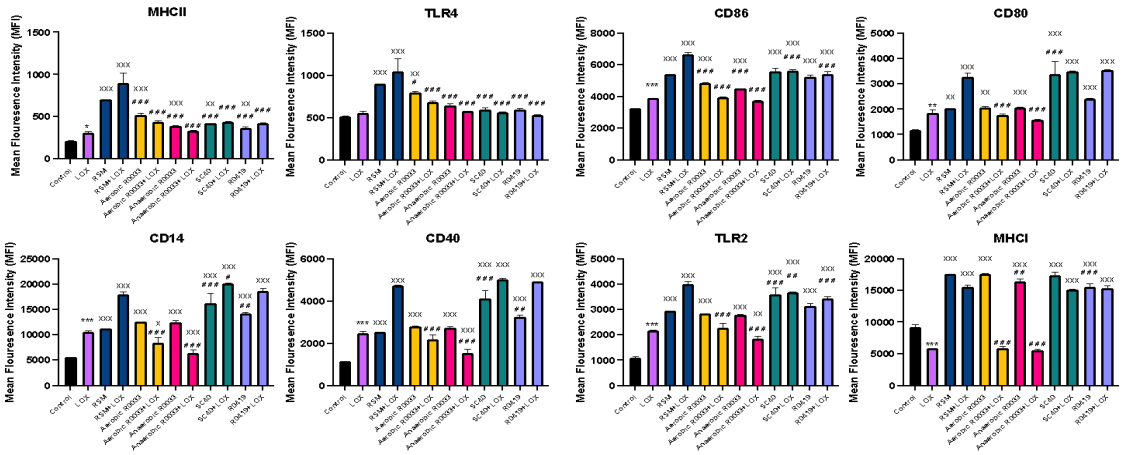

Figure 70: ***Exposure of LOX activated J774.A.1 cells to 25mg/mL sample affects Cell Surface Marker Expression.*** *J774.A.1 cells were seeded at 1x10⁶ cells/mL, incubated for 1 hour at 37°C in 5% CO_2. Cells were stimulated with 25mg/mL sample fermentate and incubated for 1 hour at 37°C in 5% CO_2 before stimulating with TLR ligands at the following concentration: LOX 0.5mM, and LPS 100ng/mL. After 24 hours cell suspensions were retained, and cell staining protocol was carried to assess the presence of cell surface markers MHCII, TLR4, CD86, CD80, CD14, CD40, TLR2 and MHCI in the presence of fermentate sample. Cells were analysed using BD FACSAria 1 system flow cytometer, raw FCS files analysed, data graphed using V10.0 FlowJo software. Data is presented as mean ± SD of two replicates. Significance determined using one- way ANOVA with a Newman-Keuls post-test. Output P value style APA: .12 (ns), .033 (*), .002(**) and <.001 (***) comparing unstimulated control cells to unstimulated sample cells"*" , compares RSM to sample equivalent"#", and comparing sample to control/TLR "x".*

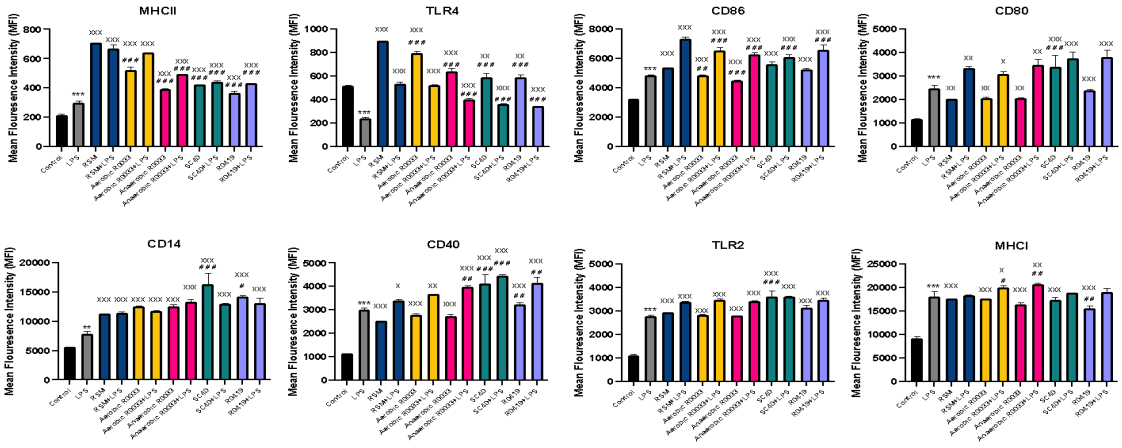

Figure 71: ***Exposure of LPS activated J774.A.1 cells to 25mg/mL sample affects Cell Surface Marker Expression.*** *J774.A. cells were seeded at 1x10⁶ cells/mL, incubated for 1 hour at 37°C in 5% CO_2. Cells were stimulated with 25mg/mL sample fermentate and incubated for 1 hour at 37°C in 5% CO_2 before stimulating with TLR ligands at the following concentration: LOX 0.5mM, and LPS 100ng/mL. After 24 hours cell suspensions were retained, and cell staining protocol was carried to assess the presence of cell surface markers MHCII, TLR4, CD86, CD80, CD14, CD40, TLR2 and MHCI in the presence of fermentate sample. Cells were analysed using BD FACSAria 1 system flow cytometer, raw FCS files analysed, data graphed using V10.0 FlowJo software. Data is presented as mean ± SD of two replicates. Significance determined using one- way ANOVA with a Newman-Keuls post-test. Output P value style APA: .12 (ns), .033 (*), .002(**) and <.001 (***) comparing unstimulated control cells to unstimulated sample cells"*" , compares RSM to sample equivalent"#", and comparing sample to control/ TLR "x".*

We clearly saw that the presence of fermentates significantly affected the expression of cell surface markers, in LOX and LPS activated J774.A.1 cells. Having completed significant analysis of fermentates affects in the J774.A.1 macrophage cell line, we wanted to examine their effects in a primary cell, BMDMs, as these are a better macrophage representative model.

Similarly to that of the BMDCs, BMDMs are easy to use and allow for a more representative assessment of how the samples will behave *in vivo*. We limited the use of BMDMs to the assessment of chemokine and cytokine secretion as limited cell concentrations were harvested and thus the more resource dependant assays were not suitable or feasible for this cell model.

4.3.2.2 BMDM screening

Initially it was important to ensure that harvested cells from the bone marrow of the mouse could be correctly differentiated into BMDMs, as the protocol for BMDC and BMDM differentiation was very similar. Therefore an initial staining for key macrophage surface marker F4/80 was carried out, for determination of differentiation between BMDM, versus BMDCs.

4.3.2.2.1 BMDM and BMDC cell lines can be differentiated and isolated by screening for expression of key surface markers of the macrophage lineage F4/80 and CD11b

BMDM and BMDC's were isolated from Balb/C mice and seeded at a concentration of $1x10^6$ cells/mL. Cells were cultured as previously described with either of 25ng/mL rM-CSF or 5ng/mL GM-CSF for differentiation of naïve monocytes into BMDM or BMDC's respectively. Labelling of both cell population with both CD11b and F4/80 allowed for the differentiation of macrophage from dendritic cells as only macrophage will express the F4/80 marker. Figure 72 demonstrated that comparable levels of CD11b are expressed in both the BMDM and BMDC cell populations, while only the BMDM cell population expresses the F4/80 marker. 68.9% of the cell population cultured with 25ng/mL rM-CSF differentiated into BMDM's, while only 29% of cells differentiated into BMDC's. 84.6% of the cell population cultured with 5ng/mL GM-CSF differentiated into BMDC's, while only 13.5% of cells differentiated into BMDM's. It is important to note that there was a limitation in the differentiation of BMDCs and BMDMs as there was a cross over of the two populations and thus the populations were not pure.

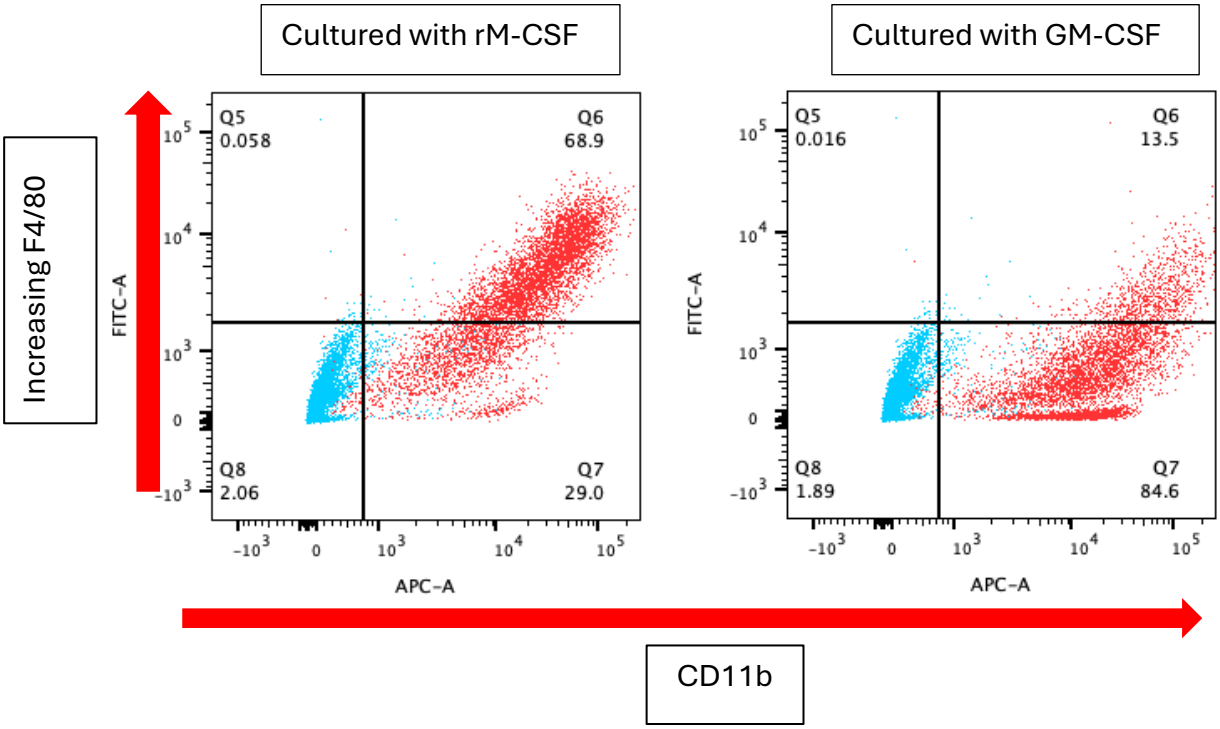

Figure 72: ***Isolated BMDM Express Key Surface Markers of the Macrophage Lineage F4/80.*** *BMDM were isolated from female Balb/C mice as previously described. Macrophage were cultured in the presence of 25ng/mL rM-CSF and dendritic cells were cultured in the presence of 5ng/mL GM-CSF. Cultured BMDMs and BMDCs were fluorescently labelled as previously described (section 2.2.16.3 BMDC and BMDM Purity Assay). BMDMs and BMDCs express comparable levels of CD11b. F4/80 a key macrophage marker is present only in cells cultured with rM-CSF, a key growth factor required for macrophage differentiation and proliferation. Blue represents unstained cells while Red represents viable populations of BMDM and BMDC cells stained with specific antibodies. % cell population highlighted per quarter.*

Therefore, only BMDMs were clearly shown to express macrophage marker F4/80, while BMDCs did not express this marker. Both BMDM, and BMDCs express the CD11b marker clearly labelling them as viable monocytes.

Having demonstrated that we were able to successfully isolate and differentiate BMDM, from BMDCs, we were now able to assess fermentate effect on cell viability, as well as cytokine and chemokine secretion in primary BMDMs. LOX and LPS were used as the key immune challenges, while availability of resources allowed for the addition of PIC, and CpG assessment also.

4.3.2.2.2 Stimulation of TLR activated BMDM with 25mg/mL raw samples Aerobic R0033, Anaerobic R0033, SC40 and R0419 doesn't affect cell viability

BMDM were seeded at a concentration of $1x10^6$ cells/mL, incubated for 24 hours before stimulating with a dose of 25mg/mL raw fermentate sample for 1 hour followed by viral TLR ligand: : LOX 0.5mM and PIC 10µg/mL or inflammatory TLR ligand: LPS 100ng/mL and CpG 5 µM respectively and subsequently incubated at 37^0C in 5% CO_2. After 24 hours an MTS assay was performed as previously outlined (section 2.2.13 MTS Cell Viability Assay).

Figure 73 demonstrates that there was no significant change in cell viability following exposure of the cells to 25mg/mL raw fermentate samples Aerobic R0033, Anaerobic R0033, SC40 and R0419 to either viral or inflammatory TLR ligand stimulations.

The RSM acted as the whole fermentate control for comparison of effects induced by each independent sample i.e., Aerobic R0033, Anaerobic R0033, SC40 and R0419. The use of the positive control of 10% DMSO provided a clear distinction between the cytotoxic effects on cell viability with the untreated control sample, as DMSO induces cell death.

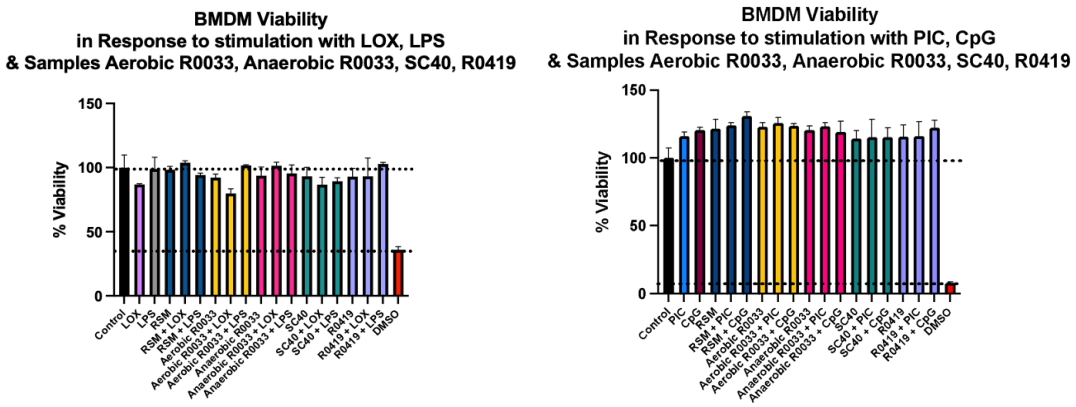

*Figure 73**: Exposure of BMDM to panel of TLRs and 25mg/mL raw sample Aerobic R0033, Anaerobic R0033, SC40 and R0419 doesn't affect cell viability.** BMDM cells were seeded at 1x10⁶ cells/mL and left overnight at 37°C in 5% CO_2. The following day cells were stimulated with 25mg/mL sample fermentate, incubated for 1 hour at 37°C in 5% CO_2 and subsequently exposed to the following concentrations of TLRs: LOX 0.5mM, LPS 100ng/mL, CpG 5 µM, PIC 10µg/mL for TLR activation before incubating overnight under the same conditions. RSM is the fermentate control. 10% DMSO was included as a positive control to induce cell death. Cells were incubated with MTS cell titre aqueous one solution for 3 hours at 37°C in 5% CO_2. Viability is represented as a percentage compared to viable, untreated cells (Control). Data is presented as mean ± SD of three replicates.*

4.3.2.2.3 Stimulation of TLR activated BMDMs with 25mg/mL raw samples Aerobic R0033, Anaerobic R0033, SC40 and R0419 affects secretion of cytokines

BMDM were seeded at a concentration of 1x10^6 cells/mL, incubated for 24 hours before stimulating with a dose of 25mg/mL raw fermentate sample for 1 hour followed by viral TLR ligand: : LOX 0.5mM and PIC 10µg/mL or inflammatory TLR ligand: LPS 100ng/mL and CpG 5 µM respectively and subsequently incubated at 37^{0}C in 5% CO_2. After 24 hours supernatants were removed and ELISA procedure for cytokines IL-1β, IL-6, IL-10 , TNF-α, IL-12p40, IL-12p70, IL-23, and IL-27 was performed according to the manufacturer's instructions (section 2.2.14 Enzyme Linked Immunosorbent Assay (ELISA)).

Figure 74 - Figure 77 demonstrate that samples significantly affected the secretion of cytokines from BMDMs in response to immune challenges LOX, PIC, LPS, and CpG when compared to the RSM. LOX significantly increased the secretion of IL-1β, TNF-α ($p<0.001$), and IL-12p40 ($p<0.033$), while non-significantly increasing IL-6, IL-10 and IL-27. PIC significantly increased TNF-α, IL-27 ($p<0.001$),

and IL-10 ($p<0.002$), and non-significantly increased IL-6 and IL-12p40. LPS significantly increased IL-6, TNF-α, and IL-27 ($p<0.001$), and non-significantly increased IL-10. CpG significantly increased IL-10, TNF-α, IL-12p40, IL-27 ($p<0.001$), and IL-1β ($p<0.002$), and non-significantly increased IL-6. Concentrations of IL-12p70 and IL-23 were very low and thus not considered significant.

In the presence of LOX, Aerobic R0033, Anaerobic R0033, and R0419 increased IL-10 ($p<0001$), Aerobic R0033 and SC40 increased IL-1β ($p<0.001$), SC40 increased IL-6 and TNF-α ($p<0.001$), while SC40 and R0419 decreased IL-12p40 and IL-27 ($p<0.001$), along with aerobic R0033 decreased IL-27 ($p<0.002$). Aerobic R0033 alone increased IL-1β ($p<0.002$), while unstimulated SC40 increased IL-1β, TNF-α ($p<0.001$), and IL-6 ($p<0.002$).

In the presence of PIC, Aerobic R0033, Anaerobic R0033,SC40 and R0419 increased IL-10 ($p<0001$), Anaerobic R0033, SC40 and R0419 increased TNF-α ($p<0.001$; $p<0.001$ $p<0.033$), SC40 and R0419 increased IL-1β ($p<0.033$; $p<0.002$), SC40 increased IL-6 ($p<0.001$) and Aerobic R0033 increased IL-27 ($p<0.002$), while Aerobic R0033, SC40 and R0419 decreased IL-12p70 ($p<0.001$).Anaerobic R0033, SC40 and R0419 alone increased IL-10 and IL-27 ($p<0.001$), Aerobic R0033 and Anaerobic R0033 increased IL-1β ($p<0.033$), SC40 increased IL-6 and TNF-α ($p<0.001$), while Aerobic R0033, Anaerobic R0033, SC40 and R0419 decreased IL-12p40 ($p<0.001$).

In the presence of LPS, Aerobic R0033, Anaerobic R0033, SC40, and R0419 increased IL-10 ($p<0.001$; $p<0.033$ $p<0.001$; $p<0.001$), Aerobic R0033 and SC40 increased IL-1β ($p<0.002$; $p<0.001$), SC40 increased IL-6, TNF-α and IL-27 ($p<0.001$), while Anaerobic R0033 and R0419 decreased IL-6 ($p<0.002$)Aerobic R0033 alone increased IL-1β and IL-10 ($p<0.001$), while unstimulated SC40 increased IL-1β, IL-6, IL-10 and TNF-α ($p<0.001$; $p<0.001$ $p<0.033$; $p<0.001$), and Anaerobic R0033 increased IL-27 ($p<0.002$).

In the presence of CpG, Aerobic R0033, Anaerobic R0033, SC40, and R0419 decreased IL-6 ($p<0.001$; $p<0.001$ $p<0.001$; $p<0.002$), Aerobic R0033, SC40 and R0419 decreased TNF-α ($p<0.001$; $p<0.001$; $p<0.002$), Aerobic R0033 and Anaerobic R0033 decreased IL-10 ($p<0.033$), SC40 decreased IL-12p40 ($p<0.033$). Aerobic R0033, Anaerobic R0033, SC40, and R0419 alone decreased IL-12p40

(p<0.001) and IL-12p70 (p<0.033), unstimulated Anaerobic R0033, SC40 and R0419 increased IL-10 and IL-27 (p<0.001), SC40 increased IL-6 and decreased TNF-α (p<0.002; p<0.001), and Aerobic R0033 increased IL-1β (p<0.033) although very low concentration.

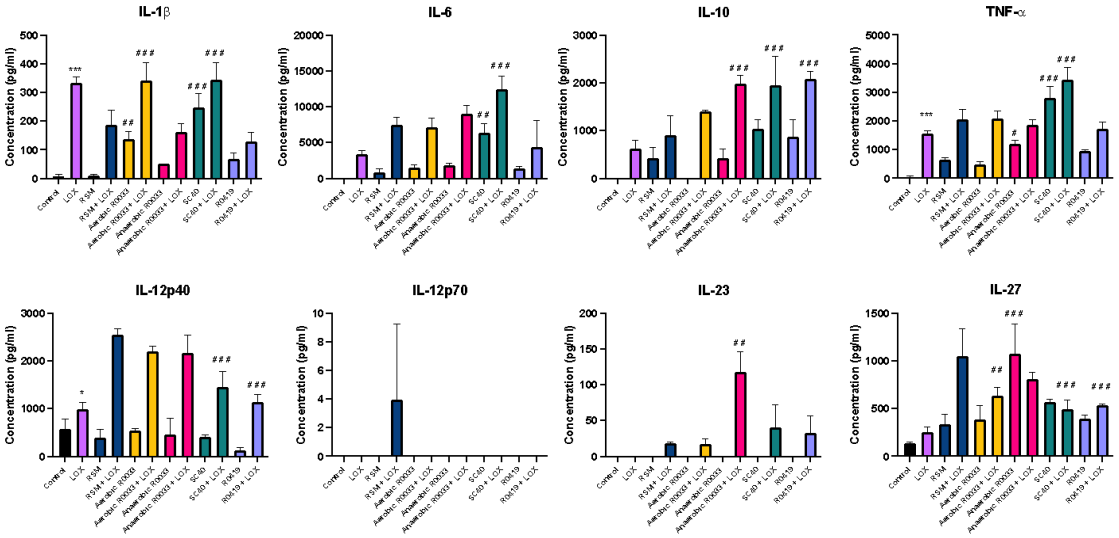

Figure 74: ***Exposure of LOX activated BMDM to 25mg/mL raw sample results in the secretion of cytokines.*** *BMDM cells were seeded at 1x10⁶ cells/mL and left overnight at 37°C in 5% CO_2. The following day cells were stimulated with 25mg/mL raw sample fermentate, incubated for 1 hour at 37°C in 5% CO_2 and 5% CO_2 and subsequently exposed to the following concentrations of TLR: LOX 0.5mM for TLR activation before incubating overnight under the same conditions. RSM is the fermentate control. Supernatants were removed after 24 hours and ELISA was performed for cytokines IL-1β, IL-6, IL-10, TNF-α, IL-12p40, IL-12p70, IL-23, and IL-27. Data is presented as mean ± SD of three replicates. Significance determined using one- way ANOVA with a Newman-Keuls post-test. Output P value style APA: .12 (ns), .033 (*), .002(**) and <.001 (***); 1) comparing unstimulated control cells to each TLR stimulated cell "*",and 2) comparing RSM to sample equivalents "#".*

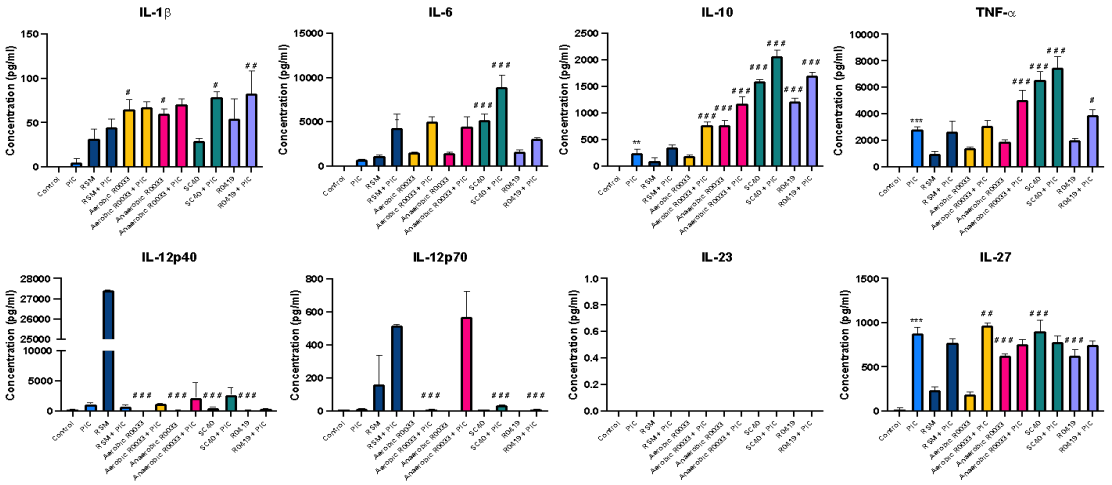

Figure 75: ***Exposure of PIC activated BMDM to 25mg/mL raw sample results in the secretion of cytokines.*** *BMDM cells were seeded at 1x10⁶ cells/mL and left overnight at 37°C in 5% CO_2. The following day cells were stimulated with 25mg/mL raw sample fermentate, incubated for 1 hour at 37°C in 5% CO_2 and 5% CO_2 and subsequently exposed to the following concentrations of TLR: PIC 10µg/mL for TLR activation before incubating overnight under the same conditions. RSM is the fermentate control. Supernatants were removed after 24 hours and ELISA was performed for cytokines IL-1β, IL-6, IL-10, TNF-α, IL-12p40, IL-12p70, IL-23, and IL-27. Data is presented as mean ± SD of three replicates. Significance determined using one- way ANOVA with a Newman-Keuls post-test. Output P value style APA: .12 (ns), .033 (*), .002(**) and <.001 (***); 1) comparing unstimulated control cells to each TLR stimulated cell "*",and 2) comparing RSM to sample equivalents "#".*

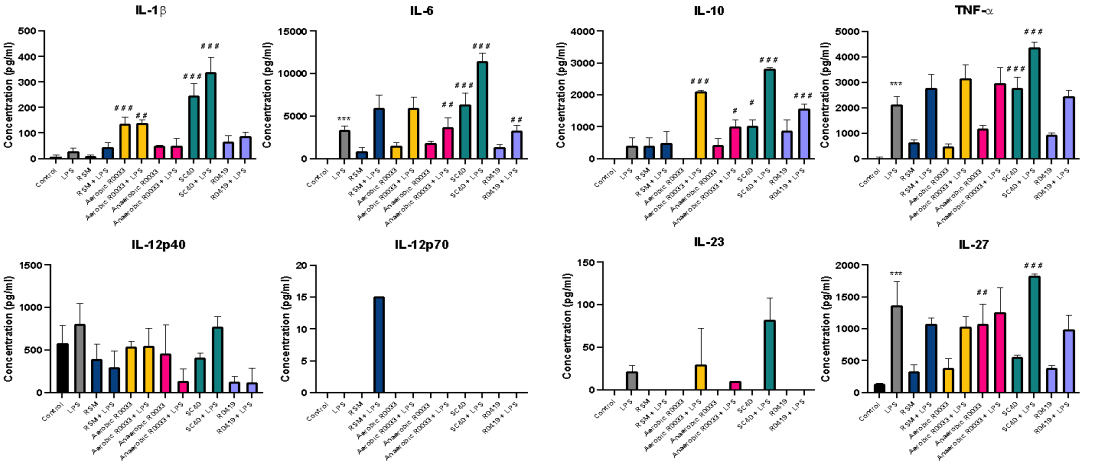

Figure 76: ***Exposure of LPS activated BMDM to 25mg/mL raw sample results in the secretion of cytokines.*** *BMDM cells were seeded at 1x10⁶ cells/mL and left overnight at 37°C in 5% CO_2. The following day cells were stimulated with 25mg/mL raw sample fermentate, incubated for 1 hour at 37°C in 5% CO_2 and 5% CO_2 and subsequently exposed to the following concentrations of TLR: LPS 100ng/mL for TLR activation before incubating overnight under the same conditions. RSM is the fermentate control. Supernatants were removed after 24 hours and ELISA was performed for cytokines IL-1β, IL-6, IL-10, TNF-α, IL-12p40, IL-12p70, IL-23, and IL-27. Data is presented as mean ± SD of three replicates. Significance determined using one- way ANOVA with a Newman-Keuls post-test. Output P value style APA: .12 (ns), .033 (*), .002(**) and <.001 (***); 1) comparing unstimulated control cells to each TLR stimulated cell "*",and 2) comparing RSM to sample equivalents "#".*

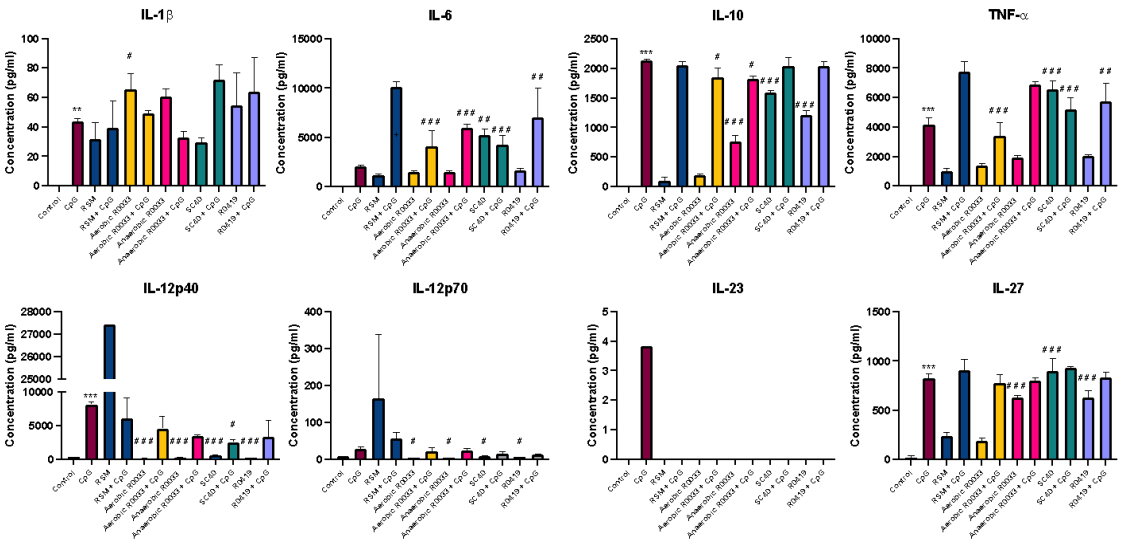

Figure 77: ***Exposure of CpG activated BMDM to 25mg/mL raw sample results in the secretion of cytokines.*** *BMDM cells were seeded at 1x10⁶ cells/mL and left overnight at 37°C in 5% CO_2. The following day cells were stimulated with 25mg/mL raw sample fermentate, incubated for 1 hour at 37°C in 5% CO_2 and 5% CO_2 and subsequently exposed to the following concentrations of TLR: CpG 5μM for TLR activation before incubating overnight under the same conditions. RSM is the fermentate control. Supernatants were removed after 24 hours and ELISA was performed for cytokines IL-1β, IL-6, IL-10, TNF-α, IL-12p40, IL-12p70, IL-23, and IL-27. Data is presented as mean ± SD of three replicates. Significance determined using one- way ANOVA with a Newman-Keuls post-test. Output P value style APA: .12 (ns), .033 (*), .002(**) and <.001 (***); 1) comparing unstimulated control cells to each TLR stimulated cell "*",and 2) comparing RSM to sample equivalents "#".*

Fermentates Aerobic R0033, Anaerobic R0033, SC40, and R0419 as demonstrated previously in cell line macrophage model J774.A.1, maintained cell viability, and bioactivity in the primary cell BMDMs. We therefore wanted to expand on this to additionally, assess their effect on chemokine secretion.

Chemokine secretion is critical to proper immune function and is a key role of the macrophage. Therefore, we wanted to assess if the presence of fermentate had the ability to impact on this parameter also.

4.3.2.2.4 Stimulation of TLR activated BMDMs with 25mg/mL raw samples Aerobic R0033, Anaerobic R0033, SC40 and R0419 affects secretion of chemokines

BMDM were seeded at a concentration of $1x10^6$ cells/mL, incubated for 24 hours before stimulating with a dose of 25mg/mL raw fermentate sample for 1 hour followed by viral TLR ligand: : LOX 0.5mM and PIC 10µg/mL or inflammatory TLR ligand: LPS 100ng/mL and CpG 5 µM respectively and subsequently incubated at 37^0C in 5% CO_2. After 24 hours supernatants were removed and ELISA procedure for chemokines MCP, MIP-1, and MIP-2 was performed according to the manufacturer's instructions (section 2.2.14 Enzyme Linked Immunosorbent Assay (ELISA)).

Figure 78 and Figure 79 demonstrate that samples significantly affected the secretion of chemokines from BMDMs in response to immune challenges LOX, PIC, LPS, and CpG when compared to the RSM. LOX and CpG significantly increased the secretion of MCP, MIP-1 and MIP-2 ($p<0.001$). PIC significantly increased MCP, MIP-1 and MIP-2 ($p<0.001$; $p<0.001$; $p<0.033$). LPS significantly increased MCP and MIP-2 ($p<0.001$), and non-significantly increased MIP-1.

In the presence of LOX, Aerobic R0033, Anaerobic R0033, SC40 and R0419 increased MCP ($p<0.001$; $p<0.002$; $p<0.001$; $p<0.001$). Aerobic R0033, Anaerobic R0033, SC40 and R0419 alone increased MIP-2 ($p<0.033$; $p<0.002$; $p<0.001$; $p<0.033$), while SC40 and R0419 increased MIP-1 ($p<0.001$; $p<0.033$).

In the presence of PIC, Anaerobic R0033, SC40 and R0419 increased MIP-2 ($p<0.002$; $p<0.001$; $p<0.033$). Aerobic R0033, Anaerobic R0033, SC40 and R0419 alone increased MIP-1 ($p<0.002$; $p<0.001$; $p<0.002$; $p<0.001$), while Anaerobic R0033, SC40 and R0419 increased MIP-2 ($p<0.033$; $p<0.001$; $p<0.033$), and SC40 and R0419 increased MCP ($p<0.002$).

In the presence of LPS, Aerobic R0033 increased MIP-1 and MIP-2 ($p<0.033$). Aerobic R0033, Anaerobic R0033, SC40 and R0419 alone increased MIP-2 ($p<0.033$;

p<0.002; p<0.001; p<0.033), while Aerobic R0033, SC40 and R0419 increased MIP-1 (p<0.033; p<0.001; p<0.033).

In the presence of CpG, Anaerobic R0033 increased MCP (p<0.033). Aerobic R0033, Anaerobic R0033, SC40 and R0419 alone increased MIP-1 (p<0.002; p<0.001; p<0.002; p<0.001), while Anaerobic R0033, SC40 and R0419 increased MIP-2 (p<0.033; p<0.001; p<0.033), and SC40 and R0419 increased MCP (p<0.033).

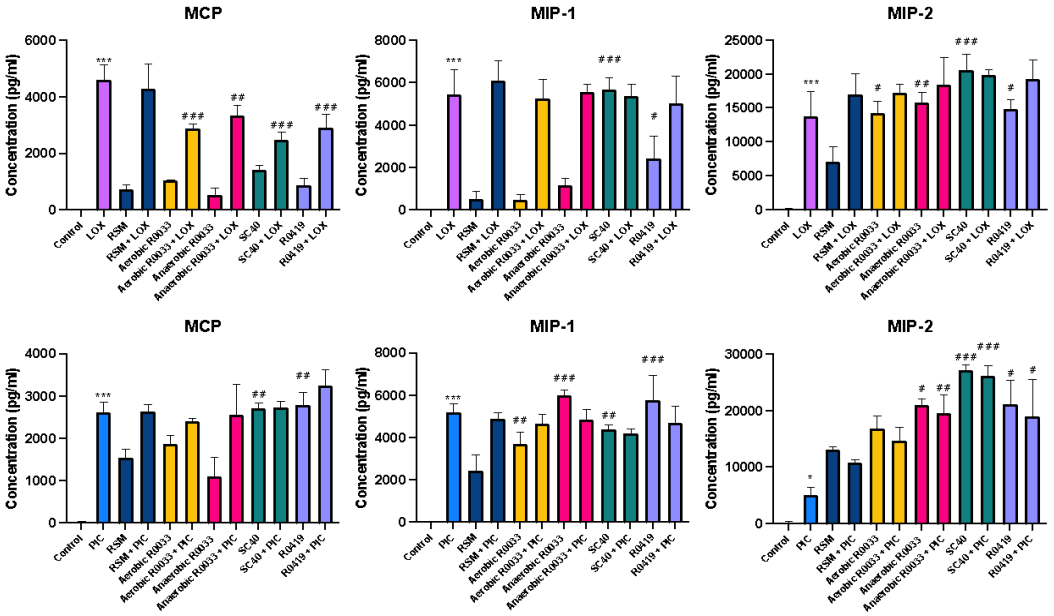

*Figure 78**: Exposure of LOX and PIC activated BMDM to 25mg/mL raw sample results in the secretion of chemokines.** BMDM cells were seeded at 1x10⁶ cells/mL and left overnight at 37°C in 5% CO_2. The following day cells were stimulated with 25mg/mL raw sample fermentate, incubated for 1 hour at 37°C in 5% CO_2 and 5% CO_2 and subsequently exposed to the following concentrations of TLRs: LOX 0.5mM, PIC 10µg/mL for TLR activation before incubating overnight under the same conditions. RSM is the fermentate control. Supernatants were removed after 24 hours and ELISA was performed MCP, MIP-1 and MIP-2. Data is presented as mean ± SD of three replicates. Significance determined using one- way ANOVA with a Newman-Keuls post-test. Output P value style APA: .12 (ns), .033 (*), .002(**) and <.001 (***); 1) comparing unstimulated control cells to each TLR stimulated cell "*", and 2) comparing RSM to sample equivalents "#".*

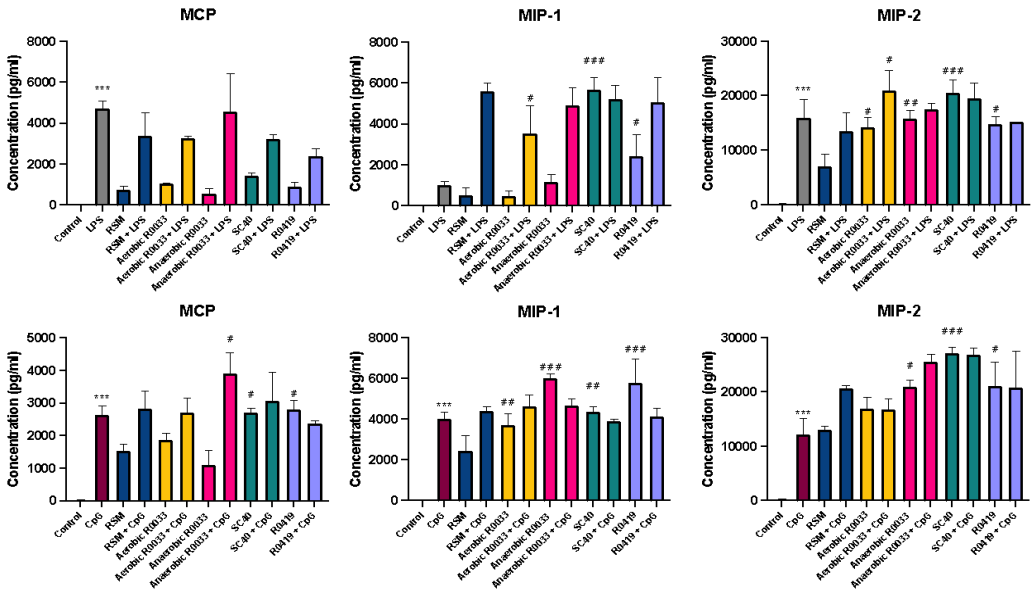

Figure 79: ***Exposure of LPS and CpG activated BMDM to 25mg/mL raw sample results in the secretion of chemokines.*** *BMDM cells were seeded at 1x10⁶ cells/mL and left overnight at 37°C in 5% CO_2. The following day cells were stimulated with 25mg/mL raw sample fermentate, incubated for 1 hour at 37°C in 5% CO_2 and 5% CO_2 and subsequently exposed to the following concentrations of TLRs: LPS 100ng/mL, CpG 5μM for TLR activation before incubating overnight under the same conditions. RSM is the fermentate control. Supernatants were removed after 24 hours and ELISA was performed MCP, MIP-1 and MIP-2. Data is presented as mean ± SD of three replicates. Significance determined using one- way ANOVA with a Newman-Keuls post-test. Output P value style APA: .12 (ns), .033 (*), .002(**) and <.001 (***); 1) comparing unstimulated control cells to each TLR stimulated cell "*", and 2) comparing RSM to sample equivalents "#".*

Thus overall, having carried out an extensive screening of fermentate effect in macrophage cells, we finally concluded that the presence of fermentates in BMDMs affected chemokine secretion.

Therefore, we concluded that the 4-candidate immune boosting fermentates Aerobic R0033, Anaerobic R0033, SC40, and R0419 maintained their bioactivity in different immune cells, and had effects on key macrophage functions, including cytokine, and chemokine secretion, phagocytosis, and cell surface marker expression.

4.4 Discussion

This chapter had two key objectives. The first was to establish whether our samples Aerobic R0033, Anaerobic R0033, SC40 and R0419 had similar effects on innate immune cells i.e. the macrophage, when these cells were activated through different TLRs. The second was to explore further the effects of our samples Aerobic R0033, Anaerobic R0033, SC40 and R0419 on macrophage function by examining their effects on phagocytosis, cell surface marker expression and cytokine/chemokine secretion.

It was clear from our data that generally the cytokine secretion in the presence of Aerobic R0033, Anaerobic R0033, SC40 and R0419 was similar in macrophages to those we observed in dendritic cells in the previous chapter with increases in IL-1β, IL-6, IL-10, TNF-α, and IL-27 in J774.A.1 and BMDM cells. There were however small deviations in secretion profiles but for the most part this remained largely unchanged in J774.A.1 and BMDM to the profiles seen in BMDCs. We also established that the effects of the fermentates were not the same when J774.A.1 and BMDM cells were activated with different TLR ligands. In general all of the fermentates elicited similar effects when the J774.A.1s, BMDM, and BMDC cells were activated with either LOX, PIC, CPG, or LPS. For example SC40 had an immune boosting profile in BMDCs, J774.A.1 cells and BMDMs activated with LPS with increased IL-1β, IL-6, IL-10, TNF-α, and IL-27, but an anti-inflammatory effect in BMDCs, J774.A.1 cells and BMDMs activated with CpG, with increased IL-10, but decreased IL-6, TNF-α, IL-12p40, IL-12p70, IL-23, and IL-27. This supported our suggestion that these fermentates may have different effects in the context of viral immunity and inflammation.

Therefore, based on our cytokine analysis we identified 4 samples possessing dual activity with potential as immune boosting samples in the context of viral immunity, or anti-inflammatory with the ability to reduce inflammation and aid in resolution of

chronic inflammation often associated with disease pathogenesis of UC and CD. (Table 23).

Given the importance of IL-6, TNF-α, IL-12p40 and IL-27 in aiding the immune system during viral infections such as influenza, vaccinia virus, HIV and herpes simplex (Amsden et al., 2022; Hamza et al., 2010; S. Y. Kim & Solomon, 2010; Novelli & Casanova, 2004; Seo & Webster, 2002b; Velazquez-Salinas et al., 2019; Y. Wang et al., 2009) and supporting viral immunity, a fermentate that can enhance these cytokines could be beneficial.

It has previously been demonstrated that an isolated acidic polysaccharide from the fungus *Cordyceps militaris* enhanced mRNA expression of IL-1β, IL-6, IL-10, and TNF-α, increased NO production and induced iNOS mRNA and protein expression in RAW 264.7 macrophage cells (Ohta et al., 2007). Additionally this also increased TNF-α and IFN-γ in mice, decreasing virus titres in the bronchoalveolar lavage fluid and the lung of mice infected with influenza A virus to increase survival rate (Ohta et al., 2007). Similarly a studying involving *Lactobacillus helveticus* was found to decrease influenza like illness in an elderly population, warranting further investigation in at risk populations (Koesnoe et al., 2021). This suggests a similar role for two of our *Lactobacillus helveticus* fermentates Aerobic R0033 and R0419 (Koesnoe et al., 2021). Another study showed that germinated *Rhynchosia nulubilis* (GRC) fermented with *Pediococcus pentosaceus* SC11 (GRC-SC11) isolated from a salted small octopus, has immune-enhancing and anti-viral effects, inhibiting 3CL protease activity in SARS-CoV in immunocompromised mice, increased T lymphocyte production and spleenocyte proliferation, increased phagocytic activity, NO production via induction of iNOS, mRNA expression of IFN-γ, IFN-α and ISG15 in RAW 264.7 macrophage, and subsequent increase in expression of TNF-α (Dhong et al., 2022)., suggesting the role of GRC-SC11 in immunosuppressed patients for the support against SARS-CoV. Similarly *Grifola frondosa* Extract (ME) can induce the expression of TNF-α mRNA in Madin-Darby canine kidney cells leading to production of TNF-α, with subsequent inhibition of viral growth of influenza A/Aichi/2/68 virus (Obi et al., 2008). Melatonin exhibits anti influenza H1N1 properties via the induction of IL-10 caused by the upregulation of

IL-27 in DCs (S.-H. Huang et al., 2019). *Rapanea melanophloeos* has been shown to increase IL-27 production ultimately increasing IL-10 production, to decrease the viral titre of influenza A virus in MDCK cells, suggesting its role as an anti-influenza treatment (Mehrbod et al., 2018). Therefore Aerobic R0033, Anaerobic R0033, SC40 and R0419 are potential novel candidates for defence against viral infection in humans due to their ability to support the secretion of antiviral cytokines such as IL-6, TNF-α, and IL-27 while increasing anti-inflammatory cytokine IL-10 in the presence of viral ligands LOX, and PIC.

As well documented in the literature, increased proinflammatory cytokine secretion, largely of IL-6, and TNF-α, has been linked to chronic inflammation and disease progression, particularly in the case of UC and CD (Arulselvan et al., 2016; Mitselou et al., 2020; Reinecker et al., 1993; Y. Song et al., 2022). Therefore, any sample that has the ability to modulate such cytokines as IL-10, IL-6, and TNF-α may have the ability to positively impact on chronic inflammation and subsequent disease development, for inflammation resolution.

In two mice models of UC and CD, LASSBio-1524 and its three analogues LASSBio-1760, LASSBio- 1763, and LASSBio-1764 reduced the secretion of TNF-α, IL-1β, IL-6, IL-12, and IFN-γ and increased secretion of IL-10, resulting in reduced disease severity, colonic tissue damage, infiltration of inflammatory cells, and production and expression of proinflammatory mediators, suggesting its role as a novel therapeutic for the treatment of UC and CD (Cordeiro et al., 2020). In another model of murine colitis, Genistein treatment led to the reduction in proinflammatory mediators IL-6, TNF-α, MCP-1 and IL-1β, as well as an increases in IL-10 from $CD4^+$ T cells, and M2 macrophage, and an increased M2 and decreased M1 macrophage phenotype, leading to reduced inflammation and disease severity, mediating colitis severity (Abron et al., 2018). Furthermore, UC has been shown to be ameliorated in the presence of Berberine hydrochloride, suppressing the expression of IL-1, IL-1β, IL-6, IL-12, TNF-α, TGF-β and IFN-γ, while enhancing the expression of IL-4 and IL-10, acting as a novel treatment of colitis in a rat DSS colitis model (L. Zhu et al., 2019). Thus, it is clear from the literature that reducing the secretion of proinflammatory cytokines such as IL-1β, IL-6, IL-12, TNF-α, while

increasing the secretion of anti-inflammatory cytokine IL-10, can be linked to improved disease prognosis for UC and CD. Therefore Aerobic R0033, Anaerobic R0033, SC40 and R0419 are potential novel candidates for the management of UC and CD in humans due to their ability to reduce the secretion of proinflammatory cytokines such as IL-1β, IL-6, IL-12, TNF-α, while increasing anti-inflammatory cytokine IL-10 in the presence of inflammatory ligands LPS, and CpG.

The second objective of this chapter was to explore the effects of our samples on macrophage cell function to include a number of parameters that would indicate how these samples might affect cells during infection.

A critical function of the macrophage in the defence against viral infection is phagocytosis, and thus an important factor to consider when establishing the best candidate sample, as hindering the cells abilities to carry out this function could impact on host immune function. For the purpose of this assessment we used LOX to mimic a viral infection, and LPS to mimic a bacterial infection. The mechanisms by which viral and bacterial phagocytosis occur are however different. Viral phagocytosis occurs through apoptosis-dependent phagocytosis (Nainu et al., 2017). This means that the host cell infected with the virus is killed via apoptosis and subsequently engulfed by the phagocyte for virus removal, antigen presentation, inflammation resolution, and trained immunity (Nainu et al., 2017). Bacterial phagocytosis on the other hand simply involves the engulfing of the invading pathogen by the phagocyte, for pathogen internalisation, destruction, and subsequent antigen presentation and immune signalling (Underhill & Goodridge, 2012). In order to assess fermentate effect on phagocytosis the cell line J774.A.1 cells were used due to the limitation of needing high volumes of viable cells, which simply are not feasible with BMDMs. In setting up the model for phagocytosis, the MFI of the latex beads, and the percentage of phagocytosing cells within the population were measured. These two parameters were then combined in order to form the overall mean MPI, the combined effect of the MFI and percentage of

phagocytosing cells, for a collective outlook of sample effect on phagocytosis. To set up the model for phagocytosis examination it was important to establish that phagocytosis could be stopped post incubation with fluorescent latex beads, in order to establish samples true independent effect on phagocytosis. Following this, establishment of the optimal time point for incubation with LOX and LPS was discovered to be either 4 or 6 hours, as these provided the most significant difference for both LOX and LPS in the MPI. The addition of the RSM further confirmed the 4 hour LOX and LPS incubation to be optimal for phagocytosis when fermentate was added for 1 hour prior. Results showed that LPS activated J774.A.1 cells, in the presence of R0419 negatively impacted MFI. Similarly LOX and LPS activated J774.A.1 cells in the presence of R0419 negatively impacted % phagocytosing cells and MPI. In contrast LOX and LPS activated J774.A.1 cells in the presence of SC40 positively impacted MFI, % phagocytosing cells and MPI. Remaining samples Aerobic R0033 and Anaerobic R0033 showed little or no effect on MFI, % phagocytosing cells or MPI in LOX or LPS activated J774.A.1 cells. RSM was included as the control and this showed that samples Aerobic R0033, Anaerobic R0033, SC40 and R0419 outperform the RSM in all measured outputs, all with higher levels of MFI, % phagocytosing cells and MPI.

Phagocytosis is traditionally known for its role in bacterial and fungal clearance (Tay et al., 2019). This is supported by the literature whereby patients with defects in phagocytic function are found to be more susceptible to common bacterial and fungal infections (Andrews & Sullivan, 2003; Tay et al., 2019). This critical role of phagocytosis in bacterial and fungal clearance highlights the importance of phagocytosis in the context of bacterial and fungal infections, versus viral infections, thus suggesting that in the context of viral immunity the role of phagocytosis may not be deemed as important as in the context of bacterial or fungal infection. Therefore the decrease seen in the MFI as a result of the presence of R0419, may still support the role of such novel fermentate in the context of viral immunity, as they provide an increase in MFI above the RSM non-fermented control.

It is clear from the literature that increases in phagocytotic activity through the use of functional foods can be linked with enhanced immunity. When RAW 264.7

murine macrophage are treated with wild simulated ginseng, increased phagocytotic activity is observed, along with increased production of immunostimulators such as NO, iNOS, COX-2, IL-1β, IL-6 and TNF-α, via LR2/4-dependent MAPK, NF-κB and PI3K/AKT signalling pathways (Um et al., 2020). Panax ginseng Meyer when administered to Balb/C mice enhanced innate and adaptive immunity via the improved cell-mediated and humoral immunity, macrophage phagocytosis capacity and NK cell activity (He et al., 2017). In this study He et al. hypothesis that the increased immunomodulating activity is due to the increased macrophage phagocytosis capacity, along with increased NK cell activity, enhancement of T and Th cells, as well as IL-2, IL-6 and IL-12 secretion and IgA, IgG1 and IgG2b production (He et al., 2017). Similarly, a study in RAW 264.7 macrophage established that a water extract (GTR-101) from Lycium chinense Miller root enhanced the innate immune system through increased induction of pro-inflammatory cytokines TNF-α and IL-6, chemokines RANTES and MIP-1α, NO, iNOS expression, and activated the Akt, NF-κB, and MAPKs ERK and p38 signalling proteins (J. Kim et al., 2020). Furthermore Lycium chinense Miller root was able to enhance phagocytic activity not only in RAW 264.7 cells but also in BMDMs (J. Kim et al., 2020). Another study demonstrates the capabilities of fermented *C.militaris* with *Pediococcus pentosaceus* ON89A (GRC-ON89A) to enhance phagocytosis in RAW 264.7 cells and primary peritoneal macrophage from normal mice and cyclophosphamide immunosuppressed mice, via the activation of MAPK and Lyn pathways (Kwon et al., 2018). It is suggested that GRC-ON89A has the potential to act as an immunostimulant for the use as an immune boosting therapy in immunosuppressed patients (Kwon et al., 2018).

Thus it is clear from current literature that functional food components which have the ability to enhance phagocytosis have the potential to aid in boosting the immune system to provide enhanced innate and adaptive immunity acting as potential immune boosting therapies.

Cell surface marker expression in J774.A.1 cells was also assessed as these cell surface proteins play a critical role in host immunity by enabling the cell to

respond and interact with the environment around them, thus playing a critical role in intracellular signalling (Bradley, 2020). Cell surface markers examined were MHCI, MHCII, CD80, CD86, TLR2, TLR4, CD40, and CD14. Our results clearly demonstrate different effects on cells depending on either LOX or LPS activation.

Our data demonstrated clear positive effects on these markers and therefore suggests that these fermentates may possess anti-viral properties. In J774.A.1 cells activated with LOX or LPS, in the presence of fermentates, no sample outperforms that of the RSM in its ability to increase cell surface markers. However, LOX and LPS activated J774.A.1 cells in the presence of only Anaerobic R0033 showed an decrease in the expression of cell surface markers CD14, CD40, TLR2, while LOX and LPS activated J774.A.1 cells in the presence of Aerobic R0033 decreased CD14. Otherwise all samples increased cell surface marker expression compared to the control or at least had little effect. LOX and LPS activated J774.A.1 cells in the presence of samples SC40 and R0419 show high increased in particular to CD80, CD14, CD40, TLR2, MHCI, however otherwise still increased MHCII, TLR4, and CD86.

MHC class molecules function to bind peptide fragments from pathogen and display them on cell surface for recognition by T cells and thus integral to the signalling of the adaptive immune system (Charles A Janeway et al., 2001). MHCI plays a particularly important role in viral immunity, for detection of virally infected cytotoxic T lymphocytes (Askew et al., 2000). CD80 and CD86 interact on APC and CD28 on T cells as costimulatory signals for the activation of T cells, and are key players in antiviral humoral and cellular immune responses, and play a critical role in the control of chronic and latent infections (Fuse et al., 2006). CD40 is a costimulatory molecule expressed by T cells, B cells, professional APCs, as well as non-immune cells and tumours, that plays pivotal roles in cellular immune processes of DCs, B cells, and endothelial cells, and many other cells including hematopoietic and non-hematopoietic, in both humoral and cellular immune responses (Elgueta et al., 2009). CD40 in particular is important for the restriction

of infection of a broad range of RNA viruses and is critical for the control of RNA viruses over the first 24 hours of infection (Rogers et al., 2021).

Additional cell surface markers MHCII, CD14, TLR2, and TLR4 are included for their overall effect on general immunity. MHCII major role is in general immunity to support and initiate antigen presentation, for antigen specific immune responses (Holling et al., 2004). CD14 is a monocyte differentiation antigen expressed on the surface of myeloid lineages, that plays a critical role in immune recognition via its interactions with TLR4 (Zamani et al., 2013). TLR2 and TLR4 have the ability to identify unique molecular patterns from invading pathogens via PRRs, acting as innate sensors against invading pathogens, while also bridging the innate and adaptive immune responses, and regulating the balance between Th1 and Th2 responses essential for host survival (Mukherjee et al., 2016). Of note, however, TLR2 has been identified to play a role in viral immunity with protective roles against viruses such as varicella zoster virus, hepatitis C virus, vaccinia virus, cytomegalovirus and respiratory syncytial virus (de Oliviera Nascimento et al., 2012). Our data demonstrates clear positive effects on these markers and therefore suggests that these fermentates may possess anti-viral properties.

As the literature demonstrates, upregulation of such cell surface markers can be of huge benefit in boosting the immune system and its host protection against viral infection. Ginseng berry extract has been shown to have antiviral, anti-tumour and immune activating effects, including the upregulation of costimulatory molecules CD86, MHCI and MHCII in vivo, as well as the promotion of L-6, IL-12 and TNF-α (W. Zhang et al., 2015). M1 and M4 metabolites of ginsenosides of root Panax ginseng C.A. Meyer have also been shown to increase cell surface expression of CD80, CD83, CD86 in human monocyte derived dendritic cells, making dendritic cells the potential targets for the immunomodulatory capacity of the ginseng components via the enhancement of differentiation and proliferation of lymphocytes (Kang & Min, 2012; Takei et al., 2004). Exopolysaccharide (EPS) from Cordyceps sinensis induce expression of MHCII, CD40, CD80, and CD86 in dendritic cell sarcoma cells, enhance their ability of antigen uptake, as well as increase secretion of IL-12 and

TNF-α, thus suggesting that EPS have a critical in initiating antitumor immunity and pro-inflammatory immune modulation (D. Song et al., 2013). Carrot pomace has been found to increase the expression of co-stimulatory molecules CD40 and CD80, and the fraction of cells CD11c+MHCII+ cells in BMDCs, increase proinflammatory cytokine production, and in cyclophosphamide immunosuppressed mice administered with influenza vaccine challenge, significantly enhanced the efficacy of the influenza vaccine(P. Sun et al., 2020). Resveratrol has been shown to enhance antigen presentation of peritoneal macrophage via the upregulation of CD86, MHCII and TLR4 levels, suggesting its role as pseudorabies virus vaccine adjuvant therapy, aiding in the host protection against viral infection (M. Chen et al., 2019).

The similar effects of our fermentates on key cell surface markers involved in viral immunity further support their potential as anti-viral and immune supportive ingredients.

Finally chemokine secretion was examined in LOX and LPS activated BMDM macrophage, as this is another critical function of the macrophage in supporting the immune system in response to viral infection and host protection. Chemokines are critical in order to mediate macrophage chemotaxis, cell trafficking, and in the regulation of M1 and M2, and regulates differentiation of monocytes into dendritic cells, to attract macrophage towards the site of injury or infection (Deshmane et al., 2009; Singh et al., 2021; Xuan et al., 2015). Chemokines are secreted in response to other immune responses such as the release of proinflammatory cytokines, where they then play a role in the recruitment of cells such as monocytes, lymphocytes and neutrophils along a chemokine gradient (Deshmane et al., 2009). The chemokines examined were MCP, MIP-1 α, and MIP-2. MCP-1 (CCL2) is a key chemokine for the regulation of migration and infiltration of monocytes, playing a critical role in inflammation (Deshmane et al., 2009). MIP-1 α (CCL3) is a chemotactic chemokine secreted by macrophage to aid in the recruitment of cells, wound healing, inhibition of stem cells, maintaining effector immune responses, and is a key mediator of virus induced inflammation (Bhavsar et al., 2014; Cook et

al., 1995). MIP-2 (CXCL2) aids in neutrophil recruitment and activation and is a potent chemoattractant secreted by macrophage and epithelial cells, that plays a critical role in LPS induced inflammation, as well as aiding in suppressing of viral replication (Chaochao et al., 2017; Han et al., 2004; Tumpey et al., 2002). Therefore, while MCP is important for inflammation, it is MIP-1 and MIP-2 that play critical roles in the context of viral infection, with their roles in virus induced inflammation and suppressing viral replication (Bhavsar et al., 2014; Chaochao et al., 2017; Cook et al., 1995; Deshmane et al., 2009; Han et al., 2004; Tumpey et al., 2002). Examining the affect samples have on the concentrations of MCP-1, MIP-1, and MIP-2 can therefore aid determining a more holistic view of how a sample would behave in vivo, due to their importance in the clearance of viral infection, as well as LPS induced inflammation via the increased recruitment of cells to the sites of infection and inflammation (Bhavsar et al., 2014; Chaochao et al., 2017; Cook et al., 1995; Deshmane et al., 2009; Han et al., 2004; Tumpey et al., 2002). It is important, however, that these chemokines are not over expressed as this leads to pathogenesis of many inflammatory diseases including cancers, rheumatoid arthritis, as well as viruses such as coronavirus (Bhavsar et al., 2014; Singh et al., 2021).

When BMDMs were activated with LOX in the presence of Aerobic R0033, Anaerobic R0033, SC40 and R0419 MCP was decreased. LPS activated BMDMs in the presence of Aerobic R0033 had decreased MIP-1, but increased MIP-2. PIC activated BMDMs in the presence of samples Anaerobic R0033, SC40 and R0419 had increased MIP-2, and CpG activated BMDMs in the presence of Anaerobic R0033 had increased MCP. Otherwise samples did not alter the expression of chemokines MCP, MIP-1, or MIP-2 in response to viral immune challenges LOX, and PIC, or inflammatory challenges LPS, or CpG in BMDMs compared to the RSM.

It is well established that decreases in MCP can be linked with the ability to inhibit viruses such as HIV (X. Chen et al., 2003). The use of the Chinese herbal medicine Shikonin, the major component of zicao, the dried root of *lithospermum erythrorhizon*, has been linked to the ability to inhibit HIV-1 through its interactions inhibiting MCP and MIP-1 (X. Chen et al., 2003). Extract of Indigo Naturalis from the

leaves of *Baphicacanthus cusia*(Nees) *Bremek*. (Fam. *Acanthaceae*), *Polygonum tinctorium Ait*. (Fam. *Polygonaceae*) or *Isatis indigotica Fort*. (Fam *Cruciferae*), has been shown to be effective in the treatment of acute lung injury induced by influenza A virus, via the reduction of high levels of MCP-1, as well as regulation of other pro-inflammatory markers (Tu et al., 2020). Furthermore, Indigo Naturalis inhibited viral adhesion to cells in vitro, thus suggesting the potential role Aerobic R0033, Anaerobic R0033, SC40 and R0429 as anti-influenza treatments (Tu et al., 2020). Similarly, Lianhuaqingwen Capsule from traditional Chinese medicine prescription, Maxing Shigan Tang and Yinqiao San, decreased the expression of MCP-1, resulting in antiviral activity for the treatment of influenza viral infection (Ding et al., 2017).

On the other hand it has been well documented in the literature that in fact a decrease in MIP-2 can be beneficial to inhibiting viral infections and inflammatory diseases, thus indicating a potential undesirable effect seen through the increased expression of MIP-2 in BMDMs activated with LOX, PIC, LPS and CpG, in the presence of Aerobic R0033, Anaerobic R0033, SC40 and R0419 (Grigore et al., 2020; Z. Wang, Chen, et al., 2021; Yeh et al., 2007). Thus overall the samples ability to largely maintain chemokine expression, and in the case of MCP and MIP-1 where this expression can be decreased, suggests a potential use of Aerobic R0033, Anaerobic R0033, SC40 and R0429 as novel anti-viral and immune supporting therapies.

In this chapter we confirmed that the fermentates Aerobic R0033, Anaerobic R0033, SC40, and R0419 had immune boosting activity in support of viral immunity enhancing viral associated cytokine production e.g. IL-6, IL-10, TNF-α, and IL-27. In addition there were positive effects on chronic inflammation in the presence of some of our fermentates, in not only dendritic cells but also in macrophage with decreased secretion of proinflammatory cytokines IL-6, TNF-α, IL-12p40, IL-12p70, IL-23, and IL-27, and increased production of anti-inflammatory cytokine IL-10. We carried out an in depth analysis of their potential as viral immune boosting samples

in support of macrophage functions, while also demonstrating their potential in chronic inflammation resolution and bacterial infection. We found that our fermentates positively impact on phagocytosis, enhanced viral immunity cell surface marker expression of MHCI, CD80, CD86, CD40, and general immunity cell surface marker expression of MHCII, CD14, TLR2, and TLR4 when compared to their starting material. Additionally our fermentates support enhanced chemokine secretion for control of chronic inflammation through decreased MCP.

5 Chapter 5

Phase 3 Fermentate Screening

5.1 Introduction

Due to the nature of this multidisciplinary project whereby FHI worked in collaboration with industry partners for commercial interest, the project evolved based on industry needs, taking into account the results and analysis of several different groups. The three different groups, working on three different aspects of the fermentates were as follows: DCU with a main focus on viral immunity, UCD with a main focus on anti-inflammatory function, and Teagasc with a main focus on the effect on the microbiome. Screening and further analysis conducted by each different group was collated by FHI and with contributions from all teams, the results were centrally analysed based not only on the scientific findings but also the feasibility and scalability of producing candidate samples at industry scale. 19 candidate samples were highlighted based on the scientific findings of the three groups for their bioactive profiles, namely their viral immune boosting capabilities (DCU), anti-inflammatory capabilities (UCD), and their effect on the microbiome (Teagasc) (Table 24). These 19 samples were then further assessed as part of the multidisciplinary team to examine candidate samples which were feasible to produce and scale up for industry. Of these 19 samples, 1 sample SC40 was highlighted as a potential sample with positive effects not only for viral immunity but also because of its additional anti-inflammatory activity, as well as its positive effect on the microbiome. This could suggest it's application in improving gut inflammation and the gut microbiome. The remaining 3 samples highlighted as candidate viral immune boosting samples, Aerobic R0033, Anaerobic R0033, and R0419 were deemed not of further interest to the companies due to difficulties in scalability, producibility at manufacturing stage, as well as regulatory issues for commercial use down the line. Thus, the overall focus of the project shifted towards investigating an immunomodulatory sample with anti-inflammatory capabilities based on consumer and industry needs. Therefore, the next step involved screening the highlighted 19 candidate samples to investigate the bioactive profiles of all samples via the examination of their cytokine profiles in BMDCs, when the cells were activated with LPS to mimic a state of inflammation. Additionally, we wanted

to examine the effect of fermentates on polarised macrophage, where an M1 profile is representative of an immune boosting phenotype, while an M2 phenotype is representative of an anti-inflammatory profile, as well as including sample effect in unpolarised BMDMs (Figure 80).

Table 24: ***Top 19 Bioactive Fermentates.*** *List of the top 19 candidate fermentates based on their bioactivity and immunomodulatory activities in viral immunity, anti-inflammatory capabilities, microbiome and gut barrier function. Collated in collaboration with scientific groups based DCU, UCD, Teagasc, and centrally managed by FHI. Samples with bioactivity in as immune boosting samples highlighted in green, anti-inflammatories groups highlighted in red, or blue with both.*

No.	Strain Code	Source	Immunity (DCU)	Inflammation (UCD)	Microbiome (Teagasc)	*Gut barrier* (Teagasc)
1	HA136	Lallemand			Top 10	
2	LH88	Sacco		Y	Top 10	*Y*
3	HA119	Lallemand			Top 10	
4	Aerobic R0033	Lallemand	Y		Top 10	
5	SC40	Teagasc (FHI2)	Y	Y	Top 10	*Y*
6	HA179	Lallemand			Top 10	
7	HA110	Lallemand			Top 10	
8	R1058	Lallemand			Top 10	
9	ST765	Sacco			Top 10	
10	ST906	Sacco			Top 10	
11	SC6	Teagasc		Y	E.coli issues	*Y*
12	R0389	Lallemand		Y	Tested	*Y*
13	Anaerobic R0700	Lallemand		Y	E.coli issues	*Y*
14	SC17	Teagasc		Y	E.coli issues	
15	DPC1817	Teagasc		Y	E.coli issues	
16	HA118	Lallemand		Y	Not analysed yet	
17	P200622	Sacco		Y	Not analysed yet	
18	Anaerobic R0033	Lallemand	Y		Not analysed yet	
19	R0419	*Lallemand*	Y		E.coli issues	

Figure 80: ***Polarisation of M0 macrophage to M1, and M2 macrophage and their subsequent phenotypes .****Polarisation compounds are highlighted that were used to polarise M0 macrophage to M1 and M2 macrophage. Summary phenotypic profile for the M1 and M2 macrophage functions.*

5.2 Chapter Aims:

The purpose of this chapter was to screen the top 19 bioactive fermentates identified in other pillars of the FHI collaborative project, to find potential candidate anti-inflammatory samples via screening in BMDCs with LPS stimulation. We next wanted to examine additional effects of the top performing bioactive immune boosting and anti-inflammatory fermentates in polarised BMDMs; M1, M2, and unpolarised M0 cells. This allowed us to determine the fermentate's effect on not only cytokine production in macrophage but also, nitric oxide production and arginase activity, the characteristic phenotypes for M1, and M2 macrophage respectively, to further establish fermentates immune boosting and/or anti-inflammatory roles.

The specific objectives included:

- Assessment of cytotoxicity of top 19 anti-inflammatory fermentates in BMDCs to ensure that samples were not negatively impacting on cell viability.
- Assessment of top 19 anti-inflammatory samples, in LPS activated BMDCs for cytokine secretion.
- Assessment of cytotoxicity of top 5 fermentates, to include candidate immune boosting and anti-inflammatory samples, in BMDCs to ensure that samples were not negatively impacting on cell viability.
- Assessment of top 5 samples, to include candidate immune boosting and anti-inflammatory samples, in LOX and LPS activated BMDCs for cytokine secretion.
- Assessment of the highlighted 2 immune boosting and 2 anti-inflammatory samples on M0, M1 and M2 macrophage phenotypes.
- Regenerated sample of SC40 was assessed to ensure accuracy, reproducibility, and scalability. Screening carried out in BMDC and BMDMs, activated with a panel of immune challenges, to assess cytokine

secretion profiles induced from Original SC40, Regenerated SC40, Powder A, Powder B both of which consist of different RSM starting concentrations, and Postbiotic SC40.

Having established that the bioactivity of the fermentates is greater than that of the RSM, statistical analysis can be compared to control cells and the TLRs examined. Data gathered from this analysis established the candidate immune boosting and anti-inflammatory fermentates to bring forward for testing in T cells.

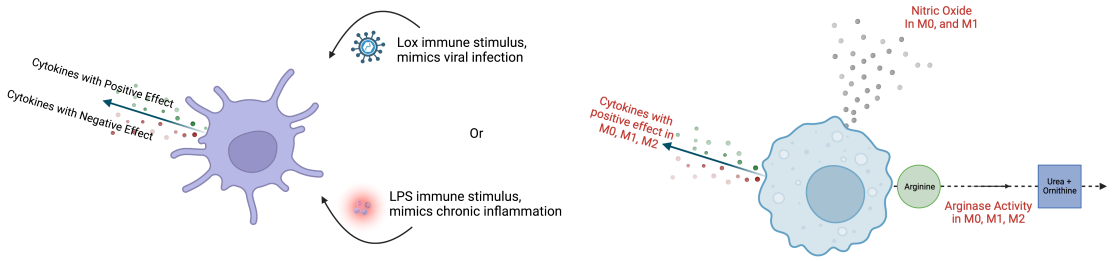

*Figure 81: **Summary of Chapter 5 Aims**. Assessing effect of sample presence on cytokine secretion profiles in dendritic cells (purple), and macrophage (blue), when activated with viral immune stimulus LOX or inflammatory stimulus LPS, or when macrophage are polarised to M1, or M2 macrophage.*

5.3 Results

Based on the multidisciplinary discussion between FHI, DCU, UCD and Teagasc, 19 top bioactive fermentates were selected as candidate fermentates for potential commercial development. Due to commercial interest and industry needs the project shifted towards identifying and producing a fermentate that acted as an anti-inflammatory and could be useful in the treatment, control, and management of self diagnosed IBDs. Therefore there was a shift in the projects main interest in DCU, and thus a smaller scale screening of the highlighted 19 candidate fermentates was carried out, to identify top preforming fermentates within the highlighted top 19 bioactive fermentates, which had anti-inflammatory capabilities.

5.3.1 Screening of Overall Top 19 bioactive Fermentates from all bioassay groups for anti-inflammatory candidate fermentates

Having highlighted the top 19 candidate samples as shown in Table 24, from each three scientific groups, it was necessary to examine each of these samples, when BMDCs were activated with LPS, mimicking an inflammatory state in the cell, to assess the samples capabilities as potential anti-inflammatory samples.

5.3.1.1 Stimulation of LPS activated BMDC with Overall Top 19 bioactive raw fermentates at 25mg/mL doesn't affect cell viability

BMDCs were seeded at a concentration of $1x10^6$ cells/mL, incubated for 24 hours before stimulating with a dose of 25mg/mL raw fermentate sample for 1 hour followed by LPS 100ng/mL and subsequently incubated at 37^0C in 5% CO_2. After 24 hours an MTS assay was performed as previously outlined (section 2.2.13 MTS Cell Viability Assay).

Figure 82 demonstrates that there was no significant change in cell viability following exposure of the cells to 25mg/mL of any of the 19 Top regenerated samples to LPS TLR ligand stimulation. The use of the positive control of 10% DMSO provided a clear distinction between the cytotoxic effects on cell viability with the untreated control sample, as DMSO induced cell death.

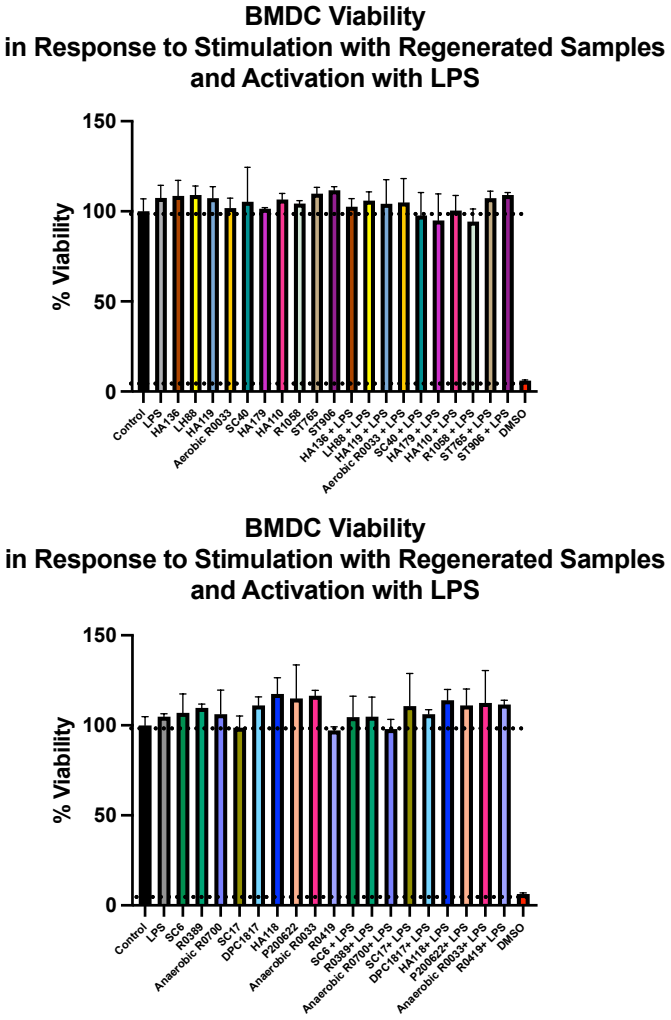

Figure 82: ***Exposure of LPS activated BMDC to 25mg/mL of top 19 Regenerated raw samples doesn't affect cell viability.*** *BMDC cells were seeded at 1x10^6 cells/mL and left overnight at 37^{0}C in 5% CO_2. The following day cells were stimulated with 25mg/mL sample fermentate, incubated for 1 hour at 37^{0}C in 5% CO_2 and subsequently exposed to LPS 100ng/mL for TLR activation before incubating overnight under the same conditions.* 10% *DMSO was included as a positive control to induce cell death. Cells were incubated with MTS cell titre aqueous one solution for 3 hours at 37^{0}C in 5% CO_2. Viability is represented as a percentage compared to viable, untreated cells (Control). Data is presented as mean ± SD of three replicates.*

5.3.1.2 Stimulation of LPS activated BMDCs with 25mg/mL top 19 raw fermentates affects secretion of cytokines

BMDCs were seeded at a concentration of $1x10^6$ cells/mL, incubated for 24 hours before stimulating with a dose of 25mg/mL raw fermentate sample for 1 hour followed by LPS 100ng/mL and subsequently incubated at 37^0C in 5% CO_2. After 24 hours supernatants were removed and ELISA procedure for cytokines IL-1β, IL-6, IL-10, TNF-α, IL-12p40, IL-12p70, IL-23, and IL-27 was performed according to the manufacturer's instructions (section 2.2.14 Enzyme Linked Immunosorbent Assay (ELISA)).

Figure 83 - Figure 86 demonstrates that samples significantly affected the secretion of cytokines in response to immune challenge LPS, when compared to the LPS control.

Figure 83 demonstrates that LPS increased TNF-α ($p<0.001$), IL-1β, and IL-6 ($p<0.002$). In the presence of LPS, LH88, HA110 and SC40, significantly increased IL-1β ($p<0.001$; $p<0.001$; $p<0.033$), IL-10 ($p<0.001$) and TNF-α ($p<0.002$; $p<0.002$; $p<0.001$). HA136, ST765, ST906 and R01058 significantly increased IL-10 and TNF-α ($p<0.001$; $p<0.001$; $p<0.001$; $p<0.002$). Unstimulated samples HA136, LH88, HA119, Aerobic R0033, SC40, HA110, R1058, ST765, and ST906 alone increased IL-1β, IL-6, IL-10 and TNF-α, while HA179 alone only increases TNF-α.

Figure 84 demonstrates that LPS increased IL-1β, TNF-α ($p<0.001$), and IL-6 ($p<0.033$), and non-significantly increased IL-10. In the presence of LPS, SC6, R0389, Anaerobic R0700, SC17, DPC1817 and P200622 significantly increased IL-1β, and IL-10 ($p<0.001$). HA118, R0419 and Anaerobic R0033 significantly increased IL-10 ($p<0.001$; $p<0.001$; $p<0.002$). SC17, R0389 and DPC1817 increased IL-6 ($p<0.001$; $p<0.033$; $p<0.033$) and TNF-α ($p<0.001$; $p<0.002$; $p<0.002$). SC6 and DPC1817 increased TNF-α ($p<0.001$; $p<0.033$), while HA118 increased TNF-α ($p<0.002$). All unstimulated samples SC6, R0389, Anaerobic R0700, SC17, DPC1817, HA118, P200622, Anaerobic R0033, and R0419 alone increased IL-1β, IL-6, IL-10 and TNF-α.

Figure 85 demonstrates that LPS increased IL-27 ($p<0.001$), and non-significantly increased IL-12p40. In the presence of LPS, HA136, LH88, HA139,

Aerobic R0033, HA110, R1058, ST765 and ST906 increased IL-23 ($p<0.001$), as well as SC40 ($p<0.002$). HA136 increased IL-12p40, IL-12p70 and IL-27 ($p<0.001$). ST765, ST906 and HA110 increased IL-12p70 ($p<0.001$; $p<0.001$; $p<0.002$) and IL-27 ($p<0.001$). LH88 increased IL-27 ($p<0.002$), while Aerobic R0033, and HA179 decreased IL-27 ($p<0.001$; $p<0.002$). Unstimulated samples HA136, LH88, HA119, SC40, HA110, R1058, ST765, and ST906 alone increased IL-23 and IL-27, HA136, R1058, and ST906 alone increased IL-12p40, and IL-12p70, and HA110 alone increased IL-12p40.

Figure 86 demonstrates that LPS increased IL-27 ($p<0.001$), and IL-12p40 ($p<0.002$), and non-significantly increased IL-23. In the presence of LPS, SC6, R0389, Anaerobic R0700, SC17, DPC1817, HA118, P200622 significantly increased IL-23 ($p<0.001$), as well as Anaerobic R0033 and R0419 ($p<0.033$). SC17 significantly increased IL-12p70, IL-12p40 and IL-27 ($p<0.001$). SC6, R0389, SC17, DPC1817, HA118, and P200622 significantly increased IL-12p40 ($p<0.033$; $p<0.001$; $p<0.001$; $p<0.001$; $p<0.033$; $p<0.033$), and IL-27 ($p<0.002$; $p<0.001$; $p<0.001$; $p<0.033$; $p<0.033$; $p<0.001$), while Anaerobic R0033 decreased IL-12p40 ($p<0.002$) and IL-27 ($p<0.033$). Unstimulated samples SC6, R0389, SC17, DPC1817, HA118, and P200622 alone increased IL-12p40, IL-23 and IL-27, while Anaerobic R0700 alone increased IL-12p40, Anaerobic R0033 alone increased IL-23, and SC17 alone also increased IL-12p70.

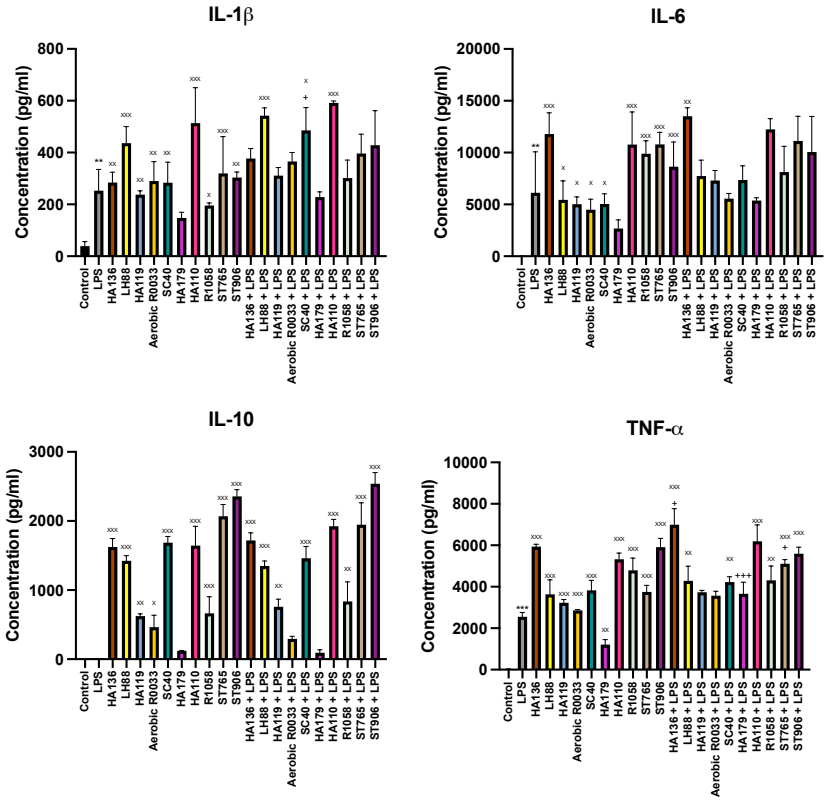

Figure 83: ***Exposure of LPS activated BMDC to 25mg/mL to top 19 raw sample fermentates results in the secretion of cytokines IL-1β, IL-6, IL-10 and TNF-α..*** *BMDC cells were seeded at 1x10^6 cells/mL and left overnight at 37^{0}C in 5% CO_2. The following day cells were stimulated with 25mg/mL raw sample fermentate, incubated for 1 hour at 37^{0}C in 5% CO_2 and % CO_2 and subsequently exposed to LPS 100ng/mL for TLR activation before incubating overnight under the same conditions. Supernatants were removed after 24 hours and ELISA was performed for cytokines IL-1β, IL-6, IL-10 and TNF-α. Data is presented as mean ± SD of three replicates. Significance determined using one- way ANOVA with a Newman-Keuls post-test. Output P value style APA: .12 (ns), .033 (*), .002(**) and <.001 (***); 1) comparing to unstimulated control cells "*", 2) comparing sample + TLR to unstimulated sample cells "+" and, 3) comparing respective control/LPS to sample +/- TLR "x".*

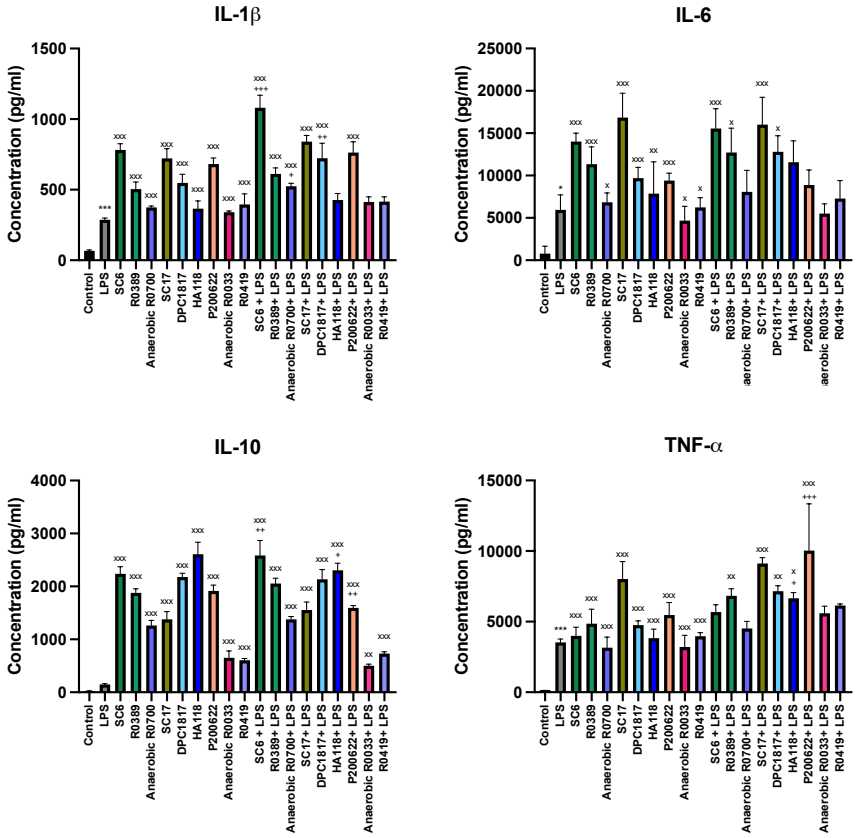

Figure 84: ***Exposure of LPS activated BMDC to 25mg/mL to top 19 raw sample fermentates results in the secretion of cytokines IL-1β, IL-6, IL-10 and TNF-α..*** *BMDC cells were seeded at 1x10^6 cells/mL and left overnight at 37^{0}C in 5% CO_2. The following day cells were stimulated with 25mg/mL raw sample fermentate, incubated for 1 hour at 37^{0}C in 5% CO_2 and % CO_2 and subsequently exposed to LPS 100ng/mL for TLR activation before incubating overnight under the same conditions. Supernatants were removed after 24 hours and ELISA was performed for cytokines IL-1β, IL-6, IL-10 and TNF-α. Data is presented as mean ± SD of three replicates. Significance determined using one- way ANOVA with a Newman-Keuls post-test. Output P value style APA: .12 (ns), .033 (*), .002(**) and <.001 (***); 1) comparing to unstimulated control cells "*", 2) comparing sample + TLR to unstimulated sample cells "+" and, 3) comparing respective control/LPS to sample +/- TLR "x".*

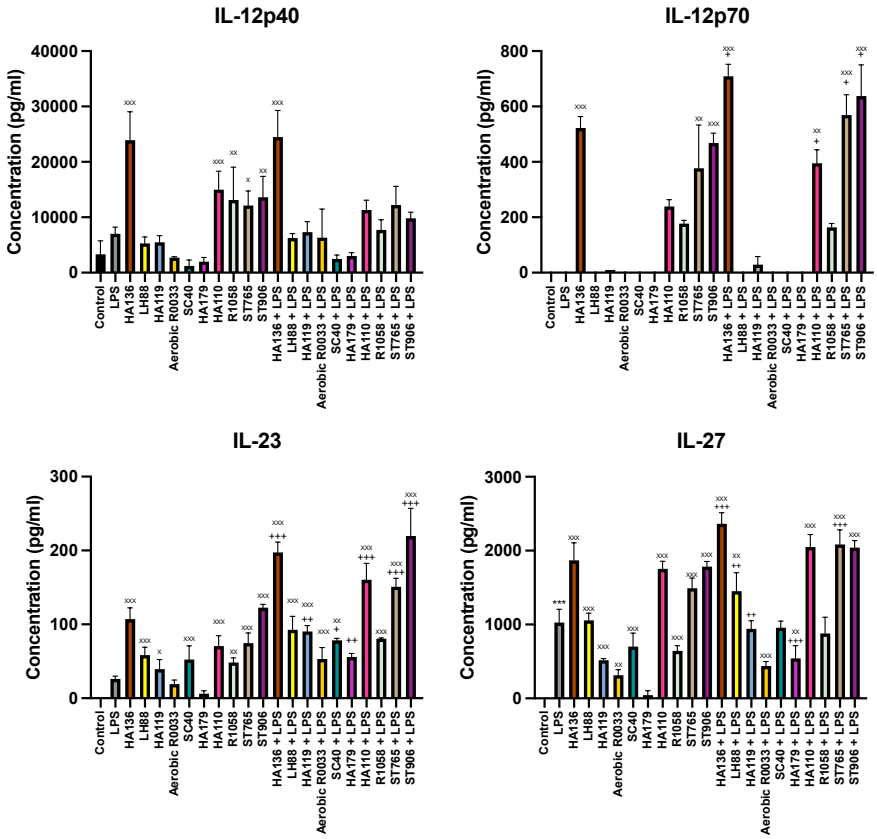

Figure 85: ***Exposure of LPS activated BMDC to 25mg/mL to top 19 raw sample fermentates results in the secretion of cytokines IL-12p40, IL-12p70, IL-23 and IL-27.*** *BMDC cells were seeded at 1x10^6 cells/mL and left overnight at 37^{0}C in 5% CO_2. The following day cells were stimulated with 25mg/mL raw sample fermentate, incubated for 1 hour at 37^{0}C in 5% CO_2 and % CO_2 and subsequently exposed to LPS 100ng/mL for TLR activation before incubating overnight under the same conditions. Supernatants were removed after 24 hours and ELISA was performed for cytokines IL-12p40, IL-12p70, IL-23 and IL-27. Data is presented as mean ± SD of three replicates. Significance determined using one- way ANOVA with a Newman-Keuls post-test. Output P value style APA: .12 (ns), .033 (*), .002(**) and <.001 (***); 1) comparing to unstimulated control cells "*", 2) comparing sample + TLR to unstimulated sample cells "+" and, 3) comparing respective control/LPS to sample +/- TLR "x".*

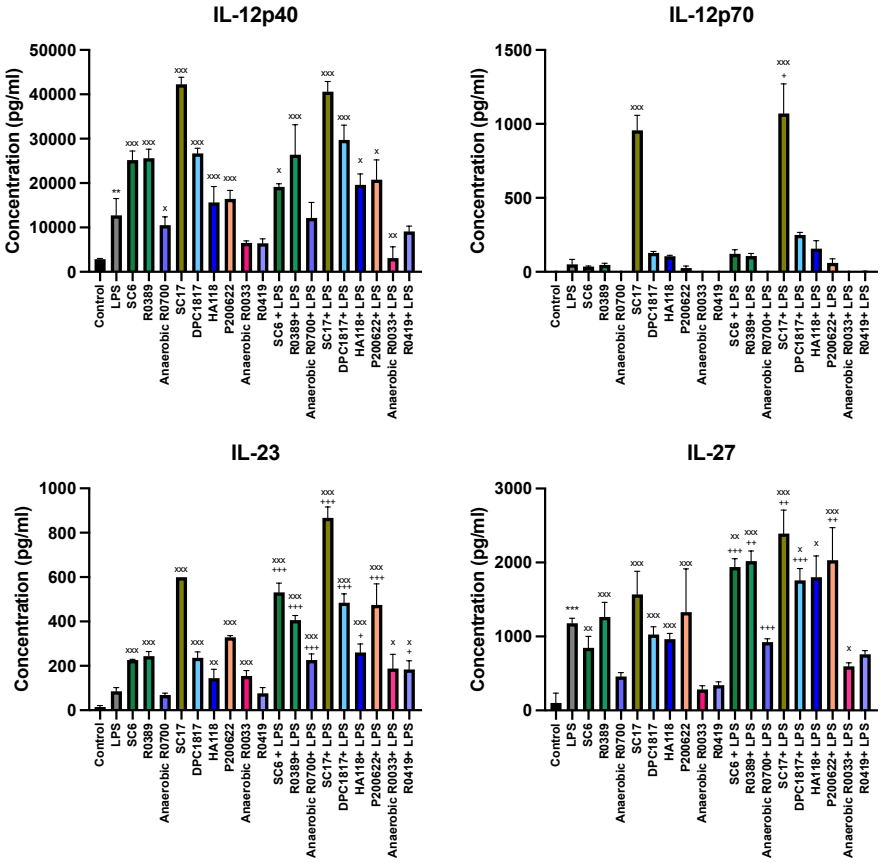

Figure 86: ***Exposure of LPS activated BMDC to 25mg/mL to top 19 raw sample fermentates results in the secretion of cytokines IL-12p40, IL-12p70, IL-23 and IL-27.*** *BMDC cells were seeded at 1x10^6 cells/mL and left overnight at 37^{0}C in 5% CO_2. The following day cells were stimulated with 25mg/mL raw sample fermentate, incubated for 1 hour at 37^{0}C in 5% CO_2 and % CO_2 and subsequently exposed to LPS 100ng/mL for TLR activation before incubating overnight under the same conditions. Supernatants were removed after 24 hours and ELISA was performed for cytokines IL-12p40, IL-12p70, IL-23 and IL-27. Data is presented as mean ± SD of three replicates. Significance determined using one- way ANOVA with a Newman-Keuls post-test. Output P value style APA: .12 (ns), .033 (*), .002(**) and <.001 (***); 1) comparing to unstimulated control cells "*", 2) comparing sample + TLR to unstimulated sample cells "+" and, 3) comparing respective control/LPS to sample +/- TLR "x".*

Therefore, we clearly saw that the top 19 bioactive fermentates do not negatively impact on cell viability, while screening in LPS activated BMDCs highlighted samples SC40, LH88, HA188 and P200622 with the most potential as anti-inflammatory samples due to their enhanced IL-10 secretion and low secretion of immune boosting cytokines.

Next, we screened our top 4 candidate anti-inflammatory samples: SC40, LH88, HA188 and P200622, but furthermore, we included Aerobic R0033 in this screening phase as a comparative for bioactivity due to its largely immune boosting profile established thus far. Additionally, although a viral immune boosting functional food was no longer the main interest for the industry partners, we continued to include Aerobic R0033 for potential future development of a viral immunity enhancing functional food. Therefore, we had top 5 candidate samples to be screened in this phase. We were now able to screen these samples further in BMDCs activated with both LOX and LPS to establish differential effects seen between uniquely bioactive candidate samples.

5.3.2 Screening of Top 5 bioactive fermentate candidates

Having screened the top 19 samples in the context of an inflammatory challenge, 5 samples of interest were determined based on their ability to modulate the immune system and maintain bioactivity. Sample Aerobic R0033 was highlighted for its immune boosting capabilities from previous chapters, while LH88, HA188 and P200622 were highlighted for their anti-inflammatory capabilities, with SC40 having its dual role as both. As samples identified had potential to act as both immune boosting and/or anti-inflammatory samples, assessment in BMDCs was carried out when cells were activated with both LOX and LPS. Aerobic R0033 as an immune boosting fermentate was included to provide contrast between anti-inflammatory and immune boosting properties.

5.3.2.1 Stimulation of LOX or LPS activated BMDC with Top 5 bioactive fermentates at 25mg/mL doesn't affect cell viability

BMDCs were seeded at a concentration of $1x10^6$ cells/mL, incubated for 24 hours before stimulating with a dose of 25mg/mL raw fermentate sample for 1 hour followed by LOX 0.5mM, or LPS 100ng/mL and subsequently incubated at 37^0C in 5% CO_2. After 24 hours an MTS assay was performed as previously outlined (section 2.2.13 MTS Cell Viability Assay).

Figure 87 demonstrates that there was no significant change in cell viability following exposure of the cells to 25mg/mL of any of the 5 Top bioactive fermentates to LPS TLR ligand stimulation. The use of the positive control of 10% DMSO provided a clear distinction between the cytotoxic effects on cell viability with the untreated control sample, as DMSO induces cell death.

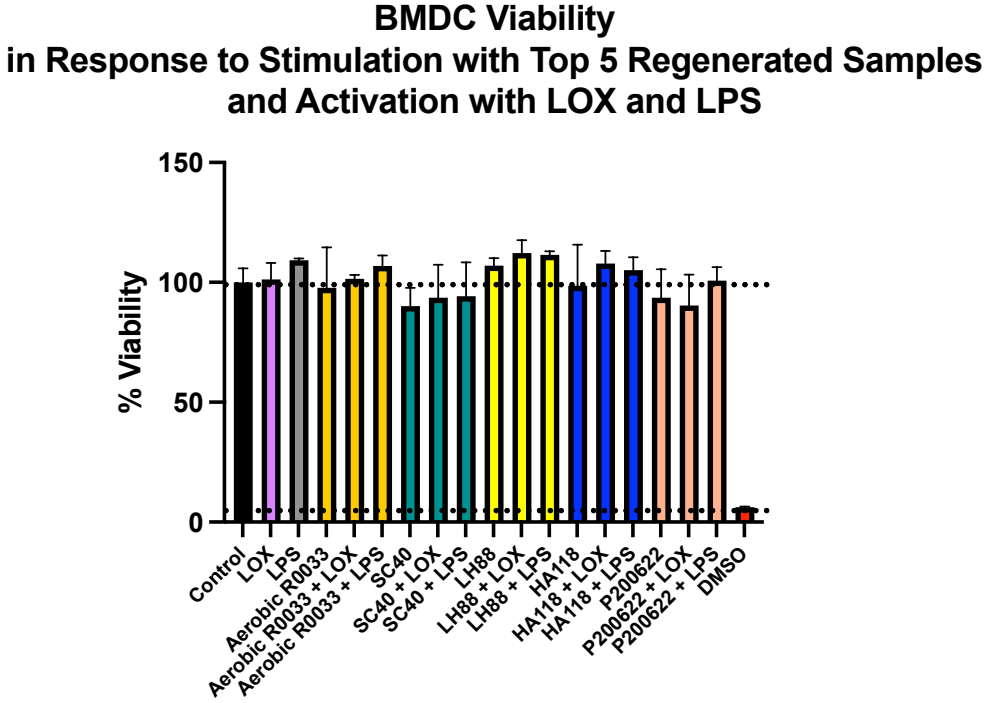

Figure 87: ***Exposure of LOX and LPS activated BMDC to 25mg/mL top 5 bioactive fermentates doesn't affect cell viability.*** *BMDC cells were seeded at $1x10^6$ cells/mL and left overnight at 37^0C in 5% CO_2. The following day cells were stimulated with 25mg/mL sample fermentate, incubated for 1 hour at 37^0C in 5% CO_2 and subsequently exposed to LOX 0.5mM or LPS 100ng/mL for TLR activation before incubating overnight under the same conditions. 10% DMSO was included as a positive control to induce cell death. Cells were incubated with MTS cell titre aqueous one solution for 3 hours at 37^0C in 5% CO_2. Viability is represented as a percentage compared to viable, untreated cells (Control). Data is presented as mean ± SD of three replicates.*

5.3.2.2 Stimulation of LOX or LPS activated BMDC with Top 5 bioactive fermentates at 25mg/mL effects cytokine secretion

BMDCs were seeded at a concentration of $1x10^6$ cells/mL, incubated for 24 hours before stimulating with a dose of 25mg/mL raw fermentate sample for 1 hour followed by LOX 0.5mM, or LPS 100ng/mL and subsequently incubated at 37^0C in 5% CO_2. After 24 hours supernatants were removed and ELISA procedure for cytokines IL-1β, IL-6, IL-10, TNF-α, IL-12p40, IL-12p70, IL-23, and IL-27 was performed according to the manufacturer's instructions (section 2.2.14 Enzyme Linked Immunosorbent Assay (ELISA)).

Figure 88 and Figure 89 demonstrate that the Top 5 bioactive fermentates affected the secretion of cytokines in response to immune challenges LOX, and LPS, when compared to the control TLRs.

Figure 88 demonstrates that LOX increased IL-1β, TNF-α, IL-12p40, IL-12p70 ($p<0.001$), IL-6, IL-10, and IL-23 ($p<0.002$). In the presence of LOX, Aerobic R0033, SC40, LH88, HA118 and P200622 significantly decreased IL-1β ($p<0.002$; $p<0.001$; $p<0.001$; $p<0.001$; $p<0.001$). Aerobic R0033, SC40, LH88, and HA118 significantly increased IL-6 ($p<0.033$). SC40, LH88, HA118 and P200622 significantly increased IL-10 ($p<0.001$), while decreasing IL-12p40 ($p<0.002$; $p<0.033$; $p<0.002$; $p<0.002$). Aerobic R0033 and HA118 increased IL-12p70 ($p<0.001$), while Aerobic R0033 increased IL-27 ($p<0.001$). SC40 decreased IL-12p70 ($p<0.002$), however concentrations of IL-12p70 are very low.

Unstimulated SC40, LH88 and P200622 significantly increased IL-1β ($p<0.033$). SC40, LH88, HA118 and P200622 increased IL-6, IL-10, TNF-α ($p<0.001$), IL-23 ($p<0.002$; $p<0.033$; $p<0.033$; $p<0.002$), and IL-27 ($p<0.033$; $p<0.001$; $p<0.001$; $p<0.001$). Aerobic R0033 increased IL-6 ($p<0.033$), and TNF-α ($p<0.002$), while HA118 increased IL-12p70 ($p<0.033$).

Figure 89 demonstrates that LPS increased IL-6, TNF-α, IL-27 ($p<0.001$), and IL-12p40 ($p<0.033$). In the presence of LPS, SC40, LH88, HA118 and P200622 significantly increased IL-10 and IL-23 ($p<0.001$). SC40, LH88, and P200622 significantly increased IL-1β IL-6 ($p<0.002$; $p<0.002$; $p<0.001$). HA118 increased IL-

6 ($p<0.033$), IL-27 ($p<0.001$), and IL-12p70 ($p<0.001$) however concentrations of IL-12p70 are very low. SC40 significantly increased TNF-α, ($p<0.033$), while LH88 decreased IL-12p40 ($p<0.033$). Aerobic R0033 significantly increased IL-23 ($p<0.002$), while decreasing IL-12p40 ($p<0.002$).

Unstimulated SC40, LH88, HA118 and P200622 significantly increased IL-6, IL-10, TNF-α ($p<0.001$), IL-23 ($p<0.001$; $p<0.002$; $p<0.002$; $p<0.001$), and IL-27 ($p<0.033$; $p<0.001$; $p<0.001$; $p<0.001$). Aerobic R0033, SC40, LH88 and P200622 significantly increased IL-1β ($p<0.001$). Aerobic R0033 significantly increased IL-6 ($p<0.033$), and TNF-α ($p<0.002$).

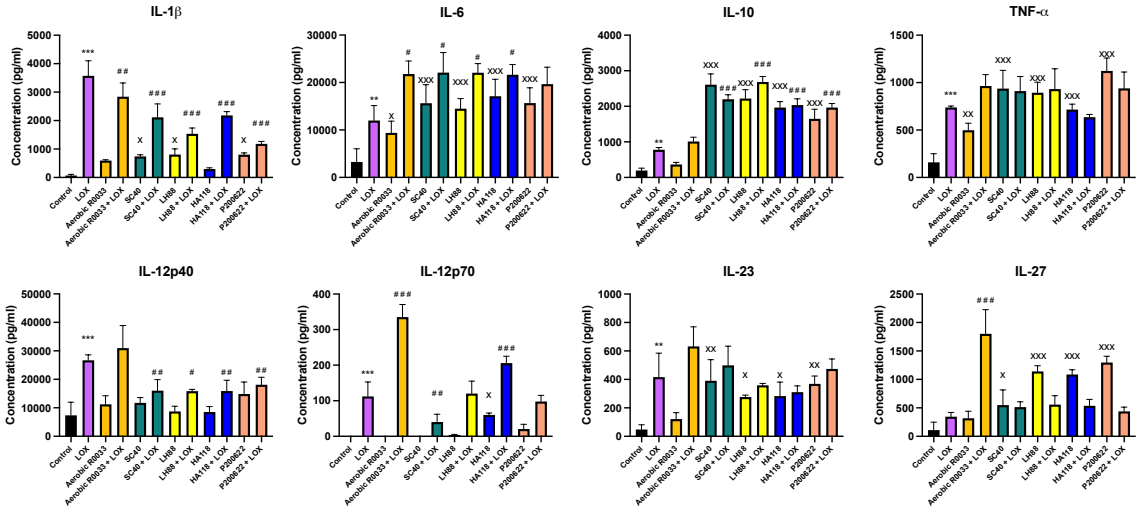

Figure 88: ***Exposure of LOX activated BMDC to 25mg/mL top 5 fermentate candidates results in the secretion of cytokines IL-1β, IL-6, IL-10, TNF-α, IL-12p40, IL-12p70, IL-23, and IL-27*** *BMDC cells were seeded at 1x10^6 cells/mL and left overnight at 37^{0}C in 5% CO_2. The following day cells were stimulated with 25mg/mL raw sample fermentate, incubated for 1 hour at 37^{0}C in 5% CO_2 and % CO_2 and subsequently exposed to LOX 0.5mM for TLR activation before incubating overnight under the same conditions. Supernatants were removed after 24 hours and ELISA was performed for IL-1β, IL-6, IL-10, TNF-α, IL-12p40, IL-12p70, IL-23, and IL-27. Data is presented as mean ± SD of three replicates. Significance determined using one- way ANOVA with a Newman-Keuls post-test. Output P value style APA: .12 (ns), .033 (*), .002(**) and <.001 (***); 1) comparing TLR to unstimulated control cells "*", 2) comparing sample to control cells "x" and, 3) comparing LOX to sample + LOX "#".*

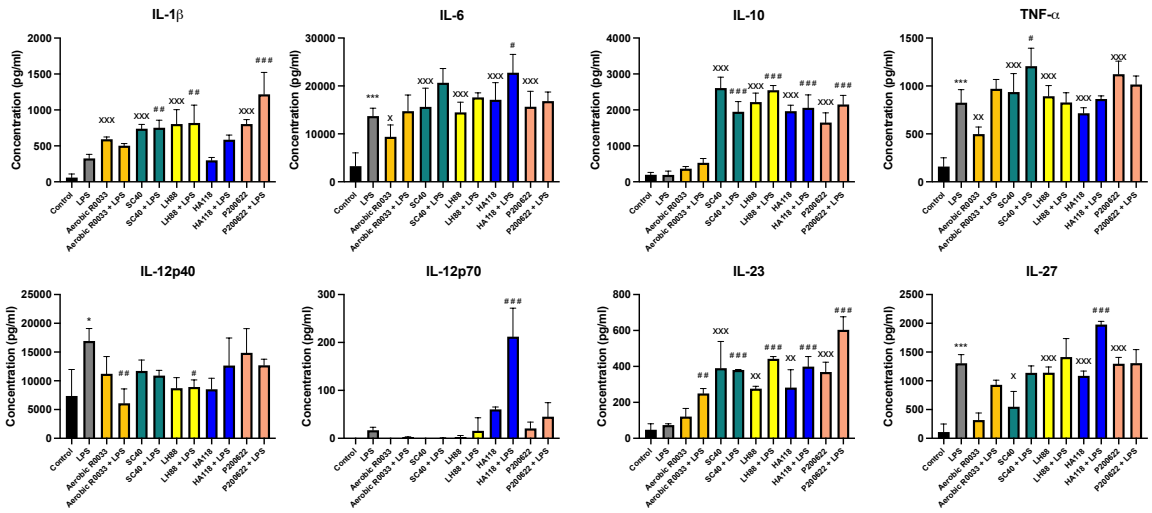

Figure 89: ***Exposure of LPS activated BMDC to 25mg/mL top 5 fermentate candidates results in the secretion of cytokines IL-1β, IL-6, IL-10, TNF-α, IL-12p40, IL-12p70, IL-23, and IL-27.*** *BMDC cells were seeded at 1x10^6 cells/mL and left overnight at 37^{0}C in 5% CO_2. The following day cells were stimulated with 25mg/mL raw sample fermentate, incubated for 1 hour at 37^{0}C in 5% CO_2 and % CO_2 and subsequently exposed to LPS 100ng/mL for TLR activation before incubating overnight under the same conditions. Supernatants were removed after 24 hours and ELISA was performed for IL-1β, IL-6, IL-10, TNF-α, IL-12p40, IL-12p70, IL-23, and IL-27 Data is presented as mean ± SD of three replicates. Significance determined using one-way ANOVA with a Newman-Keuls post-test. Output P value style APA: .12 (ns), .033 (*), .002(**) and <.001 (***); 1) comparing TLR to unstimulated control cells "*", 2) comparing sample to control cells "x" and, 3) comparing LPS to sample + LPS "#".*

Table 25 summarises the findings of the top 5 bioactive fermentates in LOX and LPS activated BMDCs. SC40, and LH88 had the most promising anti-inflammatory profile with highest IL-10 secretion, and decreased IL-12p40, and IL-12p70. HA118 and P200622 were less promising due to their enhanced IL-23, IL-27, and IL-12p70. Aerobic R0033 remained immune boosting with highest secretion of IL-1β, IL-27, and only non-significant secretion of IL-10.

Table 25: ***Summary cytokine secretion for BMDCs in the presence of Top 5 bioactive fermentates.*** *Summary of cytokines secreted in the absence/ presence of fermentates in LOX and LPS activated BMDCs. Significance determined using one- way ANOVA with a Newman-Keuls post-test. Output P value style APA: .12 (ns), .033 (*), .002(**) and <.001 (***); where unstimulated sample were compared to control cells, and samples in the presence of LOX/LPS were compared to LOX/LPS alone. Green indicates increased cytokine production, and red indicates decreased cytokine production.*

Fermentate	Aerobic R0033	SC40	LH88	HA118	P200622	
Unstimulated		*	*		*	IL-1β
	*	***	***	***	***	IL-6
		***	***	***	***	IL-10
	**	***	***	***	***	TNF-α
						IL-12p40
				*		IL-12p70
		**	*	*	**	IL-23
		*	***	***	***	IL-27
+LOX	**	***	***	***	***	IL-1β
	*	*	*	*		IL-6
		***	***	***	***	IL-10
						TNF-α
		**	*	**	**	IL-12p40
	***	**		***		IL-12p70
						IL-23
	***					IL-27
Unstimulated	***	***	***		***	IL-1β
	*	***	***	***	***	IL-6
		***	***	***	***	IL-10
	**	***	***	***	***	TNF-α
						IL-12p40
						IL-12p70
		***	**	**	***	IL-23
		*	***	***	***	IL-27
+LPS		**	**		***	IL-1β
				*		IL-6
		***	***	***	***	IL-10
		*				TNF-α
	**		*			IL-12p40
				***		IL-12p70
	**	***	***	***	***	IL-23
				***		IL-27

From this screening of the top 5 immune boosting/anti-inflammatory fermentates we can see that these fermentates did not negatively impact cell viability, while fermentates LH88, and SC40 were of most interest for their anti-inflammatory properties, in conjunction with their ability to positively affect the gut microbiome.

P200622, and HA118 were considered of less interest due to the lesser anti-inflammatory profile in comparison to LH88, and SC40, and thus were not brought forward for further testing.

Having established that SC40, in addition to LH88 were the top preforming anti-inflammatory candidates, we now brought these samples forward for an in-depth examination of their affects in polarised macrophage. We included Aerobic R0033, and R0419 for comparative purposes, and in the interest of potential future commercial interest in a viral immune boosting functional food, particularly for Aerobic R0033. This gave us our top 4 immune boosting and anti-inflammatory candidates Aerobic R0033, R0419, SC40, and LH88.

5.3.3 Extended Screening of Top 4 Immunomodulatory candidate fermentates

LH88, and SC40 had anti-inflammatory profiles, and from previous chapters, Aerobic R0033 and, R0419 had a clear immune boosting profile. In addition SC40 had a dual role also having immune boosting capabilities also, and was therefore of particular interest. Therefore, these fermentates were of key interest due to the ability to modulate the immune system. Highlighting these 4 samples as the top 4 immunomodulatory candidates enabled the examination of their extended abilities as immune boosting and anti-inflammatory candidates via the assessment of their effect on NO production, and arginase production in M0, M1, and M2 macrophage as well as the impact on IL-6, IL-10, and TNF-α production.

5.3.3.1 M0, M1 and M2 polarised BMDMs in the presence of candidate samples affect NO production via iNOS

BMDMs were seeded at a concentration of $5x10^5$ cells/mL, incubated for 1 hour before stimulating with a dose of 25mg/mL raw fermentate sample for 3 hour and subsequently incubated at 37^0C in 5% CO_2. The cells were then either polarised to

M1 phenotype by stimulating with LPS (100 ng/mL) in the presence of 20 ng/mL rIFN-γ or towards M2 cells by adding 20 ng/mL rIL-4, 20 ng/mL IL-13, and 20 ng/mL rTGF-B, or left unpolarised M0, and incubated for 24 h at 37^{0}C. Supernatants were removed after 24 hours and Griess Assay preformed according to the manufacturer's instructions (section 2.2.15.1 Griess Assay).

Figure 90A demonstrates that polarised M1 control cells significantly increased NO production ($p<0.001$), while M2 polarised control cells had no significant effect on NO production versus the control M0 unpolarised cells. Figure 90B demonstrates that all candidate samples SC40, LH88, Aerobic R0033, and R0419 significantly increased NO production ($p<0.001$) when polarised to both M1, and M2 and when left unpolarised as M0, versus their respective M0, M1, or M2 control in the absence of sample.

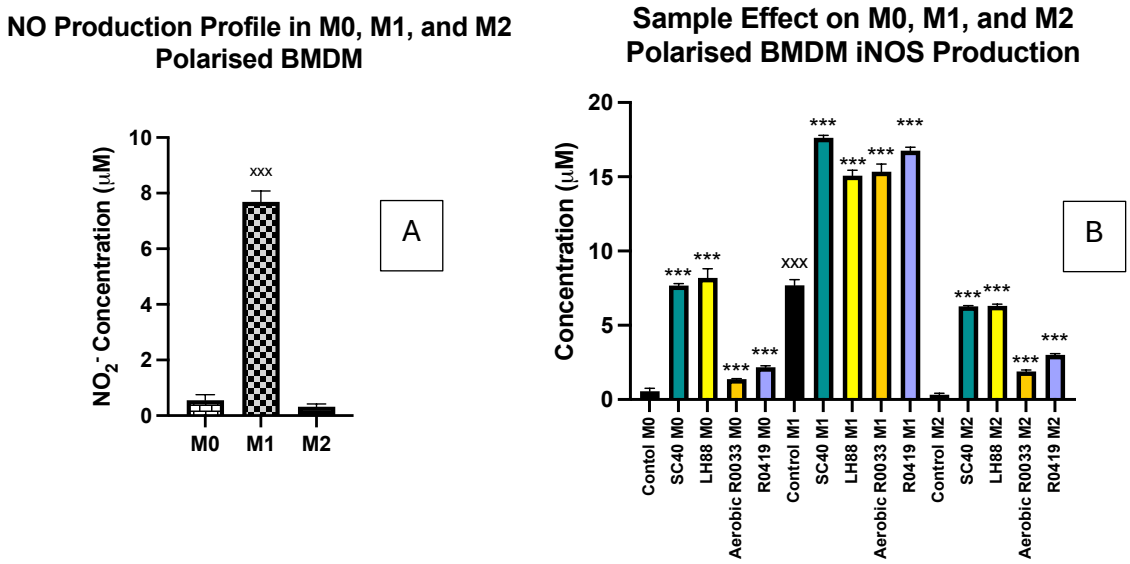

*Figure 90**: Exposure of M0, M1, and M2 BMDM to 25mg/mL top 4 raw samples affects production of NO.** *BMDM cells were seeded at 5x10^5 cells/mL and incubated for1 hour at 37^{0}C in 5% CO_2 Cells were stimulated with 25mg/mL sample fermentate, incubated for 3 hour at 37^{0}C in 5% CO_2 The cells were then either polarised to M1 phenotype by stimulating with LPS (100 ng/mL) in the presence of 20 ng/mL rIFN-γ or towards M2 cells by adding 20 ng/mL rIL-4, 20 ng/mL IL-13, and 20 ng/mL rTGF-B and incubate for 24 h at 37 C Supernatants were removed after 24 hours and Griess assay was performed as per manufacturer's instructions. Data is presented as mean ± SD of three replicates. Significance determined using one- way ANOVA with a Newman-Keuls post-test. Output P value style APA: .12 (ns), .033 (*), .002(**) and <.001 (***); 1) comparing M1 and M2 to M0 in the absence of sample "x", 2) comparing each sample M0, M1, M2 to respective M0, M1, M2 control cells "*".*

5.3.3.2 M0, M1 and M2 polarised BMDMs in the presence of candidate samples affects arginase activity

BMDMs were seeded at a concentration of $5x10^5$ cells/mL, incubated for 1 hour before stimulating with a dose of 25mg/mL raw fermentate sample for 3 hour and subsequently incubated at 37^0C in 5% CO_2. The cells were then either polarised to M1 phenotype by stimulating with LPS (100 ng/mL) in the presence of 20 ng/mL rIFN-γ or towards M2 cells by adding 20 ng/mL rIL-4, 20 ng/mL IL-13, and 20 ng/mL rTGF-B, or left unpolarised M0, and incubated for 24 h at 37^0C. Cells were harvested after 24 hours and lysates generated and protocol for Arginase Assay was performed according to the manufacturer's instructions (section 2.2.15.2 Arginase Assay).

Figure 91 demonstrates that fermentate samples affected arginase activity in response to polarisation towards an M1 and M2 macrophage phenotype, as well as when unpolarised M0, when comparing to the respective macrophage phenotype in the absence of sample i.e. M0, M1, or M2 alone.

Figure 91A demonstrates that polarised M2 control cells had significantly increased arginase activity ($p<0.033$), while M1 polarised control cells had no significant change in arginase activity versus the control M0 unpolarised cells seeing only a non-significant increase. Figure 91B demonstrates that M1 phenotypes in the presence of samples SC40, LH88, and R0419 had significantly increased arginase activity ($p<0.033$, $p<0.002$, $p<0.002$). M2 phenotypes in the presence of samples SC40, LH88, and R0419 had only non-significantly increased arginase activity. Unpolarised M0 in the presence of SC40, LH88, Aerobic R0033, and R0419 had significantly increased arginase activity ($p<0.002$, $p<0.001$; $p<0.033$; $p<0.002$), with samples SC40, LH88, and R0419 performing similar to or greater than the arginase activity of the M2 phenotype.

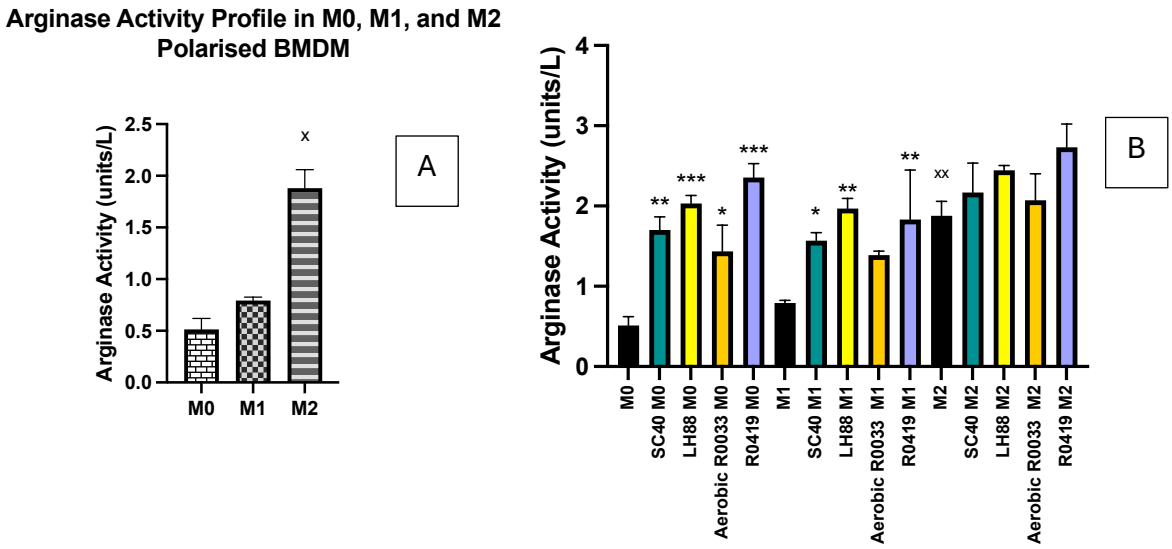

Figure 91: ***Exposure of M0, M1, and M2 BMDM to 25mg/mL top 4 raw samples affects arginase activity.*** *BMDM cells were seeded at 5x10⁵ cells/mL and incubated for1 hour at 37°C in 5% CO_2. Cells were stimulated with 25mg/mL sample fermentate, incubated for 3 hour at 37°C in 5% CO_2. The cells were then either polarised to M1 phenotype by stimulating with LPS (100 ng/mL) in the presence of 20 ng/mL rIFN-γ or towards M2 cells by adding 20 ng/mL rIL-4, 20 ng/mL IL-13, and 20 ng/mL rTGF-B and incubate for 24 h at 37 C. Cells were harvested, and lysates generated. Arginase assay was performed as per manufacturer's instructions. Data is presented as mean ± SD of two replicates. Significance determined using one- way ANOVA with a Newman-Keuls post-test. Output P value style APA: .12 (ns), .033 (*), .002(**) and <.001 (***); 1) comparing M1 and M2 to M0 in the absence of sample "x", 2) comparing each sample M0, M1, M2 to respective M0, M1, M2 control cells "*".* 1 unit arginase converts 1uMole L-arginine to omithine and urea per minute at 37°C.

5.3.3.3M0, M1 and M2 polarised BMDMs in the presence of candidate samples affects cytokine secretion

BMDMs were seeded at a concentration of $5x10^5$ cells/mL, incubated for 1 hour before stimulating with a dose of 25mg/mL raw fermentate sample for 3 hour and subsequently incubated at 37°C in 5% CO_2. The cells were then either polarised to M1 phenotype by stimulating with LPS (100 ng/mL) in the presence of 20 ng/mL rIFN-γ or towards M2 cells by adding 20 ng/mL rIL-4, 20 ng/mL IL-13, and 20 ng/mL rTGF-B, or left unpolarised M0, and incubated for 24 h at 37°C. Supernatants were removed after 24 hours and ELISA was performed for IL-6, IL-10, and TNF-α according to the manufacturer's instructions (section 2.2.14 Enzyme Linked Immunosorbent Assay (ELISA)).

Figure 92 demonstrates that fermentate samples affected the secretion of cytokines in response to polarisation towards an M1 and M2 macrophage phenotype, as well as unpolarised M0, when comparing to the respective macrophage phenotype in the absence of sample i.e. M0, M1, or M2 alone.

Figure 92A demonstrates that polarisation from an M0 to an M1 phenotype significantly increased IL-6, and TNF-α secretion ($p<0.001$), but not when polarised from an M0 to and M2 phenotype. Polarisation from an M0 to an M2 phenotype non-significantly increased IL-10, but not IL-6, and TNF-α. Figure 92B demonstrates that polarisation to an M1 phenotype in the presence of Aerobic R0033, R0419, and LH88 significantly increased IL-6 ($p<0.001$; $p<0.001$; $p<0.002$), and TNF-α ($p<0.001$; $p<0.002$; $p<0.001$). Polarisation to an M2 phenotype in the presence of SC40, LH88, Aerobic R0033, and R0419 significantly increased IL-10 ($p<0.001$), while SC40, LH88, and R0419 significantly increased TNF-α ($p<0.002$; $p<0.001$; $p<0.033$). When left unpolarised at an M0 phenotype in the presence of SC40, LH88, Aerobic R0033, and R0419 significantly increased IL-6 ($p<0.001$; $p<0.001$; $p<0.002$; $p<0.001$), and IL-10 ($p<0.001$; $p<0.001$; $p<0.033$; $p<0.002$), while only LH88, and R0419 significantly increased TNF-α ($p<0.001$).

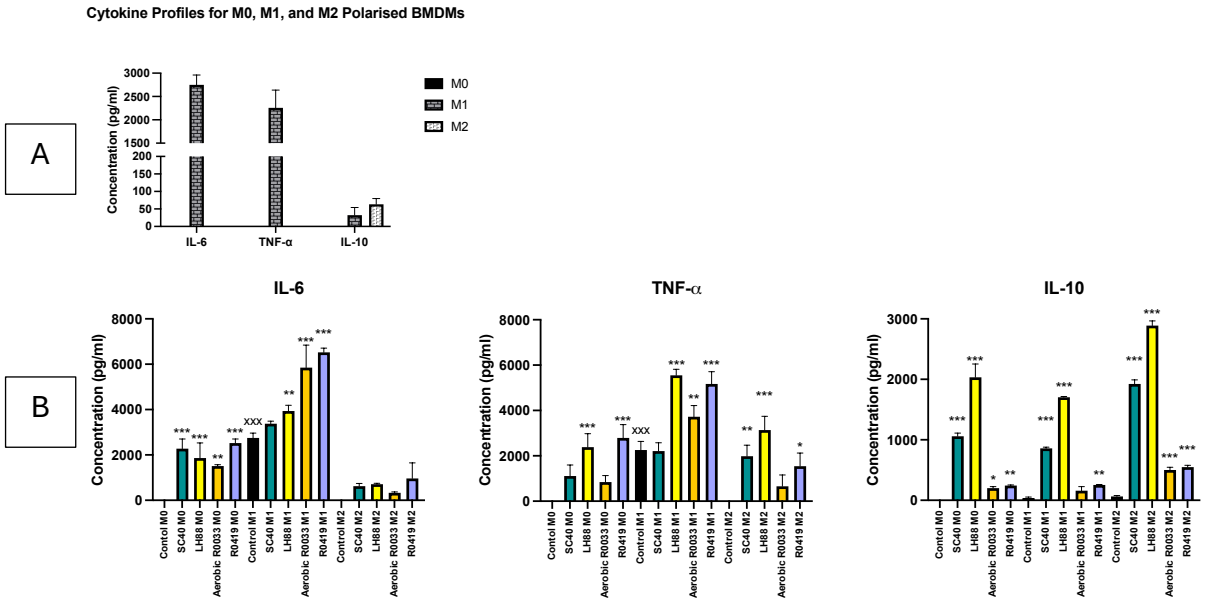

Figure 92: ***Exposure of M1/M2 polarised BMDMs to 25mg/mL top 4 Fermentate samples results in the secretion of cytokines IL-6, TNF-α, and IL-10.*** *BMDM cells were seeded at 5x10^5 cells/mL and incubated for 1 hour at 37^{0}C in 5% CO_2. Cells were stimulated with 25mg/mL sample fermentate, incubated for 3 hours at 37^{0}C in 5% CO_2 The cells were then either polarised to M1 phenotype by stimulating with LPS (100 ng/mL) in the presence of 20 ng/mL rIFN-γ or towards M2 cells by adding 20 ng/mL rIL-4, 20 ng/mL IL-13, and 20 ng/mL rTGF-B and incubate for 24 h at 37^{O}C Supernatants were removed after 24 hours and ELISA was performed for IL-6, IL-10, and TNF-α. Data is presented as mean ± SD of three replicates. Significance determined using one- way ANOVA with a Newman-Keuls post-test. Output P value style APA: .12 (ns), .033 (*), .002(**) and <.001 (***); 1) comparing to polarised control cells in the absence of sample "*" and, 2) comparing polarised M1, and M2 control cells to M0 unpolarised cells "x*

As summarised in Table 26, there was a clear distinction between each of the samples and further classification of the fermentate profiles confirmed LH88 and SC40 as an anti-inflammatory sample with increased arginase activity in M0, and M1 macrophage, and highest concentrations of IL-10 in M0, M1, and M2 macrophage, but also enhanced NO production in M0, M1, and M2 macrophage. Aerobic R0033, and R0419 were clear immune boosting fermentates with high NO production in M0, M1, and M2 macrophage, as well as enhance IL-6 secretion in M0, and M1 macrophage, and TNF-α secretion in M1 macrophage, with overall lower IL-10 secretion in M0, M1, and M2 macrophage, however there was also small levels of arginase activity in the presence of R0419 in both M0, and M1 macrophage. This demonstrates that the samples again had largely anti-inflammatory or immune

boosting profiles with some cross over in functionality also, highlighting their dual roles.

*Table 26:**Summary of the effects on cytokine secretion, NO production, and arginase activity in the presence of fermentates in M0, M1, and M2 macrophage**. Summary of cytokines secreted, NO production, arginase activity in polarised macrophage. Significance determined using one- way ANOVA with a Newman-Keuls post-test. Output P value style APA: .12 (ns), .033 (*), .002(**) and <.001 (***); where fermentates were compared to polarised macrophage in the absence of fermentate.. Green indicates increased production.*

Fermentate	SC40	LH88	Aerobic R0033	R0419	
M0	***	***	**	***	IL-6
	***	***	*	**	IL-10
		***		***	TNF-α
	***	***	***	***	NO production
	**	***	*	***	Arginase Activity
M1		**	***	***	IL-6
	***	***		**	IL-10
		***	**	***	TNF-α
	***	***	***	***	NO production
	*	**		**	Arginase Activity
M2					IL-6
	***	***	***	***	IL-10
	**	***		*	TNF-α
	***	***	***	***	NO production
					Arginase Activity

Having established the fermentates effects in a range of immune cells, and immune scenarios, it was now important to confirm that these fermentates can be upscaled to produce at a commercial rate. Upscaled production was carried out by the team in Teagasc and fermentates were generated and received in DCU for assessment of bioactivity.

5.3.4 Regeneration of fermentates has little effect on fermentate bioactivity

SC40 was chosen as the candidate fermentate for regeneration assessment as it was the key sample of interest due to its dual role in viral immunity and chronic inflammation resolution. SC40 was processed and upscaled to generate a number of SC40 spinoff samples for testing. These spinoff samples were Regenerate SC40, Powder A, Powder B, and Postbiotic SC40. Regenerated SC40 was produced in the same manner as the Original SC40. Powder A had a reduced concentration of LAB inoculum used in production at 10% w/v RSM, while Powder B had a higher concentration at 25% w/v RSM. Postbiotic SC40 was prepared in accordance with FHIs SOP for generation of postbiotic samples whereby the fermentate was grown in MRS broth before final reconstitution in RSM. Importantly the original SC40 was included for comparison for each of these regenerated fermentates. Both BMDCs and BMDMs were used when activated with both LOX/PIC and LPS/CpG for assessment of SC40 in two cell types when challenged with a range of immune stimuli. Additional regeneration of samples Aerobic R0033, Anaerobic R0033, and R0419 is attached in the appendix.

5.3.4.1 Stimulation of TLR activated BMDC and BMDM with Original vs. Regenerated raw samples at 25mg/mL doesn't affect cell viability

BMDC and BMDMs were seeded at a concentration of $1x10^6$ cells/mL, incubated for 24 hours before stimulating with a dose of 25mg/mL raw fermentate sample for 1 hour followed by viral TLR ligand: : LOX 0.5mM and PIC 10µg/mL or bacterial TLR: LPS 100ng/mL and CpG 5 µM respectively and subsequently incubated at 37^0C in 5% CO_2. After 24 hours an MTS assay was performed as previously outlined (section 2.2.13 MTS Cell Viability Assay).

Figure 93 demonstrates that there was no significant change in cell viability following exposure of the cells to 25mg/mL Original or differentially prepared SC40s when stimulated with LOX, LPS, CpG or PIC TLRs in either BMDC or BMDMs. The

use of the positive control of 10% DMSO provided a clear distinction between the cytotoxic effects on cell viability with the untreated control sample, as DMSO induced cell death.

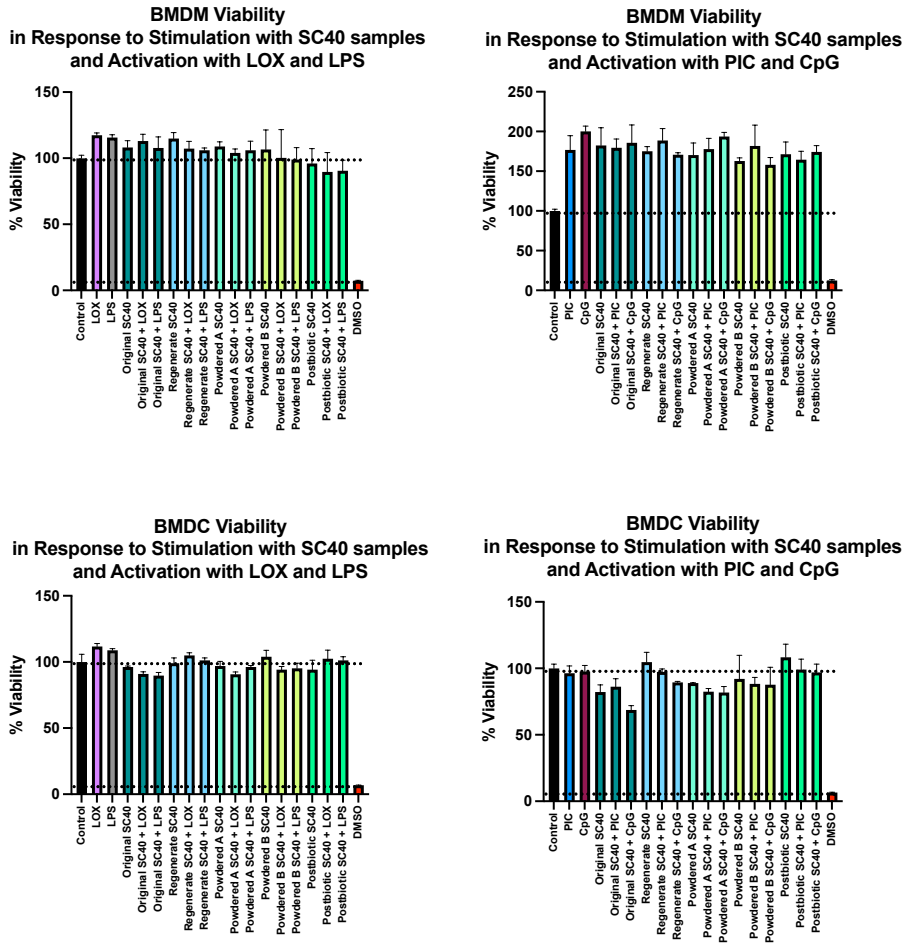

Figure 93: ***Exposure of BMDM and BMDC to panel of TLRs and 25mg/mL differentially generated raw SC40 doesn't affect cell viability.*** *J774.A.1. cells were seeded at 1x10^6 cells/mL and left overnight at 37^{0}C in 5% CO_2. The following day cells were stimulated with 25mg/mL sample fermentate, incubated for 1 hour at 37^{0}C in 5% CO_2 and subsequently exposed to the following concentrations of TLRs: : LOX 0.5mM, LPS 100ng/mL, CpG 5 µM, PIC 10µg/mL for TLR activation before incubating overnight under the same conditions.* 10% *DMSO was included as a positive control to induce cell death. Cells were incubated with MTS cell titre aqueous one solution for 3 hours at 37^{0}C in 5% CO_2. Viability is represented as a percentage compared to viable, untreated cells (Control). Data is presented as mean ± SD of three replicates.*

5.3.4.2BMDC

5.3.4.2.1 Stimulation of TLR activated BMDCs with 25mg/mL differentially generated SC40 raw sample affects secretion of cytokines

BMDCs were seeded at a concentration of $1x10^6$ cells/mL, incubated for 24 hours before stimulating with a dose of 25mg/mL raw fermentate sample for 1 hour followed by viral TLR ligand: LOX 0.5mM and PIC 10µg/mL or bacterial TLR: LPS 100ng/mL and CpG 5 µM respectively and subsequently incubated at 37^0C in 5% CO_2. After 24 hours supernatants were removed and ELISA procedure for cytokines IL-1β, IL-6, IL-10, TNF-α, IL-12p40, IL-12p70, IL-23, and IL-27 was performed according to the manufacturer's instructions (section 2.2.14 Enzyme Linked Immunosorbent Assay (ELISA)).

Figure 94 demonstrates that different SC40 regenerated samples affected the secretion of cytokines in response to immune challenges LOX, PIC, LPS, and CpG, when compared to the Original SC40. Concentrations of Il-12p70 were very low for all immune activations and thus considered insignificant.

Figure 94 demonstrates that LOX increased IL-1β, IL-12p40, IL-23($p<0.001$) and TNF-α ($p<0.033$). In the presence of LOX, Regenerate, Powder A, Powder B and Postbiotic significantly decreased IL-10 ($p<0.001$). Regenerate, Powder B and Postbiotic significantly decreased TNF-α ($p<0.033$; $p<0.033$; $p<0.002$), IL-23 ($p<0.033$; $p<0.033$; $p<0.001$), while Powder A increased IL-23 ($p<0.001$). Powder A and Powder B significantly increased IL-27 ($p<0.001$), while Regenerate and Postbiotic decreased IL-27 ($p<0.033$; $p<0.001$). Regenerate and Postbiotic decreased IL-6 ($p<0.002$; $p<0.001$), while Postbiotic decreased IL-1β ($p<0.002$). Unstimulated Regenerate, Powder A, Powder B and Postbiotic significantly decreased IL-1β ($p<0.001$). Powder A decreased IL-6 ($p<0.002$), and TNF-α ($p<0.033$). Regenerate decreased IL-27 ($p<0.002$), while Powder A and Powder B increased IL-27 ($p<0.001$), and Postbiotic decreased Il-23 ($p<0.033$).

Figure 95 demonstrates that PIC did not significantly increase any cytokines versus the control cells thus results are inconclusive, however there was clear significance seen from the samples versus the original SC40. In the presences of PIC, Regenerate, Powder A, powder B and Postbiotic significantly decreased IL-1β

($p<0.001$). Regenerate decreased IL-12p40 and IL-23 ($p<0.033$), while Postbiotic decreased IL-23 ($p<0.001$). Powder A and Powder B significantly increased IL-27 ($p<0.001$; $p<0.002$).

Unstimulated Regenerate, Powder A, Powder B and Postbiotic significantly decreased IL-1β ($p<0.001$). Regenerate and Postbiotic increased IL-10 ($p<0.033$) but decreased IL-23 ($p<0.002$; $p<0.001$). Regenerate, Powder A and Powder B significantly decreased TNF-α ($p<0.002$; $p<0.001$; $p<0.002$). Powder A and Powder B significantly increased IL-27 ($p<0.001$).

Figure 96 demonstrates that LPS increased IL-12p40 ($p<0.001$), IL-1β ($p<0.033$), and non-significantly increased IL-6, TNF-α, IL-23 and IL-27. In the presence of LPS, Regenerate, Powder A, Powder B and Postbiotic significantly decreased IL-1β ($p<0.002$; $p<0.001$; $p<0.001$; $p<0.002$). Postbiotic significantly increased IL-27 ($p<0.033$).

Unstimulated Regenerate, Powder A, Powder B and Postbiotic significantly decreased IL-1β ($p<0.001$; $p<0.001$; $p<0.001$; $p<0.002$). Powder A decreased IL-6 ($p<0.002$). Powder A and Powder B increased IL-27 ($p<0.001$; $p<0.033$), and Postbiotic decreased Il-23 ($p<0.002$).

Figure 97 demonstrates that CpG increased IL-12p40, IL-23 ($p<0.001$), IL-6 ($p<0.033$), and non-significantly increased IL-1β, TNF-α, and IL-27. In the presence of CpG, Regenerate, Powder A, Powder B and Postbiotic significantly decreased IL-1β ($p<0.001$). Powder B increased IL-10 ($p<0.002$), while Postbiotic decreased IL-23 ($p<0.001$), and Regenerate decreased IL-12p40 ($p<0.002$). Regenerate, Powder A and Powder B decreased TNF-α ($p<0.033$; $p<0.001$; $p<0.001$). Powder A and Powder B increase IL-27 ($p<0.001$).

Unstimulated Regenerate, Powder A, Powder B and Postbiotic significantly decreased IL-1β ($p<0.001$) and IL-23 ($p<0.001$; $p<0.033$; $p<0.033$; $p<0.001$). Regenerate and Postbiotic increased IL-10 ($p<0.033$). Powder A decreased TNF-α ($p<0.002$). Powder A and Powder B increased IL-27 ($p<0.001$).

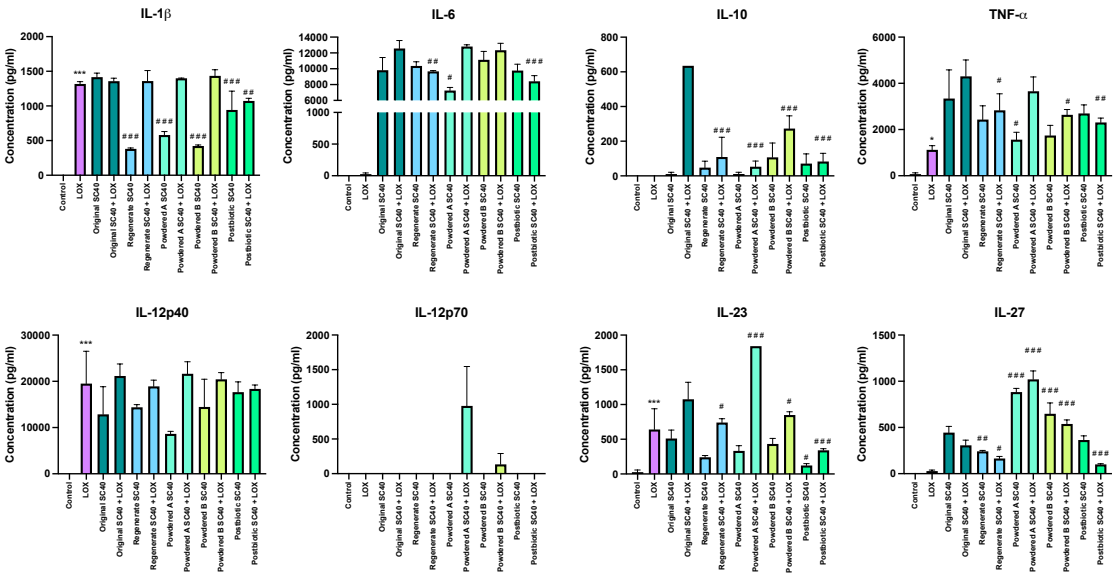

Figure 94: ***Exposure of LOX activated BMDC to 25mg/mL differentially generated SC40 raw sample results in the secretion of cytokines IL-1β, IL-6, IL-10, TNF-α, IL-12p40, IL-12p70, IL-23, and IL-27*** *BMDM cells were seeded at 1x10^6 cells/mL and left overnight at 37^{0}C in 5% CO_2. The following day cells were stimulated with 25mg/mL raw sample fermentate, incubated for 1 hour at 37^{0}C in 5% CO_2 and % CO_2 and subsequently exposed to the following concentrations of TLRs: LOX 0.5mM for TLR activation before incubating overnight under the same conditions. Supernatants were removed after 24 hours and ELISA was performed for IL-1β, IL-6, IL-10, TNF-α, IL-12p40, IL-12p70, IL-23, and IL-27. Data is presented as mean ± SD of three replicates. Significance determined using one- way ANOVA with a Newman-Keuls post-test. Output P value style APA: .12 (ns), .033 (*), .002(**) and <.001 (***); 1) comparing to unstimulated control cells "*",and 2) comparing sample to the original SC40 sample"#".*

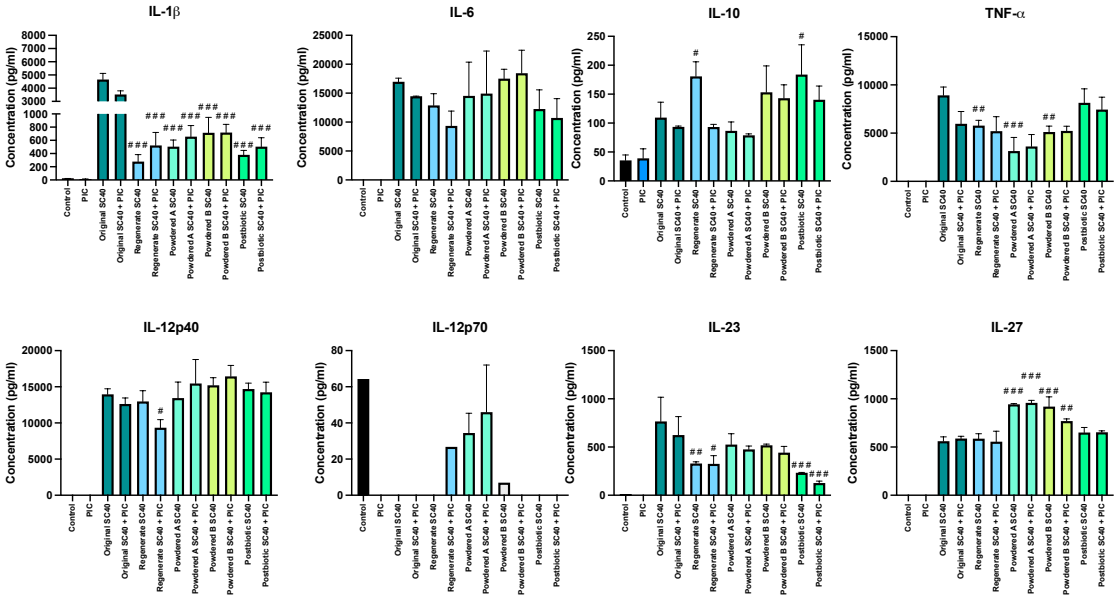

Figure 95: ***Exposure of PIC activated BMDC to 25mg/mL differentially generated SC40 raw sample results in the secretion of cytokines IL-1β, IL-6, IL-10, TNF-α, IL-12p40, IL-12p70, IL-23, and IL-27*** *BMDM cells were seeded at 1x10^6 cells/mL and left overnight at 37^{0}C in 5% CO_2. The following day cells were stimulated with 25mg/mL raw sample fermentate, incubated for 1 hour at 37^{0}C in 5% CO_2 and % CO_2 and subsequently exposed to the following concentrations of TLRs PIC 10µg/mL for TLR activation before incubating overnight under the same conditions. Supernatants were removed after 24 hours and ELISA was performed for IL-1β, IL-6, IL-10, TNF-α, IL-12p40, IL-12p70, IL-23, and IL-27. Data is presented as mean ± SD of three replicates. Significance determined using one- way ANOVA with a Newman-Keuls post-test. Output P value style APA: .12 (ns), .033 (*), .002(**) and <.001 (***); 1) comparing to unstimulated control cells "*",and 2) comparing sample to the original SC40 sample"#".*

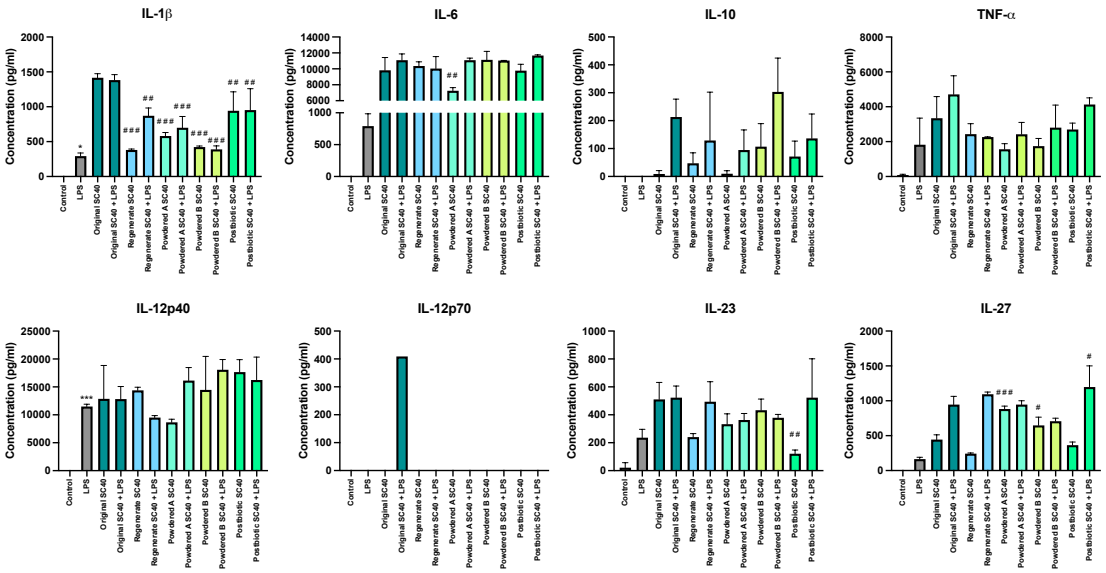

Figure 96: ***Exposure of LPS activated BMDC to 25mg/mL differentially generated SC40 raw sample results in the secretion of cytokines IL-1β, IL-6, IL-10, TNF-α, IL-12p40, IL-12p70, IL-23, and IL-27*** *BMDM cells were seeded at 1x10^6 cells/mL and left overnight at 37^{0}C in 5% CO_2. The following day cells were stimulated with 25mg/mL raw sample fermentate, incubated for 1 hour at 37^{0}C in 5% CO_2 and % CO_2 and subsequently exposed to the following concentrations of TLRs: LPS 100ng/mL for TLR activation before incubating overnight under the same conditions. Supernatants were removed after 24 hours and ELISA was performed for IL-1β, IL-6, IL-10, TNF-α, IL-12p40, IL-12p70, IL-23, and IL-27. Data is presented as mean ± SD of three replicates. Significance determined using one- way ANOVA with a Newman-Keuls post-test. Output P value style APA: .12 (ns), .033 (*), .002(**) and <.001 (***); 1) comparing to unstimulated control cells "*",and 2) comparing sample to the original SC40 sample"#".*

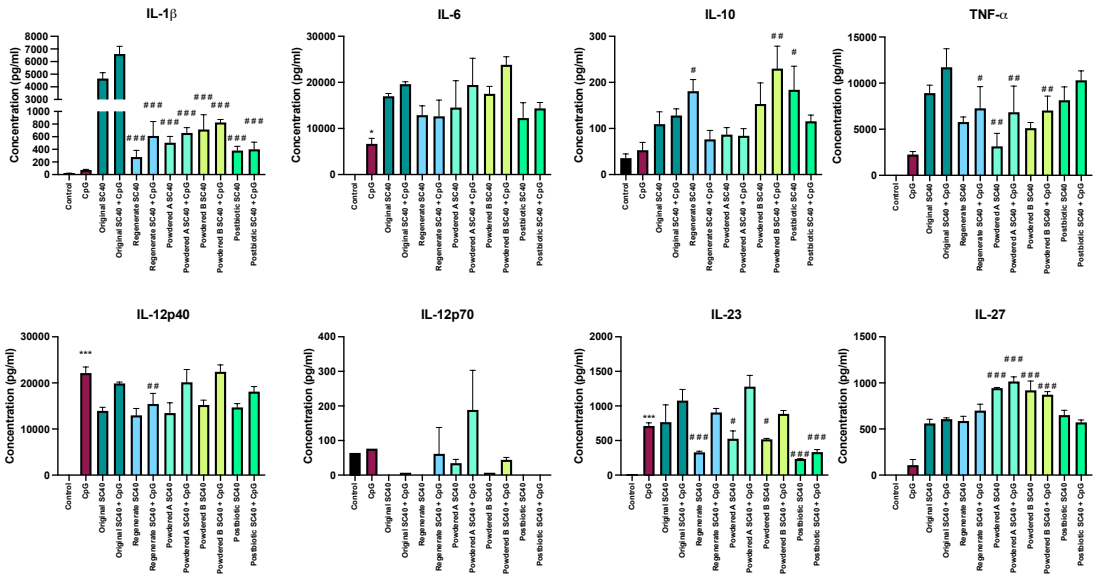

Figure 97: ***Exposure of CpG activated BMDC to 25mg/mL differentially generated SC40 raw sample results in the secretion of cytokines IL-1β, IL-6, IL-10, TNF-α, IL-12p40, IL-12p70, IL-23, and IL-27*** *BMDM cells were seeded at 1x10^6 cells/mL and left overnight at 37^{0}C in 5% CO_2. The following day cells were stimulated with 25mg/mL raw sample fermentate, incubated for 1 hour at 37^{0}C in 5% CO_2 and % CO_2 and subsequently exposed to the following concentrations of TLRs: CpG 5μM for TLR activation before incubating overnight under the same conditions. Supernatants were removed after 24 hours and ELISA was performed for IL-1β, IL-6, IL-10, TNF-α, IL-12p40, IL-12p70, IL-23, and IL-27. Data is presented as mean ± SD of three replicates. Significance determined using one- way ANOVA with a Newman-Keuls post-test. Output P value style APA: .12 (ns), .033 (*), .002(**) and <.001 (***); 1) comparing to unstimulated control cells "*",and 2) comparing sample to the original SC40 sample"#".*

5.3.4.3BMDM

5.3.4.3.1 Stimulation of TLR activated BMDMs with 25mg/mL differentially generated SC40 raw sample affects secretion of cytokines

BMDMs were seeded at a concentration of $1x10^6$ cells/mL, incubated for 24 hours before stimulating with a dose of 25mg/mL raw fermentate sample for 1 hour followed by viral TLR ligand: : LOX 0.5mM and PIC 10µg/mL or bacterial TLR: LPS 100ng/mL and CpG 5 µM respectively and subsequently incubated at 37^0C in 5% CO_2. After 24 hours supernatants were removed and ELISA procedure for cytokines IL-1β, IL-6, IL-10, TNF-α, IL-12p40, IL-12p70, IL-23, and IL-27 was performed according to the manufacturer's instructions (section 2.2.14 Enzyme Linked Immunosorbent Assay (ELISA)).

Figure 98-Figure 101 demonstrates that different SC40 regenerated samples affected the secretion of cytokines in response to immune challenges LOX, PIC, LPS, and CpG, when compared to the Original SC40. Concentrations of Il-12p70 and IL-23 were very low for all immune activations and thus considered insignificant.

Figure 98 demonstrates that LOX increased IL-1β, IL-10, and IL-12p40 ($p<0.001$). In the presence of LOX, Regenerate, Powder A, Powder B and Postbiotic significantly decreased IL-1β ($p<0.033$; $p<0.001$; $p<0.001$; $p<0.002$). Regenerate significantly decreased IL-6 and IL-12p40 ($p<0.033$). Powder A significantly increased IL-6, TNF-α and IL-12p40 ($p<0.001$; $p<0.002$; $p<0.001$). Powder A and Powder B significantly deceased IL-10 ($p<0.002$; $p<0.001$), while Powder B increased IL-12p40 ($p<0.002$).

Unstimulated Regenerate, Powder A, Powder B and Postbiotic significantly decreased IL-1β ($p<0.002$). Powder A decreased IL-6 ($p<0.033$), and TNF-α ($p<0.033$). Powder A and Powder B decreased IL-10 ($p<0.002$; $p<0.001$). Powder A and Postbiotic increased Il-12p40 ($p<0.001$; $p<0.002$).

Figure 99 demonstrates that PIC increased IL-27 ($p<0.002$) but decreased IL-1β. In the presence of PIC, Regenerate, Powder A, Powder B and Postbiotic significantly decreased TNF-α ($p<0.001$), and IL-12p40 ($p<0.001$; $p<0.001$; $p<0.001$; $p<0.002$). Regenerate and Postbiotic increased IL-10 ($p<0.002$; $p<0.001$), while

Powder A decreased IL-10 ($p<0.001$). Regenerate and Powder A decreased IL-6 ($p<0.033$), and IL-27 ($p<0.001$), along with Powder B decreasing IL-27 ($p<0.001$).
Unstimulated Regenerate significantly decreased IL-27 ($p<0.033$), while Powder A decreased IL-10 ($p<0.001$).

Figure 100 demonstrates that LPS increased IL-10, and IL-27 ($p<0.002$; $p<0.033$), and non-significantly increased IL-1β, IL-6, TNF-α, and IL-12p40. In the presence of LPS, Regenerate, Powder A, Powder B and Postbiotic significantly decreased IL-1β ($p<0.002$; $p<0.001$; $p<0.001$; $p<0.002$), and IL-6 ($p<0.033$; $p<0.001$; $p<0.033$; $p<0.033$). Powder B decreased IL-10 ($p<0.001$).
Unstimulated Regenerate, Powder A, Powder B and Postbiotic significantly decreased IL-1β ($p<0.002$; $p<0.033$; $p<0.033$; $p<0.002$). Powder A increased IL-6, TNF-α, and IL-27 ($p<0.033$). Powder A, Powder B, and Postbiotic decreased IL-10 ($p<0.001$; $p<0.001$; $p<0.033$), while Powder A and Postbiotic increased Il-12p40 ($p<0.001$; $p<0.002$).

Figure 101 demonstrates that CpG increased IL-6, IL-10, TNF-α, IL-12p40 ($p<0.001$), and IL-27 ($p<0.002$). In the presence of CpG, Regenerate, Powder A, Powder B and Postbiotic significantly decreased IL-1β ($p<0.001$). Postbiotic increased IL-10 ($p<0.001$), and Powder A increased IL-27 ($p<0.033$).
Unstimulated Powder A, and Powder B significantly increased IL-27 ($p<0.033$; $p<0.002$). Powder A decreased IL-10 ($p<0.001$), while Postbiotic increased IL-10 ($p<0.001$).

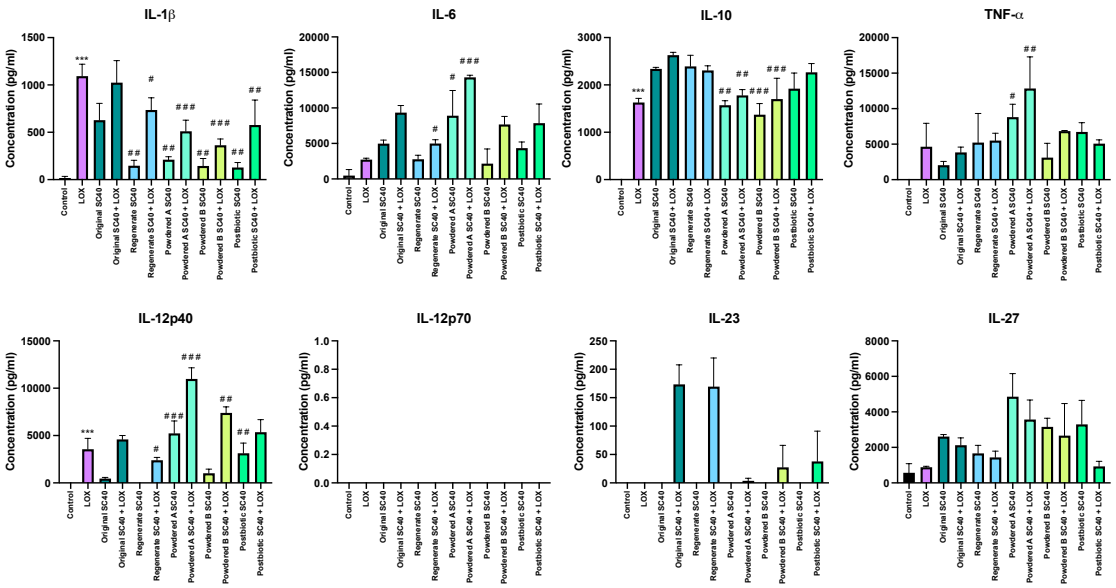

Figure 98: ***Exposure of LOX activated BMDM to 25mg/mL differentially generated SC40 raw sample results in the secretion of cytokines IL-1β, IL-6, IL-10, TNF-α, IL-12p40, IL-12p70, IL-23, and IL-27*** *BMDM cells were seeded at 1x10^6 cells/mL and left overnight at 37^{0}C in 5% CO_2. The following day cells were stimulated with 25mg/mL raw sample fermentate, incubated for 1 hour at 37^{0}C in 5% CO_2 and % CO_2 and subsequently exposed to the following concentrations of TLRs: LOX 0.5mM for TLR activation before incubating overnight under the same conditions. Supernatants were removed after 24 hours and ELISA was performed for IL-1β, IL-6, IL-10, TNF-α, IL-12p40, IL-12p70, IL-23, and IL-27. Data is presented as mean ± SD of three replicates. Significance determined using one- way ANOVA with a Newman-Keuls post-test. Output P value style APA: .12 (ns), .033 (*), .002(**) and <.001 (***); 1) comparing to unstimulated control cells "*",and 2) comparing sample to the original SC40 sample"#".*

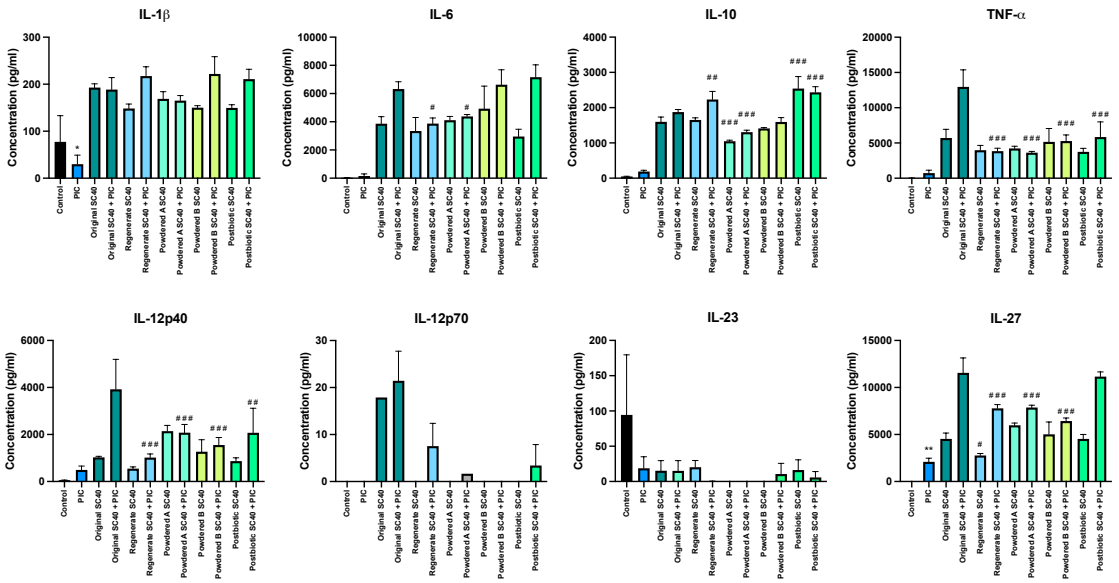

Figure 99: ***Exposure of PIC activated BMDM to 25mg/mL differentially generated SC40 raw sample results in the secretion of cytokines IL-1β, IL-6, IL-10, TNF-α, IL-12p40, IL-12p70, IL-23, and IL-27*** *BMDM cells were seeded at 1x10^6 cells/mL and left overnight at 37^{0}C in 5% CO_2. The following day cells were stimulated with 25mg/mL raw sample fermentate, incubated for 1 hour at 37^{0}C in 5% CO_2 and % CO_2 and subsequently exposed to the following concentrations of TLRs PIC 10µg/mL for TLR activation before incubating overnight under the same conditions. Supernatants were removed after 24 hours and ELISA was performed for IL-1β, IL-6, IL-10, TNF-α, IL-12p40, IL-12p70, IL-23, and IL-27. Data is presented as mean ± SD of three replicates. Significance determined using one- way ANOVA with a Newman-Keuls post-test. Output P value style APA: .12 (ns), .033 (*), .002(**) and <.001 (***); 1) comparing to unstimulated control cells "*",and 2) comparing sample to the original SC40 sample"#".*

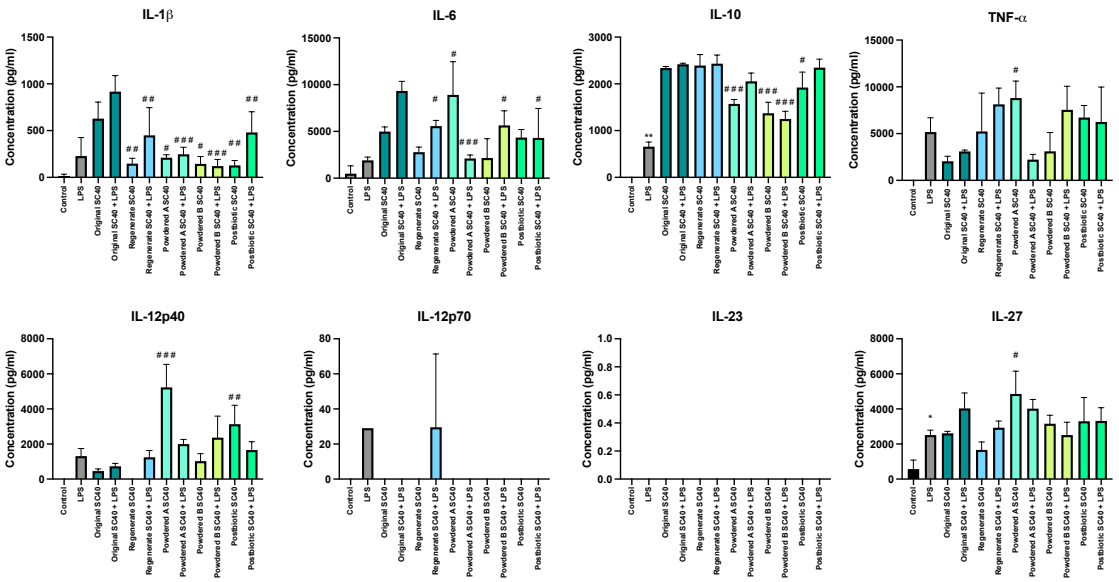

Figure 100: ***Exposure of LPS activated BMDM to 25mg/mL differentially generated SC40 raw sample results in the secretion of cytokines IL-1β, IL-6, IL-10, TNF-α, IL-12p40, IL-12p70, IL-23, and IL-27*** *BMDM cells were seeded at 1x10^6 cells/mL and left overnight at 37^{0}C in 5% CO_2. The following day cells were stimulated with 25mg/mL raw sample fermentate, incubated for 1 hour at 37^{0}C in 5% CO_2 and % CO_2 and subsequently exposed to the following concentrations of TLRs: LPS 100ng/mL for TLR activation before incubating overnight under the same conditions. Supernatants were removed after 24 hours and ELISA was performed for IL-1β, IL-6, IL-10, TNF-α, IL-12p40, IL-12p70, IL-23, and IL-27. Data is presented as mean ± SD of three replicates. Significance determined using one- way ANOVA with a Newman-Keuls post-test. Output P value style APA: .12 (ns), .033 (*), .002(**) and <.001 (***); 1) comparing to unstimulated control cells "*",and 2) comparing sample to the original SC40 sample"#".*

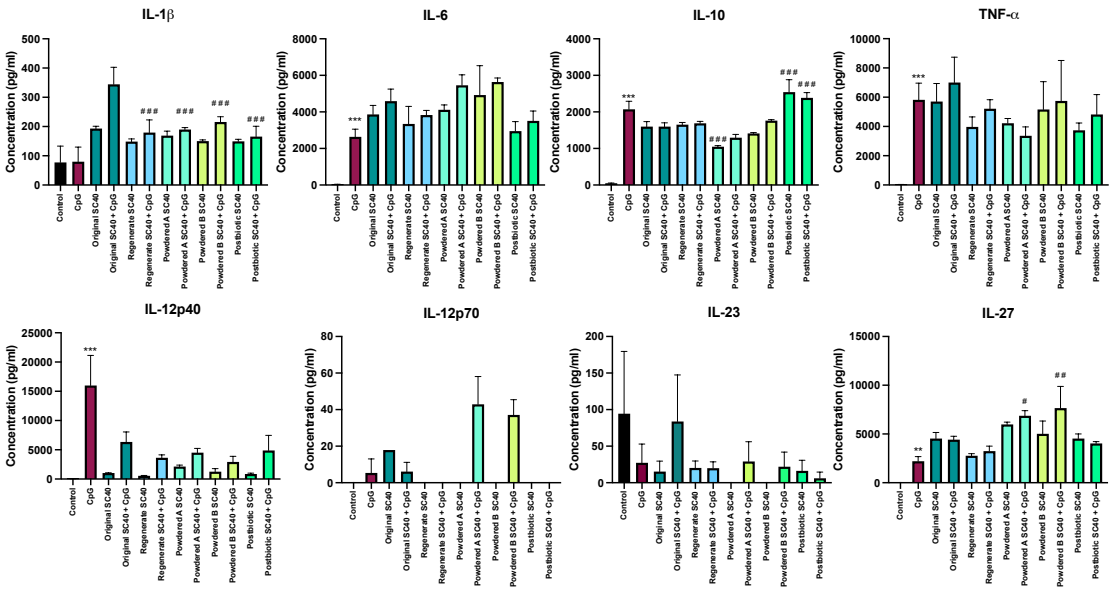

Figure 101: ***Exposure of CpG activated BMDM to 25mg/mL differentially generated SC40 raw sample results in the secretion of cytokines IL-1β, IL-6, IL-10, TNF-α, IL-12p40, IL-12p70, IL-23, and IL-27*** *BMDM cells were seeded at 1x10^6 cells/mL and left overnight at 37^{0}C in 5% CO_2. The following day cells were stimulated with 25mg/mL raw sample fermentate, incubated for 1 hour at 37^{0}C in 5% CO_2 and % CO_2 and subsequently exposed to the following concentrations of TLRs: CpG 5μM for TLR activation before incubating overnight under the same conditions. Supernatants were removed after 24 hours and ELISA was performed for IL-1β, IL-6, IL-10, TNF-α, IL-12p40, IL-12p70, IL-23, and IL-27. Data is presented as mean ± SD of three replicates. Significance determined using one- way ANOVA with a Newman-Keuls post-test. Output P value style APA: .12 (ns), .033 (*), .002(**) and <.001 (***); 1) comparing to unstimulated control cells "*",and 2) comparing sample to the original SC40 sample"#".*

Therefore overall, regeneration of SC40 didn't have too much significant effect on bioactivity of the fermentate considering the number of parameters examined. Only small differences were seen in bioactivity as highlighted in Table 27, with decreased IL-1β for all fermentates in comparison to the original SC40. Bioactivity was largely maintained and additionally, SC40 could be enhanced in its bioactivity with Powder A outperforming that of the original SC40 sample in its anti-inflammatory capabilities with decreased secretion of proinflammatory cytokines including IL-6, TNF-α, and IL-12p40.

Table 27: ***Summary of the cytokines secreted in the presence of spin-off SC40 fermentates in LOX, PIC, LPS, and CpG activated BMDC and BMDMs. Summary of cytokines secreted in the presence of fermentates in TLR activated BMDCs and BMDMs.*** *Significance determined using one- way ANOVA with a Newman-Keuls post-test. Output P value style APA: .12 (ns), .033 (*), .002(**) and <.001 (***); where TLRs in the presence of spin off fermentates were compared to TLR in the presence of original SC40. Green indicates increased cytokine production, and red indicates decreased cytokine production.*

Fermentates in BMDCs	Regenerate	Powder A	Powder B	Postbiotic	
+LOX				**	IL-1β
	**			***	IL-6
	***	***	***	***	IL-10
	*		*	**	TNF-α
					IL-12p40
					IL-12p70
	*	***	*	***	IL-23
	*	***	***	***	IL-27
+PIC	***	***	***	***	IL-1β
					IL-6
					IL-10
					TNF-α
	*				IL-12p40
					IL-12p70
	*			***	IL-23
		***	**		IL-27
+LPS	**	***	***	**	IL-1β
					IL-6
					IL-10
					TNF-α
					IL-12p40
					IL-12p70
					IL-23
				*	IL-27
+CpG	***	***	***	***	IL-1β
					IL-6
			**		IL-10
	*	**	**		TNF-α
	**				IL-12p40
					IL-12p70

				***	IL-23
		***	***		IL-27
Fermentate in BMDMs	Regenerate	Powder A	Powder B	Postbiotic	
+LOX	*	***	***	**	IL-1β
	*	***			IL-6
		**	***		IL-10
		**			TNF-α
	*	***	**		IL-12p40
					IL-12p70
					IL-23
					IL-27
+PIC					IL-1β
	*	*			IL-6
	**	***		***	IL-10
	***	***	***	***	TNF-α
	***	***	***	**	IL-12p40
					IL-12p70
					IL-23
	***	***	***		IL-27
+LPS	**	***	***	**	IL-1β
	*	***	*	*	IL-6
			***		IL-10
					TNF-α
					IL-12p40
					IL-12p70
					IL-23
					IL-27
+CpG	***	***	***	***	IL-1β
					IL-6
				***	IL-10
					TNF-α
					IL-12p40
					IL-12p70
					IL-23
		*	**		IL-27

5.4 Discussion

Based on a large multidisciplinary discussion, to incorporate all scientific aspects examined, namely the viral immunity, anti-inflammatory, microbiome and gut barrier results and analysis, the 19 samples in Table 24 were highlighted as the most promising candidates with bioactivity acting as immune boosting, anti-inflammatory, microbiome/ gut comfort supporting candidate samples. This table was collated based on discussions between all teams, DCU, UCD, Teagasc, and FHI. From this 19-candidate panel, it was further concluded that the top 5 samples were LH88, HA118, P200622 as anti-inflammatory candidates, Aerobic R0033 as an immune boosting sample, and SC40 being both immune boosting and anti-inflammatory. LH88, HA118, P200622 were included as anti-inflammatory candidates based on the screening of the top 19 bioactive candidate fermentates in BMDCs challenged with the inflammatory immune challenge LPS, where high levels of IL-10, and lower concentrations of pro-inflammatory cytokines were secreted. Aerobic R0033, and SC40 have been highlighted as immune boosting samples based on previous chapters and therefore were included in the top 5 samples analysis for BMDCs challenged with LOX and LPS. In addition to this LH88, Aerobic R0033, and SC40 all rated in the top 10 in microbiome analysis, making them of particular interest, while HA118 and P200622 being not yet analysed and already showing lower anti-inflammatory effect based on cytokine secretion profiles in BMDCs stimulated with LPS, these samples were ultimately deemed of less interest for their bioactivity and thus eliminated from further screening. Therefore, the top 4 immunomodulatory samples were chosen; immune boosting Aerobic R0033, and R0419 based on previous chapter analysis, anti-inflammatory LH88, and dual role SC40. Additionally, both LH88 and SC40 support the gut barrier integrity, while Aerobic R0033 didn't provide any significant effect. Thus, based on industry needs, the focus shifted towards an anti-inflammatory sample with the ability to support the microbiome and maintain gut barrier integrity.

Not only this but an extended analysis of the top 4 immunomodulatory was carried out to provide further insight into the fermentates capabilities in the context of polarised macrophage. Measurement of NO production, arginase activity, and cytokine secretion profiles from M0, M1, and M2 polarised macrophage allowed for the further establishment of fermentate profiles in the context of an immune boosting sample for support against viral infection or an anti-inflammatory sample for control of chronic inflammation and subsequent IBD pathogenesis.

SC40, LH88, Aerobic R0033, and R0419 all promoted the M1 phenotype with increased NO, IL-6, and TNF-α production. There was however a clear distinction between LH88, and SC40 where small increases in the M2 phenotype were seen with increased production of IL-10, and small increased arginase activity in M0, and M1 macrophage. Thus our samples SC40, LH88, Aerobic R0033, and R0419 maintained a largely immune boosting profile in the context of M1/M2 polarised macrophage, however SC40, and LH88 had more anti-inflammatory properties than Aerobic R0033, or R0419 . This further highlighted the dual role particularly of LH88, and SC40, being both immune boosting and anti-inflammatory, depending on different immune scenarios, while Aerobic R0033, and R0419 largely maintained their immune boosting profile.

NO production is necessary for viral clearance, via inducible NO synthase (iNOS), and depending on the virus can have direct antiviral properties, limiting severity of virus induced disease (Burrack & Morrison, 2014; Sodano et al., 2022). NO is a signalling molecule involved with the protective mechanisms in the gastrointestinal tract, that plays a key role in the pathogenesis of inflammation (J. N. Sharma et al., 2007; Wallace, 2019). It gives an anti-inflammatory effect under normal physiological conditions, however can also act as a pro-inflammatory mediator that induces inflammation due to over production in abnormal conditions (J. N. Sharma et al., 2007; Wallace, 2019). NO production is linked to the M1 phenotype, killing/fighting, whereby arginine is metabolised via iNOS, to NO and citrulline, to aid M1 macrophage in the production of Th1 responses for fighting infection, and aiding in the drive and recruitment of pro-inflammatory cytokines useful for the defense of the immune system against viruses (Mills, 2012; Rath et al., 2014). Arginase activity is linked to the M2 phenotype, healing/fixing, whereby arginine is

metabolised via arginase, to ornithine and urea, to aid M2 macrophage in the production of Th2 responses for infection resolution, and aiding in the drive and recruitment of anti-inflammatory cytokines useful for the defense of the immune system against chronic inflammation (Mills, 2012; Rath et al., 2014). Additionally, this arginase activity is useful for tissue repair post viral infection (Burrack & Morrison, 2014).

As highlighted in Chapter 4, compounds which increased NO production and production of IL-6, and TNF-α, and IL-10 have been associated with anti-viral immunomodulatory effects including decreased viral titres of influenza A infected mice, increased survival rates in influenza A mice, inhibitory effects in SARS-CoV in immunocompromised mice, and inhibition of viral growth of influenza A/Aichi/2/68 virus (Dhong et al., 2022; Obi et al., 2008; Ohta et al., 2007). Furthermore *Lactobacillus rhamnosus* GG induced NO production in J774.A.1 macrophage and human T84 colon epithelial cells through iNOS induction, for the treatment of viral and antibiotic associated diarrhoea, suggesting increased NO for improved gut comfort (Korhonen et al., 2001). Another study examined the effect of *Enterococcus faecium* NCIMB 10415 (*E. faecium*), in defense against enteropathogenic coronavirus transmissible gastroenteritis virus (TGEV), in swine testicle cells via reduced virus yields , reduced levels of viral structural protein, surface virus entrapment for viral infection prevention, as well as increased NO and IL-6 and IL-8 production (W. Chai et al., 2013). S-nitroso-N-acetylpenicillamine was shown to increase survival rate in SARS-CoV infected cells, via increased NO production for the inhibition of the SARS-CoV cytopathic effect (Keyaerts et al., 2004). In addition, *Lactobacillus (Lb. paracasei)* have the ability to decrease vesicular stomatitis viral infection, establishing the antiviral state in 3D4/21 macrophages, by increased production of NO and IL-6 and IFN-γ (Ivec et al., 2007). Additionally, where small increases in arginase activity and a shift towards the M2 phenotype are seen, studies have revealed that the presence of other natural compound like polyherbal tea reduced M1 activity, and enhanced arginase activity in LPS stimulated macrophage to aid in attenuation of chronic inflammation (Gahramanova et al., 2023). Similarly resveratrol, which has well documented anti-inflammatory effects in a range of inflammatory conditions, has been found to

enhance arginase activity, increasing the M2, and decrease the M1 phenotype in neuroinflammation (Saqib et al., 2018; Yang et al., 2017). Therefore, this suggests that the anti-inflammatory effect seen in the increased arginase activity could be applicable for the treatment of many of the chronic inflammatory disorders it is known to aid in, including UC and CD (M. Li et al., 2022; Shi et al., 2017; Xu et al., 2023). It is however important that arginase activity is not over promoted as increased arginase activity is associated with a range of pathological conditions including hypertension, congestive heart failure, atherosclerosis, vascular disfunction, fibrotic conditions, carcinomas and diabetes mellitus (Pernow & Jung, 2013; S. Clemente et al., 2020).

Thus one can conclude that our samples SC40, LH88, Aerobic R0033, and R0419 due to their ability to enhance the M1 phenotype, have potential as immune boosting anti-viral compounds via the increased NO, IL-6, and TNF-α production, as well as with the smaller M2 profile with just some arginase activity and increased IL-10, for promotion of tissue repair post viral infection, as well as for the resolution of chronic inflammation.

Due to the data gathered on SC40 to date, SC40 had been identified as a candidate sample for anti-inflammatory, and gut comfort support in a human intervention study. Therefore, to understand more about SC40s effect on inflammation and its dual role in boosting the immune system for viral immunity, SC40 was brought forward for testing in T cells as the core focus for the industry partners. Although not the core focus for the industry partners at present, Aerobic R0033's clear immune boosting role in the context of both a viral and inflammatory challenge, means that Aerobic R0033 was brought forward for further testing in T cells as the immune boosting candidate, with small anti-inflammatory effects for future potential commercial development.

Importantly, as SC40 was the key fermentate of interest it was important to establish that the fermentate's bioactivity was not negatively affected upon regeneration and scale-up production of this sample. Data generated on SC40, and

its regenerated forms shows that the bioactivity remained largely conserved in immune cells it was tested in and immune scenarios it was challenged with. For the most part in immune activated BMDCs Powder A performed most similar to the original SC40, followed by Powder B, then lastly by both Regenerate and Postbiotic. This was expected as the Postbiotic version was prepared in the most different way from the original SC40, where it was grown in a different culture media, MRS broth. The fact that the regenerate didn't perform most similar to the original SC40 was unexpected, however each fermentation process will have its own variables and thus cannot be replicated exactly. Therefore, with only small deviations this scaled up regenerate version was considered as a close replicate of the lab scale original SC40 where the process of scaling up changes the levels of metabolites present in comparison to the lab scale version and thus, we see small bioactive differences. Small changes in cytokine secretion included decreased IL-6, IL-10, TNF-α, and increased IL-27 in LOX activated cells, decreased IL-1β, and increased IL-12p40 in PIC activated cells, decreased IL-1β in LPS activated cells, and decreased IL-1β, TNF-α, and increased IL-27 in CpG activated cell. Powder A with its increased IL-23, and IL-27 in LOX activated cells make this a more improved sample for viral immunity. In contrast to the decreased IL-1β, IL-12p40 and IL-23 in PIC activated cells where Regenerate would be more beneficial as an anti-inflammatory sample, thus highlighting again SC40s dual role. All samples had little or no change in cytokine secretion versus the original SC40 sample in LPS activated cells. Powder A preformed best as an anti-inflammatory in CpG activated cells, decreasing IL-1β, TNF-α, and IL-12p40.

Effects of samples in activated BMDMs was more varied across the different immune challenges. For the most part in immune activated BMDMs Powder A preformed most similar to the original SC40, followed by Postbiotic, Powder B, then Regenerate. Small changes in cytokine secretion included decreased IL-1β, and increased IL-12p40 in LOX activated cells, decreased TNF-α, IL-12p40, and IL-27 in PIC activated cells, decreased IL-1β, IL-6, IL-10 and increased IL-12p40 in LPS activated cells, and decreased IL-1β in CpG activated cell. Powder A with its increased IL-6, TNF-α, and IL-12p40 in LOX activated cells make this a more

improved sample for viral immunity. In contrast to the decreased IL-6, IL-10, TNF-α, IL-12p40 and IL-27 in PIC activated cells where Powder A would be more beneficial as an anti-inflammatory sample, thus highlighting again SC40s dual role. Powder A and B decreased IL-1β, and IL-6 in LPS activated cells making these ideal anti-inflammatory candidates. Postbiotic preformed best as an anti-inflammatory in CpG activated cells, decreasing IL-1β, and increasing IL-10. Thus overall all samples had little or no negative effect in comparison to the original SC40 sample. Interestingly, Powder A in particular exerted an enhanced immunomodulatory effect depending on the immune scenario it was challenged with in both BMDCs and BMDMs.

Therefore we concluded from this chapter that SC40 and Aerobic R0033 were the candidate immunomodulatory fermentates that were to be brought forward for further assessment of their effects in T cells. We established that SC40 had a dual effect, however displayed a largely anti-inflammatory profile. This was seen through its positive anti-inflammatory effects on cytokine secretion in LPS activated BMDCs, as well as its positive impact on cytokine secretion in polarised macrophage where it leaned more towards an M2 phenotype with enahnced IL-10 in M0, M1, and M2 macrophage, but displayed a mixed M1/M2 phenotype for NO production, and arginase activity. Furthermore, we were now able to confidently proceed with testing of SC40 in T cells knowing that the key fermentate of interest was able to be produced at a commercial rate while maintaining its desired bioactivity. Additionally, we established that Aerobic R0033 had a largely immune boosting profile. This was seen through its positive immune boosting effects on cytokine secretion in LPS activated BMDCs, as well as its immune boosting impact on cytokine secretion in polarised macrophage where it leaned more towards an M1 phenotype with enhanced IL-6 and TNF-α in M0, and M1 macrophage, but similarly displayed a mixed M1/M2 phenotype for NO production, and arginase activity.

6 Chapter 6

Phase 3 Fermentate Examination

6.1 Introduction

Having established the activity of candidate immune boosting fermentate Aerobic R0033, and dual role anti-inflammatory/immune boosting fermentate SC40 in both dendritic and macrophage cells, in response to various viral and inflammatory immune challenges, we now aimed to establish their effects in T cells. T cells are the key players in the adaptive immune response and thus are a critical cell of the immune system which could be targeted by fermentates to enhance or influence immune responses in the context of both viral immunity and inflammation. Figure 102 highlights how the innate cells including the macrophage, natural killer cells and dendritic cells are first responders to immune stimuli. Dendritic cells link the innate and adaptive immune systems through interaction of the dendritic cells MHCII and CD80/CD86 cell surface markers with the naïve T cells cell surface markers TCR, and CD28 respectively. This interaction kick starts the adaptive immune response, whereby naïve T cells differentiate into cell subsets including Th1, Th2, Th17, or Treg cells. It is the Th1, and Th17 cells that are largely associated with an immune boosting proinflammatory response with secretion of IFN-γ, and IL-2 in Th1, and IL-6 and IL-17 in Th17. The Th2 and Treg responses are largely associated with the anti-inflammatory response via the secretion of IL-4, and IL-13 from Th2, and TGF-β and IL-10 from Treg cells.

As we wanted to establish a full immune profile of the fermentates effects, we examined their specific effects on T cells. With SC40 being the key fermentate of interest with its dual role as a viral immune boosting sample and an anti-inflammatory, it was critical to examine its effect in T cells to further elucidate to its potential in both these areas. Aerobic R0033 was included due to its largely pro-inflammatory immune boosting profile in order to have a comparison for SC40. We first needed to establish that we could differentiate naïve CD4+ cells in each of the subsets, Th1, Th2, Th17, and Treg cells.

Overall this in depth examination enabled the holistic assessment of the fermentate's effect on T cells, building on the data generated to date, which

established SC40 as the key sample of interest due to its immune boosting and anti-inflammatory capabilities.

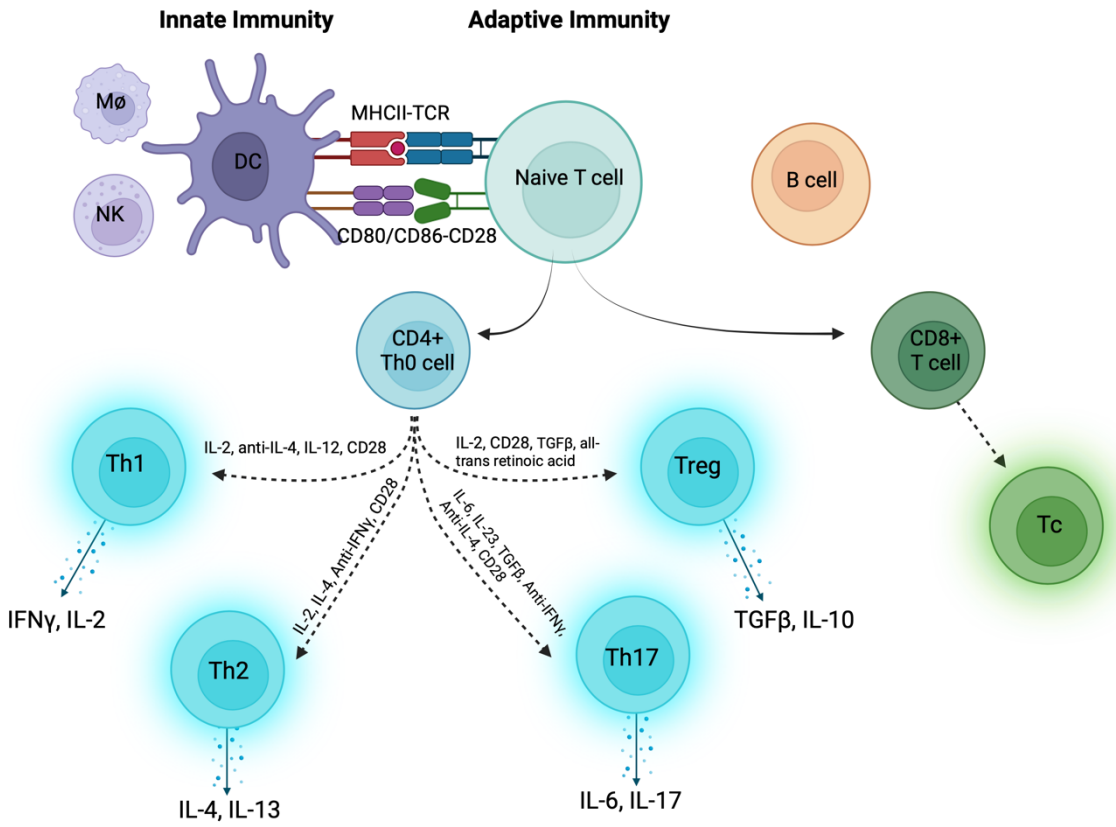

*Figure 102**: Schematic representation of T cell differentiation.** Undifferentiated naïve CD4 cells can be polarised to Th1, Th2, Th17, and Treg cells using polarising factors (dotted arrows). Polarised T cells are shown with their characteristic secretory cytokines highlighted.*

6.2 Chapter Aims:

The purpose of this chapter was to delve deeper into the capabilities of the two candidate fermentates: immune boosting Aerobic R0033, and dual role immune boosting and anti-inflammatory sample SC40, via screening in primary murine differentiated T cell subsets. Immune boosting sample Aerobic R0033 was used to contrast the findings due to its largely pro-inflammatory status identified thus far. SC40 was selected as it is the key sample of interest to the industry partners due to its ability to act as an immune boosting sample or an anti-inflammatory sample depending on the immune stimulus the cells are challenged with, suggesting its potential role in both viral immunity and as an anti-inflammatory compound. Assessing the effect of these samples in primary T cells, and further analysis of functionality in the human cell line JURKAT cells aimed to establish a full profile of their effects in adaptive immunity.

The specific objectives include:

- Establishment of the T cell profiles, for Th1, Th2, Th17, and Treg, including their transcription factor activation and cytokine secretion profiles.
- Assessment of cytotoxicity of fermentates in unpolarised T cells, Th1, Th2, Th17, and Treg cells to ensure that samples were not negatively impacting on cell viability.
- Assessment of effect of candidate fermentates on cytokine secretion in unpolarised T cells and differentiated primary T cell subtypes, Th1, Th2, Th17 and Tregs
- Assessment of effect of candidate fermentates on cell proliferation, and IL-2 production in JURKAT cells
- Assessment of effect of candidate fermentates on cell migration in JURKAT cells
- Assessment of effect of candidate fermentates on the immune synapse in JURKAT cells

- Assessment of effect of candidate fermentates on activation of signalling pathway in JURKAT cells

Data gathered from this analysis established a full profile of the most promising immune boosting and/or anti-inflammatory compounds.

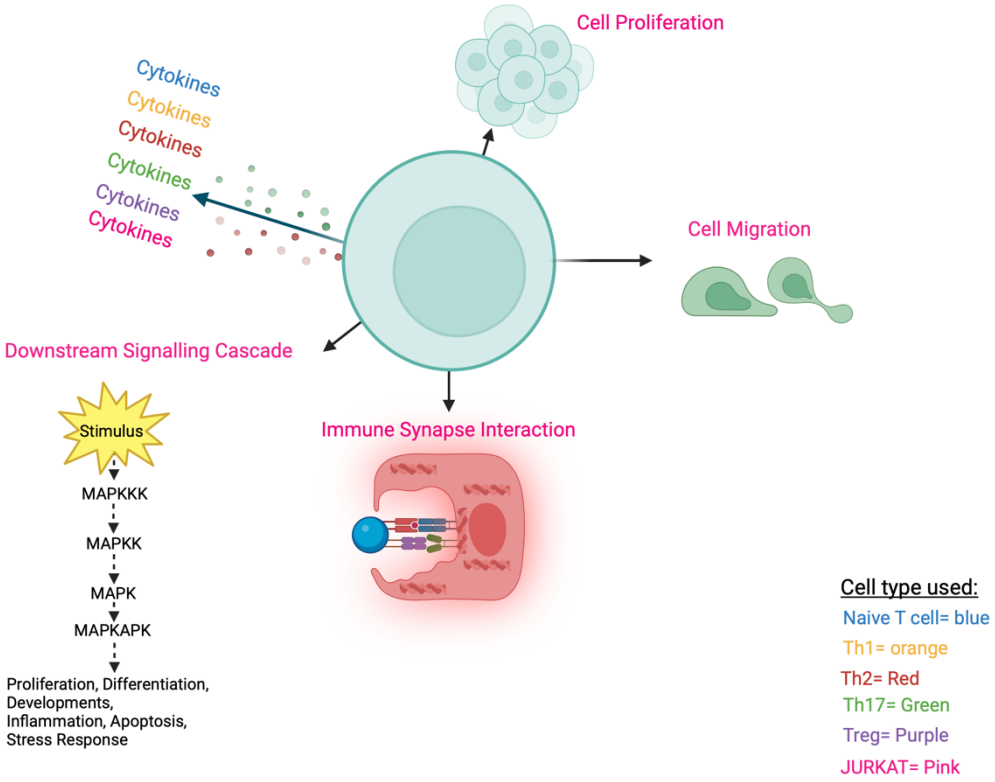

*Figure 103:**Summary of Chapter 6 Aims**. Assessing effect of sample presence on cytokine secretion profiles in naïve T cells (blue), Th1 (orange), Th2 (red), Th17 (green), Treg (purple), and IL-2 production in JURKAT cells (pink), as well as assessing sample effect on functionality in JURKAT cells to assess cell proliferation, migration, immune synapse interaction, and effect on downstream signalling cascades when activated or not activated.*

6.3 Results

In order to carry out examination of fermentate effects in T cells it was important to establish that naïve undifferentiated T cells could be isolated from the spleenocytes derived from the spleen of a female BALB/c mouse.

6.3.1 CD4+ T cells can be isolated from the spleen of Balb/C mice via magnetic separation, and express CD4, CD3 and, CD25

CD4+ T cells are found in the spleen and lymph nodes, thus to isolate CD4+ T cells from female Balb/C mice, the spleen was aseptically removed from the mouse and homogenised through a 40µm filter. CD4+ T cells were isolated from spleenocytes using easysep™ mouse CD4+ T-cell isolation kit available from Stemcell as previously described (Section 2.2.8.1 EasySep Mouse CD4+ T cell Isolation Method).

CD4 is present on T helper cells as well as on some macrophage and dendritic cells, thus purity of T cell population needed to be confirmed. CD3 composes the TCR complex and thus a marker of all T cell populations, thus double staining for CD3 and CD4 was used to confirm a CD4+ T cell population.

Figure 104 demonstrates that isolated T cells could be negatively selected from a population of spleenocytes from Balb/C mice, using magnetic separation as previously described (Section 2.2.8.1 EasySep Mouse CD4+ T cell Isolation Method). Figure 104A shows removal of debris based on the FSC and SSC via gating of spleenocytes. Figure 104B shows removal of doublets, via gating of singlets. Figure 104C shows removal of dead cells via the gating of live cells, enabled by the presence of PI-Texas red within dead cells. Figure 104D show without negative selection 90% of cells will be CD- cells, while when isolated using magnetic separation 95.5% of cells analysed are CD4+, determined via staining with primary antibody APC-Cy-7.

Figure 105 shows isolated T cells stained using primary antibodies APC-Cy-7 and FITC, for labelling of CD4 and CD3 respectively, incubated for 30 minutes at 4^{O}C, and subsequently washed, then stained with primary antibody PI-Texas Red for 5 minutes at room temperature, before analysing on BD FACS Aria. Data analysed using FlowJo software.

Figure 105A shows removal of debris based on the FSC and SSC via gating of spleenocytes. Figure 105B shows removal of doublets, via gating of singlets. Figure 105C shows removal of dead cells via the gating of live cells, enabled by the presence of PI-Texas red within dead cells. Figure 105D shows the unstained negative control cells. Figure 105E shows positively stained CD3/CD4 cells, whereby 94.7% +/- SD 0.78, of the population had been labelled with both APC-Cy-7 and FITC, and thus are confirmed CD4+ T cells.

Figure 106 demonstrates isolated T cells could be negatively selected from a population of spleenocytes from Balb/C mice, and when activated these CD4+ T cells express CD25. CD25 is a component of the IL-2 receptor, with important roles in T cell proliferation, activation induced cell death, and influences Th and Treg cells (Brusko et al. 2009). Figure 106A shows removal of debris based on the FSC and SSC via gating of spleenocytes. Figure 106B shows removal of doublets, via gating of singlets. Figure 106C shows removal of dead cells via the gating of live cells, enabled by the presence of PI-Texas red within dead cells. Figure 106D shows gating of the naïve CD4+ T cell population, at 93.6% of cell population, determined via staining with primary antibody PE. Figure 106E shows that unactivated CD4+ T cells had only 3% CD25 expressing cells, while Figure 106F shows that when naïve CD4+ T cells were activated for 3 days 81.8% of cells express CD25.

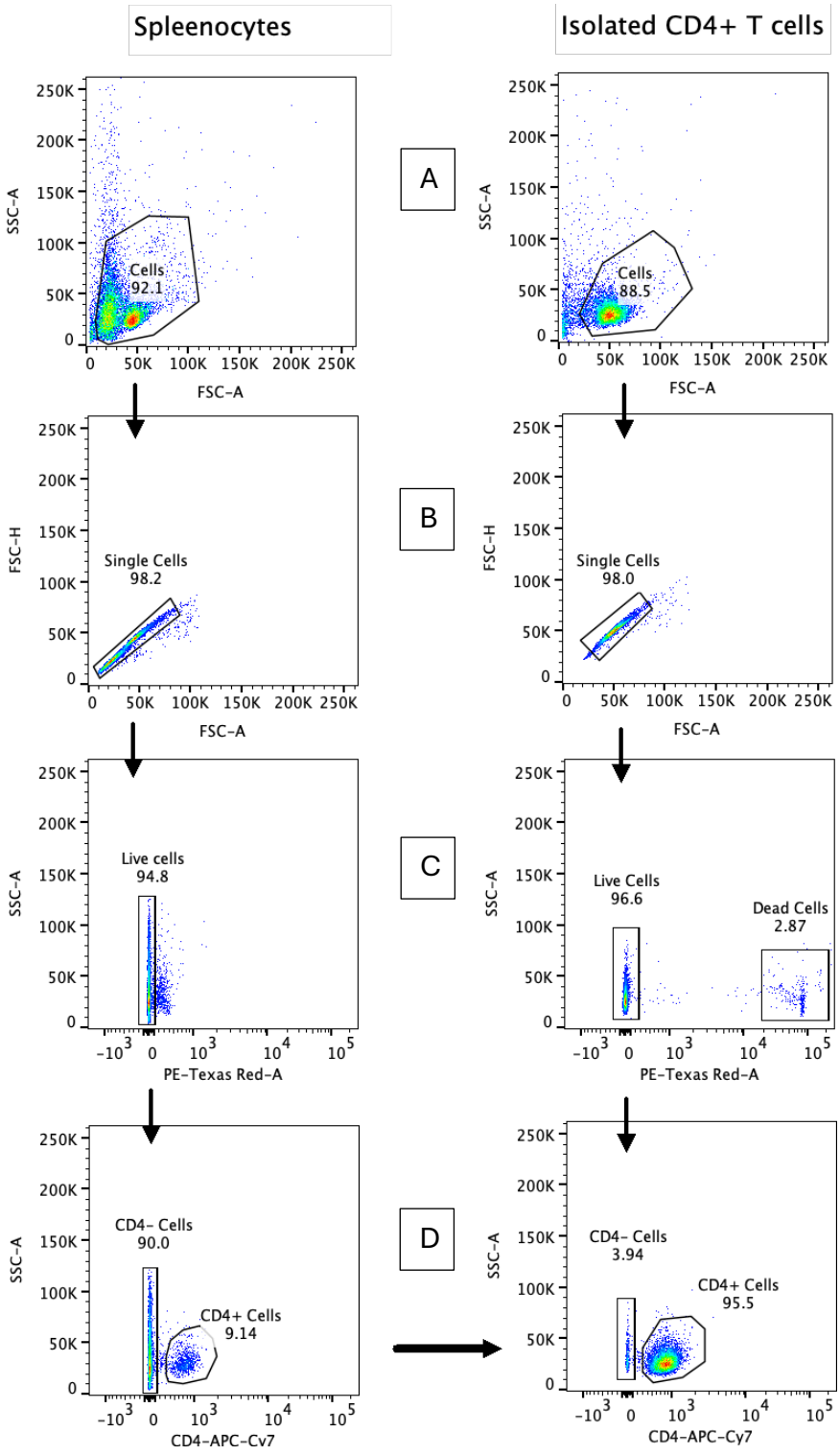

Figure 104: ***Spleenocytes do not express CD4, while Isolated T cells express CD4.*** *CD4+ T cells can be isolated from the spleens of female Balb/C mice using EasySep CD4+ Isolation kit. CD4+ T cells are negatively selected using magnetic separation (Stemcell) according to manufacturer's instructions. Cells were seeded at 1x10^6 cells/mL in round bottom 96 well plate and procedure for CD4 staining was carried out. Cells collected were stained for CD4 using primary antibody APC-Cy-7. Viability was determined via staining with primary antibody PI-Texas Red. Cells were analysed using BD FACS Aria and data analysed using Flowjo software. Cells were gated on live cells (c), excluding doublets (b) and debris (a). % cells expressed for each gated population. (d) demonstrates the CD4- population, versus the isolated CD4+ T cells.*

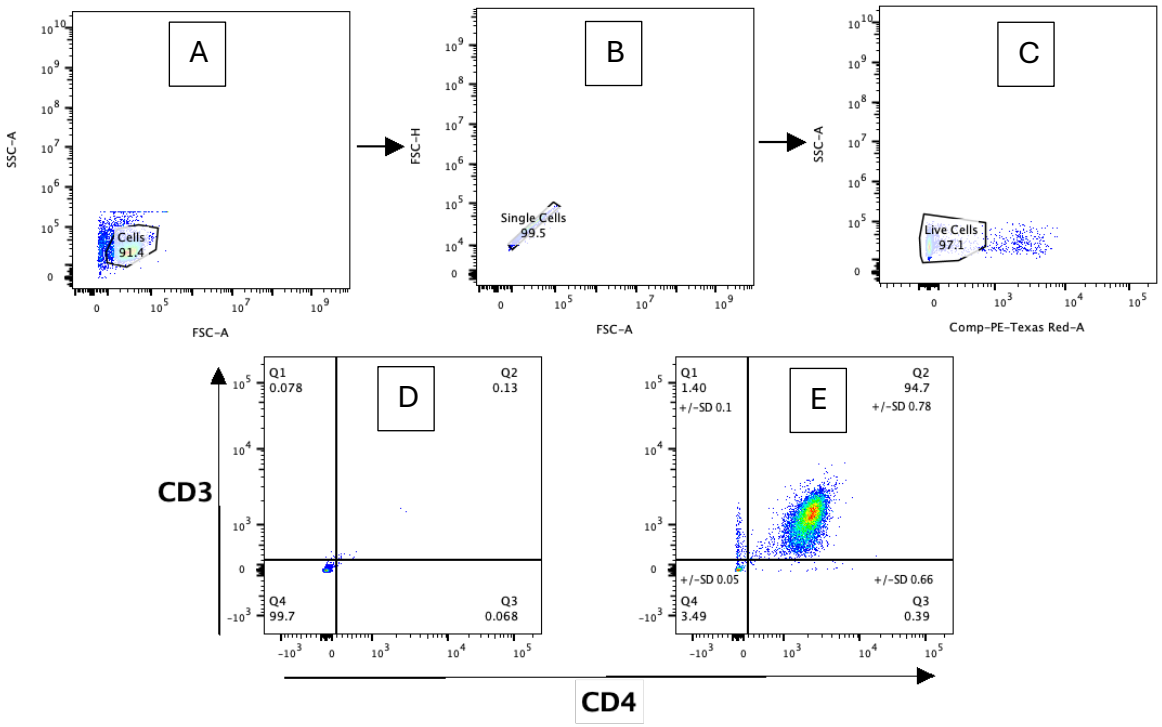

*Figure 105**: Isolated undifferentiated T cells express CD4 and CD3**. CD4+ T cells were isolated from the spleens of female Balb/C mice using EasySep CD4+ Isolation kit. CD4+ T cells were negatively selected using magnetic separation (Stemcell) according to manufacturer's instructions. Cells were seeded at 1x10^6 cells/mL in round bottom 96 well plate and procedure for CD4 CD3 staining was carried out. Cells collected were stained for CD4 and CD3 using primary antibody APC-Cy-7 and FITC respectively. Viability was determined via staining with primary antibody PI-Texas Red. Cells were analysed using BD FACS Aria and data analysed using Flowjo software. Cells were gated on live cells (c), excluding doublets (b) and debris (a). % cells expressed in each quadrant, and +/- SD of three replicates included for CD4+ T cells (e). (d) is the negative unstained control, versus (e) the positive CD4+ T cells.*

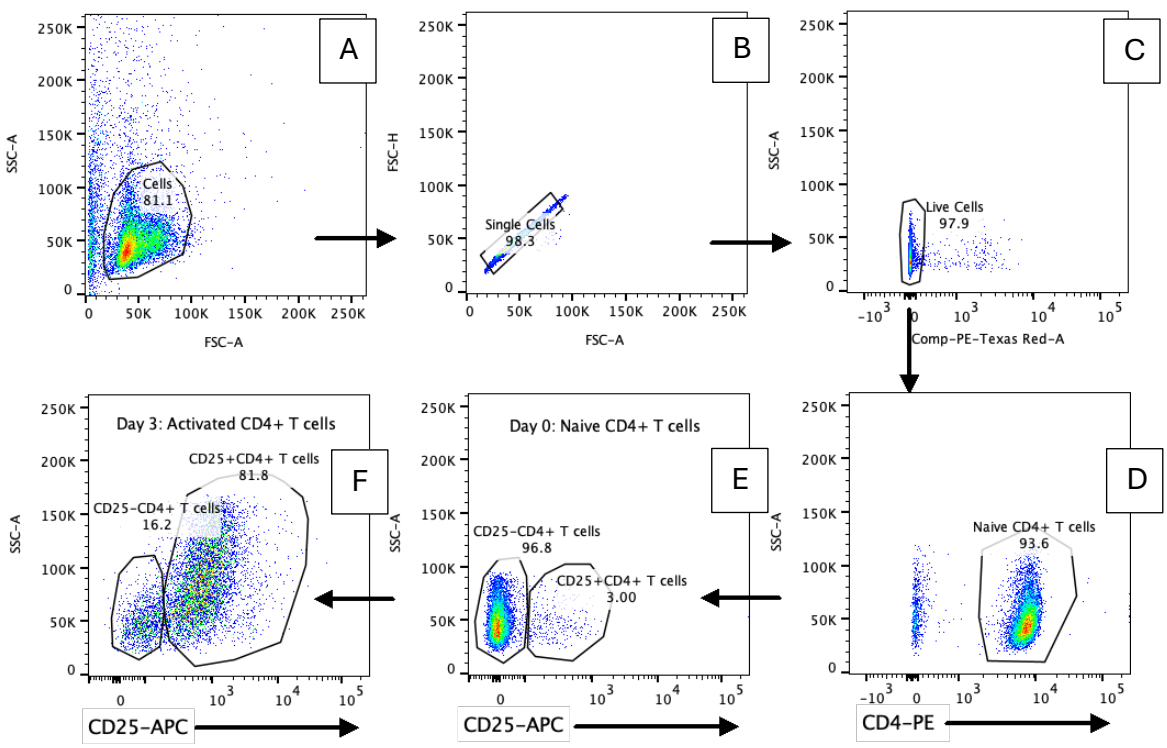

*Figure 106**: Activated CD4+ T cells express CD25**. CD4+ T cells were isolated from the spleens of female Balb/C mice using naïve EasySep CD4+ Isolation kit. CD4+ T cells were negatively selected using magnetic separation (Stemcell) according to manufacturer's instructions. Cells were seeded at 1x10^6 cells/mL in round bottom 96 well plate and procedure for CD25 staining was carried out. Cells collected were stained for CD25 using primary antibody APC-Cy-7 and for isolated CD4+ cells using PE. Viability was determined via staining with primary antibody PI-Texas Red. Cells were analysed using BD FACS Aria and data analysed using Flowjo software. Cells were gated on live cells (c), excluding doublets (b) and debris (a). % cells expressed in each gated population. (d) is the CD4+ T cell population. (e) is the control naïve T cells on day 0, while (f) shows the positive activated CD4+ T cells on day 3 expressing CD25.*

Therefore we were successfully able to isolate naïve CD25+CD4+ T cells from the spleen of Balb/C mice.

Having proven that undifferentiated naïve T cells can be isolated from the spleen of a BALB/c mouse, we next wanted to profile each of the different T cell subsets to confirm polarisation to Th1, Th2, Th17, and Treg cells. This included the profiling of cytokine secretion, followed by confirmation of T cell subset via examination of the transcription factor expression.

6.3.2 CD4+ T cells can be polarised to Th1, Th2, Th17, and Treg cells expressing signature cytokine profiles and transcription factor expression

Figure 107-Figure 111 demonstrates isolated naïve T cells can be polarised to Th1, Th2, Th17, and Treg cells. Each T cell subset can be confirmed to be differentiated to either Th1, Th2, Th17, or Treg cells through determination of their characteristic cytokine concentrations secreted from the cell, and their transcription factor expression.

Figure 107A,E demonstrates that anti-mouse CD28, clone 37.51 (3 µg/mL), anti-mouse IL-4, clone 11B11 (10 µg/mL), recombinant mouse IL-2 (20 ng/mL), and recombinant mouse IL-12 (20 ng/ml), polarised undifferentiated T cells to Th1 cells, which produce higher concentrations of IFN-γ and IL-2. Figure 107B,F demonstrate that anti-mouse CD28, clone 37.51 (3 µg/mL), recombinant mouse IL-2 (20 ng/ml), and recombinant mouse IL-4 (50 ng/ml), anti-IFN (10 ug/ml), polarised undifferentiated T cells to Th2 cells, which produce high concentrations of IL-4 and IL-13. Figure 107C,G demonstrate that anti-mouse CD28, clone 37.51 (3 µg/mL), recombinant mouse IL-6 (50 ng/mL), recombinant human TGF-β1 (2 ng/mL), recombinant mouse IL-23 (20 ng/ml), anti-mouse IL-4 (10 µg/mL), and anti-mouse IFN-γ (10 µg/mL), polarised undifferentiated T cells to Th17 cells, which produce high concentrations of IL-6 and IL-17. Figure 107D demonstrate that anti-mouse CD28, clone 37.51 (3 µg/mL), recombinant mouse IL-2 (20 ng/mL), recombinant human TGF-β1 (2 ng/mL), and all-trans retinoic acid (10 nM), polarised undifferentiated T cells to Treg cells, which produce high concentrations of TGF-β.

Figure 107H demonstrates the dual role of Th2, and Treg cells in producing IL-10, where Th2 producing IL-10 was more predominant than hypothesised but is supported in the literature. Figure 107E demonstrates that all differentiated and undifferentiated T cells produced IL-2, necessary for cell proliferation.

Similarly when differentiated to Th1, Th2, Th17, and Treg cells, each T cell subset expressed the highest percentage of the population of cells for the characteristic transcription associated with the different T cell subsets.

Figure 108 demonstrates that when polarised to Th1 cells, high levels of Tbet were expressed at 60.4% of the population. Figure 109 demonstrates that when polarised to Th2 cells, high levels of GATA were expressed at 82% of the population. Figure 110 demonstrates that when polarised to Th17 cells, high levels of RORyt were expressed at 51.7% of the population. Figure 111 demonstrates that when polarised to Treg cells, higher levels of FOXP3 were expressed at 18.8% of the population, versus Th17 cells which express only 13.5%.

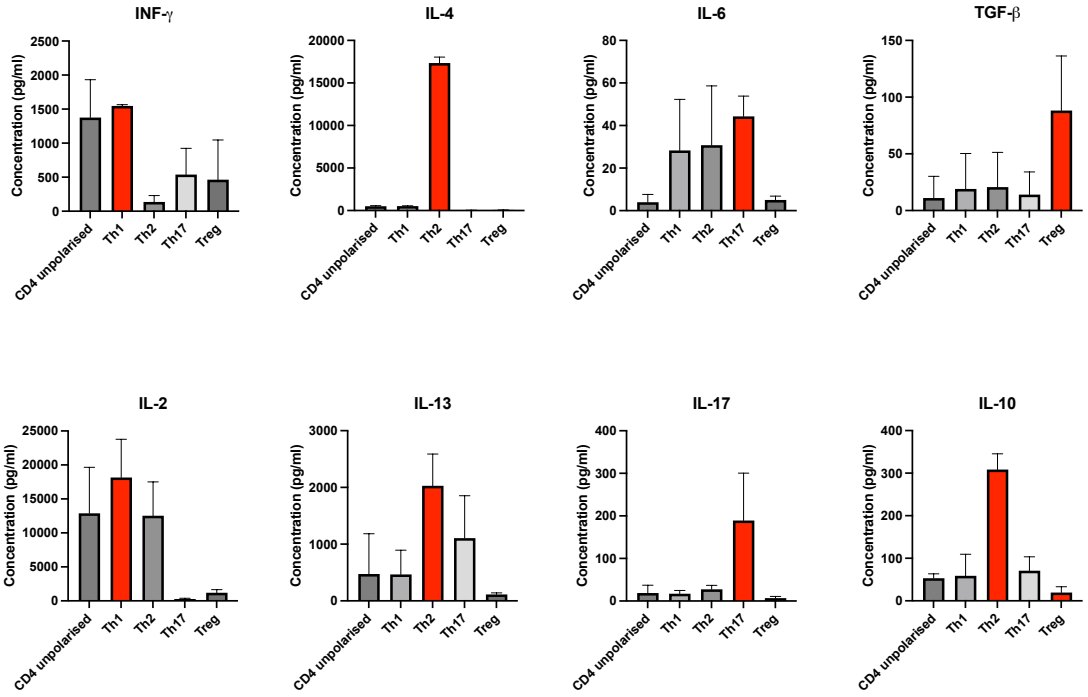

Figure 107: ***Exposure of undifferentiated CD4+ T cells to polarisation factors results in the secretion of cytokines IFN- γ, IL-2, IL-4, IL-6, IL-10, IL-13, IL-17, and TGF-β.*** *Undifferentiated CD4+ cells were seeded at 2x10^6 cells/mL, exposed to polarisation factors for Th1 (anti-mouse CD28, clone 37.51 (3 µg/mL), anti-mouse IL-4, clone 11B11 (10 µg/mL), recombinant mouse IL-2 (20 ng/mL), and recombinant mouse IL-12 (20 ng/ml)), Th2 (anti-mouse CD28, clone 37.51 (3 µg/mL), recombinant mouse IL-2 (20 ng/ml), and recombinant mouse IL-4 (50 ng/ml), anti-IFN (10 ug/ml)), Th17 (anti-mouse CD28, clone 37.51 (3 µg/mL), recombinant mouse IL-6 (50 ng/mL), recombinant human TGF-β1 (2 ng/mL), recombinant mouse IL-23 (20 ng/ml), anti-mouse IL-4 (10 µg/mL), and anti-mouse IFN-γ (10 µg/mL)), and Treg (anti-mouse CD28, clone 37.51 (3 µg/mL), recombinant mouse IL-2 (20 ng/mL), recombinant human TGF-β1 (2 ng/mL), and all-trans retinoic acid (10 nM)), and incubated for 72 hours at 37^{0}C in 5% CO_2. Supernatants were removed, and ELISA was performed for cytokines IFN- γ, IL-2, IL-4, IL-6, IL-10, IL-13, IL-17, and TGF-β. Data is presented as mean ± SD of three replicates. Red highlights the key cytokine secreted for identification of each T cell subset.*

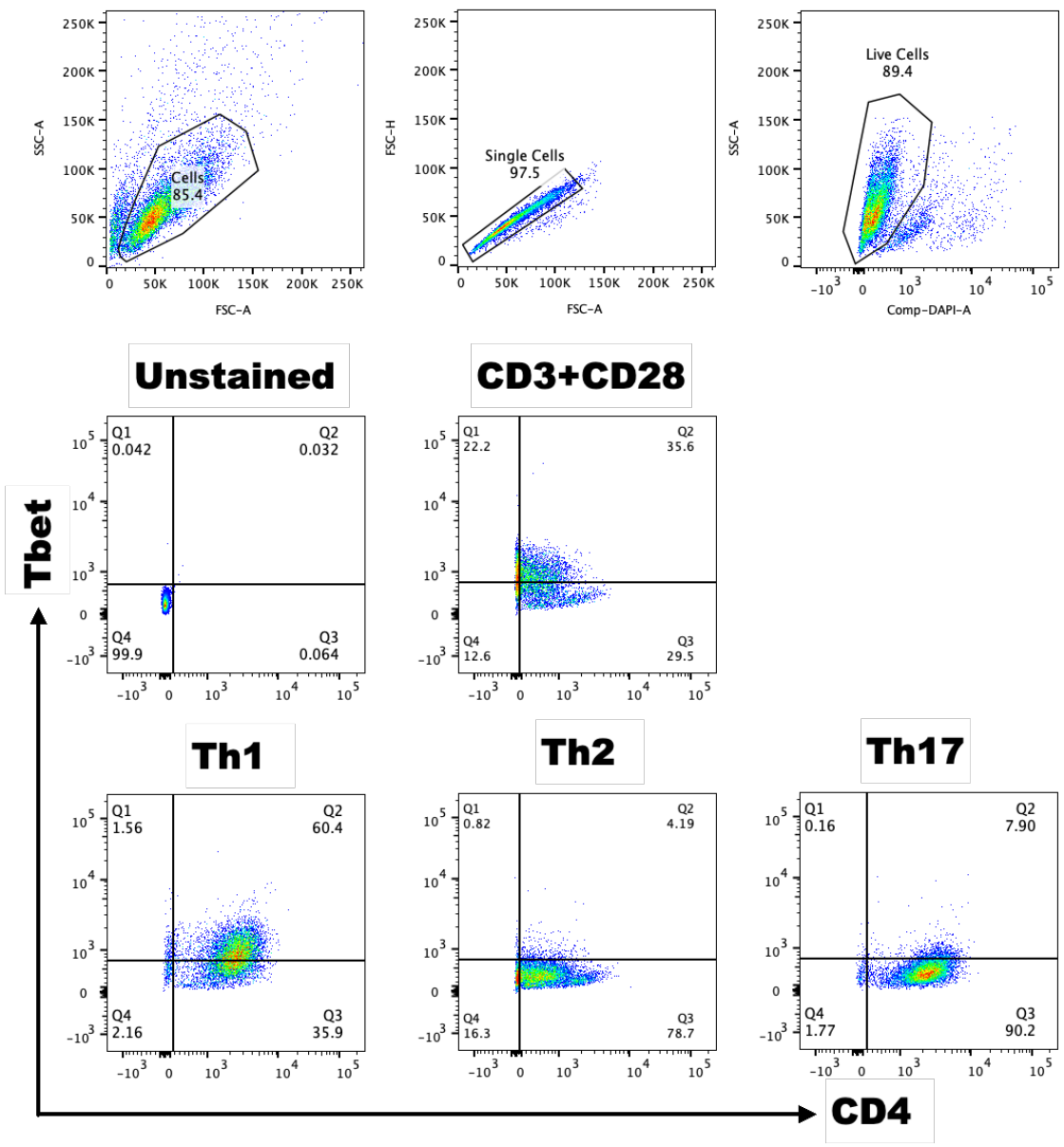

*Figure 108**: Th1 cells express high levels of Tbet.*** *CD4+ T cells can be isolated from the spleens of female Balb/C mice using EasySep CD4+ Isolation kit. CD4+ T cells are negatively selected using magnetic separation (Stemcell) according to manufacturer's instructions. Cells were seeded at 2x10^6 cells/mL in round bottom 96 well plate and procedure for transcription factor staining was carried out. Cells collected were stained for CD4 using primary antibody APC-Cy-7. Viability was determined via staining with primary antibody PI-Texas Red. Tbet was stained for using FITC. Cells were analysed using BD FACS Aria and data analysed using Flowjo software. Cells were gated on live cells (c), excluding doublets (b) and debris (a). % cells expressed in each quadrant.. Unstained control and, CD3 plus CD28 control included as positive control for polarisation to Th1, Th2, and Th17.*

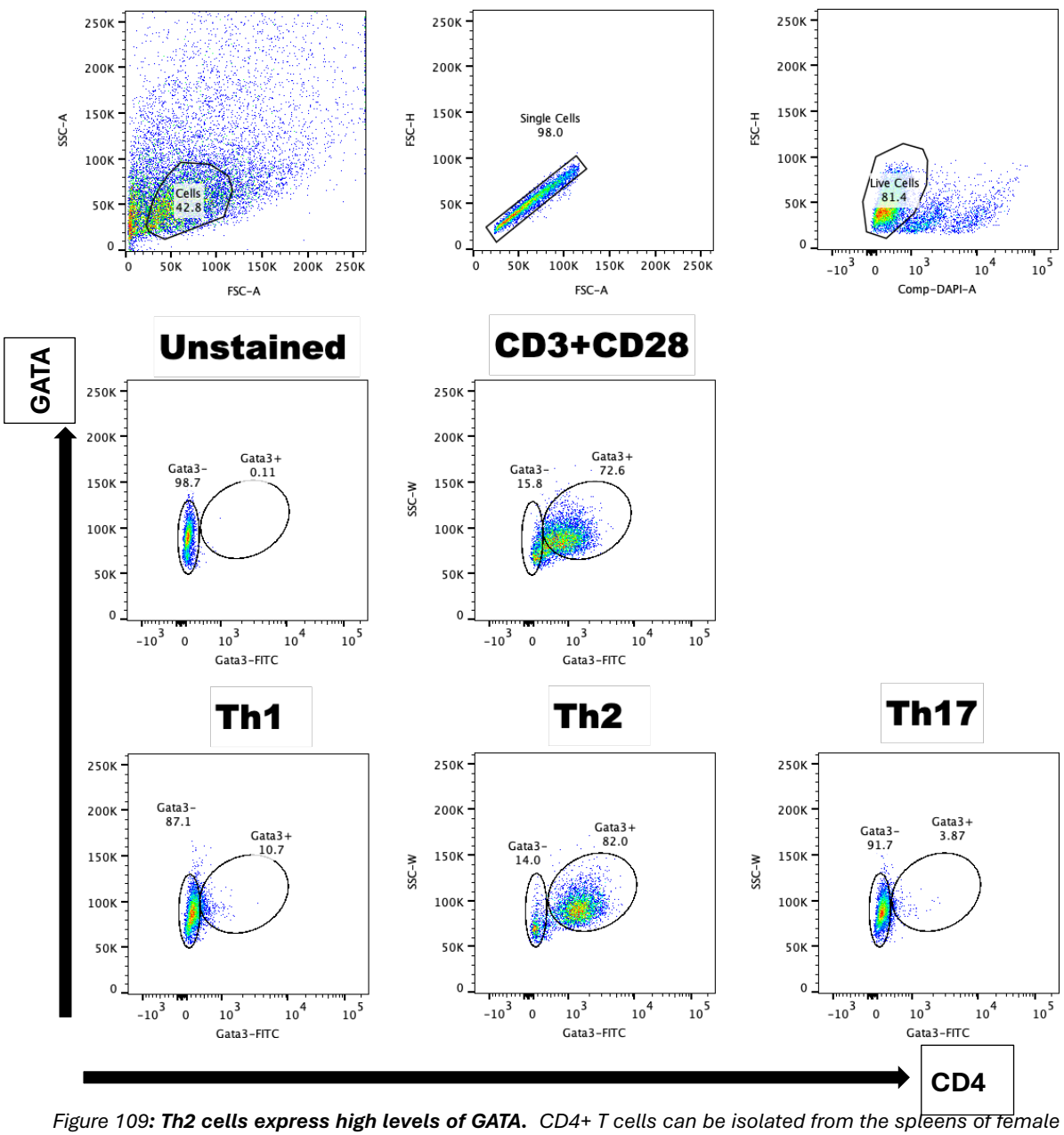

*Figure 109**: Th2 cells express high levels of GATA.*** *CD4+ T cells can be isolated from the spleens of female Balb/C mice using EasySep CD4+ Isolation kit. CD4+ T cells are negatively selected using magnetic separation (Stemcell) according to manufacturer's instructions. Cells were seeded at 2x10^6 cells/mL in round bottom 96 well plate and procedure for transcription factor staining was carried out. Cells collected were stained for CD4 using primary antibody APC-Cy-7. Viability was determined via staining with primary antibody PI-Texas Red. GATA was stained for using FITC. Cells were analysed using BD FACS Aria and data analysed using Flowjo software. Cells were gated on live cells (c), excluding doublets (b) and debris (a). % cells expressed in each quadrant.. Unstained control and, CD3 plus CD28 control included as positive control for polarisation to Th1, Th2, and Th17.*

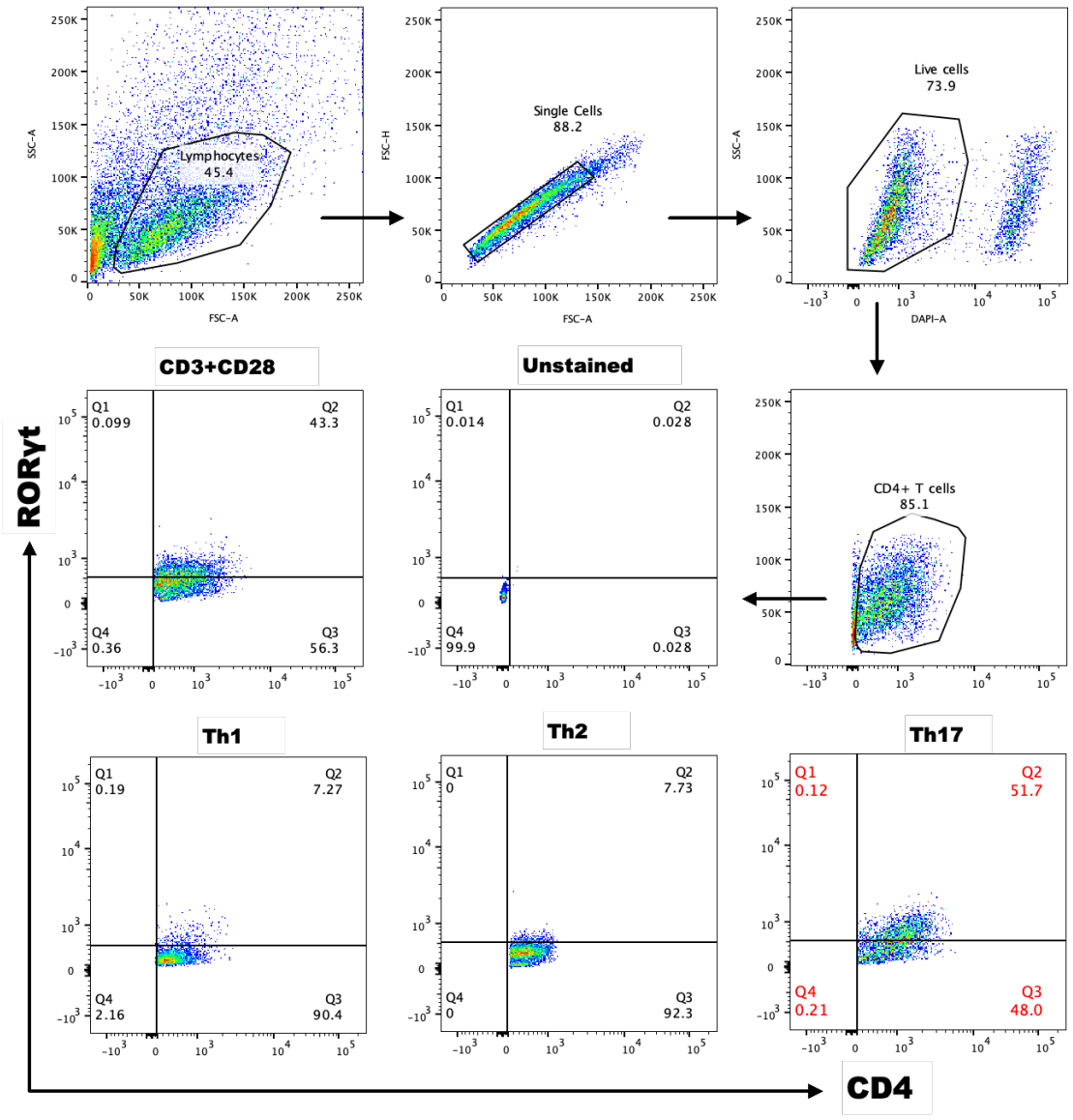

*Figure 110**: Th17 cells express high levels of RORyt.** CD4+ T cells can be isolated from the spleens of female Balb/C mice using EasySep CD4+ Isolation kit. CD4+ T cells are negatively selected using magnetic separation (Stemcell) according to manufacturer's instructions. Cells were seeded at 2x10^6 cells/mL in round bottom 96 well plate and procedure for transcription factor staining was carried out. Cells collected were stained for CD4 using primary antibody APC-Cy-7. Viability was determined via staining with primary antibody PI-Texas Red. RORyt was stained for using FITC. Cells were analysed using BD FACS Aria and data analysed using Flowjo software. Cells were gated on live cells (c), excluding doublets (b) and debris (a). % cells expressed in each quadrant.. Unstained control and, CD3 plus CD28 control included as positive control for polarisation to Th1, Th2, and Th17.*

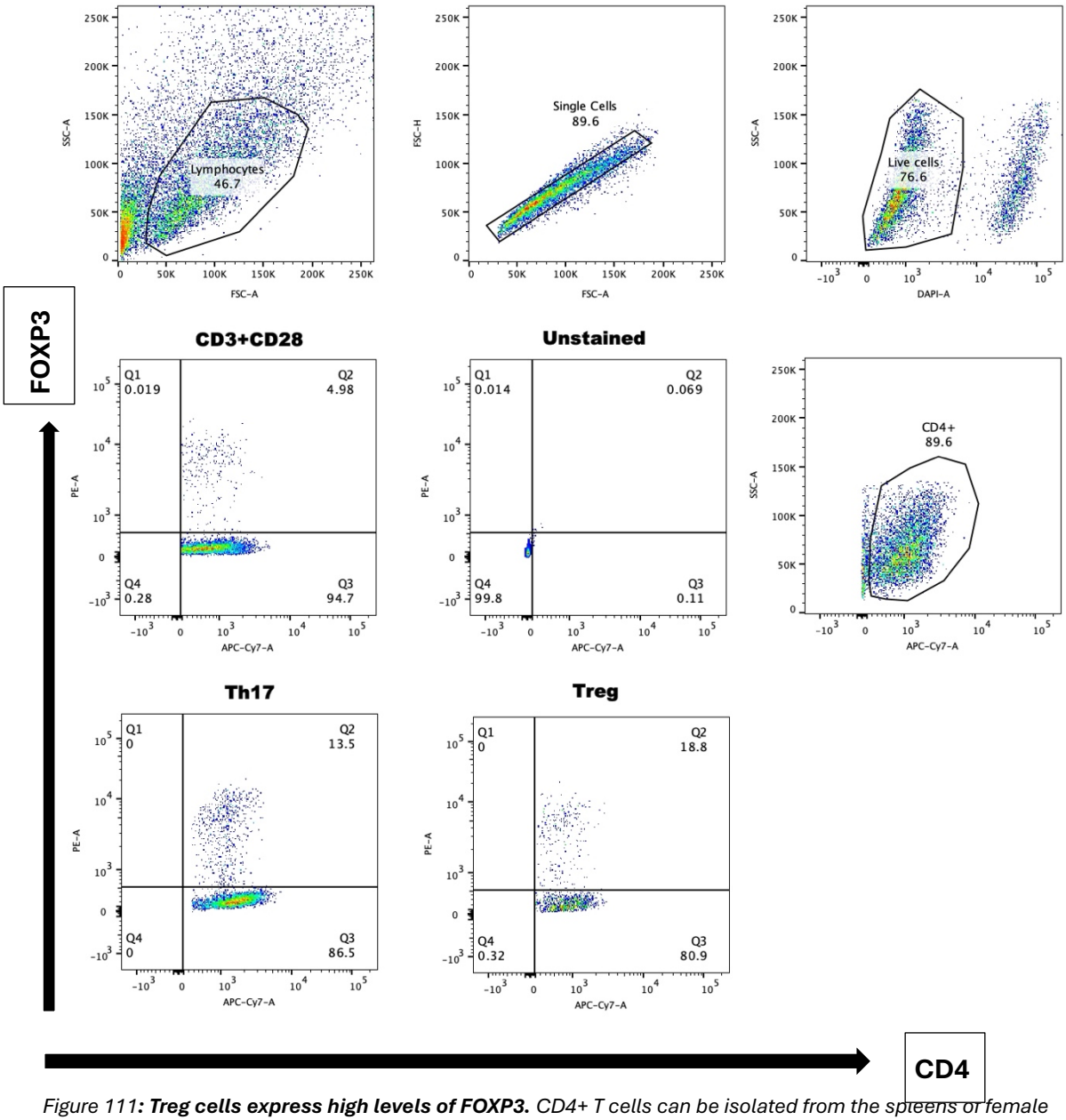

*Figure 111**: Treg cells express high levels of FOXP3.** CD4+ T cells can be isolated from the spleens of female Balb/C mice using EasySep CD4+ Isolation kit. CD4+ T cells are negatively selected using magnetic separation (Stemcell) according to manufacturer's instructions. Cells were seeded at 2x10^6 cells/mL in round bottom 96 well plate and procedure for transcription factor staining was carried out. Cells collected were stained for CD4 using primary antibody APC-Cy-7. Viability was determined via staining with primary antibody PI-Texas Red. FOXP3 was stained for using PE. Cells were analysed using BD FACS Aria and data analysed using Flowjo software. Cells were gated on live cells (c), excluding doublets (b) and debris (a). % cells expressed in each quadrant.. Unstained control and, CD3 plus CD28 control included as positive control for polarisation to Th17, and Treg.*

Therefore we were able to successfully polarise naïve CD4+ T cells to Th1, Th2, Th17, and Treg cells shown here through the production of their characteristic cytokines, and transcription marker expression.

With the profiles of the Th1, Th2, Th17, and Treg cells established, we next examined if fermentates affect these T cell subsets, by assessing their effect on cell viability and cytokine secretion, for undifferentiated T cells, Th1, Th2, Th17, and Treg cells.

6.3.3 Stimulation of differentiated T cells with raw fermentates doesn't affect cell viability

Undifferentiated T cells were isolated from the spleen of Balb/C mice and polarised to T cell subsets: Th1, Th2, Th17, and Treg as previously described (section 2.2.9 T cell polarisation) , and seeded at a concentration of $2x10^6$ cells/mL, incubated for 1 hour before stimulating with a dose of 25mg/mL raw fermentate for 5 days, incubated at 37^0C in 5% CO_2, with additional restimulation with fermentate and polarisation factors on day 3. After 5 days an MTS assay was performed as previously outlined (section 2.2.13 MTS Cell Viability Assay).

Figure 112A and B demonstrates that there was no significant change in cell viability following exposure of the cells to SC40 or Aerobic R0033 versus the control cells. Polarisation of undifferentiated CD4 cells (CD4 unpolarised) to Th1, Th2, Th17, and Tregs (controls), had no significant effect on cell viability.

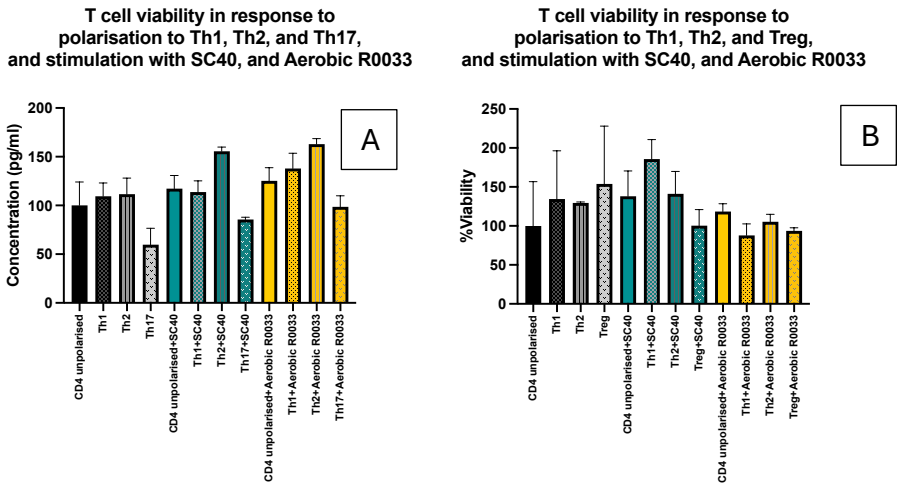

*Figure 112:**Exposure of polarised T cells to Aerobic R0033, and SC40 doesn't affect cell viability.** Undifferentiated T cells were polarised to Th1, Th2, Th17 and Treg cells and seeded at 2x10^6 cells/mL and left for 1 hour at 37^{0}C in 5% CO_2, before being stimulated with 25mg/mL raw fermentate, incubated for 5 days at 37^{0}C in 5%.* Unpolarised undifferentiated CD4 cells *were included as a positive control against differentiated CD4+ cells. Cells were incubated with MTS cell titre aqueous one solution for 3 hours at 37^{0}C in 5% CO_2. Viability is represented as a percentage compared to viable, untreated cells (CD4 unpolarised). Data is presented as mean ± SD of three replicates.*

6.3.4 Stimulation of differentiated T cells with Aerobic R0033, and SC40 affects secretion of cytokines

Undifferentiated T cells were isolated from the spleen of Balb/C mice and polarised to T cell subsets: Th1, Th2, Th17, and Treg, and seeded at a concentration of minimum 1x10^6 cells/mL, incubated for 1 hour before stimulating with a dose of 25mg/mL raw fermentate for 5 days, incubated at 37^{0}C in 5% CO_2, with additional restimulation with fermentate and polarisation factors on day 3. After 5 days supernatants were removed and ELISA procedure for cytokines IL-2, IL-4, IL-6, IL-10, IL-13, IL-17, TGF-β, and IFN-γ was performed according to the manufacturer's instructions (section 2.2.14 Enzyme Linked Immunosorbent Assay (ELISA)).

Figure 113 - Figure 114 demonstrate that fermentates affected the secretion of cytokines from polarised T cells at a dose of 25mg/mL, when compared to the unpolarised and Th1, Th2, Th17, and Treg control cells. Unpolarised cells did not secrete significant concentrations of IL-2, IL-4, IL-6, IL-10, IL-13, IL-17, TGF-β, and

IFN-γ. Polarised control cells secreted profiles of cytokines similar to previously shown in the section above in Figure 107. Figure 113, and Figure 114A and E show increased IL-2 and IFN-γ versus the unpolarised cells, characteristic of Th1 cells. Figure 113B, and Figure 114F show increased IL-4 ($p<0.001$), and IL-13 ($p<0.001$) versus the unpolarised cells, characteristic of Th2 cells. Figure 113C shows increased IL-6 and IL-17 versus the unpolarised cells, characteristic of Th17 cells, while Figure 113G shows high levels of TGF-β ($p<0.001$) from Th17 cells. Figure 114D show increased TGF-β versus the unpolarised cells, characteristic of Treg cells, however Figure 114 H demonstrates it was the Th2 cells that secrete high levels of IL-10 ($p<0.001$).

Figure 113 demonstrates that both SC40, and Aerobic R0033 non-significantly increased IL-4 , and IL-10 in Th1 cells versus the Th1 polarised control. Both SC40, and Aerobic R0033 decreased IL-4 ($p<0.001$), and non-significantly decreased IL-13, but non-significantly increased IL-2 in Th2 cells. SC40 increased TGF-β ($p<0.001$), and IL-17 ($p<0.033$), and non-significantly increased IL-2, and IL-4 in Th17 cells. Aerobic R0033 increased TGF-β ($p<0.001$), and non-significantly increased IL-4 and IL-17 in Th17 cells. Interestingly in unpolarised T cells SC40 significantly increased IFN-γ ($p<0.002$), and non-significantly increased IL-4, IL-10, and IL-13 versus unpolarised control cells. Aerobic R0033 increased IFN-γ ($p<0.033$), and TGF-β ($p<0.033$), and non-significantly increased IL-4, and IL-10 versus unpolarised control cells.

Figure 114 demonstrates that SC40 significantly increased IL-17 ($p<0.002$), and non-significantly increased IL-6, TGF-β, IL-2, IL-13 and IL-10 in Th1 cells versus the Th1 polarised control. Aerobic R0033 significantly decreased IL-2 ($p<0.002$), and non-significantly decreased IFN-γ, in contrast to the non-significant increase in TGF-β ($p<0.002$) in Th1 cells versus the Th1 polarised control. SC40 increased IL-6 ($p<0.001$), and IL-10 ($p<0.033$), and non-significantly increased IL-17, in contrast to the non-significantly decrease in IL-2 in Th2 cells. Aerobic R0033 increased IL-4 ($p<0.001$), and non-significantly increased IL-6, and TGF-β, in contrast to the non-significant decreased IL-2, and IL-13 in Th2 cells. Both SC40 and Aerobic R0033 significantly increased TGF-β ($p<0.001$; $p<0.001$), and non-significantly decreased

IFN-γ in Treg cells. Interestingly in unpolarised T cells SC40 significantly increased IL-4 ($p<0.033$), and IL-13 ($p<0.001$), but non-significantly increased IL-6, IL-2, and IL-17 versus unpolarised control cells. Aerobic R0033 non-significantly increased IL-6, IL-2, and IL-13 versus unpolarised control cells.

Table 28 summarises these findings, with a focus on the effects of fermentates seen on secretion of core cytokines of each different T cell subset, in addition to samples effect on naïve T cells.

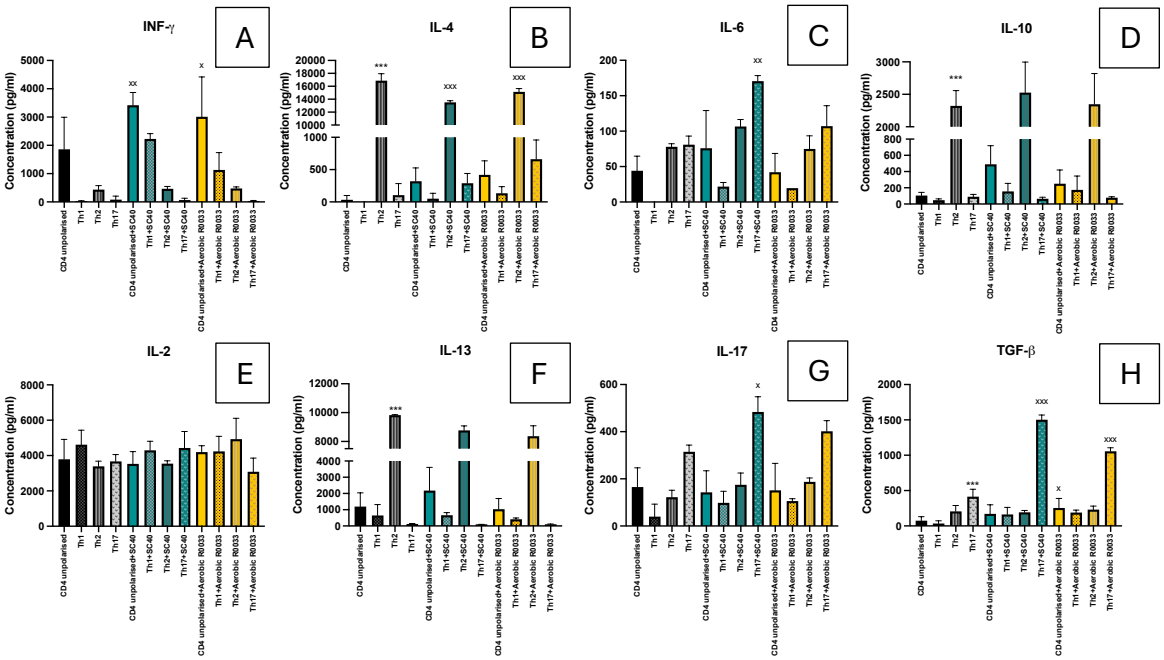

Figure 113: ***Exposure of Th1, Th2, and Th 17 cells to 25mg/mL Aerobic R0033, and SC40 results in the secretion of cytokines IL-2, IL-4, IL-6, IL-10, IL-13, IL-17, TGF-β, and IFN-γ.*** *T cells were polarised to Th1, Th2, or Th17 cells and seeded at 1.75x10^6 cells/mL and left for 1 hour at 37^{0}C in 5% CO_2., before being stimulated with 25mg/mL raw fermentate, incubated for 5 days at 37^{0}C in 5% CO_2. Supernatants were removed after 5 days and ELISA was performed for cytokines IL-2, IL-4, IL-6, IL10, IL-13, IL-17, TGF-β, and IFN-γ. Data is presented as mean ± SD of three replicates. Significance determined using one- way ANOVA with a Newman-Keuls post-test. Output P value style APA: .12 (ns), .033 (*), .002(**) and <.001 (***); 1) comparing to unstimulated control cells "*", and 2) comparing polarised controls to polarised samples "x".*

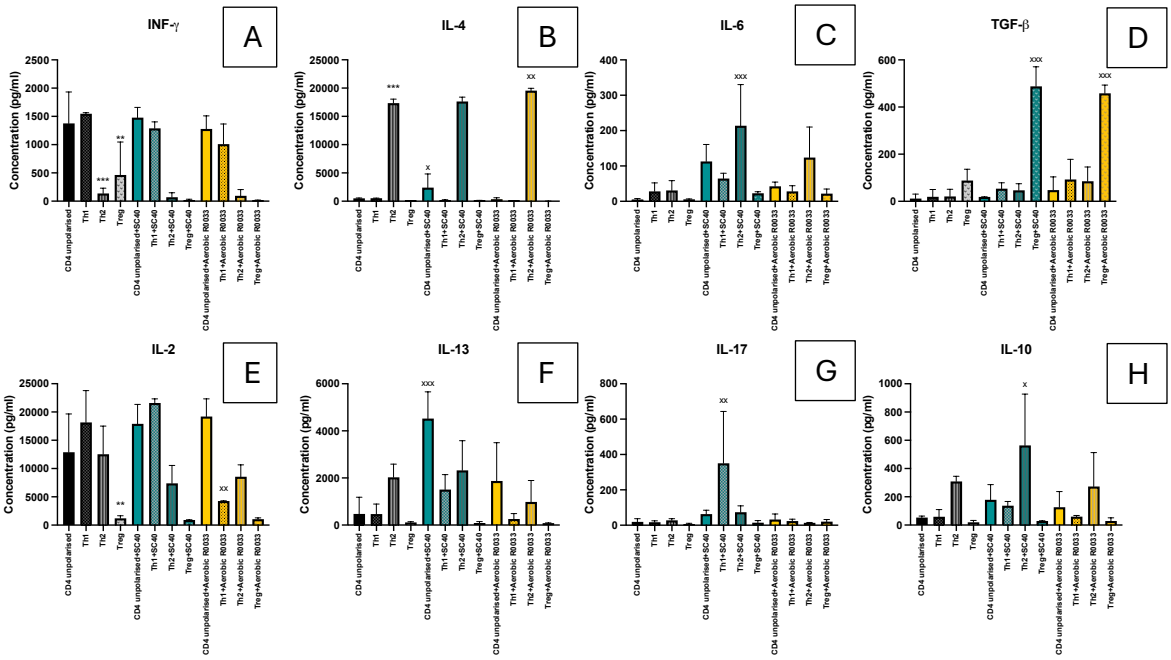

Figure 114: ***Exposure of Th1, Th2, and Treg cells to 25mg/mL Aerobic R0033, and SC40 results in the secretion of cytokines IL-2, IL-4, IL-6, IL-10, IL-13, IL-17, TGF-β, and IFN-γ.*** *T cells were polarised to Th1, Th2, or Treg cells and seeded at 2.93x10^6 cells/mL and left for 1 hour at 37^{0}C in 5% CO_2., before being stimulated with 25mg/mL raw fermentate, incubated for 5 days at 37^{0}C in 5% CO_2. Supernatants were removed after 5 days and ELISA was performed for cytokines IL-2, IL-4, IL-6, IL10, IL-13, IL-17, TGF-β, and IFN-γ. Data is presented as mean ± SD of three replicates. Significance determined using one- way ANOVA with a Newman-Keuls post-test. Output P value style APA: .12 (ns), .033 (*), .002(**) and <.001 (***); 1) comparing to unstimulated control cells "*", and 2) comparing polarised controls to polarised samples "x".*

Table 28: ***Summary of fermentate effect on key cytokines in T cell subsets.*** *Each T cell subset is shown with its characteristic cytokine secreted. Arrows indicate where the sample presence increased or decreased the secretion of this cytokine versus the control cells in the absence of sample. Effect of sample presence in naïve T cells is also shown where secretion of cytokines in naive T cells is listed. Red highlights a significant effect, while green highlights a nonsignificant effect.*

T cell subset	Characteristic cytokine	SC40	Aerobic R0033
Th1	IL-2	↑	↓
	IFN-γ		↓
Th2	IL-4	↓	↑ ↓
	IL-13	↓	↓ ↓
Th17	IL-6		
	IL-17	↑	↑
Treg	TGF-β	↑	↑
	IL-10		
Undifferentiated T cells	Sample enhances these cytokines listed:	IFN-γ, IL-4, IL-13 IL-4, IL-10, IL-13, IL-6, IL-2, IL-17	IFN-γ, TGF-β IL-4, IL-10, IL-6, IL-2, IL-13

Therefore, we were able to determine that SC40, and Aerobic R0033 had the ability to positively affect the secretion of cytokines in naïve T cells, as well as in Th1, Th2, Th17, and Treg cells. Both SC40 and Aerobic R0033, did not negatively impact of cell viability, while interestingly in T cells both had a largely anti-inflammatory cytokine secretion profile. Overall, SC40 shifted naïve T cells towards a mainly Th2 phenotype, had small enhancement of Th1 response, suppressed the Th2 response, enhanced the Th17 response, and enhanced Treg responses. Aerobic R0033 promoted mainly a Treg, and Th2 phenotype in naïve T cells, suppressed Th1 responses, suppressed Th2 responses but was context dependant with positive effects seen also, had only a small enhancement of Th17 responses, and enhanced Treg responses.

Having established the effect of SC40 and Aerobic R0033 in each of the different T cell subsets in primary cells, it was important to examine their effect on the functionality of the T cells, through various functionality assays which we carried out in JURKAT cells. Using the human cell line, JURKAT cells, allowed for the assessment of a range of parameters in T cells without the limitation of cell concentrations associated with the use of primary cells, as well as utilising a human cell model over a murine cell model. JURKAT cells is a T cell line that is well established and well documented for the use in T cell functionality assessment, and therefore were a good model for the examination of fermentate effect on T cell functionality.

6.3.5 T Cell Functionality

Initially it was important to assess the impact of prolonged exposure times of the fermentates on the JURKAT cell proliferation, at a range of doses. Additional doses were examined to provide further confirmation of final desired dose to be used for future research and potential *in vivo* models. From there we then examined the additional parameter of fermentates effect on activated T cells at various exposure times.

6.3.5.1 Fermentates effect cell proliferation

JURKAT cells were seeded at $5x10^5$ cells/mL and incubated for 24 hours at 37^0C in 5% $CO_{2.}$ Following the 24 hour incubation, cells were stimulated with a dose range of fermentates at 10mg/mL, 25mg/mL, or 50mg/mL and incubated for a further 4, 6, 18, 24, 48, and 72hrs at 37^0C in 5% $CO_{2.}$ Cells were incubated with MTS cell titre aqueous one solution and an MTS assay was performed as previously outlined (section 2.2.13 MTS Cell Viability Assay).

Figure 115 demonstrates that the 25mg/mL dose of fermentates enabled optimal cell proliferation for all time points, particularly for the RSM and SC40, with the Aerobic R0033 only having small increases at the 48hr and 72 hours at the 50mng/mL dose. Of note, the time points of 6, 24, 48, and 72 hours had enhanced

cell proliferation in comparison to the controls for all fermentates RSM, SC40, and Aerobic R0033 at each dose.

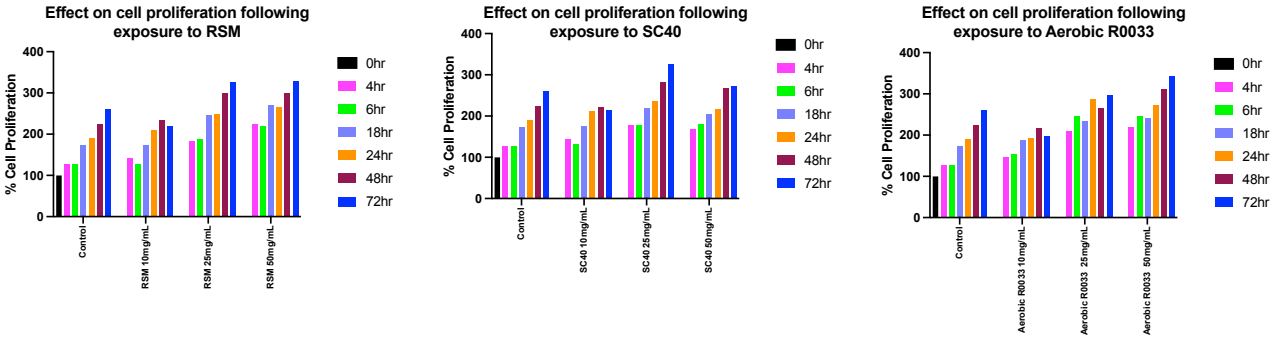

Figure 115: ***Exposure of JURKAT cells to dose range of RSM, SC40, and Aerobic R0033 influences cell proliferation****. JURKAT cells were seeded at 2.5x10^5 cells/mL and incubated for 24hrs hour at 37^{0}C in 5% CO$_2$.,* Unstimulated JURKAT cells *were included as a positive control against JURKAT cells in the presence of fermentates. The following day the cells were stimulated with 10mg/mL, 25mg/mL, and 50mg/mL doses of fermentates and incubated for 0,4, 6, 18, 24, 48, 72 hours. Cells were incubated with MTS cell titre aqueous one solution for 3 hours at 37^{0}C in 5% CO$_2$. Viability is represented as a percentage compared to viable, untreated control cells . Data is presented as mean ± SD of three replicates.*

Having determined that the 25mg/mL dose was optimal for the RSM, SC40 ,and Aerobic R0033, we next examined their effect on cell proliferation in activated T cells.

Activated T cells were an important parameter to measure to assess the effect of fermentates in an active adaptive immune response. Therefore, an optimisation for the use of plate bound rabbit anti-mouse IgG, CD3, and CD28, as T cell activators was carried out before examination of the fermentates effects on cell proliferation in activated T cells.

JURKAT cells were seeded at 5x10^5 cells/mL and activated using plate bound rabbit anti-mouse IgG and CD3, CD28 antibodies for T cell activation. Cells were incubated for 0, 6 and 24hrs hour at 37^{0}C in 5% CO$_2$. Cells were incubated with MTS cell titre aqueous one solution and an MTS assay was performed as previously outlined (section 2.2.13 MTS Cell Viability Assay).

Figure 116 demonstrates that activation of the cells at 0 hours with plate bound antibodies, CD3 and CD28, significantly enhanced cell proliferation ($p<0.001$). After

6 hours cell proliferation was significantly affected in the presence or absence of activation versus their respective 0 hour controls ($p<0.002$; $p<0.001$). After 24 hours incubation, cell proliferation increased by 79% in the absence of activation ($p<0.001$) versus the 0 hour -activation control, and 84% in the presence of the activation ($p<0.002$) versus the 0hr +activation control. Interestingly for both the – and + activation there was no significant increase in cell proliferation between the 6hr and 24hr time points.

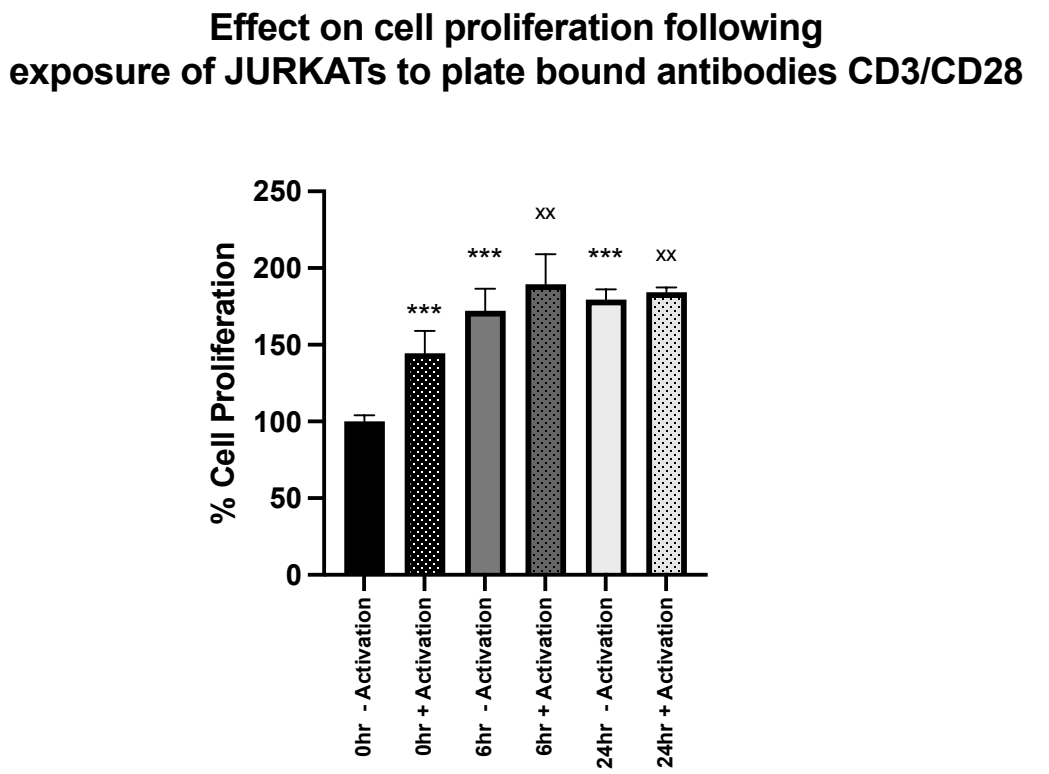

Figure 116: ***Exposure of JURKAT cells to plate bound T cell activation affects cell proliferation.*** *Plates were incubated for 24hours with 5ug/ml rabbit anti-mouse IgG at 4^0C. The following day the plates were incubated at 37^0C for 1 hour in the presence of CD3 5μg/ml, and at 1μg/ml Anti-CD28. JURKA**T** cells were seeded at $5x10^5$ cells/mL s and incubated for 0,6, and 24hrs hour at 37^0C in 5% CO_2.,* Inactivated JURKAT cells *were included as a positive control against activated JURKAT cells. Cells were incubated with MTS cell titre aqueous one solution for 3 hours at 37^0C in 5% CO_2. Viability is represented as a percentage compared to viable, untreated control cells . Data is presented as mean ± SD of three replicates. Significance determined using one- way ANOVA with a Newman-Keuls post-test. Output P value style APA: .12 (ns), .033 (*), .002(**) and <.001 (***); 1) comparing to – activation 0hr to – activation 6hr, - activation 24hr "*", and 0hr- activation to 0hr+activation, 2) comparing + activation 6hr, and 24hr to respective+ 0hr control 'x'.*

Having established that the 24 hour incubation of the JURKAT cells with plate bound CD3, and CD28 antibodies was optimal for T cell activation, we could now assess the impact of the fermentates on cell proliferation. This was done at the 25mg/mL dose of each fermentates, and for the previously highlighted optimal time points of 6, 24, 48, and 72 hours.

JURKAT cells were seeded at $5x10^5$ cells/mL and activated using plate bound rabbit anti-mouse IgG and CD3, CD28 antibodies for T cell activation. Cells were incubated for 24hrs hour at 37^0C in 5% CO_2. Cells were incubated with MTS cell titre aqueous one solution and an MTS assay was performed as previously outlined (section 2.2.13 MTS Cell Viability Assay).

Figure 117 demonstrates that cell proliferation in the absence of T cell activation, peaked at 24hours at 257% cell proliferation, followed by a decrease at later time points. Following T cell activation, T cell proliferation peaked at 6hours with 242% cell proliferation, followed by a slight decrease in proliferation at the later time points. The presence of fermentates alone in the absence of T cell activation affected cell viability. Unactivated T cells in the presence of RSM peaked in cell proliferation at 6hours and 48hours, followed by a slight decrease at the 24hour and 72hour incubations. Interestingly, activated T cells in the presence of RSM peaked at 6hours incubation, followed by a decrease in proliferation after this plateaued from 24 to the 72hours. Unactivated T cells in the presence of SC40 peaked in cell proliferation at 6hours, followed by a slight trending decrease from the 24hour to 72hour incubations. Interestingly, activated T cells in the presence of SC40 followed this same pattern. Similarly, unactivated T cells in the presence of Aerobic R0033 peaked in cell proliferation at 6hours, followed by a slight decrease at the 24hour and plateauing at the 48, and 72hour incubations. In contrast, activated T cells in the presence of Aerobic R0033 peaked at 24hours incubation, followed by a decrease in proliferation at later time points. Interestingly, all fermentates RSM, SC40, and Aerobic R0033, in the absence and in the presence of T cell activation, enhanced cell proliferation at every time point in comparison to the control time points in the absence of samples.

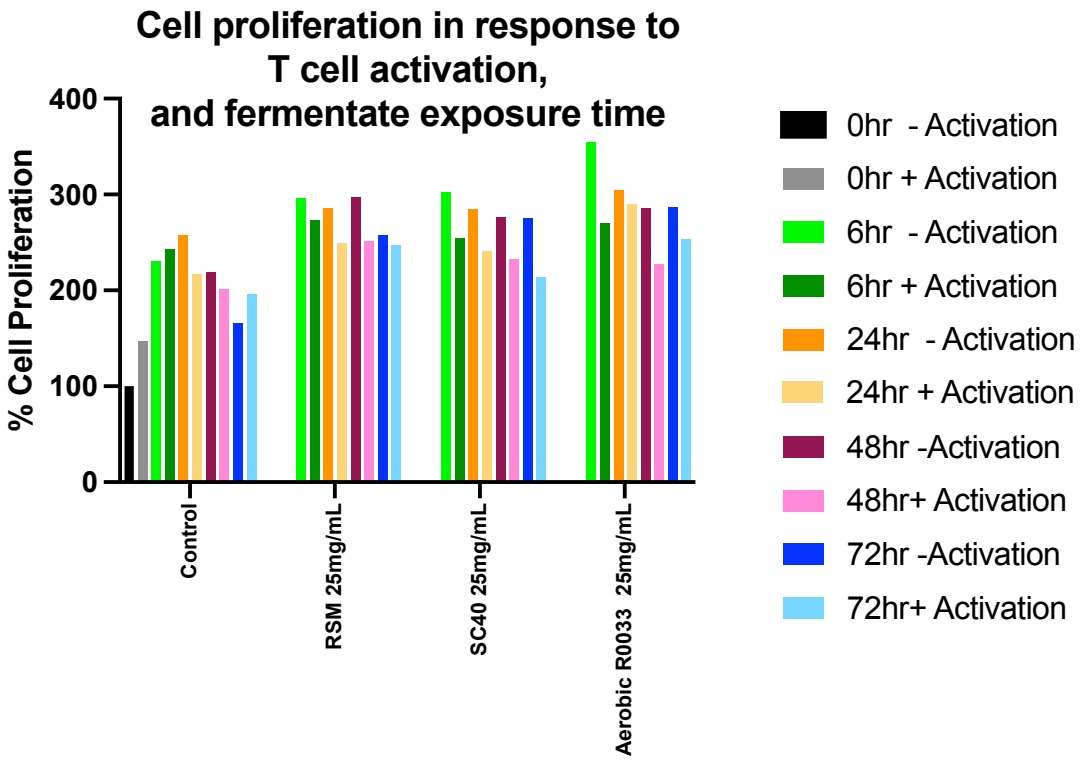

Figure 117: ***Exposure of activated JURKAT cells to fermentates affects cell proliferation.*** *Plates were incubated for 24hours with 5ug/ml rabbit anti-mouse IgG at 4^{0}C. The following day the plates were incubated at 37^{0}C for 1 hour in the presence of CD3 5μg/ml, and at 1μg/ml Anti-CD28. JURKA**T** cells were seeded at 5x10^5 cells/mL, and incubated for 0,6, and 24hrs hour at 37^{0}C in 5% CO_2.,* JURKAT cells *were included as a positive control against activated JURKAT cells. Cells were incubated with MTS cell titre aqueous one solution for 3 hours at 37^{0}C in 5% CO_2. Viability is represented as a percentage compared to viable, untreated control cells . Data is presented as mean ± SD of three replicates.*

IL-2 is another indicator of T cell proliferation and is critical for T cell functionality. Thus, we examined IL-2 secretion in JURKAT cells as an additional parameter for investigation of fermentate effect on T cell proliferation and functionality. Prior to investigation of samples effect, an optimisation for IL-2 secretion using plate bound antibodies was carried out to determine incubation time needed for sufficient activation of JURKAT cells using IgG, and CD3, and CD28 antibodies.

6.3.5.2 Fermentates effect cytokine secretion

JURKAT cells were seeded at 5x10^5 cells/mL and activated using plate bound rabbit anti-mouse IgG and CD3, CD28 antibodies for T cell activation. Cells were incubated for 0,6, and 24hrs hour at 37^{0}C in 5% CO_2. Supernatants were removed

and ELISA procedure for cytokine IL-2 was performed according to the manufacturer's instructions (section 2.2.14 Enzyme Linked Immunosorbent Assay (ELISA)).

Figure 118 demonstrates that activation of the cells at 24 hours in the presence of plate bound antibodies CD3, and CD28 significantly enhanced IL-2 ($p<0.001$) versus the 0hr +activation control. After 24 hours in the presence of plate bound antibodies IL-2 was significantly increased versus the previous time point of 6hours +activation ($p<0.001$).

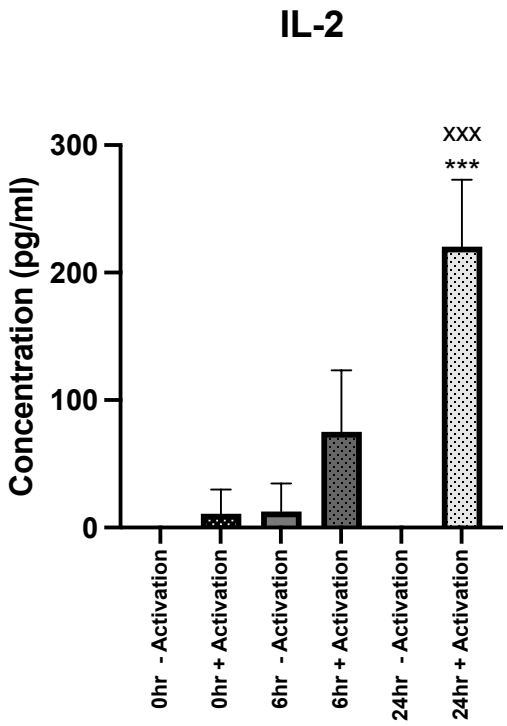

Figure 118: ***Exposure of JURKAT cells to plate bound T cell activation affects secretion of cytokines.*** *Plates were incubated for 24hours with 5ug/ml rabbit anti-mouse IgG at 4^0C. The following day the plates were incubated at 37^0C for 1 hour in the presence of CD3 5μg/ml, and at 1μg/ml Anti-CD28. JURKA**T** cells were seeded at $5x10^5$ cells/mL, and incubated for 0,6, and 24hrs hour at 37^0C in 5% CO_2., JURKA**T** cells were seeded at $5x10^5$ cells/mL and activated with immunocult at 2.5uL/ 100ul cells and left for 0,6, and 24hrs hour at 37^0C in 5% CO_2.,* Inactivated JURKAT cells *were included as a positive control against activated JURKAT cells. Data is presented as mean ± SD of three replicates. Supernatants were removed after 24 hours and ELISA was performed for cytokine IL-2. Data is presented as mean ± SD of three replicates. Significance determined using one- way ANOVA with a Newman-Keuls post-test. Output P value style APA: .12 (ns), .033 (*), .002(**) and <.001 (***); 1) comparing respective +/- 0hr controls to each +/- time point, 2) comparing +/- activation 6hr, to respective +/- 24hr time point 'x'.*

Having established that the 24 hour incubation was optimal, we could now assess the impact of the fermentates on cytokine secretion of IL-2. We used the 25mg/mL dose of each fermentates, and for the previously highlighted optimal time points of 6, 24, 48, and 72 hours.

JURKAT cells were seeded at $5x10^5$ cells/mL and activated using plate bound rabbit anti-mouse IgG and CD3, CD28 antibodies for T cell activation. Cells were incubated for 24hrs hour at 37^0C in 5% CO_2, before being stimulated with 25mg/ml of fermentates, and incubated for each different exposure times under the same conditions. Supernatants were removed and ELISA procedure for cytokine IL-2 was performed according to the manufacturer's instructions (section 2.2.14 Enzyme Linked Immunosorbent Assay (ELISA)).

Figure 119 demonstrates that in the absence of activation with the plate bound antibodies CD3, and CD28, there was no significant increase in IL-2 production at any time point, in the presence or absence of any of the fermentates. Activated JURKAT cells in the absence of fermentates significantly enhanced IL-2 versus the 0hr +activation control at 6hr, 24hr, 48hr, and 72hrs ($p<0.033$, $p<0.001$, $p<0.001$, $p<0.001$ respectively). After 48, and 72 hours in the presence of RSM, IL-2 is significantly increased versus the 48, and 72 hour controls ($p<0.002$, $p<0.001$). While after 24, 48, and 72 hours in the presence of SC40, IL-2 is significantly increased versus the 24, 48, and 72 hour controls ($p<0.033$, $p<0.002$, $p<0.002$), while only at the 72hour exposure time in the presence of Aerobic R0033 was IL-2 significantly increased ($p<0.033$). Interestingly, at the 72 hour exposure time in the presence of both SC40 and Aerobic R0033, IL-2 was significantly enhanced in comparison to the RSM at 72 hours ($p<0.001$, $p<0.001$), while in contrast the Aerobic R0033 at 48hours significantly reduced IL-2 secretion ($p<0.001$).

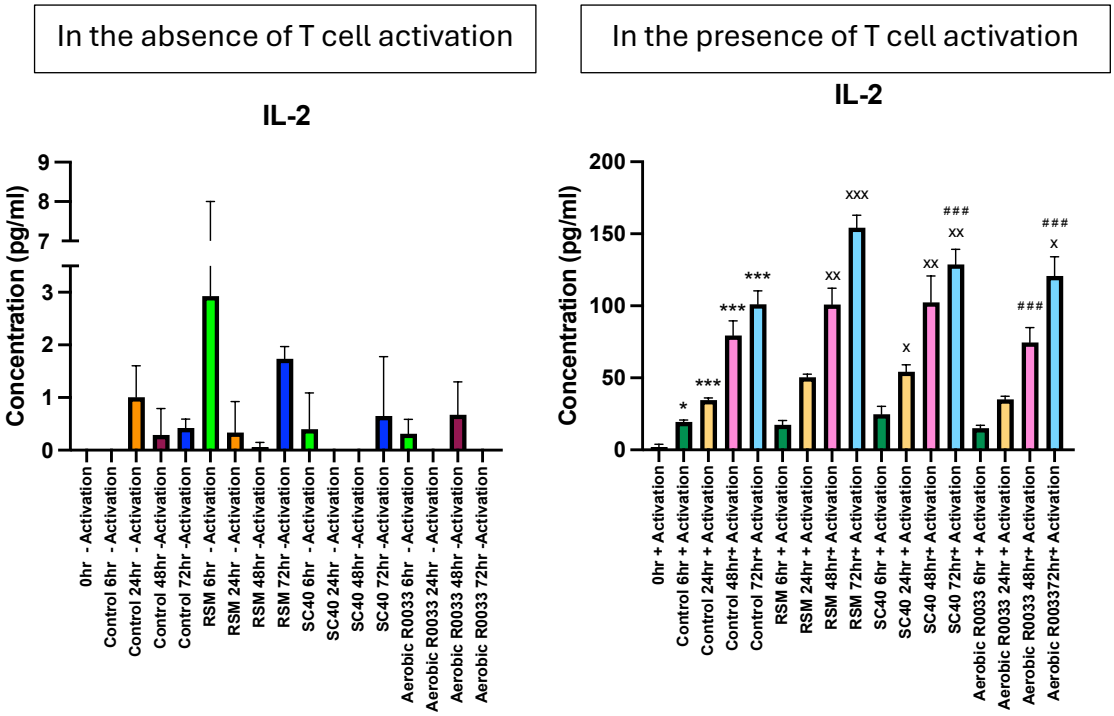

Figure 119: ***Exposure of activated JURKAT cells to fermentates affects secretion of cytokines*** *Plates were incubated for 24hours with 5ug/ml rabbit anti-mouse IgG at 4^{0}C. The following day the plates were incubated at 37^{0}C for 1 hour in the presence of CD3 5μg/ml, and at 1μg/ml Anti-CD28. JURKA**T** cells were seeded at 5x10^5 cells/mL, and incubated for 0,6, and 24hrs hour at 37^{0}C in 5% $CO_{2,}$ JURKA**T** cells were seeded at 5x10^5 cells/mL and activated with immunocult at 2.5uL/ 100ul cells and left for 0,6, and 24hrs hour at 37^{0}C in 5% $CO_{2,}$* Inactivated JURKAT cells *were included as a positive control against activated JURKAT cells. Data is presented as mean ± SD of three replicates. Supernatants were removed after 24 hours and ELISA was performed for cytokine IL-2. Data is presented as mean ± SD of three replicates. Significance determined using one- way ANOVA with a Newman-Keuls post-test. Output P value style APA: .12 (ns), .033 (*), .002(**) and <.001 (***); 1) comparing respective +/- 0hr controls to each +/- control time points '*', 2) comparing +/- activation time points to respective sample time points 'x', and 3) comparing +/- activation RSM time point to respective fermentate time point '#'.'.*

Thus, the presence of the fermentates on cell proliferation over time had little to no significant effect.

We next examined the effects of the fermentates on cell migration to determine if this could be impacted by the presence of fermentates. An initial optimisation was carried out using SDF-1 chemokine to determine the concentration of SDF-1 needed to achieve optimal cell migration through a transwell plate.

6.3.5.3 Fermentates effect cell migration

JURKATs were seeded at 1x10^6 cells/mL and serum starved for 2 hours at 37^{0}C in 5% CO_2. Procedure for migration analysis was preformed using SDF-1 chemoattractant at 0ng/mL, 3ng/mL, 10ng/mL, or 30ng/concentrations before being incubated for 2 hours at 37^{0}C in 5% CO_2 (Section 2.2.17 migration assay). Supernatants were removed and stained with Hoechst. After 24 hours incubation at 4^{0}C cells were imaged using a wide field microscope.

Figure 120 demonstrates that 3ng/mL concentration of SDF-1 chemoattractant was the most significant inducer of cell migration ($p<0.033$).

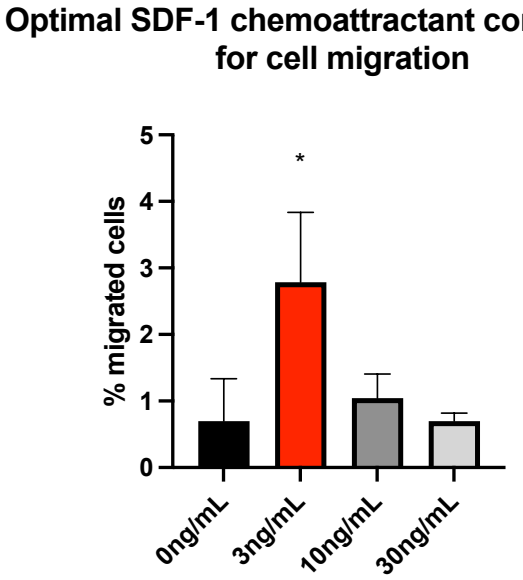

Figure 120: **Exposure of JURKAT cells to dose range of SDF-1 chemoattractant results in the migration of cells.** JURKAT cells were seeded at 1x10^6 cells/mL and serum starved for 2 hours at 37^{0}C in 5% CO_2., before being stimulated with 0ng/mL, 3ng/mL, 10ng/mL, or 30ng/mL SDF-1 chemoattractant incubated for 2 hours at 37^{0}C in 5% CO_2. Supernatants were removed after 24 hours incubation at 4^{0}C and procedure for cell migration was carried out, staining viable cells with Hoechst. Cell count analysed using Mipar software V.4.4.00 (1). Data is presented as mean ± SD of three replicates. Significance determined using one- way ANOVA with a Newman-Keuls post-test. Output P value style APA: .12 (ns), .033 (*), .002(**) and <.001 (***); 1) comparing to unstimulated control cells 0ng/mL SDF-1"*". Migrated cells are represented as a % of the total whole cell count.

Having established that 3ng/mL SDF-1 chemoattractant enabled optimal cell migration in JURKAT cells, the effect of fermentates on cell migration was assessed.

JURKATs were seeded at $1x10^6$ cells/mL and serum starved for 1 hour at 37^0C in 5% CO_2. Fermentates were used to stimulate the cells at concentrations of 10mg/mL, 25mg/mL, and 50mg/mL, and incubated under the same conditions for a further 1 hour at 37^0C in 5% CO_2 (section 2.2.17 migration assay). Supernatants were removed and stained with Hoechst. After 24 hours incubation at 4^0C cells were imaged using a wide field microscope.

Figure 121 demonstrates that there was a stepwise increase in cell migration dependent upon increasing fermentate dose. At 25mg/mL both SC40 and Aerobic R0033 significantly increased percentage of cells migrated ($p<0.033$; $p<0.033$), and similarly increased migration at 50mg/mL ($p<0.001$; $p<0.002$). Although not significant both SC40 and Aerobic R0033 increased cell migration at 10mg/mL. Interestingly, RSM at 50mg/mL significantly increased cell migration ($p<0.033$). A 50mg/mL dose of SC40 significantly increased the migration of cells compared to the previously lower dose of 25mg/mL SC40. Additionally, a 50mg/mL dose of SC40 significantly enhanced the percentage of cells migrated compared to the respective 50mg/mL RSM counterpart ($p<0.001$), while all other SC40 and Aerobic R0033 doses only non-significantly enhanced the percentage of migrated cells compared to their respective RSM counterpart.

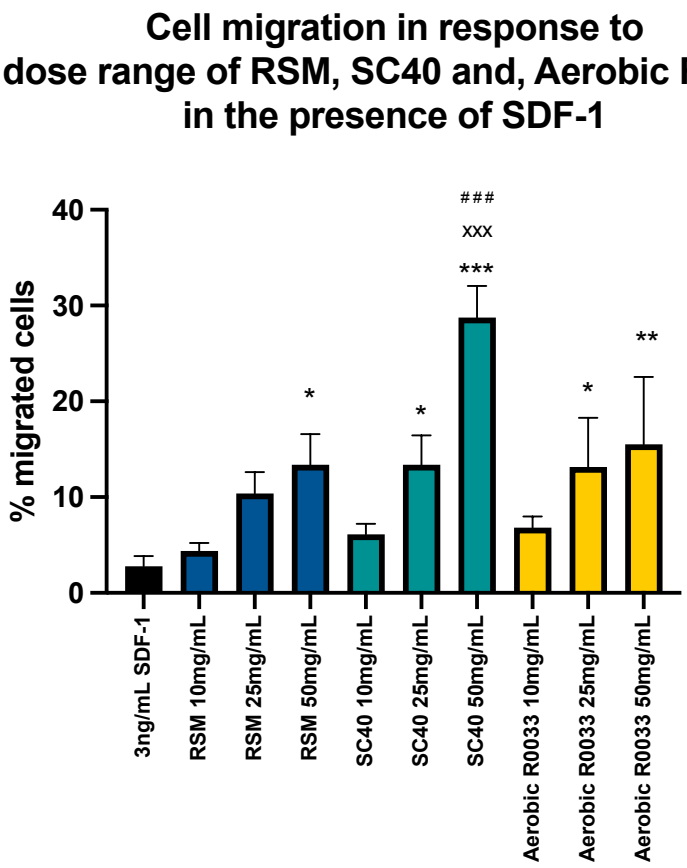

Figure 121: **Exposure of JURKAT cells to dose range of SRSM, SC40, and Aerobic R0033 results in the migration of cells.** JURKAT cells were seeded at 1x10^6 cells/mL and serum starved for 1 hours at 37^{0}C in 5% $CO_{2.,}$ before being stimulated with fermentates for a further 1 hour. Cells were activated with 3ng/mL SDF-1 chemoattractant incubated for further 2 hours at 37^{0}C in 5% CO_2 . Supernatants were removed after 24 hours incubation at 4^{0}C and procedure for cell migration was carried out, staining viable cells with Hoechst. Cell count analysed using Mipar software V.4.4.00 (1). Data is presented as mean ± SD of three replicates. Significance determined using one- way ANOVA with a Newman-Keuls post-test. Output P value style APA: .12 (ns), .033 (*), .002(**) and <.001 (***); 1) comparing to unstimulated control cells 3ng/mL SDF-1"*", 2) comparing to previous sample dose "x", and 3) comparing to the RSM "#". Migrated cells are represented as a % of the total whole cell count.

Therefore fermentates could positively affect and enhance cell migration at doses of 25mg/ml, or 50mg/ml.

Having established the fermentates effect on some T cell functionality parameters, assessment of fermentates effect on upstream and downstream signalling processes was carried out. This was in order to determine at what point the fermentates may be exerting their effects. Initially, assessment of the samples effect on immune synapse interactions was carried out, followed by examination of the sample's effect on downstream ERK1/2 signalling.

6.3.5.4 Fermentates do not affect cell activity at the immune synapse

Initial optimisations were carried out to determine optimal incubation of cells with Dynabeads needed to stimulate immune synapse interactions, Establishing this parameter then allowed for the determination of sample effect on immune synapse interactions, the point at which the adaptive immune system becomes initiated in response to T cell activation.

JURKATs were seeded at $5x10^5$ cells/mL and serum starved for 2 hours at 37^0C in 5% CO_2. DynaBeads are spherical polymer particles that were used to mimic T cell activation as they are coated with CD3 and CD28 which are essential to T cell initiation and activation. They acted as an antigen to elicit the activation of the adaptive immune response via T cell activation. DynaBeads were used to activate the T cells at a 1:1 ratio bead to cell, and were incubated under the same conditions for a either 0mins, 15mins, 30mins, 1 hour, or 4 hours. Procedure for assessing the interaction at the immune cell synapse was carried out (section 2.2.18 immune synapse assay). Cells were stained with Hoechst, and phalloidin-TRITC. Cells were imaged using a wide field microscope. See appendix for representative fluorescent images of incubation of JURKATs with Dynabeads for various times, and incubation with fermentates at each dose.

Figure 122 demonstrates the immune synapse interaction. The cell surfaces were imaged using brightfield microscopy (A, B, F, G-grey). The JURKAT cells' nucleus were stained using Hoechst (C,H-blue), while the immune synapse interaction was highlighted by staining the F-actin with Phalloidin (D, I-red). Figure 122E,J highlights the immune synapse interaction by incorporating brightfield (Figure 122B,G),

Hoechst (Figure 122C,H), and Phalloidin stains (Figure 122D,I) in the absence and presence of T cell activation beads.

Figure 122E demonstrates that in the absence of beads there was no interaction between the cell to initiate the immune synapse, with the T Phalloidin stain for F-actin remaining inactivated. Figure 122J demonstrates that in the presence of the beads there was an initiation of the immune cell synapse, which mimics antigen presentation on the T cell surface, highlighted by the Phalloidin stain for F-actin being activated.

Figure 123 demonstrates that at the 15 minute incubation of the cells with the beads that most immune cell synapse interaction occurred, where 89% of cells imaged (Figure 123) are expressing F-actin interacting on the surface of the cell nucleus. This was followed by a trending decrease in synapse interaction for the later time points of 30 minutes, 1 hour and 4hours.

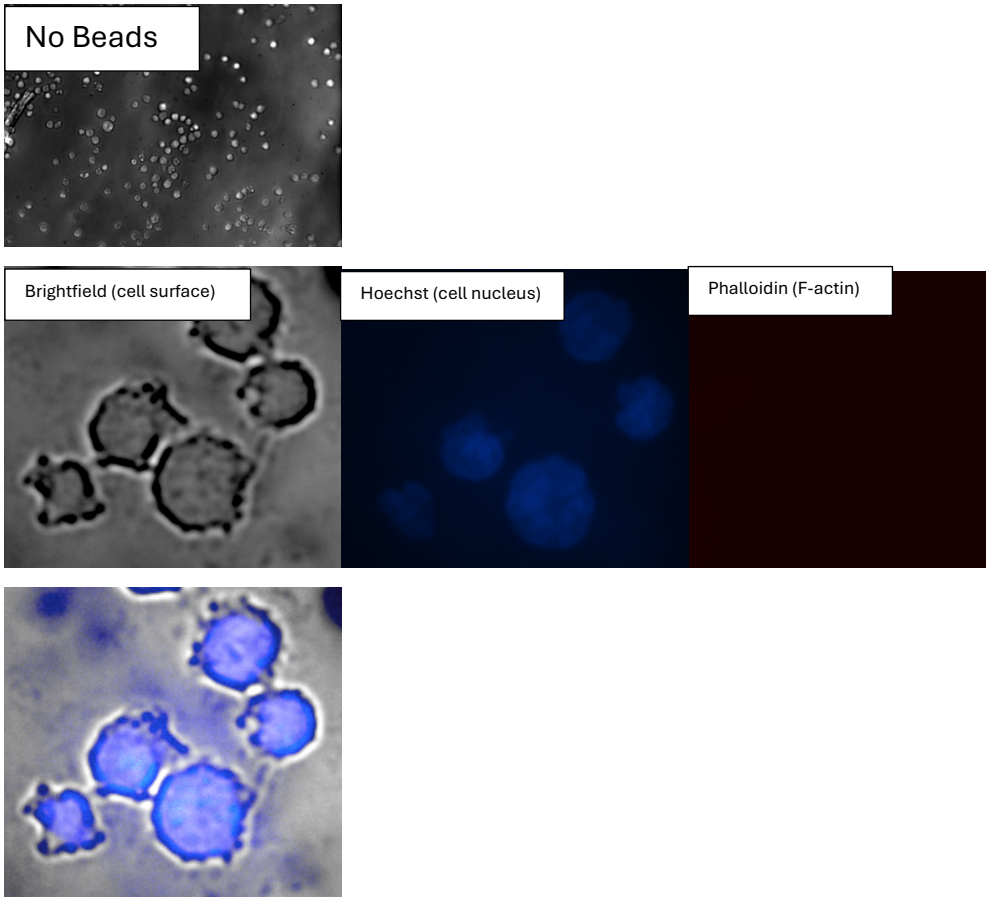
No Beads
Brightfield (cell surface)
Hoechst (cell nucleus)
Phalloidin (F-actin)
Beads
Brightfield (cell surface)
Hoechst (cell nucleus)
Phalloidin (F-actin)

Figure 122: **JURKAT cells can be stained by fluorescent microscopy to image the T cell, the nucleus, and the activated F-actin of the immune synapse.** JURKAT cells were seeded at 5x10^5 cells/mL and serum starved for 2 hours at 37^{0}C in 5% $CO_{2.,}$ before being stimulated with a 1:1 ratio of beads to cells, and incubated for either 15 minutes at 37^{0}C in 5% CO_2 . Procedure for immune synapse interaction was carried out, staining viable cells with Hoechst (nucleus), and TRITC (F-actin), while brightfield is used to image the whole cell. Cell count analysed using ImageJ JS software. Data is representative of four replicates. (A,B): brightfield cells in the absence of beads, (C) cells in absence of beads stained with Hoechst to highlight cell nucleus, (D) cells in absence of beads stained with Phalloidin to highlight F-actin, (E) cells in absence of beads combined image overlay of B,C,D, (F,G) brightfield cells in the presence of beads, (H) cells in presence of beads stained with Hoechst to highlight cell nucleus, (I) cells in presence of beads stained with Phalloidin to highlight F-actin, (J) cells in absence of beads combined image overlay of G,H,I.

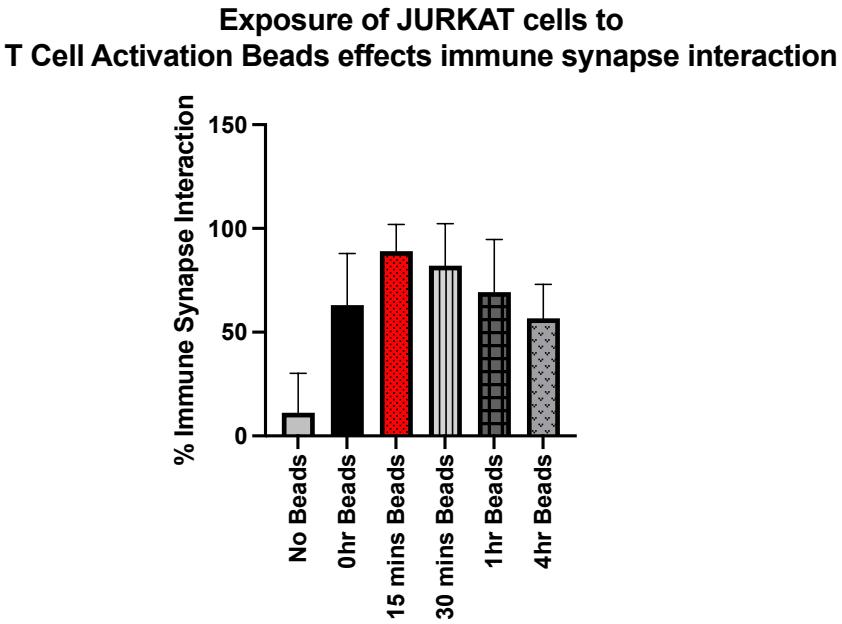

Figure 123: **Exposure of JURKAT cells to T cell activation beads results in immune synapse interaction.** JURKAT cells were seeded at 5x10^5 cells/mL and serum starved for 2 hours at 37^{0}C in 5% $CO_{2.,}$ before being stimulated with a 1:1 ratio of beads to cells, and incubated for either 0, 15, 30 minutes, or 1, or 4 hours at 37^{0}C in 5% CO_2 . Procedure for immune synapse interaction was carried out, staining viable cells with Hoechst (nucleus), and TRITC (F-actin). Cell count analysed using ImageJ JS software, and represented using GraphPad Prism V.10. Data is presented as mean ± SD of four replicates. Significance determined using one- way ANOVA with a Newman-Keuls post-test. Output P value style APA: .12 (ns), .033 (*), .002(**) and <.001 (***); 1) comparing to control cells of 0hr Beads "*". Activated T cells are represented as a % of the cells activated at the immune synapse compared to the total cell population. Negative control of cells in the presence of no activation beads is included.

Having demonstrated that 15-minute incubation of the cells with the T cell activation beads was optimal to elicit synapse interactions, the fermentates could be assessed for their effect on immune cell synapse interaction.

JURKATs were seeded at $5x10^5$ cells/mL and serum starved for 1 hour at 37^0C in 5% CO_2, before stimulating with fermentates at a dose of 10mg/mL, 25mg/mL, or 50mg/mL and incubating under the same condition, for a further 1 hour. DynaBeads were used to activate the T cells at a 1:1 ratio bead to cell, and were incubated under the same conditions for a 15mins. The procedure for assessing the interaction at the immune cell synapse was carried out (section 2.2.18 immune synapse assay). Cells were stained with Hoechst, and phalloidin-TRITC. Cells were imaged using a wide field microscope.

Figure 124 demonstrates that there was no significant effect on immune cell synapse interactions in the presence of RSM, SC40, or Aerobic R0033 at any dose. The higher dose of 50mg/mL SC40 had a slight decrease in percentage synapse interaction, while all remaining samples and doses had no significant effect on synapse interaction.

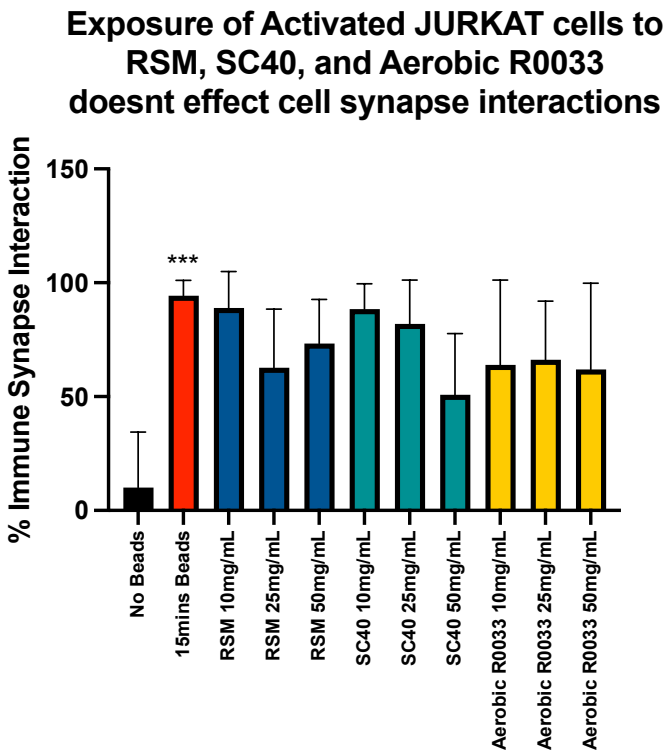

Figure 124: **Exposure of JURKAT cells to T cell activation beads results in immune synapse interaction.** JURKAT cells were seeded at $5x10^5$ cells/mL and serum starved for 1 hour at 37^0C in 5% $CO_{2.,}$ before being stimulated with a dose range of fermentates of 10mg/mL, 25mg/mL, or 50mg/mL, and then incubated for a further 1 hour. After 1 hour the cells were activated with a 1:1 ratio of beads to cells, and incubated for 15 minutes at 37^0C in 5% CO_2 . Procedure for immune synapse interaction was carried out, staining viable cells with Hoechst (nucleus), and TRITC (F-actin). Cell count analysed using ImageJ JS software, and represented using GraphPad Prism V.10. Data is presented as mean ± SD of three replicates. Significance determined using one- way ANOVA with a Newman-Keuls post-test. Output P value style APA: .12 (ns), .033 (*), .002(**) and <.001 (***); 1) comparing to control cells of 0hr Beads "*". Activated T cells are represented as a % of the cells activated at the immune synapse compared to the total cell population. Negative control of cells in the presence of no activation beads is included.

We clearly saw that the fermentates didn't have any significant effect on upstream signalling at the immune synapse. Therefore, we now moved on to assess the effects the fermentates had on downstream signalling of the ERK1/2 signalling cascade.

6.3.5.5 Fermentates effects downstream cell signalling

Prior to investigation of sample effects on downstream signalling cascades, it was necessary to generate and process the samples needed for use in the SDS-PAGE and western blot assay. In order to do so it was necessary to quantify the concentration of protein in each sample to ensure that 20-50ug of protein was added to the SDS-PAGE gel. Initial optimisations were carried out to determine optimal incubation of cells with plate bound IgG, CD3, and CD28 to initiate downstream signalling of ERK1/2 signalling cascade. Establishing this parameter then allowed for the determination of sample effect on the downstream signalling activation levels of the total extracellular signal-regulated kinase 1/2 (ERK1/2), and phosphoERK1/2 signalling cascades.

JURKAT cells were seeded at $5x10^5$ cells/mL and activated using plate bound rabbit anti-mouse IgG and CD3, CD28 antibodies for T cell activation. Cells were incubated for 0 hours, 30 minutes, and 4 hours at 37^0C in 5% CO_2, before procedure for cell lysate generation was carried out. After the cell lysates were harvested a BCA assay was carried out to quantify the concentration of protein present in each of the samples, performed according to the manufacturer's instructions (section 2.2.19 Cell lysate preparation, and section 2.2.20 BCA protein quantification).

Figure 125 demonstrates that at the 0hr activation there was 3648ug/mL of protein present. At 30 minutes incubation there was 4382ug/mL of protein present. At 4 hours there was 3835ug/mL of protein present. There was no significant difference in protein concentrations between all samples.

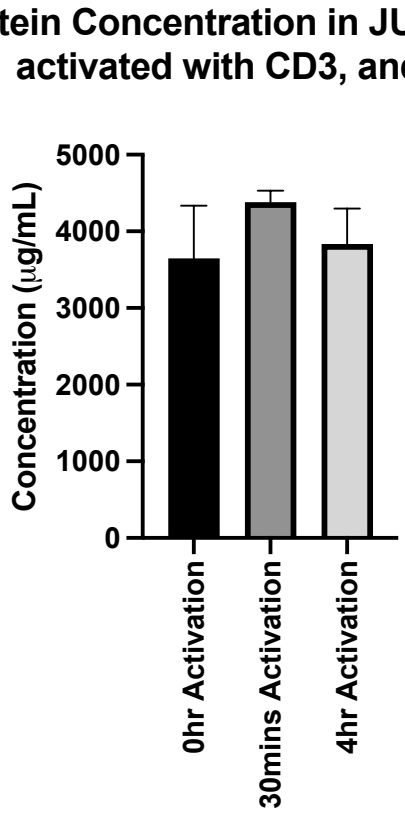

Figure 125: ***Protein quantification of JURKAT cells activated with plate bound antibodies.*** *Plates were incubated for 24hours with 5ug/ml rabbit anti-mouse IgG at 4^{0}C. The following day the plates were incubated at 37^{0}C for 1 hour in the presence of CD3 5μg/ml, and at 1μg/ml Anti-CD28. JURKA**T** cells were seeded at 5x10^5 cells/mL, and incubated for 0,30minutes, and 4hrs hour at 37^{0}C in 5% $CO_{2,}$* Inactivated JURKAT cells *were included as a positive control against activated JURKAT cells. Data is presented as mean ± SD of three replicates. Cell lysates were generated using the cell lysis buffer and procedure for quantification of protein was carried out (BCA). Significance determined using one- way ANOVA with a Newman-Keuls post-test. Output P value style APA: .12 (ns), .033 (*), .002(**) and <.001 (***); 1) comparing +activation time points to 0hr activation.*

JURKAT cells were seeded at 5x10^5 cells/mL and activated using plate bound rabbit anti-mouse IgG and CD3, CD28 antibodies for T cell activation. Cells were incubated for 0 hours, 30 minutes, and 4 hours at 37^{0}C in 5% $CO_{2,}$ before procedure for cell lysate generation, and BCA protein quantification was carried out. Samples were prepared for use in SDS-PAGE gel loading 20-50ug of protein per well. Procedure for SDS-PAGE and western blot was carried out as previously described (section 2.2.22 SDS-PAGE, and section 2.2.23 Western blot).

Figure 126 and Figure 128A demonstrates the level of Total ERK 1/2 at the 0hr, 30minutes and 4hour incubation with JURKAT cells. Total ERK1 can be seen as the

top band at approximately 44kDa, while Total ERK2 can be seen as the bottom band at approximately 42kDa. The 0hr and 30 minute incubation activated both the total ERK1 and total ERK2 pathway the most, with the 4hour incubation activating these pathways to a lesser extent.

Figure 127 and Figure 128B demonstrates the level of Phospho ERK 1/2 at the 0hr, 30minutes and 4hour incubation with JURKAT cells. Phospho ERK1 can be seen as the top band at approximately 43kDa, while phospho ERK2 can be seen as the bottom band at approximately 38kDa. The 30 minute incubation clearly activated both the phospho ERK1 and phospho ERK2 pathway the most, with the 4hour incubation only slightly more enhanced than the 0hr incubation.

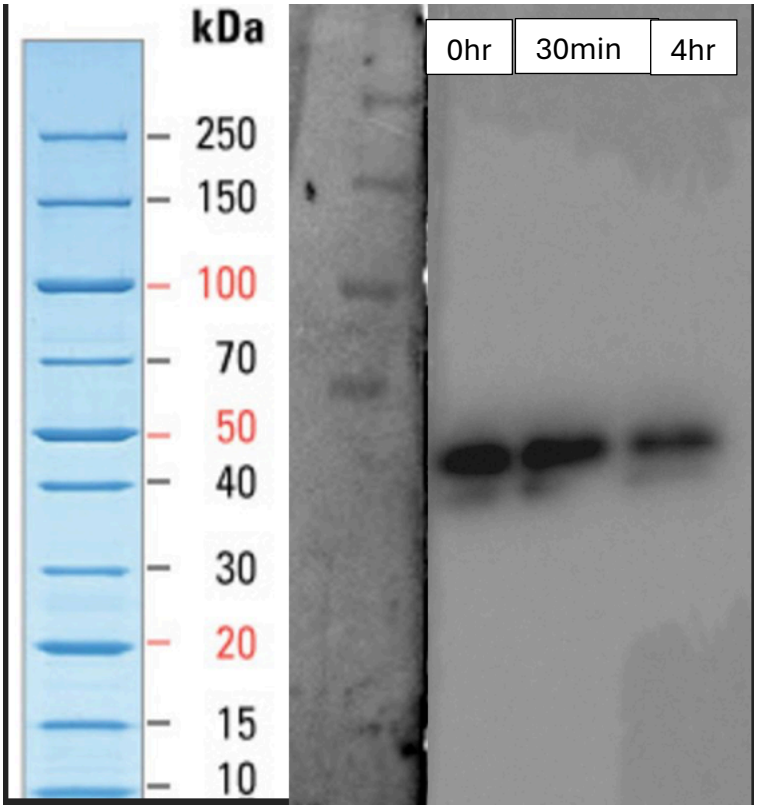

Figure 126: ***Total ERK 1/2 are expressed in JURKAT cells activated with plate bound antibodies.*** *Plates were incubated for 24hours with 5ug/ml rabbit anti-mouse IgG at 4^{0}C. The following day the plates were incubated at 37^{0}C for 1 hour in the presence of CD3 5μg/ml, and at 1μg/ml Anti-CD28. JURKA**T** cells were seeded at 5x10^5 cells/mL, and incubated for 0,30minutes, and 4hrs hour at 37^{0}C in 5% $CO_{2,}$. Cell lysates were generated using the cell lysis buffer and procedure for quantification of protein was carried out (BCA) prior to carrying out SDS-PAGE and western blot procedure. PVDF membrane was imaged using G-Box and genesys software.*

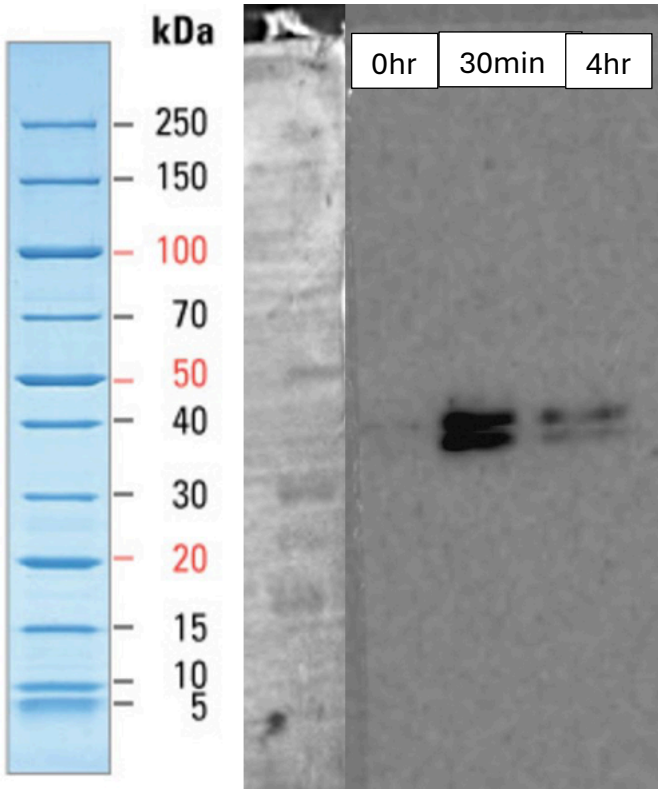

Figure 127: ***Phospho ERK 1/2 are expressed in JURKAT cells activated with plate bound antibodies.*** *Plates were incubated for 24hours with 5ug/ml rabbit anti-mouse IgG at 4^0C. The following day the plates were incubated at 37^0C for 1 hour in the presence of CD3 5μg/ml, and at 1μg/ml Anti-CD28. JURKA**T** cells were seeded at $5x10^5$ cells/mL, and incubated for 0,30minutes, and 4hrs hour at 37^0C in 5% $CO_{2,..}$ Cell lysates were generated using the cell lysis buffer and procedure for quantification of protein was carried out (BCA) prior to carrying out SDS-PAGE and western blot procedure. PVDF membrane was imaged using G-Box and genesys software.*

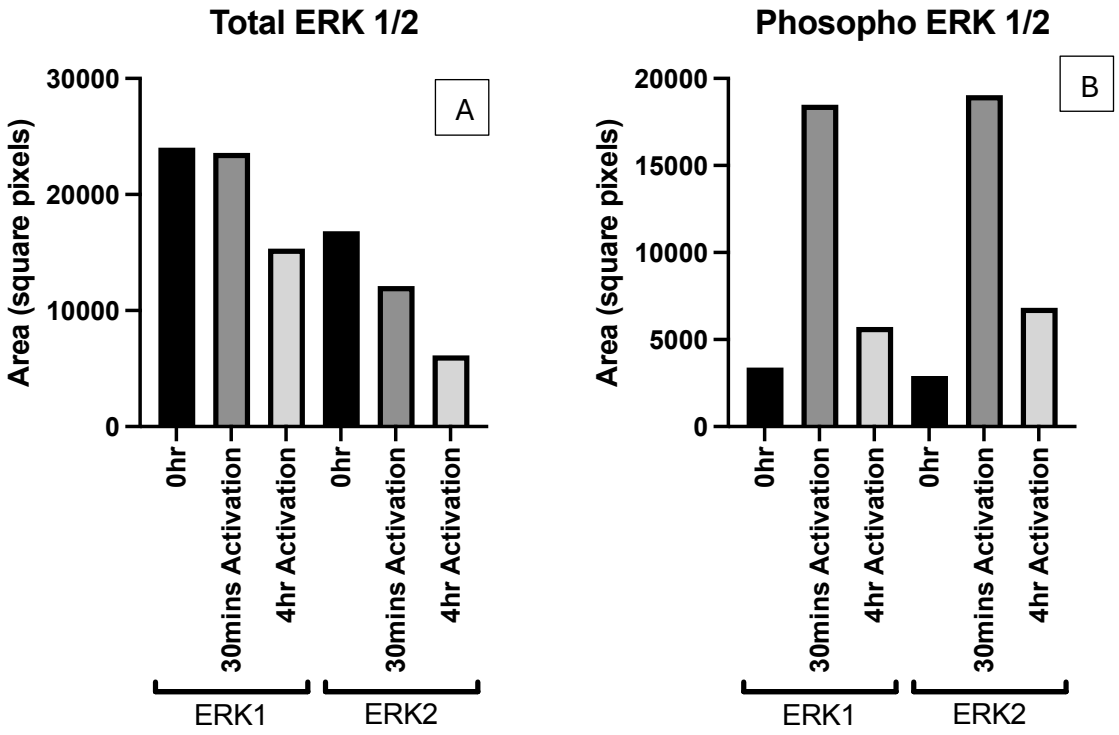

*Figure 128:**Total and Phospho ERK 1/2 are expressed in JURKAT cells activated with plate bound antibodies.** Plates were incubated for 24hours with 5ug/ml rabbit anti-mouse IgG at 4^{0}C. The following day the plates were incubated at 37^{0}C for 1 hour in the presence of CD3 5μg/ml, and at 1μg/ml Anti-CD28. JURKA**T** cells were seeded at 5x10^5 cells/mL, and incubated for 0,30minutes, and 4hrs hour at 37^{0}C in 5% $CO_{2,}$. Cell lysates were generated using the cell lysis buffer and procedure for quantification of protein was carried out (BCA) prior to carrying out SDS-PAGE and western blot procedure. PVDF membrane was imaged using G-Box and genesys software. Densitometry analysis was carried out using imageJ, and graphed using Graphpad Prism V.10.*

Having established that the 30 minute incubation was the optimal time point for induction of PhosphoERK1/2, we now were able to assess the impact of fermentates on this downstream signalling cascade.

JURKAT cells were seeded at 5x10^5 cells/mL and activated using plate bound rabbit anti-mouse IgG and CD3, CD28 antibodies for T cell activation. Cells were incubated for 30 minutes with 25mg/ml of fermentates at 37^{0}C in 5% $CO_{2,}$ before the procedure for cell lysate generation was carried out. After the cell lysates were harvested a BCA assay was carried out to quantify the concentration of protein present in each of the samples, performed according to the manufacturer's

instructions (section 2.2.19 Cell lysate preparation, and section 2.2.20 BCA protein quantification).

Figure 129 demonstrates that the control cells in the absence of activation or sample there was 6299ug/ml protein present. At 30 minutes activation in the absence of sample there was 4984ug/ml protein present. In the absence of activation, in the presence of RSM there was 6148ug/ml, SC40 5155ug/ml, and Aerobic R0033 6870ug/ml protein present in each sample. In activated JURKAT cells, in the presence of RSM there was 4970ug/ml, SC40 5765ug/ml, and Aerobic R0033 5481ug/ml protein present in each sample. There was no significant difference in protein concentrations between all samples.

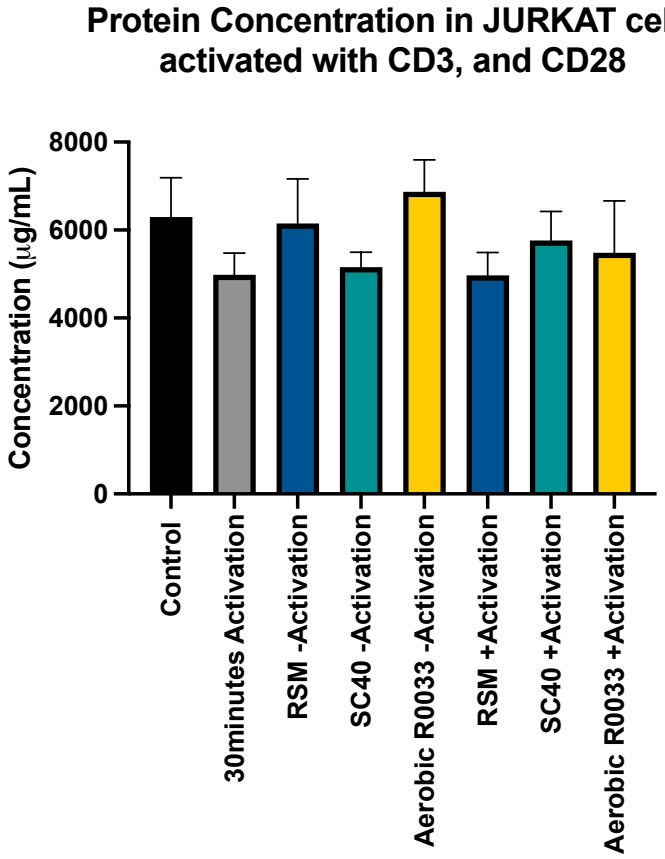

Figure 129: ***Protein quantification of JURKAT cells activated with plate bound antibodies and fermentates.*** *Plates were incubated for 24hours with 5ug/ml rabbit anti-mouse IgG at 4^0C. The following day the plates were incubated at 37^0C for 1 hour in the presence of CD3 5µg/ml, and at 1µg/ml Anti-CD28. JURKA**T** cells were seeded at $5x10^5$ cells/mL, and incubated for 0,30minutes, and 4hrs hour at 37^0C in 5% CO_2,* Inactivated JURKAT cells *were included as a positive control against activated JURKAT cells. Data is presented as mean ± SD of three replicates. Cell lysates were generated using the cell lysis buffer and procedure for quantification of protein was carried out (BCA). Significance determined using one- way ANOVA with a Newman-Keuls post-test. Output P value style APA: .12 (ns), .033 (*), .002(**) and <.001 (***); 1) comparing -/+activation samples to -/+ controls.*

JURKAT cells were seeded at $5x10^5$ cells/mL and activated using plate bound rabbit anti-mouse IgG and CD3, CD28 antibodies for T cell activation. Cells were incubated for 30 minutes, with 25mg/mL fermentates at 37^0C in 5% CO_2, before the procedure for cell lysate generation, and BCA protein quantification was carried out. Samples were prepared for use in SDS-PAGE gel loading 20-50ug of protein per well. Procedure for SDS-PAGE and western blot was carried out as previously described (section 2.2.22 SDS-PAGE, and section 2.2.23 Western blot).

Figure 130 and Figure 132A demonstrates the level of Total ERK 1/2 in the absence of activation and sample presence, and in activated JURKAT cells in the presence of samples. Total ERK1 can be seen as the top band at approximately 44kDa, while Total ERK2 can be seen as the bottom band at approximately 42kDa. In the absence of activation, SC40 increased total ERK1 the most, followed closely by RSM, but with a decrease in activation in the presence of Aerobic R0033 compared to the control cells. However in activated JURKAT cells, this is reversed and Aerobic R0033 increased total ERK1 the most, followed by a decrease in the presence of RSM, and even further for SC40 compared to the 30 minute activated control cells. Similarly, in the absence of activation SC40 increased total ERK2 the most, followed closely by RSM, but with a decrease in levels in the presence of Aerobic R0033 compared to the control cells. However in activated JURKAT cells, only the RSM increased total ERK2 slightly more than the control, followed by a slight decrease in the presence of SC40, and Aerobic R0033 compared to the 30 minute activated control cells.

Figure 131 and Figure 132B demonstrates the activation of Phospho ERK 1/2 signalling cascade in the absence of activation and sample presence, and in activated JURKAT cells in the presence of samples. Phospho ERK1 can be seen as the top band at approximately 43kDa, while phospho ERK2 can be seen as the top band at approximately 38kDa. In the absence of activation, for both the phopho ERK1 and phospho ERK 2 pathways neither the control nor the samples activated this signalling cascade. Only activated cells in the absence and presence of samples activated the phopho ERK1 and phospho ERK 2 pathways. In activated JURKAT cells, RSM activated the phospho ERK1 pathway most, followed closely by Aerobic R0033, the SC40 compared to the control cells. Similarly, in activated

JURKAT cells, RSM activated the total ERK2 pathway most, followed then by SC40, and Aerobic R0033 compared to the 30 minute activated control cells.

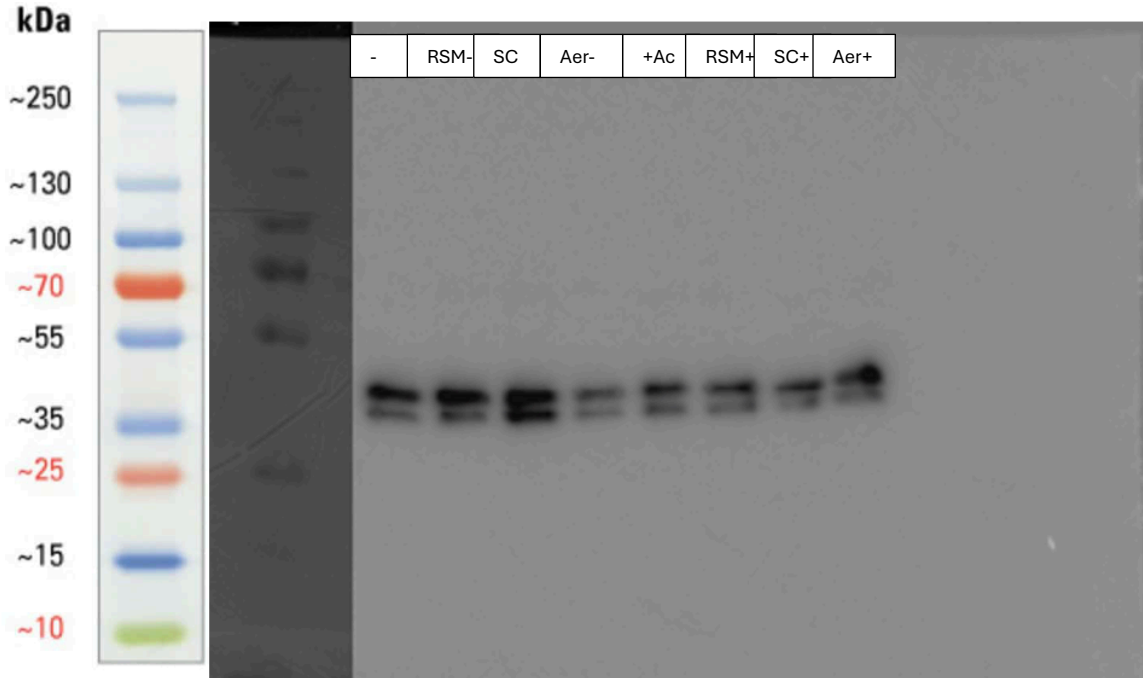

Figure 130: ***Total ERK 1/2 are expressed in activated JURKAT cells stimulated with fermentates RSM, SC40, and Aerobic R0033.*** *Plates were incubated for 24hours with 5ug/ml rabbit anti-mouse IgG at 4^{0}C. The following day the plates were incubated at 37^{0}C for 1 hour in the presence of CD3 5μg/ml, and at 1μg/ml Anti-CD28. JURKA**T** cells were seeded at 5x10^5 cells/mL, and incubated for 30minutes, and stimulated with 25mg/mL fermentates before incubating at 37^{0}C in 5% $CO_{2,..}$ Cell lysates were generated using the cell lysis buffer and procedure for quantification of protein was carried out (BCA) prior to carrying out SDS-PAGE and western blot procedure. PVDF membrane was imaged using G-Box and genesys software.*

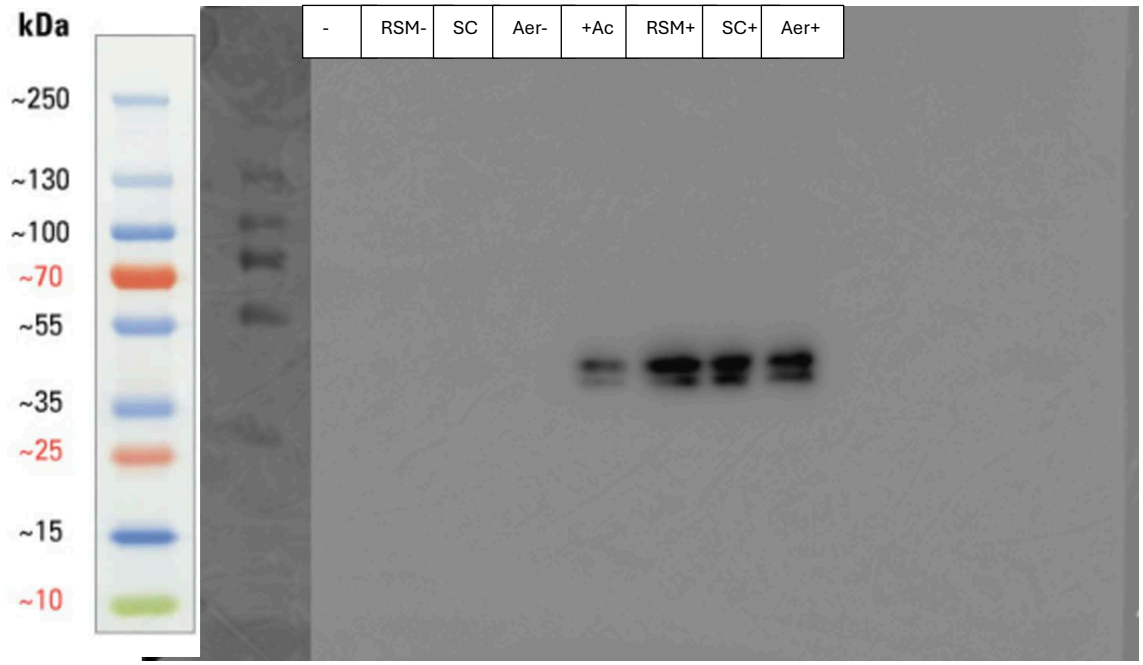

Figure 131: ***Phospho ERK 1/2 are expressed in activated JURKAT cells stimulated with fermentates RSM, SC40, and Aerobic R0033.*** *Plates were incubated for 24hours with 5ug/ml rabbit anti-mouse IgG at 4^{0}C. The following day the plates were incubated at 37^{0}C for 1 hour in the presence of CD3 5μg/ml, and at 1μg/ml Anti-CD28. JURKA**T** cells were seeded at 5x10^5 cells/mL, and incubated for 30minutes, and stimulated with 25mg/mL fermentates before incubating at 37^{0}C in 5% $CO_{2,..}$ Cell lysates were generated using the cell lysis buffer and procedure for quantification of protein was carried out (BCA) prior to carrying out SDS-PAGE and western blot procedure. PVDF membrane was imaged using G-Box and genesys software.*

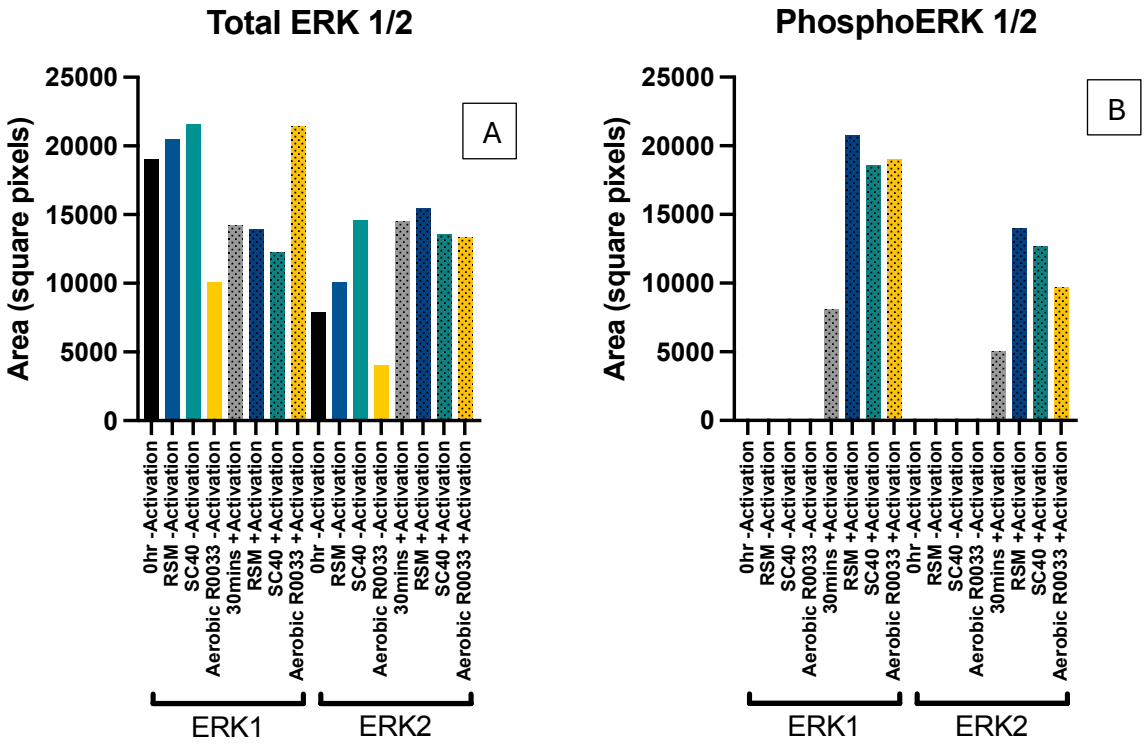

Figure 132: ***Total and Phospho ERK 1/2 are expressed in activated JURKAT cells stimulated with fermentates RSM, SC40, and Aerobic r0033.*** *Plates were incubated for 24hours with 5ug/ml rabbit anti-mouse IgG at 4^{0}C. The following day the plates were incubated at 37^{0}C for 1 hour in the presence of CD3 5μg/ml, and at 1μg/ml Anti-CD28. JURKA**T** cells were seeded at 5x10^5 cells/mL, and incubated for 30minutes, and stimulated with 25mg/mL fermentates before incubating at 37^{0}C in 5% $CO_{2,}$. Cell lysates were generated using the cell lysis buffer and procedure for quantification of protein was carried out (BCA) prior to carrying out SDS-PAGE and western blot procedure. PVDF membrane was imaged using G-Box and genesys software. Densitometry analysis was carried out using imageJ, and graphed using Graphpad Prism V.10.*

Therefore, we saw that the effect of fermentates was as a direct result of the interaction of fermentates with the signalling cascade that was the ERK1/2 signalling pathway, which resulted in the subsequent secretion of cytokines.

6.4 Discussion

This chapter aimed to explore the effects of the two candidate fermentates Aerobic R0033, and SC40 in T cells. T cells are a key cell which play a critical roles in the proper functioning of the adaptive immune system. This examination was carried out by assessing the samples effects on primary naïve CD4+ T cells, polarised Th1, Th2, Th17, and Treg cells, as well as on activated JURKAT cells, to assess cell proliferation and viability, cytokine secretion, cell migration, immune synapse interactions, and transcription marker expression.

T cells are key players in the adaptive immune response, that have receptors to recognise antigens from pathogens, tumours, and the environment, enabling them to elicit appropriate immune responses to invading pathogens, maintain immunological memory and prevent self-tolerance (Kumar et al., 2018). Upon stimulation with an antigen, the naïve T cell differentiates into a CD4+ helper T cell or an CD8+ cytotoxic effector T cell and memory T cells, to mediate direct killing, and regulate a diverse range of immunological functions, to aid in long term host protection (L. Sun et al., 2023). Abnormal T cell function can lead to disease susceptibility, autoimmunity and pathogenesis of disease. Thus T cells play a critical role in host defences and preventing disease pathogenesis, and thus it is important to understand how the fermentates affect them .

We first established that we could successfully differentiate naïve T cells into Th1, Th2, Th17, and Treg cells, with each of these subsets secreting the phenotypic cytokines and expressing the transcription factors associated with each T cell subset (Miltenyi Biotech, 2023).

In support of our findings thus far in macrophage and dendritic cells, Aerobic R0033, and SC40 maintained dual activity in T cells. The effects were dependent on the subset of T cells they were examined in, however, for the most part Aerobic R0033 and SC40 promoted a Treg phenotype, or Th2 phenotype in

undifferentiated T cells, Th1, Th17, and Treg cells. suggesting that they had more anti-inflammatory properties in T cells than immune boosting properties.

As is well documented in the literature, modulating T cell immune responses can be beneficial for both immunomodulation in support of viral immunity, and in the control of chronic inflammation for the management of diseases such as IBDs.

Viral Immunity:

It has previously been demonstrated that increasing Th1 phenotypic cytokines can aid in viral immunity. Increasing IL-2 has been found to accelerate viral clearance in mice models infected with influenza A virus , and lymphocytic choriomeningitis virus, while also regulating CD8 T cell responses (D'Souza et al., 2002; Zhou et al., 2021). IFN-γ has direct anti-viral effects in the treatment of many viruses including HCV, HPV, HSV-1, and HIV-1, in addition to its ability to activate immune cells and augment inflammation and antiviral functions, through its modulation of T cell and B cell differentiation and maturation (Kang et al., 2018). Decreased IL-2, and IFN-γ, and increased IL-4 and IL-10 has been linked with disease progression of AIDS, and thus IL-2 and IFN-γ are critical in support of viral immunity, as well as defense against viruses like HIV, highlighting the importance of the Th1/Th2 balance (Barcellini et al., 1994; Clerici et al., 1993; Spellberg & Edwards, 2001). Thus any sample that could enhance Th1 responses to increase IL-2 and IFN-γ could have the potential to support ant-viral immunity. SC40 may have the potential to aid in viral immunity as it enhanced Th1 responses, as well as increasing IL-2 secretion in Th2, and Th17 cells. Although Aerobic R0033 suppressed Th1 responses it did enhance IL-2 secretion in Th17 cells. Furthermore, SC40 and Aerobic R0033 in naïve T cells promote the secretion of IFN-γ and thus may further aid in viral immunity.

Th2 phenotypic responses typically hinder viral immunity. IL-4 is a key player in the development of Th2 cells and is therefore a regulator of Th1 type effector activity. IL-4 and IL-13 activity has been shown to negatively impact on viral clearance. In models of vaccinia virus IL-4 was proven to suppress antiviral

cytotoxicity in T cells, and number of cytotoxic T cells, coupled with a downregulation in IL-2, IFN-γ, and IL-12 gene expression, inhibiting NO production, hindering antimicrobial activity, and exacerbating viral infection (D. P. Sharma et al., 1996). In addition over production of IL-13 has been linked with the progression of severe/fatal COVID-19, (Deimel, Li, and Ranasinghe 2021). Thus any sample that could limit Th2 responses via reduced IL-4, and IL-13 may have the ability to enhance immunity against a range of different viral infections. SC40 and Aerobic R0033 suppressed Th2 responses, and thus may aid in supporting viral immunity by limiting the secretion of Th2 associated cytokines.

In contrast to the anti-viral abilities of IL-6 highlighted in previous chapters, it must be noted that Th17 phenotypic responses of increased IL-6 and IL-17 may work in synergy to suppress the ability of CD8+ cytotoxic T cells to function correctly and thus impact of the immune system's ability to fight viral infections, promoting viral persistence and inhibiting cellular apoptosis and cytotoxic cell function (Hou et al., 2014). Thus limiting a Th17 responses in viral immunity is key to enhance immunity and protection against viral infection. As SC40 enhanced the Th17 response it is important to consider that this is not overstimulated, while only a small enhancement of Th17 responses was seen in the presence of Aerobic R0033 suggests this sample may be more beneficial as an anti-viral.

Treg cells are important in viral immunity playing a protective role against viral infection (Okeke & Uzonna, 2019). In herpes simplex virus infected mice it is demonstrated that Tregs facilitate early protective responses to local viral infection to allow for the recruitment of immune cells (Lund et al., 2008). As outlined in previous chapters IL-10 is critical for the control of inflammation, and as an immune regulator in aiding in viral immunity, however in addition TGF-β is responsible for mediating tolerance, and development of and function of $FOXP3^+$ T cells (Okeke & Uzonna, 2019). Tregs are critical to viral immunity as they limit tissue damage and inflammation that occurs during viral infection (Veiga-Parga et al., 2013). Therefore any sample that could influence the Treg population has the ability to aid in viral immunity by means of restricting chronic inflammation, controlling immune responses, and producing characteristic

anti-inflammatory effects. Thus, SC40 and Aerobic R0033 not only enhance Treg responses but furthermore in the presence of Aerobic R0033 naïve T cells are promoted towards a Treg phenotype, suggests that these samples can aid in viral immunity through immune regulation, and restricting inflammation.

Previous research has demonstrated that other functional food components have the ability to positively impact on the immune system via their interactions with T cells to aid in viral immunity. Berberine has been shown to have a range of antiviral effects including anti-influenza, anti-hepatitis C, anti-cytomegalovirus, and anti-alphavirus (Z. Wang, Li, et al., 2021). In a study with influenza A/FM1/1/47 (H1N1) infected mice, berberine was shown to enhance the production of anti-inflammatory IL-4, while decreasing the excessive production of pro-inflammatory IFN-γ and TNF-α, increasing the Th1/Th2 and Th17/Treg ratios, suppressing viral replication, relieving pulmonary inflammation, and reducing necrosis, inflammatory cell infiltration, and pulmonary oedema induced by viral infection (Yan et al., 2018). Curcumin has been found to reduce the degree of severity in acute lung injury/ARDS, often an outcome of COVID-19 infection, via the promotion of the differentiation of naïve T cells to Treg cells, and the subsequent increase in anti-inflammatory IL-10 (Y. Chai et al., 2020). Additionally, nanocurcumin can upregulate Treg populations, and the expression of IL-10, IL-35, and TGF-β, in patients with mild, or severe COVID-19 infection (Tahmasebi et al., 2021). Ginseng has been found to support antiviral responses to respiratory syncytial virus (RSV), promoting a Th1 response via increased INF-γ, but simultaneously decreasing IL-4, reducing the inflammatory response (Lee et al., 2014).

Thus it is clear from current literature that functional food components which have the ability to enhance Treg differentiation, promote Th1 responses, modulate Th2 responses, enhance Treg responses, and regulate overproduction of Th17 response, such as Aerobic R0033, and SC40, could have potential to aid in the enhancement of innate and adaptive immunity.

Chronic Inflammation:

As outlined in the literature, dysregulation between the Th17/Treg balance plays a role in various chronic inflammatory disorders and enables disease progression particularly in IBDs (Luo et al., 2017). The production of proinflammatory cytokines by Th1 and Th17 cells can promote tissue inflammation, notably where increased IFN-γ, and IL-17 are significantly increased in patients with CD and murine intestinal inflammation models (Brand, 2009). Thus any sample with the ability to reduce IFN-γ (such as Aerobic R0033 in Th1 cells), and IL-17 could be considered beneficial in the management of chronic inflammation. On the other hand, IL-2 while being a pro-inflammatory cytokine secreted by Th1 cells, this cytokine is also necessary for controlling differentiation, survival, and promotion and proper functioning of Treg cells (Klatzmann & Abbas, 2015). Therefore it was important that our samples didn't over stimulate IL-2 to promote inflammation, but did however secrete this cytokine to allow for cell proliferation, and differentiation. IL-2 induces the activation of Treg cells, over Th17 cells and thus contributes to immune balance, regulating inflammation, mediating immunoregulation without immunosuppression (Klatzmann & Abbas, 2015). Low dose IL-2 has been reported to selectively expand Treg cells and is used as a therapeutic strategy in many diseases including, hepatitis C virus–induced vasculitis, systemic lupus erythematosus, Wiskott-Aldrich syndrome, and more recently UC (Goettel et al., 2019). Therefore any sample that increased IL-2 (such as SC40 in Th1 cells or SC40 and Aerobic R0033 in undifferentiated T cells) may be considered beneficial in the treatment of IBDs due to its promotion of the Treg differentiation and subsequent anti-inflammatory effect.

Due to the Treg cells roles in maintain immune homeostasis, immune balance, and antigen-specific suppressive capabilities, increasing Treg cells in IBDs is suggested as a potential therapy for IBDs, through its increased production of TGF-β, and IL-10 for resolution of chronic inflammation, characteristic to IBDs (Himmel et al., 2012). Furthermore, Treg cells have been found to be able to cure IBDs in mouse models of colitis (Mottet et al., 2003). Therefore Aerobic R0033 promoting naïve T cells into a Treg phenotype secreting

TGF-β, suggests a potentially powerful anti-inflammatory ability of this fermentate in inflammation resolution, in addition to the smaller increases in IL-10 seen in the presence of both SC40 and Aerobic R0033 in undifferentiated T cells.

Interestingly Th2 responses are situation specific and depending on the immune scenario, Th2 cells can act as anti-inflammatories to suppress IFN-γ and IL-17 inflammation, or can act as proinflammatory agents playing a role in the pathogenesis of UC (Bamias & Cominelli, 2015). Th2 cytokines are modulators of UC, and play important roles in intestinal immunity, wound healing, maintaining mucosal homeostasis, via protection from parasitic infections, and tissue repair (Bamias & Cominelli, 2015). However when Th2 responses become dysregulated they can lead to chronic inflammation, and the pathogenesis of chronic intestinal inflammation contributing to the development of UC, augmenting the mucosal and transmural fibrotic process in both CD and UC, with IL-4 and IL-13 being key drivers of this immune activation and inflammation (Bamias & Cominelli, 2015; Kasaian et al., 2014). Therefore the decrease seen in the presence of SC40 and Aerobic r0033 in IL-4, and IL-13 in Th2 cells may in fact then act as an anti-inflammatory to reduce the over secretion of IL-4, and IL-13 which can be associated with UC, and CD. It is important to consider the balance between Th1/Th2/T17 cells in the maintenance of a healthy functioning immune system for the control management and treatment of chronic inflammation associated with IBDs, where increased Tregs aid in immune balance.

Aerobic R0033, and SC40 both promoted the differentiation of naïve CD4+ T cells towards a Treg phenotype , secreting TGF-β, or Th2 cells secreting IL-4, and IL-13 suggesting it could potentially be used to control intestinal inflammation, and aid in inflammatory resolution, once these cytokines are produced in a controlled manner and do not become over stimulated to further exacerbate the chronic inflammation associated with IBDs. In Th1 cells where Aerobic R0033, and SC40 increased small concentrations of IL-4, IL-13, IL-10, TGF-β this suggests that the samples could play an anti-inflammatory role depending on the immune scenario of IL-4. In Th2 cells Aerobic R0033, and SC40 have

decreased secretion of IL-4, and IL-13, however increased IL-10, and TGF-β and thus have behave as anti-inflammatory, in conjugation with the increased IL-2 which has the potential to aid in Treg expansion and subsequent resolution of inflammation. In Th17 cells Aerobic R0033, and SC40 increased TGF-β, however in contrast there was also an increase in IL-4, and IL-17 suggesting these samples may promote further inflammation in Th17 cells. In Th17 cells SC40 also promoted IL-2, meaning SC40 may act more as an anti-inflammatory for resolution of inflammation in combination with the increased TGF-β. In Treg cells SC40, and Aerobic R0033 had clear anti-inflammatory effects with decreased IFN-γ, and increased TGF-β, both of which are so critical in the management of chronic inflammation. Therefore a role of SC40, and Aerobic R0033 as anti-inflammatories for the control and management of chronic inflammation has potential through their ability to reduce inflammatory cytokines including IFN-γ, while increasing anti-inflammatory cytokines TGF-β, and promoting Treg expansion through small increases in IL-2.

Previous research has demonstrated that other functional food components have the ability to positively impact on the immune system via their interactions with T cells to aid in the control of chronic inflammation associated with IBDs. In a study of 2,4,6-trinitrobenzene sulfonic acid (TNBS) induced colitis in mice, the traditional Chinese medicine berberine, was found to have protective effects in the mice, inhibiting levels of IFN-γ, IL-17, IL-6, IL-1β and TNF-α both in the local colon and sera, increased levels of IL-22, and increased sIgA expression in the colon, suppressing Th1 and Th17 responses, without effecting Treg cells for the treatment of IBDs (C. Li et al., 2015). Berberine has also been found to increase IL-4 expression, as well as reducing IL-1β, and TNF-α, to significantly improve colonic mucosal damage index scores in experimental rat models of UC (Jiang et al., 2021). In addition, Total glycoside of peony (TGP), has been found to increase concentrations of Treg associated immune responses to increase IL-10, and TGF-β cytokine secretion, as well as enhancing Treg differentiation and Treg cell concentrations, while simultaneously inhibiting levels of Th17-associated cytokines IL-17, IL-6, and TNF-α, suggesting TGP as a

treatment to ameliorate clinical status of colitis and reversing the severity of the disease (Lin et al., 2017). *Roseburia intestinalis* promotes the differentiation of Treg cells in TNBS-induced colitis, reducing Th17 production of IL-17 proinflammatory cytokine, to improve disease activity index scores, and improve signs of inflammation in the colon, suggesting its use in the treatment of IBDs (C. Zhu et al., 2018). Interestingly, curcumin has been found to decrease the expression of Th1 cytokines IL-12, IFN-γ, TNF-α, IL-1, while increasing the expression of Th2 cytokines IL-4, and IL-10 in colon mucosa, increasing the proportion of IFN-γ/IL-4 to therefore shift the Th1 response to a Th2 responses for therapeutic effects on TNBS-induced colitis (M. Zhang et al., 2006). Administration of Chrysanthemum polysaccharides have been found to restore levels of IL-13, IL-10, and IL-4 in TNBS-induced colitis rats, increasing the Th2 responses, while significantly decreasing the Th1 response of IL-6, IL-17, and IL-23, balancing the Th1/Th2, and Th17/Treg (Tao et al., 2017).

Thus it is clear from current literature that functional food components which have the ability to enhance Treg differentiation, balance Th1/Th2 and Th17/Treg responses, as we have shown both Aerobic R0033, and SC40 to do, have potential to aid in the control, management, and treat of inflammation.

In order to examine the effects on T cell functionality, the analysis was extended to include the human T cell line JURKAT cells, as these are a reliable, simple to use cell line, that are a good representation of how the cells would behave *in vivo*. We established that neither in the absence or presence of T cell activation, the stimulation of cells with fermentates SC40, and Aerobic R0033, or their RSM does not significantly affect cell proliferation at any exposure time to the fermentate. This confirms our hypothesis that the enhanced anti-inflammatory effects is in fact due to the fermentates ability to directly interact and aid in the differentiation of T cell subsets, shifting the T cells towards a Th2, or Treg profile, and not due to increased cell numbers present.

Additionally, the effect on IL-2 secretion was examined in JURKAT cells. IL-2 has many roles in adaptive immunity and is fundamental to the control of

differentiation and immune homeostasis, therefore it is critical in the control of immune regulation (Ross & Cantrell, 2018). IL-2 is necessary for T cell proliferation and is a key factor in T cell activation (Bachmann & Oxenius, 2007). SC40 had most impact on IL-2 secretion at exposure times of 24, 48, and 72 hours, while Aerobic R0033 had significant effect at the 72 hour exposure time. IL-2 has many benefits in controlling and enhancing both viral immunity through increased IL-2 secretion, and chronic inflammation associated with IBDs through IL-2 induction of Treg cells. It is well outlined in the literature, that increased IL-2 can aid in immune regulation. However as previously outlined it is important that this cytokine is not over produced as it is a Th1 phenotypic cytokine and over secretion could lead to inflammation. We clearly demonstrated that our samples did not promote the over secretion of IL-2.

After examining the effect on the cell proliferation and cytokine secretion we now wanted to examine the effect of fermentates on cell migration. Cell migration is critical for response to infection, tissue repair, and regeneration but also plays a role in disease progression for diseases including inflammatory diseases including CD, UC, as well as psoriasis, eczema, multiple sclerosis, Alzheimer disease, rheumatoid arthritis; asthma; arteriosclerosis; and juvenile diabetes, and cancer (Guak & Krawczyk, 2020; Luster et al., 2005; Ridley et al., 2003). Although cell migration can be considered to aid in inflammation due to the influx of cells to the site in question, it is important to consider the type of cells involved. From our analysis of fermentate effects in primary T cell subsets we know that our samples SC40, and Aerobic R0033 did in fact influence the T cell subset. SC40, and Aerobic R0033 as already highlighted, promoted a Treg or Th2 phenotype. These fermentates had the ability to alter the inflammatory status of the T cell subset, changing Th1, and Th17 cell subsets into the anti-inflammatory phenotypes of Th2, and Treg cells, while in Th2 and Treg cell subsets the samples continued to promote this phenotypic cytokine secretion. Additionally, in naïve T cells SC40 and Aerobic R0033 promote differentiation of T cells to Th2, and Treg populations. This means that in combination with this altered anti-inflammatory Treg/Th2 phenotype that cell migration to the site in

question will aid in inflammation resolution, due to the altered inflammatory status of the T cell subset. Treg cells are critical to inflammatory responses, whereby they migrate from peripheral tissues into draining lymph nodes, and together with resident lymph node Treg cells, they suppress immune responses (Ding et al., 2012). Therefore, increasing the cell migration of Treg cells can aid in inflammatory resolution, while additionally increased presence of enhanced numbers of Treg cells could also help in viral immunity as discussed. Our results showed that SC40, and Aerobic R0033 enhanced cell migration beyond that of the control chemokine of 3ng/ml SDF-1. At higher doses there was a further increase in cell migration particularly for SC40, where this significantly outperforms that of the RSM. It is important to manage this cell migration to avoid over influx of cells to the site of infection/inflammation.

Increasing cell migration as an aid in chronic inflammation is well documented in the literature. β-glucan prepared from *L. rhinocerotis* has been found to upregulate the expression of Cdc42, Rac1, and RhoA, enhance cell migration and proliferation, which ultimately lead to increased intestinal mucosal wound recovery, which is suggested as a potential candidate agent for the treatment of IBDs (X. Li et al., 2023; Veeraperumal et al., 2021). Ginseng berry extract has been found to promote the migration of $CD103^{+}CD11c^{+}$ cDCs and expansion of $Foxp3^{+}$ regulatory T cells in the colons of DSS-treated mice, leading to improved macroscopic and histological appearance of the colon wall compared to untreated control mice (W. Zhang et al., 2016). Our results could suggest a potential role for fermentates SC40, and Aerobic R0033 as compounds that increase cell migration for resolution of chronic inflammation and associated IBDs.

Having established some of the effects of fermentates on T cell functionality, it was now important to establish at what point do the fermentates exert this anti-inflammatory effect, from initiation of T cell activation at the immune cell synapse, or further downstream in the ERK1/2 signalling cascade leading to transcription marker expression and subsequent cytokine release.

Our findings showed that the fermentates had no significant effect on the immune synapse. This further confirmed for us that the effects on cytokine secretion could be considered as a direct result of the fermentates effect on T cell subsets and not enhancement of immune synapse interactions at the point of T cell activation.

Based on previous lab knowledge we hypothesised that the ERK1/2 signalling cascade may be responsible for the transcription of the observed cytokines secreted in response to fermentate presence. The ERK1/2 cascade is a key signalling pathway responsible for the regulation of stimulated cellular processes, including proliferation, survival, apoptosis, differentiation, as well as stress responses (Wortzel & Seger, 2011). ERK1/2 is a mitogen-activated protein kinase (MAPK) cascade that regulates such cellular processes via the relaying of extracellular signals to intracellular responses (Cargnello & Roux, 2011). This pathway also known as the Ras-Raf-MEK (MAP/ERK kinases)-ERK pathway is a chain of sequential phosphorylation by nearby seronine/tyrosine residues in the activation loop, leading to eventual transmission of the signal (Martin-Vega & Cobb, 2023). The ERK1 gene encodes the 44-kDa protein, while the ERK2 gene encodes the 42-kDa protein, both largely similar in functions and regulation (Wortzel & Seger, 2011).

Our results showed that both RSM, and SC40 had the ability to aid in enhancing total ERK1/2 protein present when T cells were not activated, but when T cells were activated these samples did not aid in the total ERK1/2 protein enhancement. Aerobic R0033 on the other had the opposite effect as it was only when T cells were activated and in the presence of Aerobic R0033 did the total ERK1 protein become increased, while total ERK2 remained largely unchanged. Furthermore when T cells were unactivated the presence of Aerobic R0033 decreased total ERK1/2 protein.

In the absence of T cell stimulation, the phospho ERK1/2 was not activated as expected. The presence of RSM, SC40, and Aerobic R0033 in activated T cells did however enhance phospho ERK1/2 activity. Enhancement seen on the activity of the phosphoERK1/2 pathway suggests that our samples aided in enhancing signalling activity in activated T cells, not only overall abundance of

ERK1/2 protein. Knowing that our cells shifted towards a Th2, and Treg profile in the presence of SC40, and Aerobic R0033, we can suggest that enhancement of the ERK1/2 pathway could be beneficial in aiding in the control, management, and treatment of chronic inflammation, including that of IBDs, through the subsequent enhanced release of these anti-inflammatory associated cytokines, facilitated by increased cell migration.

Other studies have exploited this knowledge of cytokine regulation through the enhancement of ERK1/2 for improvement of chronic inflammation. D-limonene has been suggested as a potential anti-inflammatory compound for treatment of UC, whereby it reduced MMP-2 and -9 mRNA expression levels via regulation of the iNOS, COX-2, PGE2, TGF-β and enhanced ERK1/2 signalling pathways in a UC rat model (Yu et al., 2017). Furthermore, luteolin, a natural bioactive compound has been found to activate the ERK1/2 signalling pathway, to attenuate symptoms of UC in DSS induced mice, improving colon tissue damage, reduced inflammation, apoptosis, and autophagy (Vukelić et al., 2020). Finally, in another study matrine an alkaloid derived from traditional Chinese herbs, aids in inflammation resolution, where it downregulated NF-κB pathway but upregulated ERK1/2 signalling pathway, and acted as an anti-rejection therapeutic post heart transplantation, but was further suggested as a novel immunosuppressive agent due to its anti-inflammatory effects, therefore suggesting its potential in IBDs (Zheng et al., 2021). Thus it is clear from the literature that enhancing downstream signalling of the ERK1/2 signalling cascade can have the potential to aid in inflammatory conditions including IBDs, thus suggesting the potential of SC40, and Aerobic R0033 in the same due to their demonstrated ability to enhance both total and phospho ERK1/2.

Therefore overall, we have demonstrated that SC40, and Aerobic R0033 interacted at the downstream signalling phase, to enhance the signalling of the ERK1/2 signalling cascade in activated T cells. Not only this but the presence of these fermentates shifted T cells towards a Th2 or a Treg profile, which in combination with the enhanced cell migration could suggest that these fermentates function in this way as anti-inflammatories and thus may be useful

for the control, and management of IBDs. Importantly we have demonstrated that this anti-inflammatory effect was due to the direct presence of sample itself, and not due to the sample enhancing cell numbers. Therefore this positioned SC40, and Aerobic R0033 as potentially powerful anti-inflammatory compounds that may be useful in the control, management and treatment of inflammatory conditions like that of IBDs.

7 Chapter 7

Final Discussion

7.1 Project Overview

Figure 133 is a diagrammatic representation of the project flow and overall chapter findings and results. Through our screening and examination, we have been able to highlight the candidate immune boosting and anti-inflammatory fermentates that we hypothesis can support viral immunity and aid in management of chronic inflammation.

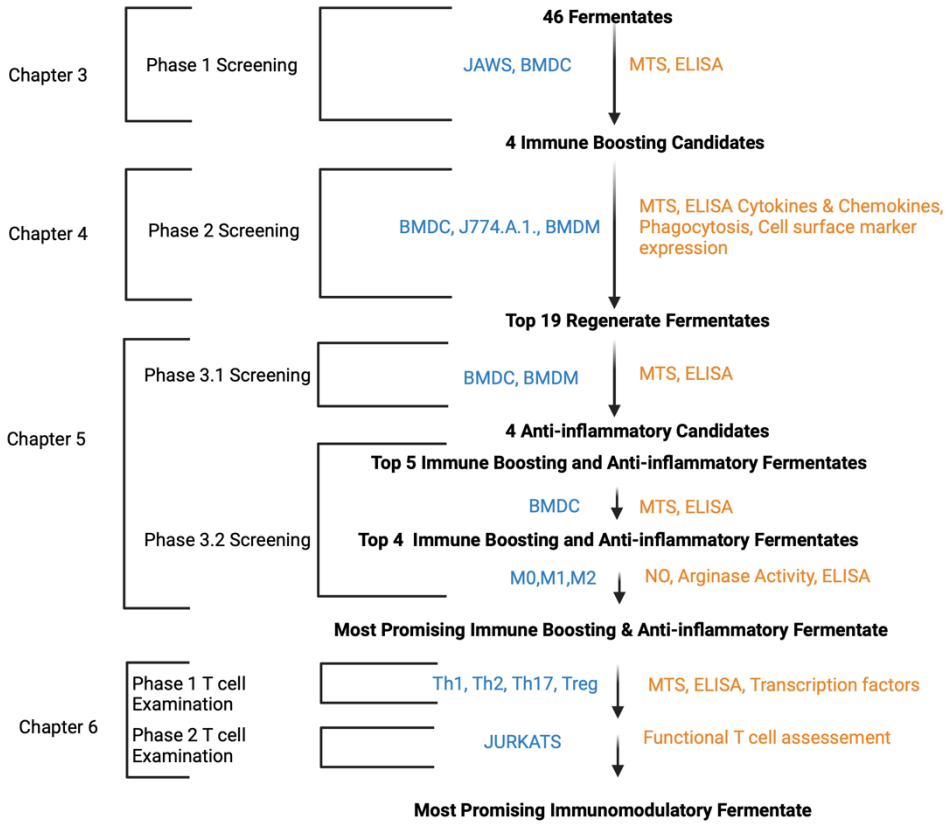

Figure 133: ***Diagrammatic representation of project.*** *Fermentates were screened starting with broad phase screening for immune boosting and anti-inflammatory capabilities. Assays used to determine candidate fermentates for further testing include MTS viability, ELISA cytokine and chemokine analysis, phagocytosis and cell surface marker expression. A range of dendritic and macrophage cell types were examined including cell lines JAWS and J774.A.1 as well as primary BMDC and BMDM. Promising candidates were regenerated and rescreened confirming bioactivity and ensuring reproducibility. Candidate numbers were filtered down to 2 immune boosting candidates and 2 anti-inflammatory candidates to undergo further examination of effect on polarised macrophage. Most promising candidate immune boosting and anti-inflammatory sample screened extensively in T cells. Cells used highlighted in blue, assay highlighted in orange and chapter outcomes highlighted in* ***bold****.* Created using BioRender.com.

7.2 Diet, global threats, and immune fitness:

In recent years, as a result of the increase in awareness of the impact of diet on health, there has been a significant shift in the interest of consumers towards food that can improve human health. As outlined in Chapter 1, there is a growing need for a more sustainable and natural way of supporting and fortifying the immune system, due to threat of virus outbreaks as well as the significant rise in chronic inflammatory disorders. Nutrition is closely linked to proper functioning of the immune system, meaning what we eat has a huge influence over our immune response, making us more or less likely to suffer from infections or inflammatory disease (Christ et al., 2019). As we have demonstrated throughout our chapters the literature clearly demonstrates that diet has a huge impact on human health and plays a key role in development of infectious disease, including viral infections such as COVID-19 and seasonal influenza. Not only this but diet also plays a role in the development of diet related disorders including IBDs such as UC, and CD, but also other diet related illnesses like diabetes, heart disease, and stroke (NIH, 2017). It is long understood that the plant-based Mediterranean diet, consisting largely of cereals, legumes, vegetables, fruits, olive oil, and nuts, provides fibre with prebiotic activity, polyunsaturated fatty acids with anti-inflammatory properties, bioactive compounds with antioxidative properties, and vitamins and minerals, all aid in the modulation of the microbiota, the activation of the host immunity, and, ultimately, promote health and disease prevention (Pérez-Cano, 2022). On the other hand, the Western diet is associated with high animal protein, digestible sugars, and fat, while also being low in fibre (Cordain et al., 2005). Observational studies have linked the Western diet to the risk and development of IBD, such as CD and UC, as well as other immune diseases, including asthma and allergy, while also coinciding with an increase in autoimmune diseases (Bach, 2002; Eder et al., 2006; Lewis, 2016; Wypych et al., 2017). The differing effects of the Mediterranean and Western diets

demonstrate that differing dietary patterns have differential effects on the immune system and overall health.

Viruses pose a significant global threat which was seen clearly during the recent COVID-19 pandemic. Not only this but we have since seen the emergence of other viral outbreaks including the monkeypox virus, pangolin virus, most recently, the Langya virus, and thus boosting the immune system is becoming increasingly important. The coronavirus became a public health emergency of international concern on the 30th January 2020, and subsequently was declared a global pandemic on the 11th March 2020 as stated by the WHO, therefore taking just 51 days to become a highly concerning international threat to human life. The scientific community came together like never before to tackle this issue as quick as possible however the high infectivity, and mutation rate made this challenge even greater than anticipated. Despite this the scientific community were able to develop a vaccine which became available on the 11th December 2020 (Office of the Food and Drug Administration, 2021). However, this meant that for 9 months all of global civilisation were in fear of contracting this potential deadly virus. In conjunction with this, a poor diet can compromise the immune system, leaving the host more susceptible to pathogenic infection, including viral infections. Viruses have the capability of spreading rapidly from person to person, causing devastating damage to humanity due to their potential for high transmissibility. Therefore, there is an urgent need to explore new ways of enhancing viral immunity, to support the body in its antiviral defense mechanisms. Fermented food has long been documented to provide antiviral protection and, therefore, can be used as a first-line strategy to boost the immune system in the form of functional foods to enhance protection against new, emerging viral infections as well as well-established viruses, including the influenza virus (Atherton et al., 1978; Chihara, G. O. R. O., 1993; Finnegan et al., 2023; Hayashi et al., 1996; Khan et al., 2005; Rahman et al., 2021; Schandalik et al., 1992; Takehara et al., 1979; Tochikura et al., 1987).

IBD prevalence is increasing globally, affecting over 10 million people worldwide and with no known cure, or cause, alternative ways of modulating the immune system to target the chronic inflammation seen in such chronic diseases is becoming increasingly important (Alatab et al., 2020; CDC, 2022a; EFCCA, 2022).

Treatment of inflammatory disorders such as IBDs, including UC and CD, often involve invasive surgical measure for the resolution of the life altering symptoms associated with IBDs. IBDs are a lifelong uncurable conditions that are often associated with the modern western diet. IBDs have painful, and life altering symptoms that effect the patient not only physically, but also mentally, with symptoms including diarrhoea, stomach cramps, incontinence, malnutrition, which can lead to poor self-image, and thus negatively can impact of mental health. Therefore, with such a devastating condition linked to diet, finding a novel functional food ingredient that can be consumed as part of a natural and healthy diet is of increasing importance. In addition, oral treatments for IBDs are often not very palatable, and therefore a more natural means of treatment is highly sought after (Lewis, 2016). Such natural functional food ingredients will have less adverse effects on the body unlike those of traditional medicine which may lead to increased prevalence of polypharmacy. This means more potential adverse effects from consumption of traditional medicines could lead to more adverse side effects including constipation, diarrhoea, or upset stomachs, and the need for further intake of traditional medicines. Thus supporting traditional medicine with functional foods may be the answer to such adverse side effects, while simultaneously supporting viral immunity and control on inflammation.

As we have demonstrated in each of our chapter discussions, functional food ingredients are powerful immunomodulators. We suggest that functional food ingredients can improve overall human health by enhancing immune fitness. Immune fitness can be viewed as the establishment of core lifestyle habits that can improve your immune capacity, including good eating habits, good social relationships, abstinence from smoking, limiting alcohol consumption, and controlling stress levels, all of which can slow down the process of aging on the immune system (Villar-Álvarez et al., 2022). Immune fitness describes the capacity of the body to respond to health challenges, such as infection, via activation of the appropriate immune response in order to prompt disease resolution, prevent pathogen infection, and promote health, thereby ensuring quality of life (van de Loo et al., 2020). Immune fitness refers to a resilient immune system with the “built-in”

capacity to adapt to challenges by establishing, maintaining, and regulating an appropriate immune response (Danone Nutricia Research, 2022). This means that the individual's immune system is robust enough to eliminate harmful pathogens, such as viruses and bacteria, while simultaneously being able to tolerate harmless ones, such as food antigens. In doing so, this prevents the body from entering into a hyporesponsive state of weakened immunity, leading to increased infection, and from entering into a hyperresponsive state, leading to allergy and autoimmune diseases including UC and CD (Danone Nutricia Research, 2022). Therefore functional foods can enhance immune fitness through improvement in diet by the addition of fortified functional food ingredients.

7.3 Traditional fermented foods and our novel fermentates:

It is well documented in the literature that fermented foods can be used to support and boost immune responses in humans. Therefore we suggest the role of fermented foods as functional foods in support of immune fitness to provide enhanced viral immunity, and aid in the control and management of chronic inflammation associated with IBDs. Traditional dairy fermented foods have been long documented for their anti-viral and anti-inflammatory qualities and include traditional functional foods such as kefir, yogurt, and Koumiss.

Kefir, has been noted for its antiviral and anti-inflammatory potential, inhibiting ACE levels and cholesterol metabolism, aiding in wound healing, suppressing tumour growth, altering the immune system to improve allergy symptoms, suppressing viral activity via modulation of immune responses, and causing disruption of viral adhesion, as well as acting as an anti-inflammatory agent inhibiting proinflammatory cytokines (Hamida et al., 2021). Kefir is thought to exert this antiviral activity by direct probiotic–virus interaction and trapping, production of antiviral inhibitory metabolites, and/or via stimulation of the immune system for the development of bacteriocins, lactic acid, and hydrogen peroxide as antiviral

agents (Al Kassaa et al., 2014). Additionally, kefir modulates gut microbiota composition, regulates low-grade inflammation, controls intestinal permeability, and regulates gut homeostasis, thus, it is a potentially powerful functional food for those suffering from IBDs (Peluzio et al., 2021; Pražnikar et al., 2020).

Similarly, yogurt is a fermented milk product containing cultures of *Lactobacillus bulgaricus* and *Streptococcus thermophilus* that are known for their ACE inhibitory effects and, therefore, may be effective in counteracting viral infection (Freitas, 2017; Gouda et al., 2021). In addition, yogurt has been linked with improvements in gut health, reduced chronic inflammation by enhancing innate and adaptive immune responses, and improved intestinal barrier function, by upregulating the expression of autophagy, tight junction proteins, and anti-microbial peptide-related genes, which all play a key role in maintaining a healthy gut barrier function through interaction with the intestinal epithelium (Freitas, 2017; Popovic et al., 2020). Furthermore, yogurt also increases anti-inflammatory cytokines while simultaneously reducing proinflammatory cytokines, thus playing a key anti-inflammatory role, and therefore overall is useful in the control, management and treatment of the chronic inflammation associated with IBDs (De Moreno de LeBlanc & Perdigón, 2010)

Lastly, koumiss is a traditional fermented dairy product made from fermented mare's milk originating in Mongolia, that has been shown to have immunomodulatory capabilities by virtue of its ability to reduce key proinflammatory cytokines involved chronic inflammation, as well being contributors to the cytokine storm seen in COVID-19 infection and thus also aids in viral infection (Tang et al., 2020; Ya et al., 2008; Yao et al., 2017). Koumiss has been shown to increase IFN-γ, playing a critical role in maintaining the gut barrier function, enhancing the production of sIgA, inducing gut mucosal responses, and preventing infection by inhibiting the attachment of bacteria and viruses within the gastrointestinal system (Fukushima et al., 1998; Ya et al., 2008).

Overall, traditional fermented dairy products can be considered functional foods with the potential to protect against viral infection, and aid in resolution of chronic inflammation associated with IBDs. Our research explored the possibility of

developing a novel fermented food ingredient for commercial use, that could potentially aid in viral immunity, and chronic inflammation associated with IBDs.

From our findings it is clear that our novel fermentates derived from fermented dairy LAB can indeed act as immunomodulators with potential not only for enhancing and supporting viral immunity but also for aiding in the control, management, and treatment of chronic inflammation, thus enhancing the body's overall immune fitness. Such ingredients could therefore be considered as functional food ingredients for enhanced immunity in the context of supporting viral immunity and anti-inflammatories for possible management of chronic inflammation. The development of such natural means of fortification of the immune system are highly desirable in the context of viral immunity, and resolution of chronic inflammation to aid in boosting and supporting immune fitness.

Throughout the course of our experiments we have been able to identify four fermentates with the ability to enhance and support viral immunity; Aerobic R0033, Anaerobic R0033, SC40, and R0419. These fermentates enhanced the secretion of immune boosting cytokines in a range of key innate immune cells, including macrophage, and dendritic cells. These samples also enhanced phagocytosis, and maintained sufficient cell surface marker expression, and chemokine secretion needed for strong viral immunity. Additionally, samples LH88, and SC40 were highlighted as anti-inflammatory, whereby these samples decreased the secretion of proinflammatory cytokine release associated with uncontrolled inflammation and cell infiltration, while simultaneously enhancing the secretion of anti-inflammatory cytokines that maintain immune homeostasis, and inflammation resolution. In the interest of the industry partners and commercial development of a functional food ingredient, two samples were deemed the lead candidates with immune boosting, and anti-inflammatory activity; Aerobic R0033, and SC40. Our further analysis of these fermentates extended to their effects on the adaptive immune response. With this examination we showed that both Aerobic R0033, and SC40 have a largely anti-inflammatory profiles in primary T cells, and the JURKAT T cell line, which positively affected cytokine secretion, and cell migration, with cell proliferation not effected. Furthermore we were able to establish the fermentates

mechanism of action was at the downstream signalling phase, as they had no effect on the immune synapse but did enhance downstream ERK1/2 activation in activated T cells. Given our data generated across all immune cell types, we propose that both Aerobic R0033, and SC40 are immunomodulators in the context of both viral immunity, and chronic inflammation.

Overall, with our knowledge of increased viral prevalence, in a world of ever-increasing accessibility and travel, we suggest a supportive role for fermentates such as SC40 and Aerobic R0033 as common ingredients to be used in fortified foods for consumption, that will aid in the improved health of the immune system against viral infection. Additionally, in the modern, fast paced life, poorer diets and higher consumption of a western diet is on the rise, and therefore we suggest a supportive role for fermentates SC40 and Aerobic R0033 as functional food ingredients to fortify foods, to aid in the control, treatment, and management of chronic inflammation often associated with dietary inflammatory disorders like UC and CD. Furthermore, given the commercial feasibility of SC40, this fermentate has now been progressed to human trials to assess its efficacy at controlling gut inflammation. Additionally SC40 has undergone tasting tests and has scored quiet successfully in such testing's. This may further support the commercial feasibility of such a functional food ingredient.

7.4 The future of functional food ingredients:

Functional foods are an evolving scientific area with expanding interest as discussed in chapter 1. We believe our research into novel fermentates grown through fermentation of LAB in reconstituted skimmed milk is novel and has the potential to go far in this area, where already we are seeing increased publication of fermented LAB as immunomodulators. The idea of "fermentates" is relativity

new, however there is already one known commercial fermentate already available on the market for support in viral immunity. This fermentate is called EpiCor, an oral fermentation product, derived from *Saccharomyces cerevisiae* (*S. cerevisiae*), with the potential of enhancing the immune system to protect and aid in defense against cold/flu-like symptoms (Moyad et al., 2008, 2010). In these two 12-week randomized, double-blind, placebo-controlled trials, it was proven that this oral over-the-counter fermentate had the ability to reduce the incidence of cold and flu-like symptoms in both individuals with and without a history of influenza vaccination (Moyad et al., 2010). These studies show the potential of fermentates for the protection and prevention of viral infections and thus warrant further investigation into their potential uses against COVID-19 as well as other viral infections. As we have previously demonstrated we can see that fermented foods have a well-established immunosupportive role, and exploiting this we can continue to consume traditional fermented foods, while it is likely that there will be an increase in the development of commercial fermented products similar to the likes of EpiCor.

Not only this but functional foods in general are potentially powerful tools in supporting human health. Using food as a means of supporting immune health and fitness is well established. Common household consumables such as milk are an obvious everyday functional food fortified to improve human health. The idea of such a product is the commercial basis for the development of other functional food ingredients like fermentates. Milk is often fortified with other functional food ingredients to provide additional positive immunosupportive effects. Such functional food ingredients used to fortify milk often include omega 3 poly unsaturated fatty acids (PUFA), and vitamin D, which are well established immunosupportive functional foods in the literature with demonstrated anti-viral, and anti-inflammatory effects for control and management of IBDs.

PUFAs act as substrates for proinflammatory and anti-inflammatory mediators, including prostaglandins, leukotrienes, thromboxanes, protectins, and resolvins, as well as for specialized pro-resolving lipid mediators (SPMs), which are critical chemical mediators needed for the stimulation of the resolution of

inflammatory responses (Chiang & Serhan, 2020; Hathaway et al., 2020). Omega-3 PUFA eicosapentaenoic acid (EPA) and docosahexaenoic acid (DHA) act as the substrate for SPM, while, in contrast, omega-6 PUFA arachidonic acid (AA) is the substrate for eicosanoids, including leukotrienes and prostaglandins, generated through the lipoxygenase and cyclooxygenase pathways (Arnardottir et al., 2021). Omega-3-derived pro-resolving mediator protectin D1 has been associated with antiviral effects and inhibiting influenza viral replication in experimental models and thus warrants further investigation for its additive effect as a potential antiviral treatment for other infections, such as COVID-19 (Arnardottir et al., 2021). Omega-3 PUFAs, including DHA-derived protectins and EPA-derived RvE1, have antiviral properties, with protectin D1 isomer (PDX) suppressing influenza virus replication through inhibition of the nuclear export of viral mRNA (Imai, 2015). Furthermore, a link has been found between the supportive role of SPMs in ARDS (acute respiratory distress syndrome) and acute lung injury (Darwesh et al., 2021). Omega-3 supplementation has been shown to significantly improve ARDS patient status, including shorter duration of mechanical ventilation, shorter ICU stay, and significant decrease in ARDS mortality, and infectious complications remained unchanged (Arnardottir et al., 2021). These studies highlight the potential of omega-3 PUFAs as natural therapeutics for the treatment and prevention of viral infection, including influenza and COVID-19, via their direct inhibition of viral replication. Additionally, it is hypothesised that by increasing omega-3 PUFAs and decreasing omega-6 PUFAs, one can skew the immune response in favour of the resolution of inflammation by favouring higher concentrations of resolvin/protectin rather than leukotriene/prostaglandin (Arnardottir et al., 2021; Thul et al., 2017). Omega-3 FAs are known to produce less pro-inflammatory cytokines; thus by increasing their intake as part of the diet, one could decrease viral entry, boost immune function, and even decrease the severity of disease in COVID-19 patients by virtue of altering the overdrive in immune response seen as the resultant cytokine storm (Hathaway et al., 2020). Furthermore, long chain AA, EPA, and DHA have been shown to enhance epithelial barrier integrity as well as reduce IL-4-mediated permeability in gut (Willemsen et al., 2008). Interestingly, a diet containing 18 g of fish oil/day for 12 weeks increased colonic concentrations of EPA and DHA while decreasing mucosal

AA content in IBD (Hillier et al., 1991). Omega-3 PUFAs have the ability to modulate the gut microbiota, and have been shown to increase the abundance of several genera of gut microbes, including *Bifidobacterium* and *Roseburia,* where *Bifidobacterium* and *Lactobacillus* have also been shown to improve clinical symptoms in IBDs (Bellenger et al., 2021; Selverajah et al., 2016; Watson et al., 2018).

Another common functional food ingredient used to fortify milk is vitamin D. Vitamin D is a crucial vitamin that helps regulate the amount of calcium and phosphate in the body in order to keep the bones and teeth strong and healthy, prevent the harmful effects of excess vitamin A, and prevent diseases like rickets and osteoporosis (Health Service Executive, 2011; National Institute of Health, 2021). Vitamin D is needed for muscle movement, nerve functioning, and for the immune system in helping to fight off invading bacteria and viruses (National Institute of Health, 2021). The vitamin D receptor is expressed on immune cells, including B cells, T cells, and APCs, which can synthesize the active vitamin D metabolite and therefore can potentially modulate both the innate and adaptive immune response, as deficiency in vitamin D is associated with increased susceptibility to infection (Aranow, 2011). It has been reported that poor nutrition and/or lack of sun exposure observed through low vitamin D levels contributes to severe disease and the progression of ARDS in some patients infected with COVID-19, while, similarly, low vitamin D levels in the active form of 1,25-dihydroxyvitamin D (1,25OHD) allow for proinflammatory molecules to trigger the subsequent development of ARDS in patients with COVID-19-associated pneumonia (Faul et al., 2021). McCartney suggests that Irish adults should have an intake of 20–25 micrograms (800–1000 iu) of vitamin D per day for the duration of the COVID-19 pandemic, taken with food in order to achieve the critical 50 nanomoles per litre blood of vitamin D where immunity against COVID-19 can be enhanced (McCartney & Byrne, 2020; Walsh, 2021). Additionally, Vitamin D is predominantly present in the skin and thus functions in its active form, 1,25-dihydroxyvitamin D, along with vitamin D receptor (1,25OHD or VDR) to aid the immune system by maintaining tight junctions, gap junctions, and adherens junctions in the innate immune system (Sundararaman et al., 2020). Vitamin D supports the integrity of the epithelial barrier

via the increased expression of VDR-associated intracellular junction proteins that constitute tight junctions between epithelial cells and include occludin, claudin, vinculin, ZO-1, and ZO-2 (Y.-G. Zhang et al., 2013). VDR is expressed in various tissues, including the skin, parathyroid gland, adipocyte, small intestines, and colon, and thus is widely expressed within the body, including within the gut; this means it could act as a therapeutic target where gut immunity is weakened and can aid in the treatment of IBDs (Battistini et al., 2021). Vitamin D and VDR deficiency are associated with the pathogenesis of IBDs and is linked to elevated claudin-2 junction protein in inflammatory responses and therefore plays a critical role in intestinal barrier function (Y.-G. Zhang et al., 2019). VDR influences individual bacterial taxa, including *Parabacteroides*, where a much lower abundance of *Parabacteroides* are seen in UC and CD patients (J. Wang et al., 2016). Deficiency in vitamin D negatively impacts Treg differentiation and weakens its function, thus leading to the triggering of autoimmune diseases, including IBDs (W.-C. Lim et al., 2005).

Further to this, in a world where increased importance needs to be put on sustainability, plant proteins are becoming an emerging area of interest in the scope of functional food ingredients. Virgin coconut oil (VCO), and extra virgin olive oil (EVOO) are two powerful natural plant based immunomodulators which may be considered the future of functional food ingredients (Finnegan et al., 2023).

VCO comes from the coconuts of coconut palm trees (Cocos nucifera), and is rich in nutrients, vitamins, and minerals, including vitamin E, palmitic acid, lauric acid, monolaurin, plant sterols, and bioactive compounds, including polyphenols, sterols, and tocopherols (Angeles-Agdeppa et al., 2021; Joshi et al., 2020; WebMD, 2020). VCO has been noted for its anti-inflammatory, analgesic, gut microbiota modulator, anti-stress, antioxidant, and antimicrobial activities (Djurasevic et al., 2018; Dumancas et al., 2016; Intahphuak et al., 2010; Yeap et al., 2015). Therefore, VCO is a potent functional food that possesses many desirable qualities that could aid in the boosting of immune fitness. VCO has been highlighted as a potential antiviral functional food with the ability to lower CRP levels among suspect and probable COVID-19-infected patients, aiding in faster recovery from viral infection (Angeles-Agdeppa et al., 2021). Additionally, VCO has been found to inhibit key

inflammatory cytokines involved in chronic inflammation and thus could be useful in the management of IBDs (Varma et al., 2018).

EVOO is the least processed variety of olive oil, extracted from olives of the olive tree (Olea europaea) (Komatsuzaki et al., 2021). EVOO is rich in vitamins and minerals, including vitamin E, vitamin K, polyunsaturated fatty acids, oleic acid, and phenolic compounds like that of oleuropein and hydroxytyrosol (Jimenez-Lopez et al., 2020; Omar, 2010; Vrdoljak et al., 2022). In the US, a patent has been created that uses a naturally occurring secoiridoid glucoside oleuropein compound from Oleaceae plants in the treatment of viral diseases, such as hepatitis, mononucleosis, shingles, herpes, influenza, the common cold, and viral types causing leukaemia (Fredrickson, 2000). Additionally, positive effects are seen on gut microbiota when EVOO is consumed via the reduction in pathogenic bacteria, the stimulation of beneficial bacteria, and the increase in the production of microbially produced short-chain fatty acids (SCFAs) to exert a wide range of anti-inflammatory effects (Millman et al., 2021). EVOO influences intestinal mucosa and supports gut homeostasis by encouraging intestinal IgA production (Martín-Peláez et al., 2016). Polyphenolic compounds from EVOO have been linked to reduced T cell activation and proliferation as well as reduced proinflammatory cytokine secretion and could have positive effects on reduction of chronic inflammation seen in IBDs (Alvarez-Laderas et al., 2020).

Going forward, research into novel functional foods may provide global supportive solutions to both the chronic health issues as well as the future food challenges. This thesis clearly demonstrates that using bacteria to generate novel fermentates could play a significant role in generating these supportive global solutions to major health concerns.

References

Aarreberg, L. D., Wilkins, C., Ramos, H. J., Green, R., Davis, M. A., Chow, K., & Gale, M. (2018). Interleukin-1β Signaling in Dendritic Cells Induces Antiviral Interferon Responses. *mBio*, *9*(2), e00342-18. https://doi.org/10.1128/mBio.00342-18

Abron, J. D., Singh, N. P., Price, R. L., Nagarkatti, M., Nagarkatti, P. S., & Singh, U. P. (2018). Genistein induces macrophage polarization and systemic cytokine to ameliorate experimental colitis. *PLOS ONE*, *13*(7), e0199631. https://doi.org/10.1371/journal.pone.0199631

Akdis, M., Aab, A., Altunbulakli, C., Azkur, K., Costa, R. A., Crameri, R., Duan, S., Eiwegger, T., Eljaszewicz, A., Ferstl, R., Frei, R., Garbani, M., Globinska, A., Hess, L., Huitema, C., Kubo, T., Komlosi, Z., Konieczna, P., Kovacs, N., … Akdis, C. A. (2016). Interleukins (from IL-1 to IL-38), interferons, transforming growth factor β, and TNF-α: Receptors, functions, and roles in diseases. *Journal of Allergy and Clinical Immunology*, *138*(4), 984–1010. https://doi.org/10.1016/j.jaci.2016.06.033

Al Kassaa, I., Hober, D., Hamze, M., Chihib, N. E., & Drider, D. (2014). Antiviral Potential of Lactic Acid Bacteria and Their Bacteriocins. *Probiotics and Antimicrobial Proteins*, *6*(3), 177–185. https://doi.org/10.1007/s12602-014-9162-6

Alatab, S., Sepanlou, S. G., Ikuta, K., Vahedi, H., Bisignano, C., Safiri, S., Sadeghi, A., Nixon, M. R., Abdoli, A., Abolhassani, H., Alipour, V., Almadi, M. A. H., Almasi-Hashiani, A., Anushiravani, A., Arabloo, J., Atique, S., Awasthi, A.,

Badawi, A., Baig, A. A. A., … Naghavi, M. (2020). The global, regional, and national burden of inflammatory bowel disease in 195 countries and territories, 1990–2017: A systematic analysis for the Global Burden of Disease Study 2017. *The Lancet Gastroenterology & Hepatology*, *5*(1), 17–30. https://doi.org/10.1016/S2468-1253(19)30333-4

Alexopoulou, L., Holt, A. C., Medzhitov, R., & Flavell, R. A. (2001). Recognition of double-stranded RNA and activation of NF-kappaB by Toll-like receptor 3. *Nature*, *413*(6857), 732–738. https://doi.org/10.1038/35099560

Allegretti, J., Canavan, J., Mitsialis, V., Hamilton, M., Carrellas, M., Freer, K., Green, J., Gringauz, J., Herwood, N., Hurtado, J., Kelly, R., Rourke, C., Whitcomb, S., Bousvaros, A., Korzenik, J., & Snapper, S. (2021). LOW DOSE IL-2 FOR THE TREATMENT OF MODERATE TO SEVERE ULCERATIVE COLITIS. *Inflammatory Bowel Diseases*, *27*(Supplement_1), S6–S7. https://doi.org/10.1093/ibd/izaa347.016

Alvarez-Laderas, I., Ramos, T. L., Medrano, M., Caracuel-García, R., Barbado, M. V., Sánchez-Hidalgo, M., Zamora, R., Alarcón-de-la-Lastra, C., Hidalgo, F. J., Piruat, J. I., Caballero-Velázquez, T., & Pérez-Simón, J. A. (2020). Polyphenolic Extract (PE) from Olive Oil Exerts a Potent Immunomodulatory Effect and Prevents Graft-versus-Host Disease in a Mouse Model. *Biology of Blood and Marrow Transplantation*, *26*(4), 615–624. https://doi.org/10.1016/j.bbmt.2019.11.019

Amsden, H., Kourko, O., Roth, M., & Gee, K. (2022). Antiviral Activities of Interleukin-27: A Partner for Interferons? *Frontiers in Immunology*, *13*, 902853. https://doi.org/10.3389/fimmu.2022.902853

Andrews, T., & Sullivan, K. E. (2003). Infections in Patients with Inherited Defects in Phagocytic Function. *Clinical Microbiology Reviews*, *16*(4), 597–621. https://doi.org/10.1128/cmr.16.4.597-621.2003

Angeles-Agdeppa, I., Nacis, J. S., Capanzana, M. V., Dayrit, F. M., & Tanda, K. V. (2021). Virgin coconut oil is effective in lowering C-reactive protein levels among suspect and probable cases of COVID-19. *Journal of Functional Foods*, *83*, 104557. https://doi.org/10.1016/j.jff.2021.104557

Apte, R. N., Dotan, S., Elkabets, M., White, M. R., Reich, E., Carmi, Y., Song, X., Dvozkin, T., Krelin, Y., & Voronov, E. (2006). The involvement of IL-1 in tumorigenesis, tumor invasiveness, metastasis and tumor-host interactions. *Cancer and Metastasis Reviews*, *25*(3), 387–408. https://doi.org/10.1007/s10555-006-9004-4

Aranow, C. (2011). Vitamin D and the immune system. *Journal of Investigative Medicine: The Official Publication of the American Federation for Clinical Research*, *59*(6), 881–886. https://doi.org/10.2310/JIM.0b013e31821b8755

Arenas-Ramirez, N., Woytschak, J., & Boyman, O. (2015). Interleukin-2: Biology, Design and Application. *Trends in Immunology*, *36*(12), 763–777. https://doi.org/10.1016/j.it.2015.10.003

Arnardottir, H., Pawelzik, S.-C., Öhlund Wistbacka, U., Artiach, G., Hofmann, R., Reinholdsson, I., Braunschweig, F., Tornvall, P., Religa, D., & Bäck, M. (2021). Stimulating the Resolution of Inflammation Through Omega-3 Polyunsaturated Fatty Acids in COVID-19: Rationale for the COVID-Omega-F Trial. *Frontiers in Physiology*, *11*. https://www.frontiersin.org/articles/10.3389/fphys.2020.624657

Arulselvan, P., Fard, M. T., Tan, W. S., Gothai, S., Fakurazi, S., Norhaizan, M. E., & Kumar, S. S. (2016). Role of Antioxidants and Natural Products in Inflammation. *Oxidative Medicine and Cellular Longevity*, *2016*, 5276130. https://doi.org/10.1155/2016/5276130

Askew, D., Chu, R. S., Krieg, A. M., & Harding, C. V. (2000). CpG DNA Induces Maturation of Dendritic Cells with Distinct Effects on Nascent and Recycling MHC-II Antigen-Processing Mechanisms. *The Journal of Immunology*, *165*(12), 6889–6895. https://doi.org/10.4049/jimmunol.165.12.6889

Atherton, J. G., Kratzing, C. C., & Fisher, A. (1978). The effect of ascorbic acid on infection of chick-embryo ciliated tracheal organ cultures by coronavirus. *Archives of Virology*, *56*(3), 195–199. https://doi.org/10.1007/BF01317848

Atzeni, F., & Sarzi-Puttini, P. (2013). *Brenner's Encyclopedia of Genetics—2nd Edition* (2nd ed.). Academic Press. https://www.elsevier.com/books/brenners-encyclopedia-of-genetics/maloy/978-0-12-374984-0

Azagra-Boronat, I., Massot-Cladera, M., Knipping, K., Garssen, J., Ben Amor, K., Knol, J., Franch, À., Castell, M., Rodríguez-Lagunas, M. J., & Pérez-Cano, F. J. (2020). Strain-Specific Probiotic Properties of Bifidobacteria and Lactobacilli for the Prevention of Diarrhea Caused by Rotavirus in a Preclinical Model. *Nutrients*, *12*(2), 498. https://doi.org/10.3390/nu12020498

Babyatsky, M., Rossiter, G., & Podolsky, D. (1996). Expression of transforming growth factors alpha and beta in colonic mucosa in inflammatory bowel

disease. *Gastroenterology*, *110*(4), 975–984. https://doi.org/10.1053/gast.1996.v110.pm8613031

Bacchetta, R. (2016). Immunodysregulation, Polyendocrinopathy, and Enteropathy, X-Linked (IPEX) Syndrome. In M. J. H. Ratcliffe (Ed.), *Encyclopedia of Immunobiology* (pp. 444–450). Academic Press. https://doi.org/10.1016/B978-0-12-374279-7.18008-7

Bach, J.-F. (2002). The Effect of Infections on Susceptibility to Autoimmune and Allergic Diseases. *New England Journal of Medicine*, *347*(12), 911–920. https://doi.org/10.1056/NEJMra020100

Bachmann, M. F., & Oxenius, A. (2007). Interleukin 2: From immunostimulation to immunoregulation and back again. *EMBO Reports*, *8*(12), 1142–1148. https://doi.org/10.1038/sj.embor.7401099

Bae, H., Barlow, A. T., Young, H., & Valencia, J. C. (2016). Interferon γ: An Overview of Its Functions in Health and Disease. In M. J. H. Ratcliffe (Ed.), *Encyclopedia of Immunobiology* (pp. 494–500). Academic Press. https://doi.org/10.1016/B978-0-12-374279-7.10006-2

Bamias, G., & Cominelli, F. (2015). Role of Th2 immunity in intestinal inflammation. *Current Opinion in Gastroenterology*, *31*(6), 471–476. https://doi.org/10.1097/MOG.0000000000000212

Barcellini, W., Rizzardi, G. P., Borgh, M. O., Fain, C., Lazzarin, A., & Meroni, P. L. (1994). TH1 and TH2 cytokine production by peripheral blood mononuclear cells from HIV-infected patients. *AIDS*, *8*(6), 757.

Battistini, C., Ballan, R., Herkenhoff, M. E., Saad, S. M. I., & Sun, J. (2021). Vitamin D Modulates Intestinal Microbiota in Inflammatory Bowel Diseases.

International Journal of Molecular Sciences, *22*(1), Article 1. https://doi.org/10.3390/ijms22010362

Bellenger, J., Bellenger, S., Bourragat, A., Escoula, Q., Weill, P., & Narce, M. (2021). Intestinal microbiota mediates the beneficial effects of n-3 polyunsaturated fatty acids during dietary obesity,. *OCL*, *28*, 21. https://doi.org/10.1051/ocl/2021006

Bettelli, E., Carrier, Y., Gao, W., Korn, T., Strom, T. B., Oukka, M., Weiner, H. L., & Kuchroo, V. K. (2006). Reciprocal developmental pathways for the generation of pathogenic effector TH17 and regulatory T cells. *Nature*, *441*(7090), Article 7090. https://doi.org/10.1038/nature04753

Bhavsar, I., Miller, C. S., & Al-Sabbagh, M. (2014). Macrophage Inflammatory Protein-1 Alpha (MIP-1 Alpha)/CCL3: As a BiomarkerMIP-1α/CCL3. In V. R. Preedy & V. B. Patel (Eds.), *General Methods in Biomarker Research and their Applications* (pp. 1–22). Springer Netherlands. https://doi.org/10.1007/978-94-007-7740-8_27-1

Boden, E. K., & Snapper, S. B. (2008). Regulatory T cells in inflammatory bowel disease. *Current Opinion in Gastroenterology*, *24*(6), 733–741. https://doi.org/10.1097/MOG.0b013e328311f26e

Boehm, U., Klamp, T., Groot, M., & Howard, J. C. (1997). Cellular responses to interferon-gamma. *Annual Review of Immunology*, *15*, 749–795. https://doi.org/10.1146/annurev.immunol.15.1.749

Bourrie, B. C. T., Willing, B. P., & Cotter, P. D. (2016). The Microbiota and Health Promoting Characteristics of the Fermented Beverage Kefir. *Frontiers in*

Microbiology, *7*. https://www.frontiersin.org/article/10.3389/fmicb.2016.00647

Bradley, Z. (2020, February 14). Technologies for Measuring Cell Surface Markers. *Cofactor Genomics*. https://cofactorgenomics.com/wk-9-2020-cell-surface-markers/

Brand, S. (2009). Crohn's disease: Th1, Th17 or both? The change of a paradigm: new immunological and genetic insights implicate Th17 cells in the pathogenesis of Crohn's disease. *Gut*, *58*(8), 1152–1167. https://doi.org/10.1136/gut.2008.163667

Brown, M. A., & Hural, J. (1997). Functions of IL-4 and control of its expression. *Critical Reviews in Immunology*, *17*(1), 1–32. https://doi.org/10.1615/critrevimmunol.v17.i1.10

Browne, E. P. (2015). An Interleukin-1 Beta-Encoding Retrovirus Exhibits Enhanced Replication In Vivo. *Journal of Virology*, *89*(1), 155–164. https://doi.org/10.1128/JVI.02314-14

Brusko, T. M., Wasserfall, C. H., Hulme, M. A., Cabrera, R., Schatz, D., & Atkinson, M. A. (2009). Influence of Membrane CD25 Stability on T Lymphocyte Activity: Implications for Immunoregulation. *PLOS ONE*, *4*(11), e7980. https://doi.org/10.1371/journal.pone.0007980

Brydon, E. W. A., Morris, S. J., & Sweet, C. (2005). Role of apoptosis and cytokines in influenza virus morbidity. *FEMS Microbiology Reviews*, *29*(4), 837–850. https://doi.org/10.1016/j.femsre.2004.12.003

Burrack, K. S., & Morrison, T. E. (2014). The Role of Myeloid Cell Activation and Arginine Metabolism in the Pathogenesis of Virus-Induced Diseases.

Frontiers in Immunology, *5*, 428. https://doi.org/10.3389/fimmu.2014.00428

Cargnello, M., & Roux, P. P. (2011). Activation and Function of the MAPKs and Their Substrates, the MAPK-Activated Protein Kinases. *Microbiology and Molecular Biology Reviews : MMBR*, *75*(1), 50–83. https://doi.org/10.1128/MMBR.00031-10

Carty, M., & Bowie, A. G. (2010). Recent insights into the role of Toll-like receptors in viral infection. *Clinical and Experimental Immunology*, *161*(3), 397–406. https://doi.org/10.1111/j.1365-2249.2010.04196.x

Castro, F., Cardoso, A. P., Gonçalves, R. M., Serre, K., & Oliveira, M. J. (2018). Interferon-Gamma at the Crossroads of Tumor Immune Surveillance or Evasion. *Frontiers in Immunology*, *9*, 847. https://doi.org/10.3389/fimmu.2018.00847

CDC. (2022a, April 27). *Prevalence of IBD | CDC*. https://www.cdc.gov/ibd/data-and-statistics/prevalence.html

CDC. (2022b, April 27). *What is inflammatory bowel disease (IBD)? | IBD*. https://www.cdc.gov/ibd/what-is-IBD.htm

CDC. (2023, September 28). *Preliminary In-Season 2021-2022 Flu Burden Estimates*. Centers for Disease Control and Prevention. https://t.cdc.gov/L9PG4

Chai, W., Burwinkel, M., Wang, Z., Palissa, C., Esch, B., Twardziok, S., Rieger, J., Wrede, P., & Schmidt, M. F. G. (2013). Antiviral effects of a probiotic Enterococcus faecium strain against transmissible gastroenteritis

coronavirus. *Archives of Virology*, *158*(4), 799–807. https://doi.org/10.1007/s00705-012-1543-0

Chai, Y., Chen, Y., Lin, S., Xie, K., Wang, C., Yang, Y., & Xu, F. (2020). Curcumin regulates the differentiation of naïve CD4+T cells and activates IL-10 immune modulation against acute lung injury in mice. *Biomedicine & Pharmacotherapy*, *125*, 109946. https://doi.org/10.1016/j.biopha.2020.109946

Chan, S. H., Kobayashi, M., Santoli, D., Perussia, B., & Trinchieri, G. (1992). Mechanisms of IFN-gamma induction by natural killer cell stimulatory factor (NKSF/IL-12). Role of transcription and mRNA stability in the synergistic interaction between NKSF and IL-2. *The Journal of Immunology*, *148*(1), 92–98.

Chaochao, Q., Lou, G., Yang, Y., Liu, Y., Hu, Y., Min, Z., Chen, P., He, J., & Chen, Z. (2017). Macrophage Inflammatory Protein-2 in High Mobility Group Box 1 Secretion of Macrophage Cells Exposed to Lipopolysaccharide. *Cellular Physiology and Biochemistry*, *42*(3), 913–928. https://doi.org/10.1159/000478646

Charles A Janeway, J., Travers, P., Walport, M., & Shlomchik, M. J. (2001). The major histocompatibility complex and its functions. *Immunobiology: The Immune System in Health and Disease. 5th Edition*. https://www.ncbi.nlm.nih.gov/books/NBK27156/

Chatterjee, P., Chiasson, V. L., Bounds, K. R., & Mitchell, B. M. (2014). Regulation of the Anti-Inflammatory Cytokines Interleukin-4 and Interleukin-10 during

Pregnancy. *Frontiers in Immunology*, *5*. https://www.frontiersin.org/articles/10.3389/fimmu.2014.00253

Chen, M., Chen, X., Song, X., Muhammad, A., Jia, R., Zou, Y., Yin, L., Li, L., He, C., Ye, G., Lv, C., Zhang, W., & Yin, Z. (2019). The immune-adjuvant activity and the mechanism of resveratrol on pseudorabies virus vaccine in a mouse model. *International Immunopharmacology*, *76*, 105876. https://doi.org/10.1016/j.intimp.2019.105876

Chen, X., Yang, L., Zhang, N., Turpin, J. A., Buckheit, R. W., Osterling, C., Oppenheim, J. J., & Howard, O. M. Z. (2003). Shikonin, a Component of Chinese Herbal Medicine, Inhibits Chemokine Receptor Function and Suppresses Human Immunodeficiency Virus Type 1. *Antimicrobial Agents and Chemotherapy*, *47*(9), 2810–2816. https://doi.org/10.1128/AAC.47.9.2810-2816.2003

Chiang, N., & Serhan, C. N. (2020). Specialized pro-resolving mediator network: An update on production and actions. *Essays in Biochemistry*, *64*(3), 443–462. https://doi.org/10.1042/EBC20200018

Chihara, G. O. R. O. (1993). Medical aspects of lentinan isolated from Lentinus edodes (Berk.) Sing. *Mushroom Biology and Mushroom Products*, 261–266.

Christ, A., Lauterbach, M., & Latz, E. (2019). Western Diet and the Immune System: An Inflammatory Connection. *Immunity*, *51*(5), 794–811. https://doi.org/10.1016/j.immuni.2019.09.020

Christmas, P. (2010). *Toll-like Receptors, Infection | Learn Science at Scitable*. https://www.nature.com/scitable/topicpage/toll-like-receptors-sensors-that-detect-infection-14396559/

Clerici, M., Lucey, D. R., Berzofsky, J. A., Pinto, L. A., Wynn, T. A., Blatt, S. P., Dolan, M. J., Hendrix, C. W., Wolf, S. F., & Shearer, G. M. (1993). Restoration of HIV-Specific Cell-Mediated Immune Responses by Interleukin-12 in Vitro. *Science*, *262*(5140), 1721–1724. https://doi.org/10.1126/science.7903123

Cleveland Clinic. (2022). *Inflammatory Bowel Disease: Symptoms, Treatment & Diagnosis*. Cleveland Clinic. https://my.clevelandclinic.org/health/diseases/15587-inflammatory-bowel-disease-overview

Cook, D. N., Beck, M. A., Coffman, T. M., Kirby, S. L., Sheridan, J. F., Pragnell, Ian B., & Smithies, O. (1995). Requirement of Mip-1α for an Inflammatory Response to Viral Infection. *Science*, *269*(5230), 1583–1585. https://doi.org/10.1126/science.7667639

Cordain, L., Eaton, S. B., Sebastian, A., Mann, N., Lindeberg, S., Watkins, B. A., O'Keefe, J. H., & Brand-Miller, J. (2005). Origins and evolution of the Western diet: Health implications for the 21st century. *The American Journal of Clinical Nutrition*, *81*(2), 341–354. https://doi.org/10.1093/ajcn.81.2.341

Cordeiro, N., Freitas, R. H. C. N., Fraga, C. A. M., & Fernandes, P. D. (2020). Therapeutic Effects of Anti-Inflammatory *N* -Acylhydrazones in the Resolution of Experimental Colitis. *Journal of Pharmacology and Experimental Therapeutics*, *374*(3), 420–427. https://doi.org/10.1124/jpet.120.000074

Covarrubias, A., & Horng, T. (2014). IL-6 strikes a balance in metabolic inflammation. *Cell Metabolism*, *19*(6), 898–899. https://doi.org/10.1016/j.cmet.2014.05.009

Danone Nutricia Research. (2022). Immune Fitness: Working towards a resilient immune system. *Danone Nutricia Research*. https://www.nutriciaresearch.com/immunology/immune-fitness-working-towards-a-resilient-immune-system/

Darwesh, A. M., Bassiouni, W., Sosnowski, D. K., & Seubert, J. M. (2021). Can N-3 polyunsaturated fatty acids be considered a potential adjuvant therapy for COVID-19-associated cardiovascular complications? *Pharmacology & Therapeutics*, *219*, 107703. https://doi.org/10.1016/j.pharmthera.2020.107703

de Mattos, B. R. R., Garcia, M. P. G., Nogueira, J. B., Paiatto, L. N., Albuquerque, C. G., Souza, C. L., Fernandes, L. G. R., Tamashiro, W. M. da S. C., & Simioni, P. U. (2015). Inflammatory Bowel Disease: An Overview of Immune Mechanisms and Biological Treatments. *Mediators of Inflammation*, *2015*, 493012. https://doi.org/10.1155/2015/493012

De Moreno de LeBlanc, A., & Perdigón, G. (2010). The application of probiotic fermented milks in cancer and intestinal inflammation | Proceedings of the Nutrition Society | Cambridge Core. *Proceedings of the Nutrition Society*, *69*(3), 421–428. https://doi.org/doi:10.1017/S002966511000159X

de Oliviera Nascimento, L., Massari, P., & Wetzler, L. (2012). The Role of TLR2 in Infection and Immunity. *Frontiers in Immunology*, *3*. https://www.frontiersin.org/articles/10.3389/fimmu.2012.00079

de Vries, J. E. (1998). The role of IL-13 and its receptor in allergy and inflammatory responses. *The Journal of Allergy and Clinical Immunology*, *102*(2), 165–169. https://doi.org/10.1016/s0091-6749(98)70080-6

Deimel, L. P., Li, Z., & Ranasinghe, C. (2021). Interleukin-13 as a target to alleviate severe coronavirus disease 2019 and restore lung homeostasis. *Journal of Clinical and Translational Research*, *7*(1), 116–120.

Deshmane, S. L., Kremlev, S., Amini, S., & Sawaya, B. E. (2009). Monocyte Chemoattractant Protein-1 (MCP-1): An Overview. *Journal of Interferon & Cytokine Research*, *29*(6), 313–326. https://doi.org/10.1089/jir.2008.0027

Dhong, K.-R., Kwon, H.-K., & Park, H.-J. (2022). Immunostimulatory Activity of Cordyceps militaris Fermented with Pediococcus pentosaceus SC11 Isolated from a Salted Small Octopus in Cyclophosphamide-Induced Immunocompromised Mice and Its Inhibitory Activity against SARS-CoV 3CL Protease. *Microorganisms*, *10*(12), Article 12. https://doi.org/10.3390/microorganisms10122321

Diebold, S. S. (2008). Recognition of viral single-stranded RNA by Toll-like receptors. *Advanced Drug Delivery Reviews*, *60*(7), 813–823. https://doi.org/10.1016/j.addr.2007.11.004

Dinarello, C. A. (2009). Immunological and inflammatory functions of the interleukin-1 family. *Annual Review of Immunology*, *27*, 519–550. https://doi.org/10.1146/annurev.immunol.021908.132612

Dinarello, C. A. (2011). Interleukin-1 in the pathogenesis and treatment of inflammatory diseases. *Blood*, *117*(14), 3720–3732. https://doi.org/10.1182/blood-2010-07-273417

Dinarello, C. A. (2018). Overview of the IL-1 family in innate inflammation and acquired immunity. *Immunological Reviews*, *281*(1), 8–27. https://doi.org/10.1111/imr.12621

Ding, Y., Xu, J., & Bromberg, J. S. (2012). T regulatory cell migration during an immune response. *Trends in Immunology*, *33*(4), 174–180. https://doi.org/10.1016/j.it.2012.01.002

Ding, Y., Zeng, L., Li, R., Chen, Q., Zhou, B., Chen, Q., Cheng, P. leng, Yutao, W., Zheng, J., Yang, Z., & Zhang, F. (2017). The Chinese prescription lianhuaqingwen capsule exerts anti-influenza activity through the inhibition of viral propagation and impacts immune function. *BMC Complementary and Alternative Medicine*, *17*(1), 130. https://doi.org/10.1186/s12906-017-1585-7

Djurasevic, S., Bojic, S., Nikolić, B., Dimkić, I., Todorovic, Z., Djordjevic, J., & Mitić-Ćulafić, D. (2018). Beneficial Effect of Virgin Coconut Oil on Alloxan-Induced Diabetes and Microbiota Composition in Rats. *Plant Foods for Human Nutrition*, *73*. https://doi.org/10.1007/s11130-018-0689-7

Dong, C. (2006). Diversification of T-helper-cell lineages: Finding the family root of IL-17-producing cells. *Nature Reviews Immunology*, *6*(4), Article 4. https://doi.org/10.1038/nri1807

D'Souza, W. N., Schluns, K. S., Masopust, D., & Lefrançois, L. (2002). Essential Role for IL-2 in the Regulation of Antiviral Extralymphoid CD8 T Cell Responses1. *The Journal of Immunology*, *168*(11), 5566–5572. https://doi.org/10.4049/jimmunol.168.11.5566

Dumancas, G., Viswanath, L., Leon, A., Ramasahayam, S., Maples, R., Hikkaduwa Koralege, R., Don, U., Perera, U. D. N., Langford, J., Shakir, A., & Castles, S. (2016). Health benefits of virgin coconut oil. In *Vegetable Oil: Properties, Uses and Benefits*.

Eder, W., Ege, M. J., & von Mutius, E. (2006). The asthma epidemic. *The New England Journal of Medicine*, *355*(21), 2226–2235. https://doi.org/10.1056/NEJMra054308

EFCCA. (2022). *About IBD (Inflammatory Bowel Diseases) organisations | World IBD Day*. World IBD Day, 19th May. https://worldibdday.org/about-us

Elgueta, R., Benson, M. J., de Vries, V. C., Wasiuk, A., Guo, Y., & Noelle, R. J. (2009). Molecular mechanism and function of CD40/CD40L engagement in the immune system. *Immunological Reviews*, *229*(1), 10.1111/j.1600-065X.2009.00782.x. https://doi.org/10.1111/j.1600-065X.2009.00782.x

Euromonitor International, a market research provider. (2022). *Market Sizes*. https://www-portal-euromonitor-com.dcu.idm.oclc.org/portal/statisticsevolution/index

Fadnes, L. T., Økland, J.-M., Haaland, Ø. A., & Johansson, K. A. (2022). Estimating impact of food choices on life expectancy: A modeling study. *PLOS Medicine*, *19*(2), e1003889. https://doi.org/10.1371/journal.pmed.1003889

Farahmnandi, F., Parhizgar, P., Tape, P. M. K., Bizhannia, F., Rohani, F. S., Bizhanzadeh, M., Alhosseini, Z. S. M., Hosseinzade, M., Farsi, Y., & Nasiri, M. J. (2023). *Antiviral effects of Lactic Acid Bacteria; a systematic review* [Preprint]. In Review. https://doi.org/10.21203/rs.3.rs-2519608/v1

Faria, A. M. C., Mucida, D., McCafferty, D.-M., Tsuji, N. M., & Verhasselt, V. (2012). Tolerance and inflammation at the gut mucosa. *Clinical & Developmental Immunology*, *2012*, 738475. https://doi.org/10.1155/2012/738475

Faul, J. L., Kerley, C. P., Love, B., O'Neill, E., Cody, C., Tormey, W., Hutchinson, K., Cormican, L. J., & Burke, C. M. (2021). *Vitamin D Deficiency and ARDS after SARS-CoV-2 Infection*. 2.

Finnegan, D., Tocmo, R., & Loscher, C. (2023). Targeted Application of Functional Foods as Immune Fitness Boosters in the Defense against Viral Infection. *Nutrients*, *15*(15), Article 15. https://doi.org/10.3390/nu15153371

Fleisch, M. C., Maxwell, C. A., & Barcellos-Hoff, M.-H. (2006). The pleiotropic roles of transforming growth factor beta in homeostasis and carcinogenesis of endocrine organs. *Endocrine-Related Cancer*, *13*(2), 379–400. https://doi.org/10.1677/erc.1.01112

Franke, A., Balschun, T., Karlsen, T. H., Sventoraityte, J., Nikolaus, S., Mayr, G., Domingues, F. S., Albrecht, M., Nothnagel, M., Ellinghaus, D., Sina, C., Onnie, C. M., Weersma, R. K., Stokkers, P. C. F., Wijmenga, C., Gazouli, M., Strachan, D., McArdle, W. L., Vermeire, S., … Schreiber, S. (2008). Sequence variants in IL10, ARPC2 and multiple other loci contribute to ulcerative colitis susceptibility. *Nature Genetics*, *40*(11), Article 11. https://doi.org/10.1038/ng.221

Fredrickson, W. R. (2000). *Method and composition for antiviral therapy* (United States Patent US6117844A). https://patents.google.com/patent/US6117844A/en

Freedman, S. B., Xie, J., Nettel-Aguirre, A., Pang, X.-L., Chui, L., Williamson-Urquhart, S., Schnadower, D., Schuh, S., Sherman, P. M., Lee, B. E., Gouin, S., Farion, K. J., Poonai, N., Hurley, K. F., Qiu, Y., Ghandi, B., Lloyd, C., & Finkelstein, Y. (2020). A randomized trial evaluating virus-specific effects of a combination probiotic in children with acute gastroenteritis. *Nature Communications*, *11*(1), 2533. https://doi.org/10.1038/s41467-020-16308-3

Freitas, M. (2017). Chapter 24—The Benefits of Yogurt, Cultures, and Fermentation. In M. H. Floch, Y. Ringel, & W. Allan Walker (Eds.), *The Microbiota in Gastrointestinal Pathophysiology* (pp. 209–223). Academic Press. https://doi.org/10.1016/B978-0-12-804024-9.00024-0

Fujii, T., Jounai, K., Horie, A., Takahashi, H., Suzuki, H., Ohshio, K., Fujiwara, D., & Yamamoto, N. (2017). Effects of heat-killed Lactococcus lactis subsp. Lactis JCM 5805 on mucosal and systemic immune parameters, and antiviral reactions to influenza virus in healthy adults; a randomized controlled double-blind study. *Journal of Functional Foods*, *35*, 513–521. https://doi.org/10.1016/j.jff.2017.06.011

Fujino, S., Andoh, A., Bamba, S., Ogawa, A., Hata, K., Araki, Y., Bamba, T., & Fujiyama, Y. (2003). Increased expression of interleukin 17 in inflammatory bowel disease. *Gut*, *52*(1), 65–70.

Fukushima, Y., Kawata, Y., Hara, H., Terada, A., & Mitsuoka, T. (1998). Effect of a probiotic formula on intestinal immunoglobulin A production in healthy children. *International Journal of Food Microbiology*, *42*(1–2), 39–44. https://doi.org/10.1016/s0168-1605(98)00056-7

Fuse, S., Obar, J. J., Bellfy, S., Leung, E. K., Zhang, W., & Usherwood, E. J. (2006). CD80 and CD86 Control Antiviral CD8+ T-Cell Function and Immune Surveillance of Murine Gammaherpesvirus 68. *Journal of Virology*, *80*(18), 9159–9170. https://doi.org/10.1128/JVI.00422-06

Gahramanova, M., Ostapchuk, A., Molozhava, O., Svyatetska, V., Rudyk, M., Hurmach, Y., Gorbach, O., & Skivka, L. (2023). Anti-inflammatory effect of polyherbal composition with hepatoprotective and choleretic properties on LPS-stimulated murine macrophages. *Journal of Complementary and Integrative Medicine*, *20*(2), 404–412. https://doi.org/10.1515/jcim-2020-0098

García-Burgos, M., Moreno-Fernández, J., J.M. Alférez, M., Díaz-Castro, J., & López-Aliaga, I. (2020). New perspectives in fermented dairy products and their health relevance—ScienceDirect. *Journal of Functional Foods*, *72*. https://doi.org/10.1016/j.jff.2020.104059

Garcia-Sastre, A., & Biron, C. (2006). Type 1 Interferons and the Virus-Host Relationship: A Lesson in Détente. *Science*, *312*(5775), 879–882. https://doi.org/DOI: 10.1126/science.1125676

Garlanda, C., Dinarello, C. A., & Mantovani, A. (2013). THE INTERLEUKIN-1 FAMILY: BACK TO THE FUTURE. *Immunity*, *39*(6), 1003–1018. https://doi.org/10.1016/j.immuni.2013.11.010

Ge, Y., Huang, M., & Yao, Y. (2020). Biology of Interleukin-17 and Its Pathophysiological Significance in Sepsis. *Frontiers in Immunology*, *11*. https://www.frontiersin.org/articles/10.3389/fimmu.2020.01558

Ghosh, S., Chaudhary, R., Carpani, M., & Playford, R. (2006). Interfering with interferons in inflammatory bowel disease. *Gut*, *55*(8), 1071–1073. https://doi.org/10.1136/gut.2005.090134

Gilliet, M., Cao, W., & Liu, Y.-J. (2008). Plasmacytoid dendritic cells: Sensing nucleic acids in viral infection and autoimmune diseases. *Nature Reviews. Immunology*, *8*(8), 594–606. https://doi.org/10.1038/nri2358

Goettel, J. A., Kotlarz, D., Emani, R., Canavan, J. B., Konnikova, L., Illig, D., Frei, S. M., Field, M., Kowalik, M., Peng, K., Gringauz, J., Mitsialis, V., Wall, S. M., Tsou, A., Griffith, A. E., Huang, Y., Friedman, J. R., Towne, J. E., Plevy, S. E., … Snapper, S. B. (2019). Low-Dose Interleukin-2 Ameliorates Colitis in a Preclinical Humanized Mouse Model. *Cellular and Molecular Gastroenterology and Hepatology*, *8*(2), 193–195. https://doi.org/10.1016/j.jcmgh.2019.05.001

Goldsby, R., Kindt, T. J., Osborne, B. A., & Kuby, J. (2003). Chapter 2: Cells and Organs of the Immune System. In *Immunology* (5th ed., pp. 24–56). W. H. Freeman and Company.

Gouda, A. S., Adbelruhman, F. G., Sabbah Alenezi, H., & Mégarbane, B. (2021). Theoretical benefits of yogurt-derived bioactive peptides and probiotics in COVID-19 patients – A narrative review and hypotheses. *Saudi Journal of Biological Sciences*, *28*(10), 5897–5905. https://doi.org/10.1016/j.sjbs.2021.06.046

Granier, A., Goulet, O., & Hoarau, C. (2013). Fermentation products: Immunological effects on human and animal models. *Pediatric Research*, *74*, 238–244. https://doi.org/10.1038/pr.2013.76

Griffin, D. E. (2008). *Encyclopedia Of Virology*. (3rd ed., pp. 620–624). Academic Press.

Grigore, A., Cord, D., Tanase, C., & Albulescu, R. (2020). Herbal medicine, a reliable support in COVID therapy. *Journal of Immunoassay and Immunochemistry*, *41*(6), 976–999. https://doi.org/10.1080/15321819.2020.1862867

Guak, H., & Krawczyk, Connie. M. (2020). Implications of cellular metabolism for immune cell migration. *Immunology*, *161*(3), 200–208. https://doi.org/10.1111/imm.13260

Guo, Y., Cao, W., & Zhu, Y. (2019). Immunoregulatory Functions of the IL-12 Family of Cytokines in Antiviral Systems. *Viruses*, *11*(9), 772. https://doi.org/10.3390/v11090772

Hamida, R. S., Shami, A., Ali, M. A., Almohawes, Z. N., Mohammed, A. E., & Bin-Meferij, M. M. (2021). Kefir: A protective dietary supplementation against viral infection. *Biomedicine & Pharmacotherapy*, *133*, 110974. https://doi.org/10.1016/j.biopha.2020.110974

Hamza, T., Barnett, J. B., & Li, B. (2010). Interleukin 12 a Key Immunoregulatory Cytokine in Infection Applications. *International Journal of Molecular Sciences*, *11*(3), Article 3. https://doi.org/10.3390/ijms11030789

Han, X.-B., Liu, X., Hsueh, W., & De Plaen, I. G. (2004). Macrophage inflammatory protein-2 mediates the bowel injury induced by platelet-activating factor. *American Journal of Physiology-Gastrointestinal and Liver Physiology*, *287*(6), G1220–G1226. https://doi.org/10.1152/ajpgi.00231.2004

Harker, J. A., Wong, K. A., Dallari, S., Bao, P., Dolgoter, A., Jo, Y., Wehrens, E. J., Macal, M., & Zuniga, E. I. (2018). Interleukin-27R Signaling Mediates Early Viral Containment and Impacts Innate and Adaptive Immunity after Chronic Lymphocytic Choriomeningitis Virus Infection. *Journal of Virology*, *92*(12), e02196-17. https://doi.org/10.1128/JVI.02196-17

Harrington, L. E., Hatton, R. D., Mangan, P. R., Turner, H., Murphy, T. L., Murphy, K. M., & Weaver, C. T. (2005). Interleukin 17–producing CD4+ effector T cells develop via a lineage distinct from the T helper type 1 and 2 lineages. *Nature Immunology*, *6*(11), Article 11. https://doi.org/10.1038/ni1254

Hasanvand, A. (2022). COVID-19 and the role of cytokines in this disease. *Inflammopharmacology*, *30*(3), 789–798. https://doi.org/10.1007/s10787-022-00992-2

Hathaway, D., Pandav, K., Patel, M., Riva-Moscoso, A., Singh, B. M., Patel, A., Min, Z. C., Singh-Makkar, S., Sana, M. K., Sanchez-Dopazo, R., Desir, R., Fahem, M. M. M., Manella, S., Rodriguez, I., Alvarez, A., & Abreu, R. (2020). Omega 3 Fatty Acids and COVID-19: A Comprehensive Review. *Infection & Chemotherapy*, *52*(4), 478–495. https://doi.org/10.3947/ic.2020.52.4.478

Hayashi, T., Hayashi, K., Maeda, M., & Kojima, I. (1996). Calcium Spirulan, an Inhibitor of Enveloped Virus Replication, from a Blue-Green Alga Spirulina platensis. *Journal of Natural Products*, *59*(1), 83–87. https://doi.org/10.1021/np960017o

He, L.-X., Ren, J.-W., Liu, R., Chen, Q.-H., Zhao, J., Wu, X., Zhang, Z.-F., Wang, J.-B., Pettinato, G., & Li, Y. (2017). Ginseng (Panax ginseng Meyer) oligopeptides regulate innate and adaptive immune responses in mice via

increased macrophage phagocytosis capacity, NK cell activity and Th cells secretion. *Food & Function*, *8*(10), 3523–3532. https://doi.org/10.1039/C7FO00957G

Head, K., & Jurenka, J. (2004). Inflammatory Bowel Disease Part II: Crohn's Disease - Pathophysiology and Conventional and Alternative Treatment Options. *Alternative Medicine Review*, *9*(4), 360–401.

Health Service Executive. (2011). *Vitamins and minerals—Vitamin D*. HSE.Ie. https://www2.hse.ie/conditions/vitamins-and-minerals/vitamin-d/

Health Service Executive. (2021, September 10). *How long does immunity last after COVID-19 vaccination? Does immunity wane faster in certain sub-populations? How safe and effective are booster doses of COVID-19 vaccine? - HLI (Health Library Ireland)*. https://hselibrary.ie/how-long-does-immunity-last-after-covid-19-vaccination-does-immunity-wane-faster-in-certain-sub-populations-how-safe-and-effective-are-booster-doses-of-covid-19-vaccine/

Hideshima, T., Nakamura, N., Chauhan, D., & Anderson, K. C. (2001). Biologic sequelae of interleukin-6 induced PI3-K/Akt signaling in multiple myeloma. *Oncogene*, *20*(42), 5991–6000. https://doi.org/10.1038/sj.onc.1204833

Hillier, K., Jewell, R., Dorrell, L., & Smith, C. L. (1991). Incorporation of fatty acids from fish oil and olive oil into colonic mucosal lipids and effects upon eicosanoid synthesis in inflammatory bowel disease. *Gut*, *32*(10), 1151–1155.

Himmel, M. E., Yao, Y., Orban, P. C., Steiner, T. S., & Levings, M. K. (2012). Regulatory T-cell therapy for inflammatory bowel disease: More questions

than answers. *Immunology*, *136*(2), 115–122. https://doi.org/10.1111/j.1365-2567.2012.03572.x

Hisamatsu, T., Kanai, T., Mikami, Y., Yoneno, K., Matsuoka, K., & Hibi, T. (2013). Immune aspects of the pathogenesis of inflammatory bowel disease. *Pharmacology & Therapeutics*, *137*(3), 283–297. https://doi.org/10.1016/j.pharmthera.2012.10.008

Hodgson, H. J. F., & Jewell, D. P. (1978). The humoral immune system in inflammatory bowel disease. *The American Journal of Digestive Diseases*, *23*(2), 123–128. https://doi.org/10.1007/BF01073186

Holling, T. M., Schooten, E., & van Den Elsen, P. J. (2004). Function and regulation of MHC class II molecules in T-lymphocytes: Of mice and men. *Human Immunology*, *65*(4), 282–290. https://doi.org/10.1016/j.humimm.2004.01.005

Horiuchi, T., Mitoma, H., Harashima, S., Tsukamoto, H., & Shimoda, T. (2010). Transmembrane TNF-α: Structure, function and interaction with anti-TNF agents. *Rheumatology*, *49*(7), 1215–1228. https://doi.org/10.1093/rheumatology/keq031

Hou, W., Jin, Y.-H., Kang, H. S., & Kim, B. S. (2014). Interleukin-6 (IL-6) and IL-17 Synergistically Promote Viral Persistence by Inhibiting Cellular Apoptosis and Cytotoxic T Cell Function. *Journal of Virology*, *88*(15), 8479–8489. https://doi.org/10.1128/JVI.00724-14

Hou, W., Kang, H. S., & Kim, B. S. (2009). Th17 cells enhance viral persistence and inhibit T cell cytotoxicity in a model of chronic virus infection. *Journal of*

Experimental Medicine, *206*(2), 313–328. https://doi.org/10.1084/jem.20082030

Hoving, J. C. (2018). Targeting IL-13 as a Host-Directed Therapy Against Ulcerative Colitis. *Frontiers in Cellular and Infection Microbiology*, *8*, 395. https://doi.org/10.3389/fcimb.2018.00395

How The Body Reacts To Viruses. (2021). HMX | Harvard Medical School. https://onlinelearning.hms.harvard.edu/hmx/immunity/

Huang, C., Hao, W., Wang, X., Zhou, R., & Lin, Q. (2023). Probiotics for the treatment of ulcerative colitis: A review of experimental research from 2018 to 2022. *Frontiers in Microbiology*, *14*, 1211271. https://doi.org/10.3389/fmicb.2023.1211271

Huang, S.-H., Liao, C.-L., Chen, S.-J., Shi, L.-G., Lin, L., Chen, Y.-W., Cheng, C.-P., Sytwu, H.-K., Shang, S.-T., & Lin, G.-J. (2019). Melatonin possesses an anti-influenza potential through its immune modulatory effect. *Journal of Functional Foods*, *58*, 189–198. https://doi.org/10.1016/j.jff.2019.04.062

Huang, Y., & Chen, Z. (2016). Inflammatory bowel disease related innate immunity and adaptive immunity. *American Journal of Translational Research*, *8*(6), 2490–2497.

Imai, Y. (2015). Role of omega-3 PUFA-derived mediators, the protectins, in influenza virus infection. *Biochimica et Biophysica Acta (BBA) - Molecular and Cell Biology of Lipids*, *1851*(4), 496–502. https://doi.org/10.1016/j.bbalip.2015.01.006

Intahphuak, S., Khonsung, P., & Panthong, A. (2010). Anti-inflammatory, analgesic, and antipyretic activities of virgin coconut oil. *Pharmaceutical Biology*, *48*(2), 151–157. https://doi.org/10.3109/13880200903062614

Ishihara, K., & Hirano, T. (2002). IL-6 in autoimmune disease and chronic inflammatory proliferative disease. *Cytokine & Growth Factor Reviews*, *13*(4), 357–368. https://doi.org/10.1016/S1359-6101(02)00027-8

Ivec, M., Botić, T., Koren, S., Jakobsen, M., Weingartl, H., & Cencič, A. (2007). Interactions of macrophages with probiotic bacteria lead to increased antiviral response against vesicular stomatitis virus. *Antiviral Research*, *75*(3), 266–274. https://doi.org/10.1016/j.antiviral.2007.03.013

Iyer, S. S., & Cheng, G. (2012). Role of Interleukin 10 Transcriptional Regulation in Inflammation and Autoimmune Disease. *Critical Reviews in Immunology*, *32*(1), 23–63.

Izcue, A., Coombes, J. L., & Powrie, F. (2006). Regulatory T cells suppress systemic and mucosal immune activation to control intestinal inflammation. *Immunological Reviews*, *212*, 256–271. https://doi.org/10.1111/j.0105-2896.2006.00423.x

Jauhiainen, T., Vapaatalo, H., Poussa, T., Kyrönpalo, S., Rasmussen, M., & Korpela, R. (2005). Lactobacillus helveticus fermented milk lowers blood pressure in hypertensive subjects in 24-h ambulatory blood pressure measurement. *American Journal of Hypertension*, *18*(12 Pt 1), 1600–1605. https://doi.org/10.1016/j.amjhyper.2005.06.006

Jelinek, I., Leonard, J. N., Price, G., Brown, K. N., Meyer-Manlapat, A., Goldsmith, P. K., Wang, Y., Venzon, D., Epstein, S. L., & Segal, D. M. (2011). Toll-Like

Receptor 3-Specific dsRNA Oligonucleotide Adjuvants Induce Dendritic Cell Cross-presentation, CTL Responses and Antiviral Protection. *Journal of Immunology (Baltimore, Md. : 1950)*, *186*(4), 2422–2429. https://doi.org/10.4049/jimmunol.1002845

Jensen, G. S., Carter, S. G., Reeves, S. G., Robinson, L. E., & Benson, K. F. (2015). Anti-inflammatory properties of a dried fermentate in vitro and in vivo. *Journal of Medicinal Food*, *18*(3), 378–384. https://doi.org/10.1089/jmf.2013.0158

Jiang, Y., Zhao, L., Chen, Q., & Zhou, L. (2021). Exploring the Mechanism of Berberine Intervention in Ulcerative Colitis from the Perspective of Inflammation and Immunity Based on Systemic Pharmacology. *Evidence-Based Complementary and Alternative Medicine : eCAM*, *2021*, 9970240. https://doi.org/10.1155/2021/9970240

Jimenez-Lopez, C., Carpena, M., Lourenço-Lopes, C., Gallardo-Gomez, M., Lorenzo, J. M., Barba, F. J., Prieto, M. A., & Simal-Gandara, J. (2020). Bioactive Compounds and Quality of Extra Virgin Olive Oil. *Foods*, *9*(8), Article 8. https://doi.org/10.3390/foods9081014

Joshi, S., Kaushik, V., Gode, V., & Mhaskar, S. (2020). Coconut Oil and Immunity: What do we really know about it so far? *The Journal of the Association of Physicians of India*, *68*, 67–72.

Jounai, K., Sugimura, T., Ohshio, K., & Fujiwara, D. (2015). Oral Administration of Lactococcus lactis Subsp. Lactis JCM5805 Enhances Lung Immune Response Resulting in Protection from Murine Parainfluenza Virus

Infection. *PLOS ONE*, *10*(3), e0119055. https://doi.org/10.1371/journal.pone.0119055

Junttila, I. S. (2018). Tuning the Cytokine Responses: An Update on Interleukin (IL)-4 and IL-13 Receptor Complexes. *Frontiers in Immunology*, *9*. https://www.frontiersin.org/articles/10.3389/fimmu.2018.00888

Kaiko, G. E., Horvat, J. C., Beagley, K. W., & Hansbro, P. M. (2008). Immunological decision-making: How does the immune system decide to mount a helper T-cell response? *Immunology*, *123*(3), 326–338. https://doi.org/10.1111/j.1365-2567.2007.02719.x

Kam, L. Y., & Targan, S. R. (2000). TNF-alpha antagonists for the treatment of Crohn's disease. *Expert Opinion on Pharmacotherapy*, *1*(4), 615–622. https://doi.org/10.1517/14656566.1.4.615

Kang, S., Brown, H. M., & Hwang, S. (2018). Direct Antiviral Mechanisms of Interferon-Gamma. *Immune Network*, *18*(5), e33. https://doi.org/10.4110/in.2018.18.e33

Kang, S., & Min, H. (2012). Ginseng, the "Immunity Boost": The Effects of Panax ginseng on Immune System. *Journal of Ginseng Research*, *36*(4), 354–368. https://doi.org/10.5142/jgr.2012.36.4.354

Kasaian, M. T., Page, K. M., Fish, S., Brennan, A., Cook, T. A., Moreira, K., Zhang, M., Jesson, M., Marquette, K., Agostinelli, R., Lee, J., Williams, C. M. M., Tchistiakova, L., & Thakker, P. (2014). Therapeutic activity of an interleukin-4/interleukin-13 dual antagonist on oxazolone-induced colitis in mice. *Immunology*, *143*(3), 416–427. https://doi.org/10.1111/imm.12319

Kawai, T., & Akira, S. (2006). TLR signaling | Cell Death & Differentiation. *Nature*, *13*, 816–825. https://doi.org/The Toll-like receptor (TLR) family plays an instructive role in innate immune responses against microbial pathogens, as well as the subsequent induction of adaptive immune responses. TLRs recognize specific molecular patterns found in a broad range of microbial pathogens such as bacteria and viruses, triggering inflammatory and antiviral responses and dendritic cell maturation, which result in the eradication of invading pathogens. Individual TLRs interact with different combinations of adapter proteins and activate various transcription factors such as nuclear factor (NF)-jB, activat- ing protein-1 and interferon regulatory factors, driving a specific immune response. This review outlines the recent advances in our understanding of TLR-signaling pathways and their roles in immune responses. Further, we also discuss a new concept of TLR-independent mechanisms for recogni- tion of microbial pathogens.

Kawai, T., Sato, S., Ishii, K. J., Coban, C., Hemmi, H., Yamamoto, M., Terai, K., Matsuda, M., Inoue, J., Uematsu, S., Takeuchi, O., & Akira, S. (2004). Interferon-alpha induction through Toll-like receptors involves a direct interaction of IRF7 with MyD88 and TRAF6. *Nature Immunology*, *5*(10), 1061–1068. https://doi.org/10.1038/ni1118

Kawashima, T., Ikari, N., Kouchi, T., Kowatari, Y., Kubota, Y., Shimojo, N., & Tsuji, N. M. (2018). The molecular mechanism for activating IgA production by Pediococcus acidilactici K15 and the clinical impact in a randomized trial. *Scientific Reports*, *8*, 5065. https://doi.org/10.1038/s41598-018-23404-4

Kedzierska, K., & Crowe, S. M. (2001). Cytokines and HIV-1: Interactions and clinical implications. *Antiviral Chemistry & Chemotherapy*, *12*(3), 133–150. https://doi.org/10.1177/095632020101200301

Keyaerts, E., Vijgen, L., Chen, L., Maes, P., Hedenstierna, G., & Van Ranst, M. (2004). Inhibition of SARS-coronavirus infection in vitro by S-nitroso-N-acetylpenicillamine, a nitric oxide donor compound. *International Journal of Infectious Diseases*, *8*(4), 223–226. https://doi.org/10.1016/j.ijid.2004.04.012

Khan, Z., Bhadouria, P., & Bisen, P. S. (2005). Nutritional and Therapeutic Potential of Spirulina. *Current Pharmaceutical Biotechnology*, *6*(5), 373–379. https://doi.org/10.2174/138920105774370607

Kim, H.-Y., Bong, Y.-J., Jeong, J.-K., Lee, S., Kim, B.-Y., & Park, K.-Y. (2016). Heterofermentative lactic acid bacteria dominate in Korean commercial kimchi. *Food Science and Biotechnology*, *25*(2), 541–545. https://doi.org/10.1007/s10068-016-0075-x

Kim, J., Na, H., Kim, J.-A., & Nam, J.-H. (2020). What we know and what we need to know about adenovirus 36-induced obesity. *International Journal of Obesity*, *44*(6), Article 6. https://doi.org/10.1038/s41366-020-0536-4

Kim, S. Y., & Solomon, D. H. (2010). Tumor necrosis factor blockade and the risk of viral infection. *Nature Reviews Rheumatology*, *6*(3), Article 3. https://doi.org/10.1038/nrrheum.2009.279

Klatzmann, D., & Abbas, A. K. (2015). The promise of low-dose interleukin-2 therapy for autoimmune and inflammatory diseases. *Nature Reviews. Immunology*, *15*(5), 283–294. https://doi.org/10.1038/nri3823

Klimpel, G. R. (1996). Immune Defenses. In *Medical Microbiology. 4th edition*. University of Texas Medical Branch at Galveston. https://www.ncbi.nlm.nih.gov/books/NBK8423/

Koesnoe, S., Masjkuri, N., Adisasmita, A., Djauzi, S., Kartasasmita, C., Sundoro, J., Nadjib, M., Korib, M., Muthia, A. N., Muzellina, V. N., Habibah, U., Nursyirwan, S. A., Djaya, K. H., Bachtiar, N. S., & Sari, R. M. (2021). A randomized controlled trial to evaluate the effect of influenza vaccination and probiotic supplementation on immune response and incidence of influenza-like illness in an elderly population in Indonesia. *PloS One*, *16*(12), e0250234. https://doi.org/10.1371/journal.pone.0250234

Kohyama, S., Ohno, S., Isoda, A., Moriya, O., Belladonna, M. L., Hayashi, H., Iwakura, Y., Yoshimoto, T., Akatsuka, T., & Matsui, M. (2007). IL-23 Enhances Host Defense against Vaccinia Virus Infection Via a Mechanism Partly Involving IL-17. *The Journal of Immunology*, *179*(6), 3917–3925. https://doi.org/10.4049/jimmunol.179.6.3917

Koithan, M., & Devika, J. (2010). New Approaches to Nutritional Therapy. *The Journal for Nurse Practitioners : JNP*, *6*(10), 805–806. https://doi.org/10.1016/j.nurpra.2010.07.001

Kollias, G., & Kontoyiannis, D. (2002). Role of TNF/TNFR in autoimmunity: Specific TNF receptor blockade may be advantageous to anti-TNF treatments. *Cytokine & Growth Factor Reviews*, *13*(4), 315–321. https://doi.org/10.1016/S1359-6101(02)00019-9

Komastu, T., Ireland, D. D. C., & Reiss, C. S. (1998). IL-12 and Viral Infections. *Cytokine & Growth Factor Reviews*, *9*(3), 277–285. https://doi.org/10.1016/S1359-6101(98)00017-3

Komatsuzaki, N., Arai, S., Fujihara, S., & Wijesekara, R. (2021). Effect of intake of virgin coconut oil (Cocos nucifera L.) on the spleen and small intestinal immune cells and liver lipid of mice. *Ceylon Journal of Science*, *50*, 103. https://doi.org/10.4038/cjs.v50i2.7871

Kondělková, K., Vokurková, D., Krejsek, J., Borská, L., Fiala, Z., & Ctirad, A. (2010). Regulatory T cells (TREG) and their roles in immune system with respect to immunopathological disorders. *Acta Medica (Hradec Kralove)*, *53*(2), 73–77. https://doi.org/10.14712/18059694.2016.63

Kopp, E., & Medzhitov, R. (2003). Recognition of microbial infection by Toll-like receptors. *Current Opinion in Immunology*, *15*(4), 396–401. https://doi.org/10.1016/S0952-7915(03)00080-3

Korhonen, R., Korpela, R., Saxelin, M., Mäki, M., Kankaanranta, H., & Moilanen, E. (2001). Induction of nitric oxide synthesis by probiotic Lactobacillus rhamnosus GG in J774 macrophages and human T84 intestinal epithelial cells. *Inflammation*, *25*(4), 223–232. https://doi.org/10.1023/a:1010971703271

Korn, T., Bettelli, E., Oukka, M., & Kuchroo, V. K. (2009). IL-17 and Th17 Cells | Annual Review of Immunology. *Annual Review of Immunology*, *27*(1), 485–517.

Kumar, B. V., Connors, T., & Farber, D. L. (2018). Human T cell development, localization, and function throughout life. *Immunity*, *48*(2), 202–213. https://doi.org/10.1016/j.immuni.2018.01.007

Kwon, H.-K., Jo, W.-R., & Park, H.-J. (2018). Immune-enhancing activity of C. militaris fermented with Pediococcus pentosaceus (GRC-ON89A) in CY-induced immunosuppressed model. *BMC Complementary and Alternative Medicine*, *18*(1), 75. https://doi.org/10.1186/s12906-018-2133-9

Laing, K., & Fred Hutchinson Cancer Research Centre. (2020). *Immune responses to viruses | British Society for Immunology*. British Society for Immunology. https://www.immunology.org/public-information/bitesized-immunology/pathogens-and-disease/immune-responses-viruses

Latz, E., Visintin, A., Espevik, T., & Golenbock, D. T. (2004). Mechanisms of TLR9 activation. *Journal of Endotoxin Research*, *10*(6), 406–412. https://doi.org/10.1177/09680519040100060501

Lee, J. S., Cho, M. K., Hwang, H. S., Ko, E.-J., Lee, Y.-N., Kwon, Y.-M., Kim, M.-C., Kim, K.-H., Lee, Y.-T., Jung, Y.-J., & Kang, S.-M. (2014). Ginseng Diminishes Lung Disease in Mice Immunized with Formalin-Inactivated Respiratory Syncytial Virus After Challenge by Modulating Host Immune Responses. *Journal of Interferon & Cytokine Research*, *34*(11), 902–914. https://doi.org/10.1089/jir.2013.0093

Lester, S. N., & Li, K. (2014). Toll-like receptors in antiviral innate immunity. *Journal of Molecular Biology*, *426*(6), 1246–1264. https://doi.org/10.1016/j.jmb.2013.11.024

Lewis, J. D. (2016). The Role of Diet in Inflammatory Bowel Disease. *Gastroenterology & Hepatology*, *12*(1), 51–53.

Li, C., Xi, Y., Li, S., Zhao, Q., Cheng, W., Wang, Z., Zhong, J., Niu, X., & Chen, G. (2015). Berberine ameliorates TNBS induced colitis by inhibiting inflammatory responses and Th1/Th17 differentiation. *Molecular Immunology*, *67*(2 Pt B), 444–454. https://doi.org/10.1016/j.molimm.2015.07.013

Li, M., Li, P., Tang, R., & Lu, H. (2022). Resveratrol and its derivates improve inflammatory bowel disease by targeting gut microbiota and inflammatory signaling pathways. *Food Science and Human Wellness*, *11*(1), 22–31. https://doi.org/10.1016/j.fshw.2021.07.003

Li, X., Zhang, M., Zhou, G., Xie, Z., Wang, Y., Han, J., Li, L., Wu, Q., & Zhang, S. (2023). Role of Rho GTPases in inflammatory bowel disease. *Cell Death Discovery*, *9*(1), Article 1. https://doi.org/10.1038/s41420-023-01329-w

Liao, W., Lin, J.-X., & Leonard, W. J. (2011). IL-2 family cytokines: New insights into the complex roles of IL-2 as a broad regulator of T helper cell differentiation. *Current Opinion in Immunology*, *23*(5), 598–604. https://doi.org/10.1016/j.coi.2011.08.003

Lim, T.-G., Jang, M., Cho, C.-W., Hong, H.-D., Kim, K.-T., Lee, S.-Y., Jung, S. K., & Rhee, Y. K. (2016). White ginseng extract induces immunomodulatory effects via the MKK4-JNK pathway. *Food Science and Biotechnology*, *25*(6), 1737–1744. https://doi.org/10.1007/s10068-016-0265-6

Lim, W.-C., Hanauer, S. B., & Li, Y. C. (2005). Mechanisms of Disease: Vitamin D and inflammatory bowel disease. *Nature Clinical Practice*

Gastroenterology & Hepatology, *2*(7), Article 7. https://doi.org/10.1038/ncpgasthep0215

Lin, H., Zhang, W., Jiang, X., Chen, R., Huang, X., & Huang, Z. (2017). Total glucosides of paeony ameliorates TNBS-induced colitis by modulating differentiation of Th17/Treg cells and the secretion of cytokines. *Molecular Medicine Reports*, *16*(6), 8265–8276. https://doi.org/10.3892/mmr.2017.7598

Loughran, S. T., Power, P. A., Maguire, P. T., McQuaid, S. L., Buchanan, P. J., Jonsdottir, I., Newman, R. W., Harvey, R., & Johnson, P. A. (2018). Influenza infection directly alters innate IL-23 and IL-12p70 and subsequent IL-17A and IFN-γ responses to pneumococcus in vitro in human monocytes. *PLoS ONE*, *13*(9), e0203521. https://doi.org/10.1371/journal.pone.0203521

Lucas, S., Ghilardi, N., Li, J., & de Sauvage J., F. (2003). IL-27 regulates IL-12 responsiveness of naïve CD4+ T cells through Stat1-dependent and -independent mechanisms. *Proceedings of the National Academy of Sciences*, *100*(25), 15047–15052. https://doi.org/10.1073/pnas.2536517100

Lund, J. M., Hsing, L., Thuy T., P., & Alexander Y., R. (2008). *Coordination of Early Protective Immunity to Viral Infection by Regulatory T Cells*. https://doi.org/10.1126/science.1155209

Luo, A., Leach, S. T., Barres, R., Hesson, L. B., Grimm, M. C., & Simar, D. (2017). The Microbiota and Epigenetic Regulation of T Helper 17/Regulatory T Cells: In Search of a Balanced Immune System. *Frontiers in Immunology*, *8*. https://www.frontiersin.org/articles/10.3389/fimmu.2017.00417

Luster, A. D., Alon, R., & von Andrian, U. H. (2005). Immune cell migration in inflammation: Present and future therapeutic targets. *Nature Immunology*, *6*(12), Article 12. https://doi.org/10.1038/ni1275

MacDermott, R. P., Nash, G. S., Bertovich, M. J., Seiden, M. V., Bragdon, M. J., & Beale, M. G. (1981). Alterations of IgM, IgG, and IgA Synthesis and Secretion by Peripheral Blood and Intestinal Mononuclear Cells from Patients with Ulcerative Colitis and Crohn's Disease. *Gastroenterology*, *81*(5), 844–852. https://doi.org/10.1016/S0016-5085(81)80107-2

Maeno, M., Yamamoto, N., & Takano, T. (1996). Identification of an Antihypertensive Peptide from Casein Hydrolysate Produced by a Proteinase from Lactobacillus helveticus CP790. *Journal of Dairy Science*, *79*(8), 1316–1321. https://doi.org/10.3168/jds.S0022-0302(96)76487-1

Makino, S., Ikegami, S., Kume, A., Horiuchi, H., Sasaki, H., & Orii, N. (2010). Reducing the risk of infection in the elderly by dietary intake of yoghurt fermented with Lactobacillus delbrueckii ssp. Bulgaricus OLL1073R-1. *The British Journal of Nutrition*, *104*(7), 998–1006. https://doi.org/10.1017/S000711451000173X

Marsh, M., & Helenius, A. (2006). Virus Entry: Open Sesame. *Cell*, *124*(4), 729–740. https://doi.org/10.1016/j.cell.2006.02.007

Martín-Peláez, S., Castañer, O., Solà, R., Motilva, M. J., Castell, M., Pérez-Cano, F. J., & Fitó, M. (2016). Influence of Phenol-Enriched Olive Oils on Human Intestinal Immune Function. *Nutrients*, *8*(4), Article 4. https://doi.org/10.3390/nu8040213

Martin-Vega, A., & Cobb, M. H. (2023). Navigating the ERK1/2 MAPK Cascade. *Biomolecules*, *13*(10), Article 10. https://doi.org/10.3390/biom13101555

Maruyama, T., Kono, K., Mizukami, Y., Kawaguchi, Y., Mimura, K., Watanabe, M., Izawa, S., & Fujii, H. (2010). Distribution of Th17 cells and FoxP3(+) regulatory T cells in tumor-infiltrating lymphocytes, tumor-draining lymph nodes and peripheral blood lymphocytes in patients with gastric cancer. *Cancer Science*, *101*(9), 1947–1954. https://doi.org/10.1111/j.1349-7006.2010.01624.x

Mathur, H., Beresford, T. P., & Cotter, P. D. (2020). Health Benefits of Lactic Acid Bacteria (LAB) Fermentates. *Nutrients*, *12*(6), Article 6. https://doi.org/10.3390/nu12061679

Matsumoto, M., & Seya, T. (2008). TLR3: Interferon induction by double-stranded RNA including poly(I:C). *Advanced Drug Delivery Reviews*, *60*(7), 805–812. https://doi.org/10.1016/j.addr.2007.11.005

McCartney, D. M., & Byrne, D. G. (2020). *Optimisation of Vitamin D Status for Enhanced Immuno-protection Against Covid-19*. 4.

Mehrbod, P., Abdalla, M. A., Fotouhi, F., Heidarzadeh, M., Aro, A. O., Eloff, J. N., McGaw, L. J., & Fasina, F. O. (2018). Immunomodulatory properties of quercetin-3-O-α-L-rhamnopyranoside from Rapanea melanophloeos against influenza a virus. *BMC Complementary and Alternative Medicine*, *18*(1), 184. https://doi.org/10.1186/s12906-018-2246-1

Millman, J. F., Okamoto, S., Teruya, T., Uema, T., Ikematsu, S., Shimabukuro, M., & Masuzaki, H. (2021). Extra-virgin olive oil and the gut-brain axis: Influence on gut microbiota, mucosal immunity, and cardiometabolic and cognitive

health. *Nutrition Reviews*, *79*(12), 1362–1374. https://doi.org/10.1093/nutrit/nuaa148

Mills, C. (2012). M1 and M2 Macrophages: Oracles of Health and Disease. *Critical Reviews™ in Immunology*, *32*(6). https://doi.org/10.1615/CritRevImmunol.v32.i6.10

Miltenyi Biotech. (2023). *TH cell differentiation | CD4 T cell differentiation | Miltenyi | Miltenyi Biotec | Ireland*. https://www.miltenyibiotec.com/IE-en/applications/by-cell-type/t-cells/polarization-of-cd4-t-helper-cells.html?filterContent=facet.filter.Content_type%3DAntibody%2Bpanel%26facet.filter.Content_type%3DApplication%2Bprotocol%26facet.filter.Cell_type%3DT%2Bcells&list=377f1f0a-7765-4d7d-8d01-5749021125c7.en_IE

Mitselou, A., Grammeniatis, V., Varouktsi, A., Papadatos, S. S., Katsanos, K., & Galani, V. (2020). Proinflammatory cytokines in irritable bowel syndrome: A comparison with inflammatory bowel disease. *Intestinal Research*, *18*(1), 115–120. https://doi.org/10.5217/ir.2019.00125

Mogensen, T. H., & Paludan, S. R. (2005). Reading the viral signature by Toll-like receptors and other pattern recognition receptors. *Journal of Molecular Medicine (Berlin, Germany)*, *83*(3), 180–192. https://doi.org/10.1007/s00109-004-0620-6

Montazersaheb, S., Hosseiniyan Khatibi, S. M., Hejazi, M. S., Tarhriz, V., Farjami, A., Ghasemian Sorbeni, F., Farahzadi, R., & Ghasemnejad, T. (2022). COVID-19 infection: An overview on cytokine storm and related

interventions. *Virology Journal*, *19*(1), 92. https://doi.org/10.1186/s12985-022-01814-1

Monteleone, G., Boirivant, M., Pallone, F., & MacDonald, T. T. (2008). TGF-beta1 and Smad7 in the regulation of IBD. *Mucosal Immunology*, *1 Suppl 1*, S50-53. https://doi.org/10.1038/mi.2008.55

Monteleone, I., Sarra, M., Pallone, F., & Monteleone, G. (2012). Th17-related cytokines in inflammatory bowel diseases: Friends or foes? *Current Molecular Medicine*, *12*(5), 592–597. https://doi.org/10.2174/156652412800620066

Moore, K. W., de Waal Malefyt, R., Coffman, R. L., & O'Garra, A. (2001). Interleukin-10 and the Interleukin-10 Receptor. *Annual Review of Immunology*, *19*(1), 683–765. https://doi.org/10.1146/annurev.immunol.19.1.683

Mottet, C., Uhlig, H. H., & Powrie, F. (2003). Cutting edge: Cure of colitis by CD4+CD25+ regulatory T cells. *Journal of Immunology (Baltimore, Md.: 1950)*, *170*(8), 3939–3943. https://doi.org/10.4049/jimmunol.170.8.3939

Moyad, M. A., Robinson, L. E., Zawada, E. T., Kittelsrud, J., Chen, D.-G., Reeves, S. G., & Weaver, S. (2010). Immunogenic Yeast-Based Fermentate for Cold/Flu-like Symptoms in Nonvaccinated Individuals. *Journal of Alternative and Complementary Medicine*, *16*(2), 213–218. https://doi.org/10.1089/acm.2009.0310

Moyad, M. A., Robinson, L. E., Zawada, E. T., Kittelsrud, J. M., Chen, D.-G., Reeves, S. G., & Weaver, S. E. (2008). Effects of a modified yeast supplement on cold/flu symptoms. *Urologic Nursing*, *28*(1), 50–55.

Mueller, S. N., & Rouse, B. T. (2008). Immune responses to viruses. *Clinical Immunology*, 421–431. https://doi.org/10.1016/B978-0-323-04404-2.10027-2

Mühl, H., & Pfeilschifter, J. (2003). Anti-inflammatory properties of pro-inflammatory interferon-γ. *International Immunopharmacology*, *3*(9), 1247–1255. https://doi.org/10.1016/S1567-5769(03)00131-0

Mukherjee, S., Karmakar, S., & Babu, S. P. S. (2016). TLR2 and TLR4 mediated host immune responses in major infectious diseases: A review. *The Brazilian Journal of Infectious Diseases: An Official Publication of the Brazilian Society of Infectious Diseases*, *20*(2), 193–204. https://doi.org/10.1016/j.bjid.2015.10.011

Mullié, C., Yazourh, A., Thibault, H., Odou, M.-F., Singer, E., Kalach, N., Kremp, O., & Romond, M.-B. (2004). Increased Poliovirus-Specific Intestinal Antibody Response Coincides with Promotion of Bifidobacterium longum-infantis and Bifidobacterium breve in Infants: A Randomized, Double-Blind, Placebo-Controlled Trial. *Pediatric Research*, *56*(5), 791–795. https://doi.org/10.1203/01.PDR.0000141955.47550.A0

Nainu, F., Shiratsuchi, A., & Nakanishi, Y. (2017). Induction of Apoptosis and Subsequent Phagocytosis of Virus-Infected Cells As an Antiviral Mechanism. *Frontiers in Immunology*, *8*, 1220. https://doi.org/10.3389/fimmu.2017.01220

National Institute of Health. (2021). *Office of Dietary Supplements—Vitamin D*. https://ods.od.nih.gov/factsheets/VitaminD-Consumer/

Negroni, A., Pierdomenico, M., Cucchiara, S., & Stronati, L. (2018). NOD2 and inflammation: Current insights. *Journal of Inflammation Research*, *11*, 49–60. https://doi.org/10.2147/JIR.S137606

Neurath, M. F., Fuss, I., Kelsall, B. L., Presky, D. H., Waegell, W., & Strober, W. (1996). Experimental granulomatous colitis in mice is abrogated by induction of TGF-beta-mediated oral tolerance. *The Journal of Experimental Medicine*, *183*(6), 2605–2616. https://doi.org/10.1084/jem.183.6.2605

Nigar, S., & Shimosato, T. (2019). Cooperation of Oligodeoxynucleotides and Synthetic Molecules as Enhanced Immune Modulators. *Frontiers in Nutrition*, *6*. https://www.frontiersin.org/article/10.3389/fnut.2019.00140

NIH. (2017, March 13). *How dietary factors influence disease risk*. National Institutes of Health (NIH). https://www.nih.gov/news-events/nih-research-matters/how-dietary-factors-influence-disease-risk

Novelli, F., & Casanova, J.-L. (2004). The role of IL-12, IL-23 and IFN-γ in immunity to viruses. *Cytokine & Growth Factor Reviews*, *15*(5), 367–377. https://doi.org/10.1016/j.cytogfr.2004.03.009

Obi, N., Hayashi, K., Miyahara, T., Shimada, Y., Terasawa, K., Watanabe, M., Takeyama, M., Obi, R., & Ochiai, H. (2008). Inhibitory Effect of TNF-α Produced by Macrophages Stimulated with Grifola frondosa Extract (ME) on the Growth of Influenza A/Aichi/2/68 Virus in MDCK Cells. *The American Journal of Chinese Medicine*, *36*(06), 1171–1183. https://doi.org/10.1142/S0192415X08006508

Office of the Food and Drug Administration. (2021, August 23). *FDA Approves First COVID-19 Vaccine*. FDA; FDA. https://www.fda.gov/news-events/press-announcements/fda-approves-first-covid-19-vaccine

Oh, S. A., & Li, M. O. (2013). TGF-β: Guardian of T Cell Function. *The Journal of Immunology*, *191*(8), 3973–3979. https://doi.org/10.4049/jimmunol.1301843

Ohta, Y., Lee, J.-B., Hayashi, K., Fujita, A., Park, D. K., & Hayashi, T. (2007). In Vivo Anti-influenza Virus Activity of an Immunomodulatory Acidic Polysaccharide Isolated from Cordyceps militaris Grown on Germinated Soybeans. *Journal of Agricultural and Food Chemistry*, *55*(25), 10194–10199. https://doi.org/10.1021/jf0721287

Okeke, E. B., & Uzonna, J. E. (2019). The Pivotal Role of Regulatory T Cells in the Regulation of Innate Immune Cells. *Frontiers in Immunology*, *10*. https://www.frontiersin.org/articles/10.3389/fimmu.2019.00680

Omar, S. H. (2010). Oleuropein in Olive and its Pharmacological Effects. *Scientia Pharmaceutica*, *78*(2), 133–154. https://doi.org/10.3797/scipharm.0912-18

Oppmann, B., Lesley, R., Blom, B., Timans, J. C., Xu, Y., Hunte, B., Vega, F., Yu, N., Wang, J., Singh, K., Zonin, F., Vaisberg, E., Churakova, T., Liu, M., Gorman, D., Wagner, J., Zurawski, S., Liu, Y.-J., Abrams, J. S., … Kastelein, R. A. (2000). Novel p19 Protein Engages IL-12p40 to Form a Cytokine, IL-23, with Biological Activities Similar as Well as Distinct from IL-12. *Immunity*, *13*(5), 715–725. https://doi.org/10.1016/S1074-7613(00)00070-4

Öztürk, H. İ., & Özel, Z. B. (2020). Antiviral Mechanisms Related to Lactic Acid Bacteria and Fermented Food Products. *Tarla Bitkileri Merkez Arastirma Enstitusu*, *29*(1), 18–28. https://doi.org/10.38042/biost.2020.29.01.03

Pahl, M., & Vaziri, N. (2015). *Chronic Renal Disease* (1st ed.). Academic Press.

Papamanoli, E., Tzanetakis, N., Litopoulou-Tzanetaki, E., & Kotzekidou, P. (2003). Characterization of lactic acid bacteria isolated from a Greek dry-fermented sausage in respect of their technological and probiotic properties. *Meat Science*, *65*(2), 859–867. https://doi.org/10.1016/S0309-1740(02)00292-9

Park, B. S., & Lee, J.-O. (2013). Recognition of lipopolysaccharide pattern by TLR4 complexes. *Experimental & Molecular Medicine*, *45*(12), Article 12. https://doi.org/10.1038/emm.2013.97

Payne, S. (2017). *Viruses: From Understanding To Investigation* (1st ed.). Academic Press.

Peck, A., & Mellins, E. D. (2010). Plasticity of T-cell phenotype and function: The T helper type 17 example. *Immunology*, *129*(2), 147–153. https://doi.org/10.1111/j.1365-2567.2009.03189.x

Peluzio, M. do C. G., Dias, M. de M. e, Martinez, J. A., & Milagro, F. I. (2021). Kefir and Intestinal Microbiota Modulation: Implications in Human Health. *Frontiers in Nutrition*, *8*. https://www.frontiersin.org/articles/10.3389/fnut.2021.638740

Pérez-Cano, F. J. (2022). Mediterranean Diet, Microbiota and Immunity. *Nutrients*, *14*(273). https://doi.org/10.3390/nu14020273

Pernow, J., & Jung, C. (2013). Arginase as a potential target in the treatment of cardiovascular disease: Reversal of arginine steal? *Cardiovascular Research*, *98*(3), 334–343. https://doi.org/10.1093/cvr/cvt036

Pessione, E. (2012). Lactic acid bacteria contribution to gut microbiota complexity: Lights and shadows. *Frontiers in Cellular and Infection Microbiology*, *2*. https://www.frontiersin.org/article/10.3389/fcimb.2012.00086

Popovic, N., Brdarić, E., Djokic, J., Dinic, M., Veljovic, K., Golić, N., & Terzic-Vidojevic, A. (2020). Yogurt Produced by Novel Natural Starter Cultures Improves Gut Epithelial Barrier In Vitro. *Microorganisms*. https://doi.org/10.3390/microorganisms8101586

Pražnikar, Z. J., Kenig, S., Vardjan, T., Bizjak, M. Č., & Petelin, A. (2020). Effects of kefir or milk supplementation on zonulin in overweight subjects. *Journal of Dairy Science*, *103*(5), 3961–3970. https://doi.org/10.3168/jds.2019-17696

Rachna, C. (2019, May 14). Difference Between Humoral and Cell-Mediated Immunity (with Comparison Chart). *Bio Differences*. https://biodifferences.com/difference-between-humoral-and-cell-mediated-immunity.html

Rahman, Md. M., Mosaddik, A., & Alam, A. K. (2021). Traditional foods with their constituent's antiviral and immune system modulating properties. *Heliyon*, *7*(1), e05957. https://doi.org/10.1016/j.heliyon.2021.e05957

Rath, M., Müller, I., Kropf, P., Closs, E. I., & Munder, M. (2014). Metabolism via Arginase or Nitric Oxide Synthase: Two Competing Arginine Pathways in

Macrophages. *Frontiers in Immunology*, *5*, 532. https://doi.org/10.3389/fimmu.2014.00532

R&D Systems Inc. (2012). *Toll-Like Receptor Signaling Pathways*. Www.Rndsystems.Com. https://www.rndsystems.com/pathways/toll-like-receptor-signaling-pathways

Reinecker, H. C., Steffen, M., Witthoeft, T., Pflueger, I., Schreiber, S., MacDermott, R. P., & Raedler, A. (1993). Enhanced secretion of tumour necrosis factor-alpha, IL-6, and IL-1 beta by isolated lamina propria mononuclear cells from patients with ulcerative colitis and Crohn's disease. *Clinical and Experimental Immunology*, *94*(1), 174–181. https://doi.org/10.1111/j.1365-2249.1993.tb05997.x

Research and Markets. (2021). *Immune Health Supplements Market—Global Outlook and Forecast 2020-2025*. https://www.researchandmarkets.com/reports/5118924/immune-health-supplements-market-global-outlook

Ridley, A. J., Schwartz, M. A., Burridge, K., Firtel, R. A., Ginsberg, M. H., Borisy, G., Parsons, J. T., & Horwitz, A. R. (2003). Cell Migration: Integrating Signals from Front to Back. *Science*, *302*(5651), 1704–1709. https://doi.org/10.1126/science.1092053

Rocamora-Reverte, L., Melzer, F. L., Würzner, R., & Weinberger, B. (2021). The Complex Role of Regulatory T Cells in Immunity and Aging. *Frontiers in Immunology*, *11*. https://www.frontiersin.org/articles/10.3389/fimmu.2020.616949

Rogers, K. J., Shtanko, O., Stunz, L. L., Mallinger, L. N., Arkee, T., Schmidt, M. E., Bohan, D., Brunton, B., White, J. M., Varga, S. M., Butler, N. S., Bishop, G. A., & Maury, W. (2021). Frontline Science: CD40 signaling restricts RNA virus replication in Mϕs, leading to rapid innate immune control of acute virus infection. *Journal of Leukocyte Biology*, *109*(2), 309–325. https://doi.org/10.1002/JLB.4HI0420-285RR

Rojas, J. M., Avia, M., Martín, V., & Sevilla, N. (2017). IL-10: A Multifunctional Cytokine in Viral Infections. *Journal of Immunology Research*, *2017*, 6104054. https://doi.org/10.1155/2017/6104054

Rook, G. A., Taverne, J., & Playfair, J. H. (1991). Evaluation of TNF as antiviral, antibacterial and antiparasitic agent. *Biotherapy (Dordrecht, Netherlands)*, *3*(2), 167–175. https://doi.org/10.1007/BF02172089

Ross, S. H., & Cantrell, D. A. (2018). Signaling and Function of Interleukin-2 in T Lymphocytes. *Annual Review of Immunology*, *36*, 411–433. https://doi.org/10.1146/annurev-immunol-042617-053352

Rouse, B. T., & Sehrawat, S. (2010). Immunity and immunopathology to viruses: What decides the outcome? *Nature Reviews Immunology*, *10*(7), Article 7. https://doi.org/10.1038/nri2802

Ruby, J., Bluethmann, H., & Peschon, J. J. (1997). Antiviral Activity of Tumor Necrosis Factor (TNF) Is Mediated via p55 and p75 TNF Receptors. *The Journal of Experimental Medicine*, *186*(9), 1591–1596.

Ruiz de Morales, J. M. G., Puig, L., Daudén, E., Cañete, J. D., Pablos, J. L., Martín, A. O., Juanatey, C. G., Adán, A., Montalbán, X., Borruel, N., Ortí, G., Holgado-Martín, E., García-Vidal, C., Vizcaya-Morales, C., Martín-Vázquez,

V., & González-Gay, M. Á. (2020). Critical role of interleukin (IL)-17 in inflammatory and immune disorders: An updated review of the evidence focusing in controversies. *Autoimmunity Reviews*, *19*(1), 102429. https://doi.org/10.1016/j.autrev.2019.102429

S. Clemente, G., van Waarde, A., F. Antunes, I., Dömling, A., & H. Elsinga, P. (2020). Arginase as a Potential Biomarker of Disease Progression: A Molecular Imaging Perspective. *International Journal of Molecular Sciences*, *21*(15), Article 15. https://doi.org/10.3390/ijms21155291

Saeed, S., Rasool, S. A., Ahmad, S., Zaidi, S. Z., & Rehmani, S. (2007). Antiviral activity of staphylococcin 188: A purified bacteriocin like inhibitory substance isolated from Staphylococcus aureus AB188. *Research Journal of Microbiology*, *2*(11), 796–806. Scopus. https://doi.org/10.3923/jm.2007.796.806

Saito, S., Nakashima, A., Shima, T., & Ito, M. (2010). REVIEW ARTICLE: Th1/Th2/Th17 and Regulatory T-Cell Paradigm in Pregnancy. *American Journal of Reproductive Immunology*, *63*(6), 601–610. https://doi.org/10.1111/j.1600-0897.2010.00852.x

Saqib, U., Sarkar, S., Suk, K., Mohammad, O., Baig, M. S., & Savai, R. (2018). Phytochemicals as modulators of M1-M2 macrophages in inflammation. *Oncotarget*, *9*(25), 17937–17950. https://doi.org/10.18632/oncotarget.24788

Schandalik, R., Gatti, G., & Perucca, E. (1992). Pharmacokinetics of silybin in bile following administration of silipide and silymarin in cholecystectomy patients. *Arzneimittel-Forschung*, *42*(7), 964–968.

Schön, M. P., & Erpenbeck, L. (2018). The Interleukin-23/Interleukin-17 Axis Links Adaptive and Innate Immunity in Psoriasis. *Frontiers in Immunology*, *9*. https://www.frontiersin.org/article/10.3389/fimmu.2018.01323

Selverajah, M., Zakaria, Z. A., Long, K., Ahmad, Z., Yaacob, A., & Somchit, M. N. (2016). Anti-ulcerogenic activity of virgin coconut oil contribute to the stomach health of humankind. *CELLMED*, *6*(2), 11.1-11.7. https://doi.org/10.5667/tang.2015.0031

Seo, S. H., & Webster, R. G. (2002a). Tumor Necrosis Factor Alpha Exerts Powerful Anti-Influenza Virus Effects in Lung Epithelial Cells. *Journal of Virology*, *76*(3), 1071–1076. https://doi.org/10.1128/JVI.76.3.1071-1076.2002

Seo, S. H., & Webster, R. G. (2002b). Tumor Necrosis Factor Alpha Exerts Powerful Anti-Influenza Virus Effects in Lung Epithelial Cells. *Journal of Virology*, *76*(3), 1071–1076. https://doi.org/10.1128/JVI.76.3.1071-1076.2002

Serkedjieva, J., Danova, S., & Ivanova, I. (2000). Antiinfluenza virus activity of a bacteriocin produced by Lactobacillus delbrueckii. *Applied Biochemistry and Biotechnology*, *88*(1), 285–298. https://doi.org/10.1385/ABAB:88:1-3:285

Sharma, D. P., Ramsay, A. J., Maguire, D. J., Rolph, M. S., & Ramshaw, I. A. (1996). Interleukin-4 mediates down regulation of antiviral cytokine expression and cytotoxic T-lymphocyte responses and exacerbates vaccinia virus infection in vivo. *Journal of Virology*, *70*(10), 7103–7107. https://doi.org/10.1128/JVI.70.10.7103-7107.1996

Sharma, J. N., Al-Omran, A., & Parvathy, S. S. (2007). Role of nitric oxide in inflammatory diseases. *Inflammopharmacology*, *15*(6), 252–259. https://doi.org/10.1007/s10787-007-0013-x

Shi, Y., Zhou, J., Jiang, B., & Miao, M. (2017). Resveratrol and inflammatory bowel disease. *Annals of the New York Academy of Sciences*, *1403*(1), 38–47. https://doi.org/10.1111/nyas.13426

Shibata, T., Kanayama, M., Haida, M., Fujimoto, S., Oroguchi, T., Sata, K., Mita, N., Kutsuzawa, T., Ikeuchi, M., Kondo, M., Naito, K., Tsuda, M., Nishizaki, Y., & Ishii, N. (2016). Lactococcus lactis JCM5805 activates anti-viral immunity and reduces symptoms of common cold and influenza in healthy adults in a randomized controlled trial. *Journal of Functional Foods*, *24*, 492–500. https://doi.org/10.1016/j.jff.2016.03.035

Silva, F. A. R., Rodrigues, B. L., Ayrizono, M. de L. S., & Leal, R. F. (2016). The Immunological Basis of Inflammatory Bowel Disease. *Gastroenterology Research and Practice*, *2016*, e2097274. https://doi.org/10.1155/2016/2097274

Singh, S., Anshita, D., & Ravichandiran, V. (2021). MCP-1: Function, regulation, and involvement in disease. *International Immunopharmacology*, *101*, 107598. https://doi.org/10.1016/j.intimp.2021.107598

Sodano, F., Gazzano, E., Fruttero, R., & Lazzarato, L. (2022). NO in Viral Infections: Role and Development of Antiviral Therapies. *Molecules (Basel, Switzerland)*, *27*(7), 2337. https://doi.org/10.3390/molecules27072337

Song, D., He, Z., Wang, C., Yuan, F., Dong, P., & Zhang, W. (2013). Regulation of the exopolysaccharide from an anamorph of Cordyceps sinensis on

dendritic cell sarcoma (DCS) cell line. *European Journal of Nutrition*, *52*(2), 687–694. https://doi.org/10.1007/s00394-012-0373-x

Song, Y., Yuan, M., Xu, Y., & Xu, H. (2022). Tackling Inflammatory Bowel Diseases: Targeting Proinflammatory Cytokines and Lymphocyte Homing. *Pharmaceuticals*, *15*(1080). https://doi.org/10.3390/ ph15091080

Sørensen, H. M., Rochfort, K. D., Maye, S., MacLeod, G., Brabazon, D., Loscher, C., & Freeland, B. (2022). Exopolysaccharides of Lactic Acid Bacteria: Production, Purification and Health Benefits towards Functional Food. *Nutrients*, *14*(14), Article 14. https://doi.org/10.3390/nu14142938

Speca, S., Giusti, I., Rieder, F., & Latella, G. (2012). Cellular and molecular mechanisms of intestinal fibrosis. *World Journal of Gastroenterology*, *18*(28), 3635–3661. https://doi.org/10.3748/wjg.v18.i28.3635

Spellberg, B., & Edwards, J. E., Jr. (2001). Type 1/Type 2 Immunity in Infectious Diseases. *Clinical Infectious Diseases*, *32*(1), 76–102. https://doi.org/10.1086/317537

Sugimura, T., Jounai, K., Ohshio, K., Tanaka, T., Suwa, M., & Fujiwara, D. (2013). Immunomodulatory effect of Lactococcus lactis JCM5805 on human plasmacytoid dendritic cells. *Clinical Immunology*, *149*(3, Part B), 509–518. https://doi.org/10.1016/j.clim.2013.10.007

Sugimura, T., Takahashi, H., Jounai, K., Ohshio, K., Kanayama, M., Tazumi, K., Tanihata, Y., Miura, Y., Fujiwara, D., & Yamamoto, N. (2015). Effects of oral intake of plasmacytoid dendritic cells-stimulative lactic acid bacterial strain on pathogenesis of influenza-like illness and immunological

response to influenza virus. *The British Journal of Nutrition*, *114*(5), 727–733. https://doi.org/10.1017/S0007114515002408

Sun, L., Su, Y., Jiao, A., Wang, X., & Zhang, B. (2023). T cells in health and disease. *Signal Transduction and Targeted Therapy*, *8*(1), Article 1. https://doi.org/10.1038/s41392-023-01471-y

Sun, P., Kim, Y., Lee, H., Kim, J., Han, B. K., Go, E., Kwon, S., Kang, J.-G., You, S., & Kwon, J. (2020). Carrot Pomace Polysaccharide (CPP) Improves Influenza Vaccine Efficacy in Immunosuppressed Mice via Dendritic Cell Activation. *Nutrients*, *12*(9), Article 9. https://doi.org/10.3390/nu12092740

Sundararaman, A., Ray, M., Ravindra, P. V., & Halami, P. M. (2020). Role of probiotics to combat viral infections with emphasis on COVID-19. *Applied Microbiology and Biotechnology*, *104*(19), 8089–8104. https://doi.org/10.1007/s00253-020-10832-4

Tahmasebi, S., Saeed, B., Temirgalieva, E., Yumashev, A., A. El-Esawi, M., Navashenaq, J., Valizadeh, H., Sadeghi, A., Aslani, S., Yousefi, M., Jadidi-Niaragh, F., Adigozalou, J., Ahmadi, M., & Roshangar, L. (2021). Nanocurcumin improves Treg cell responses in patients with mild and severe SARS-CoV2. *Life Sciences*, *276*, 119437. https://doi.org/10.1016/j.lfs.2021.119437

Takeda, S., Kawahara, S., Hidaka, M., Yoshida, H., Watanabe, W., Takeshita, M., Kikuchi, Y., Bumbein, D., Muguruma, M., & Kurokawa, M. (2013). Effects of Oral Administration of Probiotics from Mongolian Dairy Products on the Th1 Immune Response in Mice. *Bioscience, Biotechnology, and Biochemistry*, *77*(7), 1372–1378. https://doi.org/10.1271/bbb.120624

Takeda, S., Takeshita, M., Kikuchi, Y., Dashnyam, B., Kawahara, S., Yoshida, H., Watanabe, W., Muguruma, M., & Kurokawa, M. (2011). Efficacy of oral administration of heat-killed probiotics from Mongolian dairy products against influenza infection in mice: Alleviation of influenza infection by its immunomodulatory activity through intestinal immunity. *International Immunopharmacology*, *11*(12), 1976–1983. https://doi.org/10.1016/j.intimp.2011.08.007

Takehara, M., Kuida, K., & Mori, K. (1979). Antiviral activity of virus-like particles fromLentinus edodes (Shiitake). *Archives of Virology*, *59*(3), 269–274. https://doi.org/10.1007/BF01317423

Takei, M., Tachikawa, E., Hasegawa, H., & Lee, J.-J. (2004). Dendritic cells maturation promoted by M1 and M4, end products of steroidal ginseng saponins metabolized in digestive tracts, drive a potent Th1 polarization. *Biochemical Pharmacology*, *68*(3), 441–452. https://doi.org/10.1016/j.bcp.2004.04.015

Tanaka, T., Narazaki, M., & Kishimoto, T. (2014). IL-6 in Inflammation, Immunity, and Disease. *Cold Spring Harbor Perspectives in Biology*, *6*(10), a016295. https://doi.org/10.1101/cshperspect.a016295

Tang, H., Ma, H., Hou, Q., Li, W., Xu, H., Liu, W., Sun, Z., Haobisi, H., & Menghe, B. (2020). Profiling of koumiss microbiota and organic acids and their effects on koumiss taste. *BMC Microbiology*, *20*, 85. https://doi.org/10.1186/s12866-020-01773-z

Tao, J.-H., Duan, J.-A., Jiang, S., Feng, N.-N., Qiu, W.-Q., & Ling, Y. (2017). Polysaccharides from Chrysanthemum morifolium Ramat ameliorate

colitis rats by modulating the intestinal microbiota community. *Oncotarget*, *8*(46), 80790–80803. https://doi.org/10.18632/oncotarget.20477

Tau, G., & Rothman, P. (1999). Biologic functions of the IFN-γ receptors. *Allergy*, *54*(12), 1233–1251. https://doi.org/10.1034/j.1398-9995.1999.00099.x

Tay, M. Z., Wiehe, K., & Pollara, J. (2019). Antibody-Dependent Cellular Phagocytosis in Antiviral Immune Responses. *Frontiers in Immunology*, *10*. https://www.frontiersin.org/articles/10.3389/fimmu.2019.00332

The Editors of Encyclopaedia. (2020). T cell | Definition, Function, & Facts | Britannica. In *Britannica*. https://www.britannica.com/science/T-cell

Theofilopoulos, A. N., Baccala, R., Beutler, B., & Kono, D. H. (2005). TYPE I INTERFERONS (α/β) IN IMMUNITY AND AUTOIMMUNITY. *Annual Review of Immunology*, *23*(1), 307–335. https://doi.org/10.1146/annurev.immunol.23.021704.115843

Thomas, S. J., Moreira, E. D., Kitchin, N., Absalon, J., Gurtman, A., Lockhart, S., Perez, J. L., Pérez Marc, G., Polack, F. P., Zerbini, C., Bailey, R., Swanson, K. A., Xu, X., Roychoudhury, S., Koury, K., Bouguermouh, S., Kalina, W. V., Cooper, D., Frenck, R. W., … Jansen, K. U. (2021). Safety and Efficacy of the BNT162b2 mRNA Covid-19 Vaccine through 6 Months. *New England Journal of Medicine*, *385*(19), 1761–1773. https://doi.org/10.1056/NEJMoa2110345

Thomson, A. (1996). *The Cytokine Handbook* (2nd ed.). Academic Press.

Thul, S., Labat, C., Temmar, M., Benetos, A., & Bäck, M. (2017). Low salivary resolvin D1 to leukotriene B4 ratio predicts carotid intima media thickness:

A novel biomarker of non-resolving vascular inflammation. *European Journal of Preventive Cardiology*, *24*(9), 903–906. https://doi.org/10.1177/2047487317694464

Tochikura, T. S., Nakashima, H., Hirose, K., & Yamamoto, N. (1987). A biological response modifier, PSK, inhibits human immunodeficiency virus infection in vitro. *Biochemical and Biophysical Research Communications*, *148*(2), 726–733. https://doi.org/10.1016/0006-291X(87)90936-3

Travis, M. A., & Sheppard, D. (2014). TGF-β Activation and Function in Immunity. *Annual Review of Immunology*, *32*(1), 51–82. https://doi.org/10.1146/annurev-immunol-032713-120257

Trinchieri, G. (2003). Interleukin-12 and the regulation of innate resistance and adaptive immunity. *Nature Reviews Immunology*, *3*(2), Article 2. https://doi.org/10.1038/nri1001

Tsianos, E. V., & Katsanos, K. (2009). Do we really understand what the immunological disturbances in inflammatory bowel disease mean? *World Journal of Gastroenterology : WJG*, *15*(5), 521–525. https://doi.org/10.3748/wjg.15.521

Tu, P., Tian, R., Lu, Y., Zhang, Y., Zhu, H., Ling, L., Li, H., & Chen, D. (2020). Beneficial effect of Indigo Naturalis on acute lung injury induced by influenza A virus. *Chinese Medicine*, *15*(1), 128. https://doi.org/10.1186/s13020-020-00415-w

Tumpey, T. M., Fenton, R., Molesworth-Kenyon, S., Oakes, J. E., & Lausch, R. N. (2002). Role for Macrophage Inflammatory Protein 2 (MIP-2), MIP-1α, and Interleukin-1α in the Delayed-Type Hypersensitivity Response to Viral

Antigen. *Journal of Virology*, *76*(16), 8050–8057. https://doi.org/10.1128/JVI.76.16.8050-8057.2002

Um, Y., Eo, H. J., Kim, H. J., Kim, K., Jeon, K. S., & Jeong, J. B. (2020). Wild simulated ginseng activates mouse macrophage, RAW264.7 cells through TRL2/4-dependent activation of MAPK, NF-κB and PI3K/AKT pathways. *Journal of Ethnopharmacology*, *263*, 113218. https://doi.org/10.1016/j.jep.2020.113218

Underhill, D. M., & Goodridge, H. S. (2012). Information processing during phagocytosis. *Nature Reviews Immunology*, *12*(7), Article 7. https://doi.org/10.1038/nri3244

Uo, M., Hisamatsu, T., Miyoshi, J., Kaito, D., Yoneno, K., Kitazume, M. T., Mori, M., Sugita, A., Koganei, K., Matsuoka, K., Kanai, T., & Hibi, T. (2013). Mucosal CXCR4+ IgG plasma cells contribute to the pathogenesis of human ulcerative colitis through FcγR-mediated CD14 macrophage activation. *Gut*, *62*(12), 1734–1744. https://doi.org/10.1136/gutjnl-2012-303063

van de Loo, A. J. A. E., Kerssemakers, N., Scholey, A., Garssen, J., Kraneveld, A. D., & Verster, J. C. (2020). Perceived Immune Fitness, Individual Strength and Hangover Severity. *International Journal of Environmental Research and Public Health*, *17*(11), 4039. https://doi.org/10.3390/ijerph17114039

Vargas-Caraveo, A., Sayd, A., Maus, S. R., Caso, J. R., Madrigal, J. L. M., García-Bueno, B., & Leza, J. C. (2017). Lipopolysaccharide enters the rat brain by a lipoprotein-mediated transport mechanism in physiological conditions. *Scientific Reports*, *7*, 13113. https://doi.org/10.1038/s41598-017-13302-6

Vargas-Caraveo, A., Sayd, A., Robledo-Montaña, J., Caso, J. R., Madrigal, J. L. M., García-Bueno, B., & Leza, J. C. (2020). Toll-like receptor 4 agonist and antagonist lipopolysaccharides modify innate immune response in rat brain circumventricular organs. *Journal of Neuroinflammation*, *17*, 6. https://doi.org/10.1186/s12974-019-1690-2

Varma, S. R., Sivaprakasam, T. O., Arumugam, I., Dilip, N., Raghuraman, M., Pavan, K. B., Rafiq, M., & Paramesh, R. (2018). In vitro anti-inflammatory and skin protective properties of Virgin coconut oil. *Journal of Traditional and Complementary Medicine*, *9*(1), 5–14. https://doi.org/10.1016/j.jtcme.2017.06.012

Veeraperumal, S., Qiu, H.-M., Tan, C.-S., Ng, S.-T., Zhang, W., Tang, S., Cheong, K.-L., & Liu, Y. (2021). Restitution of epithelial cells during intestinal mucosal wound healing: The effect of a polysaccharide from the sclerotium of *Lignosus rhinocerotis* (Cooke) Ryvarden. *Journal of Ethnopharmacology*, *274*, 114024. https://doi.org/10.1016/j.jep.2021.114024

Veiga-Parga, T., Sehrawat, S., & Rouse, B. T. (2013). Role of Regulatory T Cells during Virus Infection. *Immunological Reviews*, *255*(1), 182–196. https://doi.org/10.1111/imr.12085

Velazquez-Salinas, L., Verdugo-Rodriguez, A., Rodriguez, L. L., & Borca, M. V. (2019). The Role of Interleukin 6 During Viral Infections. *Frontiers in Microbiology*, *10*. https://www.frontiersin.org/article/10.3389/fmicb.2019.01057

Veldhoen, M., & Stockinger, B. (2006). TGFβ1, a 'Jack of all trades': The link with pro-inflammatory IL-17-producing T cells. *Trends in Immunology*, *27*(8), 358–361. https://doi.org/10.1016/j.it.2006.06.001

Villar-Álvarez, F., de la Rosa-Carrillo, D., Fariñas-Guerrero, F., & Jiménez-Ruiz, C. A. (2022). Immunosenescence, Immune Fitness and Vaccination Schedule in the Adult Respiratory Patient. *Open Respiratory Archives*, *4*(3), 100181. https://doi.org/10.1016/j.opresp.2022.100181

Villarino, A. V., & Hunter, C. A. (2004). Biology of recently discovered cytokines: Discerning the pro- and anti-inflammatory properties of interleukin-27. *Arthritis Research & Therapy*, *6*(5), 225–233. https://doi.org/10.1186/ar1227

Vollmer, J., & Krieg, A. M. (2009). Immunotherapeutic applications of CpG oligodeoxynucleotide TLR9 agonists. *Advanced Drug Delivery Reviews*, *61*(3), 195–204. https://doi.org/10.1016/j.addr.2008.12.008

Vrdoljak, J., Kumric, M., Vilovic, M., Martinovic, D., Tomic, I. J., Krnic, M., Ticinovic Kurir, T., & Bozic, J. (2022). Effects of Olive Oil and Its Components on Intestinal Inflammation and Inflammatory Bowel Disease. *Nutrients*, *14*(4), 757. https://doi.org/10.3390/nu14040757

Vukelić, I., Detel, D., Batičić, L., Potočnjak, I., & Domitrović, R. (2020). Luteolin ameliorates experimental colitis in mice through ERK-mediated suppression of inflammation, apoptosis and autophagy. *Food and Chemical Toxicology*, *145*, 111680. https://doi.org/10.1016/j.fct.2020.111680

Wahl, S. M. (1994). Transforming growth factor beta: The good, the bad, and the ugly. *The Journal of Experimental Medicine*, *180*(5), 1587–1590.

Wallace, J. L. (2019). Nitric oxide in the gastrointestinal tract: Opportunities for drug development. *British Journal of Pharmacology*, *176*(2), 147–154. https://doi.org/10.1111/bph.14527

Walsh, L. (2021). *Please take Vitamin D to protect against Covid-19, say Irish experts*. BreakingNews.Ie. https://www.breakingnews.ie/ireland/please-take-vitamin-d-to-protect-against-covid-19-say-irish-experts-1069537.html

Wang, J., Thingholm, L. B., Skiecevičienė, J., Rausch, P., Kummen, M., Hov, J. R., Degenhardt, F., Heinsen, F.-A., Rühlemann, M. C., Szymczak, S., Holm, K., Esko, T., Sun, J., Pricop-Jeckstadt, M., Al-Dury, S., Bohov, P., Bethune, J., Sommer, F., Ellinghaus, D., … Franke, A. (2016). Genome-wide association analysis identifies variation in vitamin D receptor and other host factors influencing the gut microbiota. *Nature Genetics*, *48*(11), Article 11. https://doi.org/10.1038/ng.3695

Wang, T., Hu, Y., Wangkahart, E., Liu, F., Wang, A., Zahran, E., Maisey, K. R., Liu, M., Xu, Q., Imarai, M., & Secombes, C. J. (2018). Interleukin (IL)-2 Is a Key Regulator of T Helper 1 and T Helper 2 Cytokine Expression in Fish: Functional Characterization of Two Divergent IL2 Paralogs in Salmonids. *Frontiers in Immunology*, *9*. https://www.frontiersin.org/articles/10.3389/fimmu.2018.01683

Wang, Y., Chaudhri, G., Jackson, R. J., & Karupiah, G. (2009). IL-12p40 and IL-18 Play Pivotal Roles in Orchestrating the Cell-Mediated Immune Response to

a Poxvirus Infection1. *The Journal of Immunology*, *183*(5), 3324–3331. https://doi.org/10.4049/jimmunol.0803985

Wang, Z., Chen, W., Li, Y., Zhang, S., Lou, H., Lu, X., & Fan, X. (2021). Reduning injection and its effective constituent luteoloside protect against sepsis partly via inhibition of HMGB1/TLR4/NF-κB/MAPKs signaling pathways. *Journal of Ethnopharmacology*, *270*, 113783. https://doi.org/10.1016/j.jep.2021.113783

Wang, Z., Li, K., Maskey, A. R., Huang, W., Toutov, A. A., Yang, N., Srivastava, K., Geliebter, J., Tiwari, R., Miao, M., & Li, X. (2021). A small molecule compound berberine as an orally active therapeutic candidate against COVID-19 and SARS: A computational and mechanistic study. *The FASEB Journal*, *35*(4). https://doi.org/10.1096/fj.202001792R

Watson, H., Mitra, S., Croden, F. C., Taylor, M., Wood, H. M., Perry, S. L., Spencer, J. A., Quirke, P., Toogood, G. J., Lawton, C. L., Dye, L., Loadman, P. M., & Hull, M. A. (2018). A randomised trial of the effect of omega-3 polyunsaturated fatty acid supplements on the human intestinal microbiota. *Gut*, *67*(11), 1974–1983. https://doi.org/10.1136/gutjnl-2017-314968

WebMD. (2020). *Coconut Oil: Is It Good for You?* WebMD. https://www.webmd.com/diet/coconut-oil-good-for-you

Wehrens, E. J., Wong, K. A., Gupta, A., Khan, A., Benedict, C. A., & Zuniga, E. I. (2018). IL-27 regulates the number, function and cytotoxic program of antiviral CD4 T cells and promotes cytomegalovirus persistence. *PLOS ONE*, *13*(7), e0201249. https://doi.org/10.1371/journal.pone.0201249

Wei, H., Sun, R., Xiao, W., Feng, J., Zhen, C., Xu, X., & Tian, Z. (2004). Type two cytokines predominance of human lung cancer and its reverse by traditional Chinese medicine TTMP. *Cellular & Molecular Immunology*, *1*(1), 63–70.

Wellness Creative Co. (2019). Health & Wellness Industry Statistics 2022 [Latest Market Data & Trends]. *Wellness Creative Co*. https://www.wellnesscreatives.com/wellness-industry-statistics/

West, G. A., Matsuura, T., Levine, A. D., Klein, J. S., & Fiocchi, C. (1996). Interleukin 4 in inflammatory bowel disease and mucosal immune reactivity. *Gastroenterology*, *110*(6), 1683–1695. https://doi.org/10.1053/gast.1996.v110.pm8964392

Wheelock, E. F. (1965). Interferon-Like Virus-Inhibitor Induced in Human Leukocytes by Phytohemagglutinin. *Science*, *149*(3681), 310–311. https://doi.org/10.1126/science.149.3681.310

Willemsen, L. E. M., Koetsier, M. A., Balvers, M., Beermann, C., Stahl, B., & van Tol, E. A. F. (2008). Polyunsaturated fatty acids support epithelial barrier integrity and reduce IL-4 mediated permeability in vitro. *European Journal of Nutrition*, *47*(4), 183–191. https://doi.org/10.1007/s00394-008-0712-0

Wilson, E. B., & Brooks, D. G. (2011). The role of IL-10 in regulating immunity to persistent viral infections. *Current Topics in Microbiology and Immunology*, *350*, 39–65. https://doi.org/10.1007/82_2010_96

Wolf, S. F., Sieburth, D., & Sypek, J. (1994). Interleukin 12: A key modulator of immune function. *Stem Cells*, *12*(2), 154–168. https://doi.org/10.1002/stem.5530120203

Wortzel, I., & Seger, R. (2011). The ERK Cascade. *Genes & Cancer*, *2*(3), 195–209. https://doi.org/10.1177/1947601911407328

Wu, D., Lewis, E. D., Pae, M., & Meydani, S. N. (2018). Nutritional Modulation of Immune Function: Analysis of Evidence, Mechanisms, and Clinical Relevance. *Frontiers in Immunology*, *9*, 3160. https://doi.org/10.3389/fimmu.2018.03160

Wypych, T. P., Marsland, B. J., & Ubags, N. D. J. (2017). The Impact of Diet on Immunity and Respiratory Diseases. *Annals of the American Thoracic Society*, *14*(Supplement_5), S339–S347. https://doi.org/10.1513/AnnalsATS.201703-255AW

Xu, X., Ocansey, D. K. W., Pei, B., Zhang, Y., Wang, N., Wang, Z., & Mao, F. (2023). Resveratrol alleviates DSS-induced IBD in mice by regulating the intestinal microbiota-macrophage-arginine metabolism axis. *European Journal of Medical Research*, *28*(1), 319. https://doi.org/10.1186/s40001-023-01257-6

Xu, X., Timares, L., & Elmets, C. (2013). *Clinical Immunology* (4th ed.). Elsevier.

Xu, X., Wang, R., Su, Q., Huang, H., Zhou, P., Luan, J., Liu, J., Wang, J., & Chen, X. (2016). Expression of Th1- Th2- and Th17-associated cytokines in laryngeal carcinoma. *Oncology Letters*, *12*(3), 1941–1948. https://doi.org/10.3892/ol.2016.4854

Xuan, W., Qu, Q., Zheng, B., Xiong, S., & Fan, G.-H. (2015). The chemotaxis of M1 and M2 macrophages is regulated by different chemokines. *Journal of Leukocyte Biology*, *97*(1), 61–69. https://doi.org/10.1189/jlb.1A0314-170R

Ya, T., Zhang, Q., Chu, F., Merritt, J., Bilige, M., Sun, T., Du, R., & Zhang, H. (2008). Immunological evaluation of Lactobacillus casei Zhang: A newly isolated strain from koumiss in Inner Mongolia, China. *BMC Immunology*, *9*, 68. https://doi.org/10.1186/1471-2172-9-68

Yamada, A., Arakaki, R., Saito, M., Tsunematsu, T., Kudo, Y., & Ishimaru, N. (2016). Role of regulatory T cell in the pathogenesis of inflammatory bowel disease. *World Journal of Gastroenterology*, *22*(7), 2195–2205. https://doi.org/10.3748/wjg.v22.i7.2195

Yamashita, M., Matsumoto, K., Endo, T., Ukibe, K., Hosoya, T., Matsubara, Y., Nakagawa, H., Sakai, F., & Miyazaki, T. (2017). Preventive Effect of *Lactobacillus helveticus* SBT2171 on Collagen-Induced Arthritis in Mice. *Frontiers in Microbiology*, *8*, 1159. https://doi.org/10.3389/fmicb.2017.01159

Yan, Y.-Q., Fu, Y.-J., Wu, S., Qin, H.-Q., Zhen, X., Song, B.-M., Weng, Y.-S., Wang, P.-C., Chen, X.-Y., & Jiang, Z.-Y. (2018). Anti-influenza activity of berberine improves prognosis by reducing viral replication in mice. *Phytotherapy Research*, *32*(12), 2560–2567. https://doi.org/10.1002/ptr.6196

Yang, X., Xu, S., Qian, Y., & Xiao, Q. (2017). Resveratrol regulates microglia M1/M2 polarization via PGC-1α in conditions of neuroinflammatory injury. *Brain, Behavior, and Immunity*, *64*, 162–172. https://doi.org/10.1016/j.bbi.2017.03.003

Yao, G., Yu, J., Hou, Q., Hui, W., Liu, W., Kwok, L.-Y., Menghe, B., Sun, T., Zhang, H., & Zhang, W. (2017). A Perspective Study of Koumiss Microbiome by Metagenomics Analysis Based on Single-Cell Amplification Technique.

Frontiers in Microbiology, *8*. https://www.frontiersin.org/articles/10.3389/fmicb.2017.00165

Yeap, S. K., Beh, B. K., Ali, N. M., Yusof, H. M., Ho, W. Y., Koh, S. P., Alitheen, N. B., & Long, K. (2015). Antistress and antioxidant effects of virgin coconut oil in vivo. *Experimental and Therapeutic Medicine*, *9*(1), 39–42. https://doi.org/10.3892/etm.2014.2045

Yeh, C.-C., Lin, C.-C., Wang, S.-D., Hung, C.-M., Yeh, M.-H., Liu, C.-J., & Kao, S.-T. (2007). Protective and immunomodulatory effect of Gingyo-san in a murine model of acute lung inflammation. *Journal of Ethnopharmacology*, *111*(2), 418–426. https://doi.org/10.1016/j.jep.2006.12.014

Yoneyama, M., & Fujita, T. (2010). Recognition of viral nucleic acids in innate immunity. *Reviews in Medical Virology*, *20*(1), 4–22. https://doi.org/10.1002/rmv.633

Yu, L., Yan, J., & Sun, Z. (2017). D-limonene exhibits anti-inflammatory and antioxidant properties in an ulcerative colitis rat model via regulation of iNOS, COX-2, PGE2 and ERK signaling pathways. *Molecular Medicine Reports*, *15*(4), 2339–2346. https://doi.org/10.3892/mmr.2017.6241

Yun, S.-M., Kim, S.-H., & Kim, E.-H. (2019). The Molecular Mechanism of Transforming Growth Factor-β Signaling for Intestinal Fibrosis: A Mini-Review. *Frontiers in Pharmacology*, *10*. https://www.frontiersin.org/articles/10.3389/fphar.2019.00162

Zamani, F., Zare Shahneh, F., Aghebati-Maleki, L., & Baradaran, B. (2013). Induction of CD14 Expression and Differentiation to Monocytes or Mature Macrophages in Promyelocytic Cell Lines: New Approach. *Advanced*

Pharmaceutical Bulletin, *3*(2), 329–332. https://doi.org/10.5681/apb.2013.053

Zhang, M., Deng, C., Zheng, J., & Xia, J. (2006). Curcumin regulated shift from Th1 to Th2 in trinitrobenzene sulphonic acid-induced chronic colitis. *Acta Pharmacologica Sinica*, *27*(8), 1071–1077. https://doi.org/10.1111/j.1745-7254.2006.00322.x

Zhang, W., Cho, S.-Y., Xiang, G., Min, K.-J., Yu, Q., & Jin, J.-O. (2015). Ginseng Berry Extract Promotes Maturation of Mouse Dendritic Cells. *PLoS ONE*, *10*(6), e0130926. https://doi.org/10.1371/journal.pone.0130926

Zhang, W., Xu, L., Cho, S.-Y., Min, K.-J., Oda, T., Zhang, L., Yu, Q., & Jin, J.-O. (2016). Ginseng Berry Extract Attenuates Dextran Sodium Sulfate-Induced Acute and Chronic Colitis. *Nutrients*, *8*(4), 199. https://doi.org/10.3390/nu8040199

Zhang, Y.-G., Lu, R., Xia, Y., Zhou, D., Petrof, E., Claud, E. C., & Sun, J. (2019). Lack of Vitamin D Receptor Leads to Hyperfunction of Claudin-2 in Intestinal Inflammatory Responses. *Inflammatory Bowel Diseases*, *25*(1), 97–110. https://doi.org/10.1093/ibd/izy292

Zhang, Y.-G., Wu, S., & Sun, J. (2013). Vitamin D, Vitamin D Receptor, and Tissue Barriers. *Tissue Barriers*, *1*(1), e23118. https://doi.org/10.4161/tisb.23118

Zhang, Z., Ohto, U., Shibata, T., Krayukhina, E., Taoka, M., Yamauchi, Y., Tanji, H., Isobe, T., Uchiyama, S., Miyake, K., & Shimizu, T. (2016). Structural Analysis Reveals that Toll-like Receptor 7 Is a Dual Receptor for Guanosine and Single-Stranded RNA. *Immunity*, *45*(4), 737–748. https://doi.org/10.1016/j.immuni.2016.09.011

Zhang, Z., Ohto, U., & Shimizu, T. (2017). Toward a structural understanding of nucleic acid-sensing Toll-like receptors in the innate immune system. *FEBS Letters*, *591*(20), 3167–3181. https://doi.org/10.1002/1873-3468.12749

Zhao, C. J., Kinner, M., Wismer, W., & Gänzle, M. G. (2015). Effect of Glutamate Accumulation During Sourdough Fermentation with Lactobacillus reuteri on the Taste of Bread and Sodium-Reduced Bread. *Cereal Chemistry*, *92*(2), 224–230. https://doi.org/10.1094/CCHEM-07-14-0149-R

Zheng, S., Chen, Y., Wang, Z., Che, Y., Wu, Q., Yuan, S., & Zhong, X. (2021). Combination of matrine and tacrolimus alleviates acute rejection in murine heart transplantation by inhibiting DCs maturation through ROS/ERK/NF-κB pathway. *International Immunopharmacology*, *101*, 108218. https://doi.org/10.1016/j.intimp.2021.108218

Zhou, P., Chen, J., He, J., Zheng, T., Yunis, J., Makota, V., Alexandre, Y. O., Gong, F., Zhang, X., Xie, W., Li, Y., Shao, M., Zhu, Y., Sinclair, J. E., Miao, M., Chen, Y., Short, K. R., Mueller, S. N., Sun, X., … Li, Z. (2021). Low-dose IL-2 therapy invigorates CD8+ T cells for viral control in systemic lupus erythematosus. *PLOS Pathogens*, *17*(10), e1009858. https://doi.org/10.1371/journal.ppat.1009858

Zhu, C., Song, K., Shen, Z., Quan, Y., Tan, B., Luo, W., Wu, S., Tang, K., Yang, Z., & Wang, X. (2018). Roseburia intestinalis inhibits interleukin-17 excretion and promotes regulatory T cells differentiation in colitis. *Molecular Medicine Reports*, *17*(6), 7567–7574. https://doi.org/10.3892/mmr.2018.8833

Zhu, L., Gu, P., & Shen, H. (2019). Protective effects of berberine hydrochloride on DSS-induced ulcerative colitis in rats. *International Immunopharmacology*, *68*, 242–251. https://doi.org/10.1016/j.intimp.2018.12.036

Zhu, X., Hu, Z., Yu, T., Hu, H., Zhao, Y., Li, C., Zhu, Q., Wang, M., Zhai, P., He, L., Riaz Rajoka, M. S., Song, X., & He, Z. (2022). The Antiviral Effects of Jasminin via Endogenous TNF-α and the Underlying TNF-α-Inducing Action. *Molecules*, *27*(5), Article 5. https://doi.org/10.3390/molecules27051598

Appendix

Chapter 3:

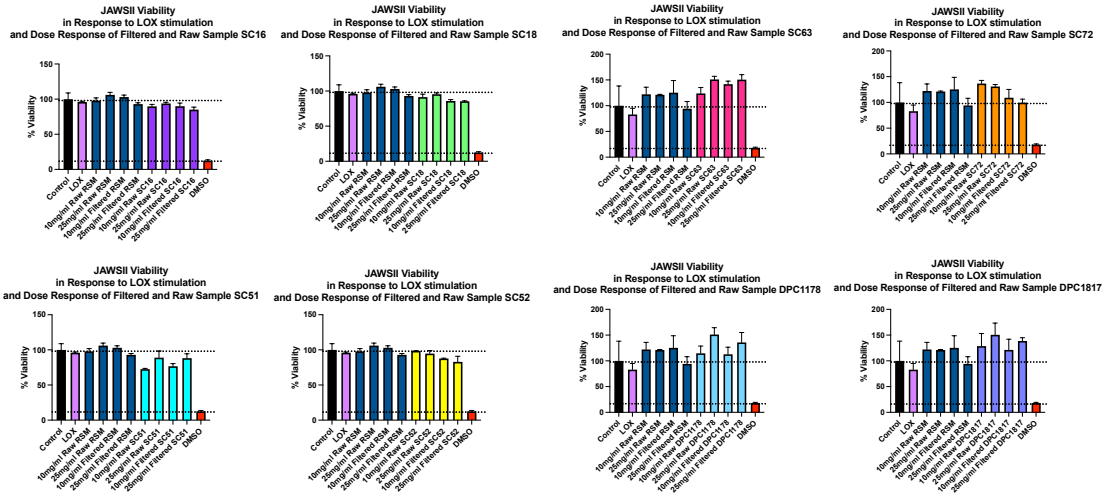

Figure 134: ***Exposure of JAWS to dose response of raw or filtered fermentates doesn't affect cell viability.*** *JAWS cells were seeded at 1x10^6 cells/mL and left overnight at 37^{0}C in 5% CO_2. The following day cells were stimulated with 10mg/mL and 25mg/mL raw and filtered fermentate sample, incubated for 1 hour at 37^{0}C in 5% CO_2 and subsequently exposed to LOX 0.5mM for viral TLR activation before incubating overnight under the same conditions. RSM is the fermentate control.* 10% *DMSO was included as a positive control to induce cell death. Cells were incubated with MTS cell titre aqueous one solution for 3 hours at 37^{0}C in 5% CO_2. Viability is represented as a percentage compared to viable, untreated cells (Control). Data is presented as mean ± SD of three replicates.*

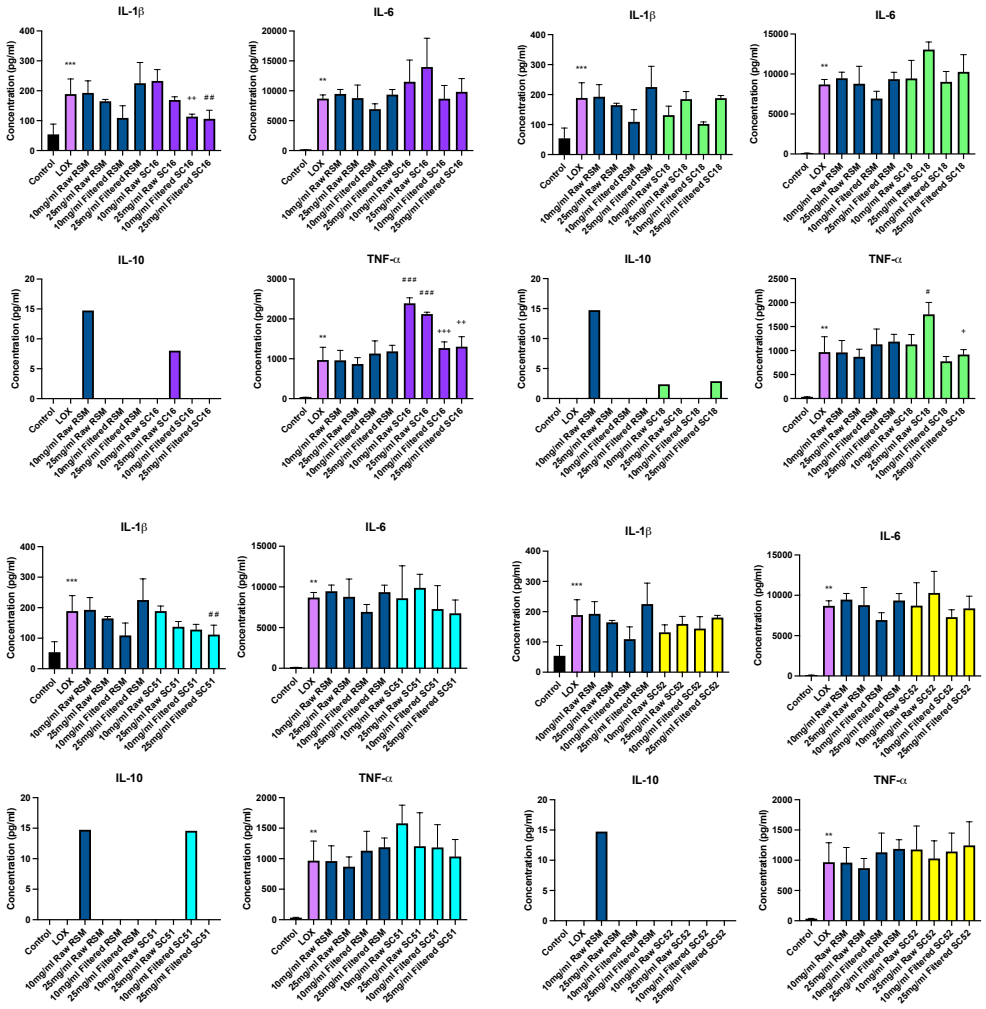

Figure 135: ***Exposure of LOX activated JAWS to sample SC16, SC18, SC51, and SC52 results in the secretion of cytokines.*** *JAWS cells were seeded at 1x10^6 cells/mL and left overnight at 37^{0}C in 5% CO_2. The following day cells were stimulated with 10mg/mL and 25mg/mL raw and filtered sample fermentate, incubated for 1 hour at 37^{0}C in 5% CO_2 and subsequently exposed to LOX 0.5mM for viral TLR activation before incubating overnight under the same conditions. RSM is the fermentate control. Supernatants were removed after 24 hours and ELISA was performed for cytokines IL-1β, IL-6, IL-10 and TNF-α. Data is presented as mean ± SD of three replicates. Significance determined using one- way ANOVA with a Newman-Keuls post-test. Output P value style APA: .12 (ns), .033 (*), .002(**) and <.001 (***) comparing unstimulated control cells to LOX TLR stimulated cells "*", comparing respective dose and processing of sample to its appropriate RSM counterpart "#" and comparing filtered dose to raw unprocessed sample dose "+".*

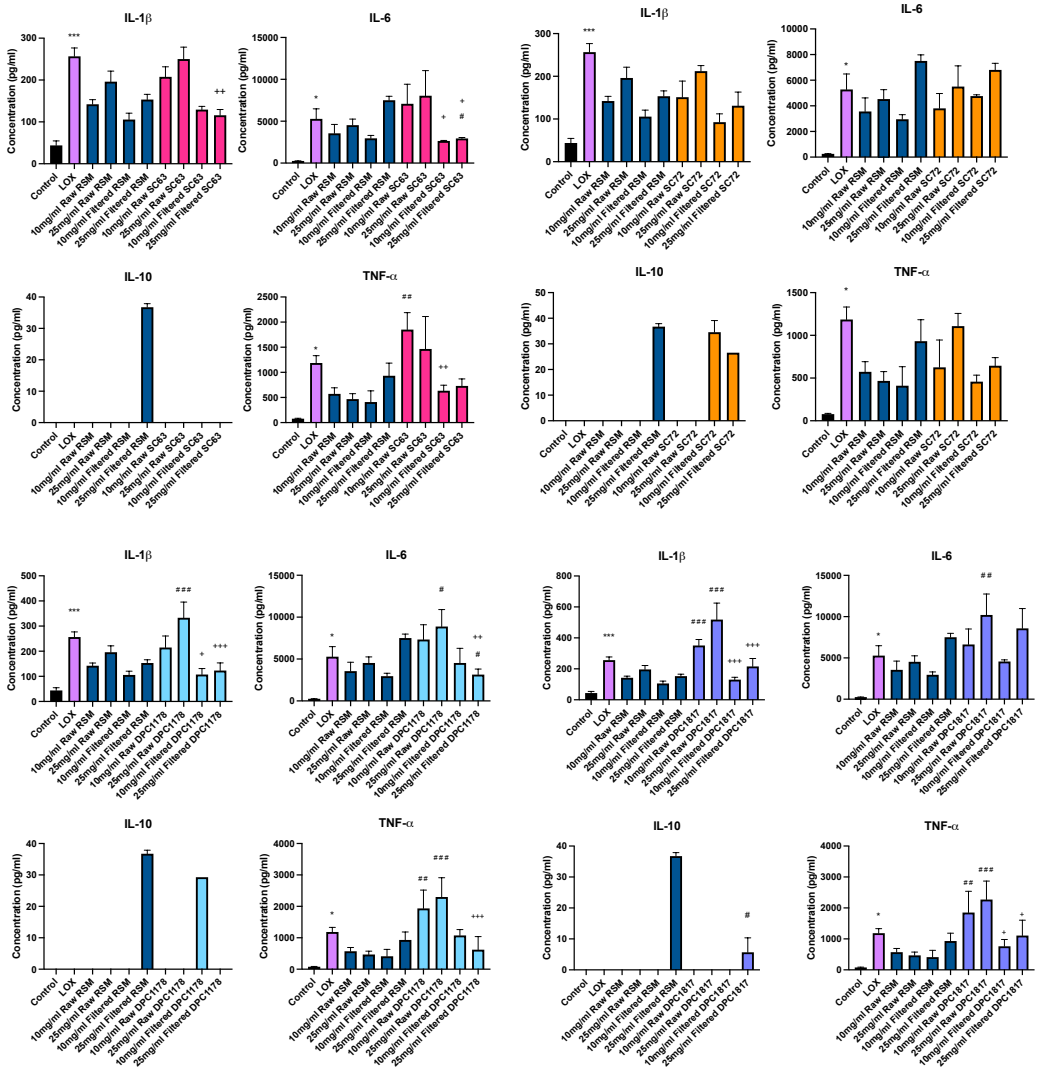

Figure 136: ***Exposure of LOX activated JAWS to sample SC63, SC72, DPC1178, and DPC1817 results in the secretion of cytokines.*** *JAWS cells were seeded at 1x10^6 cells/mL and left overnight at 37^{0}C in 5% CO_2. The following day cells were stimulated with 10mg/mL and 25mg/mL raw and filtered sample fermentate, incubated for 1 hour at 37^{0}C in 5% CO_2 and subsequently exposed to LOX 0.5mM for viral TLR activation before incubating overnight under the same conditions. RSM is the fermentate control. Supernatants were removed after 24 hours and ELISA was performed for cytokines IL-1β, IL-6, IL-10 and TNF-α. Data is presented as mean ± SD of three replicates. Significance determined using one- way ANOVA with a Newman-Keuls post-test. Output P value style APA: .12 (ns), .033 (*), .002(**) and <.001 (***) comparing unstimulated control cells to LOX TLR stimulated cells "*", comparing respective dose and processing of sample SC63 to its appropriate RSM counterpart "#" and comparing filtered dose to raw unprocessed sample dose "+".*

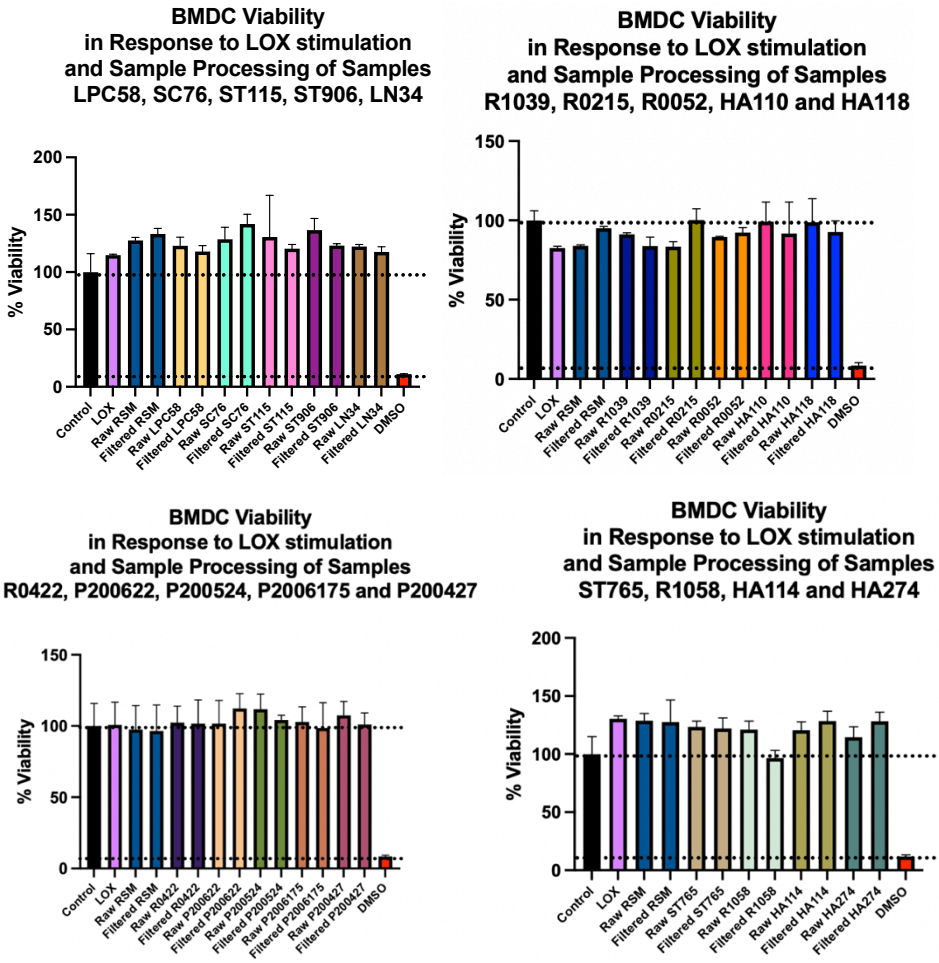

Figure 137: ***Exposure of BMDC to 25mg/mL raw and filtered samples doesn't affect cell viability.*** *BMDC cells were seeded at 1x10^6 cells/mL and left overnight at 37^{0}C in 5% CO_2. The following day cells were stimulated with 25mg/mL sample fermentate, incubated for 1 hour at 37^{0}C in 5% CO_2 and subsequently exposed to LOX 0.5mM for viral TLR activation before incubating overnight under the same conditions. RSM is the fermentate control.* 10% *DMSO was included as a positive control to induce cell death. Cells were incubated with MTS cell titre aqueous one solution for 3 hours at 37^{0}C in 5% CO_2. Viability is represented as a percentage compared to viable, untreated cells (Control). Data is presented as mean ± SD of three replicates.*

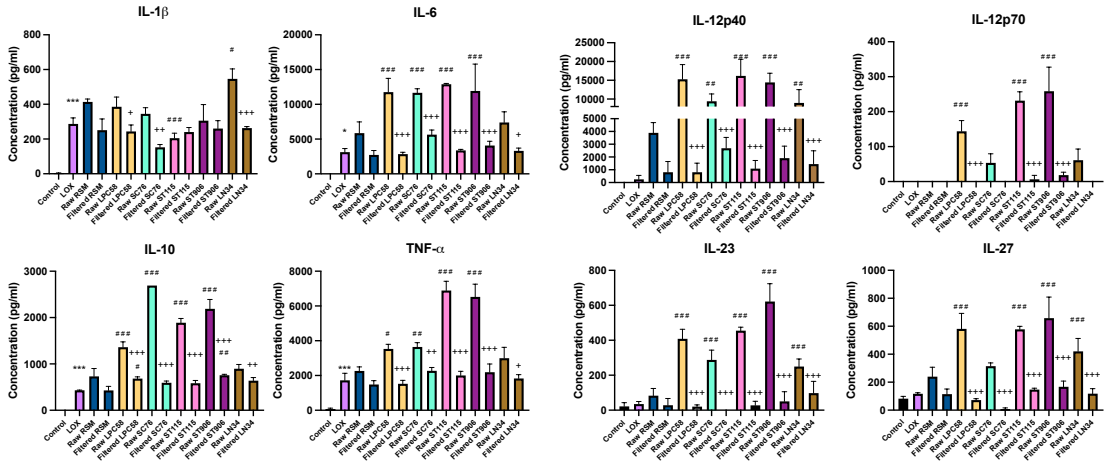

Figure 138: ***Exposure of LOX activated BMDC to sample LPC58, SC76, ST115, ST906 and LN34 results in the secretion of cytokines.*** *BMDC cells were seeded at 1x10^6 cells/mL and left overnight at 37^{0}C in 5% CO_2. The following day cells were stimulated with 25mg/mL raw and filtered sample fermentate, incubated for 1 hour at 37^{0}C in 5% CO_2 and subsequently exposed to LOX 0.5mM for viral TLR activation before incubating overnight under the same conditions. RSM is the fermentate control. Supernatants were removed after 24 hours and ELISA was performed for cytokines IL-1β, IL-6, IL-10, TNF-α, IL-12p40, IL-12p70, IL-23 and IL-27. Data is presented as mean ± SD of three replicates. Significance determined using one- way ANOVA with a Newman-Keuls post-test. Output P value style APA: .12 (ns), .033 (*), .002(**) and <.001 (***) comparing unstimulated control cells to LOX TLR stimulated cells "*", comparing processed or unprocessed sample LPC58, SC76, ST115, ST906 and LN34 to its appropriate RSM counterpart "#" and comparing filtered sample to raw unprocessed sample "+".*

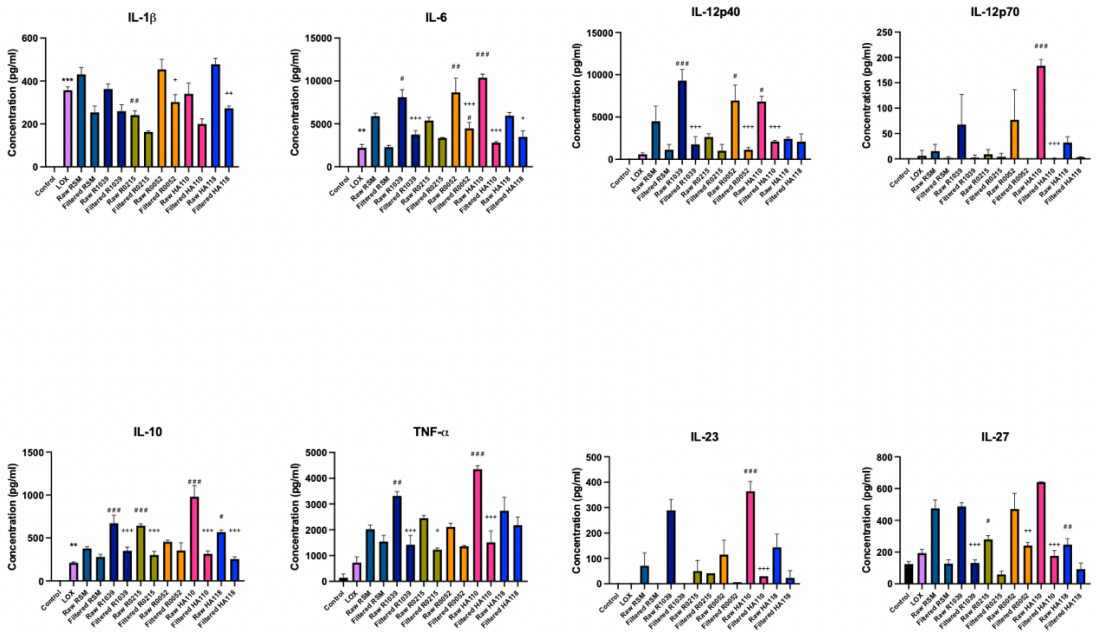

Figure 139: ***Exposure of LOX activated BMDC to sample R1039, R0215, R0052, HA110 and HA118 results in the secretion of cytokines.*** *BMDC cells were seeded at 1x10^6 cells/mL and left overnight at 37^{0}C in 5% CO_2. The following day cells were stimulated with 25mg/mL raw and filtered sample fermentate, incubated for 1 hour at 37^{0}C in 5% CO_2 and subsequently exposed to LOX 0.5mM for viral TLR activation before incubating overnight under the same conditions. RSM is the fermentate control. Supernatants were removed after 24 hours and ELISA was performed for IL-1β, IL-6, IL-10, TNF-α, IL-12p40, IL-12p70, IL-23 and IL-27. Data is presented as mean ± SD of three replicates. Significance determined using one- way ANOVA with a Newman-Keuls post-test. Output P value style APA: .12 (ns), .033 (*), .002(**) and <.001 (***) comparing unstimulated control cells to LOX TLR stimulated cells "*", comparing processed or unprocessed sample R1039, R0215, R0052, HA110 and HA118 to its appropriate RSM counterpart "#" and comparing filtered sample to raw unprocessed sample "+".*

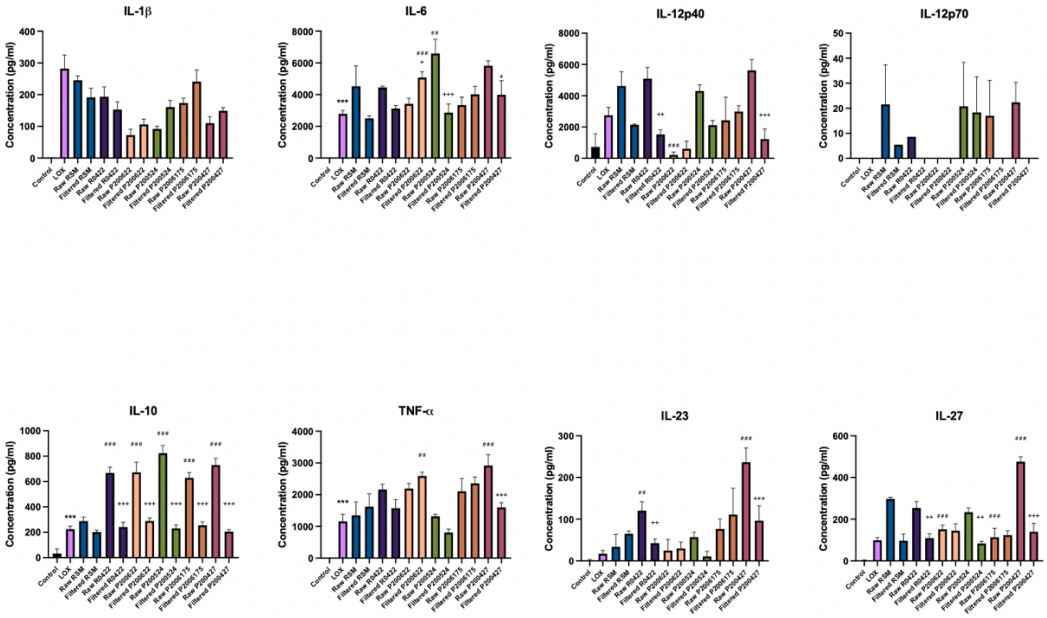

Figure 140: ***Exposure of LOX activated BMDC to sample R0422, P200622, P200524, P2006175 and P200427 results in the secretion of cytokines.*** *BMDC cells were seeded at 1x10^6 cells/mL and left overnight at 37^{0}C in 5% CO_2. The following day cells were stimulated with 25mg/mL raw and filtered sample fermentate, incubated for 1 hour at 37^{0}C in 5% CO_2 and subsequently exposed to LOX 0.5mM for viral TLR activation before incubating overnight under the same conditions. RSM is the fermentate control. Supernatants were removed after 24 hours and ELISA was performed for IL-1β, IL-6, IL-10 TNF-α, IL-12p40, IL-12p70, IL-23 and IL-27. Data is presented as mean ± SD of three replicates. Significance determined using one- way ANOVA with a Newman-Keuls post-test. Output P value style APA: .12 (ns), .033 (*), .002(**) and <.001 (***) comparing unstimulated control cells to LOX TLR stimulated cells "*", comparing processed or unprocessed sample R0422, P200622, P200524, P2006175 and P200427 to its appropriate RSM counterpart "#" and comparing filtered sample to raw unprocessed sample "+".*

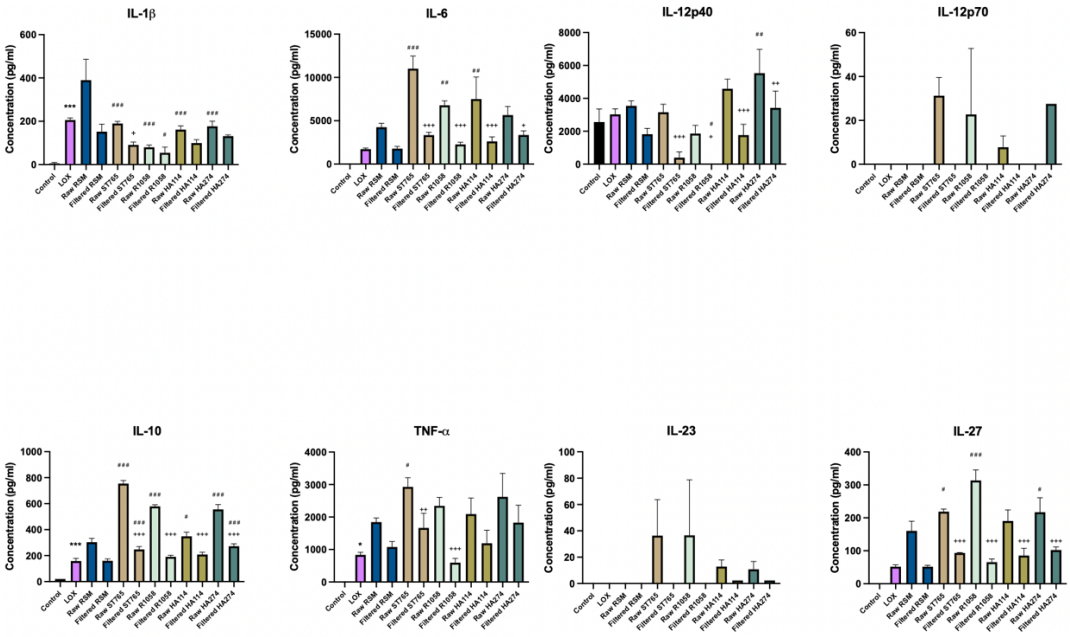

Figure 141: ***Exposure of LOX activated BMDC to sample ST765, R1058, HA114 and HA274 results in the secretion of cytokines.*** *BMDC cells were seeded at 1x10^6 cells/mL and left overnight at 37^{0}C in 5% CO_2. The following day cells were stimulated with 25mg/mL raw and filtered sample fermentate, incubated for 1 hour at 37^{0}C in 5% CO_2 and subsequently exposed to LOX 0.5mM for viral TLR activation before incubating overnight under the same conditions. RSM is the fermentate control. Supernatants were removed after 24 hours and ELISA was performed for IL-1β, IL-6, IL-10, TNF-α, IL-12p40, IL-12p70, IL-23 and IL-27. Data is presented as mean ± SD of three replicates. Significance determined using one- way ANOVA with a Newman-Keuls post-test. Output P value style APA: .12 (ns), .033 (*), .002(**) and <.001 (***) comparing unstimulated control cells to LOX TLR stimulated cells "*", comparing processed or unprocessed sample ST765, R1058, HA114 and HA274 to its appropriate RSM counterpart "#" and comparing filtered sample to raw unprocessed sample "+".*

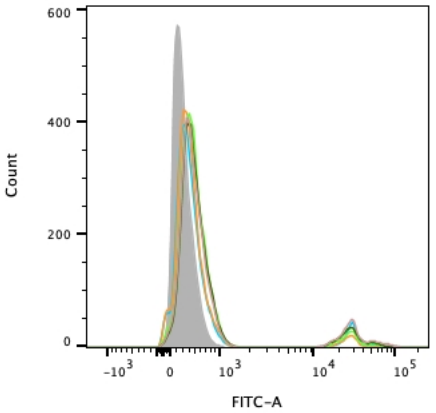

	Sample Name	Subset Name	Count	Mean : FITC-A
	Specimen_001_6HR LPS A.fcs	Viable Cells	9149	4818
	Specimen_001_4HR LPS A.fcs	Viable Cells	9006	3659
	Specimen_001_3HR LPS B.fcs	Viable Cells	9259	2541
	Specimen_001_1HR LPS A.fcs	Viable Cells	8739	2080
	Specimen_001_C A.fcs	Viable Cells	8563	3106
	Specimen_001_US A.fcs	Viable Cells	8527	321

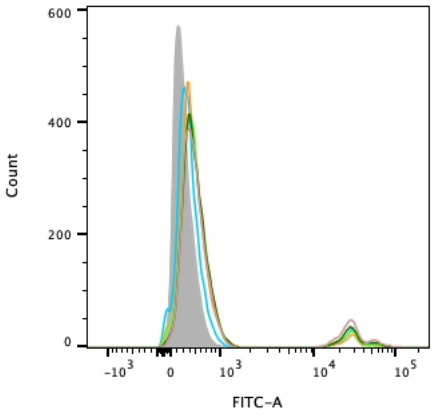

	Sample Name	Subset Name	Count	Mean : FITC-A
	Specimen_001_6HR LPS B.fcs	Viable Cells	9119	4797
	Specimen_001_4HR LPS B.fcs	Viable Cells	9088	3489
	Specimen_001_3HR LPS B.fcs	Viable Cells	9259	2541
	Specimen_001_1HR LPS B.fcs	Viable Cells	9321	2081
	Specimen_001_C B.fcs	Viable Cells	9051	3067
	Specimen_001_US A.fcs	Viable Cells	8527	321

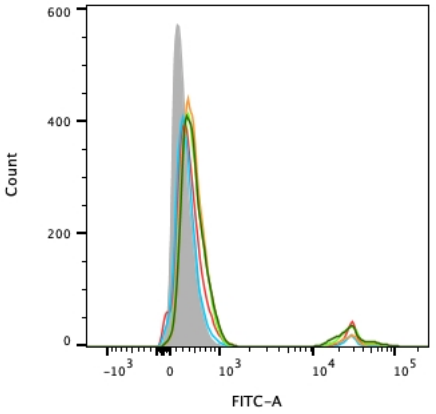

	Sample Name	Subset Name	Count	Mean : FITC-A
	Specimen_001_6HR LOX A.fcs	Viable Cells	9072	4064
	Specimen_001_4HR LOX A.fcs	Viable Cells	8806	3475
	Specimen_001_3HR LOX A.fcs	Viable Cells	9086	2271
	Specimen_001_1HR LOX A.fcs	Viable Cells	7315	2247
	Specimen_001_C A.fcs	Viable Cells	8563	3106
	Specimen_001_US A.fcs	Viable Cells	8527	321

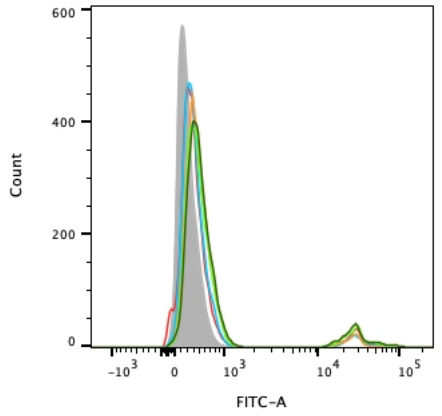

	Sample Name	Subset Name	Count	Mean : FITC-A
	Specimen_001_6HR LOX B.fcs	Viable Cells	9024	4161
	Specimen_001_4HR LOX B.fcs	Viable Cells	8620	3760
	Specimen_001_3HR LOX B.fcs	Viable Cells	8692	2153
	Specimen_001_1HR LOX B.fcs	Viable Cells	8841	2401
	Specimen_001_C B.fcs	Viable Cells	9051	3067
	Specimen_001_US A.fcs	Viable Cells	8527	321

Figure 142: ***Exposure of J774.A.1 to time course of LOX and LPS activated TLRs results in phagocytosis.*** *J774.A.1. cells were seeded at 1x10^6 cells/mL and left overnight at 37^{0}C in 5% CO_2. The following day cells were stimulated with the following concentrations of TLRs: LPS 100ng/ml, LOX 0.5mM, incubated for 1, 3, 4 and 6 hours at 37^{0}C in 5% CO_2. Cell suspensions were retained, and cells were stimulated with 1µm fluorescent latex beads at a concentration of 20 beads per cell, for 1 hour at 37^{o}C in 5% CO_2. Cells were analysed using BD FACSAria 1 system flow cytometer, raw FCS files analysed, data graphed using V10.0 FlowJo software.*

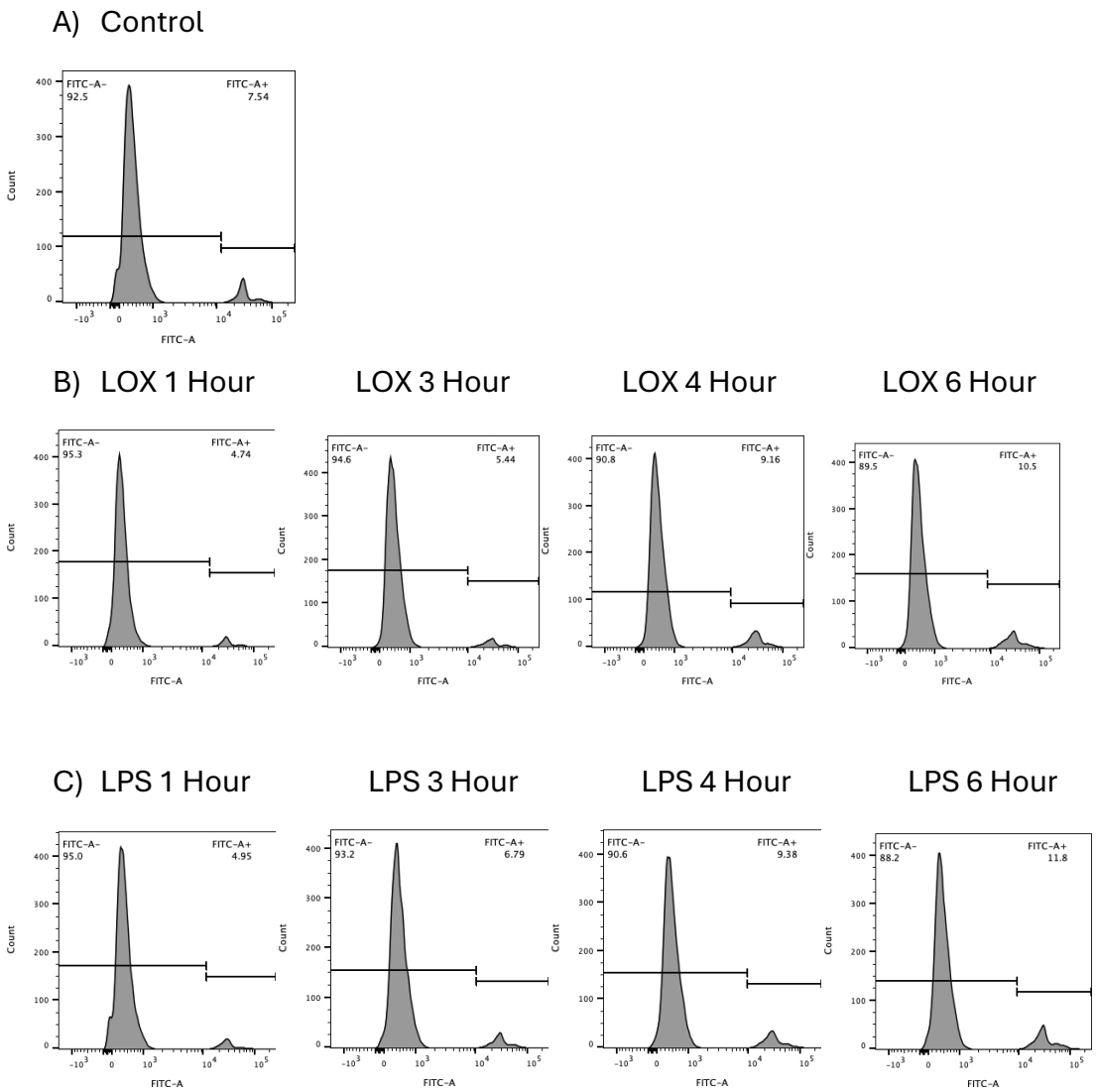

Figure 143: ***Activation of J774.A.1 Macrophage time course of LOX and inflammatory LPS TLRs affects phagocytic activity****. J774.A.1. cells were seeded at 1x10^6 cells/mL and left overnight at 37^{0}C in 5% CO_2. The following day cells were stimulated with LOX 0.5mM (B) and LPS 100ng/mL (C) and incubated for 1, 3, 4 and 6 hours at 37^{0}C in 5% CO_2. Cell suspensions were retained, and cells were stimulated with 1µm fluorescent latex beads at a concentration of 20 beads per cell, for 1 hour at 37^{o}C in 5% CO_2. Cells were analysed using BD FACSAria 1 system flow cytometer, raw FCS files analysed, data graphed using V10.0 FlowJo software. Data is presented as mean ± SD of two replicates. Histograms represent FITC-A- the % cells that do not contain beads (non-phagocytes) vs. FITC-A+ representing the % of cells containing beads (phagocytes) within the viable cell population.*

RSM:

Replicate A

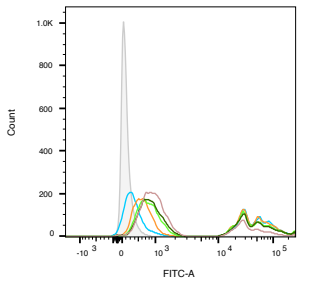

Sample Name	Subset Name	Count	Mean : FITC-A
Specimen_001_RSM 6 A.fcs	Viable Cells	9633	12907
Specimen_001_RSM 4 A.fcs	Viable Cells	9680	24279
Specimen_001_RSM 3 A.fcs	Viable Cells	9554	26165
Specimen_001_RSM 1 A.fcs	Viable Cells	9589	29322
Specimen_001_C A.fcs	Viable Cells	9468	29474
Specimen_001_US.fcs	Viable Cells	9450	213

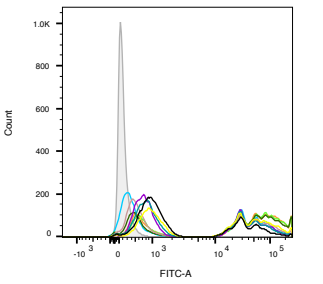

Sample Name	Subset Name	Count	Mean : FITC-A
Specimen_001_RSM LOX 6 A.fcs	Viable Cells	9153	19202
Specimen_001_RSM LOX 4 A.fcs	Viable Cells	9301	38834
Specimen_001_RSM LOX 3 A.fcs	Viable Cells	9342	26888
Specimen_001_RSM LOX 1 A.fcs	Viable Cells	9648	26640
Specimen_001_6 LOX A.fcs	Viable Cells	8921	34799
Specimen_001_4 LOX A.fcs	Viable Cells	8985	58387
Specimen_001_3 LOX A.fcs	Viable Cells	8989	61788
Specimen_001_1 LOX A.fcs	Viable Cells	9016	61888
Specimen_001_C A.fcs	Viable Cells	9468	29474
Specimen_001_US.fcs	Viable Cells	9450	213

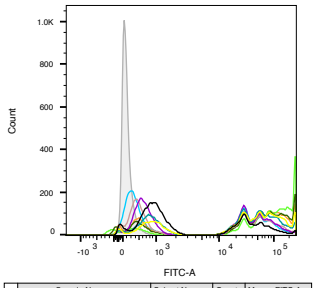

Sample Name	Subset Name	Count	Mean : FITC-A
Specimen_001_RSM LPS 6 A.fcs	Viable Cells	8967	22779
Specimen_001_RSM LPS 4 A.fcs	Viable Cells	9020	60454
Specimen_001_RSM LPS 3 A.fcs	Viable Cells	9266	49800
Specimen_001_RSM LPS 1 A.fcs	Viable Cells	9476	32710
Specimen_001_6 LPS A.fcs	Viable Cells	8639	35784
Specimen_001_4 LPS A.fcs	Viable Cells	8788	77070
Specimen_001_3 LPS A.fcs	Viable Cells	8520	103999
Specimen_001_1 LPS A.fcs	Viable Cells	8924	71353
Specimen_001_C A.fcs	Viable Cells	9468	29474
Specimen_001_US.fcs	Viable Cells	9450	213

Replicate B

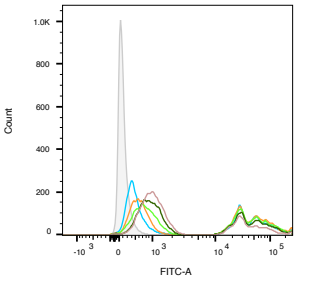

Sample Name	Subset Name	Count	Mean : FITC-A
Specimen_001_RSM 6 B.fcs	Viable Cells	9722	17442
Specimen_001_RSM 4 B.fcs	Viable Cells	9695	25853
Specimen_001_RSM 3 B.fcs	Viable Cells	9631	30873
Specimen_001_RSM 1 B.fcs	Viable Cells	9643	33204
Specimen_001_C B.fcs	Viable Cells	9437	29491
Specimen_001_US.fcs	Viable Cells	9450	213

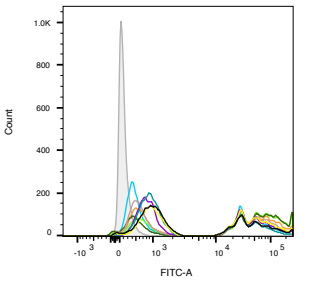

Sample Name	Subset Name	Count	Mean : FITC-A
Specimen_001_RSM LOX 6 B.fcs	Viable Cells	9042	28980
Specimen_001_RSM LOX 4 B.fcs	Viable Cells	9419	35714
Specimen_001_RSM LOX 3 B.fcs	Viable Cells	9529	20907
Specimen_001_RSM LOX 1 B.fcs	Viable Cells	9615	31344
Specimen_001_6 LOX B.fcs	Viable Cells	9079	36405
Specimen_001_4 LOX B.fcs	Viable Cells	8783	62847
Specimen_001_3 LOX B.fcs	Viable Cells	8928	61000
Specimen_001_1 LOX B.fcs	Viable Cells	9143	46110
Specimen_001_C B.fcs	Viable Cells	9437	29491
Specimen_001_US.fcs	Viable Cells	9450	213

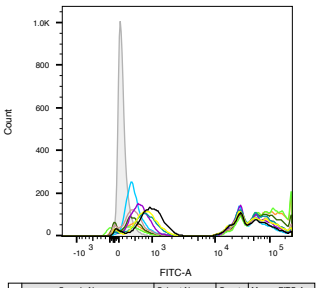

Sample Name	Subset Name	Count	Mean : FITC-A
Specimen_001_RSM LPS 6 B.fcs	Viable Cells	9188	31037
Specimen_001_RSM LPS 4 B.fcs	Viable Cells	9284	40720
Specimen_001_RSM LPS 3 B.fcs	Viable Cells	9345	43508
Specimen_001_RSM LPS 1 B.fcs	Viable Cells	9357	36029
Specimen_001_6 LPS B.fcs	Viable Cells	8706	45716
Specimen_001_4 LPS B.fcs	Viable Cells	8837	61507
Specimen_001_3 LPS B.fcs	Viable Cells	8904	85399
Specimen_001_1 LPS B.fcs	Viable Cells	8849	80683
Specimen_001_C B.fcs	Viable Cells	9437	29491
Specimen_001_US.fcs	Viable Cells	9450	213

Figure 144: ***Exposure of J774.A.1 to 25mg/mL RSM sample and LOX or LPS activated TLRs results in phagocytosis.*** *J774.A.1. cells were seeded at 1x10^6 cells/mL and left overnight at 37^{0}C in 5% CO_2. The following day cells were stimulated with 25mg/mL RSM sample fermentate for 1 hour prior to stimulating with the following concentrations of TLRs: LPS 100ng/ml, LOX 0.5mM and incubated for 1, 3, 4 and 6 hours at 37^{0}C in 5% CO_2. Cell suspensions were retained, and cells were stimulated with 1µm fluorescent latex beads at a concentration of 20 beads per cell, for 1 hour at 37^{0}C in 5% CO_2. Cells were retained and analysed using BD FACSAria 1 system flow cytometer, raw FCS files analysed, data graphed using V10.0 FlowJo software.*

A) Control

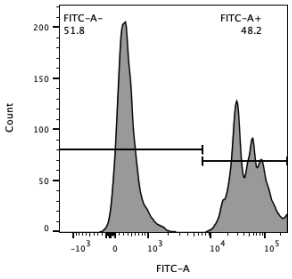

B) LOX 1 Hour LOX 3 Hour LOX 4 Hour LOX 6 Hour

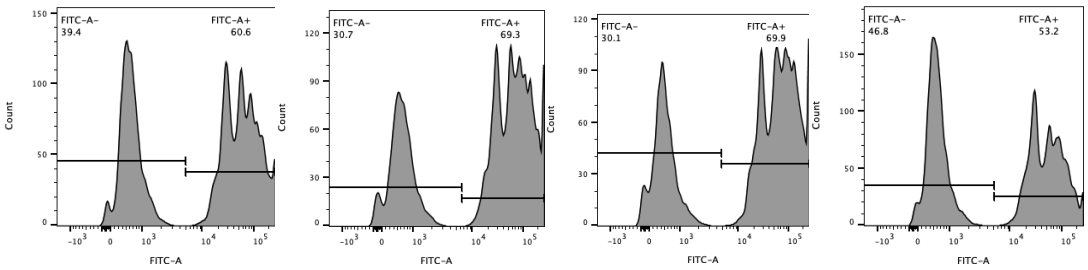

C) RSM+LOX 1 Hour RSM+LOX 3 Hour RSM+LOX 4 Hour RSM+LOX 6 Hour

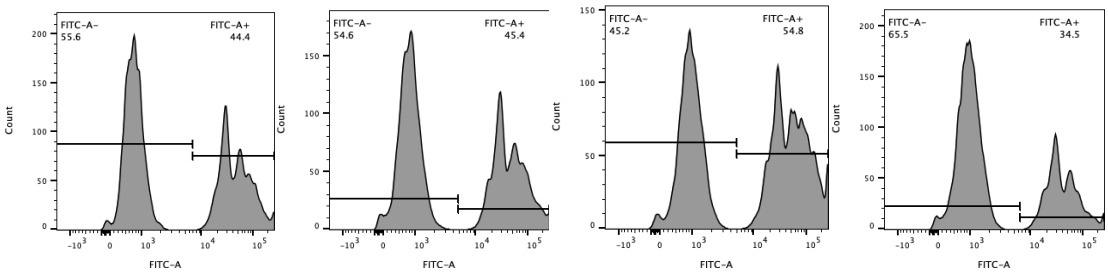

D) RSM 1 Hour RSM 3 Hour RSM 4 Hour RSM 6 Hour

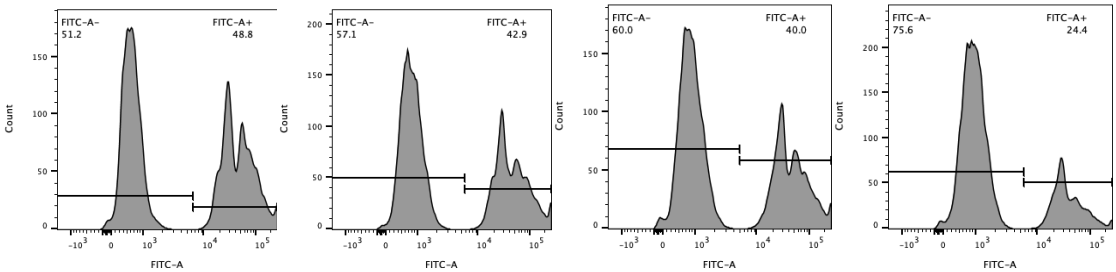

Figure 145: ***Activation of J774.A.1 Macrophage with sample and viral TLR LOX affects phagocytic activity****. J774.A.1. cells were seeded at 1x10^6 cells/mL and left overnight at 37^{0}C in 5% CO_2. The following day cells were stimulated for 1 hour with 25mg/mL raw RSM fermentate (C,D) prior to stimulation with LOX 0.5mM (C-D) and incubated for 1, 3, 4 and 6 hours at 37^{0}C in 5% CO_2. Cell suspensions were retained, and cells were stimulated with 1µm fluorescent latex beads at a concentration of 20 beads per cell, for 1 hour at 37^{o}C in 5% CO_2. Cells were analysed using BD FACSAria 1 system flow cytometer, raw FCS files analysed, data graphed using V10.0 FlowJo software. Data is presented as mean ± SD of two replicates. Histograms represent FITC-A- the % cells that do not contain beads (non-phagocytes) vs. FITC-A+ representing the % of cells containing beads (phagocytes) within the viable cell population.*

A) Control

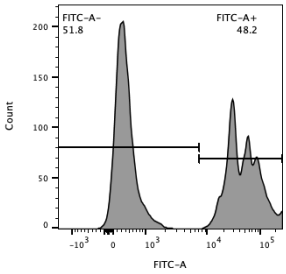

B) LPS 1 Hour LPS 3 Hour LPS 4 Hour LPS 6 Hour

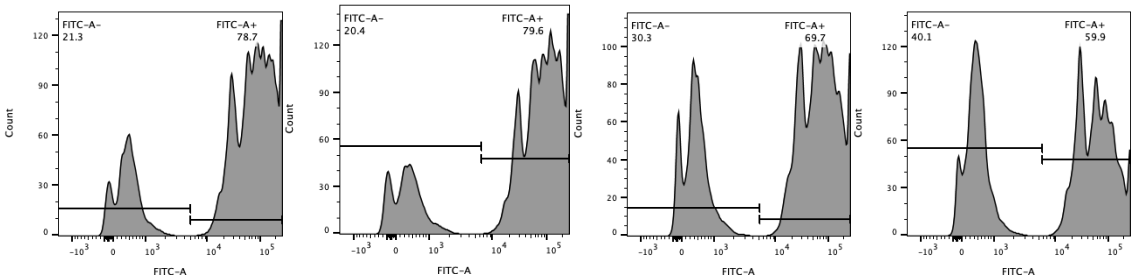

C) RSM+LPS 1 Hour RSM+LPS 3 Hour RSM+LPS 4 Hour RSM+LPS 6 Hour

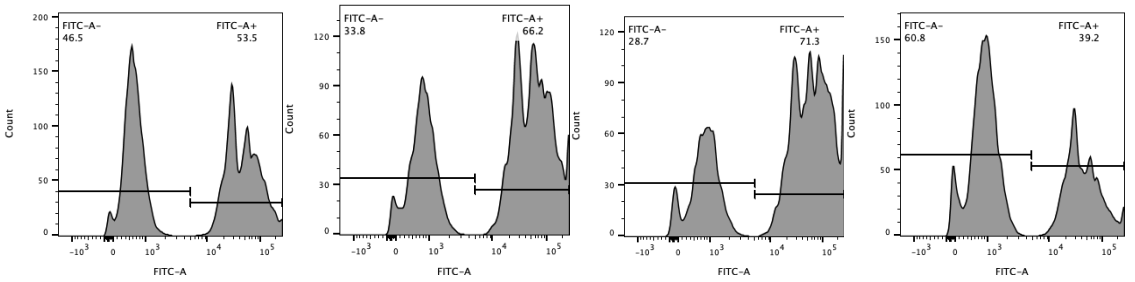

D) RSM 1 Hour RSM 3 Hour RSM 4 Hour RSM 6 Hour

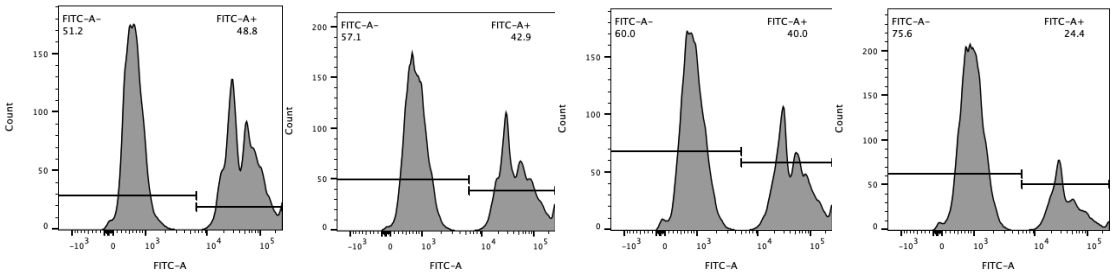

Figure 146: ***Activation of J774.A.1 Macrophage with sample and inflammatory TLR LPS affects phagocytic activity****. J774.A.1. cells were seeded at 1x10^6 cells/mL and left overnight at 37^{0}C in 5% CO_2. The following day cells were stimulated for 1 hour with 25mg/mL raw RSM fermentate (C,D) prior to stimulation with LPS 100ng/mL (C-D) and incubated for 1, 3, 4 and 6 hours at 37^{0}C in 5% CO_2. Cell suspensions were retained, and cells were stimulated with 1µm fluorescent latex beads at a concentration of 20 beads per cell, for 1 hour at 37^{0}C in 5% CO_2. Cells were analysed using BD FACSAria 1 system flow cytometer, raw FCS files analysed, data graphed using V10.0 FlowJo software. Data is presented as mean ± SD of two replicates. Histograms represent FITC-A- the % cells that do not contain beads (non-phagocytes) vs. FITC-A+ representing the % of cells containing beads (phagocytes) within the viable cell population.*

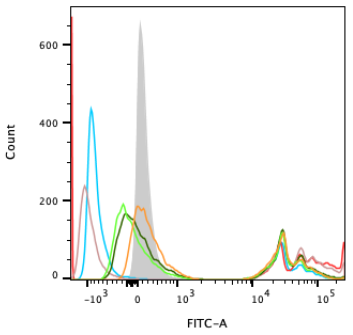

	Sample Name	Subset Name	Count	Mean : FITC-A
	Specimen_001_RSM LPS A.fcs	Viable cells	8928	16363
	Specimen_001_RSM LOX A.fcs	Viable cells	8949	14922
	Specimen_001_RSM A.fcs	Viable cells	9343	17038
	Specimen_001_LPS A.fcs	Viable cells	8346	34196
	Specimen_001_LOX A.fcs	Viable cells	7380	45043
	Specimen_001_C A.fcs	Viable cells	8450	12221
	Specimen_001_US.fcs	Viable cells	7887	250

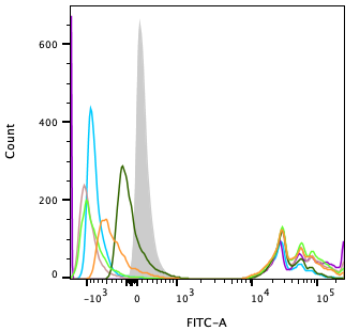

	Sample Name	Subset Name	Count	Mean : FITC-A
	Specimen_001_AER LPS A.fcs	Viable cells	8669	29082
	Specimen_001_AER LOX A.fcs	Viable cells	9064	33318
	Specimen_001_AER A.fcs	Viable cells	9324	14181
	Specimen_001_LPS A.fcs	Viable cells	8346	34196
	Specimen_001_LOX A.fcs	Viable cells	7380	45043
	Specimen_001_C A.fcs	Viable cells	8450	12221
	Specimen_001_US.fcs	Viable cells	7887	250

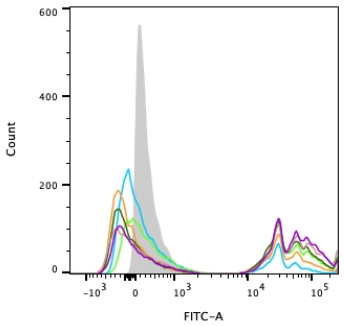

	Sample Name	Subset Name	Count	Mean : FITC-A
	Specimen_001_SC40 LPS A.fcs	Viable cells	8760	40106
	Specimen_001_SC40 LOX A.fcs	Viable cells	8820	39032
	Specimen_001_SC40 A.fcs	Viable cells	9007	30460
	Specimen_001_LPS A.fcs	Viable cells	8752	29417
	Specimen_001_LOX A.fcs	Viable cells	8490	18149
	Specimen_001_C A.fcs	Viable cells	8966	8245
	Specimen_001_US.fcs	Viable cells	8978	350

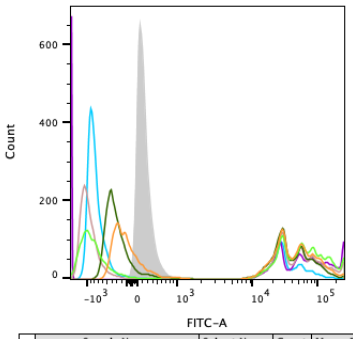

	Sample Name	Subset Name	Count	Mean : FITC-A
	Specimen_001_ANAER LPS A.fcs	Viable cells	8599	32444
	Specimen_001_ANAER LOX A.fcs	Viable cells	8445	45015
	Specimen_001_ANAER A.fcs	Viable cells	9056	24387
	Specimen_001_LPS A.fcs	Viable cells	8346	34196
	Specimen_001_LOX A.fcs	Viable cells	7380	45043
	Specimen_001_C A.fcs	Viable cells	8450	12221
	Specimen_001_US.fcs	Viable cells	7887	250

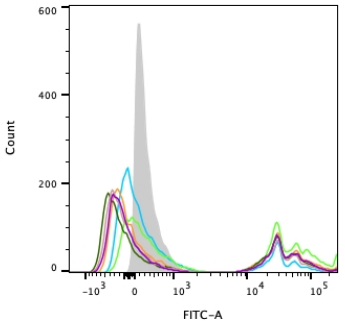

	Sample Name	Subset Name	Count	Mean : FITC-A
	Specimen_001_R0419 LPS A.fcs	Viable cells	7756	16591
	Specimen_001_R0419 LOX A.fcs	Viable cells	7815	12815
	Specimen_001_R0419 A.fcs	Viable cells	7947	15811
	Specimen_001_LPS A.fcs	Viable cells	8752	29417
	Specimen_001_LOX A.fcs	Viable cells	8490	18149
	Specimen_001_C A.fcs	Viable cells	8966	8245
	Specimen_001_US.fcs	Viable cells	8978	350

Figure 147: ***Exposure of J774.A.1 to LOX and LPS TLRs and 25mg/mL sample affects phagocytosis.*** *J774.A.1. cells were seeded at 1x10^6 cells/mL and left overnight at 37^{0}C in 5% CO_2. The following day cells were stimulated with 25mg/mL RSM, Aerobic R0033, Anaerobic R0033, SC40 and R0419 for 1 hour before activating with the following concentrations of TLRs: LPS 100ng/ml, LOX 0.5mM, and incubated for 4 hours at 37^{0}C in 5% CO_2. Cell suspensions were retained, and cells were stimulated with 1µm fluorescent latex beads at a concentration of 20 beads per cell, for 1 hour at 37^{0}C in 5% CO_2. Cells were analysed using BD FACSAria 1 system flow cytometer, raw FCS files analysed, data graphed using V10.0 FlowJo software.*

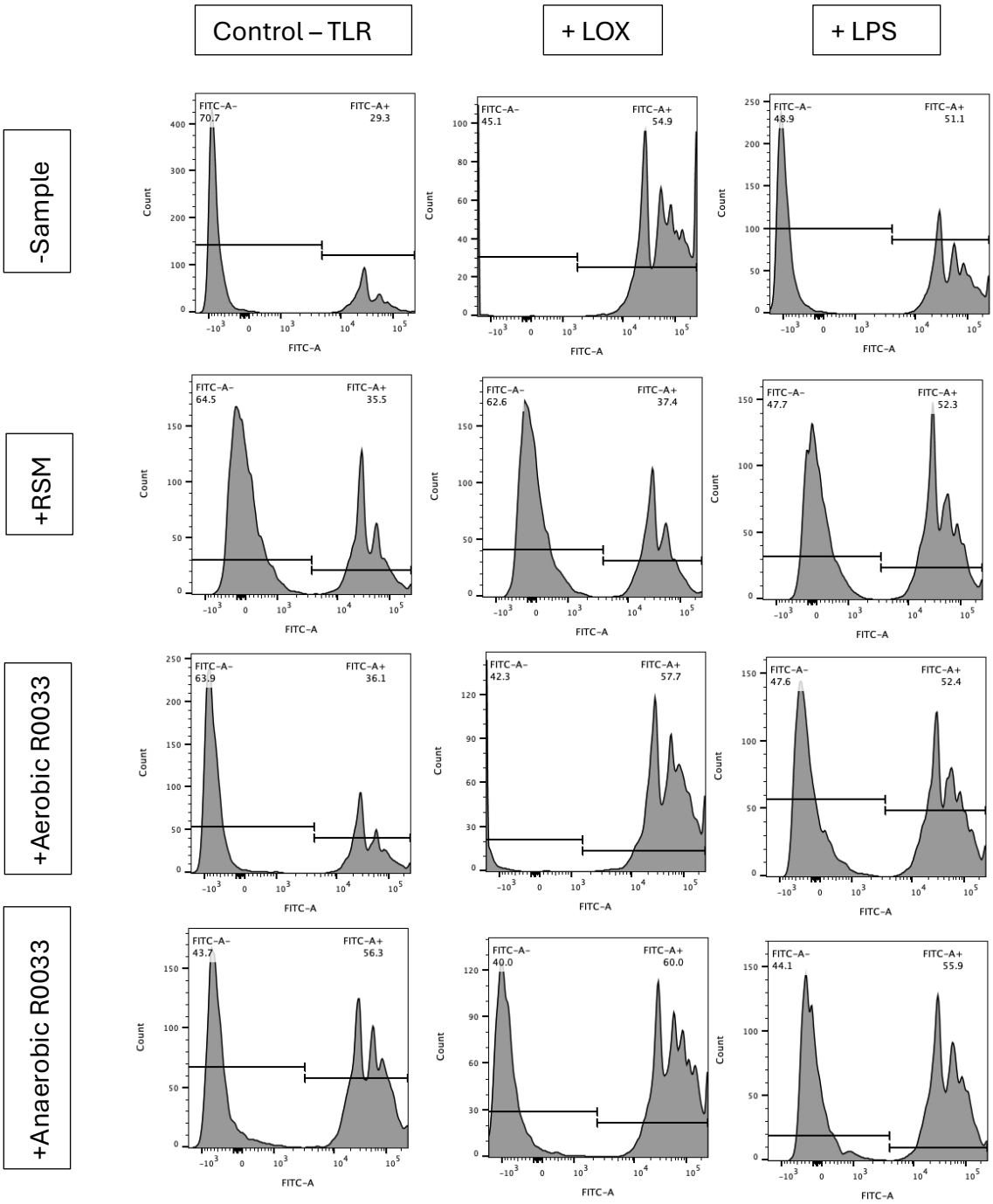

Figure 148: ***Stimulation of LOX and LPS activated J774.A.1 Macrophage with RSM, Aerobic R0033 and Anaerobic R0033 affects phagocytic activity****. J774.A.1. cells were seeded at 1x10^6 cells/mL and left overnight at 37^{0}C in 5% CO_2. The following day cells were stimulated for 1 hour with 25mg/mL raw sample fermentate prior to stimulation with LOX 0.5mM or LPS 100ng/mL and incubated for 4 hours at 37^{0}C in 5% CO_2. Cell suspensions were retained, and cells were stimulated with 1µm fluorescent latex beads at a concentration of 20 beads per cell, for 1 hour at 37^{o}C in 5% CO_2. Cells were analysed using BD FACSAria 1 system flow cytometer, raw FCS files analysed, data graphed using V10.0 FlowJo software. Data is presented as mean ± SD of two replicates. Histograms represent FITC-A- the % cells that do not contain beads (non-phagocytes) vs. FITC-A+ representing the % of cells containing beads (phagocytes) within the viable cell population.*

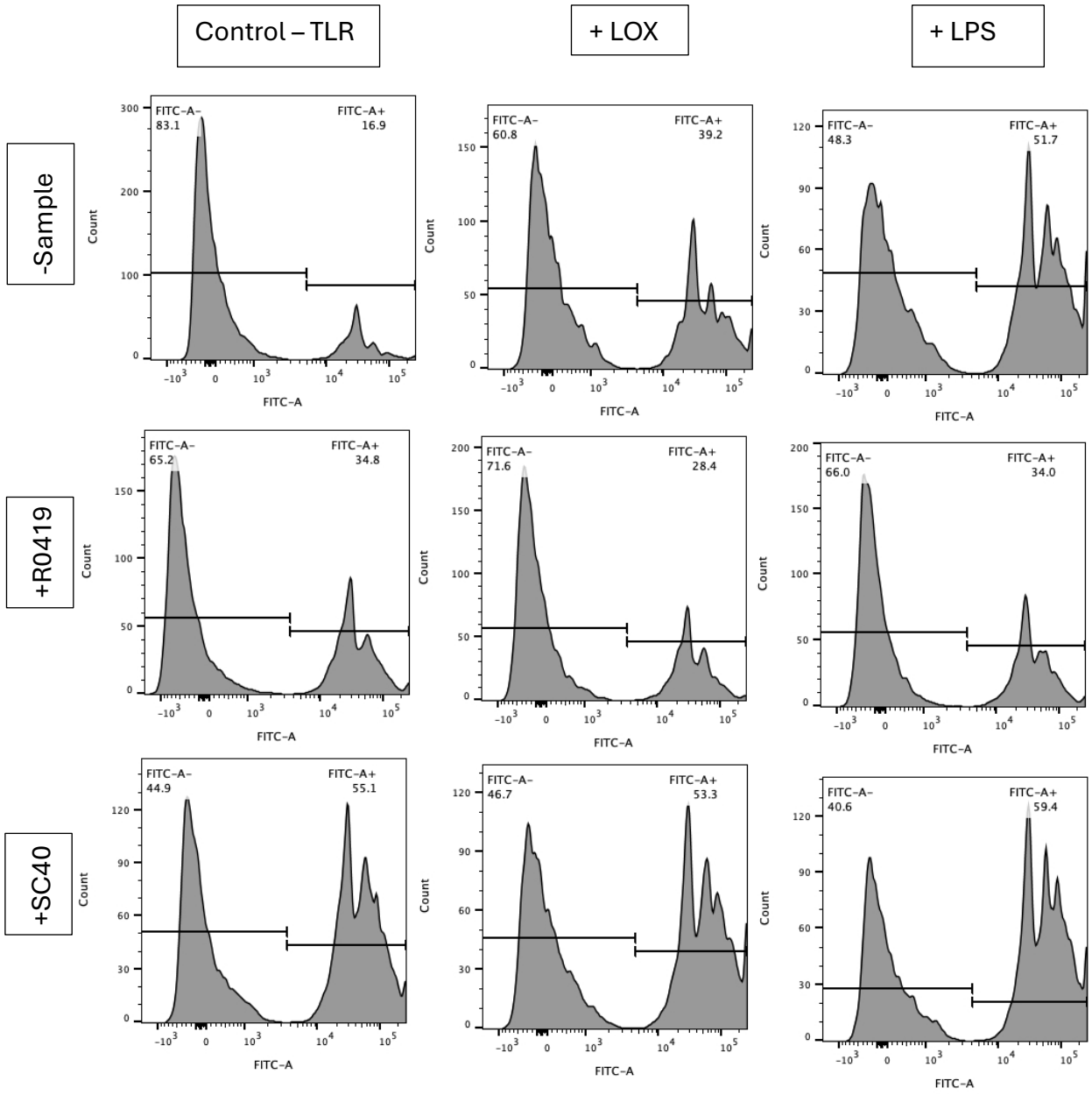

Figure 149: ***Stimulation of LOX and LPS activated J774.A.1 Macrophage with RSM, R0419 and SC40 affects phagocytic activity****. J774.A.1. cells were seeded at 1x10^6 cells/mL and left overnight at 37^{0}C in 5% CO_2. The following day cells were stimulated for 1 hour with 25mg/mL raw sample fermentate prior to stimulation with LOX 0.5mM or LPS 100ng/mL and incubated for 4 hours at 37^{0}C in 5% CO_2. Cell suspensions were retained, and cells were stimulated with 1µm fluorescent latex beads at a concentration of 20 beads per cell, for 1 hour at 37^{o}C in 5% CO_2. Cells were analysed using BD FACSAria 1 system flow cytometer, raw FCS files analysed, data graphed using V10.0 FlowJo software. Data is presented as mean ± SD of two replicates. Histograms represent FITC-A- the % cells that do not contain beads (non-phagocytes) vs. FITC-A+ representing the % of cells containing beads (phagocytes) within the viable cell population.*

RSM:

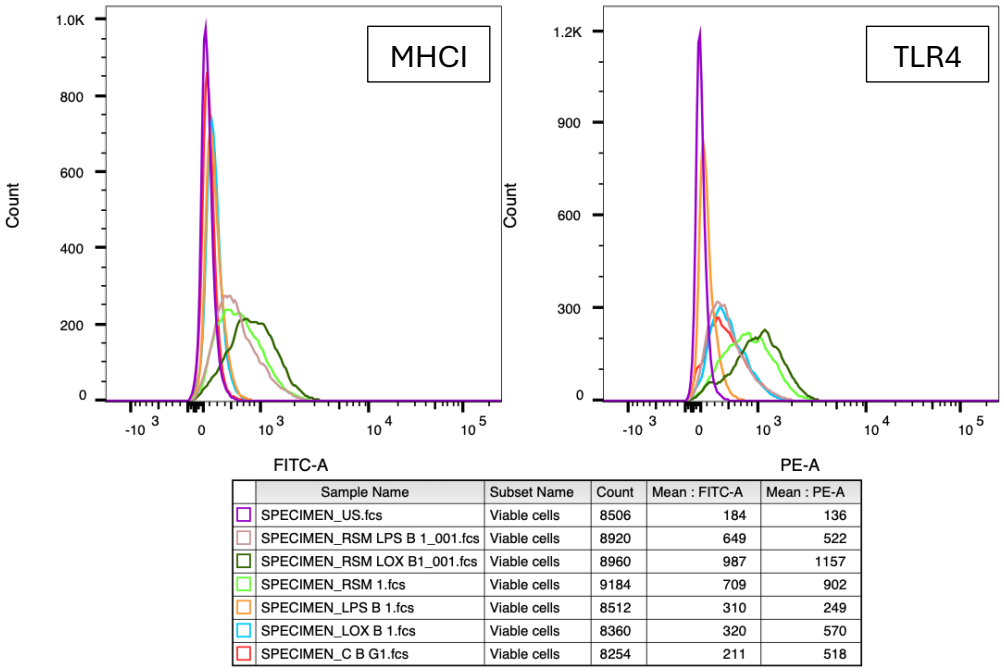

	Sample Name	Subset Name	Count	Mean : FITC-A	Mean : PE-A
	SPECIMEN_US.fcs	Viable cells	8506	184	136
	SPECIMEN_RSM LPS B 1_001.fcs	Viable cells	8920	649	522
	SPECIMEN_RSM LOX B1_001.fcs	Viable cells	8960	987	1157
	SPECIMEN_RSM 1.fcs	Viable cells	9184	709	902
	SPECIMEN_LPS B 1.fcs	Viable cells	8512	310	249
	SPECIMEN_LOX B 1.fcs	Viable cells	8360	320	570
	SPECIMEN_C B G1.fcs	Viable cells	8254	211	518

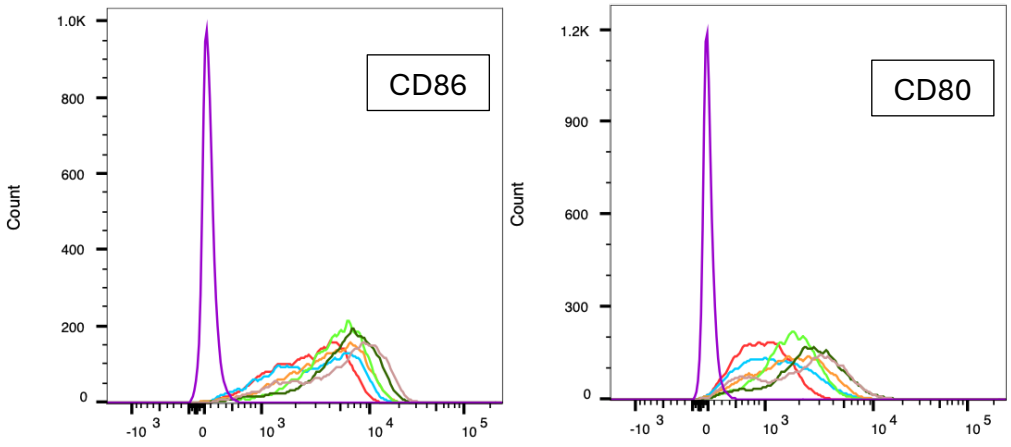

	Sample Name	Subset Name	Count	Mean : FITC-A	Mean : PE-A
	SPECIMEN_US.fcs	Viable cells	8506	184	136
	SPECIMEN_RSM B LPS 2_001.fcs	Viable cells	9000	7285	3399
	SPECIMEN_RSM LOX B 2_001.fcs	Viable cells	8851	6770	3386
	SPECIMEN_RSM 2.fcs	Viable cells	9275	5421	2062
	SPECIMEN_LPS B 2_001.fcs	Viable cells	8903	4832	2421
	SPECIMEN_LOX B 2_001.fcs	Viable cells	8858	3906	1784
	SPECIMEN_C B 2_001.fcs	Viable cells	9190	3254	1155

Figure 150: ***Cell Surface Marker Expression Profile is affected by Specific TLR Activation and RSM presence.*** *J774.A.1. cells were seeded at 1x10^6 cells/mL and incubated overnight at 37^{0}C in 5% CO_2. Cells were stimulated with 25mg/mL raw sample fermentate, incubated for 1 hour at 37^{0}C in 5% CO_2 before stimulating with TLR ligands at the following concentrations: LPS 100ng/mL and LOX 0.5mM and incubated overnight at 37^{0}C in 5% CO_2. Cell suspensions were retained, and cell staining protocol was carried out for activated TLR ligands LPS and LOX in the presence of fermentates, to assess the presence of cell surface markers MHCII, TLR4, CD86 and CD80. Cells were analysed using BD FACSAria 1 system flow cytometer, raw FCS files analysed, data graphed using V10.0 FlowJo software.*

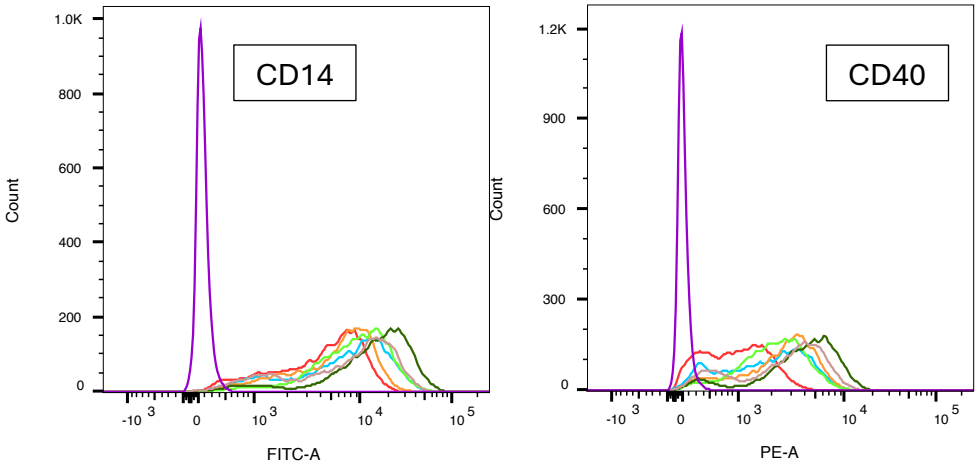

	Sample Name	Subset Name	Count	Mean : FITC-A	Mean : PE-A
	SPECIMEN_US.fcs	Viable cells	8506	184	136
	SPECIMEN_RSM LPS B 3_001.fcs	Viable cells	9057	11269	3376
	SPECIMEN_RSM LOX B 3_001.fcs	Viable cells	9042	18344	4769
	SPECIMEN_RSM 3.fcs	Viable cells	9422	11335	2561
	SPECIMEN_LPS B 3_001.fcs	Viable cells	8992	7515	2966
	SPECIMEN_LOX B 3_003.fcs	Viable cells	9083	10312	2432
	SPECIMEN_C B 3_001.fcs	Viable cells	9356	5633	1149

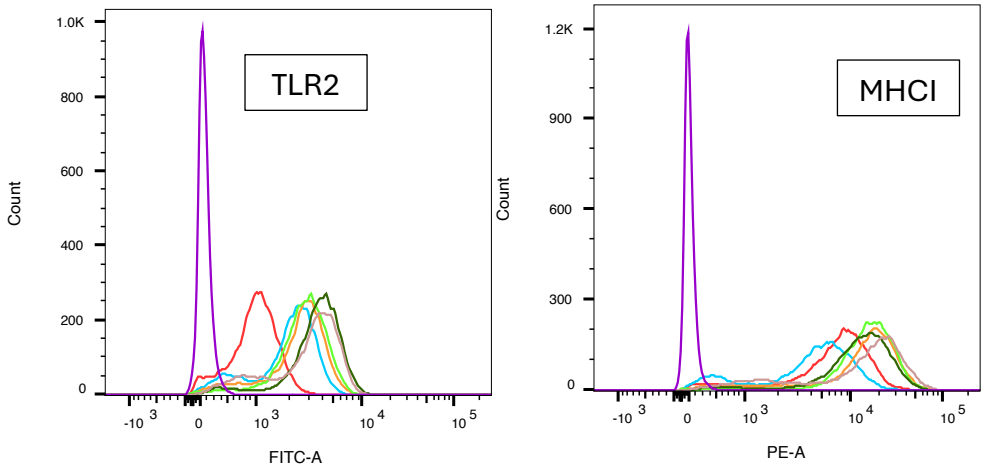

	Sample Name	Subset Name	Count	Mean : FITC-A	Mean : PE-A
	SPECIMEN_US.fcs	Viable cells	8506	184	136
	SPECIMEN_RSM LPS A 4.fcs	Viable cells	9054	3407	18499
	SPECIMEN_RSM LOX A 4.fcs	Viable cells	9052	3935	15814
	SPECIMEN_RSM 4.fcs	Viable cells	9427	2953	17625
	SPECIMEN_LPS A 4.fcs	Viable cells	8814	2729	17380
	SPECIMEN_LOX A 4.fcs	Viable cells	8984	2198	5896
	SPECIMEN_C A 4.fcs	Viable cells	9347	1080	8936

Figure 151: ***Cell Surface Marker Expression Profile is affected by Specific TLR Activation and RSM presence.*** *J774.A.1. cells were seeded at 1x10^6 cells/mL and incubated overnight at 37^{0}C in 5% CO_2. Cells were stimulated with 25mg/mL raw sample fermentate, incubated for 1 hour at 37^{0}C in 5% CO_2 before stimulating with TLR ligands at the following concentrations: LPS 100ng/mL and LOX 0.5mM and incubated overnight at 37^{0}C in 5% CO_2. Cell suspensions were retained, and cell staining protocol was carried out for activated TLR ligands LPS and LOX in the presence of fermentates to assess the presence of cell surface markers CD14, CD40, TLR2 and MHCI. Cells were analysed using BD FACSAria 1 system flow cytometer, raw FCS files analysed, data graphed using V10.0 FlowJo software.*

Aerobic R0033:

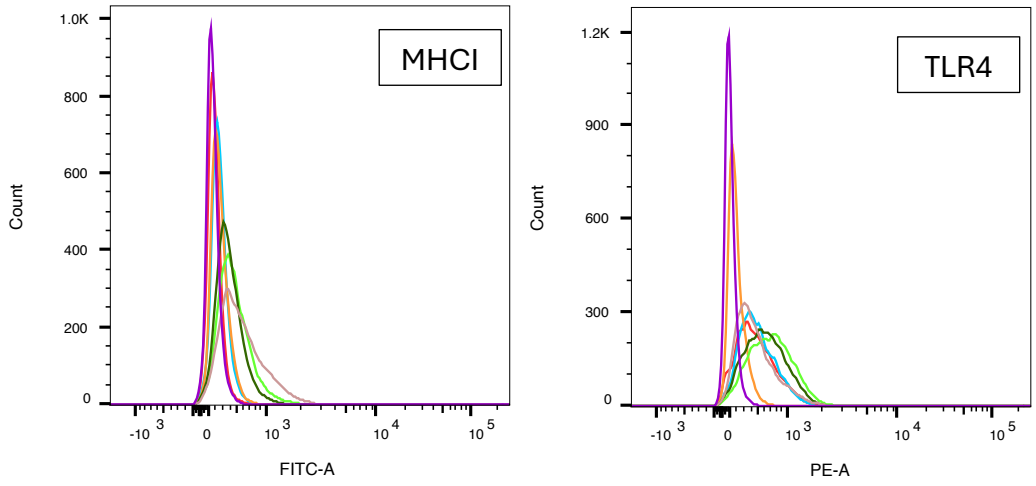

	Sample Name	Subset Name	Count	Mean : FITC-A	Mean : PE-A
	SPECIMEN_US.fcs	Viable cells	8506	184	136
	SPECIMEN_AER LPS B 1.fcs	Viable cells	8725	641	530
	SPECIMEN_AER LOX B 1_001.fcs	Viable cells	8823	432	675
	SPECIMEN_AER B 1.fcs	Viable cells	8807	508	783
	SPECIMEN_LPS B 1.fcs	Viable cells	8512	310	249
	SPECIMEN_LOX B 1.fcs	Viable cells	8360	320	570
	SPECIMEN_C B G1.fcs	Viable cells	8254	211	518

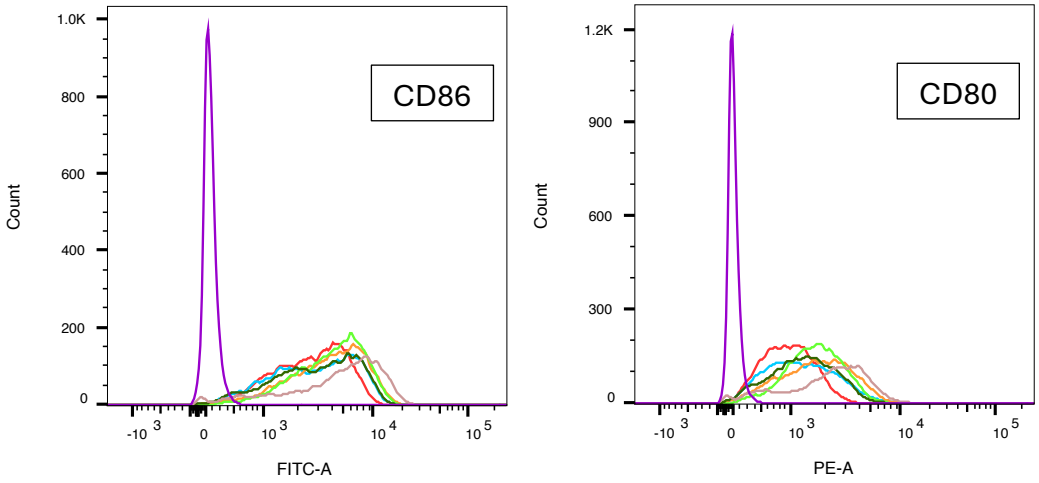

	Sample Name	Subset Name	Count	Mean : FITC-A	Mean : PE-A
	SPECIMEN_US.fcs	Viable cells	8506	184	136
	SPECIMEN_AER LPS B 2_001.fcs	Viable cells	7104	6383	3044
	SPECIMEN_AER LOX B 2_001.fcs	Viable cells	8674	4009	1723
	SPECIMEN_AER B 2_001.fcs	Viable cells	9197	4896	2046
	SPECIMEN_LPS B 2_001.fcs	Viable cells	8903	4832	2421
	SPECIMEN_LOX B 2_001.fcs	Viable cells	8858	3906	1784
	SPECIMEN_C B 2_001.fcs	Viable cells	9190	3254	1155

Figure 152: ***Cell Surface Marker Expression Profile is affected by Specific TLR Activation and Aerobic R0033 presence.*** *J774.A.1. cells were seeded at 1x10^6 cells/mL and incubated overnight at 37^{0}C in 5% CO_2. Cells were stimulated with 25mg/mL raw sample fermentate, incubated for 1 hour at 37^{0}C in 5% CO_2 before stimulating with TLR ligands at the following concentrations: LPS 100ng/mL and LOX 0.5mM and incubated overnight at 37^{0}C in 5% CO_2. Cell suspensions were retained, and cell staining protocol was carried out for activated TLR ligands LPS and LOX in the presence of fermentates, to assess the presence of cell surface markers MHCII, TLR4, CD86 and CD80. Cells were analysed using BD FACSAria 1 system flow cytometer, raw FCS files analysed, data graphed using V10.0 FlowJo software.*

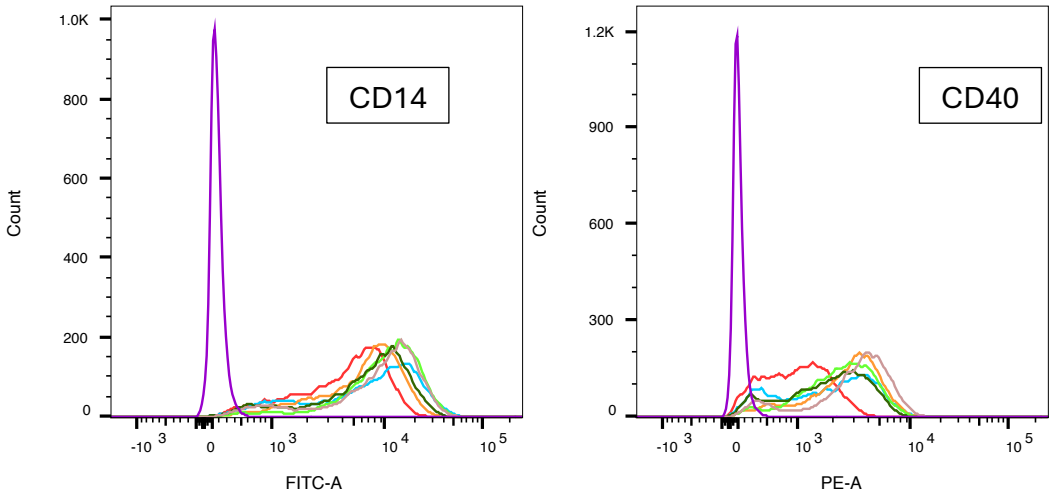

	Sample Name	Subset Name	Count	Mean : FITC-A	Mean : PE-A
	SPECIMEN_US.fcs	Viable cells	8506	184	136
	SPECIMEN_AER LPS A 3.fcs	Viable cells	9082	11825	3677
	SPECIMEN_AER LOX A 3.fcs	Viable cells	8940	9186	2353
	SPECIMEN_AER A 3.fcs	Viable cells	9289	12561	2766
	SPECIMEN_LPS A 3.fcs	Viable cells	9055	8164	3086
	SPECIMEN_LOX A 3_002.fcs	Viable cells	8822	10826	2543
	SPECIMEN_C A 3.fcs	Viable cells	9571	5614	1163

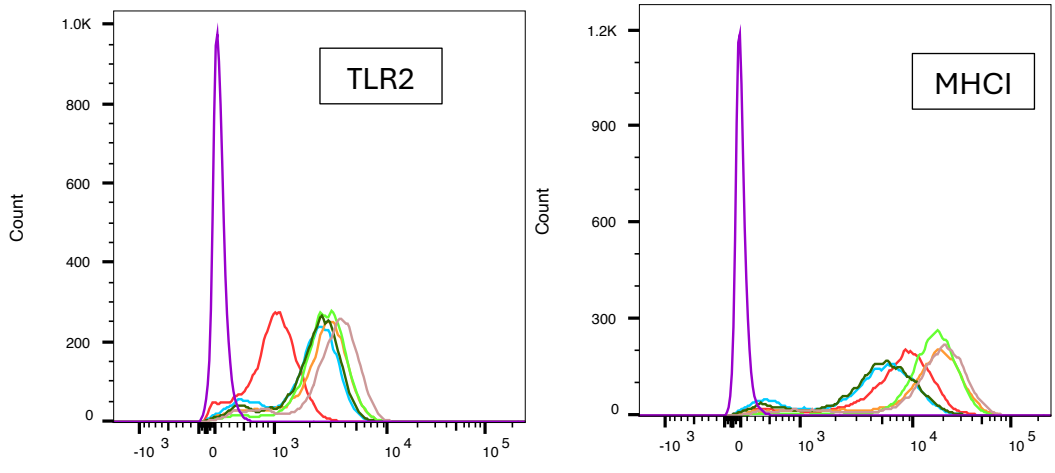

	Sample Name	Subset Name	Count	Mean : FITC-A	Mean : PE-A
	SPECIMEN_US.fcs	Viable cells	8506	184	136
	SPECIMEN_AER LPS A 4.fcs	Viable cells	8998	3423	19855
	SPECIMEN_AER LOX A 4.fcs	Viable cells	9084	2409	6105
	SPECIMEN_AER A 4.fcs	Viable cells	9352	2827	17601
	SPECIMEN_LPS A 4.fcs	Viable cells	8814	2729	17380
	SPECIMEN_LOX A 4.fcs	Viable cells	8984	2198	5896
	SPECIMEN_C A 4.fcs	Viable cells	9347	1080	8936

Figure 153: ***Cell Surface Marker Expression Profile is affected by Specific TLR Activation and Aerobic R0033 presence****. J774.A.1. cells were seeded at 1x10^6 cells/mL and incubated overnight at 37^{0}C in 5% CO_2. Cells were stimulated with 25mg/mL raw sample fermentate, incubated for 1 hour at 37^{0}C in 5% CO_2 before stimulating with TLR ligands at the following concentrations: LPS 100ng/mL and LOX 0.5mM and incubated overnight at 37^{0}C in 5% CO_2. Cell suspensions were retained, and cell staining protocol was carried out for activated TLR ligands LPS and LOX in the presence of fermentates to assess the presence of cell surface markers CD14, CD40, TLR2 and MHCI. Cells were analysed using BD FACSAria 1 system flow cytometer, raw FCS files analysed, data graphed using V10.0 FlowJo software.*

Anaerobic R0033:

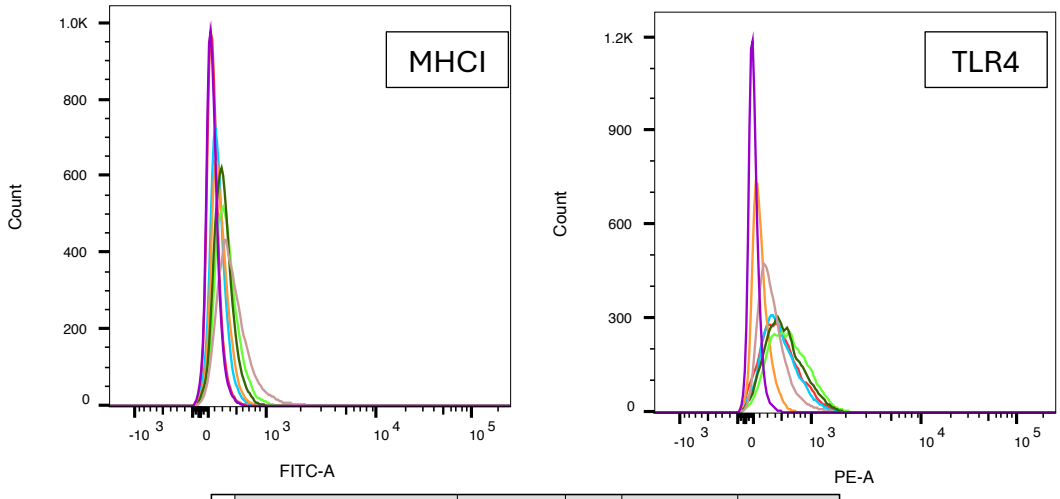

	Sample Name	Subset Name	Count	Mean : FITC-A	Mean : PE-A
	SPECIMEN_US.fcs	Viable cells	8506	184	136
	SPECIMEN_ANAER LPS A 1.fcs	Viable cells	8899	496	409
	SPECIMEN_ANAER LOX A 1.fcs	Viable cells	8956	339	581
	SPECIMEN_ANAER A 1.fcs	Viable cells	8831	390	662
	SPECIMEN_LPS A 1.fcs	Viable cells	8086	289	233
	SPECIMEN_LOX A 1.fcs	Viable cells	8187	299	538
	SPECIMEN_C A G1.fcs	Viable cells	8713	223	523

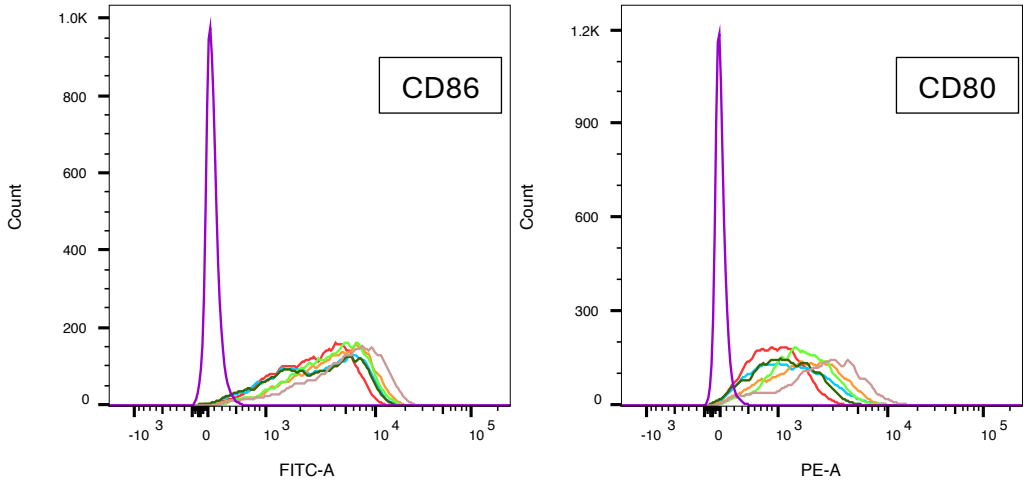

	Sample Name	Subset Name	Count	Mean : FITC-A	Mean : PE-A
	SPECIMEN_US.fcs	Viable cells	8506	184	136
	SPECIMEN_ANAER LPS B 2_001.fcs	Viable cells	8695	6373	3675
	SPECIMEN_ANAER LOX B 2_001.fcs	Viable cells	8566	3789	1555
	SPECIMEN_ANAER B 2_001.fcs	Viable cells	9105	4533	2049
	SPECIMEN_LPS B 2_001.fcs	Viable cells	8903	4832	2421
	SPECIMEN_LOX B 2_001.fcs	Viable cells	8858	3906	1784
	SPECIMEN_C B 2_001.fcs	Viable cells	9190	3254	1155

Figure 154: ***Cell Surface Marker Expression Profile is affected by Specific TLR Activation and Anaerobic R0033 presence.*** *J774.A.1. cells were seeded at 1x10^6 cells/mL and incubated overnight at 37^{0}C in 5% CO_2. Cells were stimulated with 25mg/mL raw sample fermentate, incubated for 1 hour at 37^{0}C in 5% CO_2 before stimulating with TLR ligands at the following concentrations: LPS 100ng/mL and LOX 0.5mM and incubated overnight at 37^{0}C in 5% CO_2. Cell suspensions were retained, and cell staining protocol was carried out for activated TLR ligands LPS and LOX in the presence of fermentates, to assess the presence of cell surface markers MHCII, TLR4, CD86 and CD80. Cells were analysed using BD FACSAria 1 system flow cytometer, raw FCS files analysed, data graphed using V10.0 FlowJo software.*

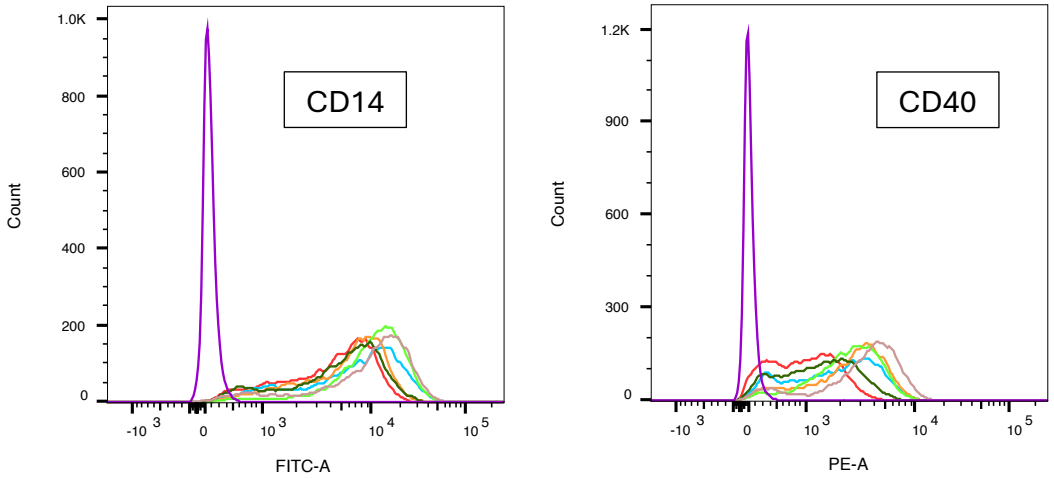

	Sample Name	Subset Name	Count	Mean : FITC-A	Mean : PE-A
	SPECIMEN_US.fcs	Viable cells	8506	184	136
	SPECIMEN_ANAER LPS B 3_001.fcs	Viable cells	8917	13115	3955
	SPECIMEN_ANAER LOX B 3_001.fcs	Viable cells	8850	6877	1682
	SPECIMEN_ANAER B 3_001.fcs	Viable cells	9290	12785	2796
	SPECIMEN_LPS B 3_001.fcs	Viable cells	8992	7515	2966
	SPECIMEN_LOX B 3_003.fcs	Viable cells	9083	10312	2432
	SPECIMEN_C B 3_001.fcs	Viable cells	9356	5633	1149

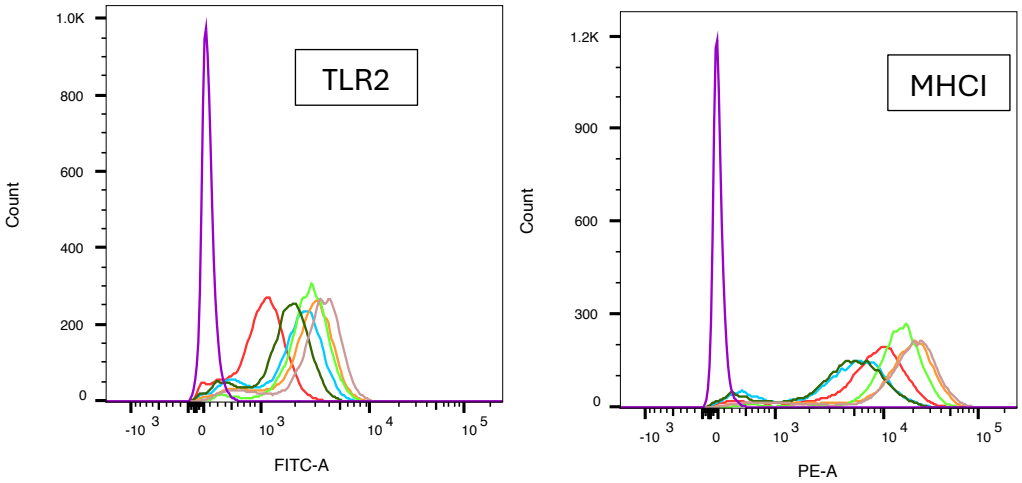

	Sample Name	Subset Name	Count	Mean : FITC-A	Mean : PE-A
	SPECIMEN_US.fcs	Viable cells	8506	184	136
	SPECIMEN_ANAER LPS B 4_001.fcs	Viable cells	8925	3426	20938
	SPECIMEN_ANAER LOX B 4_001.fcs	Viable cells	9005	1783	5701
	SPECIMEN_ANAER B 4_001.fcs	Viable cells	9250	2806	16056
	SPECIMEN_LPS B 4_001.fcs	Viable cells	8959	2822	18899
	SPECIMEN_LOX B 4_001.fcs	Viable cells	8952	2178	5877
	SPECIMEN_C B 4_001.fcs	Viable cells	9298	1141	9506

Figure 155: ***Cell Surface Marker Expression Profile is affected by Specific TLR Activation and Anaerobic R0033 presence.*** *J774.A.1. cells were seeded at 1x10^6 cells/mL and incubated overnight at 37^{0}C in 5% CO_2. Cells were stimulated with 25mg/mL raw sample fermentate, incubated for 1 hour at 37^{0}C in 5% CO_2 before stimulating with TLR ligands at the following concentrations: LPS 100ng/mL and LOX 0.5mM and incubated overnight at 37^{0}C in 5% CO_2. Cell suspensions were retained, and cell staining protocol was carried out for activated TLR ligands LPS and LOX in the presence of fermentates to assess the presence of cell surface markers CD14, CD40, TLR2 and MHCI. Cells were analysed using BD FACSAria 1 system flow cytometer, raw FCS files analysed, data graphed using V10.0 FlowJo software.*

SC40:

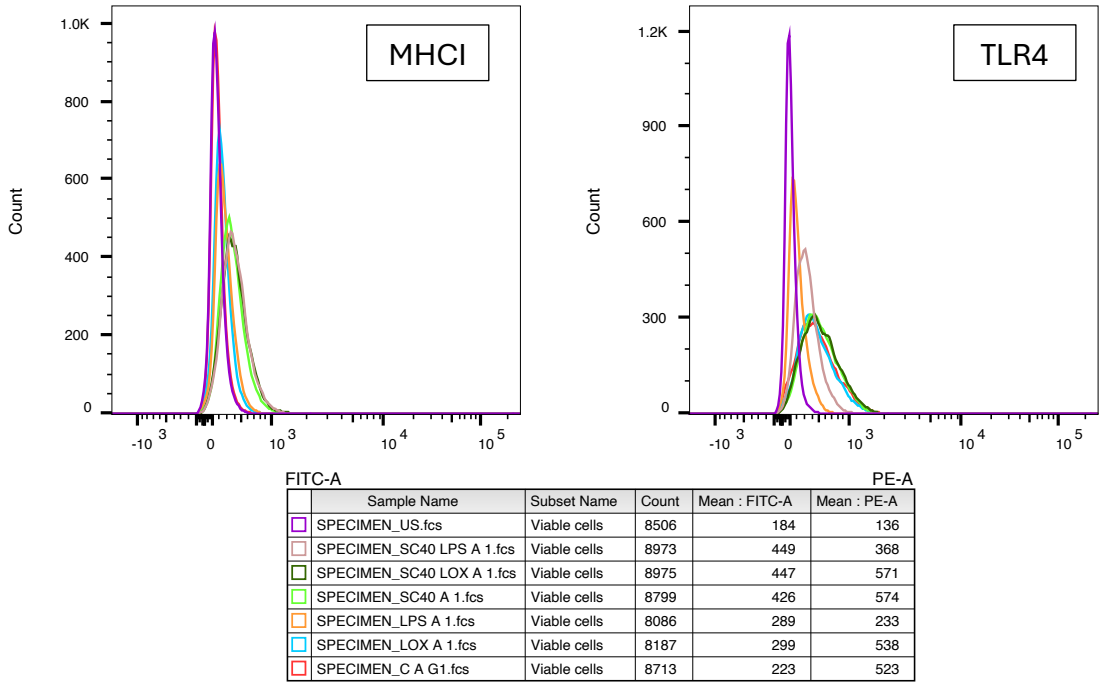

	Sample Name	Subset Name	Count	Mean : FITC-A	Mean : PE-A
☐	SPECIMEN_US.fcs	Viable cells	8506	184	136
☐	SPECIMEN_SC40 LPS A 1.fcs	Viable cells	8973	449	368
☐	SPECIMEN_SC40 LOX A 1.fcs	Viable cells	8975	447	571
☐	SPECIMEN_SC40 A 1.fcs	Viable cells	8799	426	574
☐	SPECIMEN_LPS A 1.fcs	Viable cells	8086	289	233
☐	SPECIMEN_LOX A 1.fcs	Viable cells	8187	299	538
☐	SPECIMEN_C A G1.fcs	Viable cells	8713	223	523

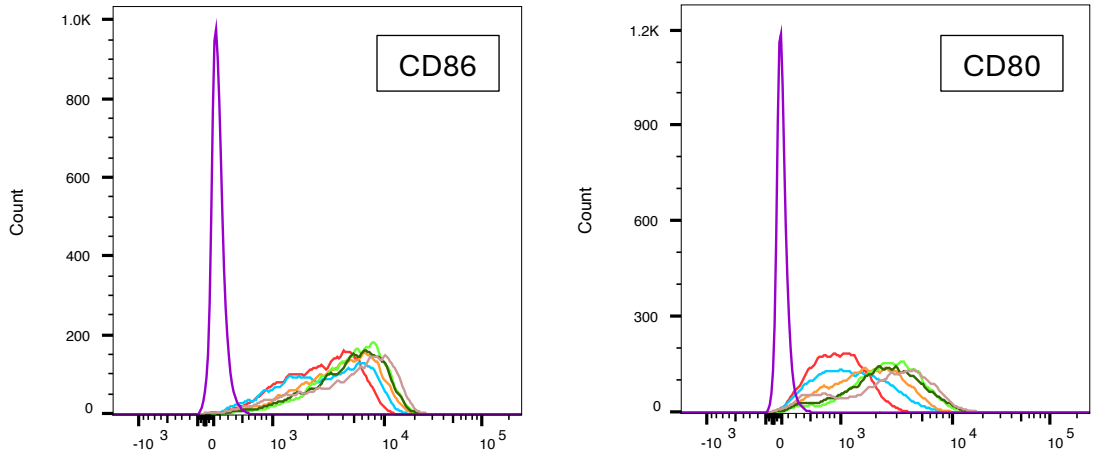

	Sample Name	Subset Name	Count	Mean : FITC-A	Mean : PE-A
☐	SPECIMEN_US.fcs	Viable cells	8506	184	136
☐	SPECIMEN_SC40 LPS B 2_001.fcs	Viable cells	8742	6259	3961
☐	SPECIMEN_SC40 LOX B 2_001.fcs	Viable cells	8729	5615	3509
☐	SPECIMEN_SC40 B 2_001.fcs	Viable cells	9062	5761	3759
☐	SPECIMEN_LPS B 2_001.fcs	Viable cells	8903	4832	2421
☐	SPECIMEN_LOX B 2_001.fcs	Viable cells	8858	3906	1784
☐	SPECIMEN_C B 2_001.fcs	Viable cells	9190	3254	1155

Figure 156: ***Cell Surface Marker Expression Profile is affected by Specific TLR Activation and SC40 presence.*** *J774.A.1. cells were seeded at 1x10^6 cells/mL and incubated overnight at 37^{0}C in 5% CO_2. Cells were stimulated with 25mg/mL raw sample fermentate, incubated for 1 hour at 37^{0}C in 5% CO_2 before stimulating with TLR ligands at the following concentrations: LPS 100ng/mL and LOX 0.5mM and incubated overnight at 37^{0}C in 5% CO_2. Cell suspensions were retained, and cell staining protocol was carried out for activated TLR ligands LPS and LOX in the presence of fermentates, to assess the presence of cell surface markers MHCII, TLR4, CD86 and CD80. Cells were analysed using BD FACSAria 1 system flow cytometer, raw FCS files analysed, data graphed using V10.0 FlowJo software.*

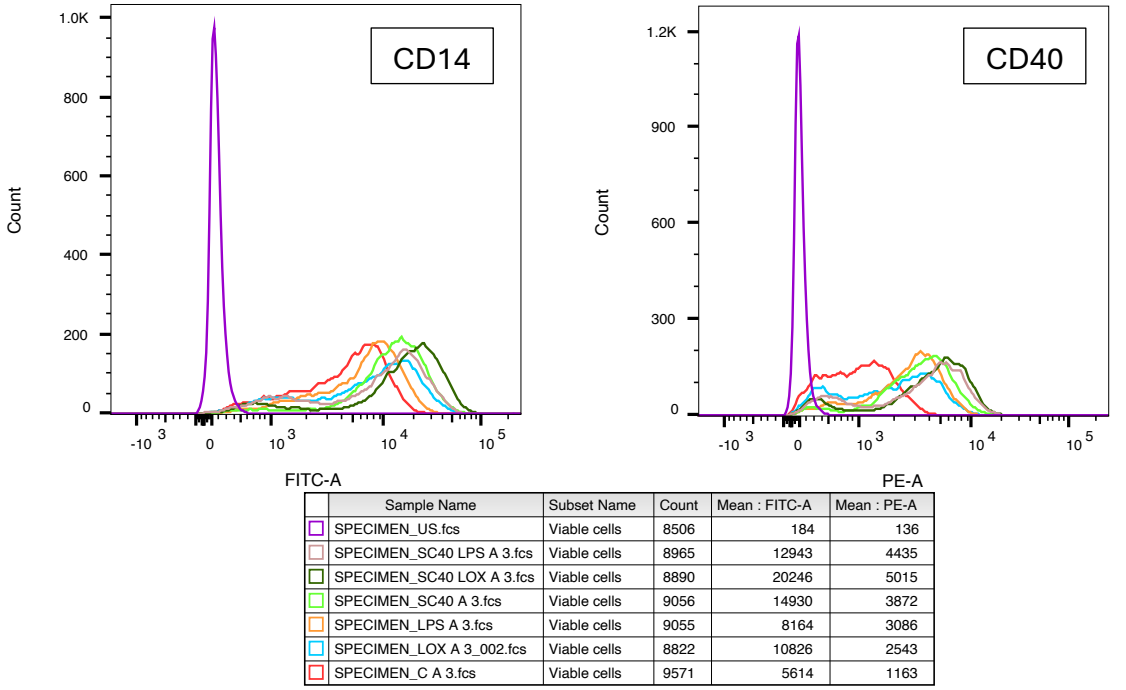

	Sample Name	Subset Name	Count	Mean : FITC-A	Mean : PE-A
	SPECIMEN_US.fcs	Viable cells	8506	184	136
	SPECIMEN_SC40 LPS A 3.fcs	Viable cells	8965	12943	4435
	SPECIMEN_SC40 LOX A 3.fcs	Viable cells	8890	20246	5015
	SPECIMEN_SC40 A 3.fcs	Viable cells	9056	14930	3872
	SPECIMEN_LPS A 3.fcs	Viable cells	9055	8164	3086
	SPECIMEN_LOX A 3_002.fcs	Viable cells	8822	10826	2543
	SPECIMEN_C A 3.fcs	Viable cells	9571	5614	1163

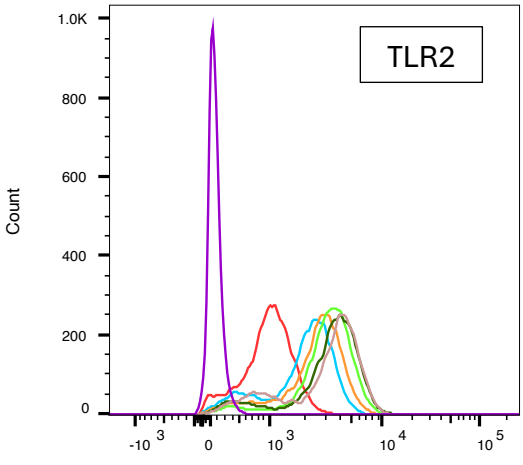

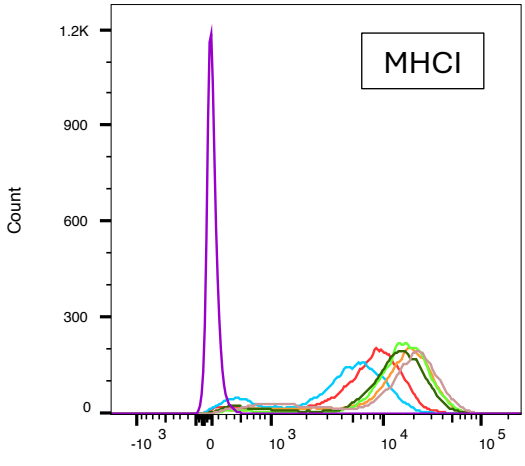

	Sample Name	Subset Name	Count	Mean : FITC-A	Mean : PE-A
	SPECIMEN_US.fcs	Viable cells	8506	184	136
	SPECIMEN_SC40 LPS A 4.fcs	Viable cells	9081	3568	18920
	SPECIMEN_SC40 LOX A 4.fcs	Viable cells	8940	3698	15219
	SPECIMEN_SC40 A 4.fcs	Viable cells	9117	3424	17789
	SPECIMEN_LPS A 4.fcs	Viable cells	8814	2729	17380
	SPECIMEN_LOX A 4.fcs	Viable cells	8984	2198	5896
	SPECIMEN_C A 4.fcs	Viable cells	9347	1080	8936

Figure 157: ***Cell Surface Marker Expression Profile is affected by Specific TLR Activation and SC40 presence.*** *J774.A.1. cells were seeded at 1x10^6 cells/mL and incubated overnight at 37^{0}C in 5% CO_2. Cells were stimulated with 25mg/mL raw sample fermentate, incubated for 1 hour at 37^{0}C in 5% CO_2 before stimulating with TLR ligands at the following concentrations: LPS 100ng/mL and LOX 0.5mM and incubated overnight at 37^{0}C in 5% CO_2. Cell suspensions were retained, and cell staining protocol was carried out for activated TLR ligands LPS and LOX in the presence of fermentates to assess the presence of cell surface markers CD14, CD40, TLR2 and MHCI. Cells were analysed using BD FACSAria 1 system flow cytometer, raw FCS files analysed, data graphed using V10.0 FlowJo software.*

R0419:

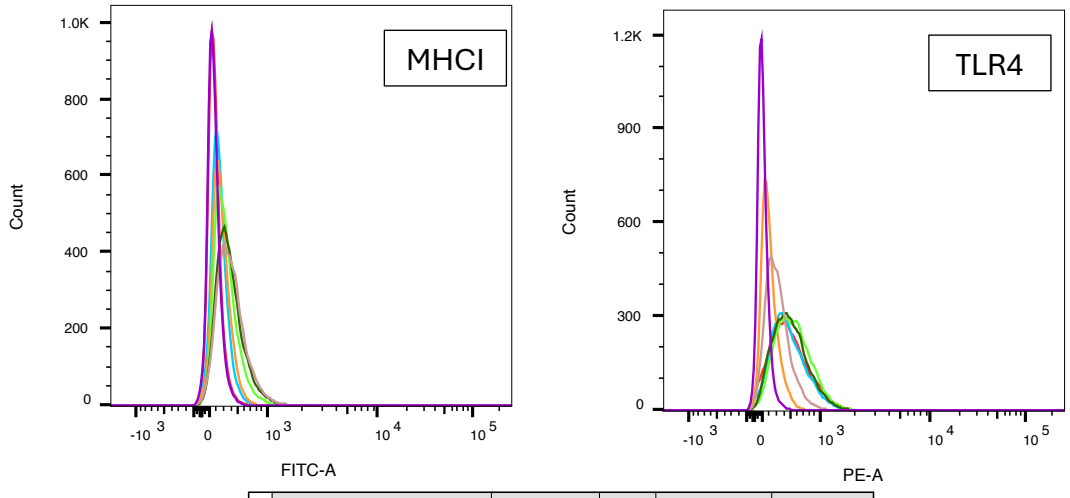

	Sample Name	Subset Name	Count	Mean : FITC-A	Mean : PE-A
	SPECIMEN_US.fcs	Viable cells	8506	184	136
	SPECIMEN_R0419 LPS A 1.fcs	Viable cells	8872	435	346
	SPECIMEN_R0419 LOX A 1.fcs	Viable cells	8896	430	536
	SPECIMEN_R0419 A 1.fcs	Viable cells	9055	359	580
	SPECIMEN_LPS A 1.fcs	Viable cells	8086	289	233
	SPECIMEN_LOX A 1.fcs	Viable cells	8187	299	538
	SPECIMEN_C A G1.fcs	Viable cells	8713	223	523

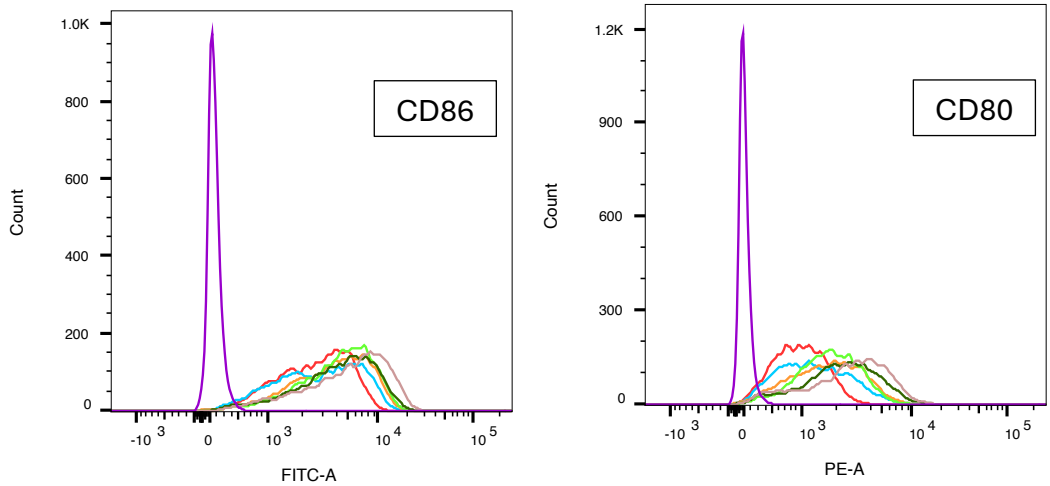

	Sample Name	Subset Name	Count	Mean : FITC-A	Mean : PE-A
	SPECIMEN_US.fcs	Viable cells	8506	184	136
	SPECIMEN_R0419 LPS A 2.fcs	Viable cells	8912	6854	4047
	SPECIMEN_R0419 LOXA 2.fcs	Viable cells	8564	5535	3548
	SPECIMEN_R0419 A 2.fcs	Viable cells	9133	5203	2448
	SPECIMEN_LPS A 2.fcs	Viable cells	8816	4909	2583
	SPECIMEN_LOX A 2.fcs	Viable cells	8879	3899	1954
	SPECIMEN_C A 2.fcs	Viable cells	9200	3280	1193

Figure 158: ***Cell Surface Marker Expression Profile is affected by Specific TLR Activation and R0419 presence.*** *J774.A.1. cells were seeded at 1x10^6 cells/mL and incubated overnight at 37^{0}C in 5% CO_2. Cells were stimulated with 25mg/mL raw sample fermentate, incubated for 1 hour at 37^{0}C in 5% CO_2 before stimulating with TLR ligands at the following concentrations: LPS 100ng/mL and LOX 0.5mM and incubated overnight at 37^{0}C in 5% CO_2. Cell suspensions were retained, and cell staining protocol was carried out for activated TLR ligands LPS and LOX in the presence of fermentates, to assess the presence of cell surface markers MHCII, TLR4, CD86 and CD80. Cells were analysed using BD FACSAria 1 system flow cytometer, raw FCS files analysed, data graphed using V10.0 FlowJo software.*

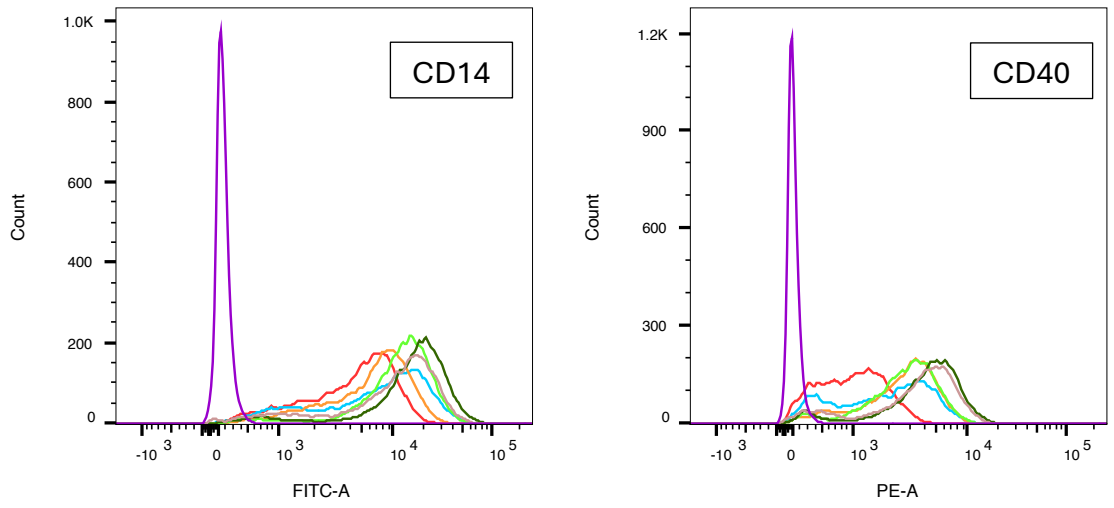

	Sample Name	Subset Name	Count	Mean : FITC-A	Mean : PE-A
	SPECIMEN_US.fcs	Viable cells	8506	184	136
	SPECIMEN_R0419 LPS A 3.fcs	Viable cells	8736	13736	4338
	SPECIMEN_R0419 LOX A 3.fcs	Viable cells	8798	19029	4941
	SPECIMEN_R0419 A 3.fcs	Viable cells	9087	14013	3188
	SPECIMEN_LPS A 3.fcs	Viable cells	9055	8164	3086
	SPECIMEN_LOX A 3_002.fcs	Viable cells	8822	10826	2543
	SPECIMEN_C A 3.fcs	Viable cells	9571	5614	1163

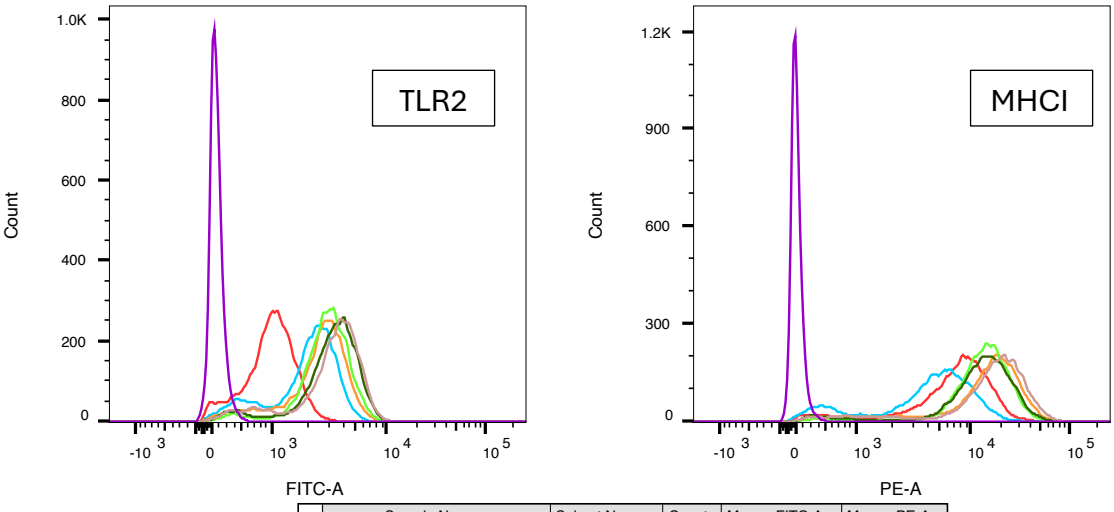

	Sample Name	Subset Name	Count	Mean : FITC-A	Mean : PE-A
	SPECIMEN_US.fcs	Viable cells	8506	184	136
	SPECIMEN_R0419 LPS A 4.fcs	Viable cells	8958	3525	19711
	SPECIMEN_R0419 LOX A 4.fcs	Viable cells	8893	3489	15687
	SPECIMEN_R0419 A 4.fcs	Viable cells	9081	3077	15310
	SPECIMEN_LPS A 4.fcs	Viable cells	8814	2729	17380
	SPECIMEN_LOX A 4.fcs	Viable cells	8984	2198	5896
	SPECIMEN_C A 4.fcs	Viable cells	9347	1080	8936

Figure 159: ***Cell Surface Marker Expression Profile is affected by Specific TLR Activation and R04190 presence.*** *J774.A.1. cells were seeded at 1x10^6 cells/mL and incubated overnight at 37^{0}C in 5% CO_2. Cells were stimulated with 25mg/mL raw sample fermentate, incubated for 1 hour at 37^{0}C in 5% CO_2 before stimulating with TLR ligands at the following concentrations: LPS 100ng/mL and LOX 0.5mM and incubated overnight at 37^{0}C in 5% CO_2. Cell suspensions were retained, and cell staining protocol was carried out for activated TLR ligands LPS and LOX in the presence of fermentates to assess the presence of cell surface markers CD14, CD40, TLR2 and MHCI. Cells were analysed using BD FACSAria 1 system flow cytometer, raw FCS files analysed, data graphed using V10.0 FlowJo software.*

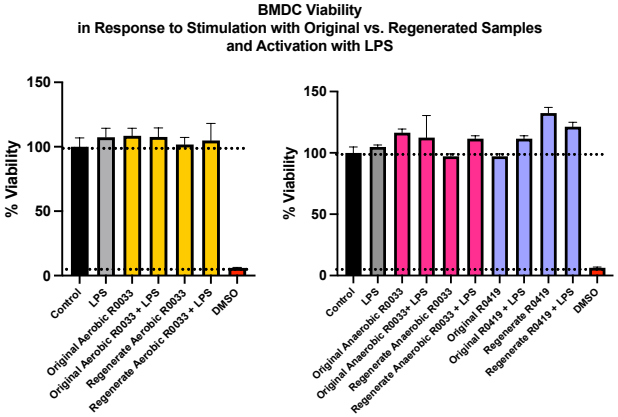

Figure 160: ***Exposure of LPS activated BMDC to 25mg/mL Original or Regenerated raw samples doesn't affect cell viability.*** *BMDC cells were seeded at 1x10^6 cells/mL and left overnight at 37^{0}C in 5% CO_2. The following day cells were stimulated with 25mg/mL sample fermentate, incubated for 1 hour at 37^{0}C in 5% CO_2 and subsequently exposed to LPS 100ng/mL for TLR activation before incubating overnight under the same conditions. 10% DMSO was included as a positive control to induce cell death. Cells were incubated with MTS cell titre aqueous one solution for 3 hours at 37^{0}C in 5% CO_2. Viability is represented as a percentage compared to viable, untreated cells (Control). Data is presented as mean ± SD of three replicates.*

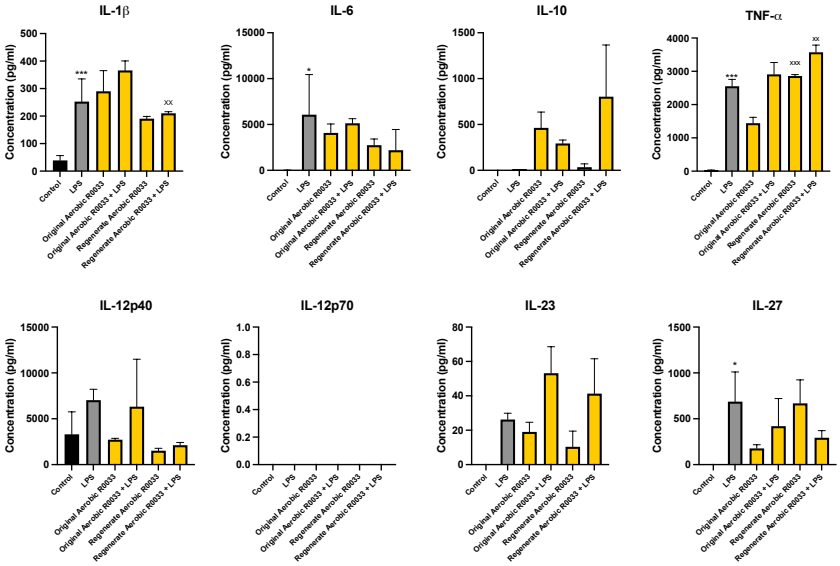

Figure 161: ***Exposure of LPS activated BMDC to 25mg/mL Original or Regenerated raw Aerobic R0033 results in the secretion of cytokines IL-1β, IL-6, IL-10, TNF-α, IL-12p40, IL-12p70, IL-23, and IL-27.*** *BMDC cells were seeded at 1x10^6 cells/mL and left overnight at 37^{0}C in 5% CO_2. The following day cells were stimulated with 25mg/mL raw sample fermentate, incubated for 1 hour at 37^{0}C in 5% CO_2 and % CO_2 and subsequently exposed to the following concentrations of TLRs: LPS 100ng/mL for TLR activation before incubating overnight under the same conditions. Supernatants were removed after 24 hours and ELISA was performed for cytokines IL-1β, IL-6, IL-10, TNF-α, IL-12p40, IL-12p70, IL-23, and IL-27. Data is presented as mean ± SD of three replicates. Significance determined using one- way ANOVA with a Newman-Keuls post-test. Output P value style APA: .12 (ns), .033 (*), .002(**) and <.001 (***); 1) comparing TLR to unstimulated control cells "*" and 2) comparing original sample -/+ LPS to regenerate sample -/+ LPS "x".*

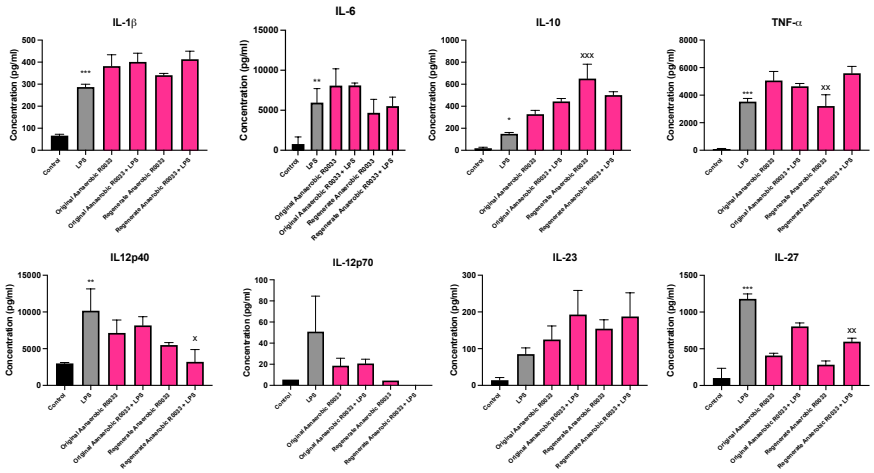

Figure 162: ***Exposure of LPS activated BMDC to 25mg/mL Original or Regenerated raw Anaerobic R0033 results in the secretion of cytokines IL-1β, IL-6, IL-10, TNF-α, IL-12p40, IL-12p70, IL-23, and IL-27.*** *BMDC cells were seeded at 1x10^6 cells/mL and left overnight at 37^{0}C in 5% CO_2. The following day cells were stimulated with 25mg/mL raw sample fermentate, incubated for 1 hour at 37^{0}C in 5% CO_2 and % CO_2 and subsequently exposed to the following concentrations of TLRs: LPS 100ng/mL for TLR activation before incubating overnight under the same conditions. Supernatants were removed after 24 hours and ELISA was performed for cytokines IL-1β, IL-6, IL-10, TNF-α, IL-12p40, IL-12p70, IL-23, and IL-27. Data is presented as mean ± SD of three replicates. Significance determined using one- way ANOVA with a Newman-Keuls post-test. Output P value style APA: .12 (ns), .033 (*), .002(**) and <.001 (***); 1) comparing TLR to unstimulated control cells "*" and 2) comparing original sample -/+ LPS to regenerate sample -/+ LPS "x".*

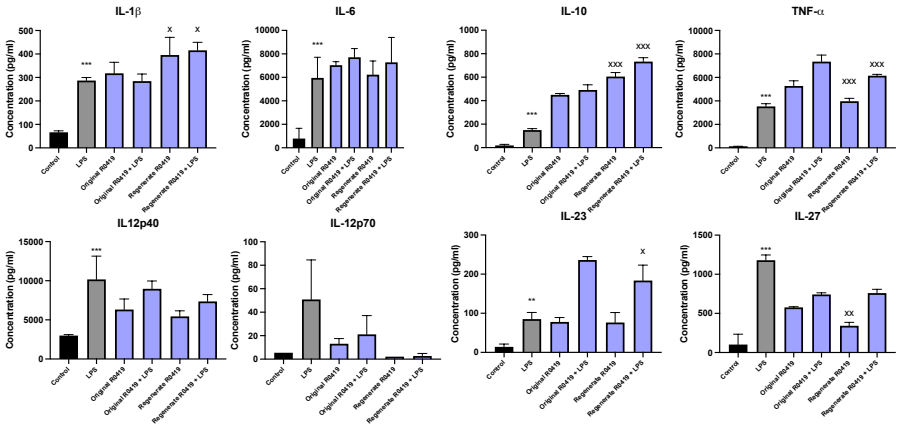

Figure 163: ***Exposure of LPS activated BMDC to 25mg/mL Original or Regenerated R0419 results in the secretion of cytokines IL-1β, IL-6, IL-10, TNF-α, IL-12p40, IL-12p70, IL-23, and IL-27.*** *BMDC cells were seeded at 1x10^6 cells/mL and left overnight at 37^{0}C in 5% CO_2. The following day cells were stimulated with 25mg/mL raw sample fermentate, incubated for 1 hour at 37^{0}C in 5% CO_2 and % CO_2 and subsequently exposed to the following concentrations of TLRs: LPS 100ng/mL for TLR activation before incubating overnight under the same conditions. Supernatants were removed after 24 hours and ELISA was performed for cytokines IL-1β, IL-6, IL-10, TNF-α, IL-12p40, IL-12p70, IL-23, and IL-27. Data is presented as mean ± SD of three replicates. Significance determined using one- way ANOVA with a Newman-Keuls post-test. Output P value style APA: .12 (ns), .033 (*), .002(**) and <.001 (***); 1) comparing TLR to unstimulated control cells "*" and 2) comparing original sample -/+ LPS to regenerate sample -/+ LPS "x".*

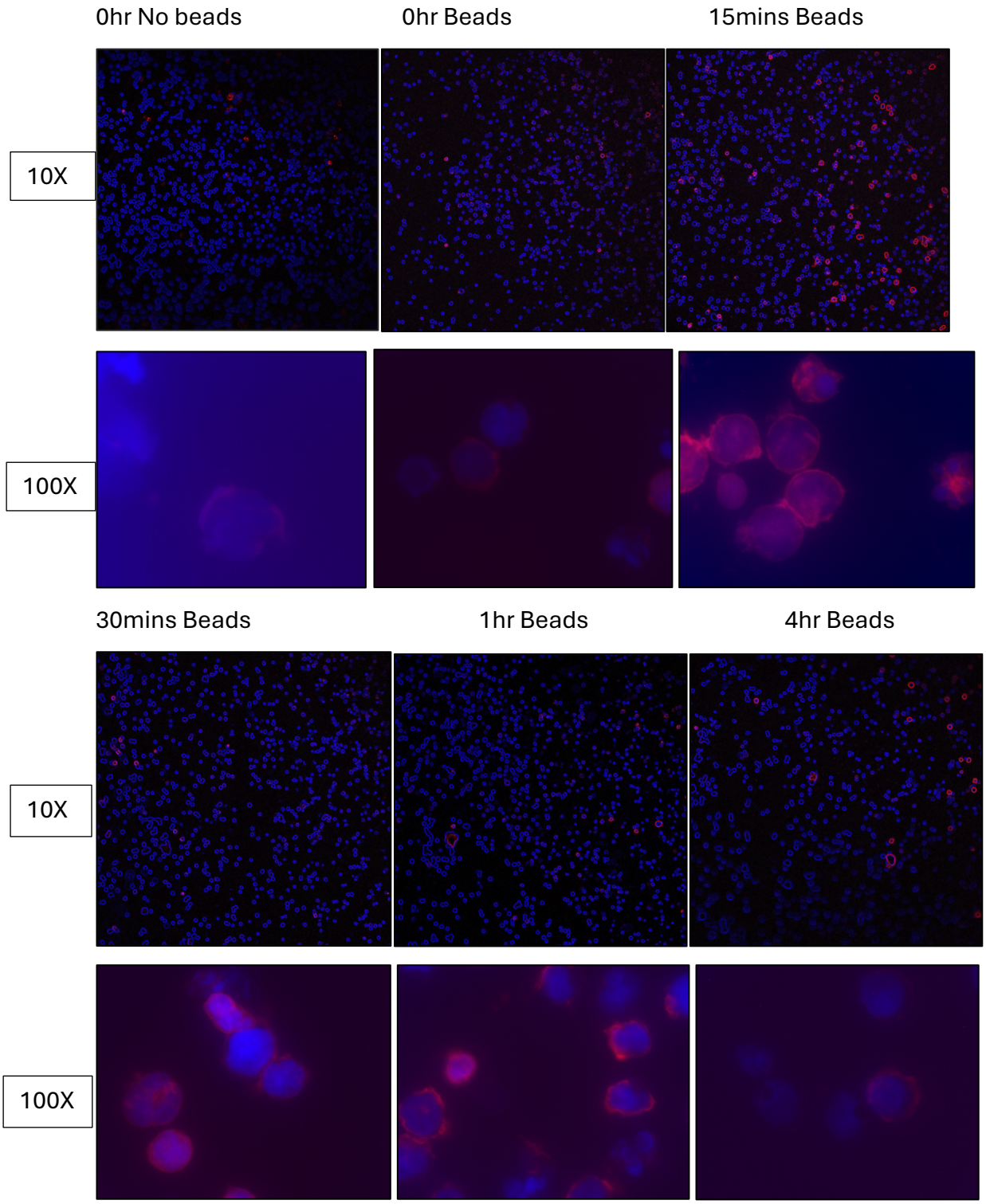

Figure 164: **Exposure of JURKAT cells to T cell activation beads results F-ACTIN.** JURKAT cells were seeded at $5x10^5$ cells/mL and serum starved for 2 hours at 37^0C in 5% $CO_{2.}$, before being stimulated with a 1:1 ratio of beads to cells, and incubated for either 0, 15, 30 minutes, or 1, or 4 hours at 37^0C in 5% CO_2 . Procedure for immune synapse interaction was carried out, staining viable cells with Hoechst (nucleus), and TRITC (F-actin). Cell count analysed using ImageJ JS software. Negative control of cells in the presence of no activation beads is included.

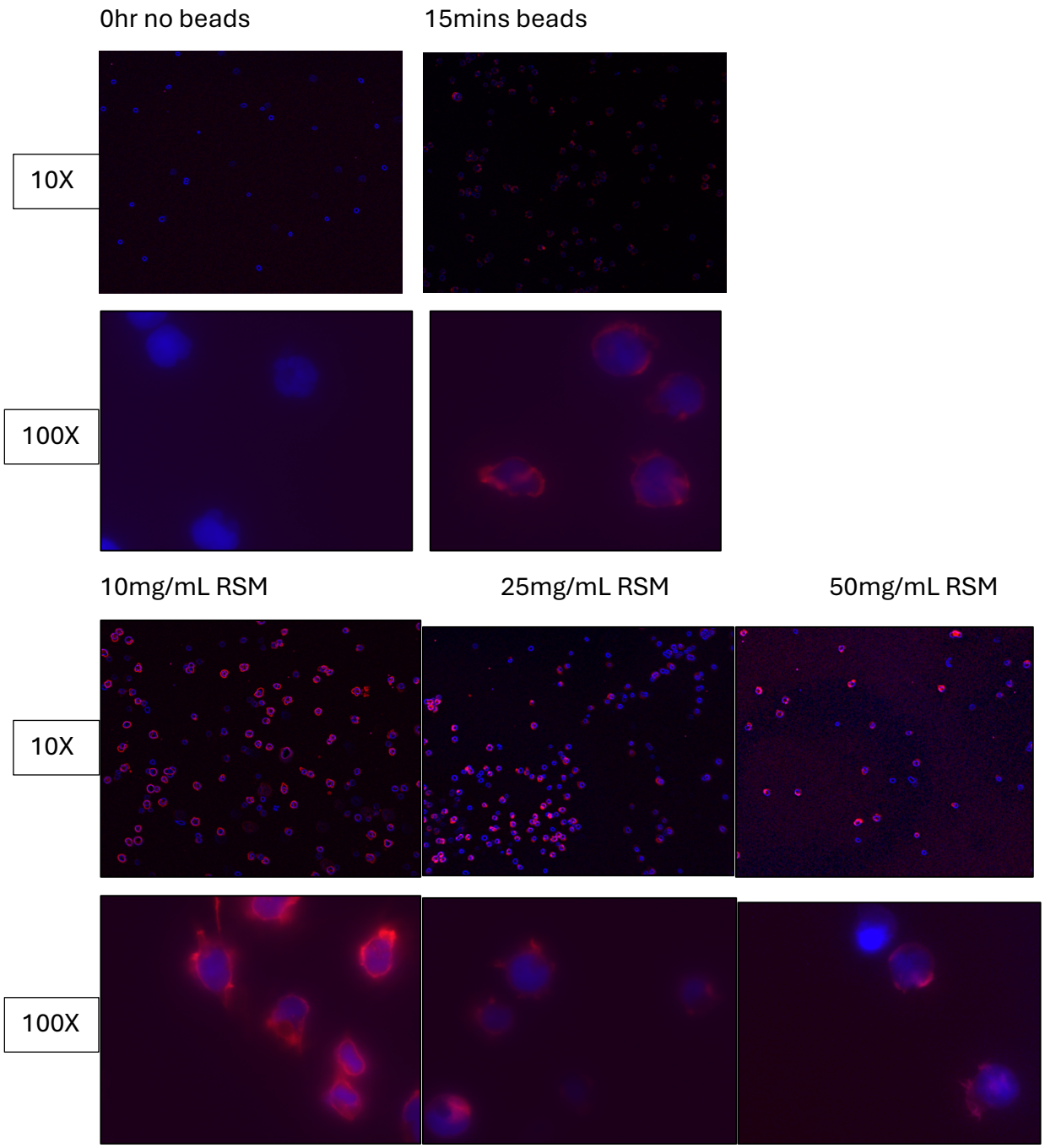
0hr no beads
15mins beads
10X
100X
10mg/mL RSM
25mg/mL RSM
50mg/mL RSM
10X
100X

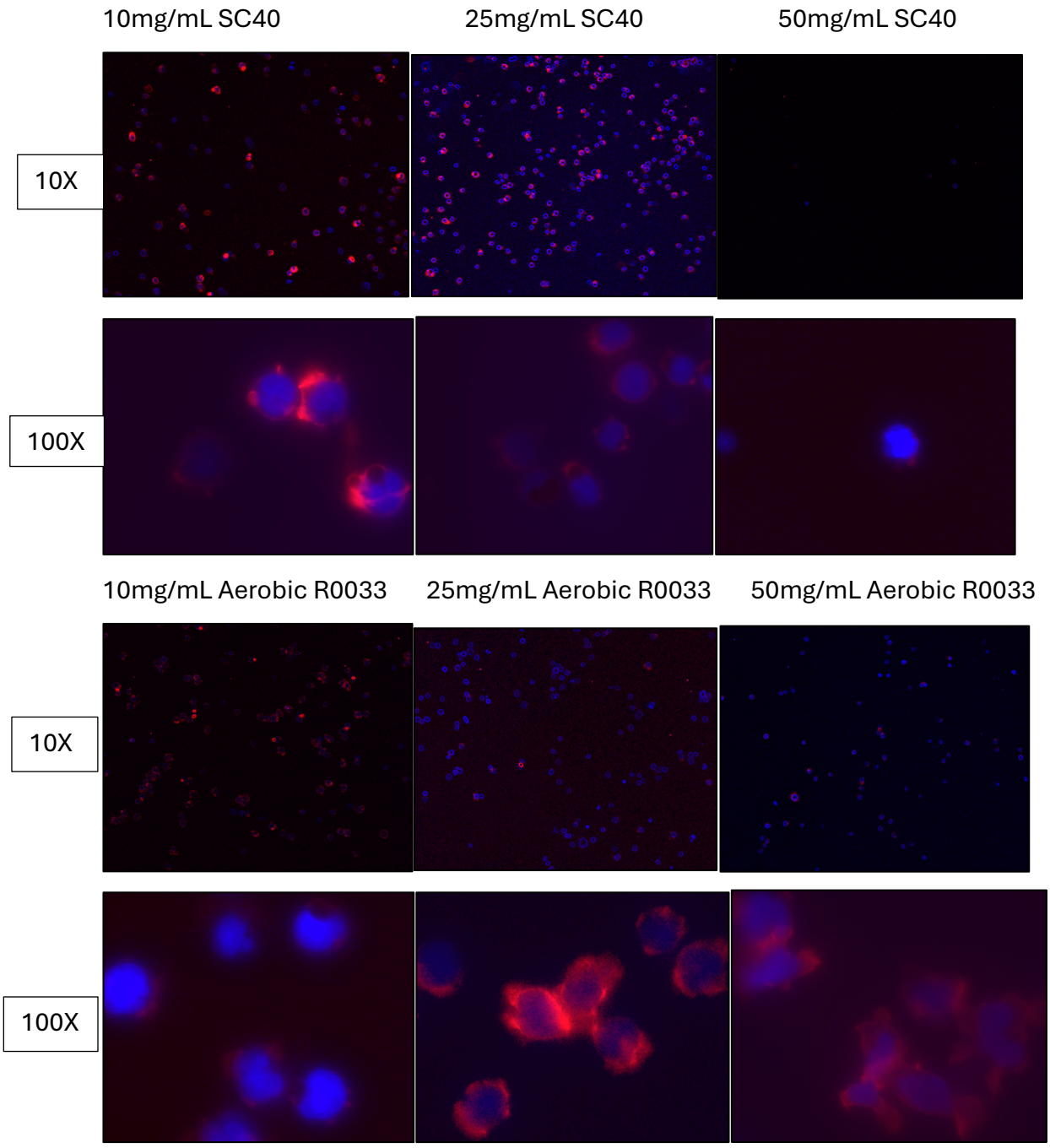

Figure 165: **Exposure of JURKAT cells to T cell activation beads results in immune synapse interaction.** JURKAT cells were seeded at $5x10^5$ cells/mL and serum starved for 1 hour at 37^0C in 5% $CO_{2.,}$ before being stimulated with a dose range of fermentates of 10mg/mL, 25mg/mL, or 50mg/mL, and then incubated for a further 1 hour. After 1 hour the cells were activated with a 1:1 ratio of beads to cells, and incubated for 15 minutes at 37^0C in 5% CO_2 . Procedure for immune synapse interaction was carried out, staining viable cells with Hoechst (nucleus), and TRITC (F-actin). Data displayed is as representative of four replicates. Activated T cells are represented as a % of the cells activated at the immune synapse compared to the total cell population. Negative control of cells in the presence of no activation beads is included.